

NASA CR- 168301



National Aeronautics and
Space Administration

R82AEB472
March 1984

*P-474
#304580*

ENERGY EFFICIENT ENGINE

**COMBUSTOR TEST HARDWARE
DETAILED DESIGN REPORT**

By

- D.L. Burrus
- C.A. Chahrour
- H.L. Foltz
- P.E. Sabla
- S.P. Seto
- J.R. Taylor

AIRCRAFT ENGINE BUSINESS GROUP
ADVANCED TECHNOLOGY
PROGRAMS DEPARTMENT
CINCINNATI, OHIO 45215

Prepared for
NATIONAL AERONAUTICS AND SPACE ADMINISTRATION
LEWIS RESEARCH CENTER
21000 BROOKPARK ROAD
CLEVELAND, OHIO 44135

These limitations shall be con-
sidered void after two (2) years after date of such data.

**NASA - LEWIS RESEARCH CENTER
Contract NAS3-20643**

(NASA-CR-168301) ENERGY EFFICIENT ENGINE
COMBUSTOR TEST HARDWARE DETAILED DESIGN
REPORT (GE) 474 p CSCL 21E

N90-28554

Unclass

TABLE OF CONTENTS

<u>Section</u>		<u>Page</u>
1.0	SUMMARY	1
2.0	INTRODUCTION	2
3.0	DESIGN SELECTION	4
	3.1 Objectives and Goals	4
	3.2 Design Approach	6
4.0	AERO DESIGN	12
	4.1 Requirements	12
	4.2 Key Design Studies	14
	4.2.1 Cycle Studies	14
	4.2.2 Diffuser	18
	4.2.3 Fuel Nozzle	21
	4.2.4 Starting	24
	4.2.5 Emissions	34
	4.3 Combustor Design Features	41
	4.4 Design Summary	50
5.0	MECHANICAL DESIGN	52
	5.1 Requirements	52
	5.2 General Design Features	52
	5.3 Design Selection	55
	5.3.1 Materials	55
	5.3.2 Design Description and Geometry	55
	5.4 Design Analysis	81
	5.4.1 Heat Transfer	81
	5.4.2 Stress and Life	106
	5.4.3 Fuel Nozzle Vibratory Analysis	124
6.0	COMBUSTOR TEST RESULTS	136
	6.1 Subcomponent Testing	136
	6.1.1 Combustion System Diffuser Test	136
	6.1.2 Swirl Cup Development Tests	175
	6.1.3 Dome Metal Temperature Tests	190
	6.1.4 Sector Combustor Tests	200
	6.2 Full-Annular Test	260
	6.2.1 Test Hardware Description	262
	6.2.2 Screening Combustor Test Results	283
	6.2.3 Development Testing	364

TABLE OF CONTENTS (Concluded)

<u>Section</u>		<u>Page</u>
7.0	CONCLUDING REMARKS	415
	APPENDIX A	419
	APPENDIX B	422
	APPENDIX C	439
	APPENDIX D	447
	APPENDIX E	448
	APPENDIX F	449
	REFERENCES	459

LIST OF ILLUSTRATIONS

<u>Figure</u>		<u>Page</u>
1.	E ³ Combustor Cross Section.	7
2.	NASA/GE Double-Annular Combustors.	8
3.	Comparison of QCSEE and E ³ Double-Annular Combustors.	9
4.	E ³ Combustor Film/Impingement Liner Design.	11
5.	Turbine Inlet Radial Temperature Profile Requirements.	13
6.	Effect of Pilot Dome Airflow on CO Emissions.	15
7.	E ³ Double-Annular Combustor Airflow Distribution, Baseline.	16
8.	E ³ Combustor Design Airflow Distribution, Core Engine (% W _c).	17
9.	Split Duct Diffuser Design.	20
10.	E ³ Double-Annular Combustor Fuel Nozzle Design.	22
11.	E ³ Fuel Nozzle Flow Characteristics.	23
12.	Combustor Fuel/Air Ratio Versus Core Compressor Flow.	26
13.	Combustor Exit Temperature Profile.	28
14.	Double-Annular Combustor Dome Velocity Comparison.	29
15.	Comparison of Combustor Fuel Staging Sequence.	30
16.	Comparison of Core Engine Start Models.	32
17.	Emissions Comparison.	36
18.	Low Power Emissions Comparison.	37
19.	High Power Emissions Comparison.	38
20.	Trade-Off in CO Emissions Index Between Idle and Approach Conditions to Meet E ³ CO EPAP Goal.	39
21.	Swirl Cup Design.	43
22.	Combustor Emissions - Reduction Sleeves.	44
23.	Recirculation Flow Compared to Sleeve "Included Angle."	45
24.	Venturi Anticarboning Design Criteria.	47
25.	E ³ Dilution Thimble Designs.	48
26.	Comparison of E ³ Dilution Jet Penetration.	49
27.	Fuel Nozzle Staging - Pilot to Main Stage.	51
28.	Assembled E ³ Combustor.	53
29.	Combustor Materials Selection.	54

LIST OF ILLUSTRATIONS (Continued)

<u>Figure</u>		<u>Page</u>
30.	E ³ Fuel Nozzle Materials.	56
31.	Combustor Inner Support Liner.	58
32.	Assembled Combustor Inner Liner.	59
33.	E ³ /GE23 Shingle - Comparison of Support Foot Spacings.	61
34.	Comparison of Shingle Edge Seal Configurations.	62
35.	Effect of Shingle Edge Leakage on Shingle Configurations.	64
36.	E ³ Dilution Thimbles.	65
37.	E ³ Combustor Casing Hardware.	66
38.	E ³ Combustor Casing Features.	67
39.	E ³ Combustor Casing Rollout.	68
40.	E ³ Combustor Support Pin Design.	69
41.	E ³ Combustor Dome (Forward Looking Aft).	71
42.	E ³ Combustor Dome Design Features.	72
43.	E ³ Combustor Centerbody Structure.	73
44.	Detailed View of Centerbody and Domes.	75
45.	E ³ Combustor Centerbody Design.	76
46.	E ³ Centerbody Configuration.	77
47.	E ³ Combustor Fuel Delivery System.	78
48.	E ³ Fuel Nozzle Mechanical Features.	79
49.	E ³ Fuel Nozzle Assembly.	80
50.	Design Calculation Flow Chart for Combustor Heat Transfer Analysis.	83
51.	Node Model for a Machined Ring Combustor Showing Heat Transfer Quantities.	85
52.	Flow Distribution Used For Heat Transfer Analysis of Liners.	86
53.	Comparison of Liner Cooling Rate Parameters, Outer Liners.	87
54.	Comparison of Liner Cooling Rate Parameters, Inner Liners.	88
55.	Heat Transfer Input/Output Data.	90
56.	Panel 1 Inner Axial Temperature Profile Growth +27° F Hot Day Takeoff.	93
57.	Three-Dimensional Model.	94
58.	Three-Dimensional Temperature Profile - Full Foot Width.	95

LIST OF ILLUSTRATIONS (Continued)

<u>Figure</u>		<u>Page</u>
59.	Three-Dimensional Temperature Profile - One-Half Foot Width.	96
60.	Flow Distribution Used in the Analysis of the Centerbody.	98
61.	Centerbody Panel Temperature - Baseline Standard Day Takeoff.	99
62.	Centerbody Tip Surface Temperature - Baseline Standard Day Takeoff.	101
63.	Centerbody Tip Metal Temperature Distribution.	103
64.	Effect of Inlet Fuel Temperature on Fuel Nozzle Temperatures.	105
65.	Recommended Mission Mix for E ³ .	107
66.	Shingle Structural Model.	108
67.	Analytically Predicted Pressure Stresses for Shingle.	110
68.	Shingle Foot Size Versus Rupture Life Capability.	111
69.	Shingle Low Cycle Fatigue Model Temperature Distribution.	112
70.	Analytically Predicted Shingle Stress in Hot Streak.	113
71.	E ³ Combustor Shingle Predicted LCF Life.	114
72.	Predicted Stress for Combustor Support Outer Liners.	117
73.	Predicted Stress for Combustor Support Inner Liners.	118
74.	Support Liner Buckling Analysis Model.	119
75.	Outer Support Liner Critical Buckling Pressures.	120
76.	Effect of Out-of-Roundness on Buckling Characteristics.	121
77.	Predicted Axial Stress Distribution for Casing.	122
78.	Predicted Centerbody Structure Life Levels.	123
79.	E ³ Combustor Design.	125
80.	E ³ Combustor Fuel Nozzle Vibration Analysis.	126
81.	E ³ Fuel Nozzle Design Features.	127
82.	E ³ Fuel Nozzle Campbell Diagram.	128
83.	E ³ Fuel Nozzle Aerodynamic Impact.	130
84.	Comparison of Outer Passage Blockage for E ³ Fuel Nozzle Designs.	131
85.	Comparison of E ³ Combustor Fuel Nozzle Stem Designs.	132
86.	E ³ Combustor Geometric Constraints.	133
87.	E ³ Mechanical Vibration Test Setup.	134
88.	E ³ Combustor Development Test Schedule.	137

LIST OF ILLUSTRATIONS (Continued)

<u>Figure</u>		<u>Page</u>
89.	Combustor Inlet Prediffuser Wall Contours (Inches).	140
90.	Combustor Inlet Prediffuser Wall Contours (Centimeters).	141
91.	Diffuser Inlet Velocity Profile Streamline Plot.	142
92.	Combustor Inlet Diffuser CAFD Analysis.	144
93.	Split Duct Diffuser Flow Regimes.	145
94.	Split Duct Diffuser, 2-D Water Table Model.	148
95.	Split Duct Diffuser, 2-D Water Table Test.	149
96.	Combustor Cowling Modifications.	150
97.	Diffuser Model in Test Cell.	152
98.	Diffuser Model, Forward View.	153
99.	Diffuser Model, Aft View.	154
100.	Annular Diffuser Model Instrumentation Layout.	156
101.	Keil Probe.	157
102.	Diffuser Inlet Velocity Profiles.	162
103.	Prediffuser Velocity Profiles.	163
104.	Static Pressure Recovery Levels, Center Peaked Profile.	165
105.	Static Pressure Recovery Levels, Outer Peaked Profile.	166
106.	Static Pressure Recovery Levels, Inner Peaked Profile.	167
107.	Static Pressure Rise Coefficients, Center Peaked Profile.	169
108.	Static Pressure Rise Coefficients, Outer Peaked Profile.	170
109.	Static Pressure Rise Coefficients, Inner Peaked Profile.	171
110.	Total Pressure Loss Coefficients, Center Peaked Profile.	172
111.	E ³ Spray Characteristics Test Dome Assembly Cross Section.	177
112.	Visual Test Setup.	179
113.	Wedge Probe Test Schematic, Flow Stand.	180
114.	Development Swirl Cup Sleeve Configurations.	183
115.	Fuel Spray Patternation Test Results, Pilot Stage Dome Cup.	184
116.	Fuel Spray Patternation Test Results, Main Stage Dome Cup.	185
117.	Swirl Cup Axial Velocity Profiles, Pilot Stage Cup.	187
118.	Swirl Cup Axial Velocity Profiles, Main Stage Cup.	188
119.	Recirculation Test Schematic (Halogen Detector).	189

LIST OF ILLUSTRATIONS (Continued)

<u>Figure</u>		<u>Page</u>
120.	Dome Metal Temperature Test Hardware.	192
121.	Dome Metal Temperature Test Instrumentation.	193
122.	Dome Metal Temperature Test Rig.	194
123.	Dome Metal Temperature Test Results.	198
124.	E ³ Sector Combustor Test Schedule.	201
125.	E ³ Sector Combustor Cross Section.	203
126.	Sector Combustor Hardware.	204
127.	E ³ Sector Combustor Test Rig Schematic.	207
128.	Sector Test Rig Inlet Diffuser.	208
129.	Test Rig and Instrumentation Emission Tests.	209
130.	Sector Test Rig Gas Sampling Rake.	211
131.	Schematic of Typical Rake Sampling Element.	212
132.	Sector Combustor Baseline Ignition Results.	224
133.	Sector Combustor Mod I Ignition Results, Pilot Stage.	225
134.	Sector Combustor Mod I Ignition Results, Main Stage.	227
135.	Sector Combustor Mod I Ignition Results Versus Cycle Requirement.	228
136.	Sector Combustor Mod III Ignition Results.	229
137.	Sector Combustor Mod II and III Main Stage Ignition Results.	231
138.	Sector Combustor Mod III Ignition Results Versus Cycle Requirement.	232
139.	Sector Combustor Mod IV Ignition Results at Actual Inlet Pressure.	233
140.	Sector Combustor Mod V Ignition Results at Actual Inlet Pressure.	235
141.	Sector Combustor Mod VI Ignition Results.	236
142.	E ³ Sector Combustor Subidle EGT Profiles (Pilot Only).	237
143.	E ³ Sector Combustor Subidle EGT Profiles (Staged).	238
144.	E ³ Sector Combustor EGT Profiles at Simulated SLTO.	239
145.	Sector Combustor Pressure Drop Versus Flow Function Parameter.	241
146.	E ³ Sector Combustor Emissions Results, Baseline Configuration.	242

LIST OF ILLUSTRATIONS (Continued)

<u>Figure</u>		<u>Page</u>
147.	E ³ Sector Combustor Emissions Results, Mod I Configuration.	243
148.	E ³ Sector Combustor Emissions Results, Mod II Configuration.	245
149.	E ³ Sector Combustor Emissions Results, Mod III Configuration.	246
150.	E ³ Sector Combustor Emissions Results, Fuel Nozzle Type.	247
151.	E ³ Sector Combustor Emissions Results, Mod IV Configuration.	248
152.	E ³ Sector Combustor Emissions Results, Mod V Configuration.	249
153.	E ³ Sector Combustor Emissions Results, Mod VI Configuration.	251
154.	E ³ Sector Combustor Emissions Results, Approach Conditions.	252
155.	E ³ Sector Combustor Emissions Results, EI _{NO_x} .	254
156.	E ³ Sector Combustor Altitude Relight Test Results, Mod VI Configuration.	255
157.	Full-Annular Test Schedule.	261
158.	E ³ Full-Annular Development Combustor Design.	263
159.	E ³ Test Rig Fuel Nozzle Assembly.	266
160.	E ³ Full-Annular Combustor Component Test Rig.	267
161.	Test Rig Bleed Simulation System.	270
162.	Test Rig Instrumentation Spool.	272
163.	ACTS Traverse System.	274
164.	E ³ Full-Annular Combustor EGT Thermocouple Rakes.	277
165.	E ³ Full-Annular Combustor Gas Sampling Rakes.	279
166.	Gas Sampling Rake Instrumentation for Ignition Testing.	280
167.	Effect of Gas Rake Cooling Medium on CO and HC Emissions.	282
168.	Development Combustor Baseline Atmospheric Ignition Test Results.	286
169.	Development Combustor Baseline EGT Performance Test Results, Idle.	290
170.	Development Combustor Baseline EGT Performance Test Results, SLTO.	291
171.	Development Combustor Baseline EGT Performance Test Results, Circumferential Temperatures.	292
172.	Baseline Combustor Instrumentation Layout, Pilot Stage.	295

LIST OF ILLUSTRATIONS (Continued)

<u>Figure</u>		<u>Page</u>
173.	Baseline Combustor Instrumentation Layout, Main Stage.	296
174.	Baseline Combustor Instrumentation Layout, Liners.	297
175.	Baseline Combustor Instrumentation Layout, Centerbody and Fuel Nozzles.	298
176.	Combustor Test Rig Instrumentation.	299
177.	Baseline Combustor Emissions Results, Idle, EI _{CO} .	301
178.	Baseline Combustor Emissions Results, Idle, EI _{HC} .	302
179.	Baseline Combustor Emissions Results, 30% Power.	303
180.	Baseline Combustor Emissions Results, at Staging.	305
181.	Baseline Combustor Emissions Results, EI _{NO_x} .	306
182.	Diffuser Inlet Mach Number Profile (Baseline Test).	309
183.	Measured Combustor Pressure Losses for Baseline.	311
184.	Measured Combustor Metal Temperatures for Baseline Test, Panel 1, Outer Liner.	313
185.	Measured Combustor Metal Temperatures for Baseline Test, Panel 2, Outer Liner.	314
186.	Measured Combustor Metal Temperatures for Baseline Test, Panel 3, Outer Liner.	315
187.	Measured Combustor Metal Temperatures for Baseline Test, Panel 1, Inner Liner.	316
188.	Measured Combustor Metal Temperatures for Baseline Test, Panel 2, Inner Liner.	317
189.	Measured Combustor Metal Temperatures for Baseline Test, Panel 3, Inner Liner.	318
190.	Measured Combustor Metal Temperatures for Baseline Test, Centerbody, Pilot Side.	319
191.	Measured Combustor Metal Temperatures for Baseline Test, Centerbody, Main Stage Side.	320
192.	Measured Combustor Metal Temperatures for Baseline Test, Splash Plate.	321
193.	Mod I Combustor Hardware Modifications.	324
194.	Mod I Atmospheric Ignition Test Results, Pilot Stage.	327
195.	Mod I Atmospheric Ignition Test Results, Main Stage.	328
196.	Mod I EGT Performance Test Results, Pilot Only.	331

LIST OF ILLUSTRATIONS (Continued)

<u>Figure</u>		<u>Page</u>
197.	Mod I EGT Performance Test Results, 50/50 Fuel Flow Split.	333
198.	Mod I EGT Performance Test Results, 40/60 Fuel Flow Split.	334
199.	Mod I EGT Performance Test Results, 30/70 Fuel Flow Split.	335
200.	Mod I Ignition Results at True Cycle Conditions.	337
201.	Mod I Combustor Instrumentation Layout, Pilot Stage.	340
202.	Mod I Combustor Instrumentation Layout, Main Stage.	341
203.	Mod I Combustor Instrumentation Layout, Outer and Inner Liners.	342
204.	Mod I Combustor Instrumentation Layout, Centerbody.	343
205.	Mod I Emissions Test Results, EI_{CO} at Idle.	344
206.	Mod I Emissions Test Results, EI_{HC} at Idle.	345
207.	Rake Gas Sample Level at Idle.	347
208.	Mod I Emissions Test Results, EI_{NO_x} .	348
209.	Diffuser Inlet Mach Number Profile (Mod I Test).	351
210.	Measured Pressure Losses for Mod I Combustor.	353
211.	Measured Combustor Metal Temperatures for Mod I Test, Panel 1, Outer Liner.	354
212.	Measured Combustor Metal Temperatures for Mod I Test, Panel 2, Outer Liner.	355
213.	Measured Combustor Metal Temperatures for Mod I Test, Panel 3, Outer Liner.	356
214.	Measured Combustor Metal Temperatures for Mod I Test, Panel 1, Inner Liner.	357
215.	Measured Combustor Metal Temperatures for Mod I Test, Panel 2, Inner Liner.	358
216.	Measured Combustor Metal Temperatures for Mod I Test, Panel 3, Inner Liner.	359
217.	Measured Combustor Metal Temperatures for Mod I Test, Splash Plate, Pilot.	360
218.	Measured Combustor Metal Temperatures for Mod I Test, Splash Plate, Main.	361
219.	Measured Combustor Metal Temperatures for Mod I Test, Centerbody, Pilot Side.	362
220.	Measured Combustor Metal Temperatures for Mod I Test, Centerbody, Main Side.	363

LIST OF ILLUSTRATIONS (Concluded)

<u>Figure</u>		<u>Page</u>
221.	Mod II-A Combustor Hardware Modification.	367
222.	Mod III-A Combustor Hardware Modification.	368
223.	Mod III-A Atmospheric Ignition Test Results.	372
224.	Mod III-B Atmospheric Ignition Test Results.	374
225.	Mod IV Combustor Hardware Modification.	376
226.	Mod V Combustor Hardware Modification.	377
227.	Mod IV Atmospheric Ignition Test Results.	379
228.	Mod V Atmospheric Ignition Test Results.	380
229.	Mod V EGT Performance Test Results.	383
230.	Mod V EGT Performance Test Results.	384
231.	Mod VI Atmospheric Ignition Test Results.	389
232.	Mod VI EGT Performance Test Results, SLTO.	393
233.	Mod VI EGT Performance Test Results, Pilot Only.	394
234.	Mod VII EGT Performance Test Results, SLTO.	398
235.	Mod VII EGT Performance Test Results, Low Power.	399
236.	Mod VII Ignition Results at True Cycle Conditions.	402
237.	Mod VII Emissions Test Results, Idle Conditions.	404
238.	Mod VII Emissions Test Results, EI _{NO_x} .	406
239.	Engine Combustor Atmospheric Ignition Test Results.	408

LIST OF TABLES

<u>Table</u>	<u>Page</u>
I. E ³ Combustor - Emissions Goals.	4
II. E ³ Combustor - Key Performance/Operating Requirements.	5
III. E ³ Combustor - Parts Life Goals.	5
IV. Performance Requirements.	12
V. Cycle Comparison.	18
VI. Starting Background.	24
VII. E ³ Starting Studies Chronology.	25
VIII. Adverse Impacts of Pilot and Main Stage Ground Start Ignition.	31
IX. Revised Engine Start Analysis.	33
X. Ignition Study Results.	33
XI. Ground Idle Cycle Comparison.	34
XII. E ³ Emissions Adjustment Relationships.	40
XIII. E ³ Combustor Estimated Emissions.	41
XIV. Engine Fuel Nozzle Features.	50
XV. Combustor Mechanical Design Objectives.	52
XVI. Shingle Geometry Comparison.	60
XVII. Summary of Two-Dimensional Temperature Calculations and Cycle Data.	92
XVIII. Summary of Predicted Liner Temperatures for the Baseline Development Combustor - Baseline Standard Day Takeoff.	97
XIX. E ³ Combustor Shingle Predicted Life Levels.	115
XX. Comparison of Fuel Nozzle First Flex Frequencies.	129
XXI. Diffuser Pressure Loss Goals.	146
XXII. Diffuser Performance with Center, Outboard, and Inboard Peaked Profiles.	173
XXIII. Diffuser Model Performance Comparison.	174
XXIV. Test Conditions for Fuel Spray Visualization Testing.	181
XXV. E ³ Combustor Swirl Cup Flow Visualization Test Results.	186
XXVI. Dome Metal Temperature Test Point Schedule.	195
XXVII. Estimated Dome Metal Temperatures for Full-Annular Combustor Testing.	199

LIST OF TABLES (Continued)

<u>Table</u>	<u>Page</u>
XXVIII. Flow Area Distribution for Baseline Sector Combustor Configuration.	205
XXIX. Sector Combustor Ignition Test Point Schedule.	215
XXX. Sector Combustor Emissions Test Point Schedule.	217
XXXI. Altitude Ignition Testing Summary, Mod V Configuration, 11.8 Kg/Hr (26 Lb/Hr) Nozzles.	257
XXXII. Altitude Ignition Testing Summary, Mod V Configuration, 2.3 Kg/Hr (5.1 Lb/Hr) Nozzles.	257
XXXIII. Altitude Ignition Testing Summary, Mod VI Configuration, 2.3 Kg/Hr (5.1 Lb/Hr) Nozzles.	258
XXXIV. Altitude Ignition Testing Summary, Mod VI Configuration, 11.3 Kg/Hr (26 Lb/Hr) Nozzles.	258
XXXV. Sector Combustor Ignition Test Results.	259
XXXVI. Combustor Test Matrix.	265
XXXVII. CAROL Calibration Gases.	283
XXXVIII. Baseline Atmospheric Ignition Test Point Schedule.	284
XXXIX. Baseline Atmospheric EGT Performance Test Point Schedule.	288
XL. Baseline Emissions Test Point Schedule.	293
XLI. Baseline Combustor EPAP Results.	307
XLII. Baseline Combustor Smoke Results.	307
XLIII. Calculated Diffuser Performance for Baseline Test.	310
XLIV. Combustor Mod I Atmospheric Ignition Test Point Schedule.	325
XLV. Combustor Mod I Atmospheric EGT.	330
XLVI. Combustor Mod I Emissions Test Point Schedule.	339
XLVII. Mod I Combustor EPAP Results.	349
XLVIII. Calculated Diffuser Performance for Mod I Test.	350
XLIX. Mod II and III Atmospheric Ignition Test Point Schedule.	370
L. Mod V Atmospheric EGT Performance Test Point Schedule.	382
LI. Mod VI and VII Atmospheric Ignition Test Point Schedule.	388
LII. Mod VI Atmospheric EGT Performance Test Point Schedule.	391
LIII. Mod VII Atmospheric EGT Performance Test Point Schedule.	396
LIV. Mod VII Emissions Test Point Schedule.	401
LV. Mod VII Emissions Results at Approach Power.	403

LIST OF TABLES (Concluded)

<u>Table</u>	<u>Page</u>
LVI. Mod VII EPAP Results.	405
LVII. Summary of Full-Annular Combustor Configurations.	410
LVIII. Summary of Full-Annular Combustor Test Results.	411
LIX. Subidle Ignition Test Results.	413
LX. Combustor Emissions Summary.	414
LXI. E ³ Development Combustor Exit Temperature Distribution Results.	414
LXII. E ³ FPS Emissions Predictions.	415

1.0 SUMMARY

The Energy Efficient Engine (E³) combustor development effort was conducted as part of the overall NASA/GE E³ Program. The key elements of this 5-year effort included the selection of an advanced double-annular combustion system design based on technology derived from the NASA/GE Experimental Clean Combustor and QCSEE Clean Combustor Development Programs. Numerous preliminary and detailed design studies were conducted to define the features of the combustion system design. Development test hardware was fabricated, and an extensive testing effort was undertaken to evaluate the combustion system sub-components in order to verify and refine the design. This testing effort included full-scale diffuser model testing to develop diffuser performance, sector combustor testing to develop acceptable ignition and emissions characteristics, and full-annular combustor development testing to further develop ignition and emissions characteristics as well as develop acceptable exit temperature performance. Technology derived from this development testing effort will be incorporated into the engine combustion system hardware design. This advanced engine combustion system will then be evaluated in component testing to verify that it satisfies the design intent. What will evolve is an advanced combustion system capable of satisfying all of the E³ combustion system design objectives and requirements.

2.0 INTRODUCTION

The General Electric Company is currently engaged in the Energy Efficient Engine (E³) Project under Contract NAS3-20643 to the NASA-Lewis Research Center. The purpose of the E³ Project is to develop and demonstrate the technology for obtaining higher thermodynamic and propulsive efficiencies in advanced, environmentally acceptable, turbofan engines for possible use in future commercial transport aircraft. The Project involves technology development for engine components, including the design of an advanced, low emissions combustor.

The purpose of the E³ combustor development effort is to develop an advanced combustion system capable of meeting both the stringent emissions and long life goals of the E³, as well as meeting all of the usual performance requirements of combustion systems for modern turbofan engines. Aerothermo and mechanical analyses were conducted to define a design of this advanced combustor. To meet the emissions and performance requirements, an advanced, short length, double-annular dome, combustor design concept was adopted. To meet the long life goals, an advanced, double-walled segmented liner concept using impingement and film cooling was selected. This design approach was chosen based on the low emissions combustor design technology developed in both the NASA Experimental Clean Combustor Program (ECCP) (Reference 1) and the NASA Quiet Clean Short Haul Experimental Engine (QSCEE) Program (Reference 2). In these development programs, it was demonstrated that low emissions levels could be obtained with the double-annular combustor design concept in addition to obtaining the other combustor performance capabilities required for satisfactory operation of a turbofan such as the E³.

This report summarizes the results of the detailed design and analysis efforts, to date, on the combustion system for General Electric's Energy Efficient Engine. This report includes a general description of the combustion system and represents the current status of the design.

This report also includes a presentation of the results for development tests carried out during the detail design and hardware procurement phase of the combustor program. These development tests included subcomponent as well as full-annular tests of prototype designs to evolve the current core engine combustor configuration.

3.0 DESIGN SELECTION

3.1 OBJECTIVES AND GOALS

The key objectives of this program are to design and develop an advanced combustion system capable of meeting both the stringent emissions and long life goals of the E³, as well as meeting all of the usual performance requirements of combustion systems for modern turbofan engines.

As presented in Table I, the E³ program goals for carbon monoxide (CO), unburned hydrocarbons (HC), and oxides of nitrogen (NO_x) emissions are equivalent to the current requirements specified by the Environmental Protection Agency (EPA) for Class T2 [rated thrust greater or equal to 89 kN (20,000 pounds), subsonic application] aircraft engines newly certified after 1981 (Reference 3).

Table I. E³ Combustor - Emission Goals.

EPA 1981 Standards for Newly Certified Engines			
•	Carbon Monoxide	(CO) kgn per kilonewton hour	1.49 (3.0)
•	Hydrocarbons	(HC) cycle (lb per 1000 lb thrust hour cycle)	0.2 (0.4)
•	Nitrogen Oxides	(NO _x) SAE smoke number	1.49 (3.0)
•	Smoke		20.0

Revisions to the EPA standards have been proposed and finalized. These final standards still impose very challenging emission requirements for HC to become effective after 1984. However, the CO and NO_x requirements were eliminated. Therefore, the E³ program emissions goals are much more challenging than the goals imposed by the current standards. The E³ combustion system also must produce an invisible exhaust plume which corresponds to an SAE smoke number of 20 or lower.

The key combustor performance goals for the E³ program are presented in Table II. Most of the current conventional combustor designs developed by General Electric already provide performance levels generally equal to or better than the goals established for the E³ combustor.

Table II. E₃ Combustor - Key Performance Operating Requirements.

●	Combustion efficiency at SLTO (%)	99.5 Min.
●	Total pressure drop at SLTO (%)	5.0 Max.
●	Exit temperature pattern factor at SLTO	0.250 Max.
●	Exit temperature profile factor at SLTO	0.125 Max.
●	Altitude relight capability, km (feet)	9.1 (30,000) Min.
●	Ground idle thrust (% of SLTO)	6.0 Max.

The E³ combustor life requirements are summarized in Table III. General Electric design standards require that all combustor designs meet twice the technical life goals in order to assure adequate design margin. Thus, for technical life goals of 9000 cycles to repair, the GE design standard requires a design with 18,000 cycles predicted capability. It is observed from Table III that the E³ combustor life goals represent a significant advancement over current GE combustor life goals.

Table III. E³ Combustor - Parts Life Goals.

	<u>Hours</u>	<u>Flight Cycle</u>
●	Hot parts	
	- First repair	9,000
	- Total	18,000
●	Cold parts	
	- Total	36,000
●	Current goal for CF6-50 rolled ring combustor - 3000 cycles before first repair	

3.2 DESIGN APPROACH

To meet the emissions goals and other performance requirements of the E³, an advanced, double-annular, short length dome combustor design concept was chosen for the E³ combustion system. A cross section of the E³ combustor design and some of its key features are shown in Figure 1. This combustor concept is based on the technology developed in two NASA/GE combustor programs conducted prior to the start of the E³ program. A brief description of these two programs is given below.

The NASA/GE Experimental Clean Combustor Program involved the design and development of a CF6-50 sized, double-annular dome combustor. This program was directed at developing a large size combustor design with very low CO, HC, and NO_x emissions, compared to a conventional CF6-50 combustor design, over the range of operating conditions of a modern high-pressure-ratio turbofan engine.

The NASA/GE Clean Combustor Program was used as a base for the design and development of a double-annular dome combustor as part of the Quiet Clean Short Haul Experimental Engine Program. This program was similar to the NASA/GE ECCP except that the QCSEE combustor is much smaller and more compact than the CF6-50 combustor design, as shown in Figure 2. However, in order to meet the very challenging NO_x emissions goals of the E³ program, the combustor design was made shorter and more compact than the design evolved in the QCSEE program. This comparison is presented in Figure 3.

To obtain very low CO and HC emission levels at ground idle and low NO_x emission levels at high power conditions requires a staged combustion process. At low power settings, only the outer dome is fueled, providing a rich combustion zone for rapid consumption of the CO and HC emissions; while, at high power settings, both domes are fueled and are designed for very lean fuel/air ratio operation of the combustion zone. This lean combustion is accomplished for the most part by introducing large quantities of airflow into the inner dome annulus. The introduction of these large quantities of airflow in the combustion zone severely limits the availability of air to perform the other aerodynamic functions.

ORIGINAL PAGE IS
OF POOR QUALITY

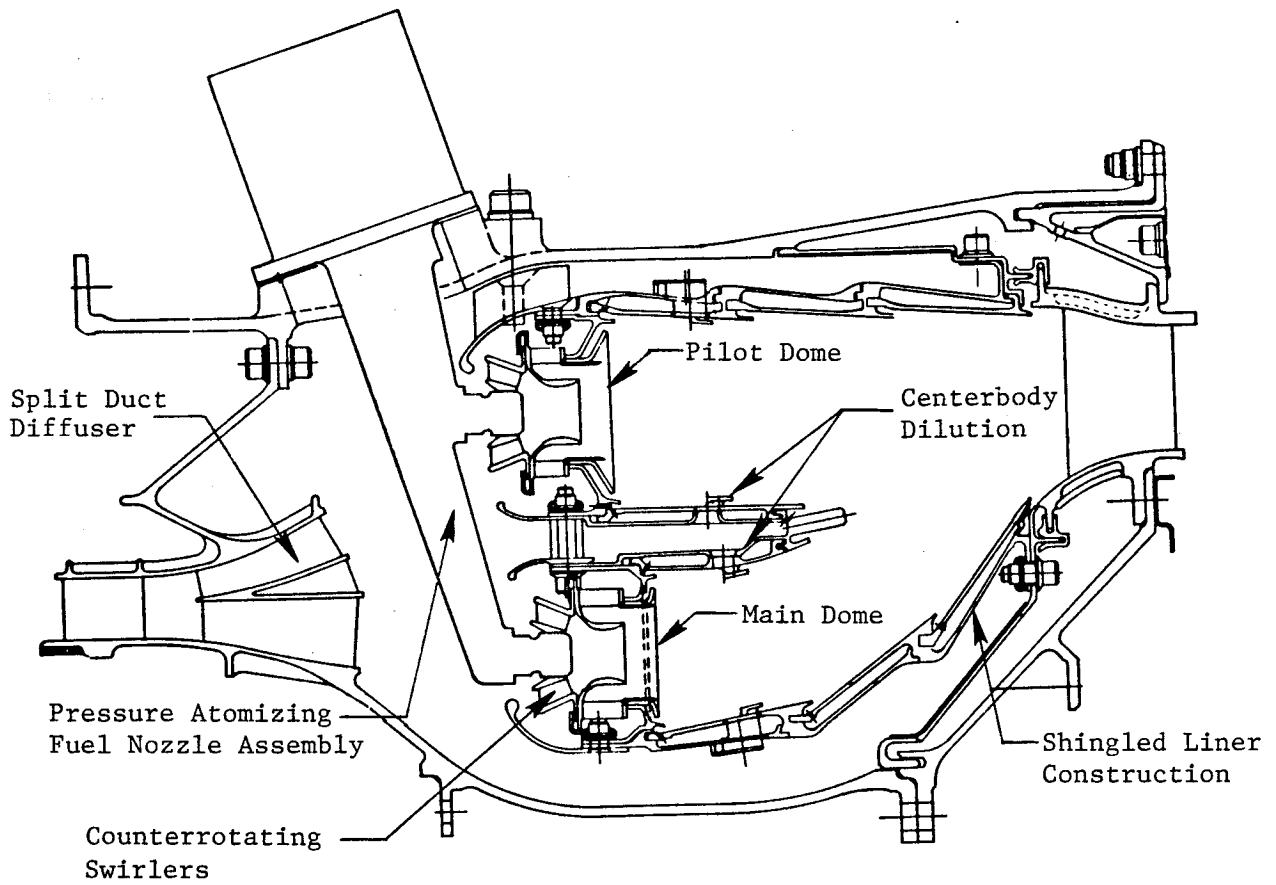
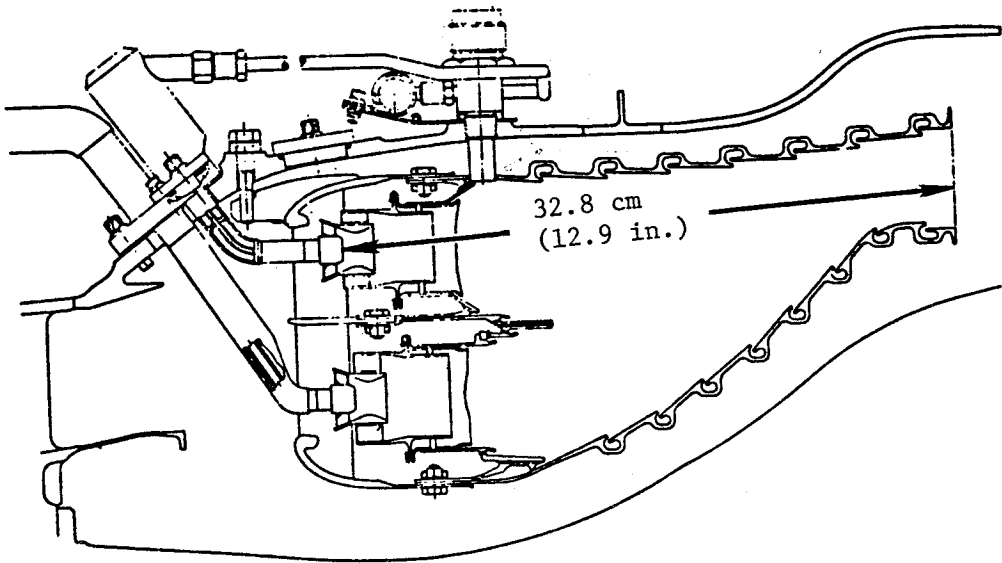


Figure 1. E³ Combustor Cross Section.

ORIGINAL PAGE IS
OF POOR QUALITY

NASA/GE
ECCP
(CF6-50)



NASA/GE QCSEE

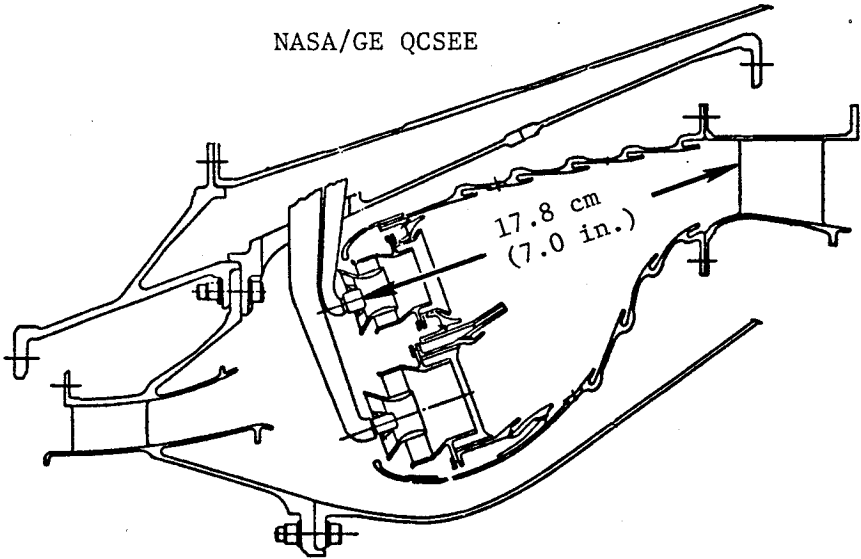


Figure 2. NASA/GE Double-Annular Combustors.

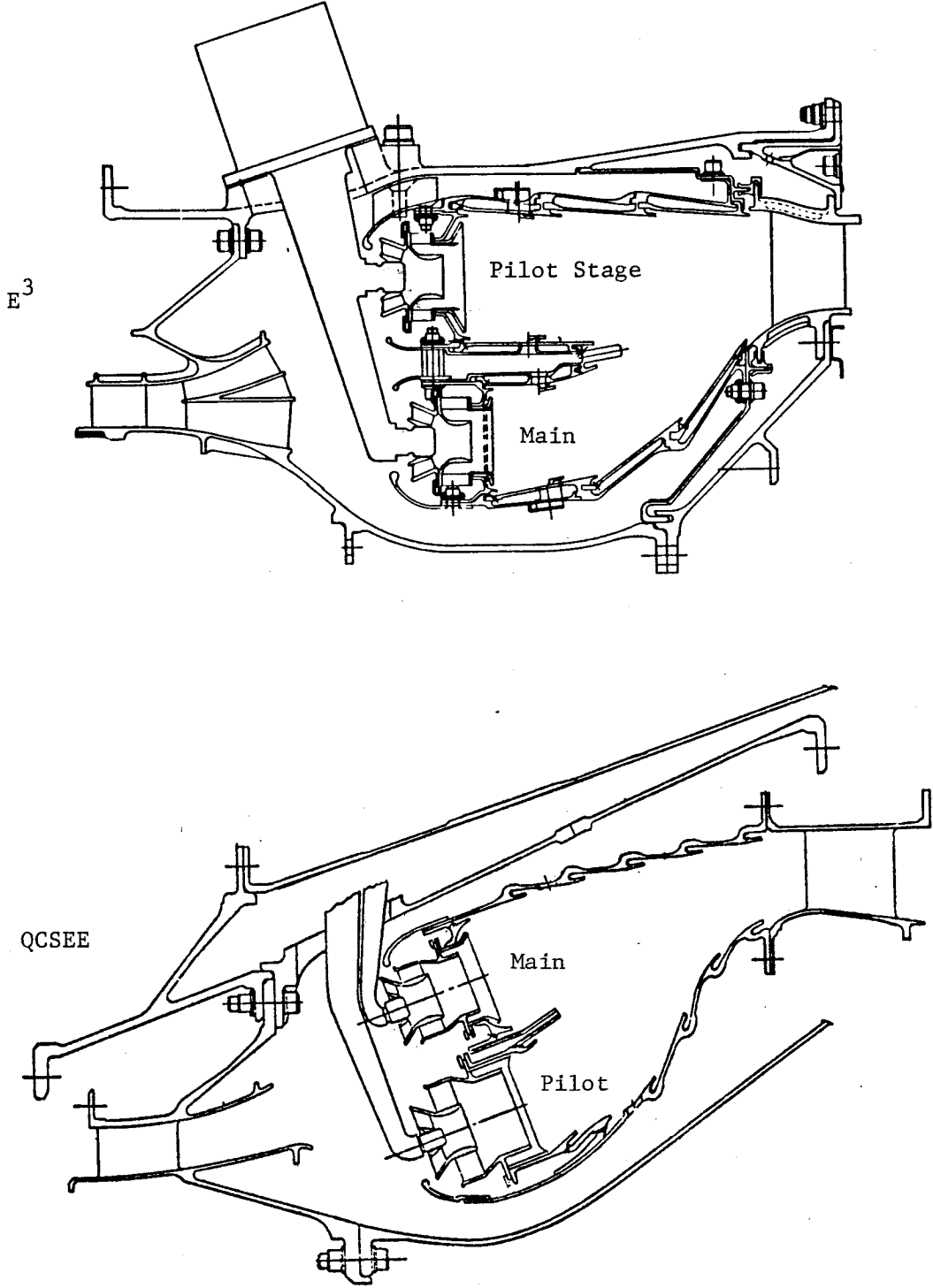


Figure 3. Comparison of QCSEE and E³ Double-Annular Combustors.

To meet the life goals of the E³ combustor program, studies of various liner configurations were conducted to identify a design which would provide the required long life characteristics. These studies were devoted to analysis of advanced film plus impingement-cooled liner designs. This design concept features a two piece liner construction; that is, a film liner, and an impingement liner. An illustration of this advanced liner design is presented in Figure 4. Preliminary analysis of an advanced machined ring film plus impingement-cooled liner design indicated that it would not satisfy the E³ technical life goal of 9000 flight cycles to first repair. Because of the uncertainty in meeting the E³ life goals with this liner design concept, a segmented film liner version of this design approach (the shingle liner) was evaluated. This even more advanced liner design concept has been developed specially for applications with very high peak combustor liner metal temperatures and for long life.

The desirable features of using a shingle liner approach are summarized as follows:

- Segmented axial and circumferential panels
- Reduced stress
- 360° support structure carries mechanical loads
- Maintainability
- Life greater than 10⁵ cycles
- Cooling levels consistent with NO_x requirements
- Required for growth engine cycles.

Consistent with the double-annular dome and shingled liner design selections, other design features chosen for the E³ combustor system include a short length, high-area-ratio, split-step diffuser for a low loss, high pressure recovery system, and duplex fuel tips for the fuel nozzles. The combustor dome has counterrotating airblast swirl cups for improved fuel atomization and controlled discharge angle and opposed dilution jet mixing through the liners to further mix and distribute the byproducts of combustion to achieve uniform exit temperature distributions.

ORIGINAL PAGE IS
OF POOR QUALITY

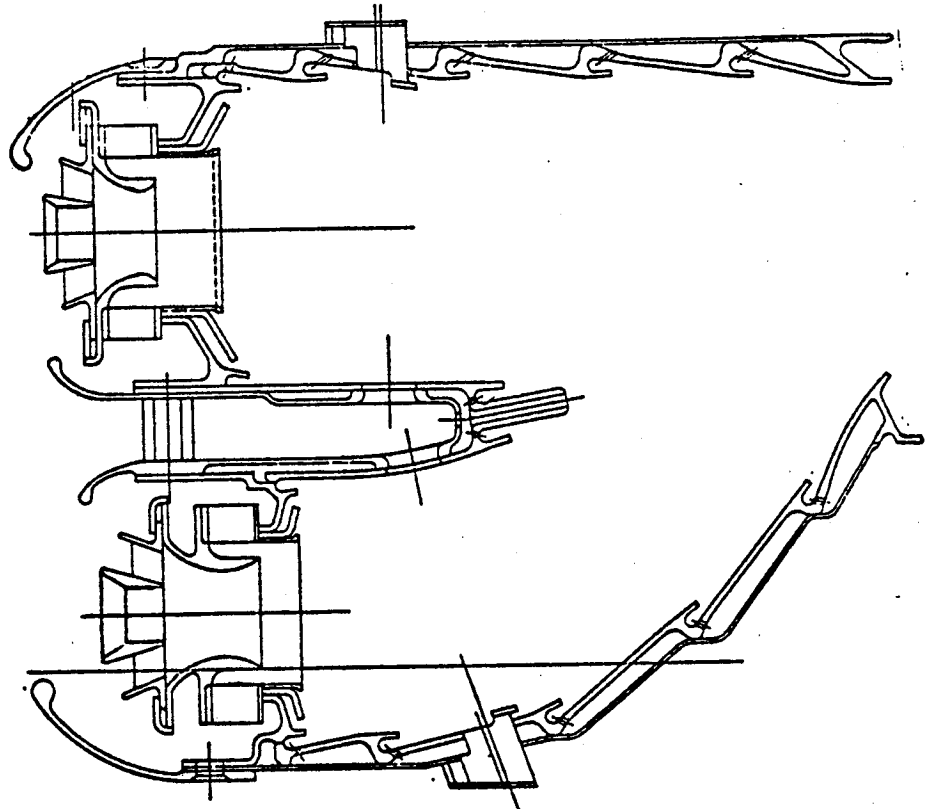


Figure 4. E³ Combustor Film/Impingement Liner Design.

4.0 AERO DESIGN

4.1 REQUIREMENTS

The major emphasis in the combustion system design is directed at meeting the very technically challenging emissions and life goals of the program; however, the combustion system must also provide the performance characteristics required for operation of a typical modern turbofan engine.

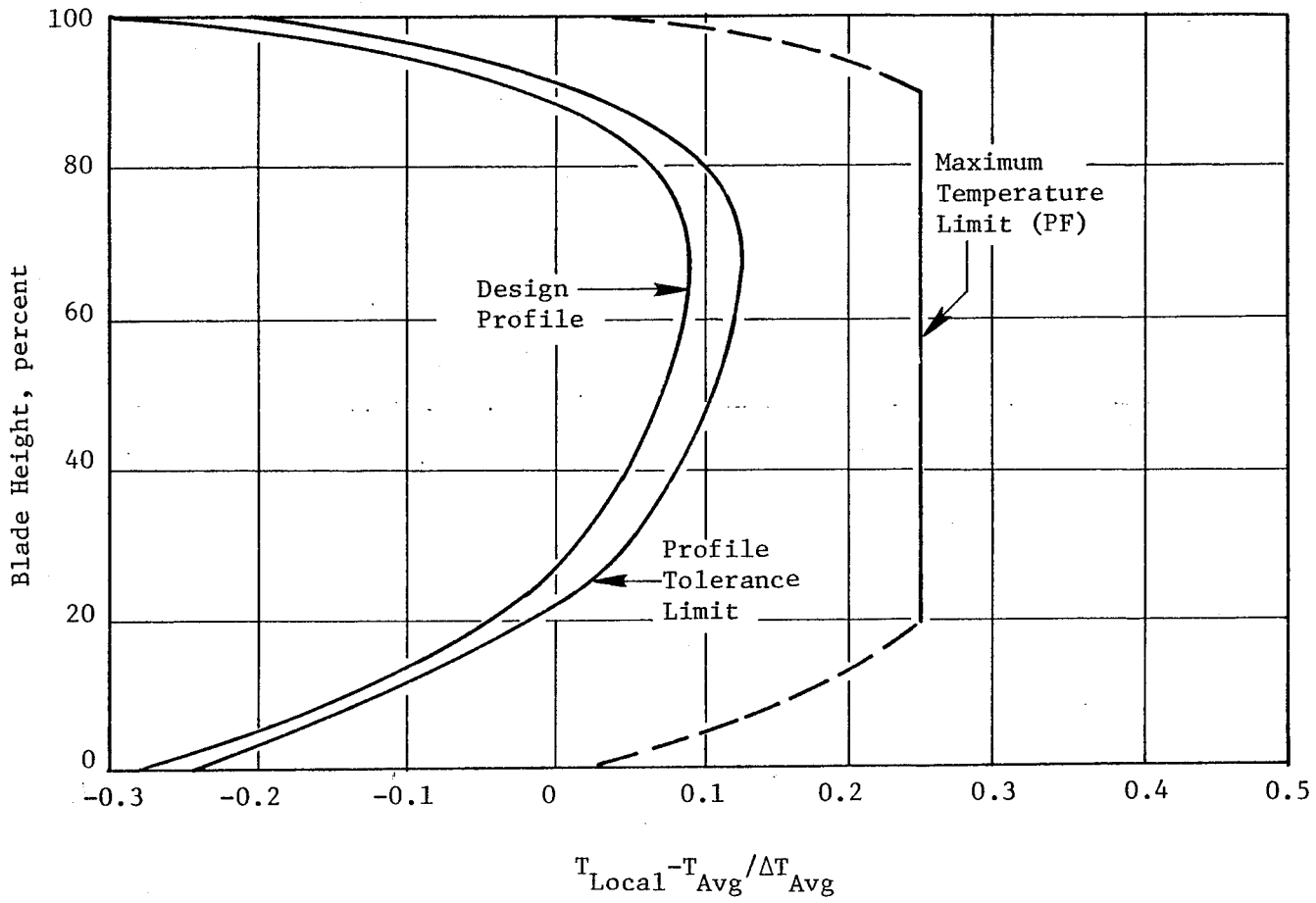
The performance parameters generally considered most important in a combustion system are shown in Table IV and Figure 5. It should be noted that not only is high combustion efficiency required at sea level takeoff (SLTO) conditions for this design, it must be maintained at a level greater than 99% at idle in order to meet the CO and HC emissions goals of the program.

Table IV. Performance Requirements.

●	Combustion Efficiency (Minimum)	99.5%
●	Total Pressure Drop (Maximum)	5.0%
●	Exit Temperature Pattern Factor (Maximum)	0.250
●	Exit Temperature Profile Factor (Maximum)	0.125
●	Ground start ignition to ground idle within 60 seconds	
●	Stable combustion within the flight envelope	
●	Altitude relight capability up to 9.1 km (30,000 feet)	
●	Carbon-free operation	
●	No resonance or starting growl within the flight envelope	

Achievement of the E³ emissions goals required that the liner cooling flows be minimized. Additionally, with the emphasis on low emissions, the amount of trim air necessary for low pattern factor and profile peak value would be limited. Hence, the development challenge was to obtain an equitable balance between emissions, life, and performance goals through the application of aerodynamic analysis.

● SLTO SLS Standard Day



ORIGINAL PAGE IS
OF POOR QUALITY

Figure 5. Turbine Inlet Temperature Radial Profile Requirements.

4.2 KEY DESIGN STUDIES

In the process of evolving the preliminary design of the combustor and refining the design features into the detailed design for the core engine, a large number of design studies were conducted.

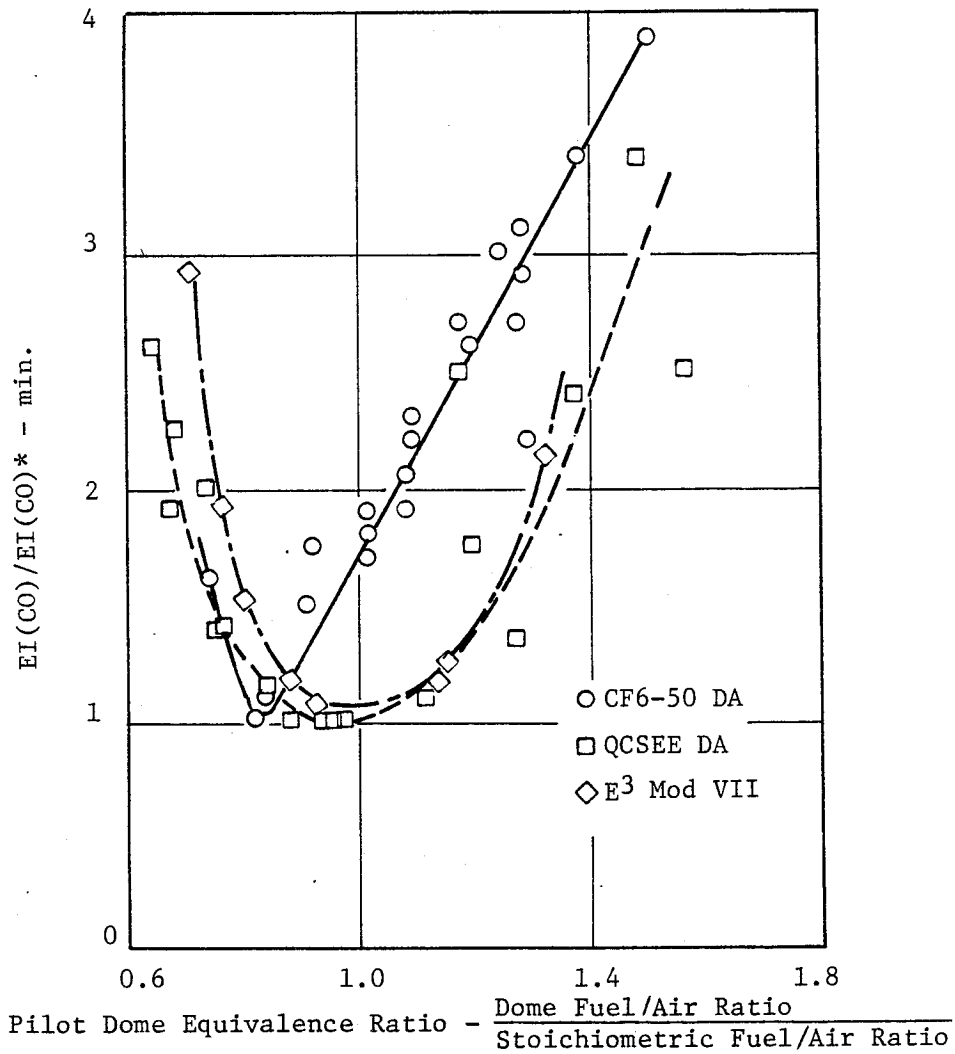
The four major areas of study were related to detail component and systems design which included aerodynamic analysis, ground start sequence, fuel staging modes, and estimates of the emissions levels to be expected from the core, ICLS, and FPS engine designs.

The major objective of the aerodynamic analysis was to define a desirable combustor flowpath within the constraints of the engine envelope and to develop the required distribution of airflow within the flowpath to meet all of the combustor performance, emissions, and life objectives.

4.2.1 Cycle Studies

One of the key inputs in evolving the airflow distribution was the engine operating cycle. Two of the most important operating modes are ground idle and sea level takeoff. Both of these cycle conditions are utilized in the EPA landing takeoff (EPA-LTO) cycle to calculate emissions performance, and sea level takeoff is generally selected as the combustor design point for combustor sizing and analysis. Of the four EPA-LTO conditions, the ground idle is extremely important for a staged combustor design such as the double-annular since the pilot stage dome design is based primarily on this operating condition. The CO emissions levels are very sensitive to the pilot dome equivalence ratio at this condition as shown in Figure 6. However, the ground idle combustor inlet conditions may vary as the engine cycle is refined, as shown in Table V. Therefore, several iterations on the airflow distribution may be required to satisfy the requirements of the emissions goals, establish cooling airflows to maintain metal temperatures, and select combustion zone airflows to meet performance. Figure 7 shows the airflow distribution evolved for the baseline design and can be compared to the airflow distributions finally evolved for the core engine in Figure 8. This comparison illustrates how significantly the aerodynamics can change.

ORIGINAL PAGE IS
OF POOR QUALITY



$\frac{*EI(CO) \text{ measured on any of the three configurations tested.}}{EI(CO) \text{ minimum value measured on any of the three configurations.}}$

In this case, the minimum value was measured on QCSEE DA.

Figure 6. Effect of Pilot Dome Airflow on CO Emissions.

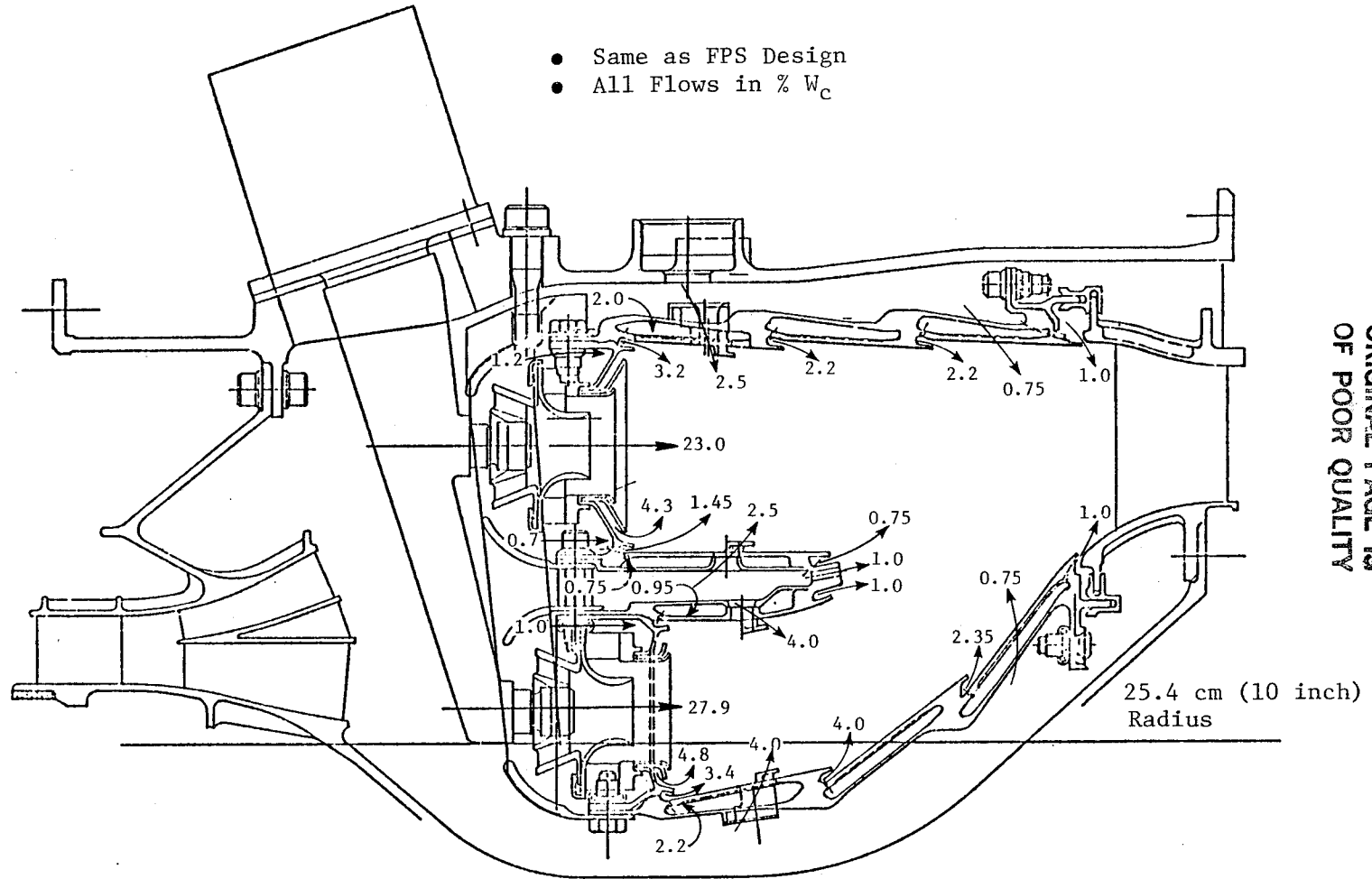
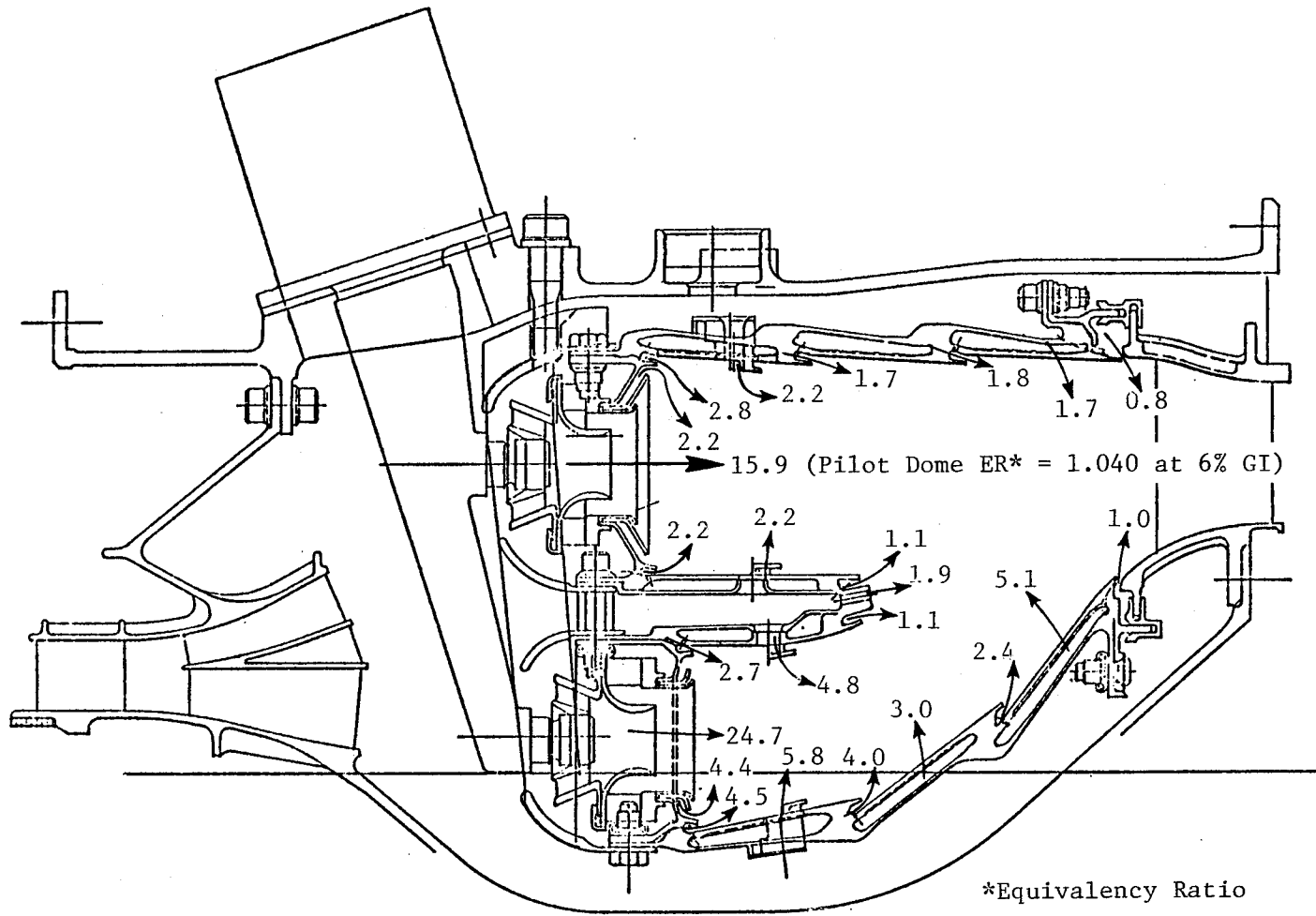


Figure 7. E³ Double-Annular Combustor Airflow Distribution, Baseline.



ORIGINAL PAGE IS
OF POOR QUALITY

Figure 8. E³ Combustor Design Airflow Distribution, Core Engine (% W_C).

Table V. Cycle Comparison.

	PDR (7/78)	IDR (4/79)	DDR (8/81)
Ground Idle (6% F_N)			
T_3 - K ($^{\circ}$ R)	485 (873)	517 (931)	497 (894)
P_3 - MPa (psia)	0.40 (58)	0.043 (62)	0.43 (63)
FAR 4	0.012	0.0141	0.0123
SLTO (100% F_N)			
T_3 K ($^{\circ}$ R)	814 (1465)	815 (1467)	815 (1467)
P_3 MPa (psia)	3.01 (438)	3.02 (439)	3.02 (439)
FAR 4	0.0244	0.0244	0.0245

4.2.2 Diffuser

One of the key components in the combustion system which directly affects combustor as well as engine performance is the diffuser. The diffuser accepts air from the compressor discharge and directs it to the combustor. The key design requirements for the diffuser are:

- Positive flow distribution
- Stable flow, separation-free
- Short length
- Low pressure losses
- Bleed airflow capability.

The design of the combustor diffuser depended on selection of a turbine cooling air extraction configuration, definition of the diffuser wall contours, and modeling of the diffuser system aerodynamics. The design approach selected was a dual passage, step diffuser system to provide for the large area change between compressor discharge and the double-dome height of the combustor. This diffuser design is defined as a split duct.

Two approaches for extracting turbine cooling air from the compressor airstream were considered for the split duct diffuser design. The configurations investigated were a leading edge design and a trailing edge design.

The leading edge approach, which extracts the turbine cooling air from the centerline location of the compressor flowpath, offers the advantage of a positive total pressure feed and lower air temperature. The airflow is metered through a circumferential slot located at the leading edge of the splitter vane. The airflow is then diffused into the strut cavity and routed through the hollow strut passage into the cooling circuit. Since the flow metering is done at the leading edge slot, very accurate dimensional control is required. The leading edge design also has higher frontal blockage which results in a higher OGV Mach number, requiring longer diffuser passages.

The trailing edge approach has positive design features, such as dirt separation, enhanced diffuser stability, and good mechanical strength. However, the trailing edge design depends on static pressure feed and has slightly higher cooling air temperatures due to mixing in the prediffuser passages. In this design, the airflow is metered through circular orifices in the discharge base of the splitter vane and dumps into the strut cavity. This approach permits accurate metering and easy modification of bleed flow quantity.

Although the leading edge design does offer the advantage of slightly improved sfc due to the lower cooling air temperature and higher combustor inlet temperature, the disadvantages of increased hardware cost, cooling air metering dimensional sensitivity, and rework difficulty were considered critical risks and led to the selection of the trailing edge approach shown in Figure 9. Additional design studies using conventional design practices, such as the Stanford Diffuser Separation Correlations, and analyses using the General Electric Compressor Axisymmetric Flow Determination (CAFD) computer program, were conducted on the prediffuser design to determine the passage Mach numbers and pressure distributions. The configuration analyzed included the effects of blockage from the 30 prediffuser struts and an estimated compressor discharge airflow radial profile. These analyses provided information concerning the velocity characteristics, and permitted selection of the prediffuser wall coordinates. After the coordinates were defined, the system was analyzed to determine the expected performance for comparison to the design requirements. The results predicted a mass-weighted total pressure loss of 1.5%. No major problem areas were identified for the diffuser; therefore, the identified

ORIGINAL PAGE IS
OF POOR QUALITY

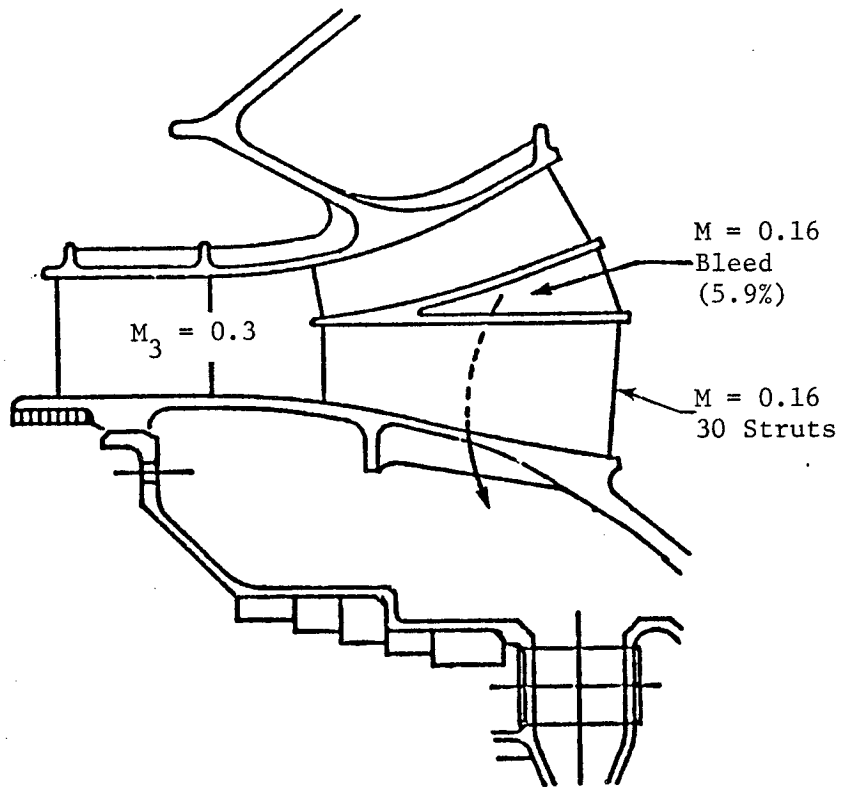


Figure 9. Split Duct Diffuser Design.

design was transmitted to the General Electric Corporate Research and Development Center for fabrication of a water table model and full-annular, full-scale, aerodynamic model.

4.2.3 Fuel Nozzle

The fuel nozzle for the E³ double-annular combustor had the following requirements as its development criteria:

- Maximum fuel nozzle pressure drop of 3102 KPa (450 psid) to obtain reasonable fuel pump pressures and provide for pumping margin
- Separate primary and secondary fuel delivery circuits to provide for both ground/altitude starting and flow capacity at takeoff
- Pilot-to-total fuel split flexibility necessary for final combustor fuel staging flow selection.

Figure 10 shows the fuel nozzle design which evolved from these requirements. Figure 11 shows the nozzle fuel flow characteristics versus nozzle pressure drop. The nozzle hydraulic system features a primary and secondary duplex fuel nozzle system in both the pilot and main stage systems. The primary system provides excellent fuel atomization at low power operating conditions where the combustor inlet environment is less favorable for combustion. At high power where combustor inlet conditions are favorable, the secondary system provides excellent fuel atomization and the desired flow capacity to achieve full engine power. The valve mechanism mounted above the flange provides the fuel metering schedule between primary and secondary nozzle flow and is cooled by fan air to reduce thermal problems.

Because the combustor was in the stage of development where the optimum proportion of fuel between the pilot dome and main dome had not yet been determined, it was necessary to provide a degree of flexibility in the amount of fuel which could be scheduled to each system without exceeding the flow capacity of the engine fuel system. The fuel system was oversized to incorporate this flexibility. By installing a fixed orifice in the main stage fuel system, the fuel flow split between the pilot stage and main stage could be adjusted to provide the desired flow split. Following completion of the core engine combustor component test program, the hydraulic characteristics for the two fuel systems will be selected and the appropriate orifice size will be installed.

ORIGINAL PAGE IS
OF POOR QUALITY

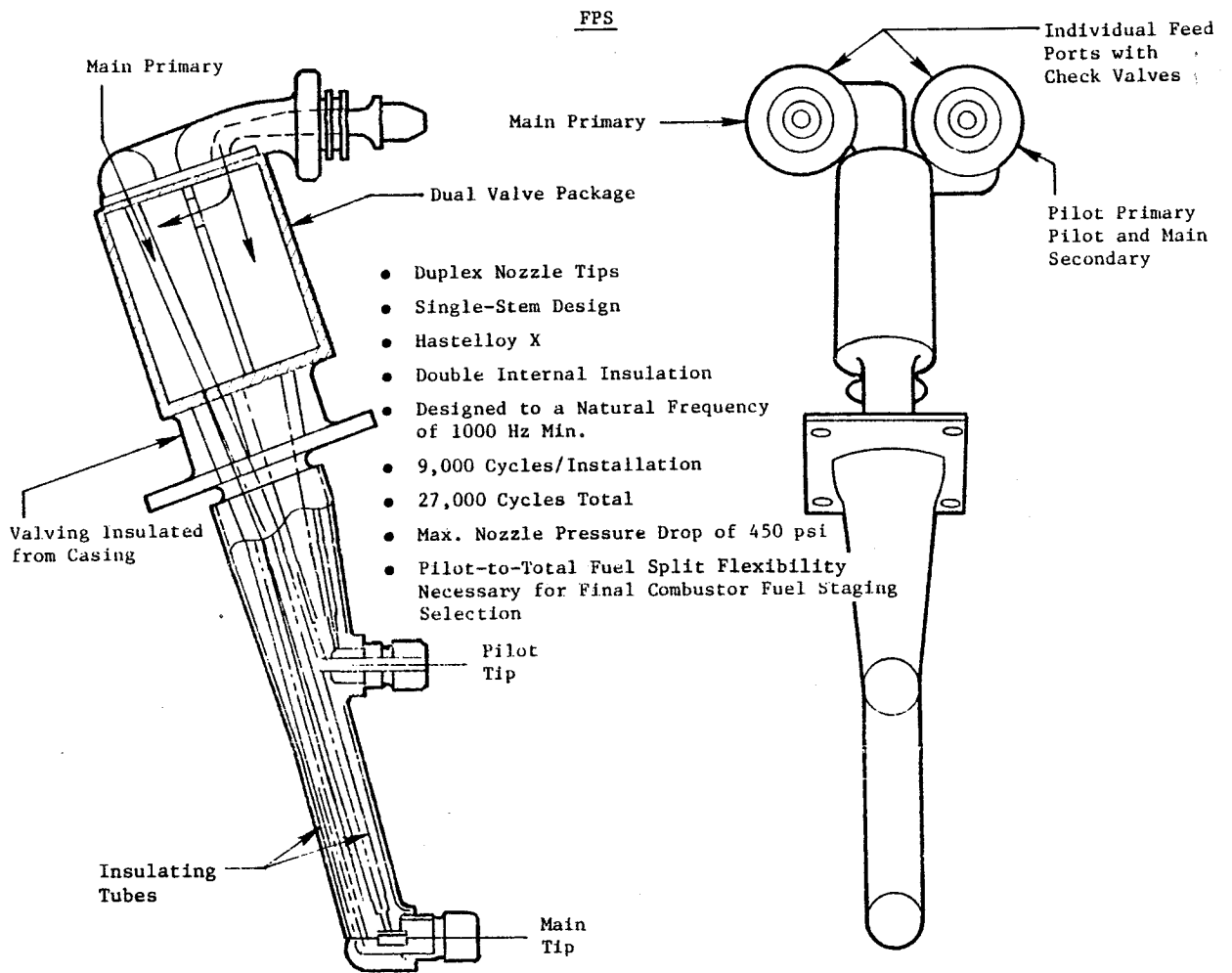


Figure 10. E³ Double-Annular Combustor Fuel Nozzle Design.

ORIGINAL PAGE IS
OF POOR QUALITY

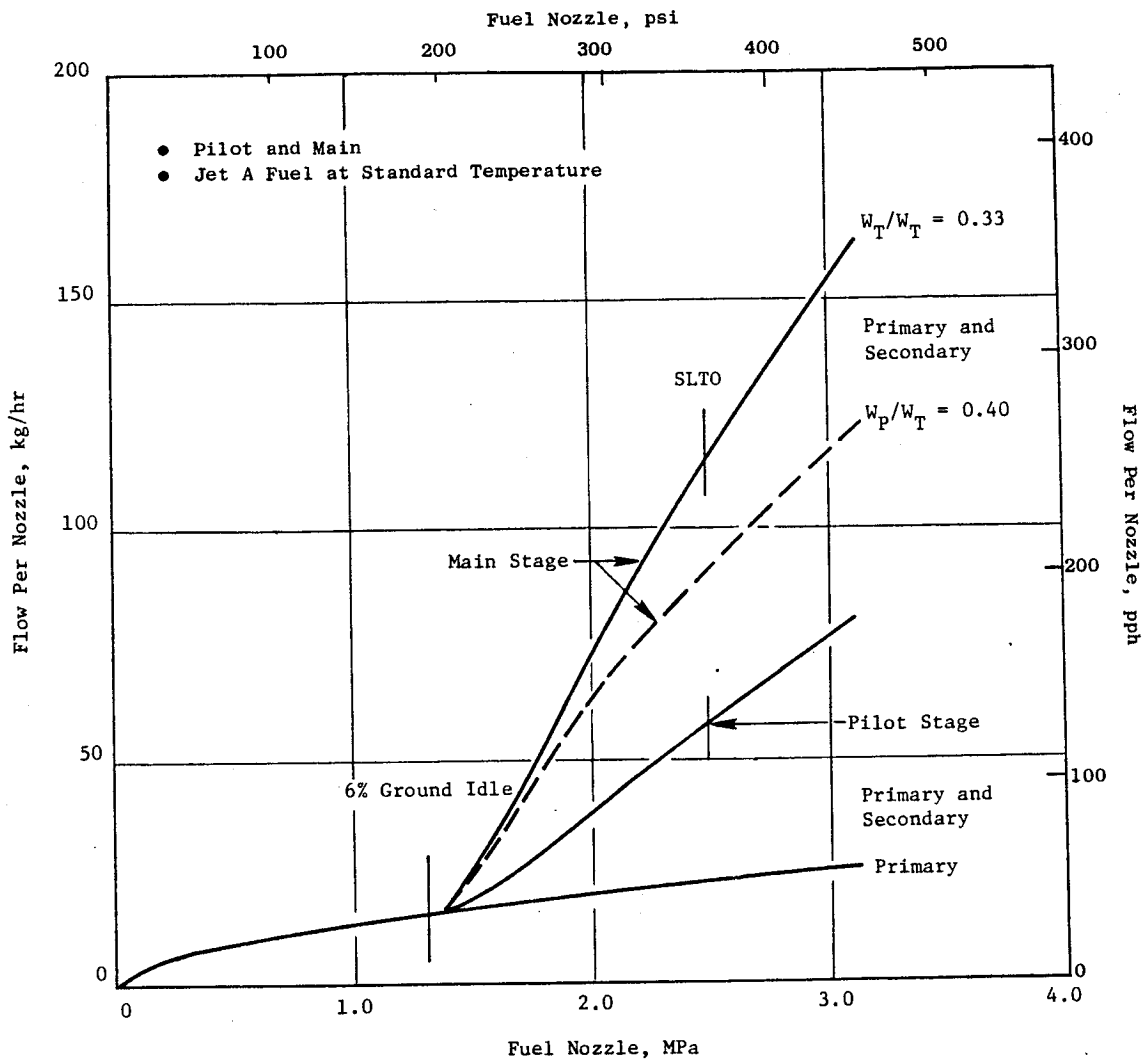


Figure 11. E³ Fuel Nozzle Flow Characteristics.

4.2.4 Starting

One of the major and most intensive studies conducted on the combustor system dealt with obtaining an acceptable ground start ignition sequence⁴ for the E³ equipped with the parallel-staged combustor design. The ignition requirements for the E³ are typical of those for conventional commercial aircraft engine applications. These requirements were:

- Stable ignition and propagation
- 60-second accel to idle
- Start free of stall and noise.

A substantial amount of experience in starting engines equipped with a parallel-staged combustor, such as the E³, had been obtained in the NASA/GE ECCP conducted earlier. As shown in Table VI, the CF6-50 sized, parallel-staged design tested in the ECCP had demonstrated very satisfactory experience for engine ground starts.

Table VI. Starting Background.

- | |
|--|
| <ul style="list-style-type: none">• CF6-50 Double-Annular (ECCP)<ul style="list-style-type: none">- Staged Combustor- Extensive Component Tests- Engine Tested• Staging Procedure<ul style="list-style-type: none">- Ground Start to Approach Power (Pilot Only)- Above Approach (Pilot and Main)• Starting History<ul style="list-style-type: none">- Satisfactory Main Stage Ignition in Component Tests- Fifty-six Successful Engine StartsOne Unsuccessful Start (Aborted Exceeded T_{4.9} Limit) |
|--|

Ground start ignition was a key factor in the design development of the E₃ combustor. Table VII is a chronology of the starting studies conducted during design development. This history indicates the progression of the development effort and key turning points in the design based on the availability of improved and more current compressor component data and the dynamic analysis of the starting sequence.

Table VII. E³ Starting Studies Chronology.

January 1978 - October 1978	Combustor Design - Original Concept - Pilot Only Ignition Through Ground Idle
December 1978 - September 1979	Engine Start Studies Initiated- Model Predicts High T _{4.1} max. With Pilot Only Fueled
February 1979 - March 1980	Combustor Ignition Studies Conducted to Develop Capability to Start Engine With Both Domes Fueled
January 1980 - May 1981	Development Combustor Activity Directed at Evolving Satisfactory Ignition With Both Domes Fueled From Light-off Through Ground Idle
May 1981 -	Start Studies Resumed With New Component Data Input That Indicate Pilot Only Start Will Be Satisfactory

The key differences between the previously successful ECCP design and the E³ design centered around the ground start compressor bleed flows required to prevent compressor stall, the associated combustor fuel/air ratios, and their impact on turbine metal temperatures. Figure 12 shows the initial estimates of starting compressor bleed required resulted in very high combustor fuel/air ratios. These high overall fuel/air ratios coupled with the tip

ORIGINAL PAGE IS
OF POOR QUALITY

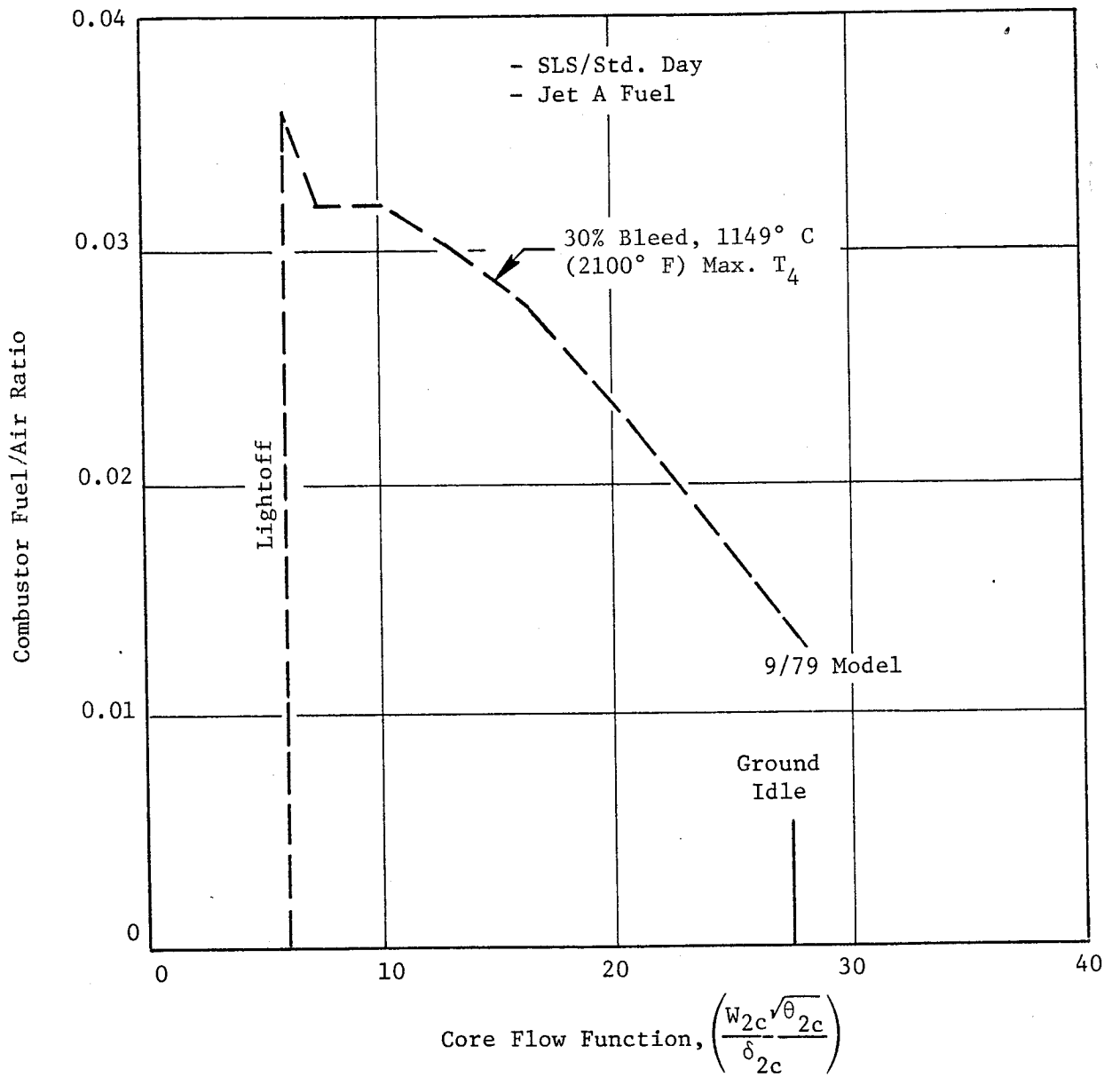


Figure 12. Combustor Fuel/Air Ratio Versus Core Compressor Flow.

peaked exit temperature profiles, shown in Figure 13, associated with fueling only the pilot stage dome during ground start resulted in unacceptable turbine metal temperatures, particularly in the uncooled low pressure turbine hardware. In order to attenuate the temperature profiles associated with operation of the pilot stage only during ground start, an alternative fueling mode was evolved. This alternate approach involved staging the combustor from the pilot only mode to pilot and main during the ground start sequence to divide the fuel between both pilot and main stages, providing a flatter exit temperature profile similar to that shown in Figure 13. Since the main stage was originally intended only for operation at high power operating modes where the combustor inlet conditions are more favorable for ignition, several approaches were considered:

- Primary-secondary fuel nozzle
- Alternate fuel nozzles fueled, subidle
- Rich domes, reduced main dome airflow.

This redirection in operating requirements for the combustor and, in particular, the main stage combustion system resulted in major changes to the design. These design changes are outlined below:

- Duplex fuel nozzles in pilot and main dome
- Complex control staging at ignition
- Reduced main dome airflow
- Crossfire tube improvements.

As shown in Figure 14 with the lean main stage dome evolved as the baseline design, the main stage dome velocities are considerably higher than in the pilot stage dome. Even with major reductions in airflow designed to obtain a rich main stage dome configuration, the dome velocities remain high due to the smaller annulus area of the main dome. Figure 15 shows that fuel staging becomes much more complex, requiring significantly more manipulation of the pilot and main stage fuel flows during the start sequence. The undesirable features of the rich dome design approach are outlined in Table VIII. Of particular concern were the higher NO_x emission levels expected with the rich main stage dome design. However, the greatest concern was centered around the capability to start the engine satisfactorily without sustaining any damage to

CONFIDENTIAL: PAGE 12
OF 100A-01A-01-01

- 46% Core Speed Operating Condition
- 9/79 Start Cycle

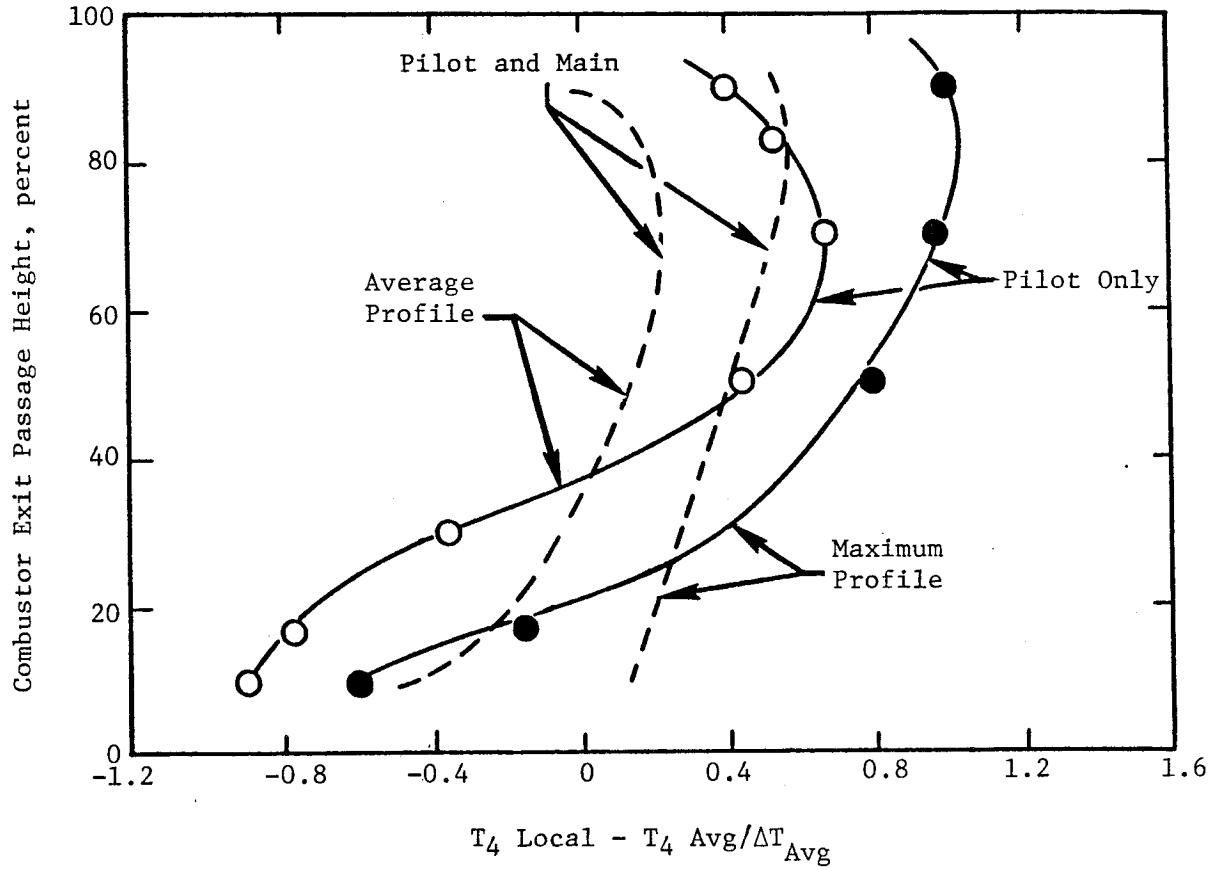


Figure 13. Combustor Exit Temperature Profile.

ORIGINAL PAGE IS
OF POOR QUALITY

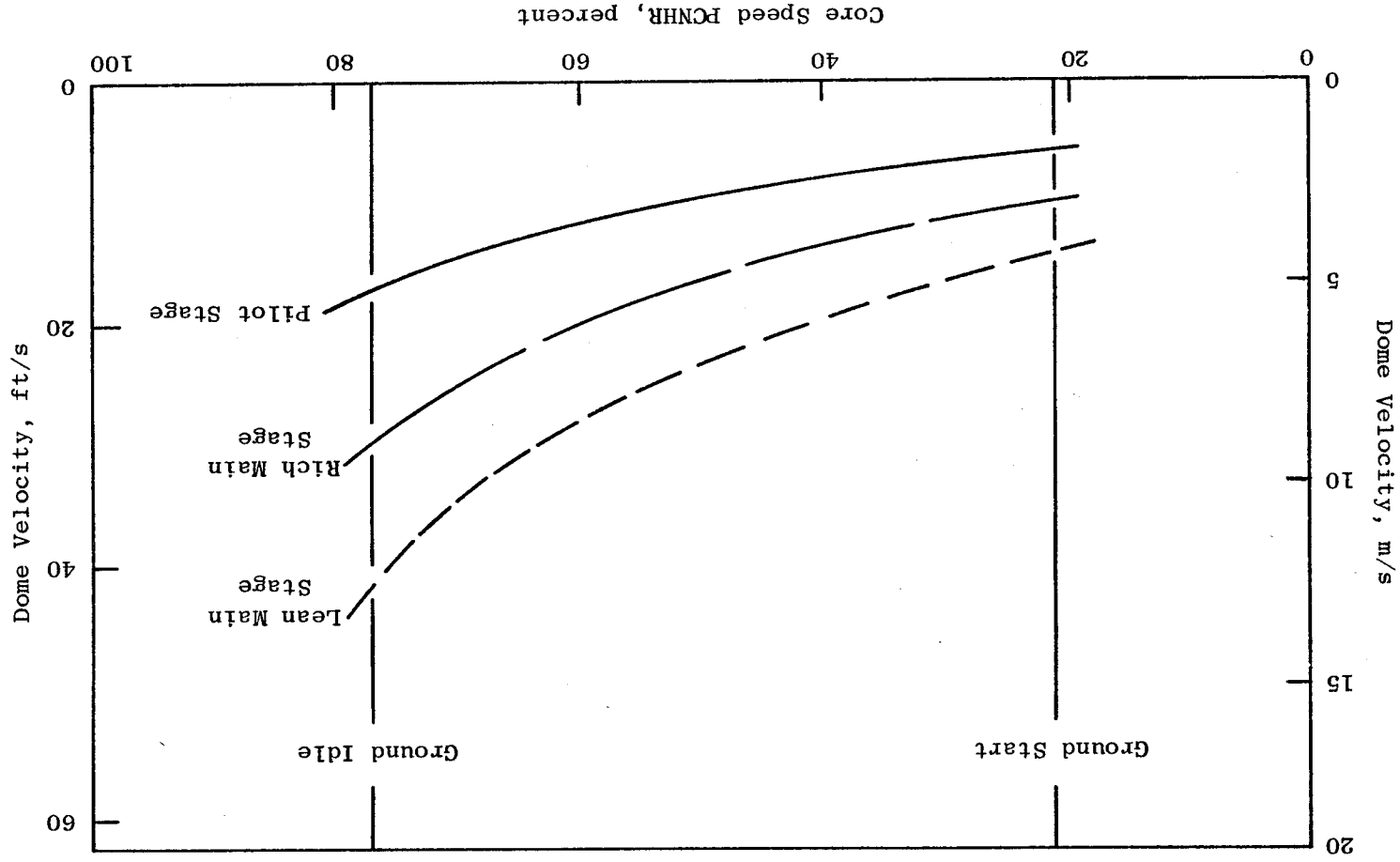


Figure 14. Double-Annular Combustor Dome Velocity Comparison.

ORIGINAL PAGE IS
OF POOR QUALITY

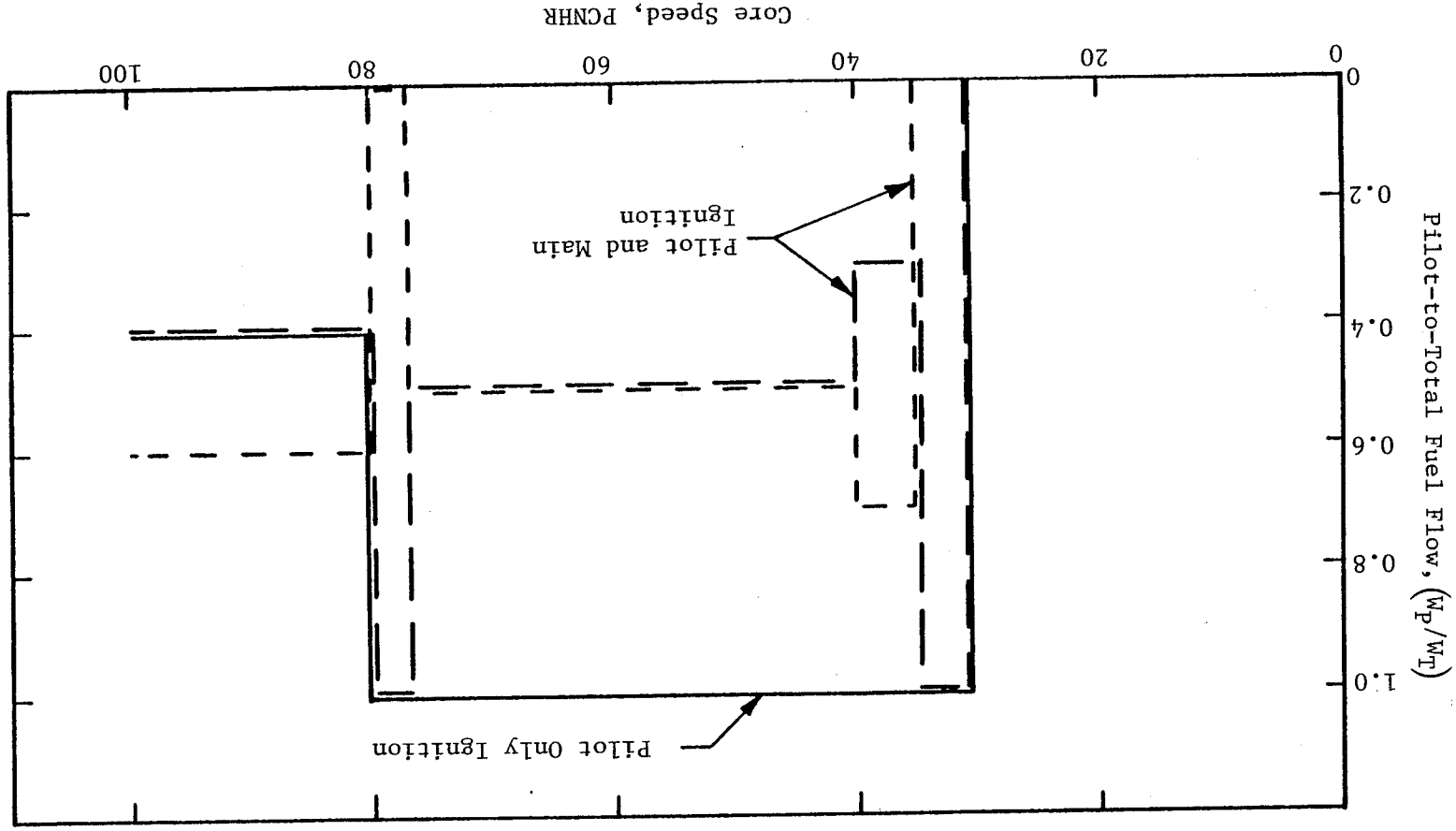


Figure 15. Comparison of Comustor Fuel Staging Sequence.

the engine components. Therefore, the combustor development activity was redirected toward evolving a rich main dome configuration.

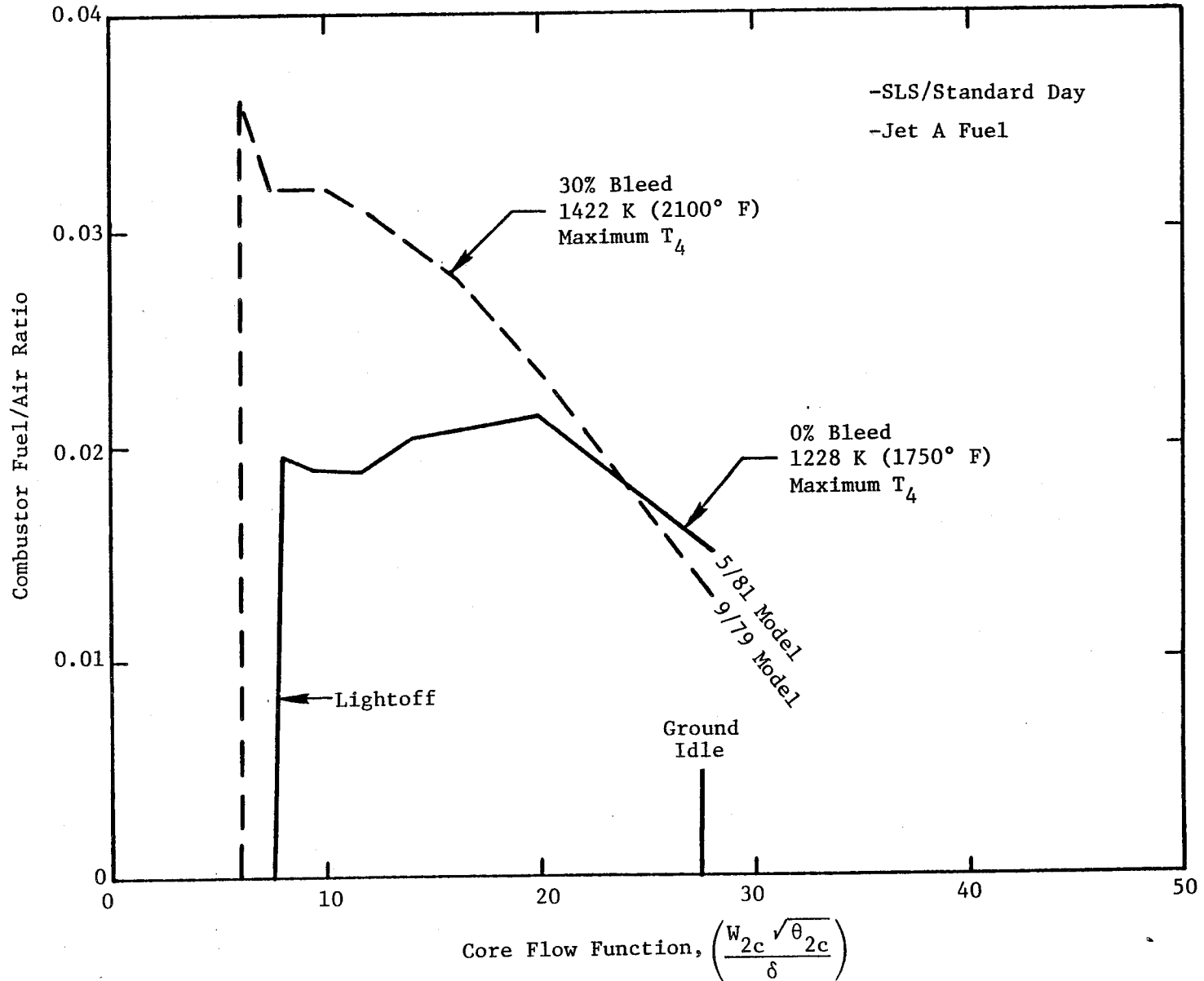
Table VIII. Adverse Impacts of Pilot and Main Stage Ground Start Ignition.

- Increased Fuel Staging Complexity
- Additional Control Logic Required
- More Complex Main Stage Fuel Nozzle
 - Added Hydraulic Features (Primary Orifice)
 - Additional Fuel Tube Insulation
 - Larger Envelope (Heavier)
 - More Expensive
- Richer Main Dome Operation at High Power
 - Increased NO_x Emissions
 - Increased Liner Temperatures

During the first quarter of 1981, key component test results were obtained relative to the E³ compressor and turbine low speed performance. Utilizing this most recent component test data, the engine starting analysis was updated. The key points of this study are presented in Table IX. The results of the study were:

- Satisfactory 60-second ground start
- 10% stall margin below 65% N_c
- Maximum average T_{4.1} at 1228 K (1750° F) as compared to previous 1422 K (2100° F)
- Satisfactory ground start obtained operating on pilot only.

The key finding of this updated study was that considerably less compressor bleed was required during start than had originally been determined. As a result, the combustor overall fuel/air ratios encountered during start were greatly reduced as shown in Figure 16.



ORIGINAL PAGE IS
OF POOR QUALITY

Figure 16. Comparison of Core Engine Start Models.

Table IX. Revised Engine Start Analysis.

- Start Model Updated 5/81
 - New Compressor Subidle Representation Based on 1 - 10 Test Results
 - Improved Low Speed Turbine Efficiency Levels Based on E³ Turbine Component Tests
 - Lower Bleed Flows Required
- Improved Profile Mixing Through High Pressure Turbine

A comparison of the study results for the two operating modes for the combustor during ground start is summarized in Table X. Based on these results, it was concluded that engine ground start with the pilot stage only fueled was the preferred mode of operation due to the very favorable ignition characteristics of the pilot dome and the significantly reduced complexity required for the control system. These conclusions obtained from the starting studies led to another redirection in the combustor development effort back to the original lean main stage dome design, but considerable development effort had been expended in designing a rich main stage dome.

Table X. Ignition Study Results.
(Pilot Stage Only Versus Both Stages Fueled)

- Light-off to Ground Idle in 60 Seconds
 - Both Approaches Meet Objective
 - Both Domes Fueled Require More Complex, Heavier Fuel System and Control Logic
- Stable Ignition and Flame Propagation
 - Pilot Stage Design Most Amenable to Good Ignition and Flame Propagation
 - Both Domes Require Crossfire to Main Stage
- Stall- and Growl-Free Operation in Subidle Range
 - Pilot Stage Only Provides Most Potential for Growl-Free Operations
 - Both Domes Fueled Provides Most Potential for Stall-Free Operation Due to Lower, More Uniform Combustor Exit Temperature

4.2.5 Emissions

One of the key concerns during the preliminary and detail design phases was the predicted emissions levels of the E³ combustor design and how these would compare with the program goals. The key considerations affecting the results of the E³ combustor emissions study effort were:

- Previous development experience on CF6 ECCP, QCSEE, and LOPER
- E₃ cycle conditions
- E³ emissions adjustment relationships.

GE has acquired considerable experience in designing advanced, low emissions combustors. The NASA/GE ECCP involved development of an advanced, parallel-staged, full-annular combustor sized to fit a CF6-50 engine. The NASA/GE QCSEE Program also involved an advanced, parallel-staged combustor similar in size to an F101/CFM56 combustor which was developed in sector combustor tests. The NASA/GE LOPER Program was directed at obtaining ultra-low CO and HC emissions at low power operating conditions in a single-annular design. These single-annular designs utilized such advanced concepts as recuperative cooled liners, hot wall liners, and catalytic combustion.

The ground idle combustor inlet conditions for these development combustors are compared to the E³ combustor ground idle conditions in Table XI. As observed, the E³ combustor inlet conditions are more favorable for reduced levels of CO and HC emissions than the previously tested ECCP, QCSEE, and LOPER development combustors which have already demonstrated low CO and HC emissions in their respective programs.

Table XI. Ground Idle Cycle Comparison.

	T ₃ , K (°R)	P ₃ MPa (psia)	f/a	V _{ref} MPa (fps)
QCSEE	414 (745)	0.25 (36)	0.016	14.9 (49)
CF6 ECCP	429 (772)	0.30 (43)	0.0110	18.3 (60)
LOPER	422 (760)	0.30 (44)	N/A	22.9 (75)
E ³	497 (894)	0.43 (63)	0.0123	14.6 (48)

Figure 17 shows a comparison of the idle emission indices of CO and HC and sea level takeoff levels of NO_x of the previously tested development combustors with the target levels of the E^3 combustor superposed for each of the contaminants. It can be seen that the E^3 target levels represent achievable goals based on past technology.

Therefore, it was expected that the E^3 combustor design would have the potential for low CO and HC emissions at low power operating conditions.

In order to estimate the expected emissions levels for the E^3 combustor, adjustments were made to an existing data base to determine the impact of combustor inlet parameters and combustor aero design features on emissions. The relationship used in making the E^3 combustor estimates is shown in Table XII. The key parameters affecting CO and HC emissions at low power are inlet pressure, bulk residence time, and inlet temperature. The key parameters affecting emissions at high power where NO_x emissions are of primary concern are inlet pressure, inlet temperature, bulk residence time, inlet air humidity, and fuel split between the pilot and main stage domes. Applying these relationships to the data base for the ECCP, QCSEE, and LOPER, Figures 18 and 19 show plots of these data bases corrected to E^3 operating conditions, and with E^3 target emissions levels indicated. With the more favorable combustor inlet parameters of the E^3 cycle, the expected CO and HC emissions levels of the E^3 were estimated to be below the target level with margin. The NO_x emissions were expected to approach the goal closely for both designs when the adjustment to residence time is made for the short length of the E^3 combustor. The similarity of design features and airflow distributions in the ECCP and QCSEE combustors cause their emissions characteristics to closely approach those anticipated for the E^3 combustor. However, the LOPER incorporates more advanced state-of-the-art and unique emissions reduction concepts which result in ultra-low levels of CO and HC emissions.

Figure 20 shows the trade-off of CO needed to meet the required E^3 goals with fuel staging of the main dome at the approach power condition.

The CO, HC, and NO_x emissions estimates were generated from the above study and are presented in Table XIII.

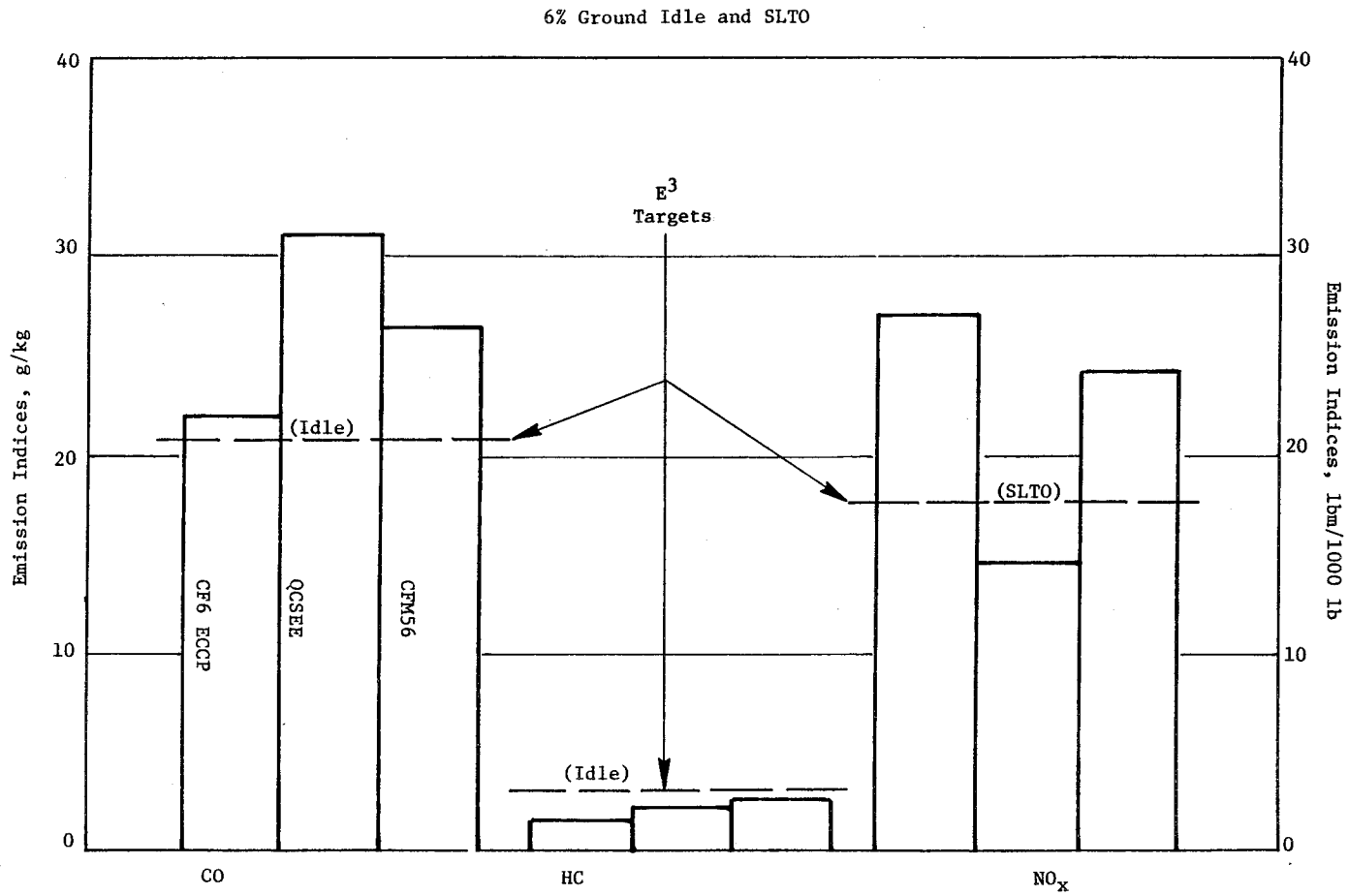


Figure 17. Emissions Comparison.

ORIGINAL PAGE IS
OF POOR QUALITY

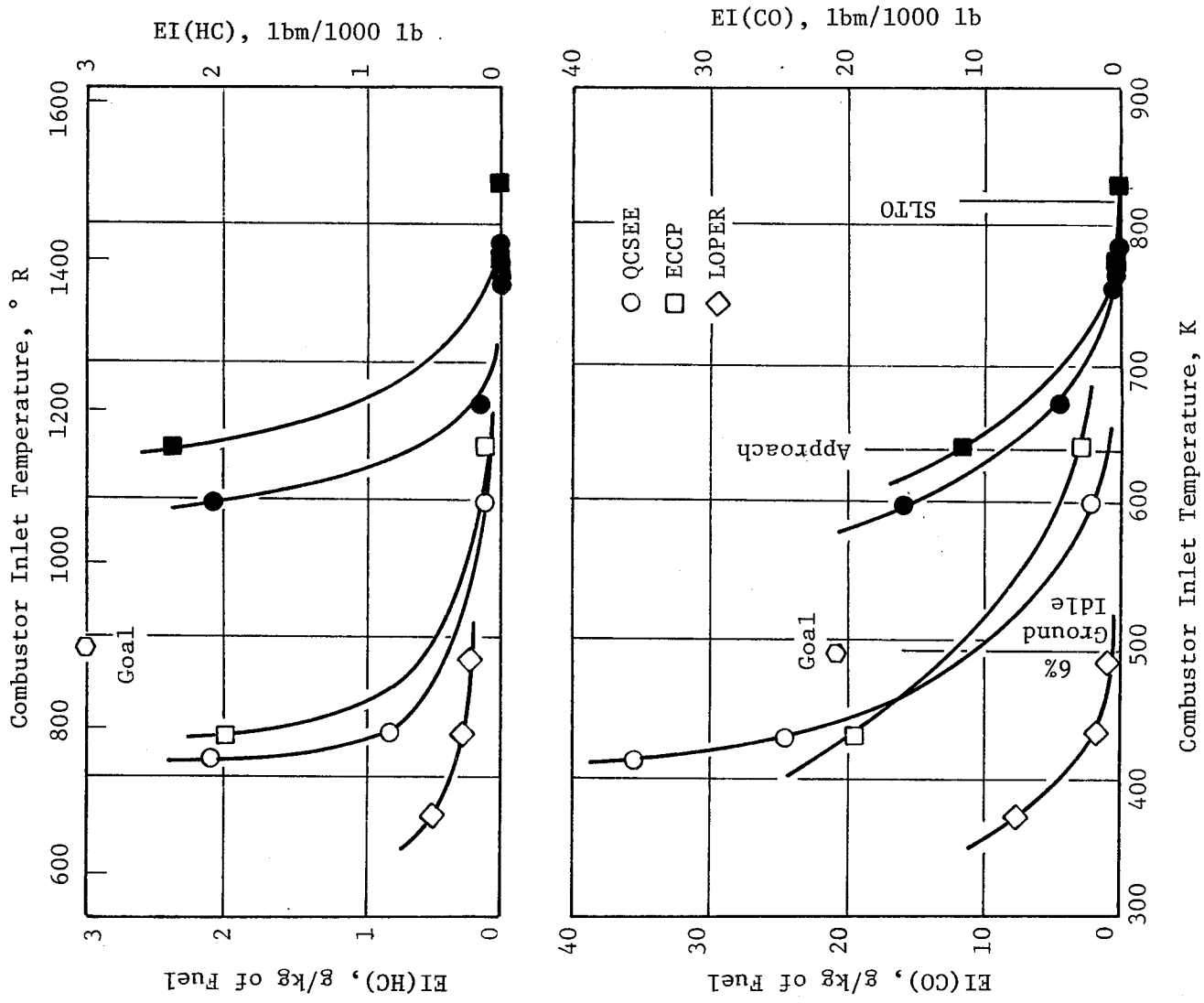


Figure 18. Low Power Emissions Comparison.

ORIGINAL PAGE IS
OF POOR QUALITY

-0.40 Pilot-to-Main Fuel Split
- NO_x Emissions Adjusted to E³ Engine Cycle

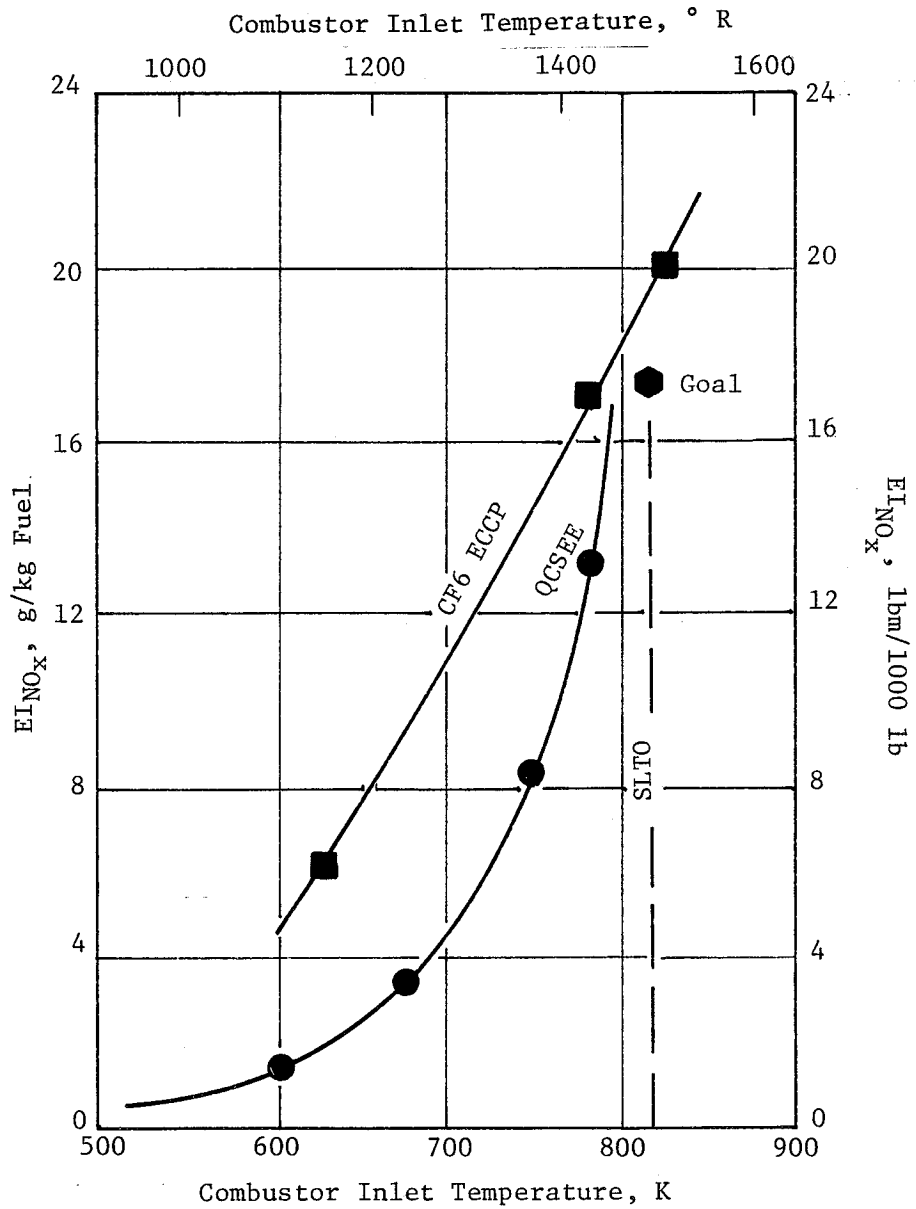


Figure 19. High Power Emissions Comparison.

ORIGINAL PAGE IS
OF POOR QUALITY

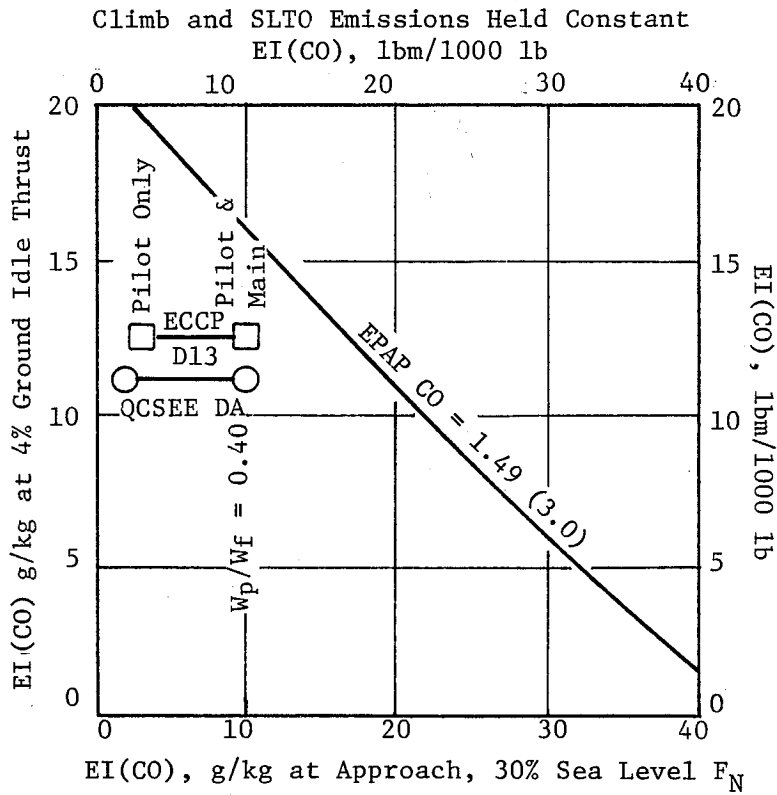


Figure 20. Tradeoff in CO Emissions Index Between Idle and Approach Conditions to Meet E³ CO EPAP Goal.

Table XII. E3 Emissions Adjustment Relationships.

$$EI_{CO} = EI_{CO} \text{ Meas} * \left(\frac{P_3}{P_{3_{cyc}}} \right)^a \left(\frac{V_{ref}}{V} \right) \exp \left(\frac{T_3 - T_{3_{cyc}}}{b} \right); a = 1.5, b = \infty$$

$$EI_{HC} = EI_{HC} \text{ Meas} * \left(\frac{P_3}{P_{3_{cyc}}} \right)^A \left(\frac{V_{ref}}{V} \right) \exp \left(\frac{T_3 - T_{3_{cyc}}}{B} \right); A = 2.5, B = \infty$$

$$EI_{NO_x} = EI_{NO_x} \text{ Meas} * \left(\frac{P_{3_{cyc}}}{P_3} \right)^M \left(\frac{V}{V_{ref}} \right)^N \left(\frac{FP}{FP_{cyc}} \right)^P \left(\frac{FM}{FM_{cyc}} \right) \exp \left(\frac{T_{3_{cyc}} - T_3}{R} + \frac{H_{std} - H}{S} \right); M = 0.37,$$

$$N = 1.0; P = 0; R = 345, S = 53.19$$

$$SN = SN \text{ Meas} * \left(\frac{P_3 \text{ ER Dome}}{T_3} \right)^Z \left(\frac{W_c}{P_3 N_F} \right) * \left(\frac{W_c}{W_c/P_3 N_F} \right); Z = 1.5$$

Cycle

ORIGINAL PAGE IS
OF POOR QUALITY

Based on these predicted levels, it is expected that the E³ combustor would meet the CO and HC emissions goals for the program with both pilot and main stage fueled at the approach (30% F_N) operating condition. With the very favorable cycle conditions at low power and the short residence time associated with the short combustor length, the E³ combustor was expected to meet all of the program goals with considerable margin even taking into account engine-to-engine variability.

Table XIII. E³ Combustor Estimated Emissions.

<ul style="list-style-type: none"> ● Pilot and Main at Approach ● Pilot Only at Ground Idle 				
	6% Idle	Target Level	Goal	Grams per kilonewtons (pounds per 1000 pounds) Thrust - Hour - Cycle
EPAP CO	0.94 (1.9)	1.24 (2.5)	1.49 (3.0)	
HC	0.02 (0.05)	0.15 (0.30)	0.2 (0.4)	
NOx	1.34 (2.7)	1.34 (2.7)	1.49 (3.0)	
Smoke - SN	15	16	20	

4.3 COMBUSTOR DESIGN FEATURES

The key combustor component areas where the design features were expected to significantly impact performance were:

- Counterrotating swirl cups
- Dilution thimbles
 - Full ΔP/P
 - Spent impingement
- Emission reduction sleeves
- Fuel nozzles.

The airblast swirl cup is one of the most important components of the combustor since it atomizes, mixes the fuel and air, and prepares the fuel for burning in the combustion zone. The design features of the swirl cups for the E³ combustor were:

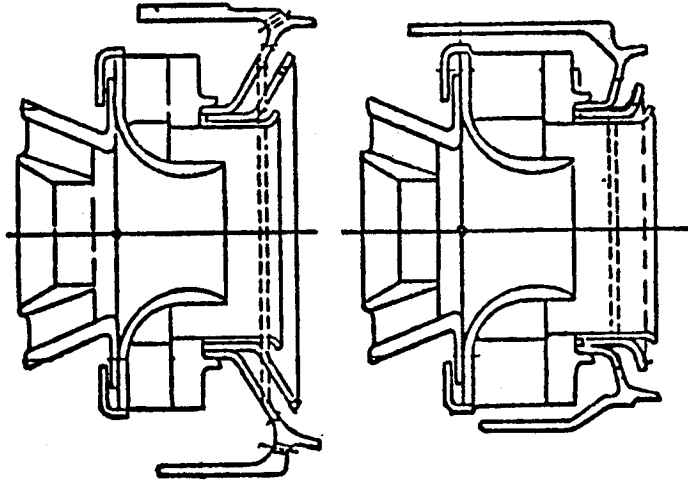
- Axial flow primary swirler
- Counterrotating radial inflow secondary swirler
- Venturi for carbon prevention
- Slip joint between primary-secondary for thermal growth
- Simple mechanical design.

The aero features are shown in Figure 21. The key design properties for the swirl cup are:

- Fuel spray quality
- Recirculation strength
- Velocity through venturi
- Primary-to-secondary swirler airflow ratio
- Fuel nozzle eccentricity and immersion.

These properties are important since they control the combustion zone performance and durability. The swirl cup must provide a stable spray at the proper ejection angle and the fuel must be well atomized and properly distributed. The combustor flame is stabilized and seated in the dome by the recirculation zone formed by the vortex action of the fuel/air mixture exiting the swirl cup. The recirculation zone pulls hot exhaust products from the primary combustion zone upstream into the unburned mixture which helps vaporization and initiation of the combustion process. However, this recirculation zone must be well controlled to prevent possible combustion instability, carboning of the swirl cup components, and/or possible damage to combustor dome components due to excessive heating and to provide flame stability. One of the swirl cup features which controls recirculation in the E³ design is the emissions reduction sleeve located at the cup discharge as shown in Figure 22. As shown in Figure 23, the exit angle of the sleeve controls the amount of recirculation flow. The sleeve exit angle initially selected for the E³ swirl cup was 45°, but component performance testing revealed that a 90° angle sleeve was better. Another important design feature of the swirl cup is the venturi. The venturi prevents the hot combustion gases from reaching the fuel nozzle face and creating carbon deposits. A parametric development study was conducted earlier as part of the ECCP to determine the key design values of the venturi which would prevent carbon buildup. The results of this study are

ORIGINAL PAGE IS
OF POOR QUALITY



		<u>Pilot</u>	<u>Main</u>
Primary	Vane Angle	60°	60°
	Inlet Angle	23°	23°
	Effective Area, cm (in ²)	0.92 (0.143)	0.92 (0.143)
	Venturi Throat Diameter, cm ² (in ²)	1.58 (0.623)	1.58 (0.623)
Secondary	Vane Angle	80°	80°
	Vane Height, cm (in)	0.70 (0.275)	1.02 (0.400)
	Effective Area, cm ² (in ²)	1.38 (0.214)	1.87 (0.290)

Figure 21. Swirl Cup Design.

ORIGINAL PAGE 127
OF POOR QUALITY

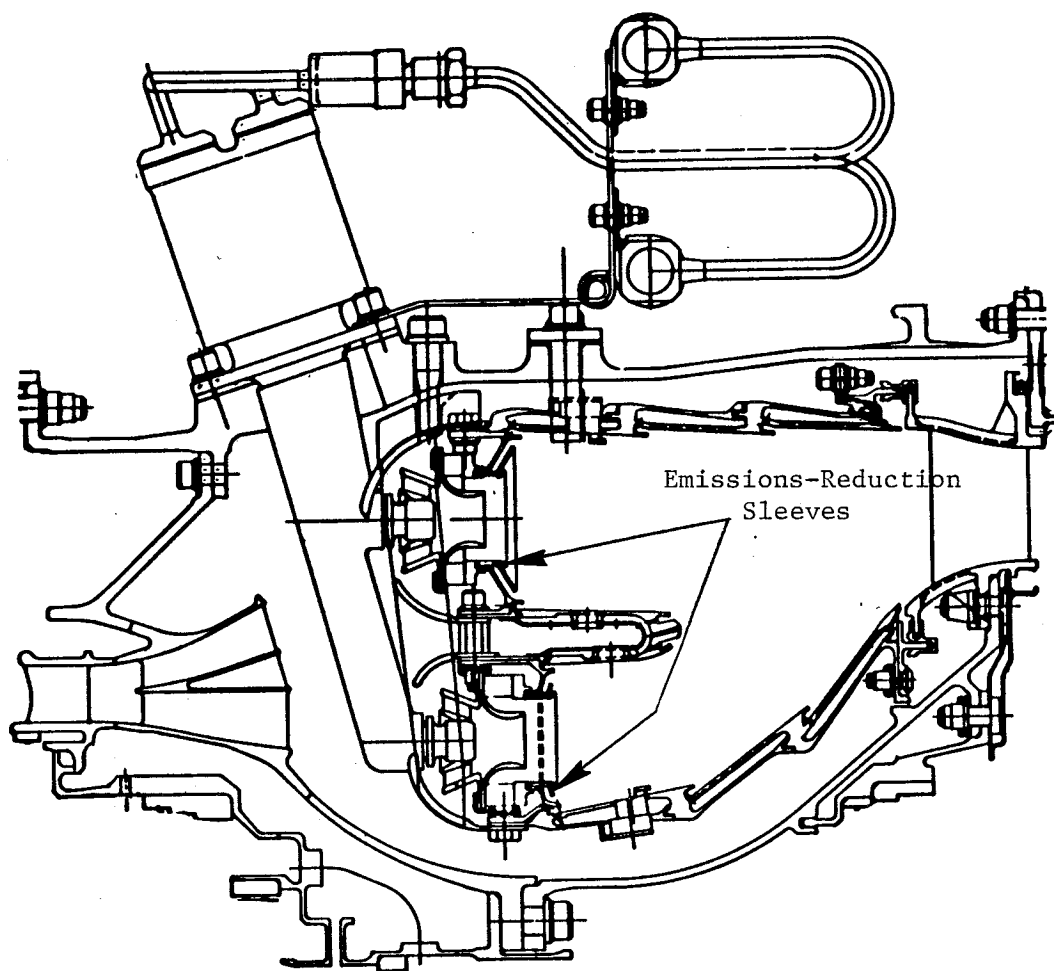


Figure 22. Combustor Emissions - Reduction Sleeves.

ORIGINAL PAGE IS
OF POOR QUALITY

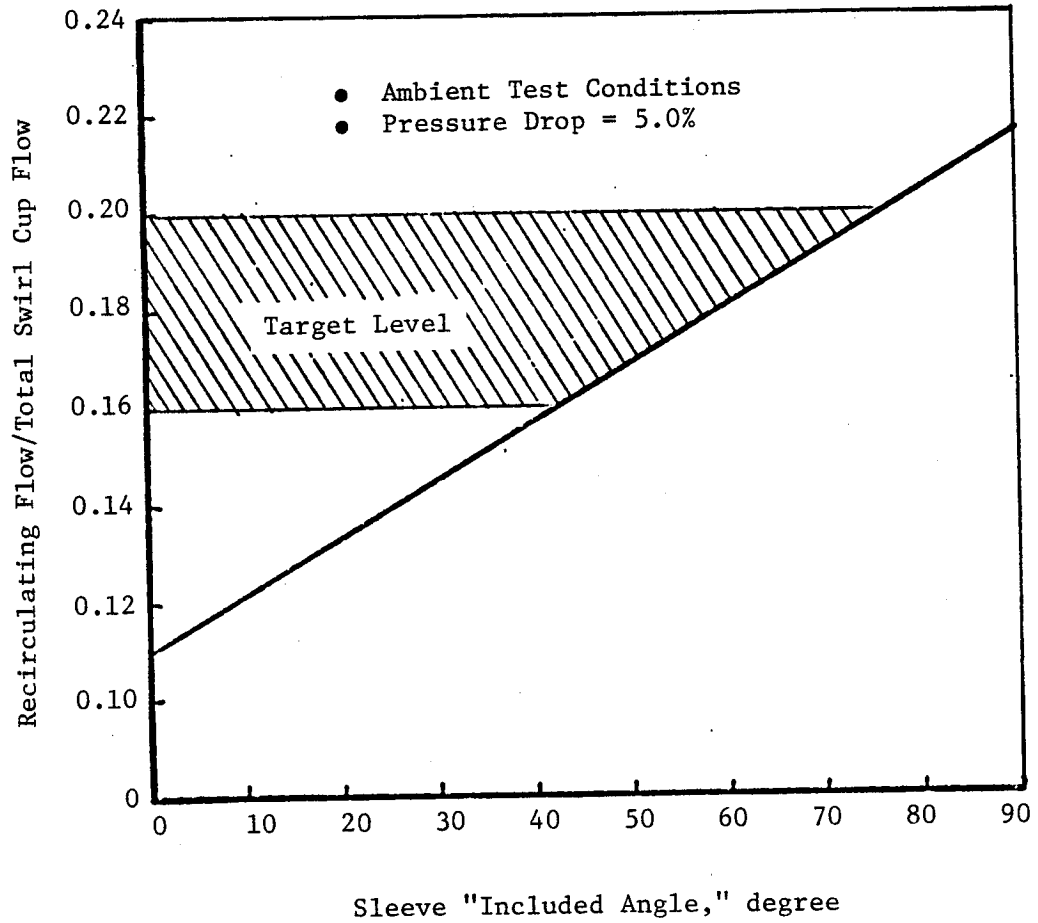


Figure 23. Recirculation Flow Compared to Sleeve "Included Angle."

shown in Figure 24. Using this design criteria, the E³ swirl cup venturi parameters were selected to assure that carboning of the fuel nozzle or venturi surfaces would not occur.

A unique feature of the advanced, film impingement liner construction selected for the E³ combustor is that dilution air can be introduced either at full liner pressure drop or at a lower pressure drop level. These two dilution designs are illustrated in Figure 25. Figure 26 illustrates that these concepts provide different jet penetration characteristics. This provides additional design flexibility when trying to control the exit temperature profile characteristics of the combustor.

The fuel nozzle for the E³ combustor is similar in design to the type used in conventional combustion systems except it provides fuel for both the pilot and main stage systems. The key fuel nozzle spray characteristics are controlled spray angle, stable operation, good atomization, and uniform distribution. The hydraulic flow schedule is also shown in Figure 11. Specific design features of the fuel nozzle are shown in Table XIV. The combustor operates on the small size primary system to assure high nozzle pressure drop and good atomization in the low engine speed region where combustion conditions are most severe. The primary systems of the pilot and main stage nozzles are identical. Therefore, when both primary systems are operating, the fuel flow is split equally between the pilot and main stage domes. At engine speeds above ground idle, the metering valve opens and permits fuel into the high flowing secondary system. At these more favorable inlet conditions where combustor inlet pressures and temperatures are higher, the larger spray droplets from the secondary system are more easily vaporized. The main stage total flow is about twice that of the pilot above the secondary cut-in, to bias the fuel flow to the lean main stage dome at high power operating conditions for NO_x emissions control. However, the exact flow split has not been selected. Therefore, the fuel systems were oversized to provide some flow split flexibility. The pilot and main fuel systems are supplied from a common line and, therefore, operate from a common fuel flow and pressure source. By installing a restriction in the main or pilot stage fuel inlet line, the flow split can be shifted by inducing additional pressure drop into that system. As an example, if the pilot stage fuel system was operating at 2.41 MPa (349.5 psi) and

ORIGINAL PAGE IS
OF POOR QUALITY

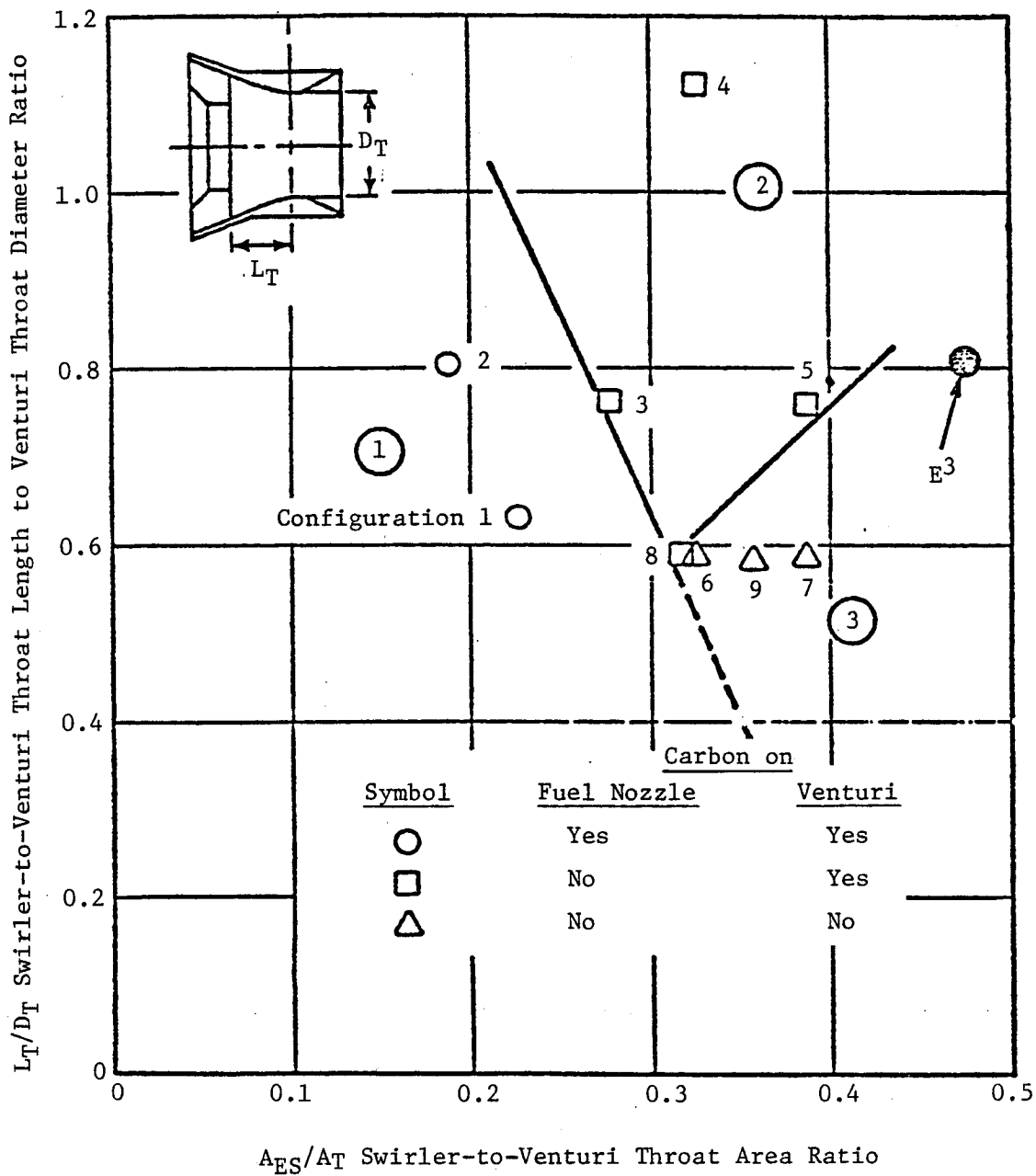
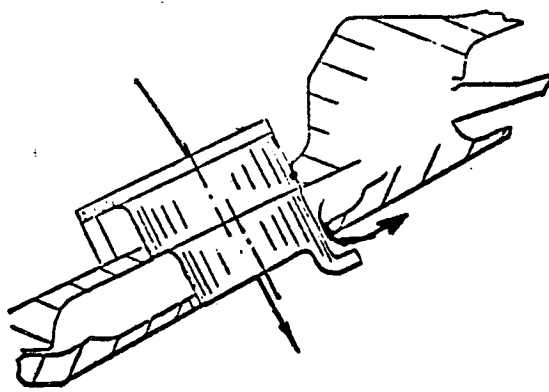
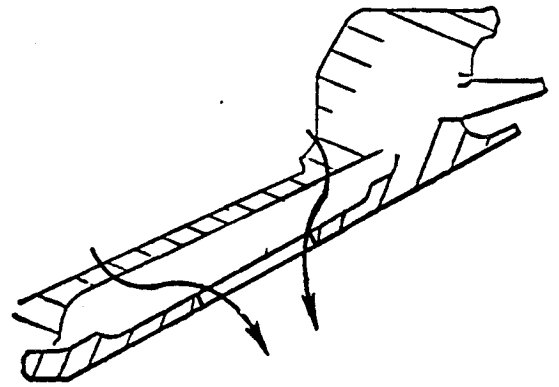


Figure 24. Venturi Anticarboning Design Criteria.

ORIGINAL PAGE IS
OF POOR QUALITY



Full Pressure Drop



Spent Impingement Dilution

Figure 25. E^3 Dilution Thimble Designs.

ORIGINAL PAGE IS
OF POOR QUALITY

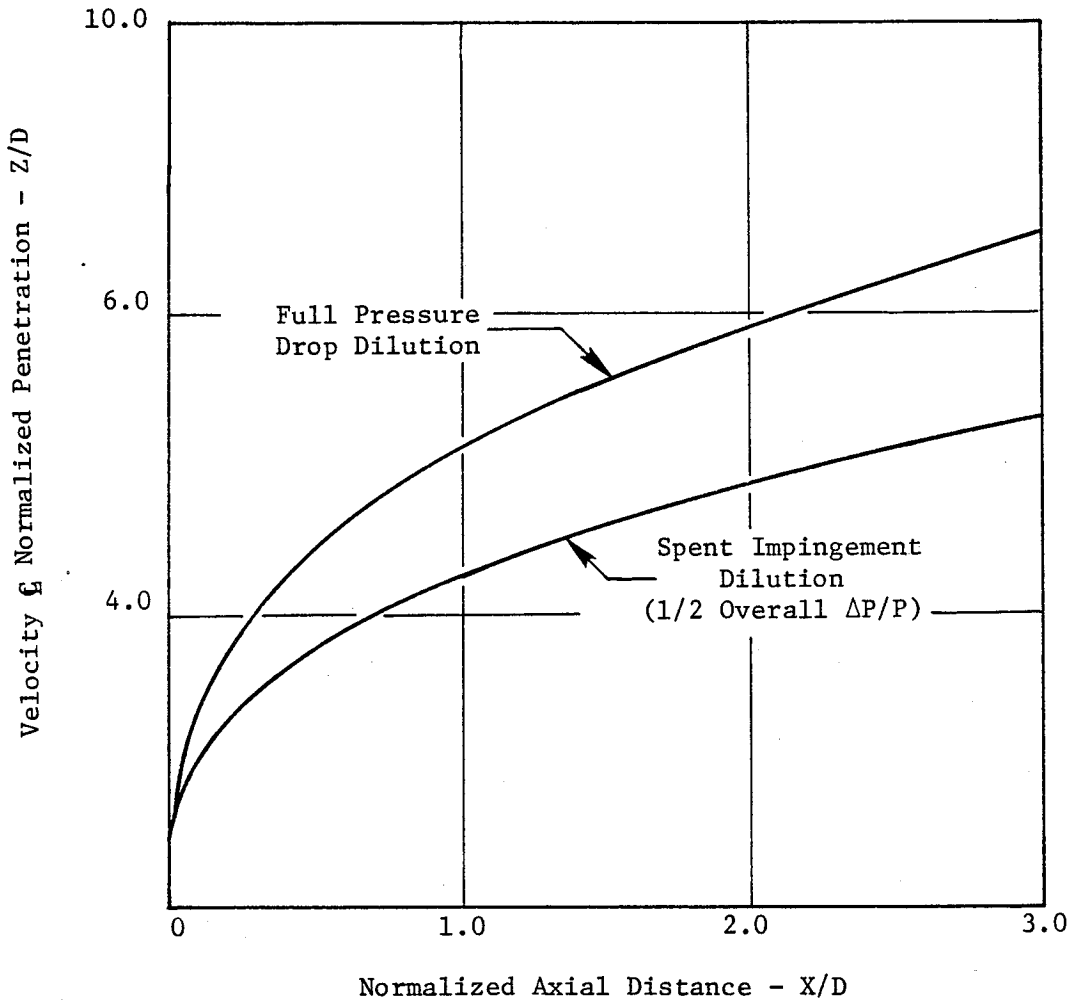


Figure 26. Comparison of E^3 Dilution Jet Penetration.

a restriction was added to the main supply line to provide an additional pressure drop of 0.35 MPa (50.8 psi), the resulting flow curve would look like the one shown in Figure 11 for the 40% pilot-to-total flow split. The operating characteristics of the pilot and main stage fuel systems across the E³ FPS standard day operating line are presented in Figure 27.

Table XIV. Engine Fuel Nozzle Features.

- | |
|---|
| <ul style="list-style-type: none">● Flight-Type Fuel Schedule - Oversize to Permit Flow Split Variation● Duplex Spray Tips - Primary and Secondary● Primary Spray Angle of 50° for Emissions Reduction and Ignition and Secondary Spray Angle of 70° for Uniform Exit Temperature Distribution● Shutoff and Metering Valves - Pilot and Main● Heat Shielded and Insulated |
|---|

4.4 DESIGN SUMMARY

The design studies completed to date in E³ combustor development have resulted in the following progress:

- The preliminary aerodynamic design for the combustor has been selected.
- Definition has been provided for the swirl cups, emissions reduction sleeves, and fuel nozzles.
- Selection of the ground starting operating mode has been made. Pilot stage operation only has been selected to provide for the least complex control system and most favorable ignition characteristics.
- The results of the component testing, discussed in the next section, have been factored into the initial aero design effort, and these further studies have resulted in selection of the final combustor aero design definition shown in Figure 8.

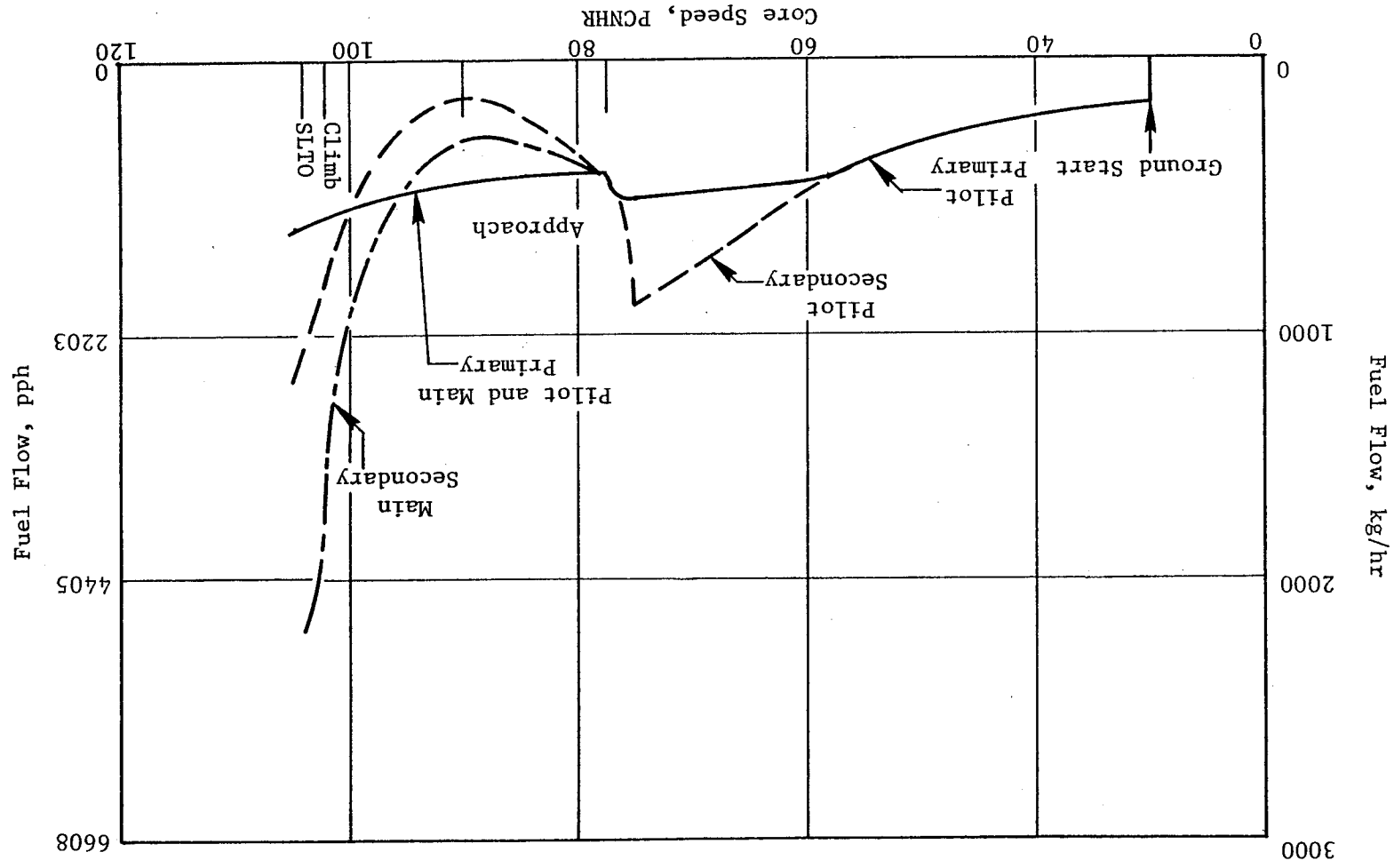


Figure 27. Fuel Nozzle Staging - Pilot to Main Stage.

5.0 MECHANICAL DESIGN

5.1 REQUIREMENTS

The E³ combustor mechanical design life objectives, shown in Table XV, are consistent with the engine technical requirements. The combustion system hot parts were designed to a cyclic life capability of 9000 cycles to first repair with an ultimate life of 18,000 cycles for these parts. Based on the typical engine mission of 2-hour duration, the cyclic life requirement translates to 18,000 hours to first repair with an ultimate life of 36,000 hours.

Table XV. Combustor Mechanical Design Objectives.

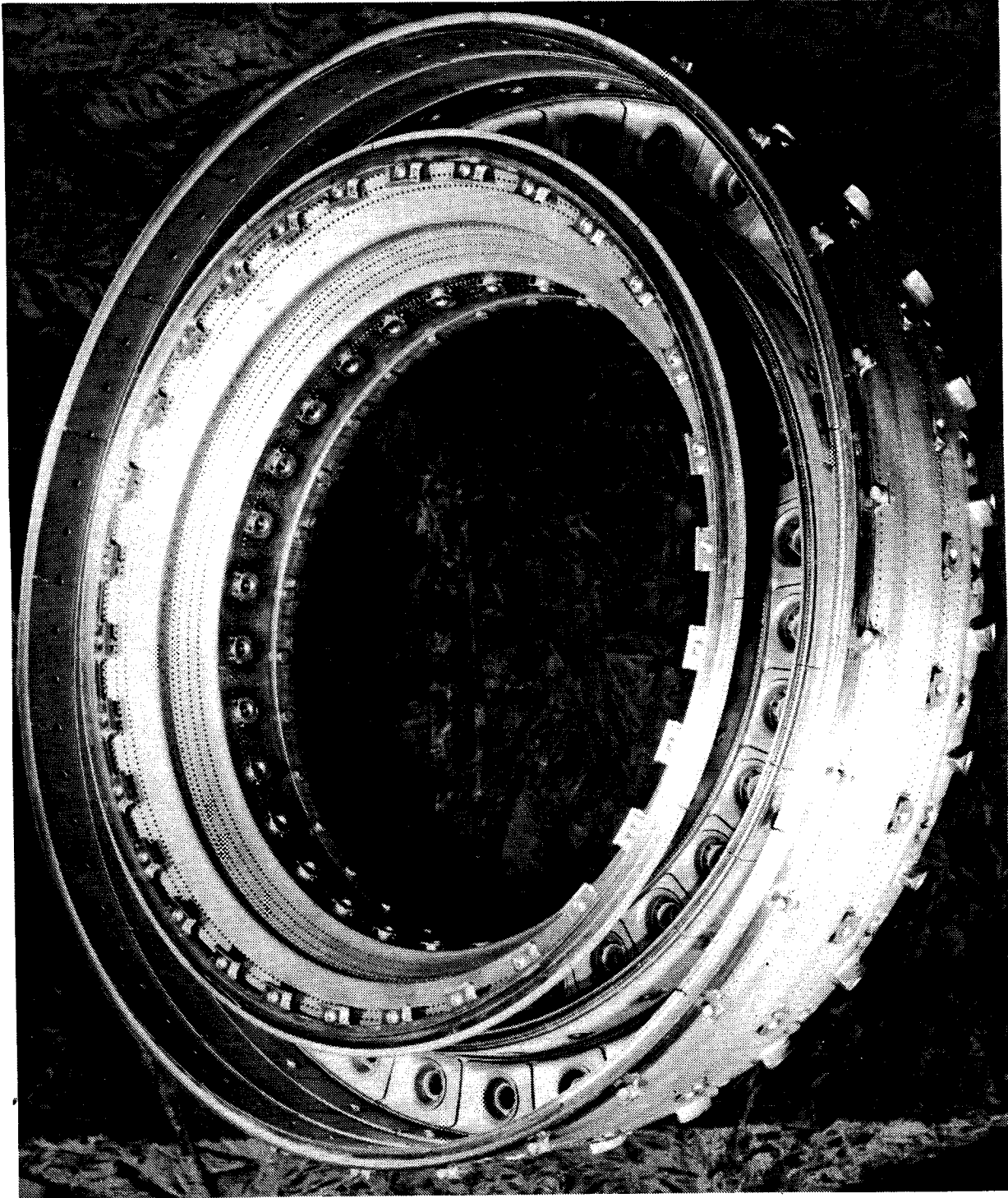
	<u>Operating Time</u>	
	<u>Hours</u>	<u>Cycles</u>
To First Repair	18,000	9,000
Total Life	36,000	18,000
Maximum Operating Conditions (Growth Engine)		
Inlet Temperature	927 K (1669° R)	
Inlet Pressure	3.91 MPa (567 psia)	
Fuel-to-Air Ratio	0.025	

The components were designed to operate at the most severe anticipated engine operating condition. This corresponds to growth engine hot day takeoff.

5.2 GENERAL DESIGN FEATURES

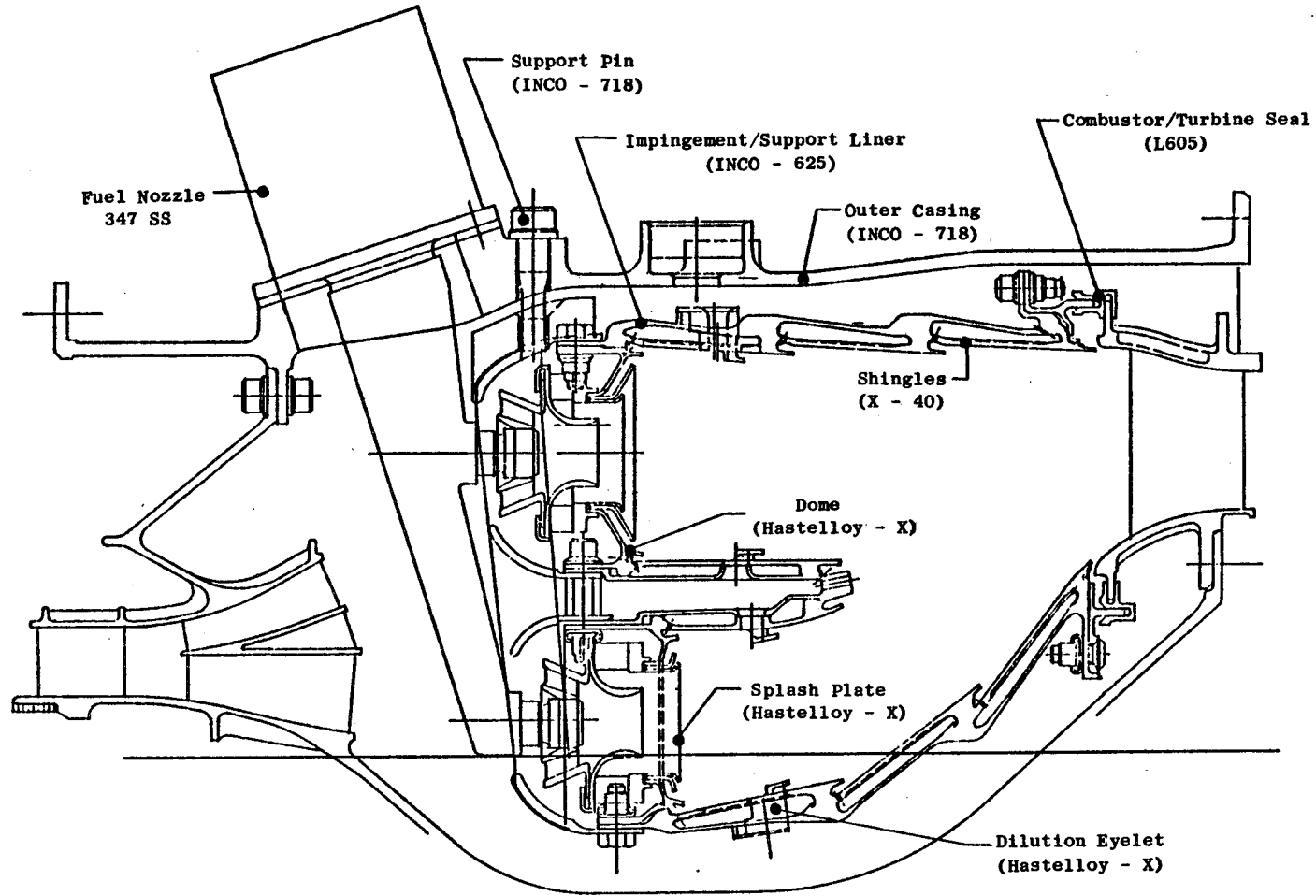
Figure 28 shows the assembled E³ combustor. A cross section of the combustor design is shown in Figure 29. The E³ combustor design features a double-annular dome with a common swirl cup design used in each dome. A centerbody structure separates the outer pilot dome from the inner main stage dome. Fuel is introduced to the combustor through 30 dual tip fuel nozzles. Each fuel nozzle features a completely independent fuel metering for each dome. The combustor liners utilize a double-walled, shingled liner concept to provide

Figure 28. Assembled F₃ Combusstor.



ORIGINAL PAGE IS
OF POOR QUALITY

ORIGINAL PAGE
BLACK AND WHITE PHOTOGRAPH



ORIGINAL PAGE IS
OF POOR QUALITY

Figure 29. Combustor Materials Selection.

long life. The combustor is supported at the upstream end by 30 support pins. These support pins transmit all the mechanical force loads from the liners and dome to the outer combustor case. The combustor turbine interface is sealed with machined fishmouth seals which accommodate the relative growth and mechanical stackups between the two components.

The outer casing supports the combustor, the fuel nozzles, fuel delivery system, the ignition system, and the engine firewall. Ports are provided in the casing for borescope inspection, compressor discharge bleed, and instrumentation leadout.

5.3 DESIGN SELECTION

5.3.1 Materials

The materials selected for the combustion system are shown in Figure 29. Conventional combustor high temperature alloys, such as Hastelloy X and X-40 (a high temperature cobalt-based alloy which has demonstrated excellent durability), were chosen for the components which are exposed to hot combustion gases: the dome, centerbody, shingles, and dilution eyelets. Supporting structures, such as the outer casing and the impingement liners, are made of nickel-based alloys. The fuel system was fabricated from stainless steel alloys as shown in Figure 30.

A stable thermal barrier coating material will be applied to the flame side surfaces of the centerbody to provide for reduced metal temperatures and longer life.

5.3.2 Design Description and Geometry

After the preliminary design review, several changes were incorporated into the combustor mechanical design. These changes affected the following components. Liner shingle geometry was optimized to a shingle array which featured three axial rows. The shingle edges were designed with circumferential overlap seals thereby eliminating 105 leaf seals in the combustor assembly. The turbine cooling air filtration screens located at the combustor aft end were removed to be consistent with current commercial engine design philosophy and to reduce system weight complexity and cost. The combustor centerbody was

ORIGINAL PAGE IS
OF POOR QUALITY

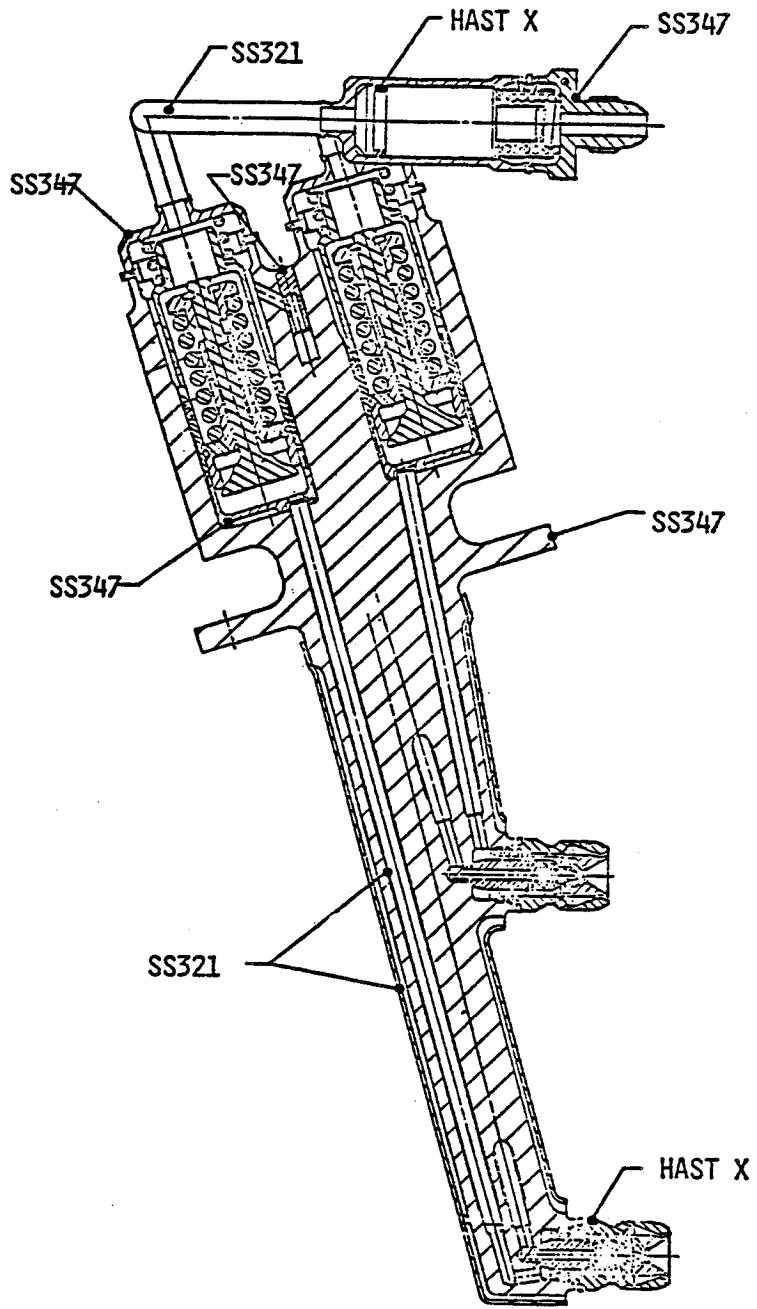


Figure 30. E³ Fuel Nozzle Materials.

shortened from the original configuration to provide a more rigid, more readily cooled design. In addition, centerbody thermal relief slots were incorporated to reduce thermal stress and provide adequate component life capability.

The design details of the combustor will be summarized by major component: liners, casing, domes, centerbody, and fuel delivery stem. A detailed description of each component follows.

Combustor Liner Design

The combustor liners utilize a double-walled, shingled liner concept similar to the liners developed in the GE/ATEGG engine program. The liners consist of a load carrying 360° turning which supports individual heat shields or shingles. The shingles are segmented axially and circumferentially to reduce stress and provide long life. The support liner, in addition to supporting the shingles, provides impingement cooling to the shingle. Figure 31 shows the inner support liner. All of the cooling and dilution holes in both support liners were laser drilled. Laser hole drilling of combustors is a new application of this technology with savings in both time and cost over conventional hole drilling methods such as electrodischarge machining (EDM). Figure 32 shows the assembled inner liner.

The E³ shingle design is similar to the ATEGG/GE23 shingle design. The GE23 combustor features a cast shingle design. This design background provided the basis for the E³ combustor liner design. A comparison between the GE23 shingle geometry and the E³ shingle geometry is shown in Table XVI. One significant difference in design configuration between the E³ and GE23 combustor shingles is the support foot configuration. A comparison of the two support foot designs is provided in Figure 33. The E³ design was optimized to allow the maximum coolant flow introduction between feet while maintaining sufficient foot width for mechanical strength. The optimization consisted of trading off cyclic fatigue life against rupture life capability for the shingle design.

Another significant difference in shingle design is the method of controlling leakage between adjacent shingles. Figure 34 illustrates the GE23 and E³ edge seal configuration. The GE23 shingle utilizes individual sheet metal

ORIGINAL PAGE IS
OF POOR QUALITY

ORIGINAL PAGE
BLACK AND WHITE PHOTOGRAPH



Figure 31. Combustor Inner Support Liner.

ORIGINAL PAGE IS
OF POOR QUALITY

ORIGINAL PAGE
BLACK AND WHITE PHOTOGRAPH

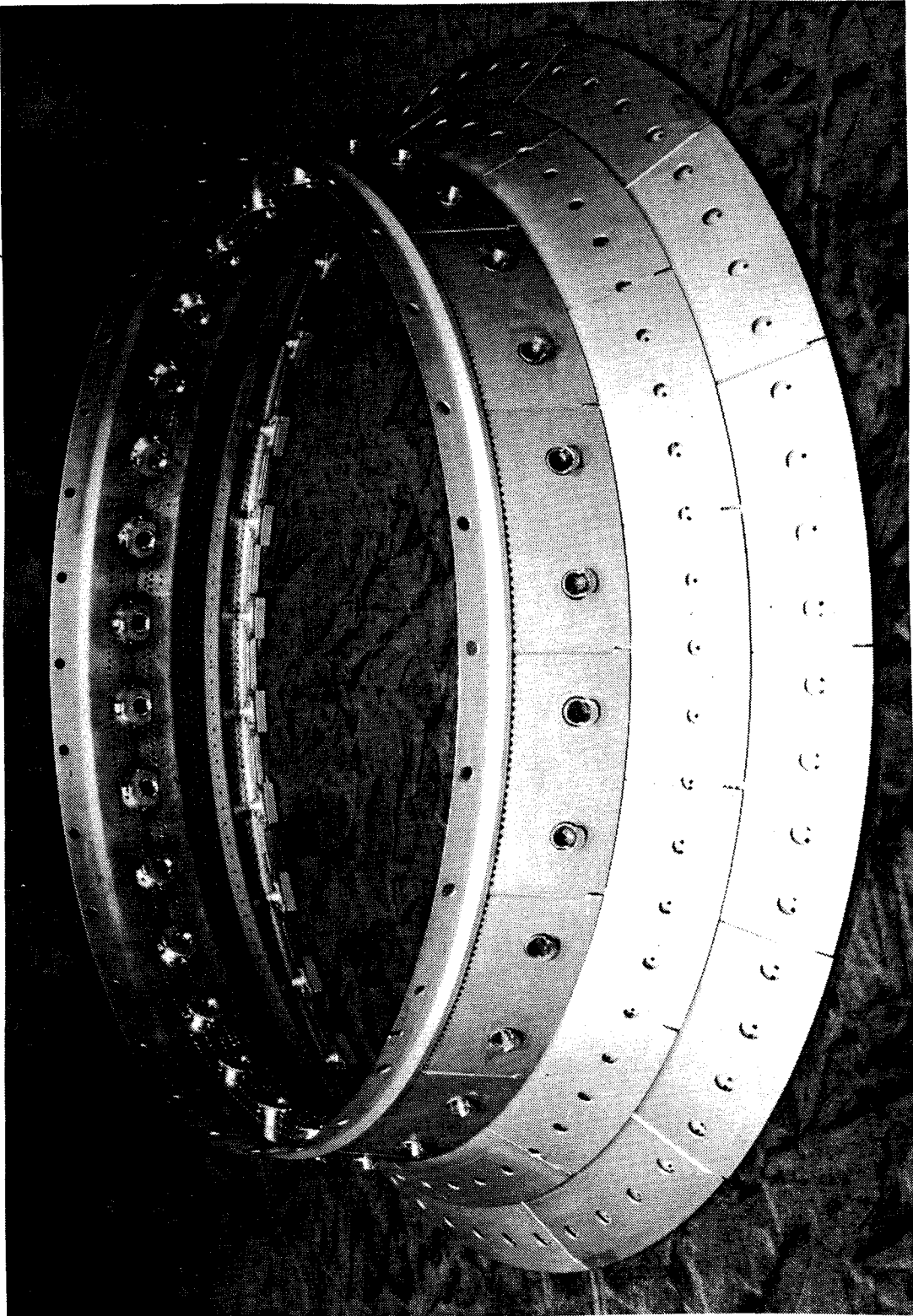


Figure 32. Assembled Combustor Inner Liner.

Table XVI. Shingle Geometry Comparison.

Design		No. of Axial Panels	Number of Circumferential Segments	Panel Length L, cm (inch)	Number Feet	Thickness cm (inch)	Shingle Arc Width, cm (inch)
E ³	Outer Liner	3	20	4.47 (1.76)	11	0.127 (0.050)	11.76 (4.63)
	Inner Liner	3	15	4.78 (1.88)	11	0.127 (0.050)	12.24 (4.82)
GE23	Outer Liner	4	20	4.62 Max. (1.82)	11	0.127 (0.050)	11.41 (4.49)
	Inner Liner	4	20	3.56 Max. (1.40)	9	0.127 (0.050)	9.68 (3.81)

CONTINUED FROM PREVIOUS PAGE

ORIGINAL PAGE IS
OF POOR QUALITY

	$W,$ cm (inch)	$S,$ cm (inch)	W/S
<u>GE23</u>			
Outer Liner	0.58 → 0.66 (0.23) → (0.26)	0.33 → 0.38 (0.13) → (0.15)	1.8
Inner Liner	0.51 → 0.66 (0.20) → (0.26)	0.31 → 0.38 (0.12) → (0.15)	1.9
<u>E³</u>			
Outer Liner	0.51 (0.20)	0.51 (0.20)	1.0
Inner Liner	0.46 → 0.56 (0.18) → (0.22)	0.46 → 0.56 (0.18) → (0.22)	1.0

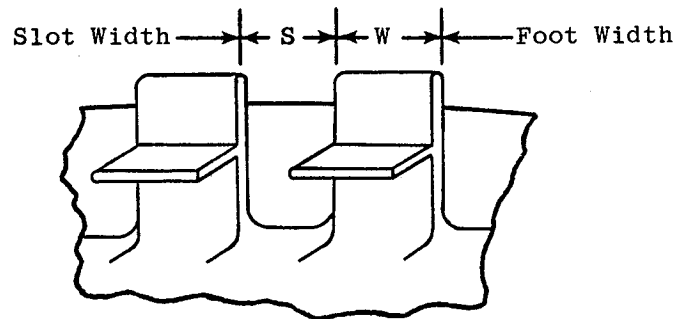
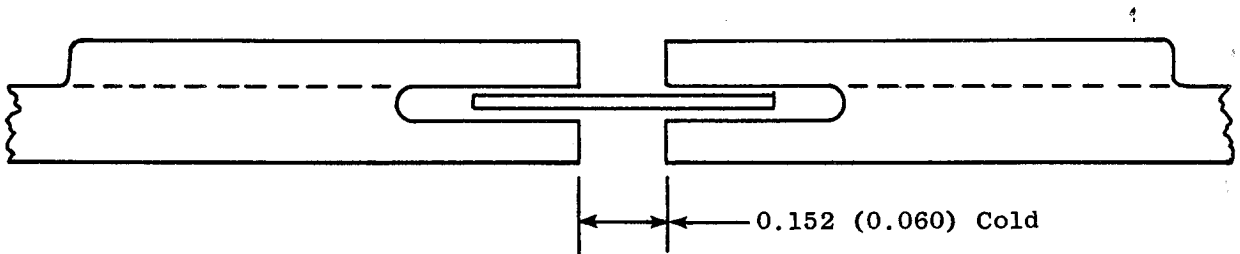


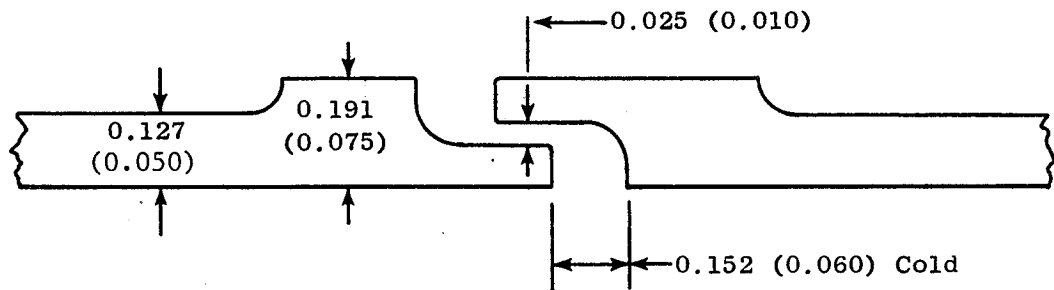
Figure 33. E³/GE23 Shingle - Comparison of Support Foot Spacings.

ORIGINAL FIGURE
OF POOR QUALITY



GE23 Shingle

• All Dimensions Are in cm and (inch)



E³ Shingle

Advantage: Elimination of 105 Parts

Figure 34. Comparison of Shingle Edge Seal Configurations.

leaf seals which fit into slots along the edges of the shingle. The E³ shingle introduces a novel concept for between-shingle leakage control. This shingle design has overlapping edges which eliminate the need for individual edge seals. The edge leakage flow is controlled by closely dimensioning the gap between the overlapping shingle edges. The elimination of the shingle edge seal does introduce a controlled leakage and a slight penalty in loss of shingle coolant and slightly increased operating temperature. Figure 35 shows the effect of shingle edge leakage on shingle operating temperature. The maximum increase in metal temperature due to this leakage is on the order of 19 K (34° F). The E³ design can accommodate this metal temperature increase penalty in light of the significant reduction in component pieces and the easier liner assembly achieved with the overlapping shingle design.

Another combustor liner feature similar to the GE23 combustor design is the liner dilution eyelet. The liner dilution eyelet is supported by the support liner. As shown in Figure 36, a coannular gap is utilized at the shingle interface to avoid interference between the "hot" shingle and the "cold" eyelet during engine operation. The aft portion of the annular gap flow is directed onto the shingle with a film restarter lip to restore the dilution jet stripped cooling film. This technique was developed on the ATEGG combustors and has demonstrated significant shingle temperature reduction in the areas downstream of the dilution holes.

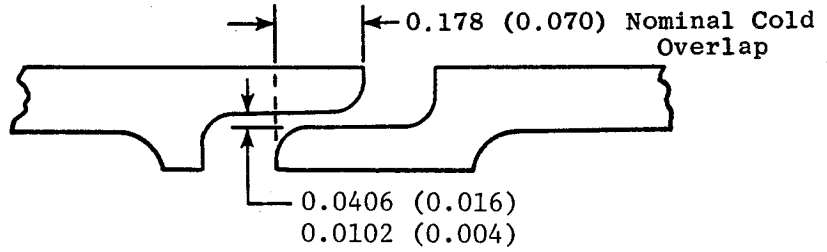
Combustor Casing

Figure 37 shows the combustor casing. The primary function of the combustor casing is to support the combustor and its fuel delivery and ignition systems. The casing features mounting pads for the fuel nozzles, ignitors, and combustor mounting pins. In addition, the casing has compressor discharge bleed ports, instrumentation ports, and borescope inspection ports. The location and orientation of these features are shown in Figures 38 and 39.

Combustor Support Pins

Figure 40 shows the combustor support pin design. This design is similar to the CF6 support pin design. The 30 support pins are bolted to the

• Dimensions Are in cm and (inch)



E³ Combustor Shingle Overlap Detail

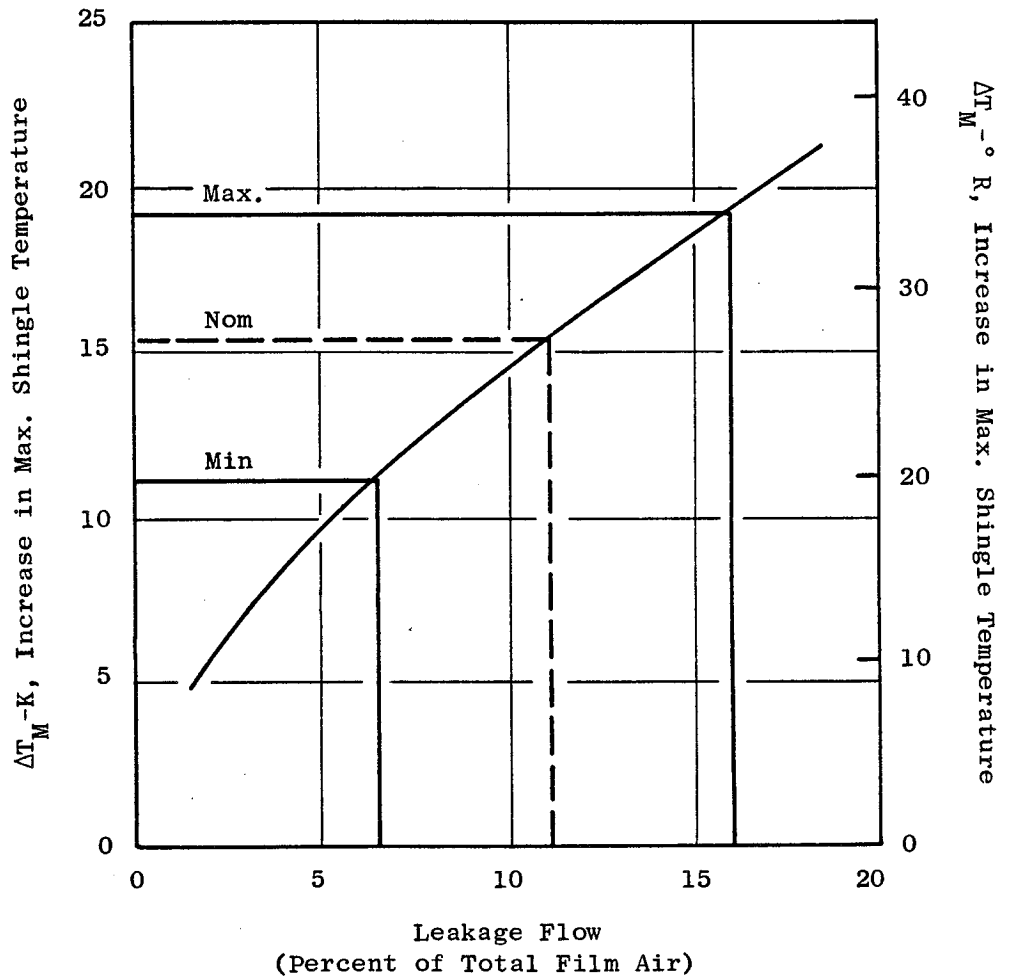


Figure 35. Effect of Shingle Edge Leakage on Shingle Configurations.

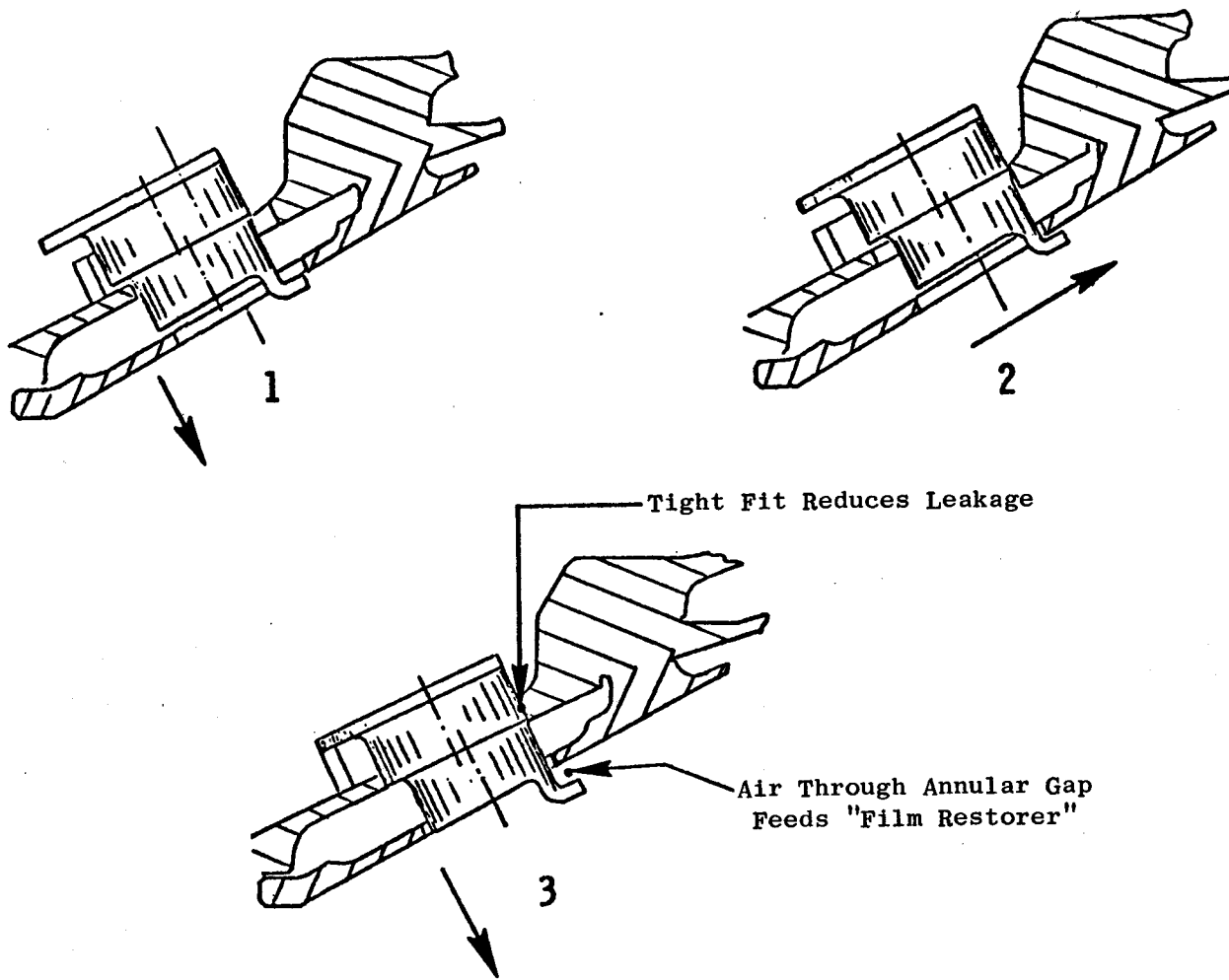


Figure 36. E³ Dilution Thimbles.

ORIGINAL PAGE IS
OF POOR QUALITY

ORIGINAL PAGE
OF POOR QUALITY

ORIGINAL PAGE
BLACK AND WHITE PHOTOGRAPH

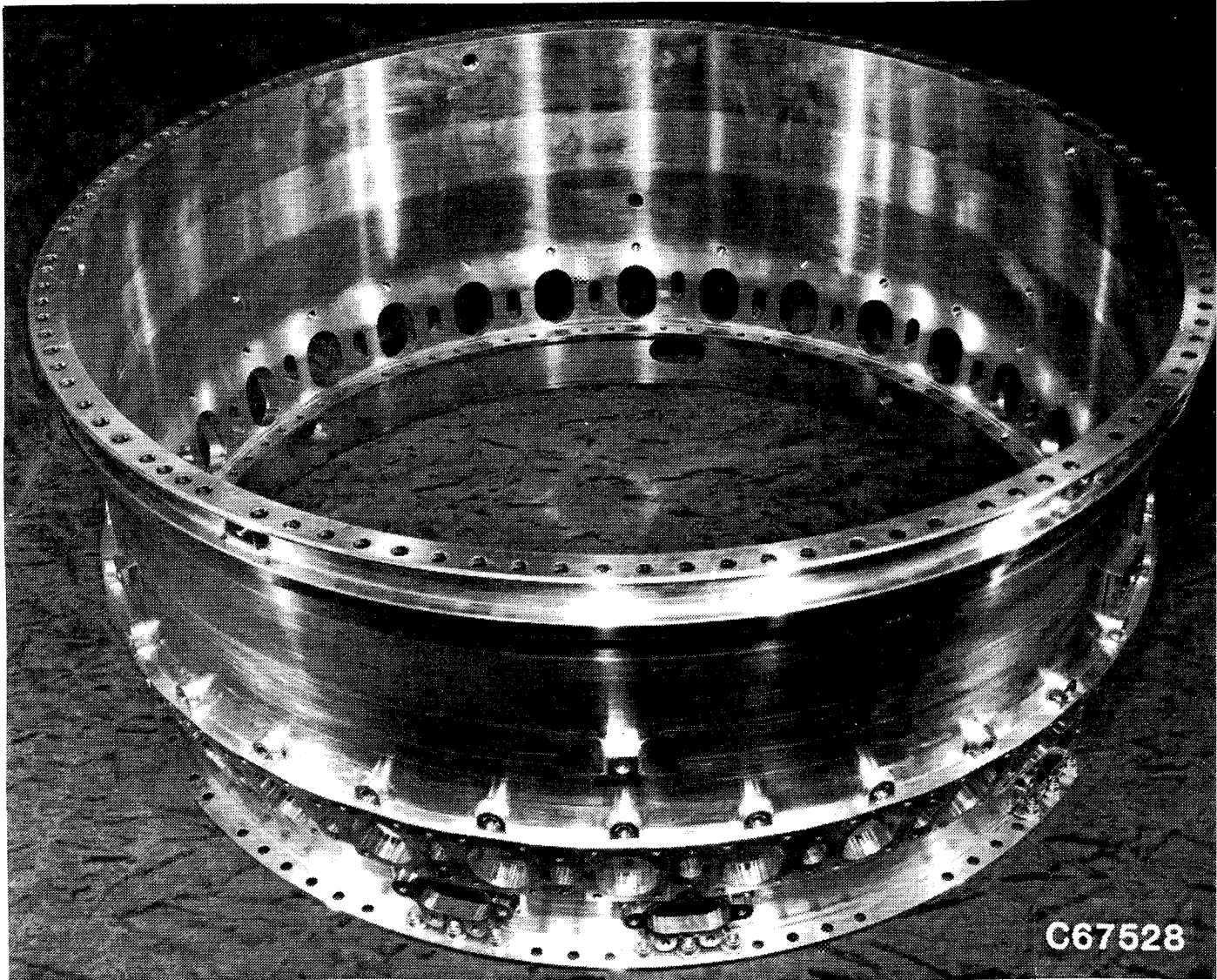


Figure 37. E³ Combustor Casing Hardware.

ORIGINAL PAGE IS
OF POOR QUALITY

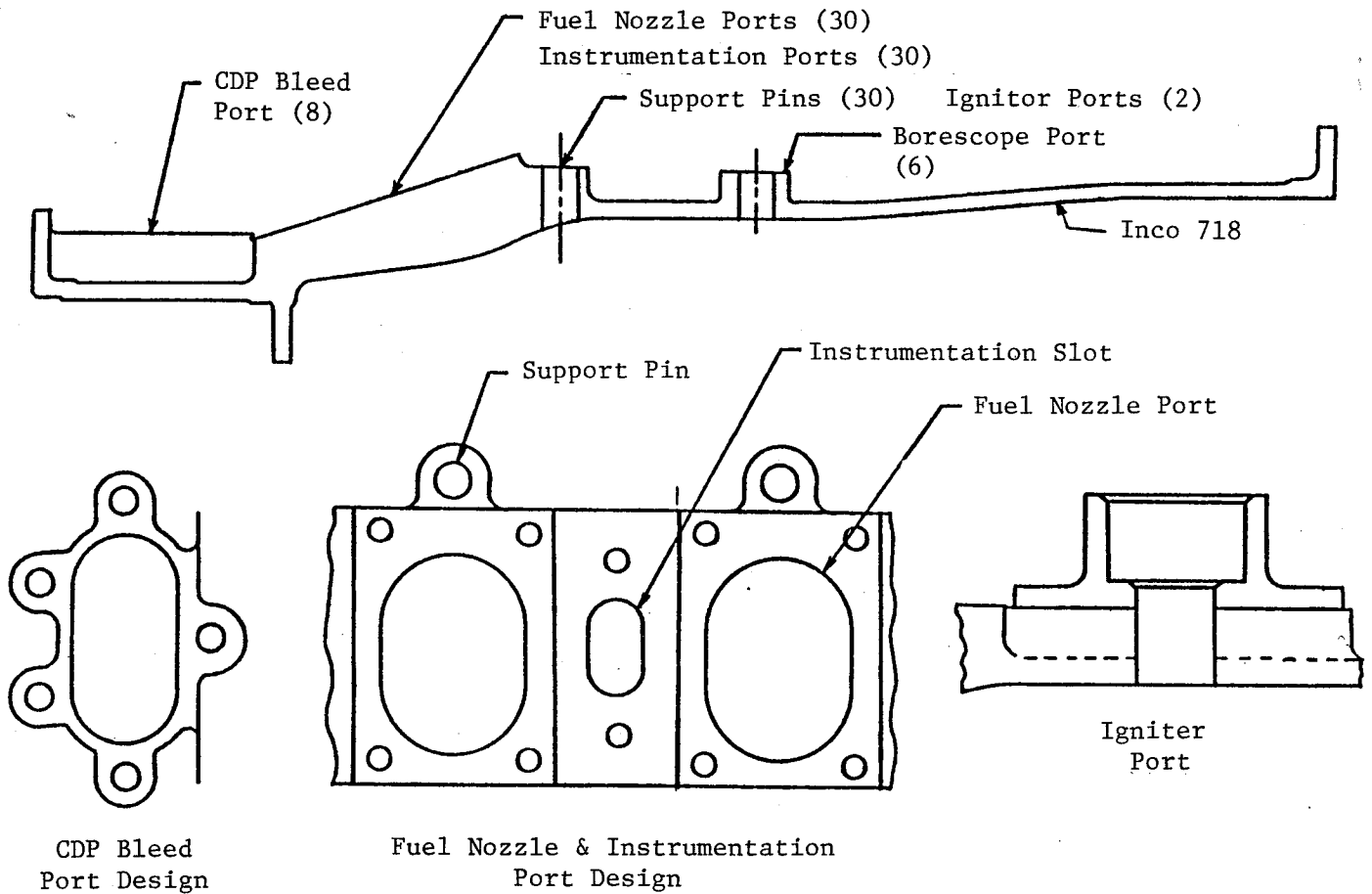


Figure 38. E³ Combustor Casing Features.

ORIGINAL PAGE IS
OF POOR QUALITY

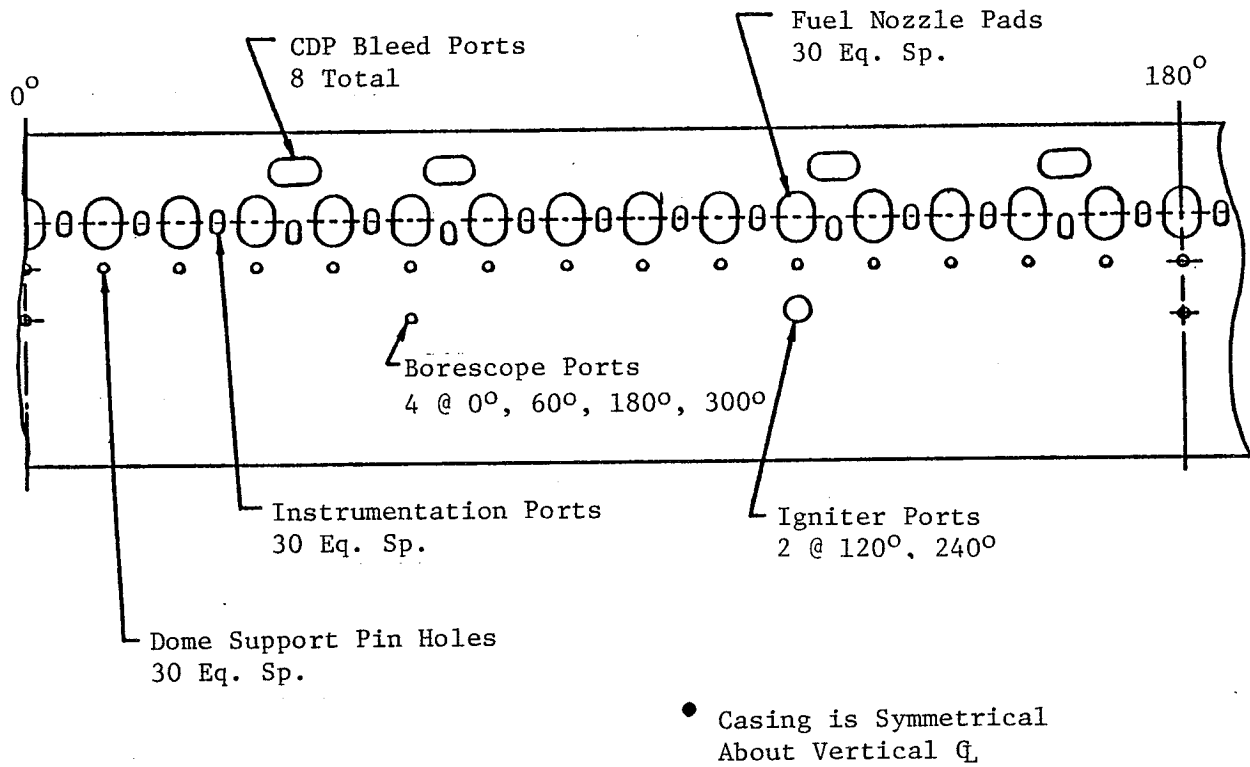


Figure 39. E³ Combustor Casing Rollout.

ORIGINAL PAGE IS
OF POOR QUALITY

30 Total
Max. Load = 805 N (181 lb) Each Pin
Max. Stress = 345 MPa (50 ksi) Bending
Yield = 793 MPa (115 ksi) Avg -3σ

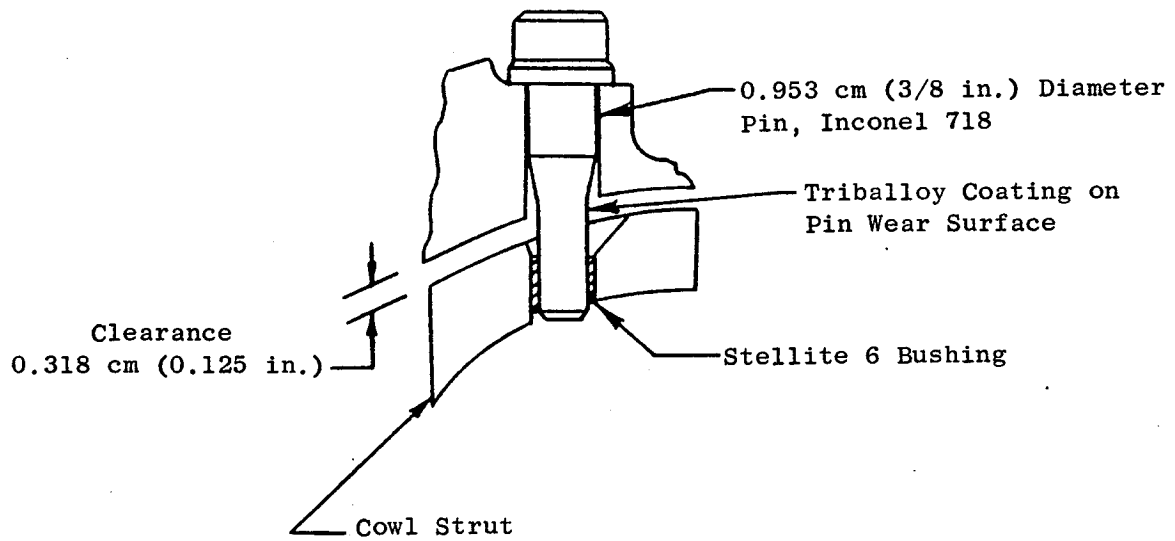


Figure 40. Combustor Support Pin Design.

outer case and establish the axial location of the combustor through mating holes in the cowl struts. The combustor force aerodynamic loads are transmitted to the combustor case through the support pins. A wear-resistant surface is provided at the support pin/cowl interface with a Triballoy coating on the support pin and a Stellite 6 bushing in the cowl.

Double-Annular Dome Design

Figure 41 shows a forward looking aft view of the combustor dome assembly. Each of the domes consist of 30 swirl cups supported by a 360° spectacle plate. The spectacle plate is the main structural member of the dome and is protected from the hot gases by individual splash plates at each swirl cup location. The swirl cups are comprised of counterrotating primary and secondary swirlers. The swirlers are machined from adjustable area swirler castings which allow flexibility in flow sizing.

The primary swirler features a slip joint attachment to the swirler cup which allows the primary vane assembly to "float" within certain limits. This floating primary vane arrangement allows for assembly stackup and thermal expansion between the dome and fuel nozzle.

The domes are bolted to the cowl assembly. The cowl struts transmit the aerodynamic loads from the domes and liners through the support pins to the combustor casing. Scallops are provided on the inner and outer cowls to allow installation and removal of the fuel nozzles without major engine disassembly. A cutaway of the dome features is shown in Figure 42.

Dome Centerbody Design

Figure 43 shows the centerbody structure. Its primary function is to separate the primary burning zones of the pilot and main stage domes. The main structure of the centerbody consists of a 360° machined piece with both film and impingement cooling. A sheet metal impingement baffle is brazed inside the centerbody cavity. Each dome has dilution air introduced through 30 dilution eyelets which are brazed to the main structure. Two crossfire

ORIGINAL PAGE
BLACK AND WHITE PHOTOGRAPH

ORIGINAL PAGE IS
OF POOR QUALITY

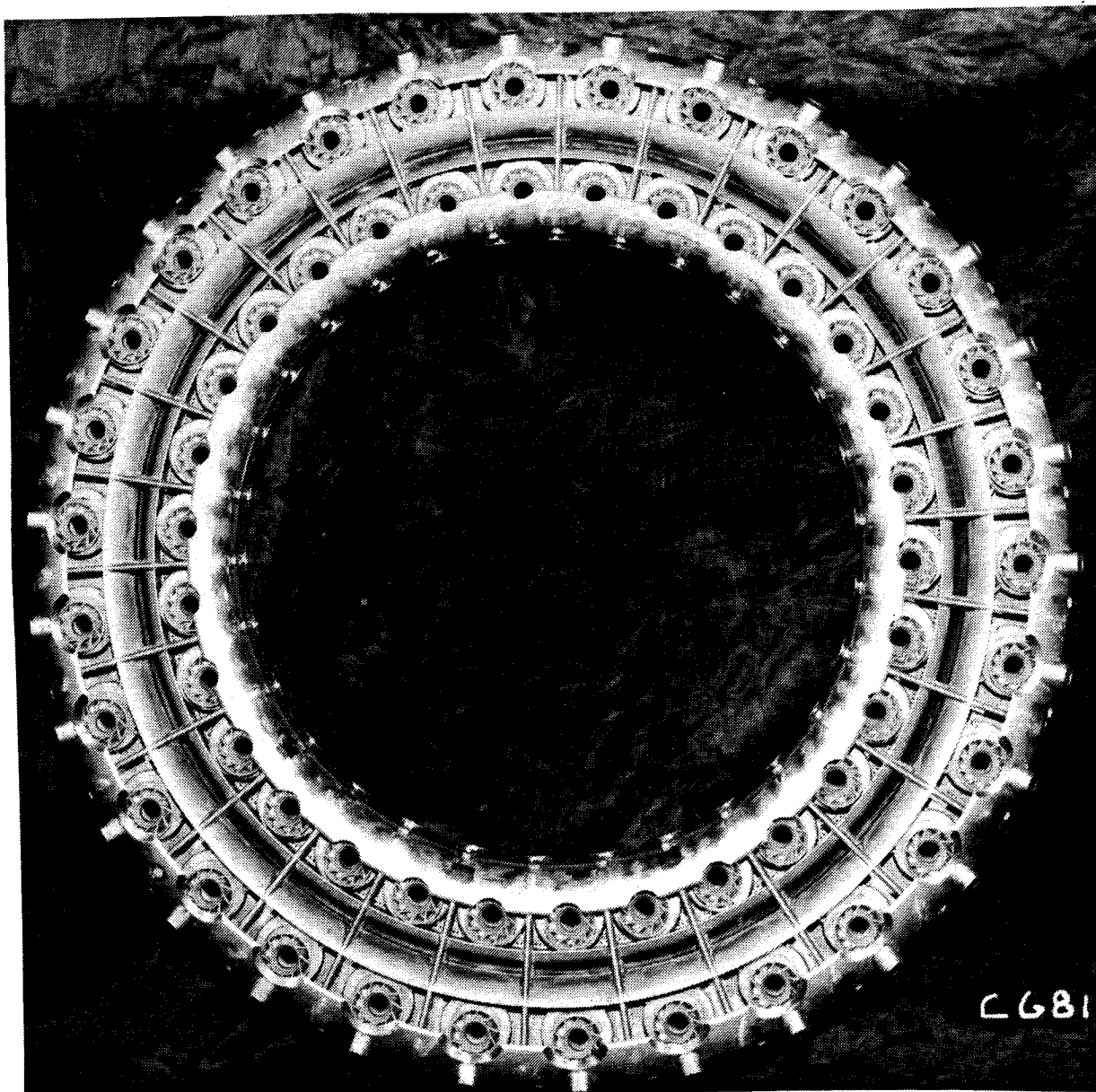
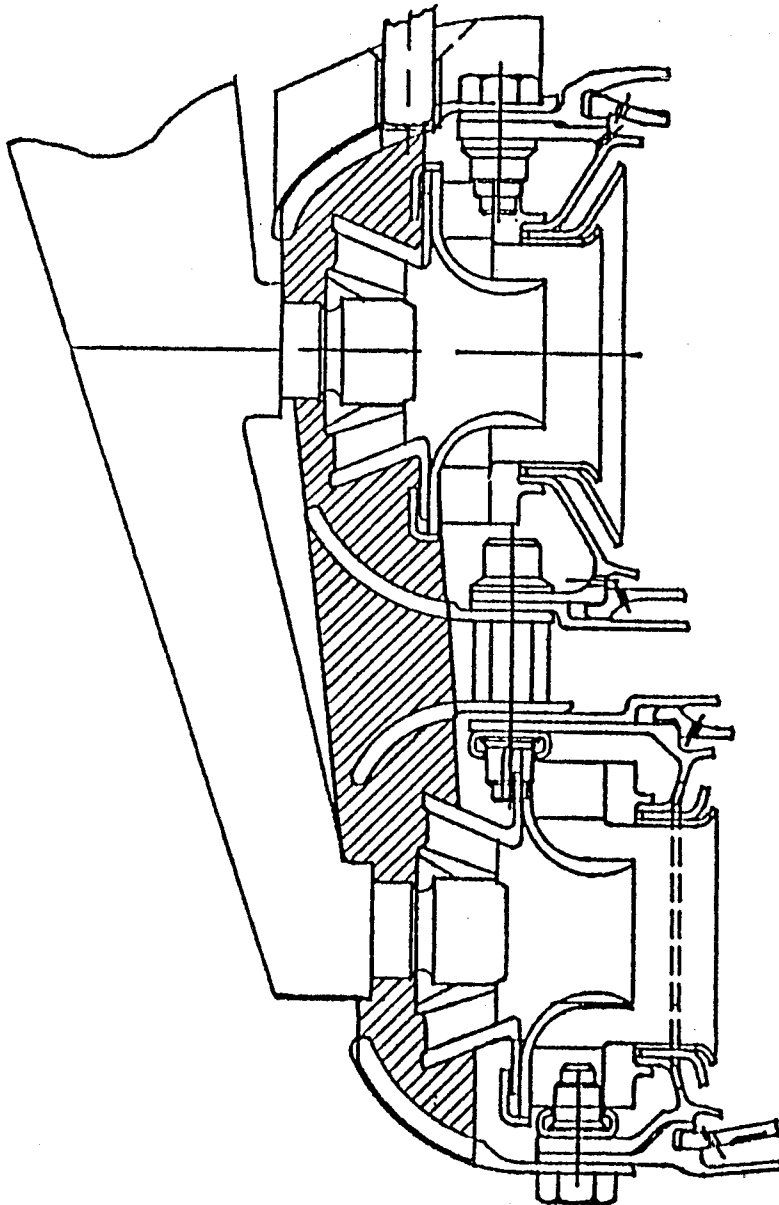


Figure 41. E³ Combustor Dome (Forward Looking Aft).

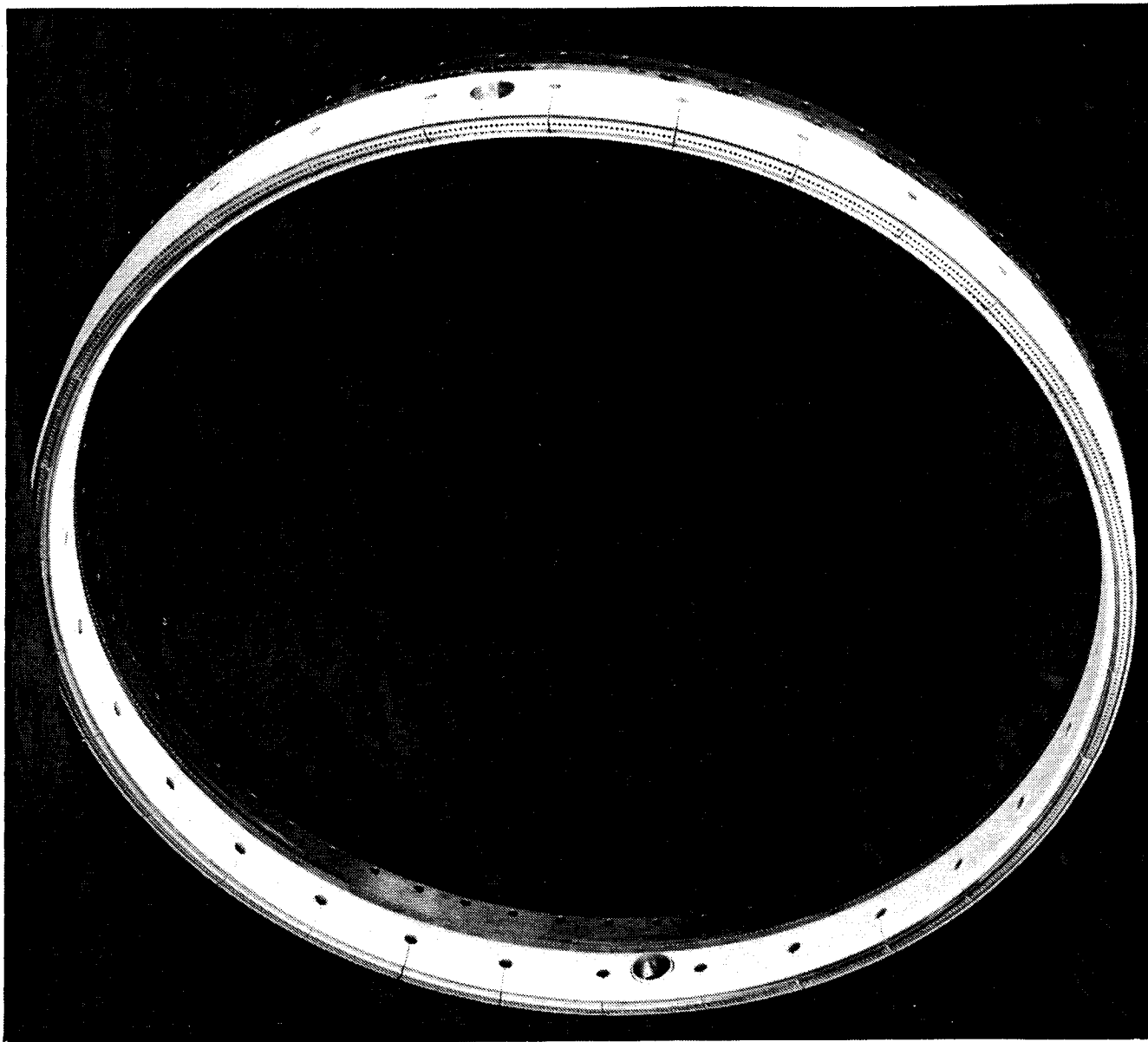


- Dome Structure Fully Shielded From Hot Gases
- Adjustable Area Swirler Castings
- Floating Primary Vane Assembly
 - Minimizes Nozzle Tip Load
 - Maintains Concentric Swirler Exit
- Cowl Struts to Transmit Dome and Liner Loads
- Potential ODS Alloy for Splashplate

ORIGINAL PAGE IS
OF POOR QUALITY

Figure 42. E³ Combustor Dome Design Features.

Figure 43. E₃ Combusstor Centerbody Structure.



ORIGINAL PAGE IS
BLACK AND WHITE PHOTOGRAPH

ORIGINAL PAGE IS
OF POOR QUALITY

tubes in line with the two igniters provide flame propagation across the centerbody to the main stage dome. Figure 44 shows a closeup view of the combustor illustrating the centerbody region near a crossfire tube. Other features shown are the pilot side dilution holes and the tip cooling holes.

Several design changes to the centerbody were incorporated since the preliminary design review. The centerbody tip was shortened to add rigidity and to eliminate a difficult tip hole drilling operation. This tip was also slotted to reduce thermal stress. A stable thermal barrier coating material was applied to reduce the metal temperature. "Gill" cooling holes were provided downstream of each crossfire tube to increase the film cooling in that region. These design changes are shown in Figures 45 and 46.

Fuel Delivery System

The fuel delivery system, shown in Figure 47, consists of two completely independent systems which feed each dome through a single stem fuel nozzle. The fuel manifolds and pigtail assemblies are fabricated from stainless steel. The fuel nozzle is made from a stainless steel forging. The material selection is based on extensive demonstrated commercial engine experience and reduced fabrication costs.

The fuel nozzle mechanical design features are shown in Figure 48. Each circuit has its own positive check valve to maintain fuel in the manifolds and reduce system fill time. Double heat insulation is provided by a stem heat shield and a coking gap around each fuel passage to prevent fuel boiling. Each nozzle tip is fed through individual primary and secondary fuel tubes to accommodate off-design conditions. An extended valve standoff is provided to isolate the metering valve from the engine casing and its associated heat loads which might cause fuel gumming or varnishing of the valve components. Figure 49 shows the fuel nozzle assembly.

Extensive vibration and geometric studies were conducted to ensure that the fuel nozzle design would avoid critical frequencies on the high power operating range, meet geometric constraints, and minimize aerodynamic losses.

ORIGINAL PAGE IS
OF POOR QUALITY

ORIGINAL PAGE
BLACK AND WHITE PHOTOGRAPH

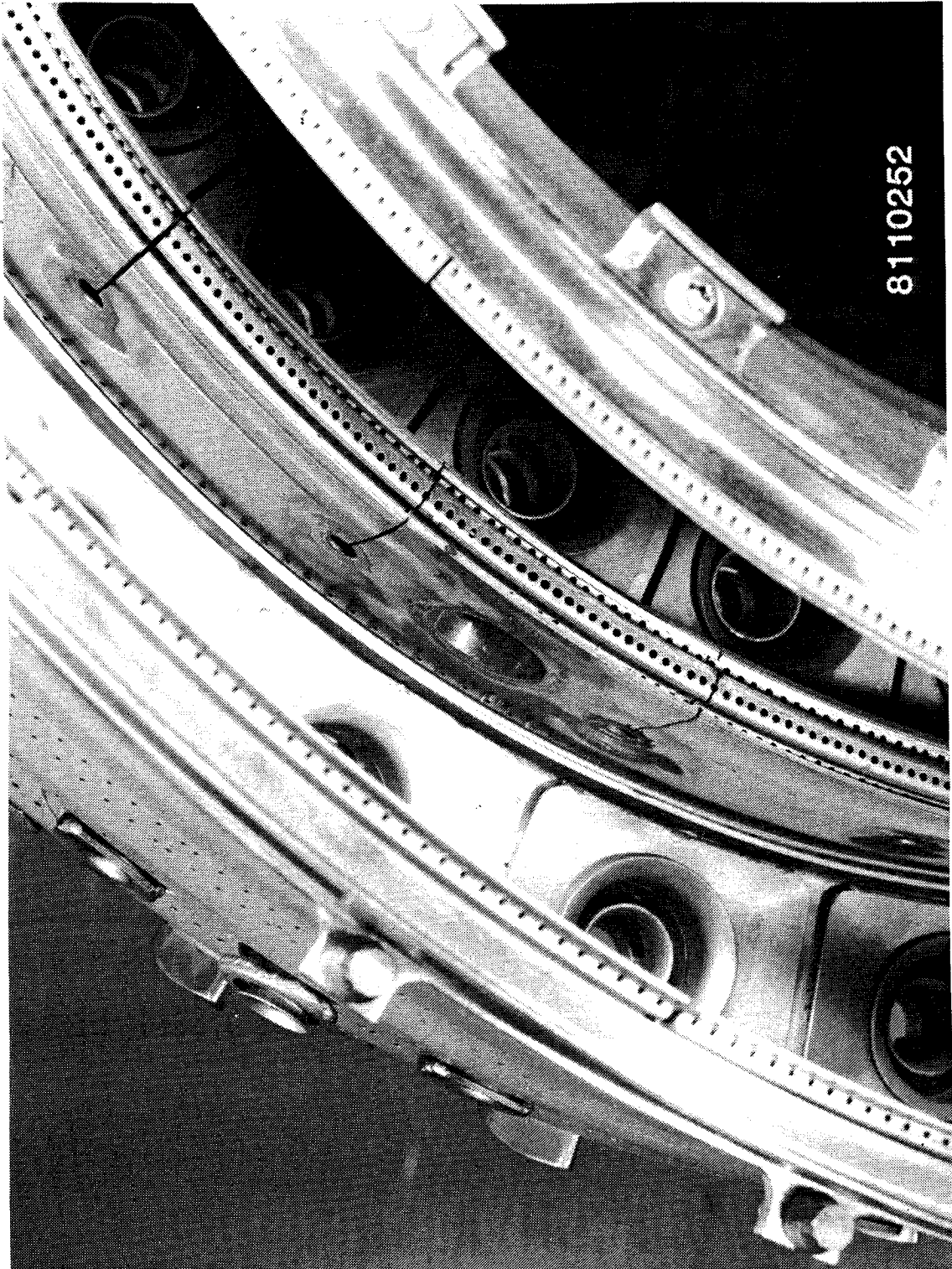
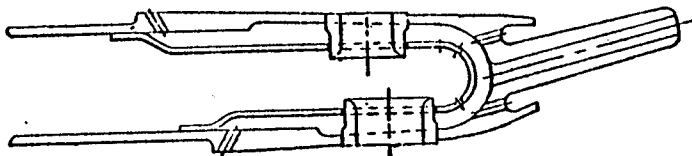
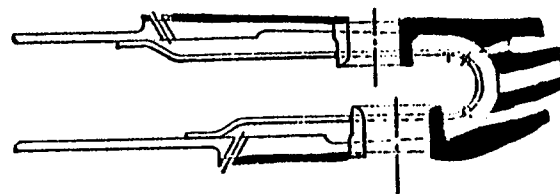


Figure 44. Detailed View of Centerbody and Domes.



Initial Design

- Uncoated Hastelloy X
- Tip First Flex
Frequency: 800 Hz
(4.0/Rev)

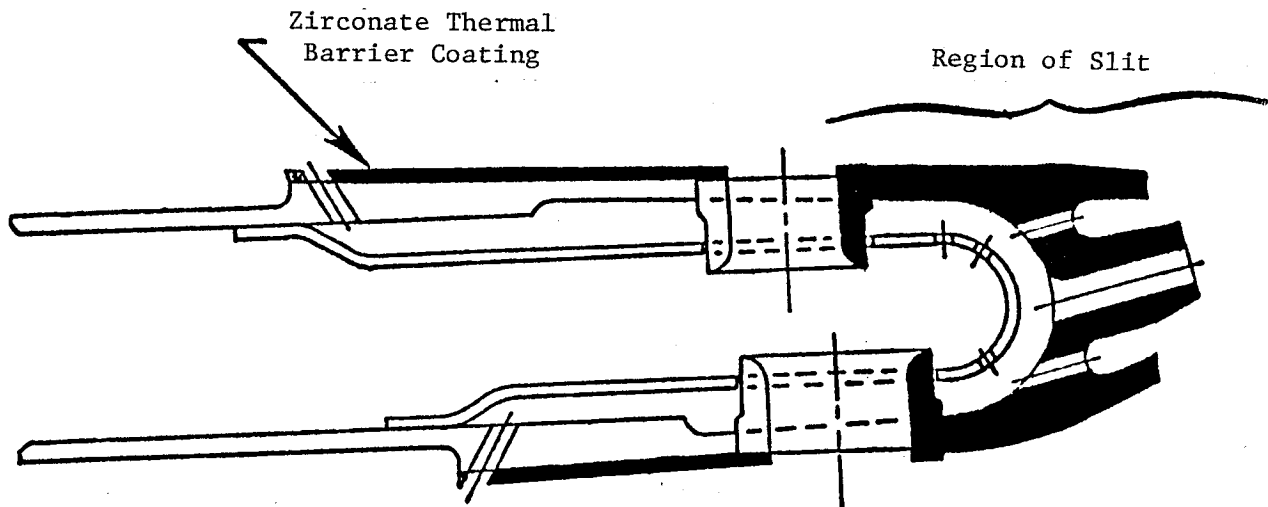


Chosen Engine Configuration

- Thermal Barrier-Coated
- Slotted Tip
- Tip First Flex Frequency: 3000 Hz
(15/Rev)

Figure 45. E³ Combustor Centerbody Design.

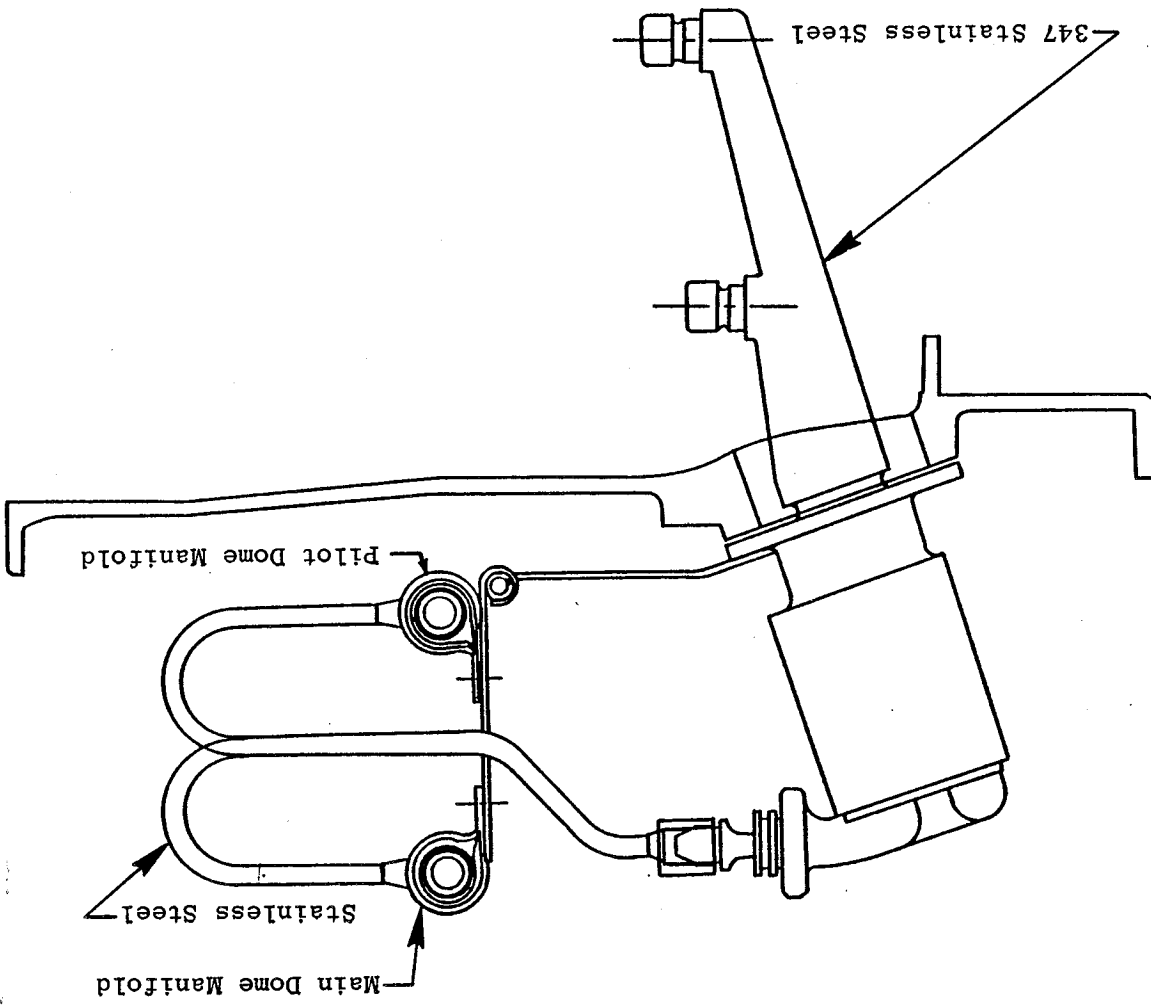
ORIGINAL PAGE IS
OF POOR QUALITY



- Brazed Construction
- Thermal Barrier-Coated
- Slit for Stress Relief
- Adequate Stiffness (3000 Hz)
- Difficult Tip Hole Drill Eliminated

Figure 46. E³ Centerbody Configuration.

Figure 47. E₃ Fuel Delivery System.



ORIGINAL PAGE IS
OF POOR QUALITY

ORIGINAL PAGE IS
OF POOR QUALITY

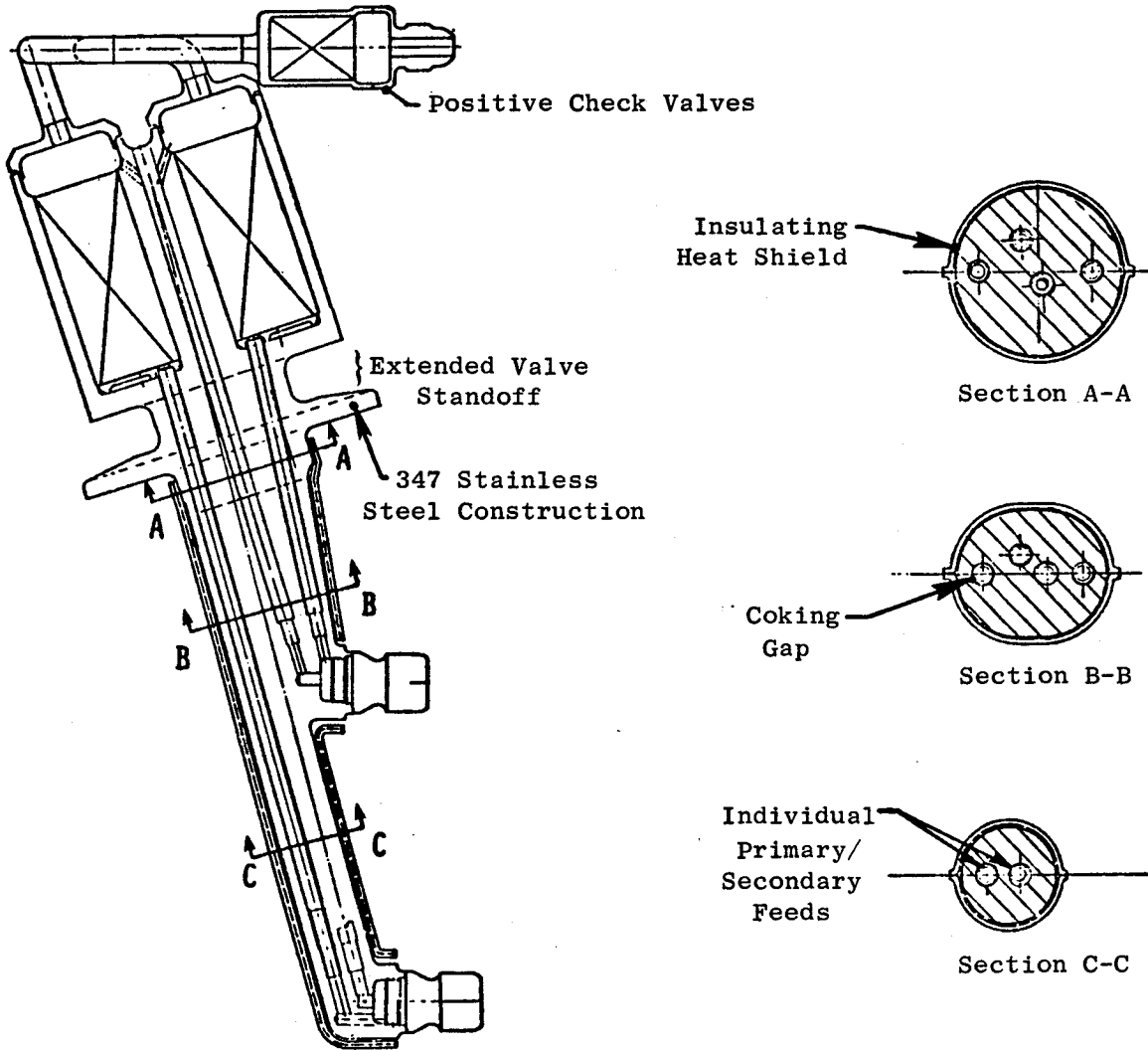


Figure 48. E³ Fuel Nozzle Mechanical Features.

ORIGINAL PAGE
BLACK AND WHITE PHOTOGRAPH

ORIGINAL PAGE IS
OF POOR QUALITY.

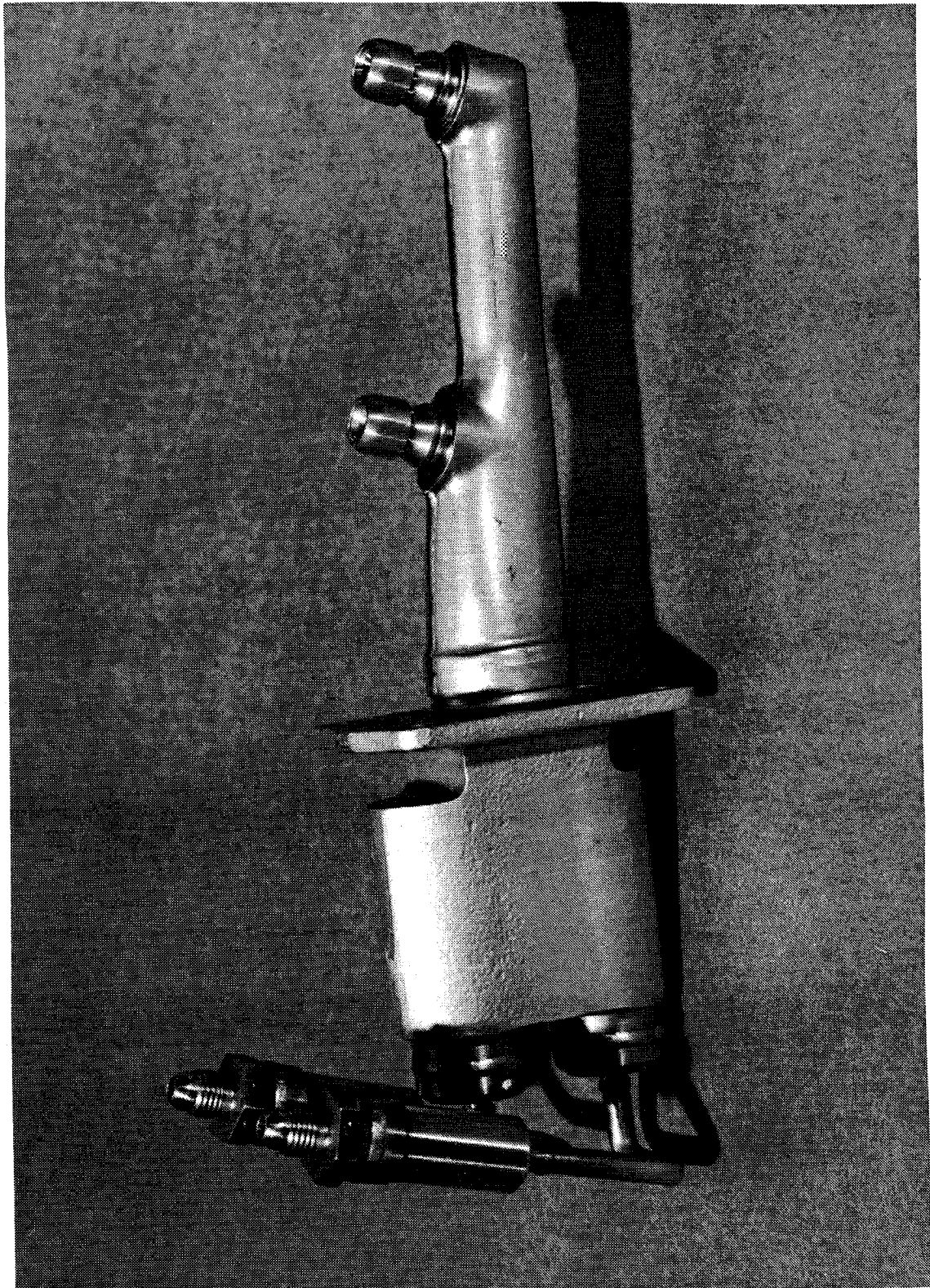


Figure 49. E³ Fuel Nozzle Assembly.



5.4 DESIGN ANALYSIS

5.4.1 Heat Transfer

5.4.1.1 General Information

5.4.1.1.1 Summary

The heat transfer design calculation procedure applied to the Energy Efficient Engine combustor liner design is presented. This procedure uses General Electric's standard design practice equations and has been successfully used in the past to analyze and design both standard convection-cooled and impingement-cooled designs. Calculations were made at various E³ cycle conditions for the liner and centerbody and the resulting temperature distributions served as input to stress analyses. Test data from the baseline development combustor were used to verify inputs in the heat transfer calculation. Typical temperature predictions are shown for the engine combustor liner design.

For a number of reasons, the final engine design has significant flow distribution differences from the original design; but since the original design had adequate calculated life margin, no reanalysis was judged to be needed for the new flow distributions, at least until after engine test data became available.

5.4.1.1.2 Introduction

Heat transfer analyses of the dome and combustor liners were required in order to establish cooling levels and to identify design changes which were needed to achieve allowable temperature levels. The allowable temperature levels were established so that the calculation of stresses and expected life of the combustor would meet design requirements. Preliminary calculations were based on one-dimensional procedures; and as the design became finalized, two-dimensional calculations were made to provide detailed temperature distributions which served as input to stress calculations. Large circumferential temperature variations exist in main combustors, usually one hot streak for each fuel injector. Procedures have been developed in the past, based on matching measured temperatures, to estimate the hot streak temperature levels.

Calculations were made to provide both maximum and nominal two-dimensional temperature distributions, thus providing the needed information for the three-dimensional circumferential effect which was input to the stress programs. The cooling flows were then adjusted, as needed, to meet the allowable temperature limits. In the case of severe hot streaks, the amount of cooling air was varied around the circumference to preferentially treat the local hot streaks and thus minimize the total amount of cooling air. Details of the calculation procedure are given below.

5.4.1.1.3 Calculation Procedure

The calculation procedure currently used follows the design calculation flow chart shown in Figure 50. Following the definition of design requirements and conceptual design, a cooling flow distribution was selected. The flow was estimated from similar or related designs. This cooling flow distribution was input to a computer program to calculate the pressure, velocity, and gas temperature distributions. This information was used to calculate the heat transfer input for one-dimensional temperature calculations. Based on these results, the cooling flow distribution was adjusted as required to achieve the desired temperature levels. As test data became available, the radiation level or film effectiveness assumptions in the calculations were adjusted as needed to match the measured temperature levels. The adjusted flow distribution and radiation or film effectiveness levels were then used to calculate two-dimensional temperature distributions which served as input to stress calculations. Figure 51 indicates how the combustor is heated by convection and radiation from the hot combustion gases. The local gas velocities and temperatures are calculated by the SODAC computer program. The combustor liner is protected by the film air introduced through the film cooling slots. The rate at which the hot combustion gases mix through this protective film has been established from both laboratory wind tunnel test data and modified by combustor experience. The convective heat transfer coefficients were calculated from correlations developed from open literature data or from wind tunnel test results for specific geometries. These correlations for heat transfer coefficients and film effectiveness were incorporated into the Steady

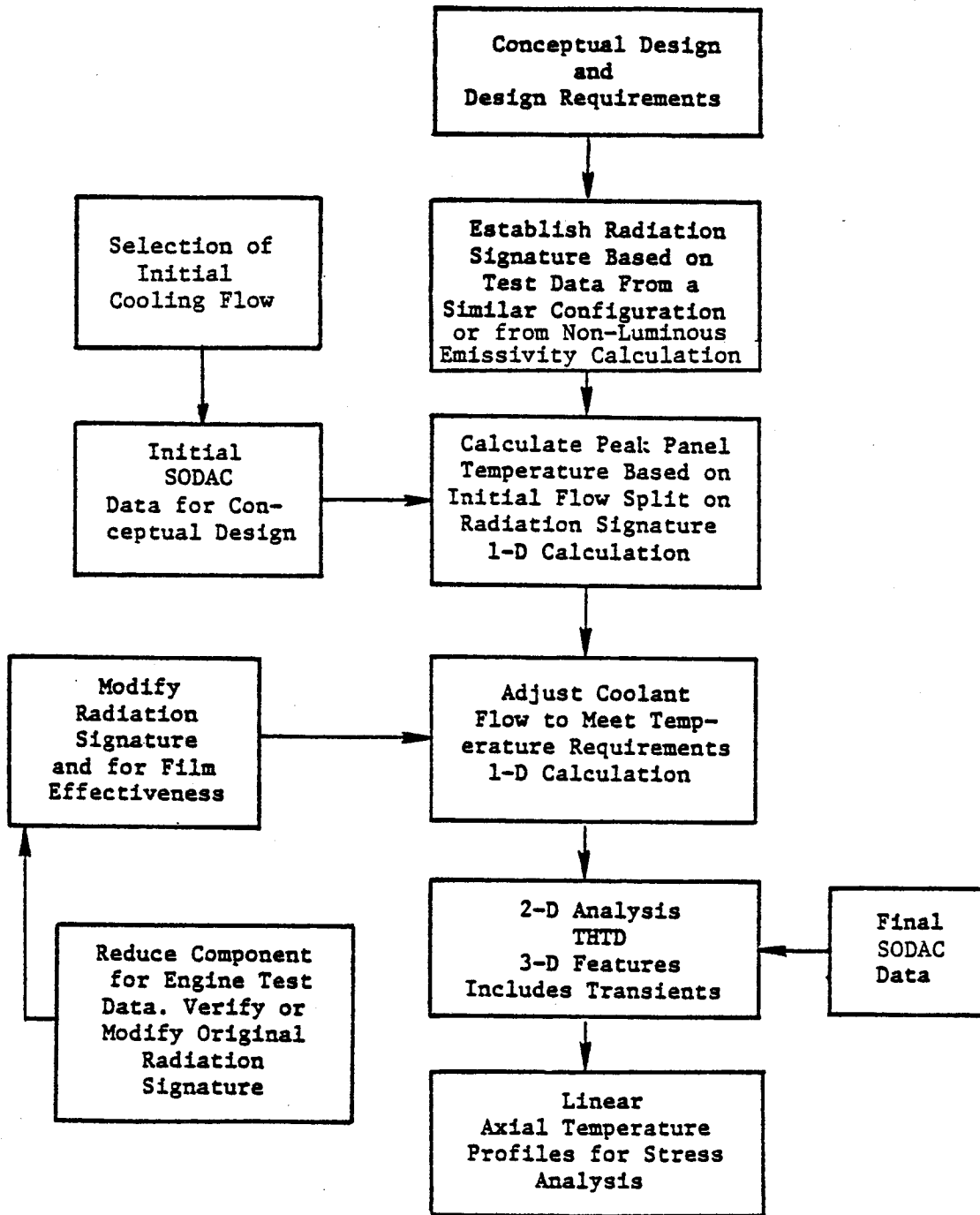


Figure 50. Design Calculation Flow Chart for Combustor Heat Transfer Analysis.

State Heat Transfer (SSHT) computer program which calculates the model geometry input for each node (Figure 51), the convective heat transfer coefficients and film temperatures, and then calculates the steady-state centroid temperatures for each node accounting for thermal conduction in this structure. The Transient Heat Transfer - Version D (THTD) computer program is another program which calculates the temperature distribution within the structure for both steady-state and transient conditions and is widely used in the General Electric Company for all types of heat transfer calculations. The flame radiation is the least well-defined term in the heat balance and is either back-calculated from measured liner temperature data or is calculated from a nonluminous flame emissivity correlation.

The initial total coolant flow and distribution can be estimated from the flow required to cool similar or related designs for similar cycle conditions. The parameter which is used was the coolant flow per unit of cooled surface area per atmosphere of combustor pressure. This guide, along with the total target coolant flow, was used to determine the initial coolant flow distribution. After the initial flow distribution has been selected, the individual panel flows were examined to ensure that the levels were not less than a lower limit which had been established to maintain a protective film over the entire panel length. The CF6-50 double-annular combustor (Reference 1) and a combustor with shingle liner construction similar to the E³ served as a guide in selecting the E³ cooling flow distribution. These two combustors were selected since the CF6-50 configuration was also a lean dome, low emission, double-annular design and the shingle liner combustor was the most recently tested impingement/film cooled design. Figure 52 shows the selected cooling flow distribution. The cooling rate comparisons with the CF6-50 combustor and the shingle liner combustor are shown in Figures 53 and 54. This distribution, selected early in the development program, was used in all of the liner heat transfer analyses. The analysis of the centerbody was conducted later in the design effort and was based on a cooling flow distribution tested in an early development configuration. This flow distribution is shown in a later section of this report.

The correlations for the heat transfer coefficients and film temperatures were programmed into the SSHT computer program which calculates and

η = Film Effectiveness

$$T_{\text{Film}} = T_{\text{Gas}} - \eta (T_{\text{Gas}} - T_{\text{Coolant}})$$

T_{Gas} = Flame Temperature

T_{Coolant} = Coolant Temperature

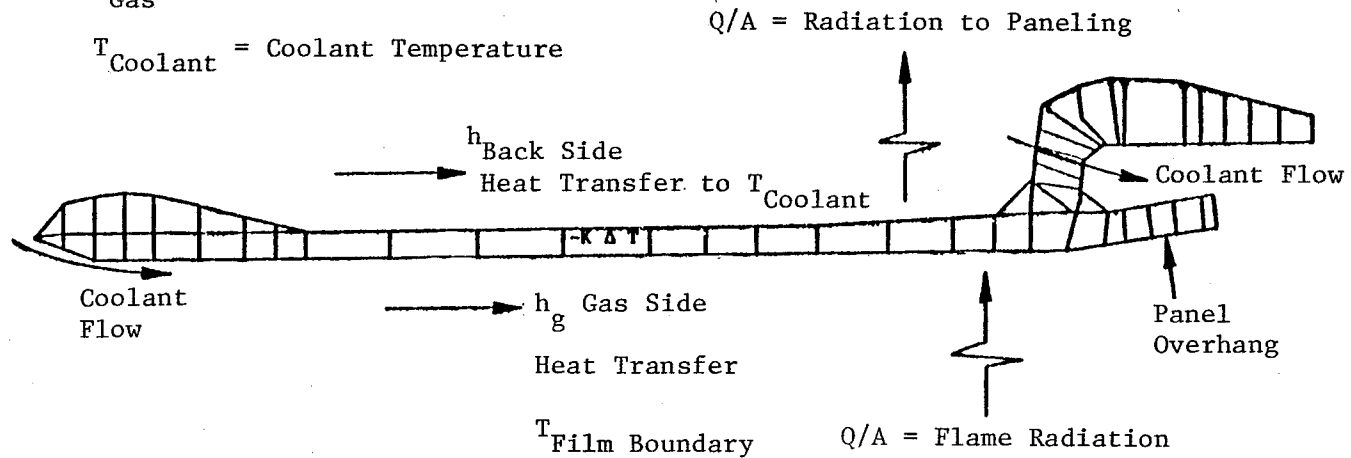
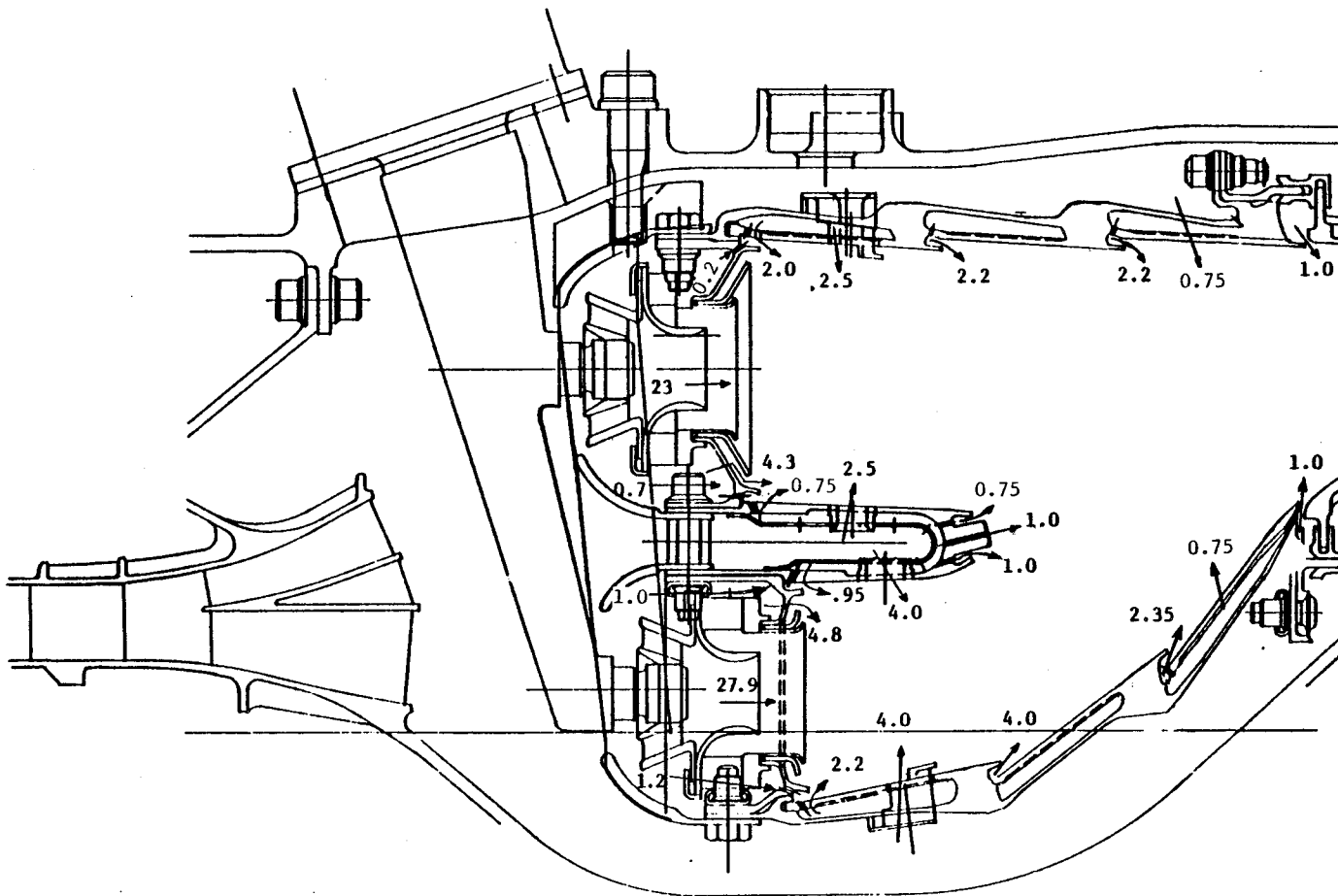


Figure 51. Node Model for a Machined Ring Combustor Showing Heat Transfer Quantities.

ORIGINAL PAGE IS
OF POOR QUALITY



All Flows in % WC

ORIGINAL PAGE IS
OF POOR QUALITY

Figure 52. Flow Distribution Used for Heat Transfer Analysis of Liners.

ORIGINAL PAGE IS
OF POOR QUALITY

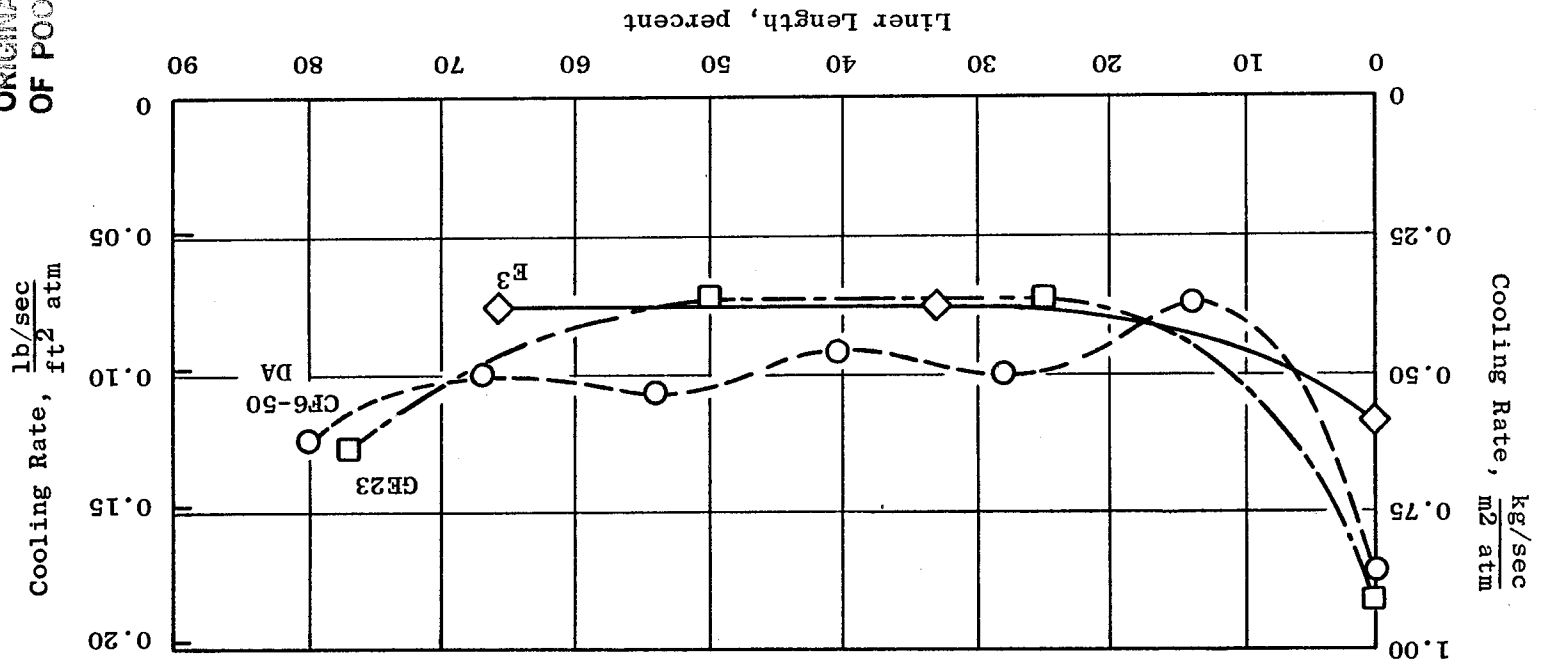


Figure 53. Comparison of Liner Cooling Rate Parameters, Outer Liners.

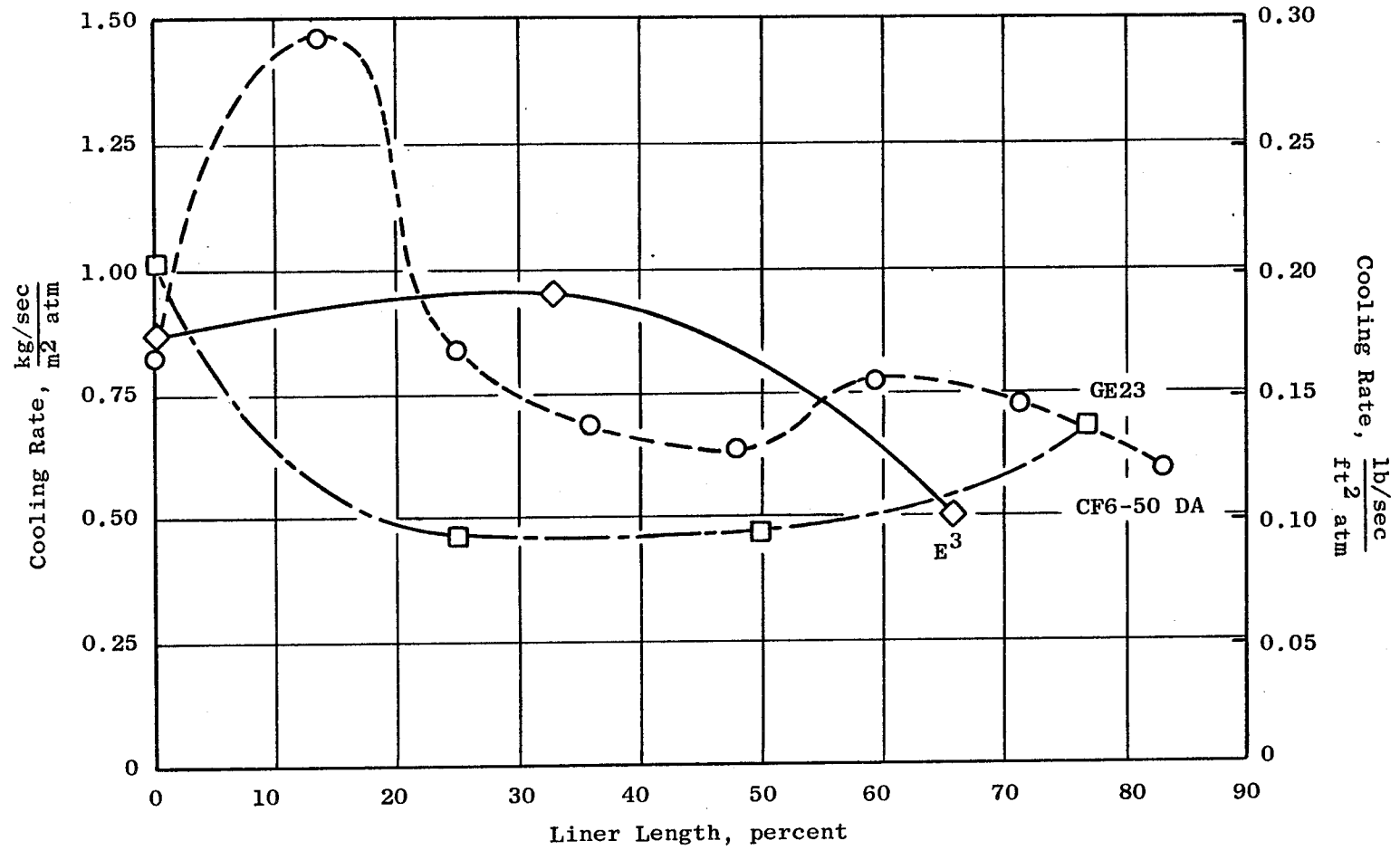


Figure 54. Comparison of Liner Cooling Rate Parameters, Inner Liners.

applies the heat transfer coefficients and boundary temperatures to each node in the heat transfer model. The program then calculates the centroid temperature for each node. The program has the capability of handling two materials; thus thermal barrier coatings can be handled in the calculation.

A flow chart of the input/output data of this program is shown in Figure 55. The first step in the procedure was to lay out the node network as shown in Figure 51 on a 10X cross section of the liner and then to digitize the coordinates. One program, the Steady-State Heat Transfer Node Hookup Generator (SSHTNHGN), prepares a node hookup file and a second program, the Node Plot Steady-State Heat Transfer (NPLTSSHT), prepares the X, Y coordinate file in an SSHT main program format. Other options are available in the NPLTSSHT program. One option prepares a plot of the coordinate data which serves as a check for possible errors in the model. Another option can increase or decrease the length of the model so that an existing model can be used where panel lengths have been changed. Next, the cycle data (flow data, gas and coolant temperature, etc.) have been changed. Then, the cycle data (flow data, gas and coolant temperature, etc.) and combustor geometry data (engine diameters, cooling metering holes sizes, film slot heights, etc.) time-sharing files were assembled. The cycle and geometry files, the node hookup file, and the X, Y coordinate files were merged to prepare a complete input file for the main program. The output from the main program was in the form of a printed copy of the input/output and a time-sharing file of the calculated centroid temperatures. The time-sharing film was input to the NPLTSSHT Program and prepared a temperature distribution plot.

5.4.1.2 Liners

The above procedure was used to calculate one-dimensional temperatures at various cycle conditions. The calculations were made very early in the program; thus component test data were not available to adjust the heat transfer input values. The CF6-50 double-annular configuration was used as a guide to adjust the heat transfer input. Based on liner temperature data matching calculations for the CF6-50 double-annular combustor, the radiation and film effectiveness levels were determined and were adjusted to the E³ cycle condition.

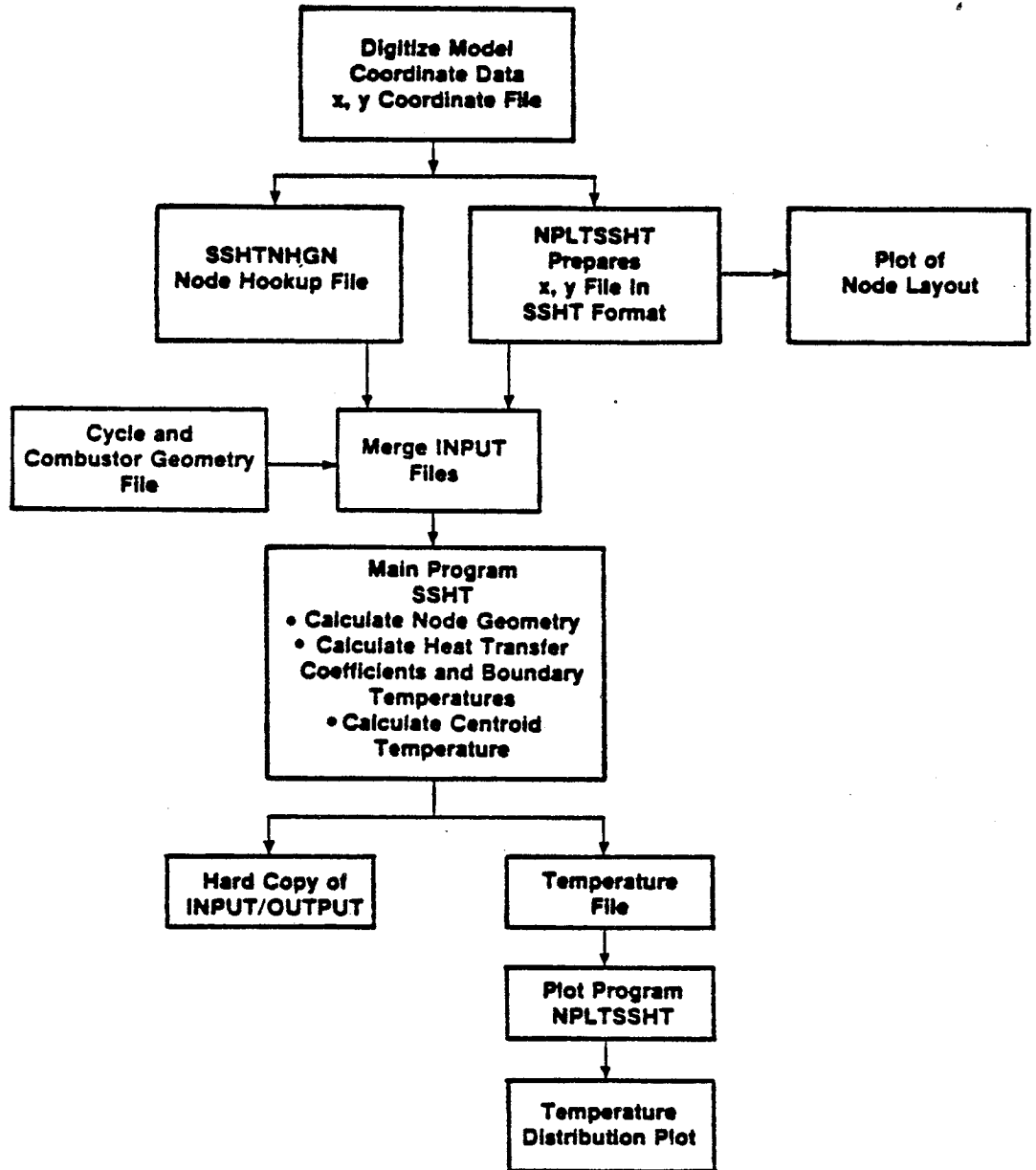


Figure 55. Heat Transfer Input/Output Data.

These input definitions were then used in all of the temperature predictions for the E³ liner design. It was determined from these calculations that the limiting panel was Panel 1 of the inner liner and that most of the two-dimensional calculations were done on this panel. A summary of the two-dimensional calculations is given in Table XVII. These calculations were made for both hot streak conditions and for nominal conditions. A typical temperature distribution curve is shown in Figure 56. The temperatures plotted in the figure are for the layer of nodes adjacent to the hot gases. The maximum temperature occurs in the region of the panel "feet" which cannot be effectively convection-cooled. Cooling in this region depends on conduction to the highly cooled overhang or to the impingement-cooled region just upstream of the foot or between the feet. These feet are not continuous in the circumferential direction but occupy about two-thirds of the circumference in the model shown in Figure 56. Impingement air is introduced between the feet to aid in cooling this region. Two three-dimensional models of the region were made in order to supply temperature distributions which could be used to optimize the foot width. One model was made in which the foot occupied two-thirds of the circumference. The foot occupied only one-third of the circumference in the second model. Both models are shown in Figure 57. The calculated temperatures for the full foot design and half-foot design are shown in Figures 58 and 59, respectively. Note that both the circumferential gradient and the absolute temperature level are reduced with the half-foot design. These temperature distributions were used in stress calculations that led to the final design, which is about one-half way between these two analyzed designs.

In addition to these detailed studies based on the original design flow distribution involving two-dimensional calculations in the shingle structure accounting for the three-dimensional hot streak pattern, one-dimensional calculations were made for the somewhat different flow distribution in the baseline development combustor. A summary is shown for takeoff conditions in Table XVIII. For a number of reasons, the final engine combustor has a still different flow distribution. However, since the baseline combustor calculated temperatures were within limits to achieve adequate life, no further reanalysis of the engine combustor heat transfer was judged to be necessary at least until after engine test data became available. It would be expected, based on

Table XVII. Summary of Two-Dimensional Temperature Calculations and Cycle Data.

	Baseline Std. Day Takeoff		Growth Approach		Growth (+27° F) Hot Day Takeoff		Growth (+63° F) Hot Day Takeoff		Growth Max. Climb		Growth 90% Takeoff Power		Growth Flight Idle	
T3 K (° R)	815 (1467)		668 (1201)		909 (1638)		922 (1660)		893 (1607)		884 (1592)		584 (1051)	
P3 MPa (psia)	3.03 (439)		1.44 (209)		3.75 (544)		3.22 (467)		3.75 (544)		3.41 (494)		0.66 (95.5)	
W _{comb} kg/s (pps)	55.3 (122)		30.7 (67.6)		65.3(144.0)		65.3 (123.8)		67.0 (147.8)		60.4 (133.2)		15.1 (33.25)	
f/a	0.024		0147		0.0282		0.0278		0.0253		0.0266		0.0127	
$\frac{W_{\text{fuel Main}}}{W_{\text{fuel Total}}}$	0.7		0		0.7		0.7		0.7		0.7		0.7	
Panel	Max.(1)	Nom.(2)	Max.	Nom	Max.	Nom	Max.	Nom	Max.	Nom	Max.	Nom	Max.	Nom
1 Outer	X	X												
2 Outer	X													
3 Outer	X	X												
1 Inner	X	X			X	X	X	X	X		X		X	
2 Inner														
3 Inner														
Centerbody Tip	X(3)		X											
<p>(1) Hot Streak Calculation (2) Average Temperature Calculation (3) Also Calculated for Component Test, T3 = 814 K (1465° F), psia, W_{comb} = 30.1 kg/s (66.3 pps) f/a = 0.0244, $\frac{W_{\text{fuel Main}}}{W_{\text{fuel Total}}} = 0.8$.</p>														

ORIGINAL PART OF POOR QUALITY

ORIGINAL PAGE IS
OF POOR QUALITY

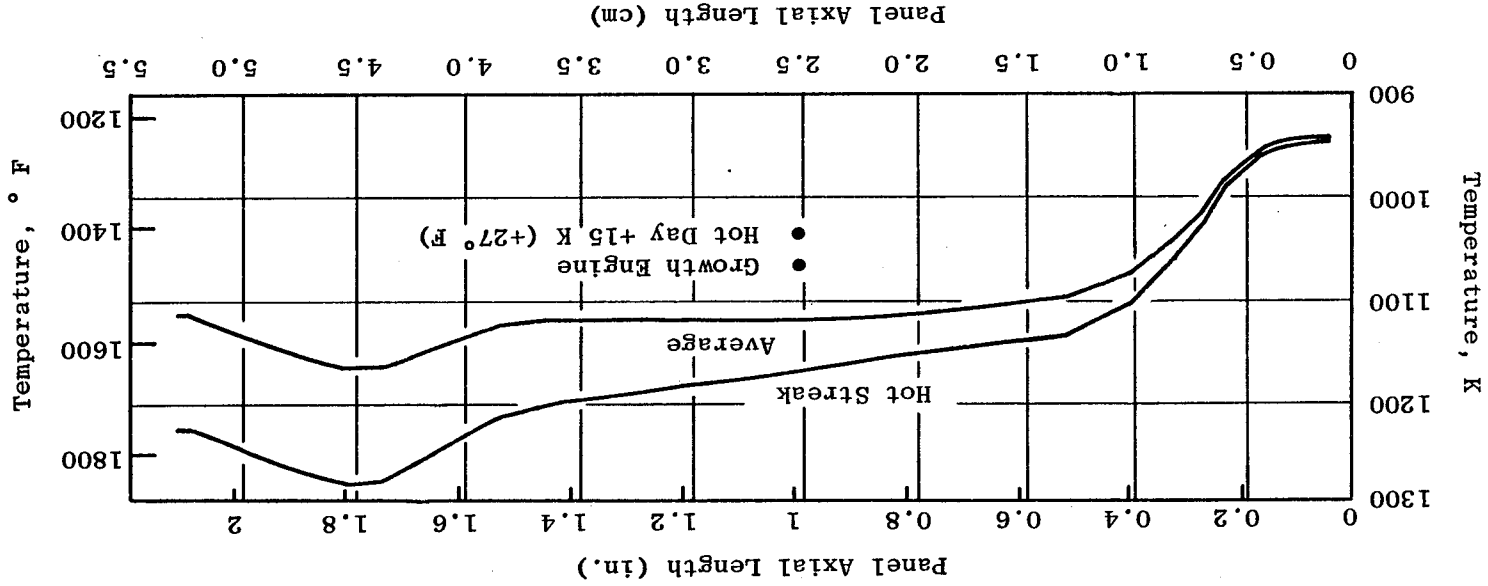
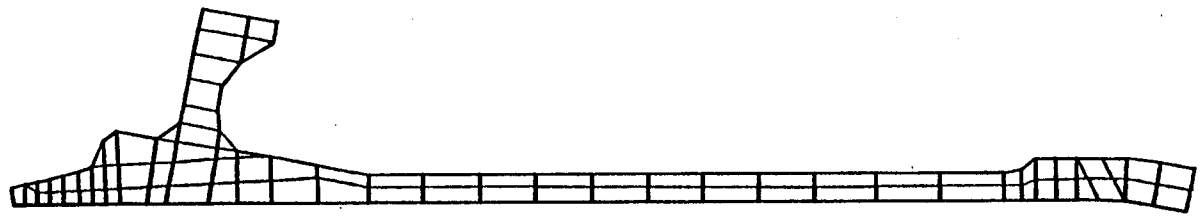


Figure 56. Panel 1 Inner Axial Temperature Profile Growth +27° F
Hot Day Takeoff.



ORIGINAL PAGE IS
OF POOR QUALITY

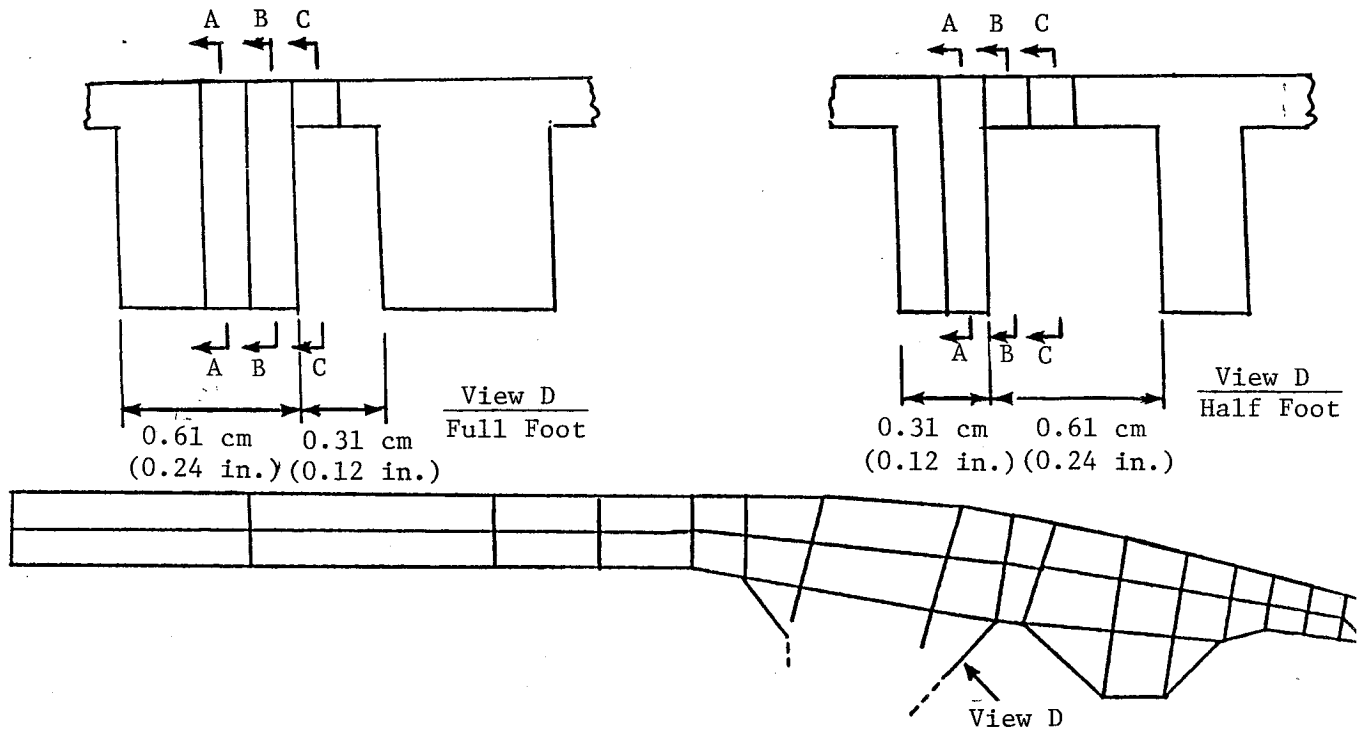


Figure 57. Three-Dimensional Model.

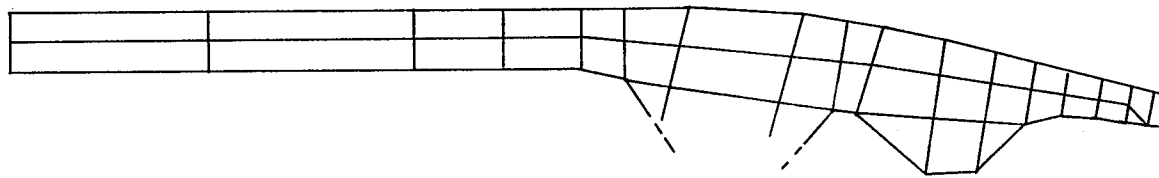
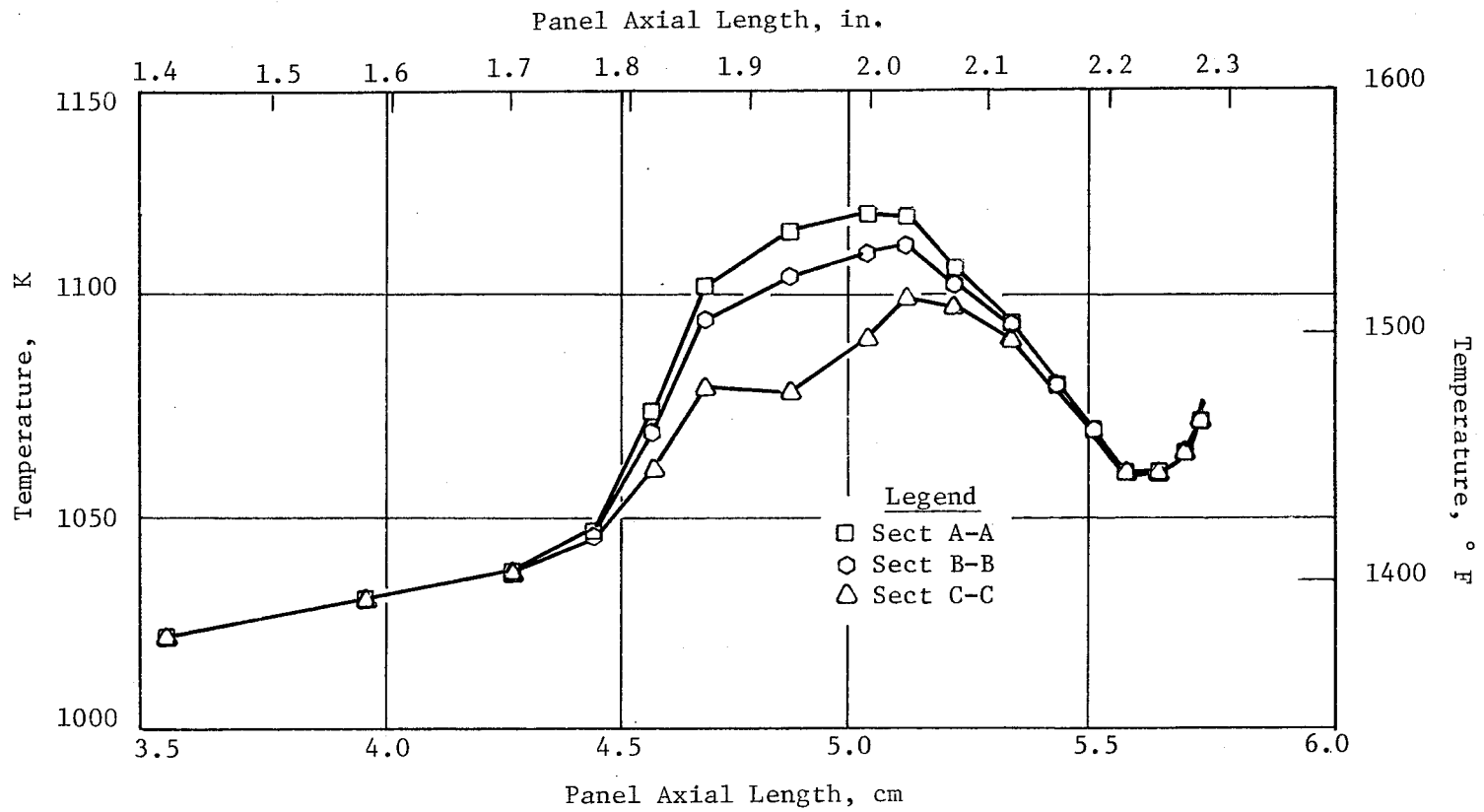


Figure 58. Three-Dimensional Temperature Profile - Full Foot Width.

ORIGINAL PAGE IS
OF POOR QUALITY

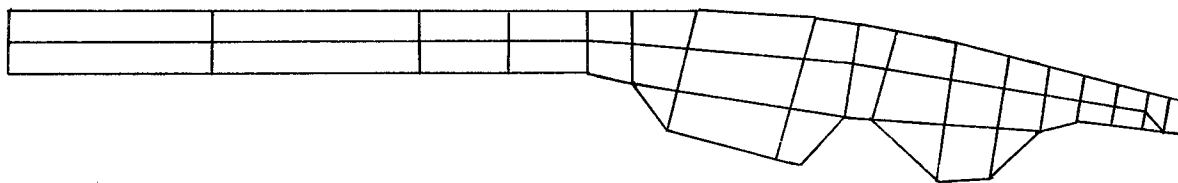
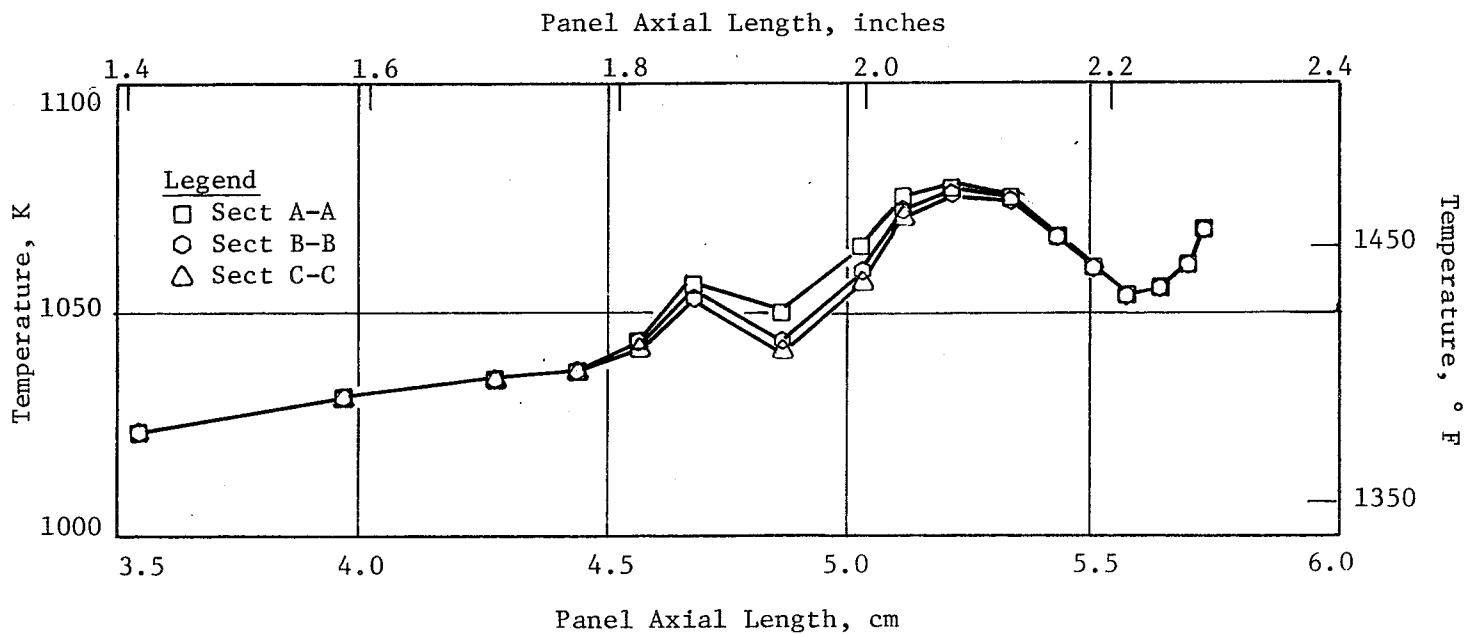


Figure 59. Three-Dimensional Temperature Profile - One-Half Foot Width.

ORIGINAL PAGE IS
OF POOR QUALITY

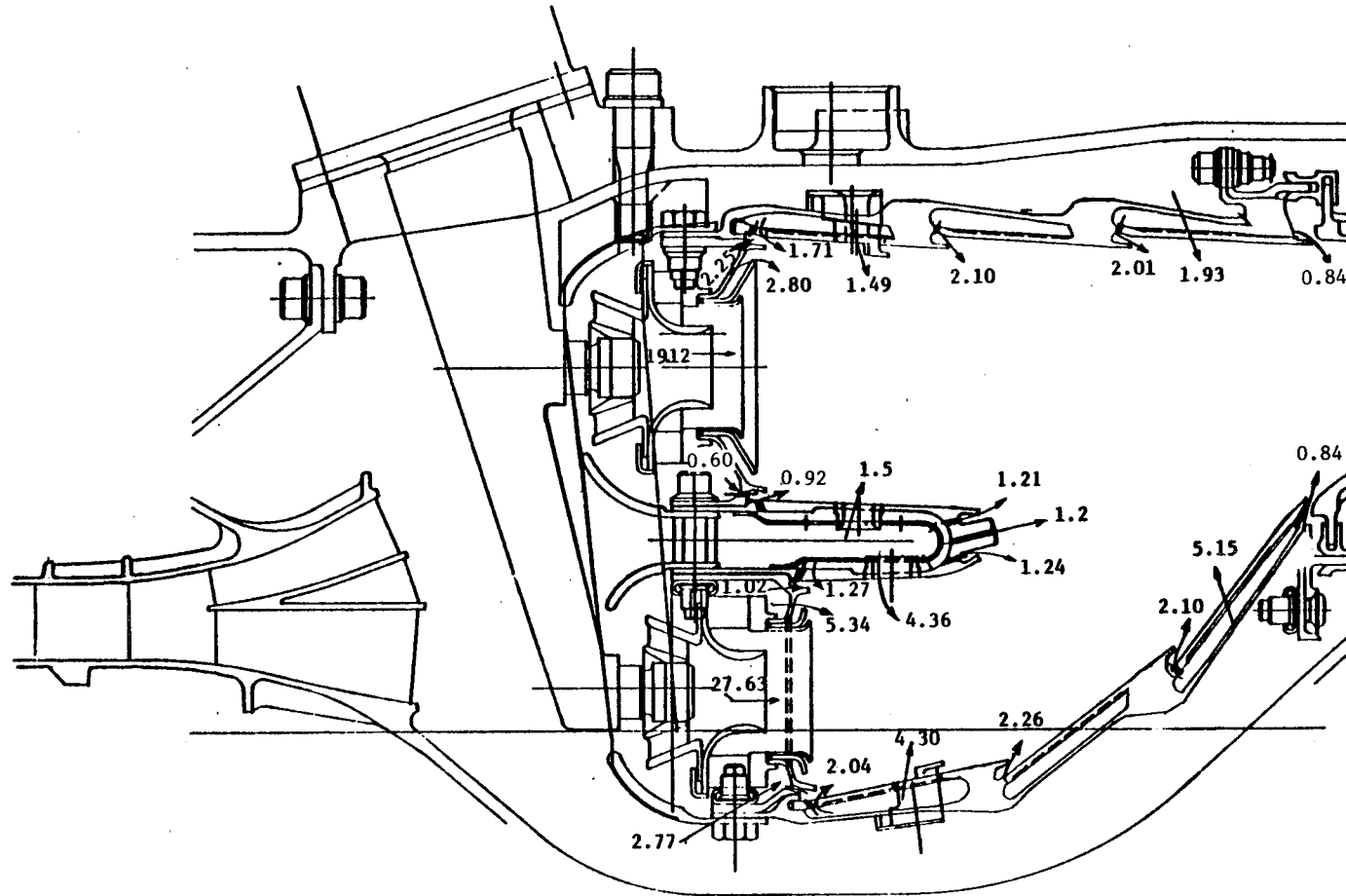
the existing analysis, that if excessive temperatures were encountered anywhere in the engine combustor, appropriate cooling flow adjustments could be made at that time.

Table XVIII. Summary of Predicted Liner Temperatures for the Baseline Development Combustor - Baseline Standard Day Takeoff.

Panel	Predicted Temperature, K (° F)
1 Outer	1090 (1501)
2 Outer	1072 (1471)
3 Outer	1039 (1410)
1 Inner	1172 (1651)
2 Inner	1131 (1576)
3 Inner	1085 (1493)

5.4.1.3 Centerbody

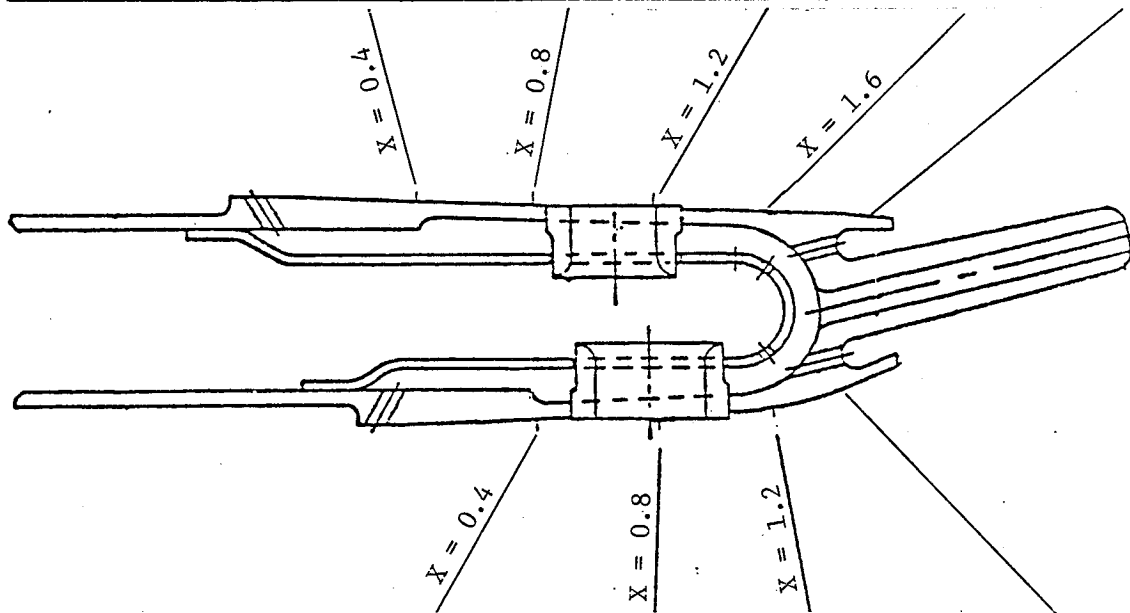
One-dimensional temperature calculations were made for the centerbody panels and two-dimensional calculations were made at two axial locations on the centerbody tip. These calculations were made using film effectiveness and radiation levels consistent with the test data from the baseline development combustor. The calculations were made for standard day takeoff conditions and main dome to total fuel flow splits of 50%, 60%, and 70%. In addition, the predictions were made for both uncoated metal and for the surface coated with 0.02 inch of thermal barrier coating. The flow distribution for these calculations was based on the development combustor Mod 1 configuration, flow split shown in Figure 60. Figures 61a and 61b show the calculated panel temperatures at several axial locations measured from the upstream overhang. The centerbody tip metal surface temperatures are shown in Figures 62a and 62b. A complete metal temperature distribution around the convective cooling hole is shown in Figure 63. These temperature distributions were used in the stress analysis of the centerbody which led to the selection of the final configuration.



ORIGINAL PAGE IS
OF POOR QUALITY

Figure 60. Flow Distribution Used in the Analysis of the Centerbody.

Pilot/Main Fuel Split	1		2		1		2		1		2	
50-50	989	947	1018	972	1034	985	1048	997	962	927		
	1034		1072		1092		1111		1043			
40-60	943	914	968	934	982	945	992	953	926	901		
	980		1009		1026		1039		988			
30-70	905	884	922	899	932	908	941	915	894	877		
	931		953		966		977		938			



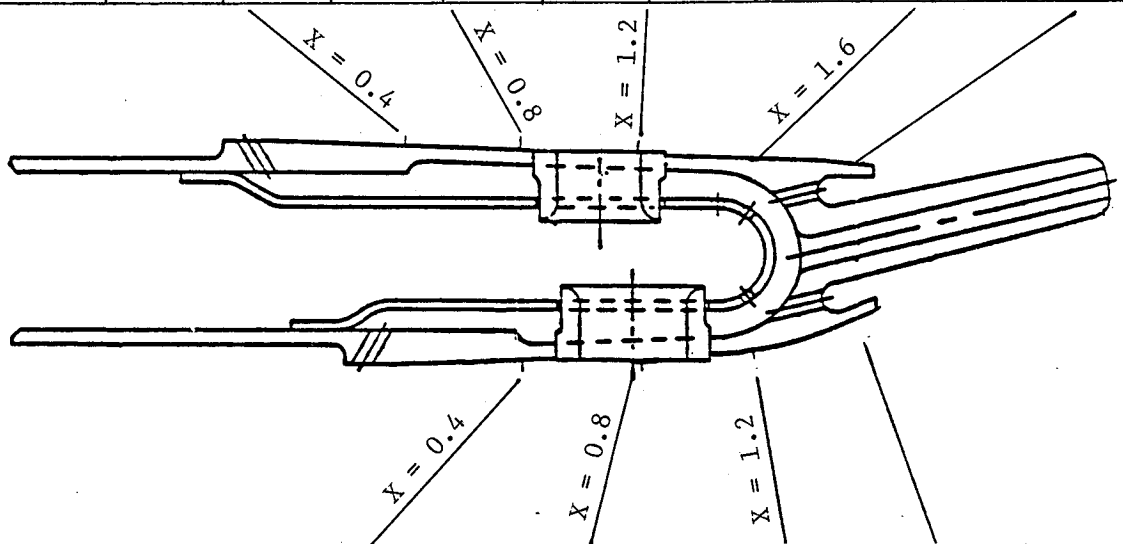
Pilot/Main Fuel Split	1		2		1		2		1		2	
50-50	971	922	1009	950	1038	973	1010	947				
	1016		1065		1103		1094					
40-60	769	942	1045	976	1084	1002	1048	973				
	1057		1112		1157		1149					
30-70	1035	965	1086	1002	1129	1033	1094	1001				
	1100		1160		1215		1207					

1 - Uncoated Cold Surface
Hot Surface

2 - 0.051 cm (0.02 in.) Thermal Barrier Coating Cold Surface

Figure 61a. Centerbody Panel Temperature - Baseline Standard Day Takeoff (K).

Pilot/Main Fuel Split	1		2		1		2		1		2	
50-50	1319 1402	1245	1372 1470	1289	1401 1506	1313	1427 1539	1334	1271 1417	1208		
40-60	1238 1305	1185	1283 1356	1221	1307 1387	1241	1325 1410	1256	1207 1318	1162		
30-70	1169 1216	1132	1200 1255	1158	1218 1279	1174	1234 1299	1188	1150 1228	1118		



Pilot/Main Fuel Split	1		2		1		2		1		2	
50-50	1288 1369	1199	1356 1457	1249	1408 1525	1291	1358 1510	1245				
40-60	1344 1442	1236	1421 1542	1296	1491 1622	1344	1426 1608	1291				
30-70	1404 1520	1277	1495 1628	1343	1573 1727	1399	1510 1713	1341				

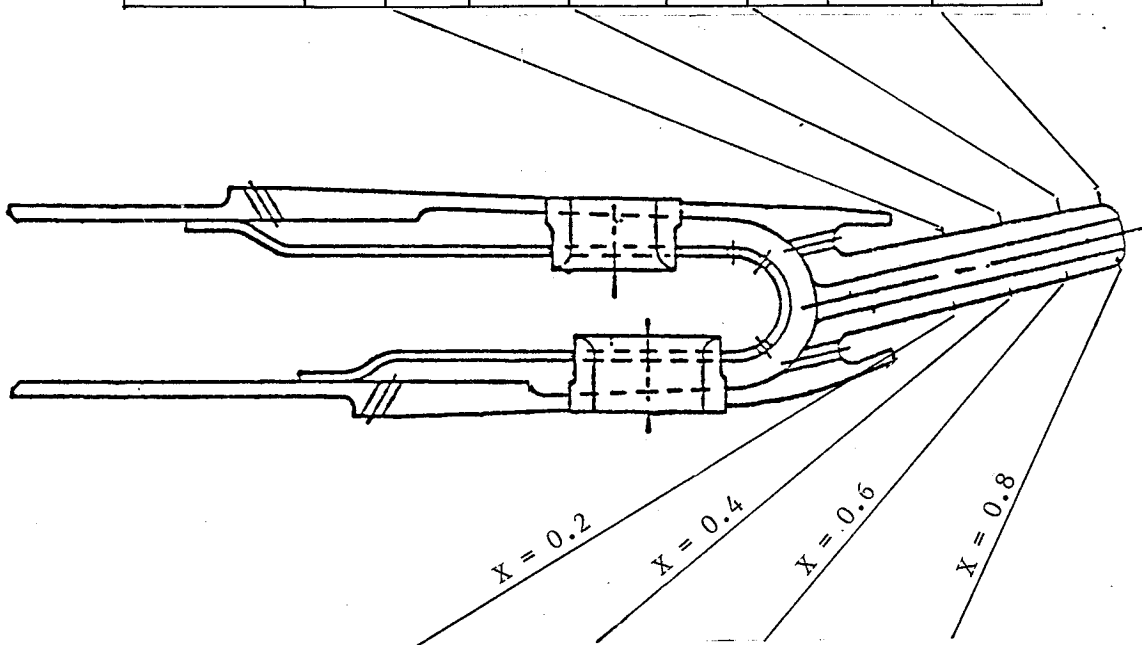
1 - Uncoated Cold Surface
Hot Surface

2 - 0.051 cm (0.02 in.) Thermal Barrier Coating Cold Surface

Figure 61b. Centerbody Panel Temperature - Baseline Standard Day Takeoff (° F).

ORIGINAL PAGE IS
OF POOR QUALITY

Pilot/Main Fuel Split			1	2			1	2
50-50			1498	1417			1595	1510
40-60			1463	1381			1569	1479
30-70			1435	1352			1550	1455



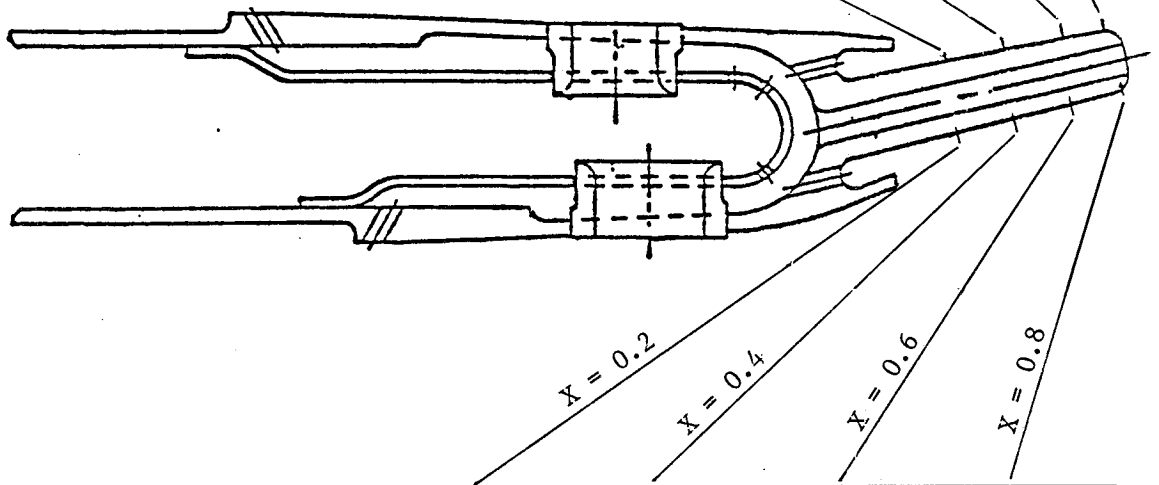
Pilot/Main Fuel Split			1	2			1	2
50-50			1502	1404			1465	1526
40-60			1544	1425			1707	1563
30-70			1588	1451			1770	1603

1 - Uncoated
2 - 0.051 cm (0.02 in.) Thermal Barrier Coating

Figure 62a. Centerbody Tip Surface Temperature - Baseline Standard Day Takeoff ($^{\circ}$ F).

ORIGINAL PAGE IS
OF POOR QUALITY

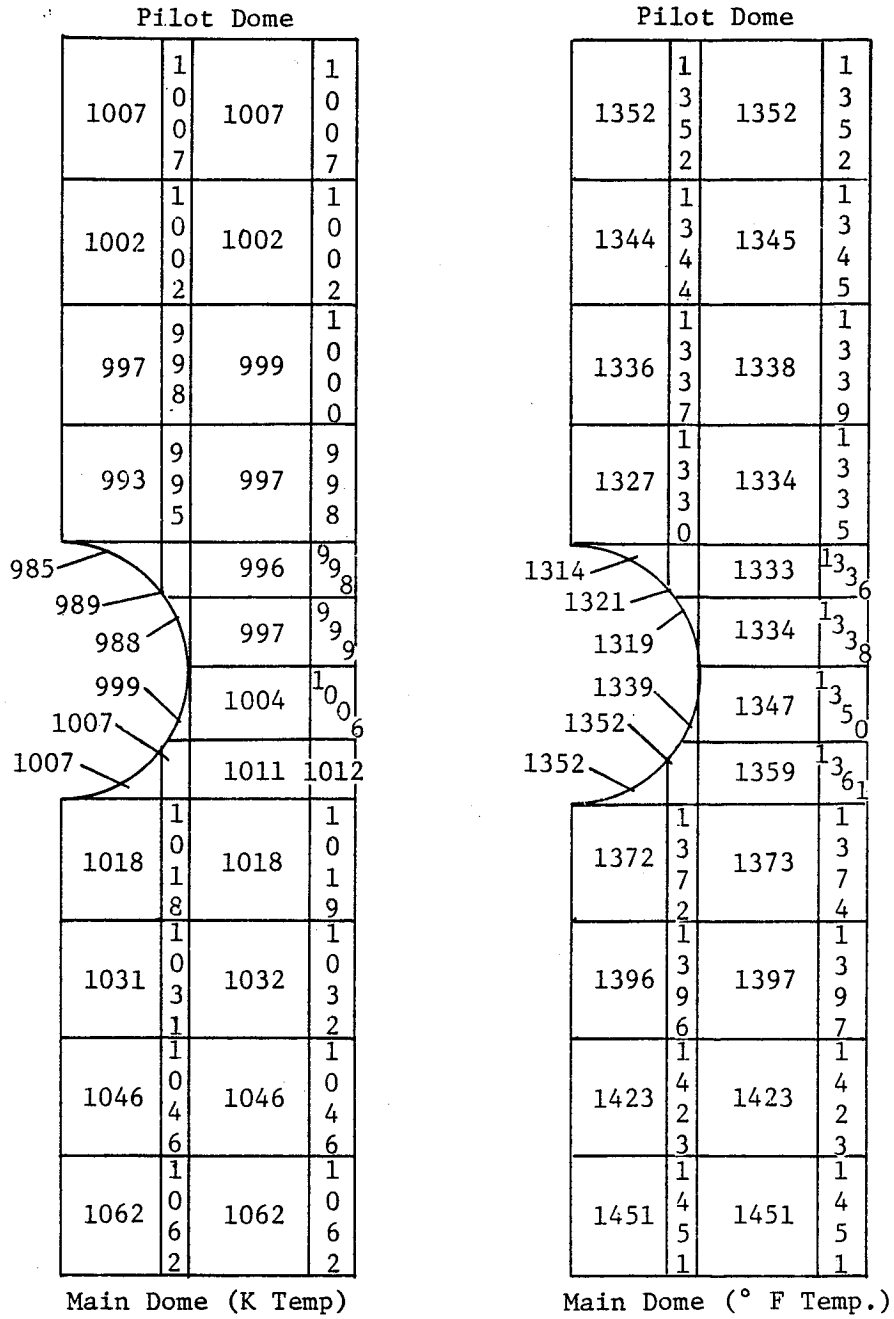
Pilot/Main Fuel Split		1	2			1	2
50-50		1088	1043			1142	1094
40-60		1068	1023			1127	1077
30-70		1053	1007			1117	1064



Pilot/Main Fuel Split		1	2			1	2
50-50		1090	1036			1069	1103
40-60		1113	1047			1204	1124
30-70		1138	1062			1239	1146

1 - Uncoated
2 - 0.051 cm (0.02 in.) Thermal Barrier Coating

Figure 62b. Centerbody Tip Surface Temperature - Baseline Standard Day Takeoff (K).



Baseline Standard Day Takeoff
 $X = 1.016 \text{ cm (0.4 in.)}$, $W_{\text{fuel}}/(\text{PILOT})/W_{\text{fuel}}(\text{TOTAL}) = 0.4$
 0.051 cm (0.02 in.) Thermal Barrier Coating

Figure 63. Centerbody Tip Metal Temperature Distribution.

5.4.1.4 Fuel Nozzle

A major design effort was directed at heat transfer analyses of the fuel nozzle designs for the core and Integrated Core Low Spool (ICLS) systems. These design studies were conducted to assure that no fuel gumming or carboning would occur during the demonstrator program which will be conducted with ambient fuel temperatures at sea level conditions. Additional studies were conducted on the Flight Propulsion System (FPS) where fuel inlet temperatures as high as 408 K (734° R) would be expected, and where the nozzles would be exposed to high heat loads with low fuel flows that exist during high altitude operation.

The heat loading conditions selected for the design of the annular test rig fuel nozzles were simulated sea level takeoff conditions. The estimated critical temperature range for incipient carbon formation is 422 to 450 K (760° to 810° R). Without any insulating features, the fuel-wetted wall temperatures of the test rig nozzle assemblies were expected to exceed 478 K (860° R). This could result in a marginal design. The wall temperatures are reduced markedly to levels well below the critical limit with the addition of insulating tubes in the fuel passages. This design feature was incorporated into the annular test rig fuel nozzle assemblies.

The core engine and ICLS fuel nozzle design was analyzed in a similar fashion. However, the core and ICLS design featured an external heat shield as well as fuel passage insulating tubes, Figure 49. The heat load conditions selected for this design study were the ICLS SLTO conditions. As expected, with ambient inlet fuel temperatures, the wall temperatures were very low. However, as shown in Figure 64, at higher fuel inlet temperatures, the wall temperatures approached the critical limit. Based on these results, a more rigorous analysis was conducted on the FPS design where more severe operating conditions might exist. The analysis indicates that the worst heating condition is near the flange where the heat shield is in contact with the stem and forms a heat conduction path. The analysis showed that the tube wall temperature can be reduced significantly if the original fuel tube insulating gap is increased from 0.02 to 0.051 cm (0.008 to 0.020 inch). As long as the duration of exposure to the maximum inlet fuel temperature of 408 K (734° R) is short, carbon buildup or fuel gumming is expected to be negligible.

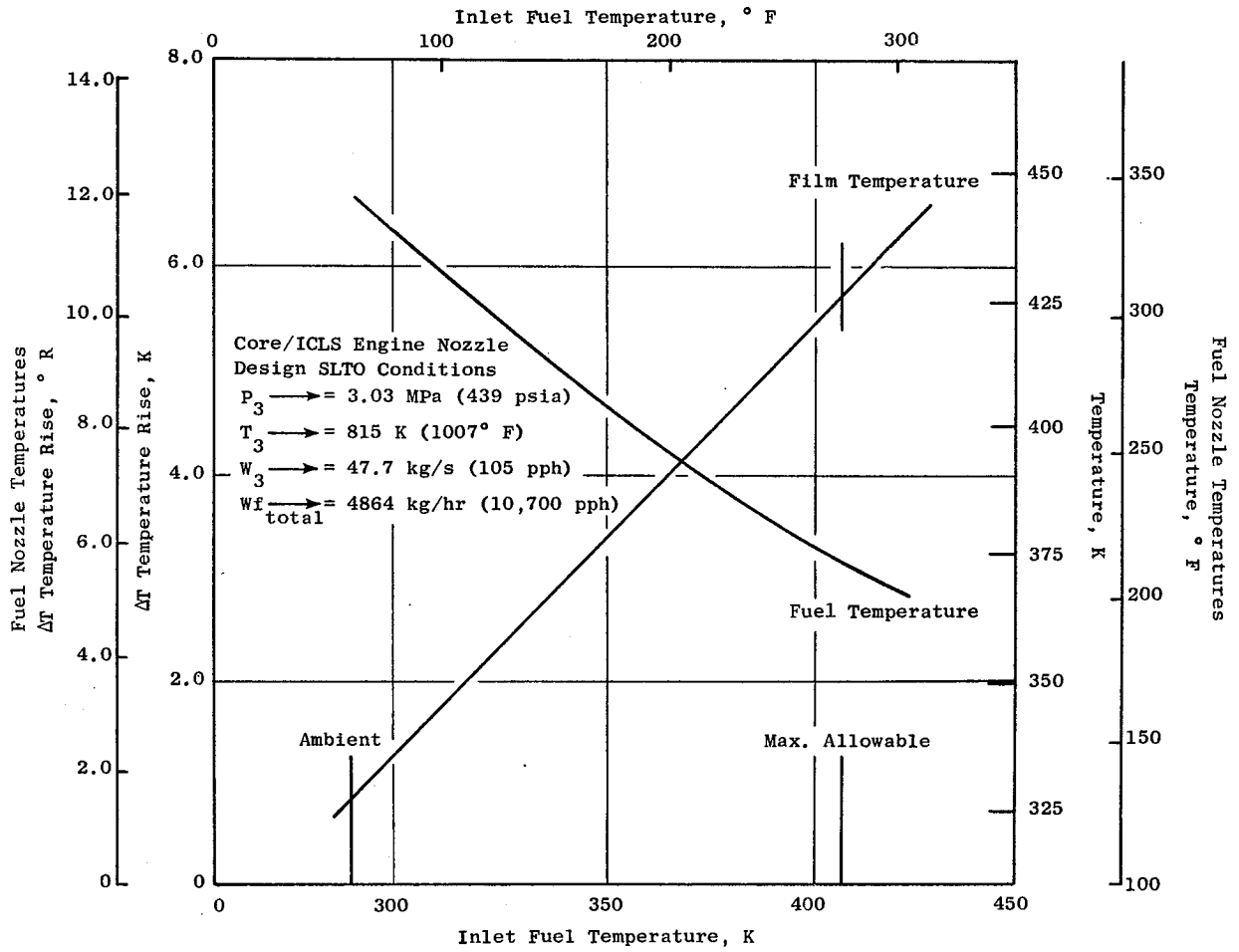


Figure 64. Effect of Inlet Fuel Temperature on Fuel Nozzle Temperatures.

5.4.1.5 Ignition System

One additional design study conducted was related to the ICLS ignition system. The mounting provisions for the ICLS ignition system require that the igniter lead be routed underneath the core cowl to connect the spark igniter to the ignition exciter box. Generally, the core cowl region is purged with fan air at about 478 K (860° R). However, a more severe condition is expected to exist on a shutdown from maximum power where casing temperatures heat the core cavity air to higher levels than the fan purge air. A transient heat transfer analysis was conducted based on measured core cavity temperature responses in a CF6-50 on shutdown from maximum power. Based on these analyses using the E³ core cavity geometry, a peak air temperature of 616 K (1109° R) would be expected during soak back. The Teflon lining of the ignition lead will withstand 700 K (1260° R) without material damage. Therefore, it was concluded that a standard lead design without auxiliary cooling would be adequate.

5.4.2 Stress and Life

5.4.2.1 Shingles

A recommended mission mix provided in E³ technical requirements is shown in Figure 65. This mission indicates engine operation at the most severe condition, hot day, on only 20% of the total flights. However, in order to provide a conservative approach to the shingle liner durability assessment, life studies evaluated cyclic life assuming constant hot day engine operation. A comparison of liner heat loads for the growth engine tropical day +15 K (27° F) and hot day +35 K (63° F) indicates that the tropical day condition is life limiting due to higher metal temperature gradients.

In order to assess shingle operating stresses, a finite element model of the shingle was constructed. The Mechanical Analysis of Space Structures (MASS) computer program was employed. Figure 66 shows the MASS model of the shingle. The model consisted of a series of curved plates and beams and accurately modeled the actual shingle casting. Only half the shingle was modeled as it is symmetric about the axial centerline. Boundary conditions on the model accurately simulate the combustor environment and structural attachment.

Life Assessment Approach
Evaluate Life at Constant
Hot Day +15 K (27° F)
Operation

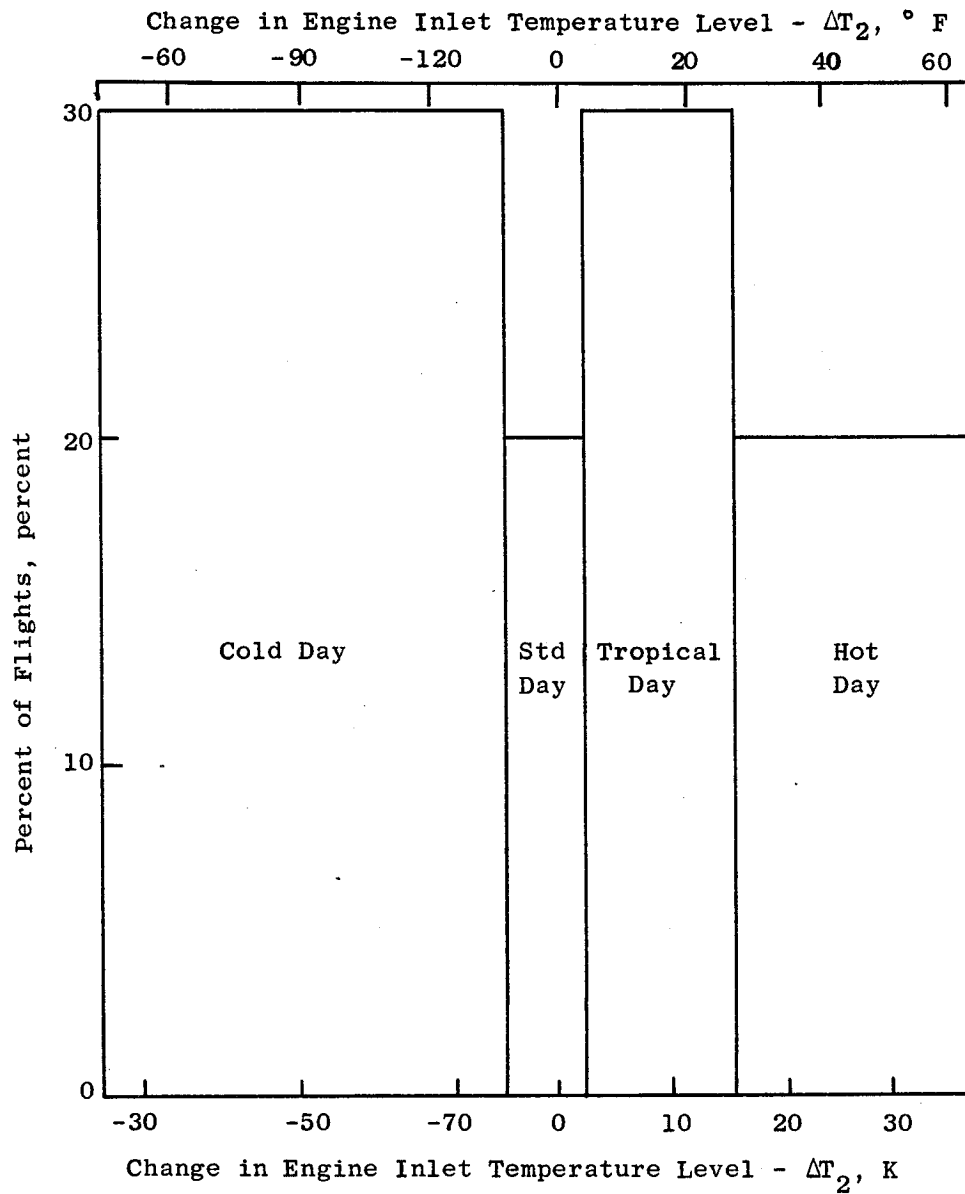


Figure 65. Recommended Mission Mix for E³.

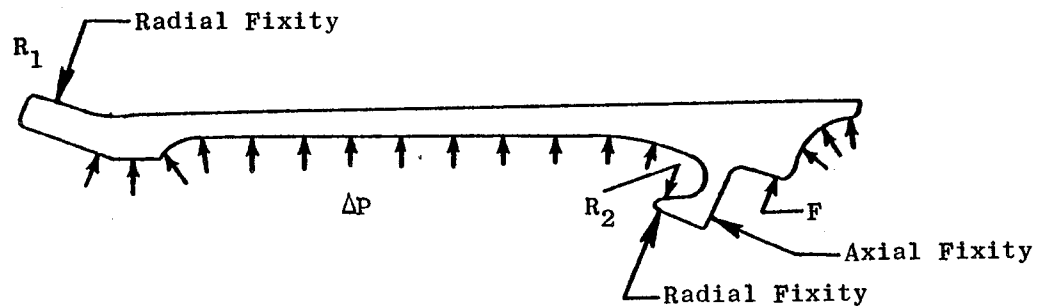
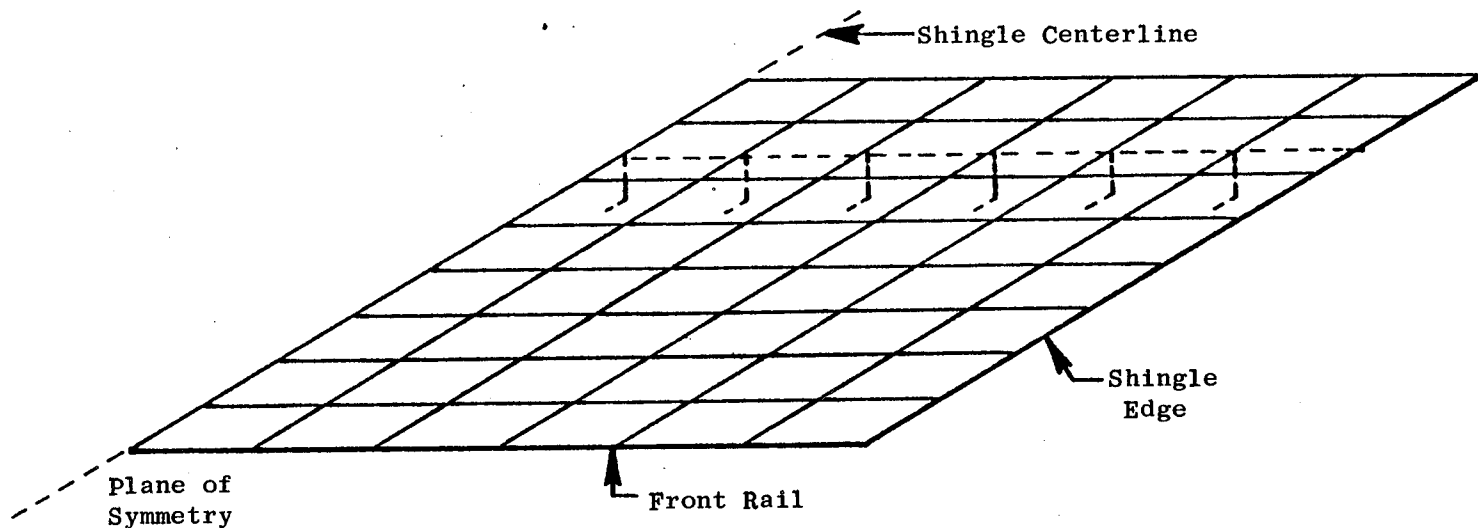


Figure 66. Shingle Structural Model.

ORIGINAL PAGE IS
OF POOR QUALITY

The MASS program is capable of calculating stress levels due to pressure, mechanical, and temperature loading.

The shingle MASS model was employed to determine shingle pressure stresses. The maximum anticipated combustor liner pressure drop was imposed across the panel. A safety factor of 1.5 was applied to account for engine surges during transient operation. As shown in Figure 67, the maximum pressure stress occurred in the support foot region of the shingle; this stress determines the ultimate rupture life of the liner.

A shingle support foot rupture life was estimated based on the foot operating stress and temperature. Increased rupture life can be obtained by increasing the shingle foot width relative to the slot between feet, by increasing foot cross-sectional area. Figure 68 shows that the chosen E^3 design meets the engine life goal with margin.

The low cycle fatigue life of the shingle was assessed at the hot day growth takeoff condition with a hot streak located at the quarter shingle position as shown in Figure 69. The hot streak was modeled as a narrow axial band. Various locations were evaluated and the quarter-shingle position produced the highest shingle stress level. Figure 70 shows the stress distribution at the hot streak location. The life-limited region of the shingle was the aft support foot region.

An estimate of cycle life was made utilizing the shingle thermal stress and operating temperature predictions. The cyclic life was estimated based on the effects of foot-width-to-slot-width-ratio and operating temperature. Cyclic life capability can be increased by opening the slot width, thereby allowing increased coolant flow introduction. However, this slot width size is limited by rupture life considerations. Adequate foot width must be maintained to provide sufficient rupture life as shown in the prior rupture analysis. As shown in Figure 71, the chosen shingle configuration provides adequate fatigue life. For constant hot day operation, degraded material properties, and hold time effects included, the shingle design meets the life goal with margin.

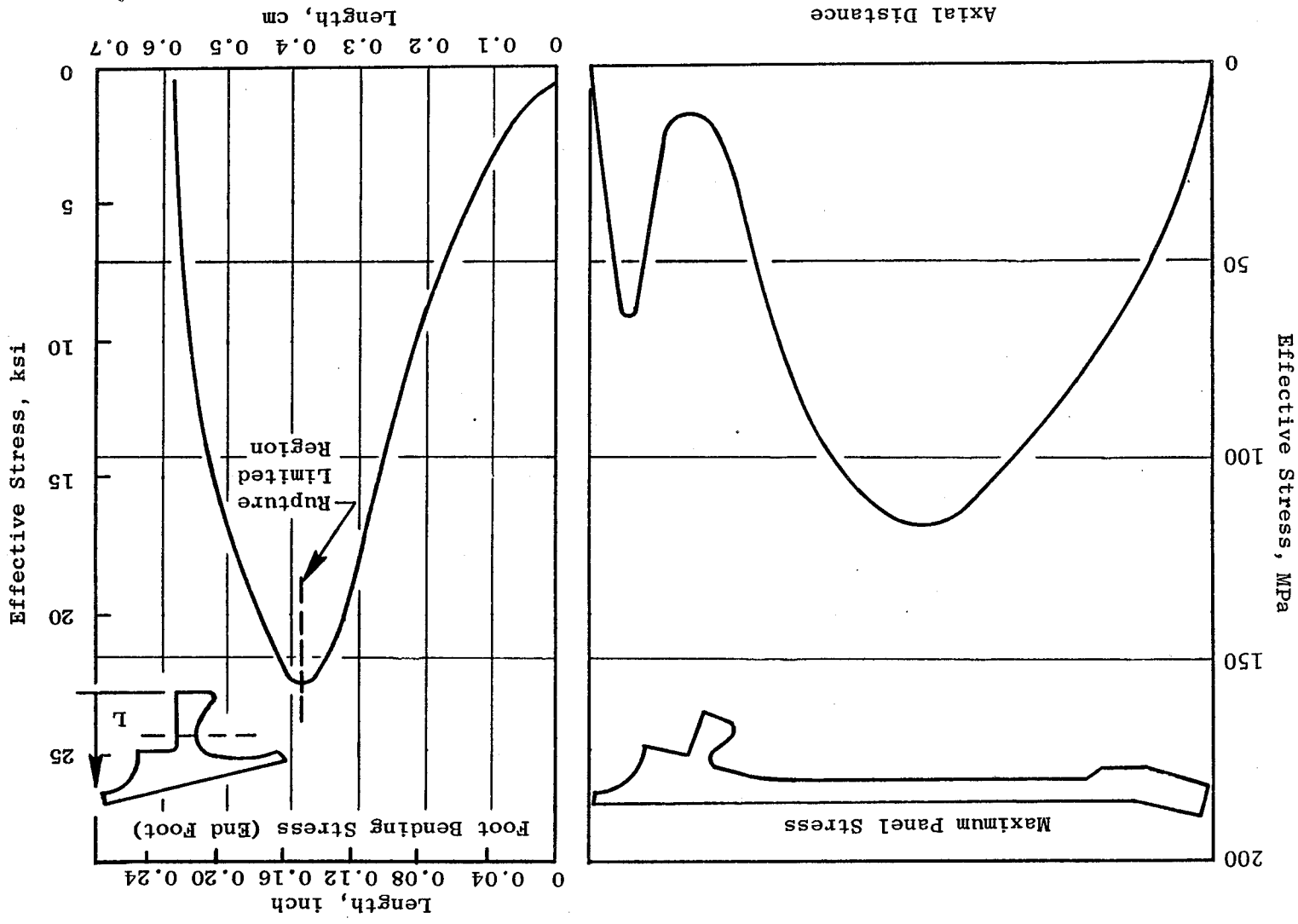


Figure 67. Analytically Predicted Pressure Stresses for Shingle.

ORIGINAL PAGE IS
OF POOR QUALITY

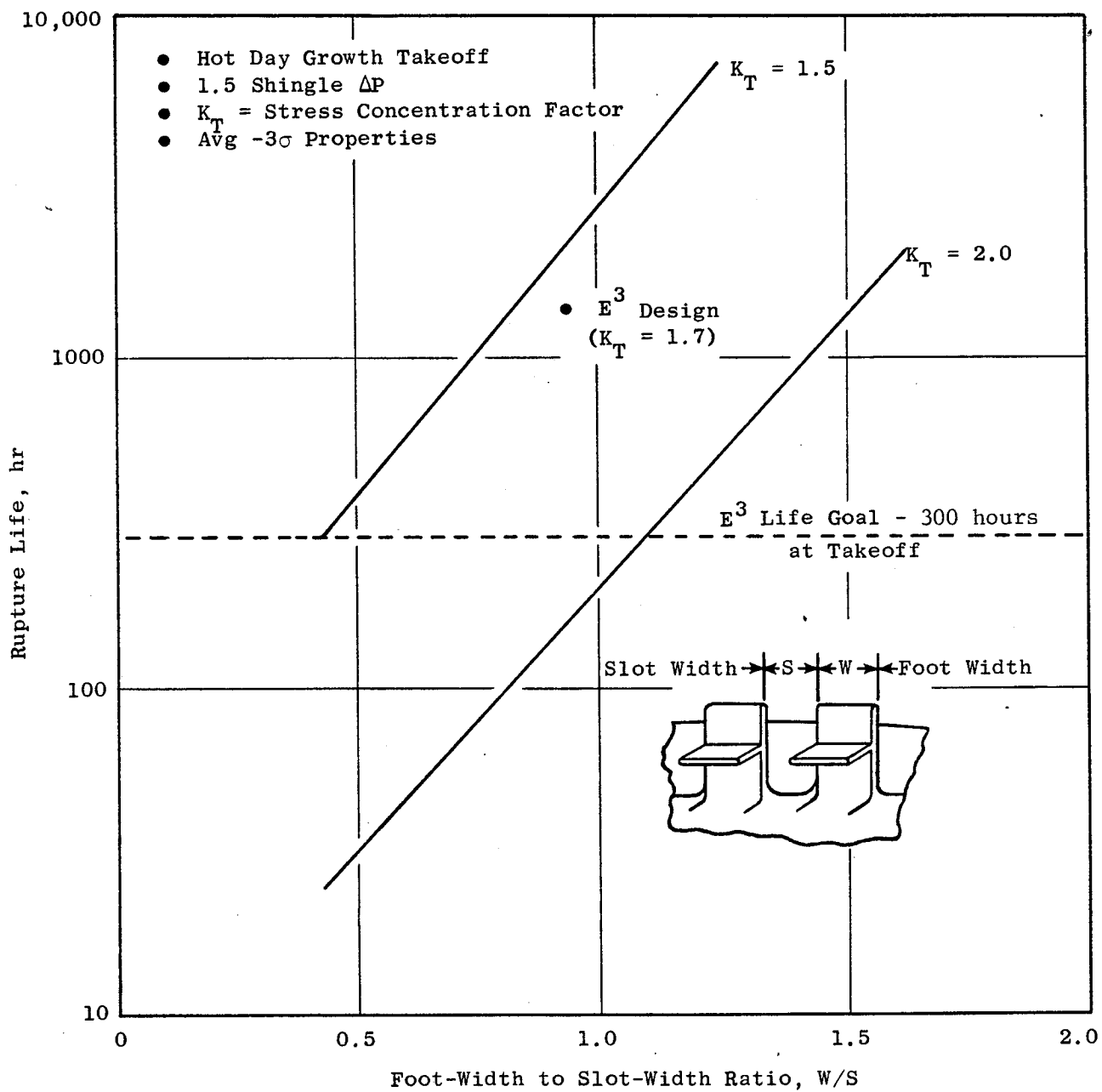


Figure 68. Shingle Foot Size Versus Rupture Life Capability.

ORIGINAL PAGE IS
OF POOR QUALITY

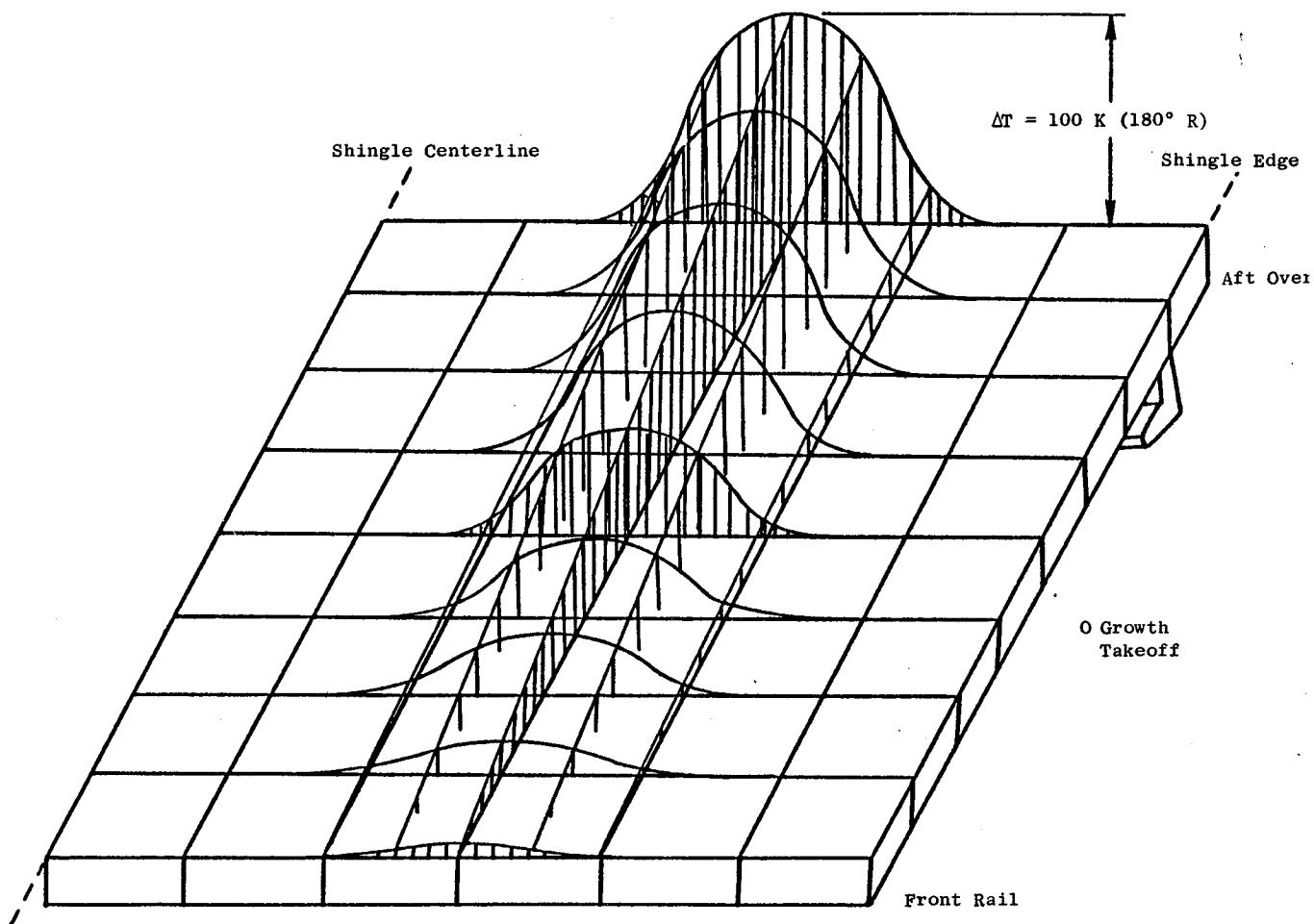


Figure 69. Shingle Low Cycle Fatigue Model Temperature Distribution.

ORIGINAL PAGE IS
OF POOR QUALITY.

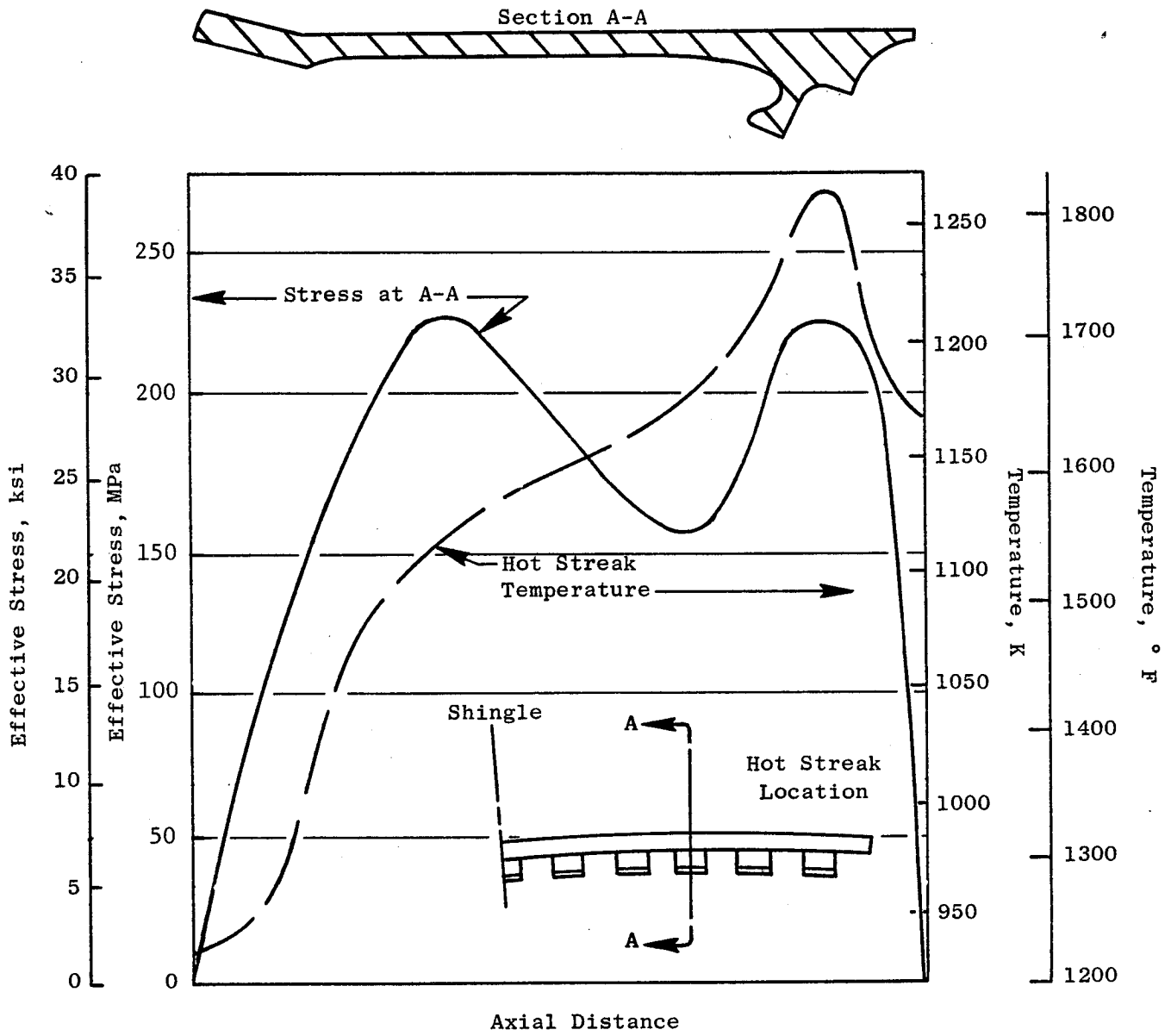


Figure 70. Analytically Predicted Shingle Stress in Hot Streak.

ORIGINAL PAGE IS
OF POOR QUALITY.

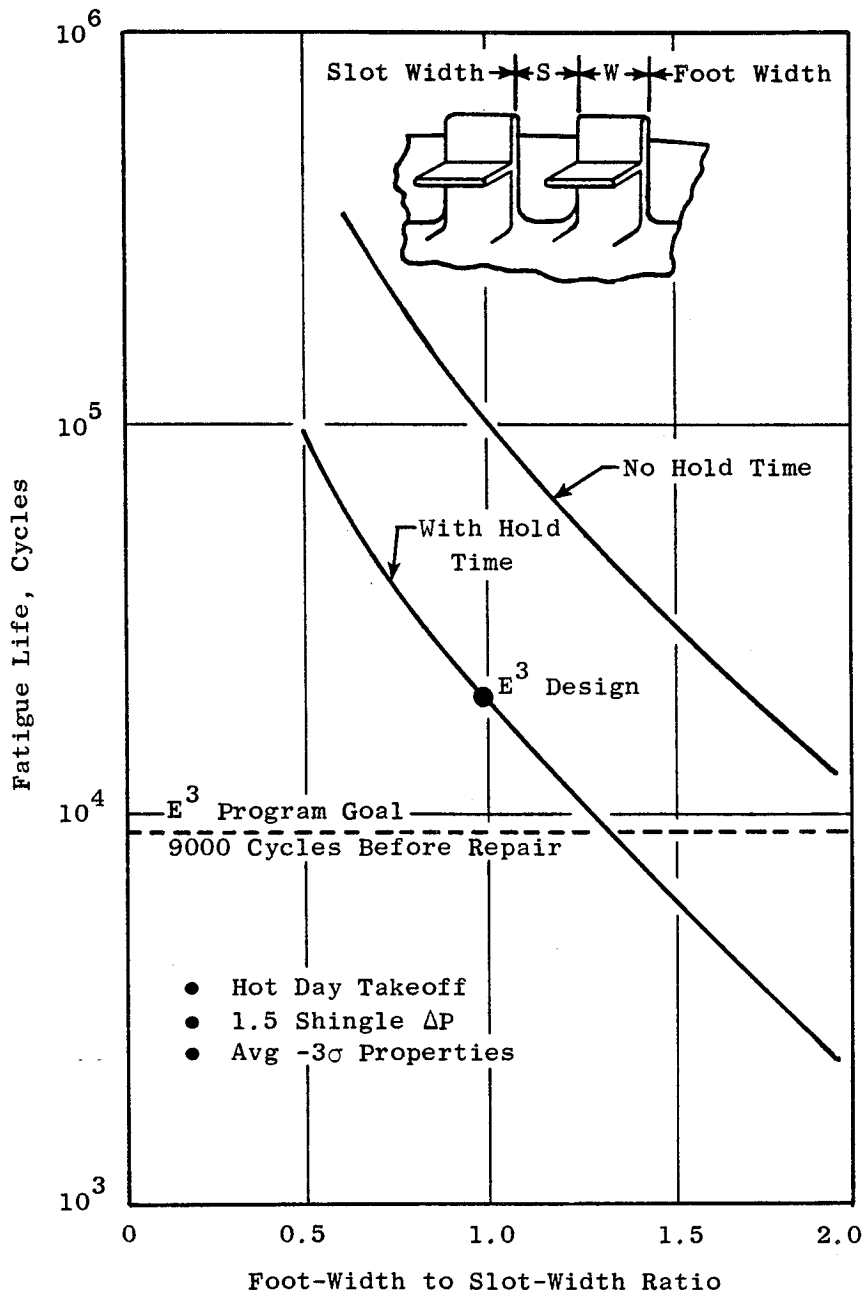


Figure 71. E³ Combustor Shingle Predicted LCF Life.

The shingle cyclic life capability is very sensitive to operating temperature. A moderate increase in shingle temperature results in a significant loss in cyclic life capability. If shingle temperature predictions are exceeded during actual engine operation, then liner cooling distributions would be adjusted to ensure adequate component life.

Table XIX shows a comparison of the predicted shingle life capability to the program design goals. Adequate rupture and fatigue life are provided with the chosen design. The growth engine combustor would utilize Mar-M-509 as the cast shingle alloy to meet the cyclic life requirement.

Table XIX. E³ Combustor Shingle Predicted Life Levels.

	Low Cycle Fatigue Life (Hold Time Effects Included)	Rupture Life, Hours (Stress Concentration Effects Included)
E ³ Goal	9,000	300
Baseline Engine - X-40 Shingle [T _{max} = 1111 K (1540° F)]	105	5000
Growth Engine - Mar-M-509 Shingle [T _{max} = 1283 K (1850° F)]	26,000	1000

5.4.2.2 Support Liners

The combustor support liners were analyzed using CLASS-MASS and Buckling of Shells of Revolution (BOSOR) computer programs. The CLASS-MASS model was used to predict the stress levels due to pressure, mechanical, and temperature loadings. The BOSOR model was used to identify critical buckling pressures and mode shapes of the outer liner. Adjustments were made to the critical buckling pressure level to allow for out-of-roundness effects.

The CLASS-MASS analysis of the shingle support liners was conducted to assess the operating stress levels at the most adverse operating conditions.

The models simulated the growth engine maximum pressure conditions and the actual structural attachment boundary conditions. The effective stress distributions for the outer and inner support liners are shown in Figures 72 and 73, respectively.

An important design consideration in the liner design is the buckling capability of the outer liner. The liner shell is subjected to the buckling loads resulting from the combustor pressure drop. The E³ design was analyzed using the model shown in Figure 74. Various liner thicknesses were evaluated over a range of 0.76 to 1.27 mm (0.038 to 0.050 inch) thick. The buckling analysis utilized the maximum growth engine pressure drop condition.

The critical pressure drop across the outer liner which produces buckling of the shell is dependent on several factors: the end fixity of the shell, the thickness of the shell, the number of nodes of the deflected structure, and the roundness of the initial structure. Figure 75 shows that for a round structure with a thickness of 1.02 mm (0.04 inch) a minimum critical pressure of approximately 1.24 MPa (180 psi) is indicated. This pressure is well above the anticipated operating pressure drop of the liner. However, when the liner out-of-roundness effects are considered, the margin of safety is reduced. Figure 76 shows the effect of out-of-roundness on the buckling characteristics. The chosen E³ liner thickness and radial concentricity requirements provide a 2X safety margin at maximum growth engine operation.

5.4.2.3 Casing

The combustor casing was analyzed using the CLASS-MASS computer program. Figure 77 shows the stress levels of the casing at the growth engine maximum pressure loading conditions. In this analysis, the casing temperature is assumed fairly uniform and slightly less than compressor discharge temperature. The casing thickness was chosen so that the maximum stress levels would be 50% yield strength of the casing material.

5.4.2.4 Centerbody

Figure 78 shows the results of the centerbody life analysis. A comparison was made between different centerbody configurations to determine the

ORIGINAL PAGE IS
OF POOR QUALITY

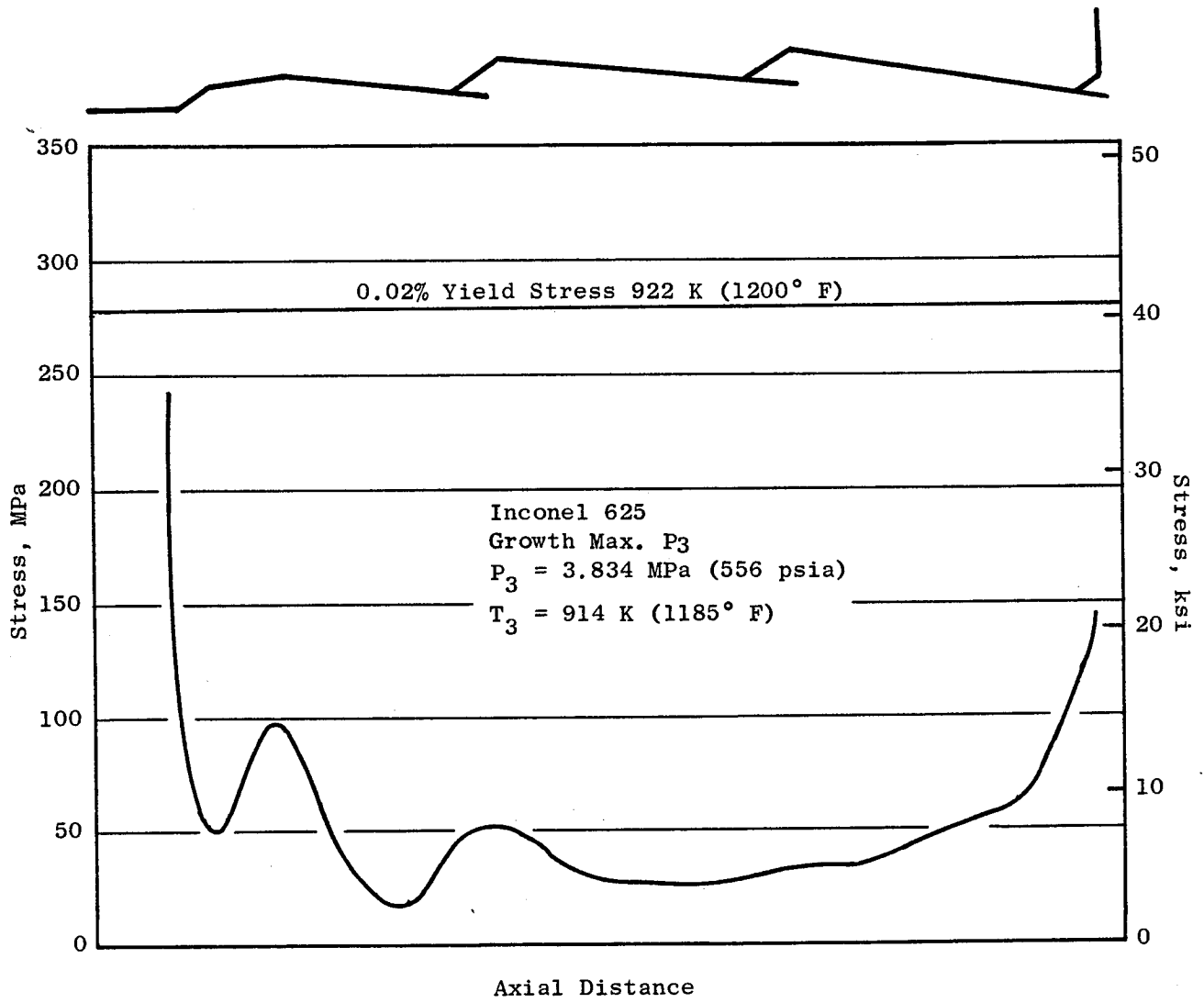


Figure 72. Predicted Stress for Combustor Support Outer Liners.

ORIGINAL PAGE IS
OF POOR QUALITY

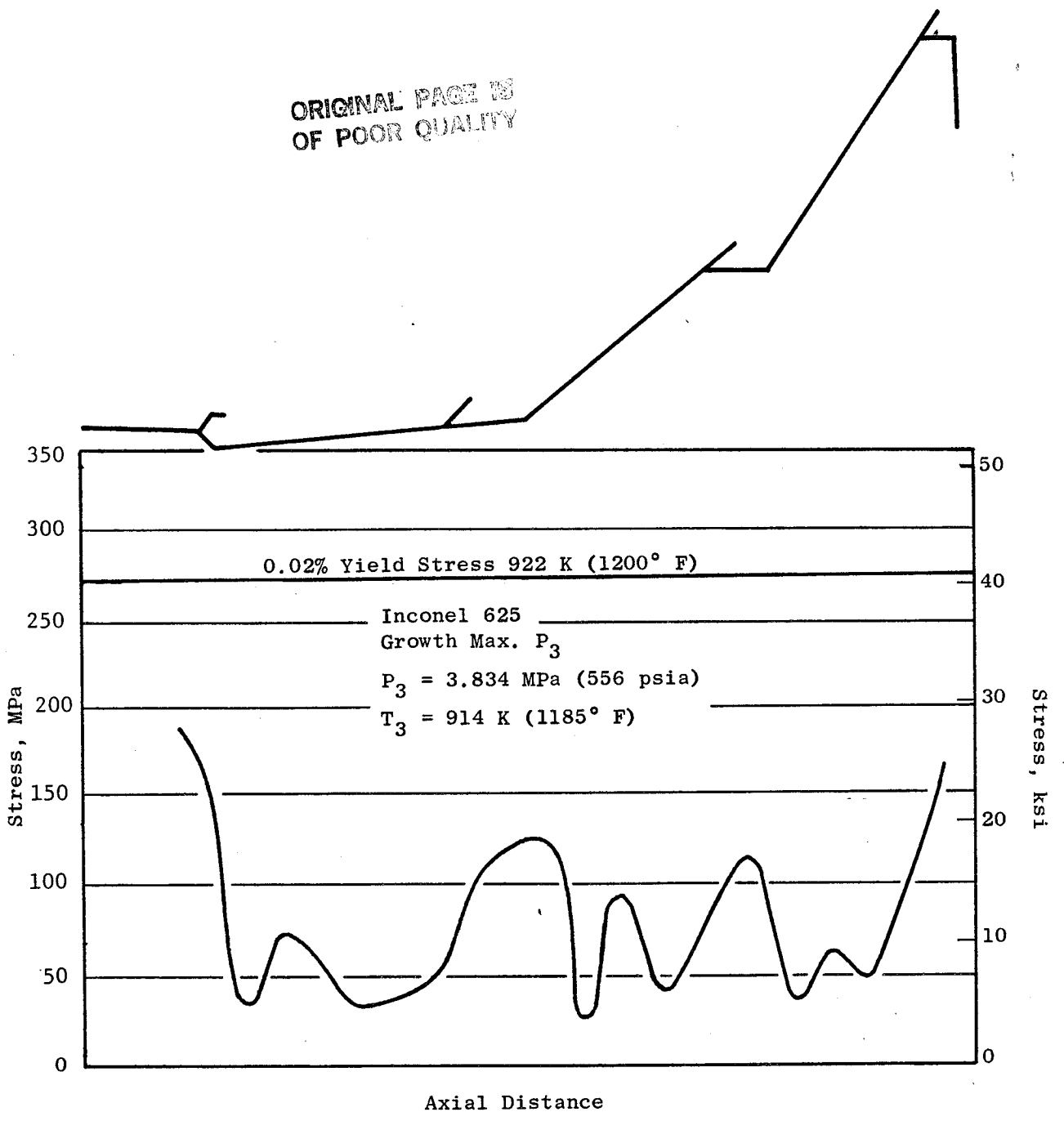
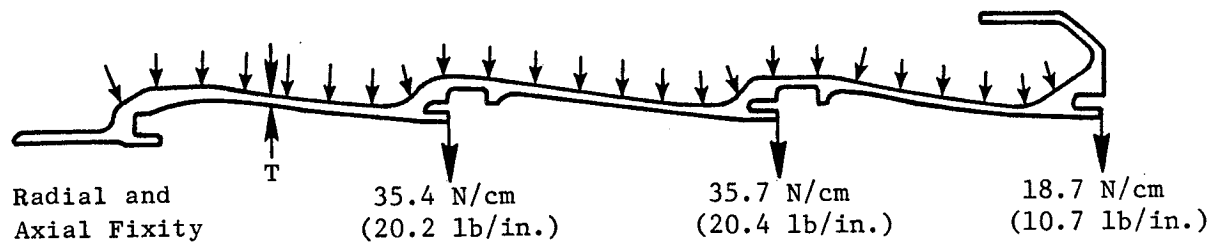


Figure 73. Predicted Stress for Combustor Support Inner Liners.

ORIGINAL PAGE IS
OF POOR QUALITY

$$\Delta P = 0.193 \text{ MPa (28 psia)}$$



- Growth, Max. P_3 Condition
- $P_3 = 3.91 \text{ MPa (567 psia)}$
- $T_3 = 94 \text{ K (1185}^\circ \text{ F)}$
- Inconel 625
- BOSOR Program
- Liner Thickness, $T = 0.26\text{--}1.27 \text{ mm (0.03\text{--}0.05 \text{ in.})}$

Figure 74. Support Liner Buckling Analysis Model.

ORIGINAL PAGE IS
OF POOR QUALITY

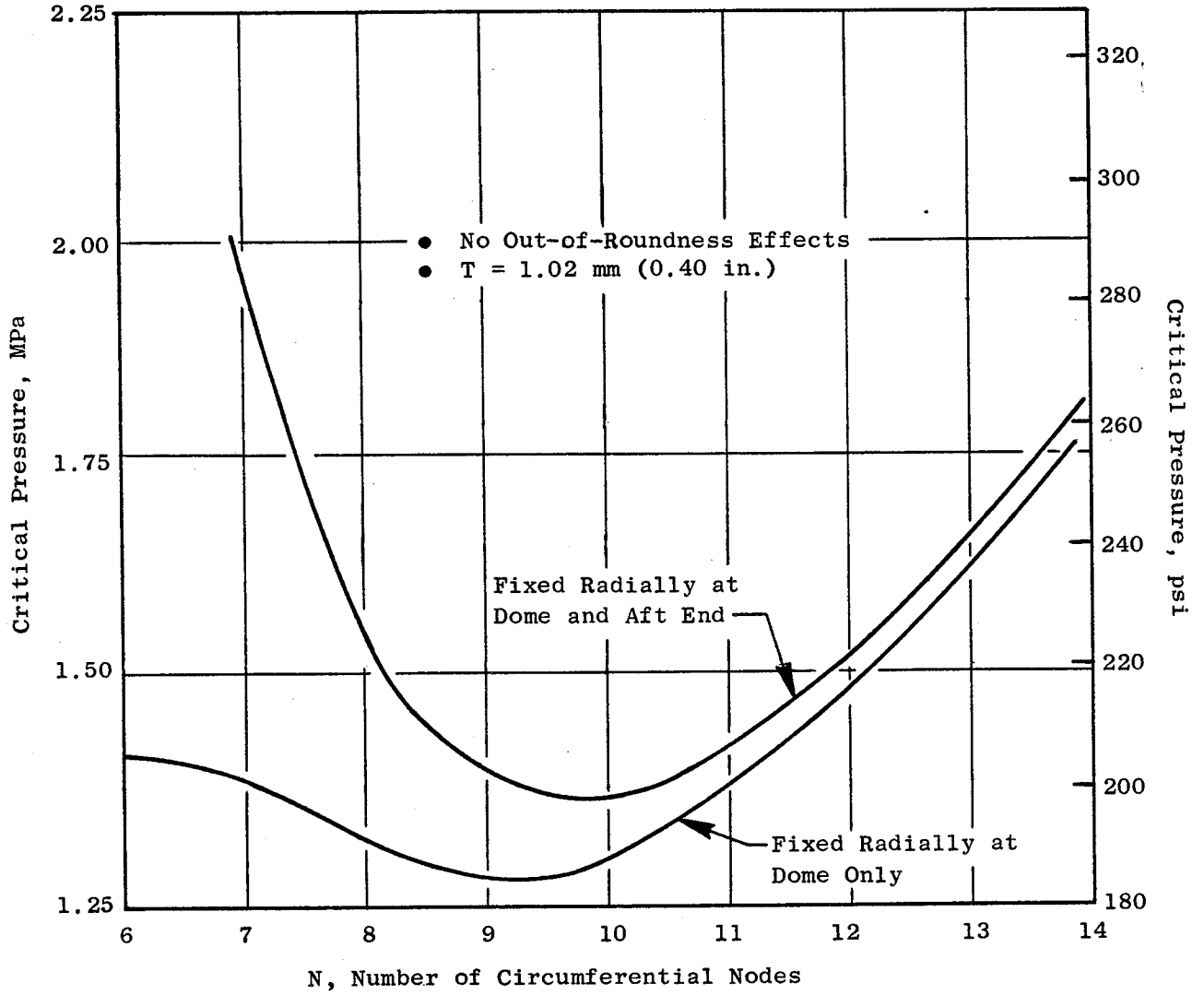


Figure 75. Outer Support Liner Critical Buckling Pressures.

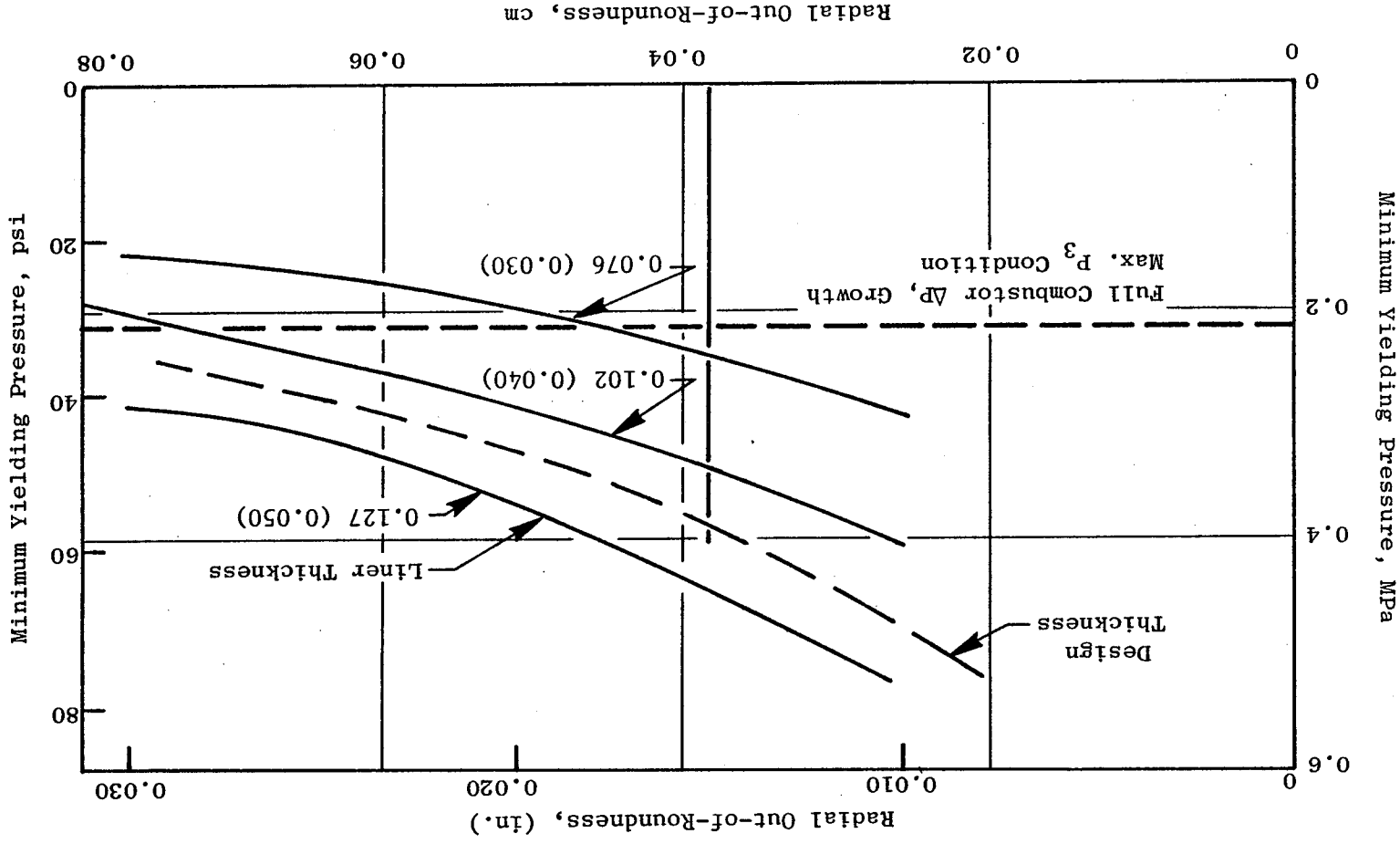
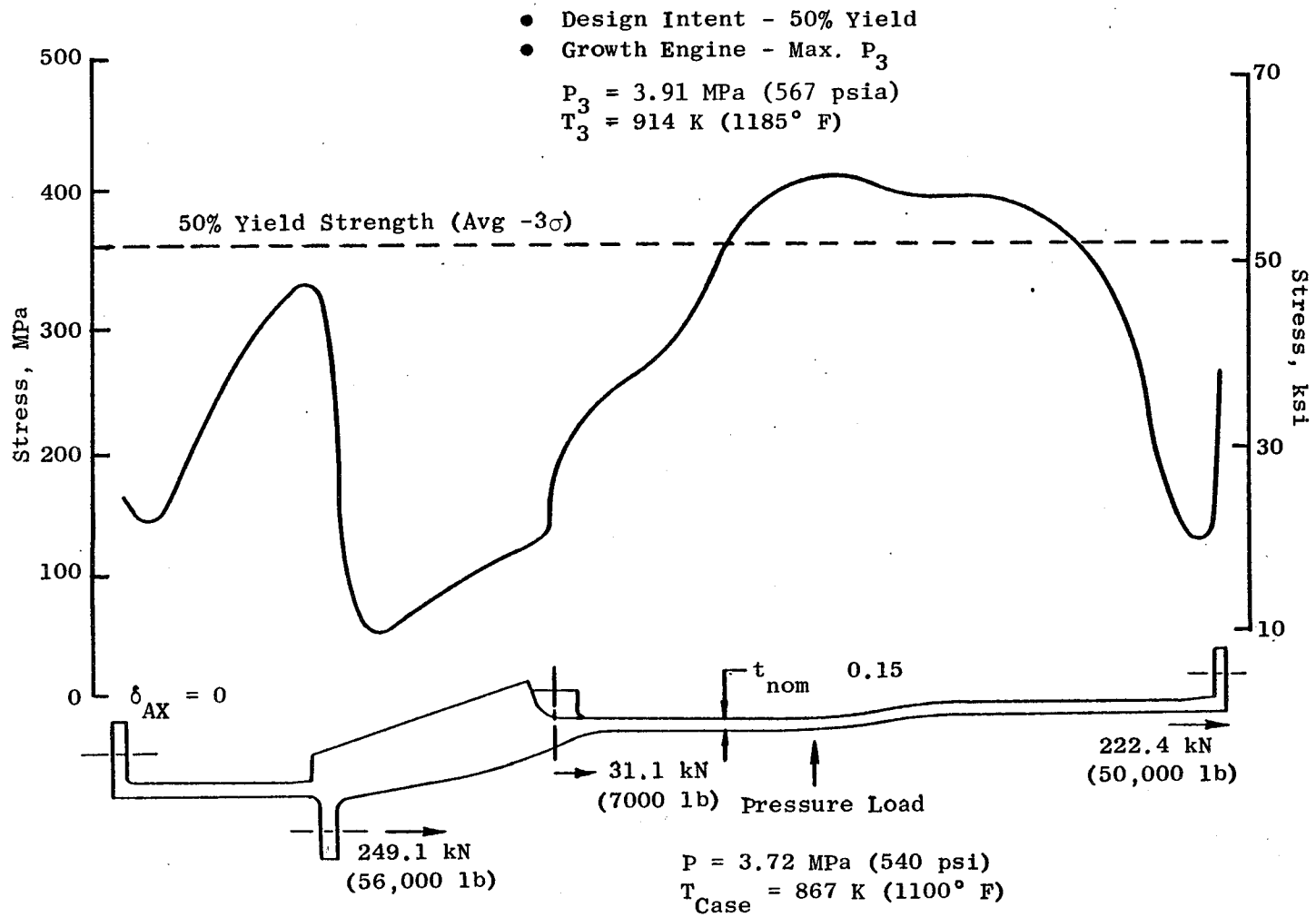


Figure 76. Effect of Out-of-Roundness on Buckling Characteristics.



ORIGINAL PAGE IS
OF POOR QUALITY

Figure 77. Predicted Axial Stress Distribution for Casing.

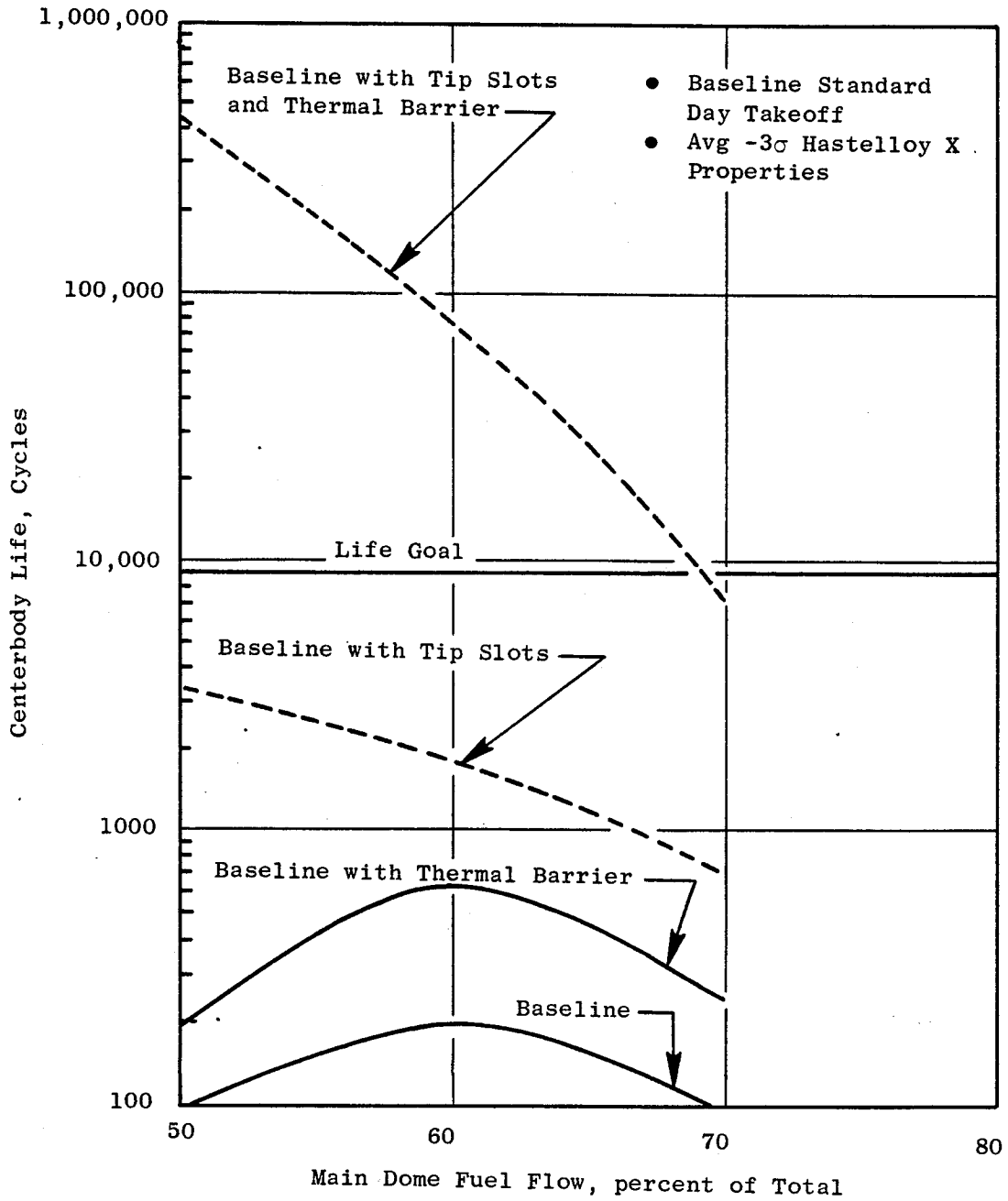


Figure 78. Predicted Centerbody Structure Life Levels.

effect the design changes have on cyclic life. As shown, the baseline configuration with tip slots and thermal barrier coating provides a life level in excess of the requirement of 9000 cycles.

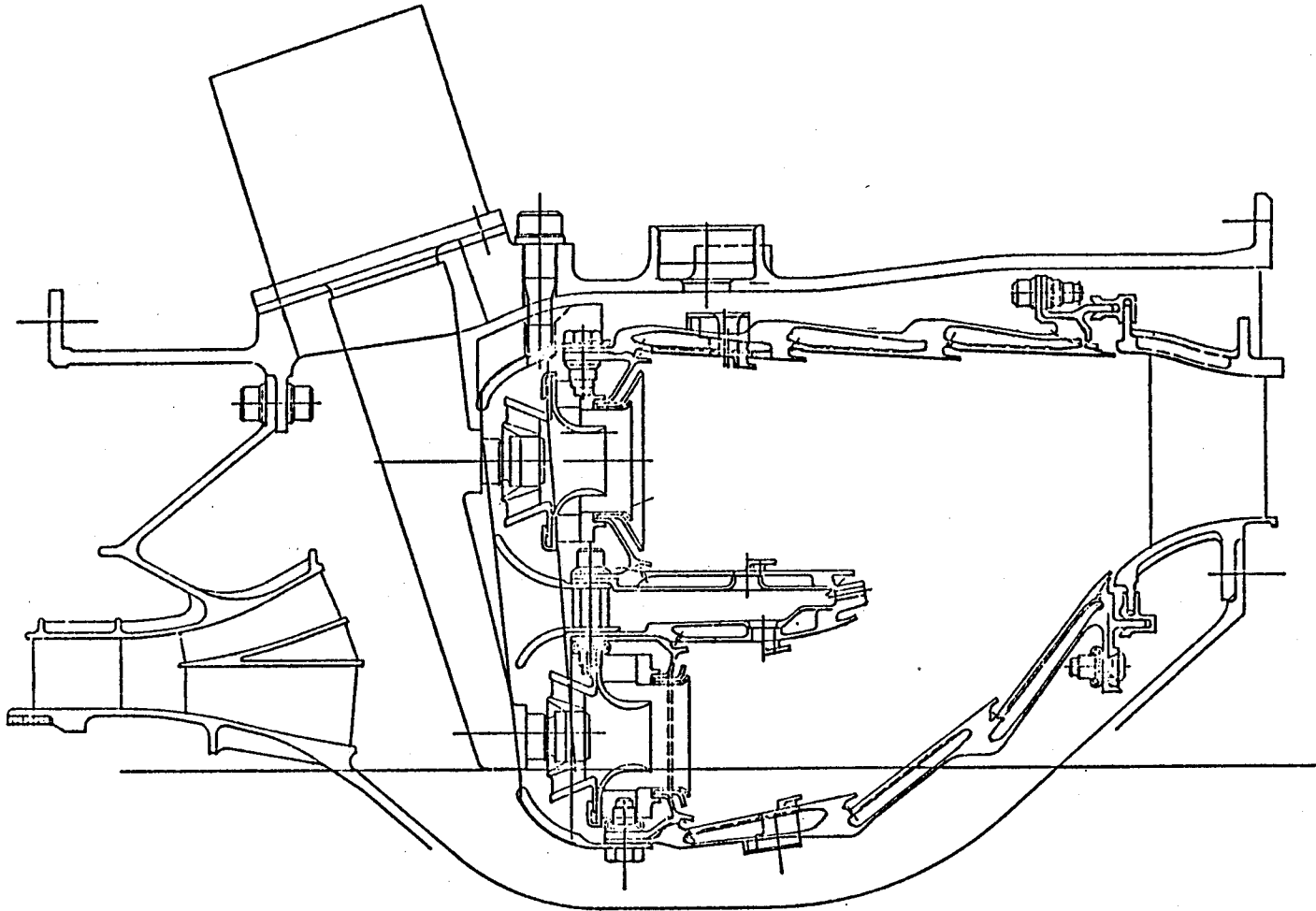
5.4.3 Fuel Nozzle Vibratory Analysis

5.4.3.1 Background

The objective of the fuel nozzle vibration studies was to identify a fuel nozzle stem configuration with adequate rigidity to avoid criticals in the engine high power operating range. The original design goal was a minimum natural frequency of 1000 hertz. In addition, the nozzle must meet the combustion system geometric constraints and the nozzle stem must be configured to minimize aerodynamic drag losses to the turbine cooling circuits. The double-annular combustion system, with the fuel nozzle installed, is shown in Figure 79. Applicable prior commercial engine experience, primarily the CF6 engine, was reviewed.

The fuel nozzle design experience of the CF6 indicated that forged construction was a necessity. In addition, the blend radii between the stem and flange should be maximized and the metering valve should be isolated from the stem to avoid the high casing heat loads. These features were incorporated into the E³ fuel nozzle design.

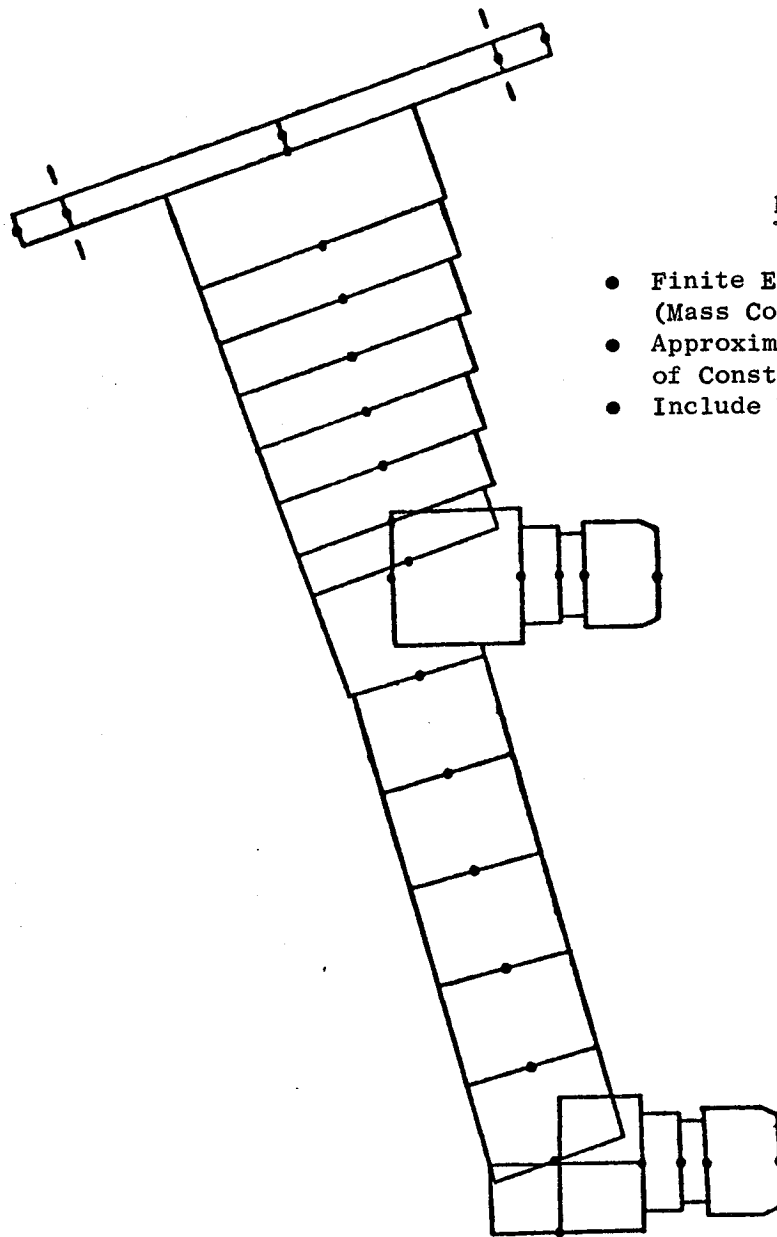
The fuel nozzle vibration analyses were conducted with the MASS computer program. The program utilizes finite element techniques to predict operating stresses and vibratory stiffness. The fuel nozzle stem was approximated as a series of constant area beams as shown in Figure 80. The stem model included the loss of cross-sectional area due to the internal fuel passages and insulating features. These internal features are illustrated in Figure 81. Extensive studies were conducted to identify two designs, a 750 and a 1000 hertz configuration. These designs are shown on a Campbell diagram in Figure 82. As shown, a given stem frequency decreases slightly with increasing engine speed. This occurs because vibration frequency is proportional to the square root of Young's Modulus and Young's Modulus decreases with increasing operating temperature. Therefore, to obtain a 750 hertz stiffness at takeoff conditions, a stem frequency of 816 hertz is required at room temperature.



ORIGINAL PART IS
OF POOR QUALITY

Figure 79. E³ Combustor Design.

ORIGINAL PAGE 19
OF POOR QUALITY



Method

- Finite Element Model
(Mass Computer Program)
- Approximate Stem with a Series
of Constant Area Beams
- Include Effect of Fuel Passages

Figure 80. E³ Combustor Fuel Nozzle Vibration Analysis.

ORIGINAL PAGE IS
OF POOR QUALITY.

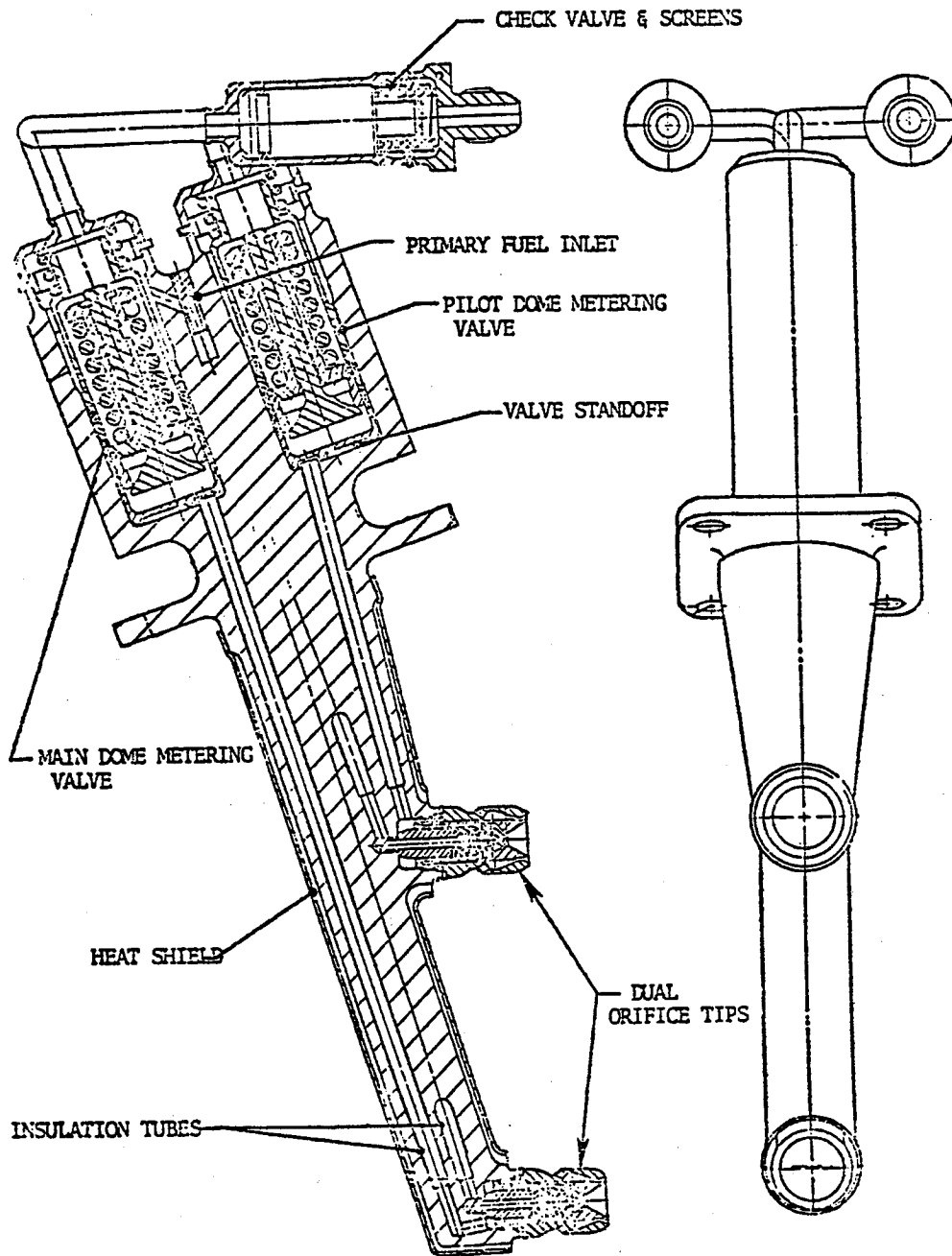


Figure 81. E³ Fuel Nozzle Design Features.

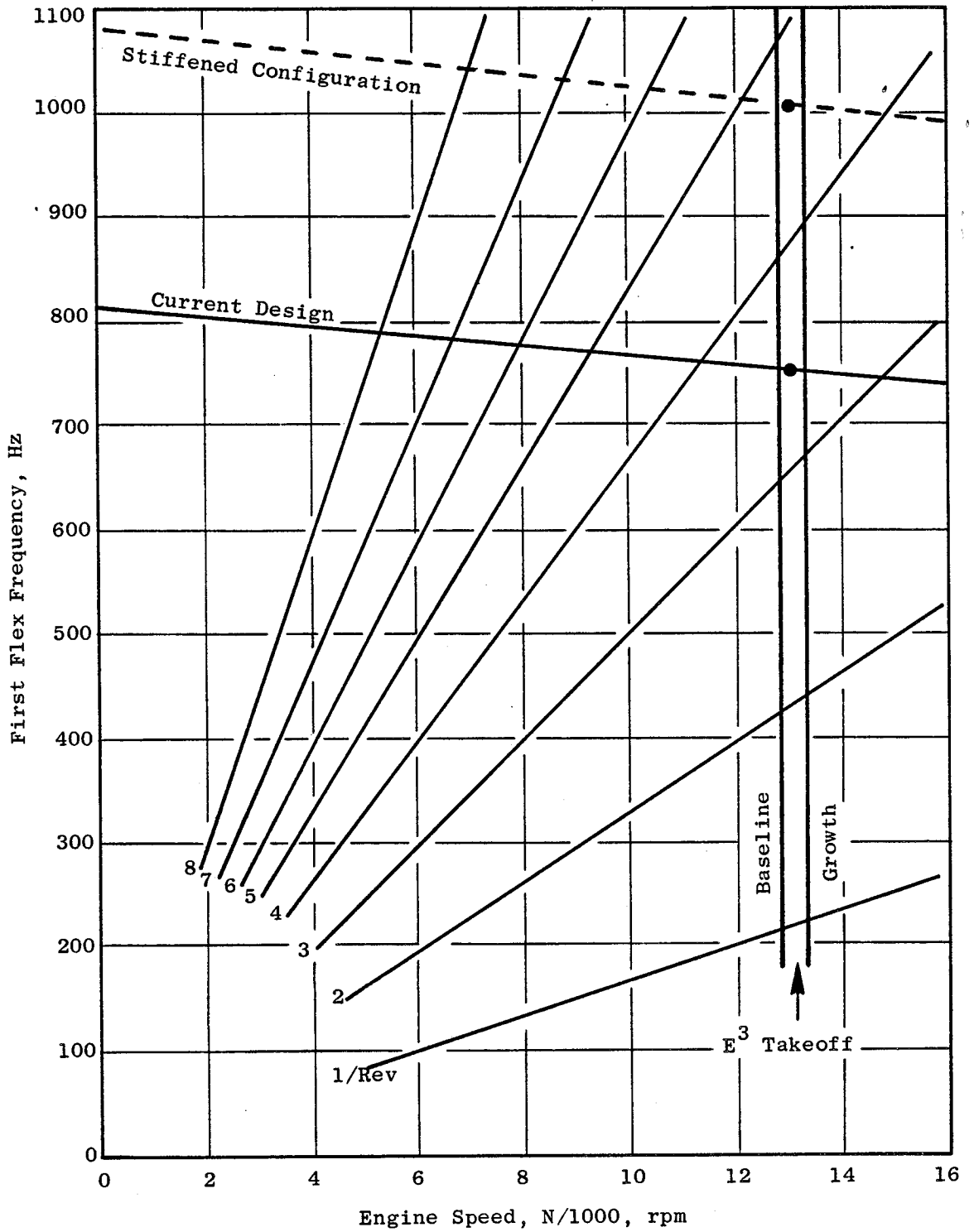


Figure 82. E³ Fuel Nozzle Campbell Diagram.

The stiffer (1000 hertz) configuration exhibits several significant drawbacks when compared to the 750 hertz design. Turbine cooling air is conducted through the outer combustor passage as shown in Figure 83. The stiffer fuel nozzle configuration has a larger stem cross section and, consequently, higher flow blockage. This blockage effect is illustrated in Figures 84 and 85. As shown, the 1000 hertz design has approximately 50% higher stem blockage. The fuel nozzle design must be removable from the engine with the combustor assembly intact. Figure 86 shows this removal and installation through the combustor casing port are severely restricted by the proximity of the diffuser and combustor cowlings. The stiffer configuration would not interface with the geometric constraints due to its larger size. In consideration of the stem blockage and geometric constraints, the 750 hertz configuration was chosen for the E³ application. A comparison of the chosen design with other GE commercial designs is provided in Table XX. The E³ chosen design is within the range of these other designs. The E³ fuel nozzle is shown pictorially in Figure 49.

Table XX. Comparison of Fuel Nozzle First Flex Frequencies.

Fuel Nozzle Design	First Flex Natural Frequency, Hz	Per Rev Excitation at Takeoff
CF6-50 Ruggedized	900	5.5
CFM56/F101 Current Engine Design	500	2
Current E ³ Design	750	3.5

5.4.3.2 Laboratory Testing

In order to confirm the fuel nozzle stem vibratory analysis predictions, a laboratory test was conducted.

The test setup is shown in Figure 87. The fuel nozzle was mounted to a rigid plate which simulated the casing attachment. The fuel nozzle stem was

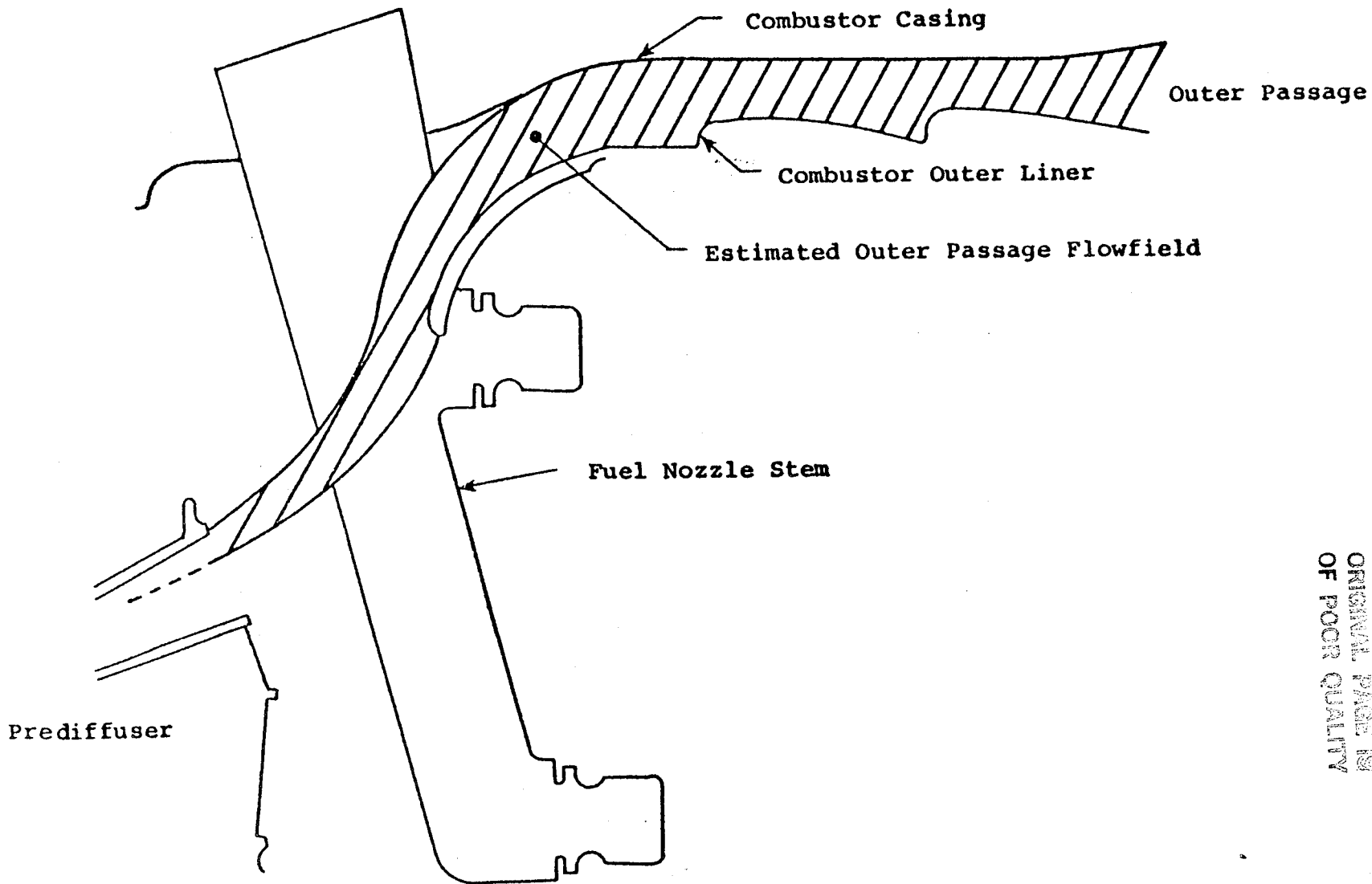
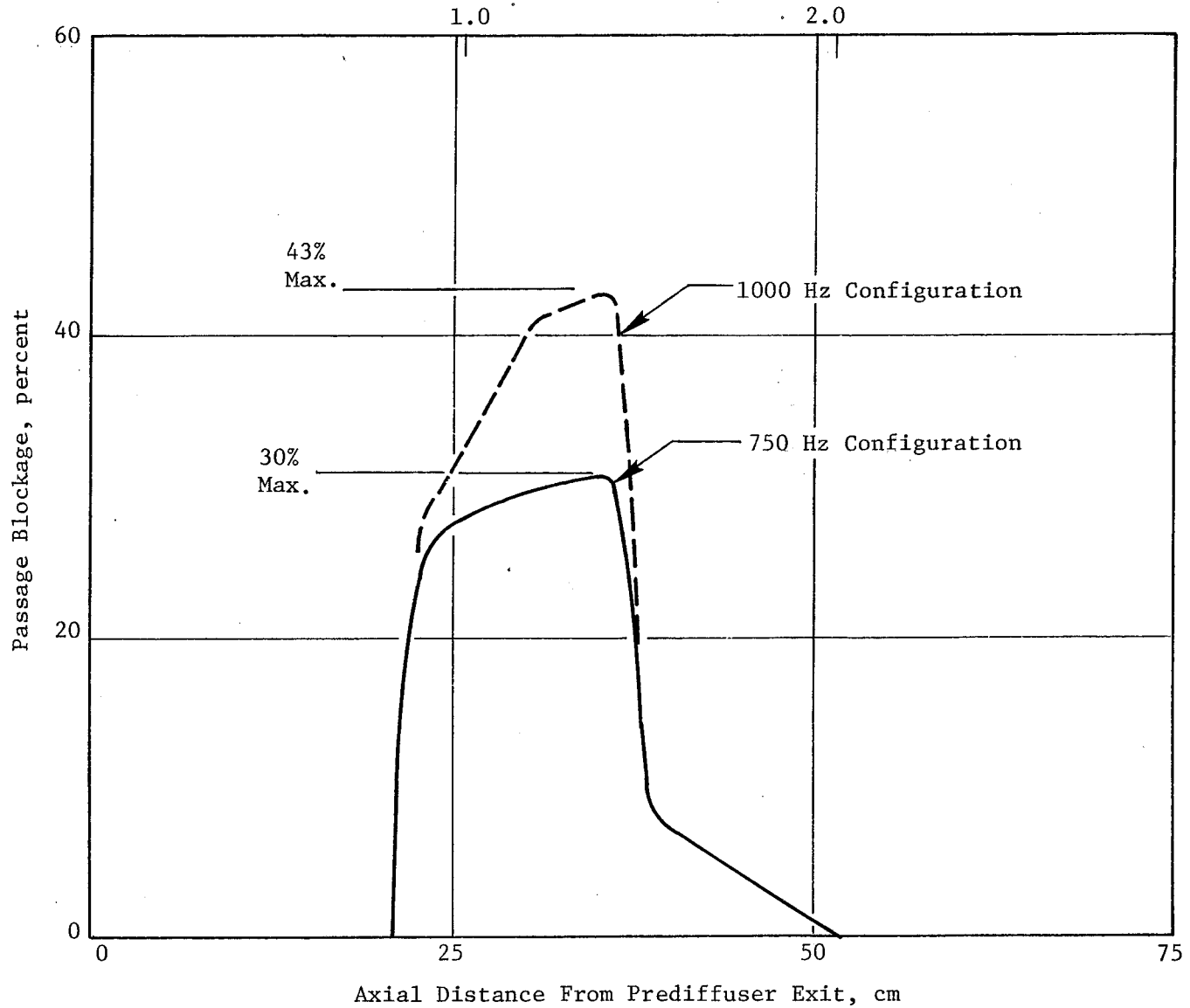


Figure 83. E³ Fuel Nozzle Aerodynamic Impact.

ORIGINAL PAGE IS
OF POOR QUALITY

Axial Distance From Prediffuser Exit, inches



ORIGINAL PAGE IS
OF POOR QUALITY

Figure 84. Comparison of Outer Passage Blockage for E³ Fuel Nozzle Designs.

ORIGINAL PAGE IS
OF POOR QUALITY

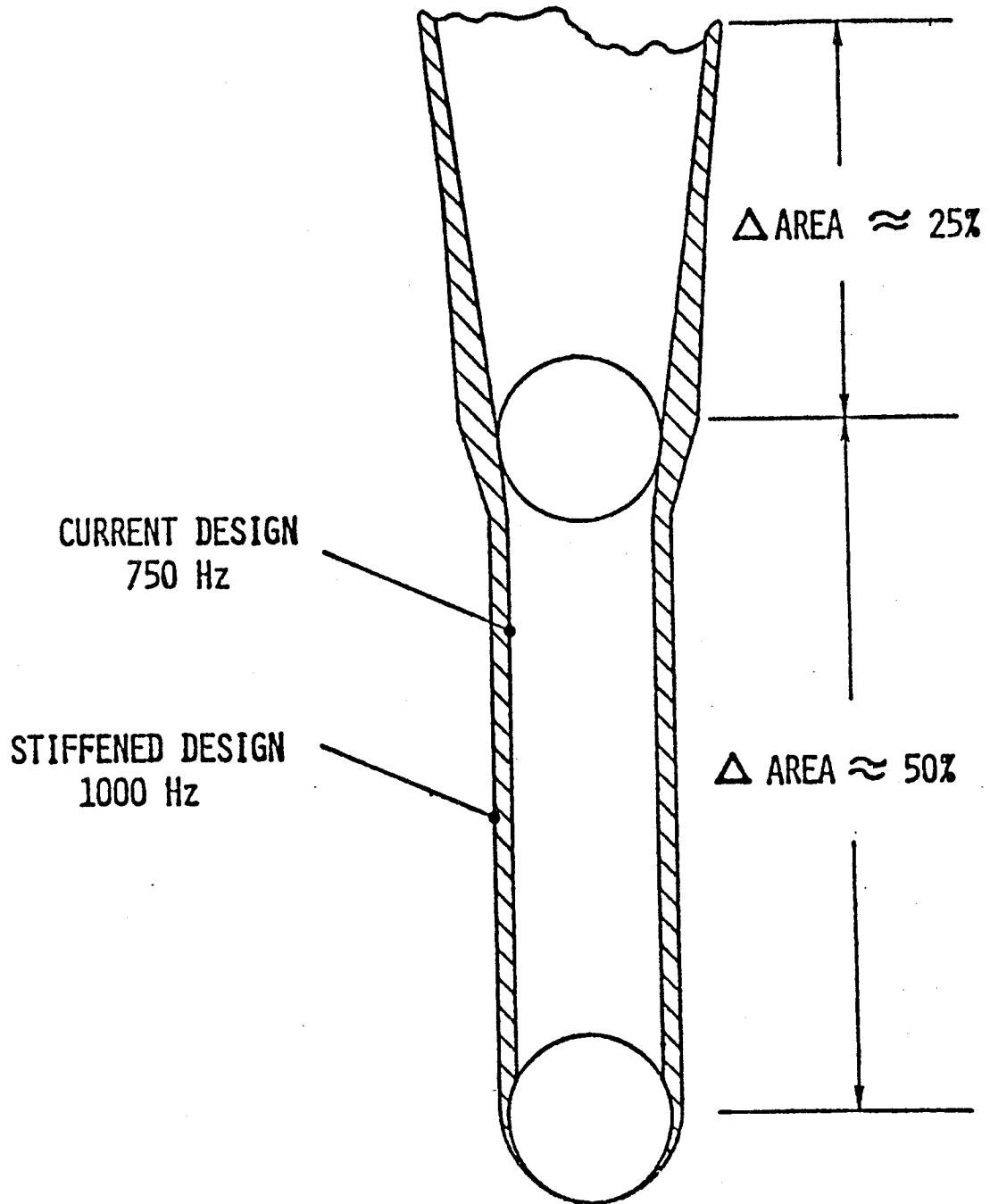


Figure 85. Comparison of E³ Combustor Fuel Nozzle Stem Designs.

ORIGINAL PAGE IS
OF POOR QUALITY

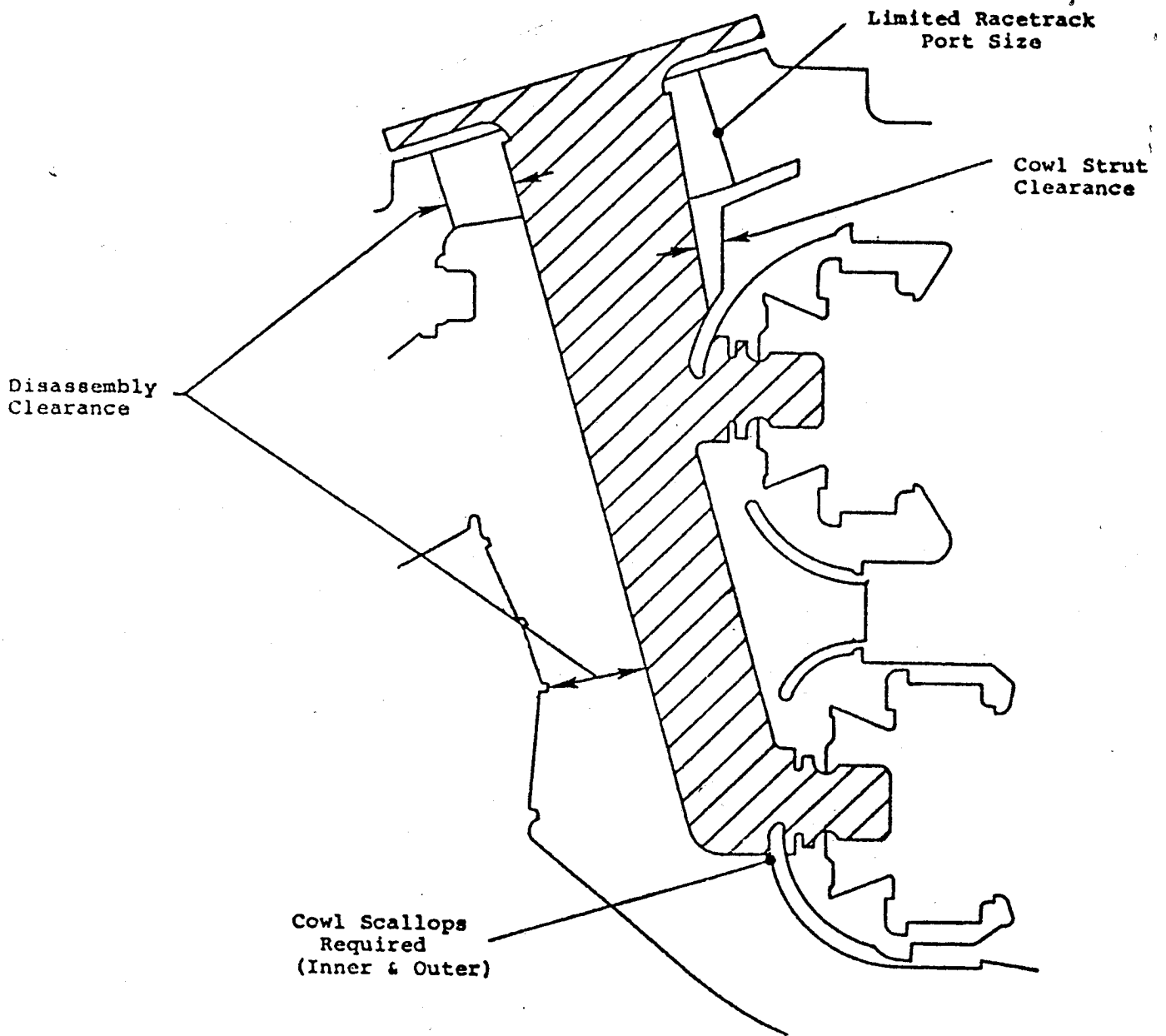
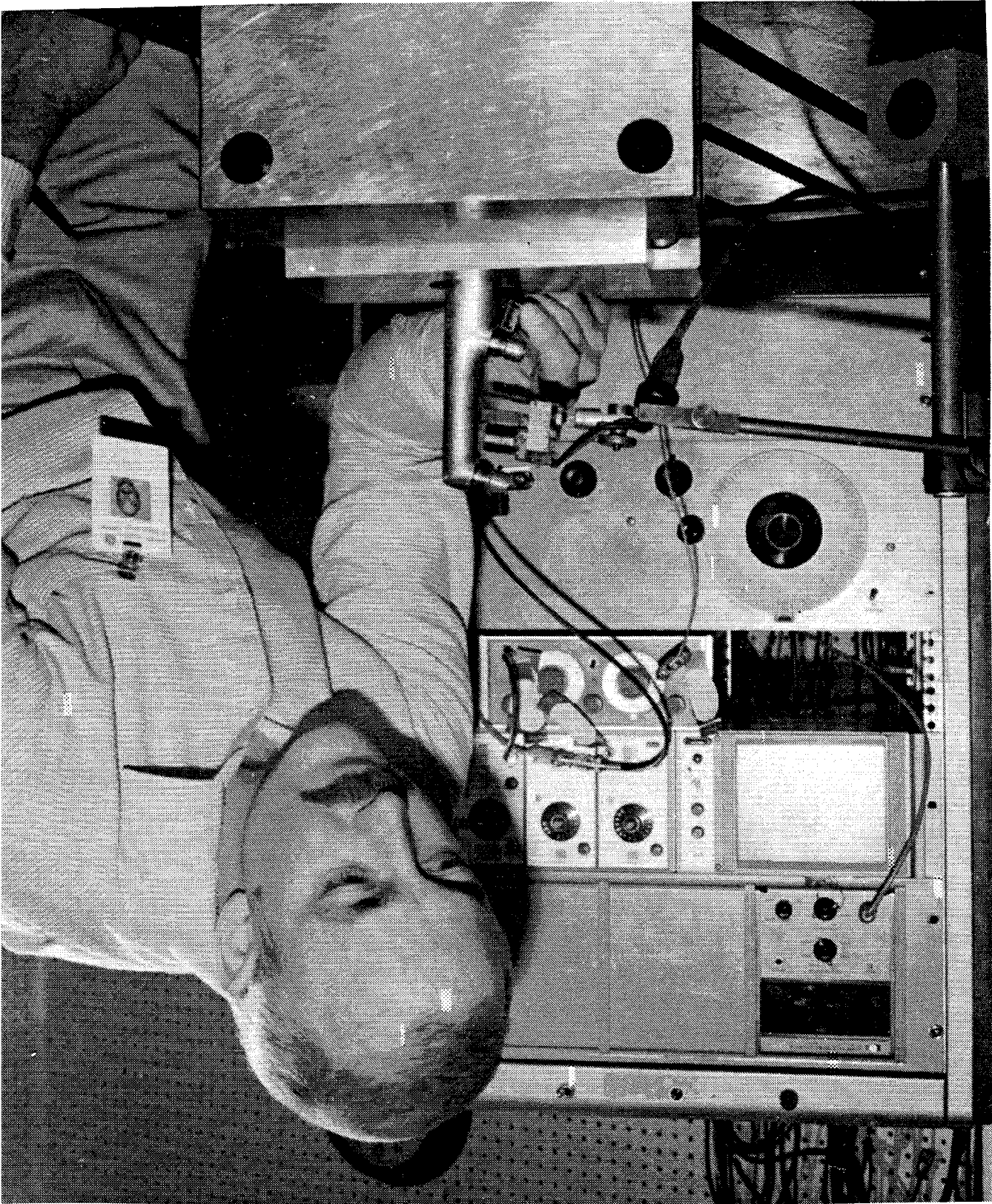


Figure 86. E³ Combustor Geometric Constraints.

Figure 87. E₃ Mechanical Vibration Test Setup.



ORIGINAL PAGE IS
OF POOR QUALITY

ORIGINAL PAGE
BLACK AND WHITE PHOTOGRAPH

vibrated by means of an electromagnet. A hand-held electromagnetic probe was used to monitor stem responses as a frequency search was conducted to evaluate vibration nodes.

The results of this frequency search indicated the following first flex frequencies for the E³ fuel nozzle:

<u>Mode</u>	<u>Frequency, Hz</u>
Circumferential	822
Axial	864
Predicted First Flex (Circumferential)	816

The predicted level is based on a 750 hertz frequency at an elevated temperature of 1000° F. Due to Young's Modulus effects, this translates to 816 Hz at room temperature conditions. The demonstrated first flex frequency agrees very well with the analytically predicted level.

5.4.3.3 Conclusions and Summary

Excellent agreement was obtained between laboratory data and pretest predictions. A first flex frequency of 822 Hz was obtained in the laboratory as compared to a predicted 816 Hz. The fuel nozzle stiffness is adequate for the E³ application. A summary of the design is shown below:

<u>Parameter</u>	<u>Current Design</u>	<u>Stiffened Configuration</u>
First Flex Natural Frequency, Hz	750	1000
Frequency-to-Engine-Speed Ratio at T/O	3.5	4.5
Outer Passage Blockage, %	30	43
Estimated Stem Blockage Pressure Loss, %	0.5	0.8
Fits Current Combustor Envelope	Yes	No
Stem Weight, kg (lb) Per Set	13.6 (30)	18.1 (40)

6.0 COMBUSTOR TEST RESULTS

This section describes the subcomponent and component test programs which were used to assist in the development of the E³ combustor system. Testing was used to verify analytical aerodynamic designs for the combustor diffuser system and for development of the combustor swirl cups. This effort was followed by component tests for performance development in annular sector combustors in parallel to, but in advance of, the full-annular combustor development program. This method was used to ensure that performance goals were attainable and to quickly solve annular performance problems related to aerodynamics, thermodynamics performance, and emissions.

Use of subcomponent and component testing for these purposes greatly facilitates the overall development of the full-annular combustor and provides an inexpensive and rapid means for problem solving during the development cycle. In addition, hardware changes can be evaluated separately from the annular effort to provide necessary alternative approaches for changes in design philosophy or engine system modifications.

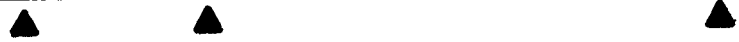
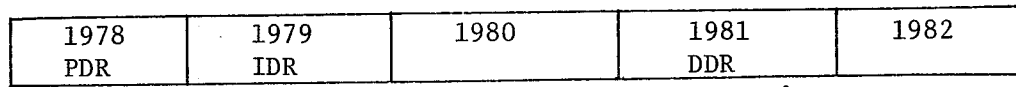
Figure 88 presents the E³ combustor development test schedule and shows current progress plus work remaining to release of the core engine combustor for engine assembly.

6.1 SUBCOMPONENT TESTING

6.1.1 Combustion System Diffuser Test

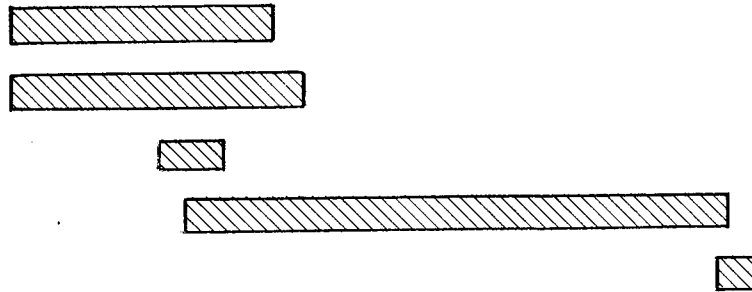
6.1.1.1 Introduction

The purpose of this test program was to develop and characterize the aerodynamic performance of the E³ combustor inlet diffuser as a supporting effort to the E³ combustor development program. This diffuser is an advanced, short length design that is closely integrated with the low emissions, double-annular E³ combustor system. For this program, a full-scale annular model of the E³ diffuser was built and tested at the General Electric Corporate Research and Development Center (CR&DC) in Schenectady, New York. This model



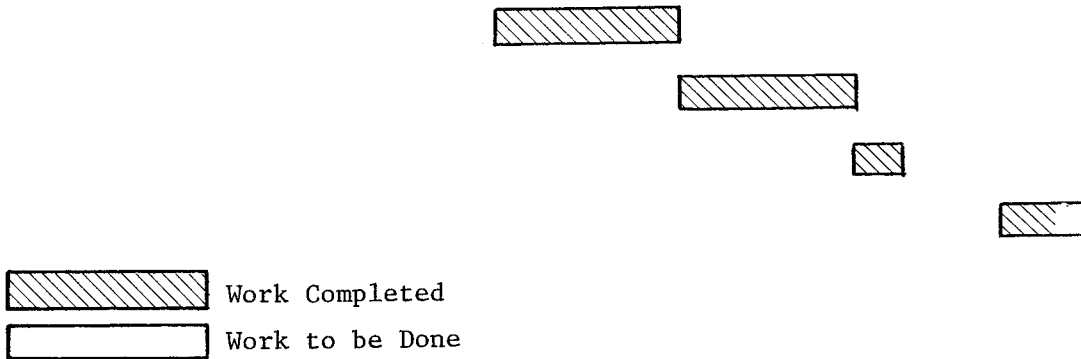
Subcomponent Tests

- Diffuser
- Swirl Cup
- Dome Temperature
- Sector Combustor
- Fuel Nozzles



Full-Annular Tests

- Screening
- Development
- Engine Component
- Core Engine



Work Completed
 Work to be Done

ORIGINAL PAGE IS OF POOR QUALITY

Figure 88. E³ Combustor Development Test Schedule.

was constructed of wood and aluminum and was designed to accurately duplicate the E³ diffuser flow passages from the compressor outlet guide vanes (OGV's) to the five coaxial combustor annular flow passages downstream of the combustor dome region. A metering plate at the exit end of the model was used to independently vary the flow in each passage.

Static pressure recovery characteristics and total pressure loss coefficients were measured for a wide range of flow splits in each of the five flow passages. These measurements were made for three different inlet velocity profiles with the final modified version of the E³ flowpath contours.

Diagnostic tests with a two-dimensional water table were conducted earlier in the test program and revealed excessive flow spillage from the combustor dome cowlings with the original flowpath contours. Several cowling contours were tested on the water table, and a design was selected for the airflow model that had significantly reduced flow spillage from the dome region.

Test results for the final version of this diffuser design show that the pressure losses in the outer flow passage are about 0.5% higher than expected. Pressure losses in the remaining four passages are nearly the same or somewhat less than anticipated. The test results also show that all of the individual passage static pressure recovery characteristic curves have negative slopes at the design flow conditions which indicates that this diffuser design has a high degree of flow stability. High turbulence levels generated by the inlet velocity profilers for the peaked-out and peaked-in profiles resulted in significantly lower diffuser pressure losses when testing with these profilers.

6.1.1.2 Design Features

The design configuration of the split-duct diffuser was selected to obtain a short-length prediffuser, positive flow direction to the combustor domes, reduced air temperature extraction for turbine rotor cooling, and low pressure losses.

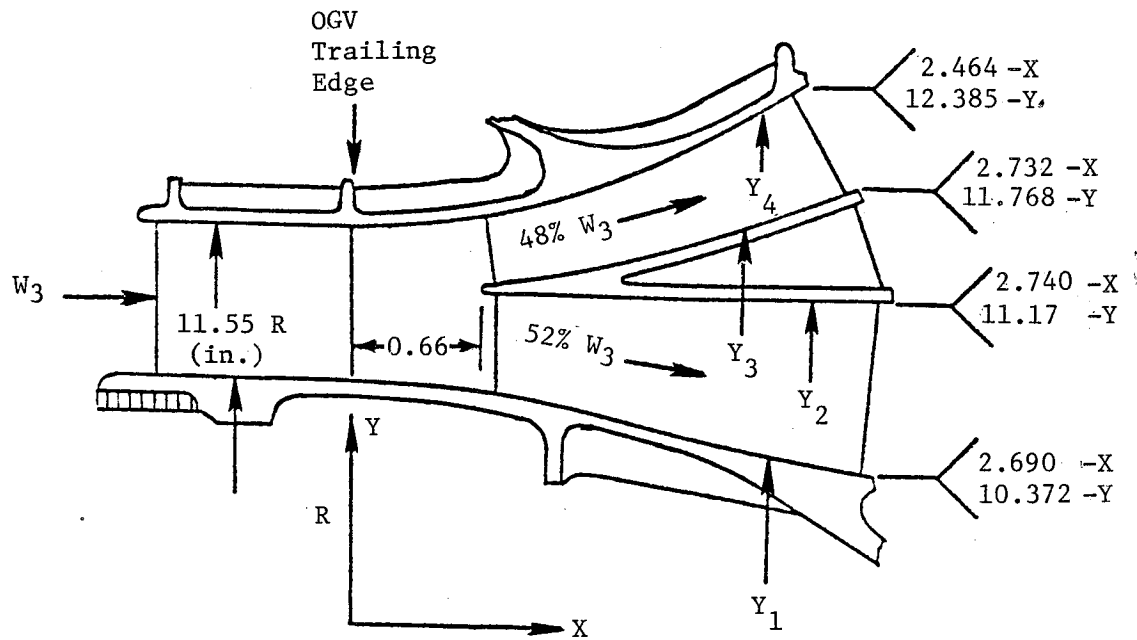
As illustrated in Figures 89 and 90, the E³ combustor inlet diffuser accepts core engine airflow from the compressor OGV's and divides this flow into two parallel prediffuser passages. The outer passage curves outward and directs about 48% of the airflow toward the outer dome annulus of the combustor. The inner passage directs the remaining 52% of the airflow toward the inner dome annulus of the combustor. Each of these two passages has a diffuser area ratio of 1.8.

Flow leaving this short prediffuser is dumped into the combustor liner passages and into the plenum region upstream of the combustor domes. The dumping area ratio in the liner passages is 2.5. The resulting dumping pressure loss is small because the compressor exit velocity head is reduced from 5.8% of the total pressure at takeoff conditions to 1.7% by the prediffuser. Nearly all of this prediffuser exit velocity head is recovered in a "free stream" diffusion region which enters each of the plenums ahead of the two combustor domes. Total pressure losses from the compressor OGV's to the combustor domes are very small with this configuration.

A short, constant-area section is provided in the diffuser passage immediately downstream of the OGV's to permit the wakes from the OGV's to mix and decay before the flow is diffused. Downstream of this section, the outer and inner walls of the prediffuser begin to diverge; and a single-annular splitter vane is positioned in the passage to divide the prediffuser into two parallel annular passages. The splitter contours, along with the outer and inner wall surfaces of the prediffuser, are designed to provide the desired rate of diffusion through these passages. Each passage is designed to fall below the line of no appreciable stall on the Stanford diffuser flow regime correlation (Reference 5). The splitter vane reduces the length required for the prediffuser and also directs the airflow leaving the prediffuser into the combustor dome regions.

A compressible, axisymmetric potential flow computer program (CAFD) was used to analyze several contour configurations for the E³ prediffuser. A streamline plot of the final selected version is presented in Figure 91. The CAFD Program accounts for the flow blockage of the support struts by introducing a distributed blockage as a function of radial position at each axial

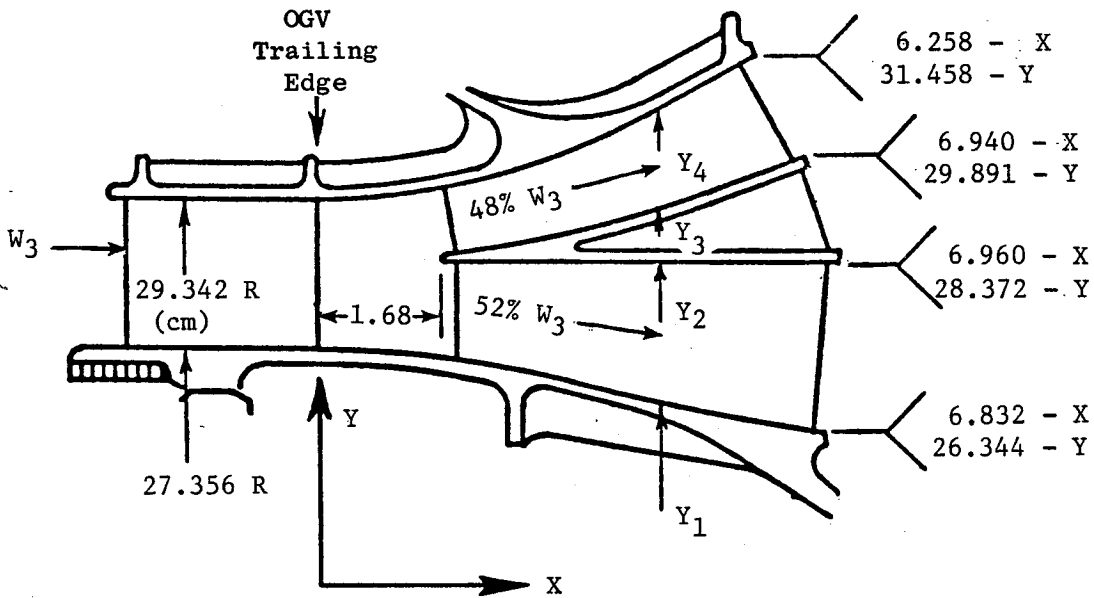
ORIGINAL PAGE IS
OF POOR QUALITY



X	Y ₁	Y ₂	Y ₃	Y ₄
0	10.77		-	11.552
0.2	10.76	-	-	11.557
0.4	10.75	-	-	11.574
0.6	10.74	-	-	11.602
0.66	10.73	11.195	11.193	11.612
0.7	10.72	11.17	11.222	11.620
0.8	10.71		11.235	11.637
1.0	10.68		11.265	11.691
1.2	10.64		11.302	11.754
1.4	10.59		11.346	11.830
1.6	10.55		11.398	11.920
1.8	10.51		11.457	12.025
2.0	10.47		11.532	12.133
2.2	10.44		11.590	12.242
2.395	10.41		11.656	12.348
2.4	10.41		11.657	-
2.6	10.38		11.724	-
2.604	10.38		11.725	-
2.69	10.37		-	-
2.74	-	11.17	-	-

Figure 89. Combustor Inlet Prediffuser Wall Contours (Inches).

ORIGINAL PAGE IS
OF POOR QUALITY



X	Y_1	Y_2	Y_3	Y_4
0	27.356	-	-	29.342
0.508	27.347	-	-	29.356
1.016	27.319	-	-	29.398
1.524	27.272	-	-	29.468
1.676	27.255	28.430	28.430	29.494
1.778	27.242	28.372	28.504	29.514
2.032	27.207	↓	28.536	29.557
2.540	27.123		28.613	29.696
3.048	27.019		29.708	29.856
3.556	26.906		28.820	30.049
4.064	26.799		28.952	30.278
4.572	26.700		29.102	30.542
5.080	26.608		29.269	30.818
5.588	26.523		29.439	31.094
6.084	26.446		29.605	31.363
6.096	26.445		29.609	-
6.604	26.374	29.779	-	
6.613	26.373	29.782	-	
6.832	26.344	-	-	
6.960	-	28.372	-	

Figure 90. Combustor Inlet Prediffuser Wall Contours (Centimeters).

ORIGINAL PAGE IS
OF POOR QUALITY

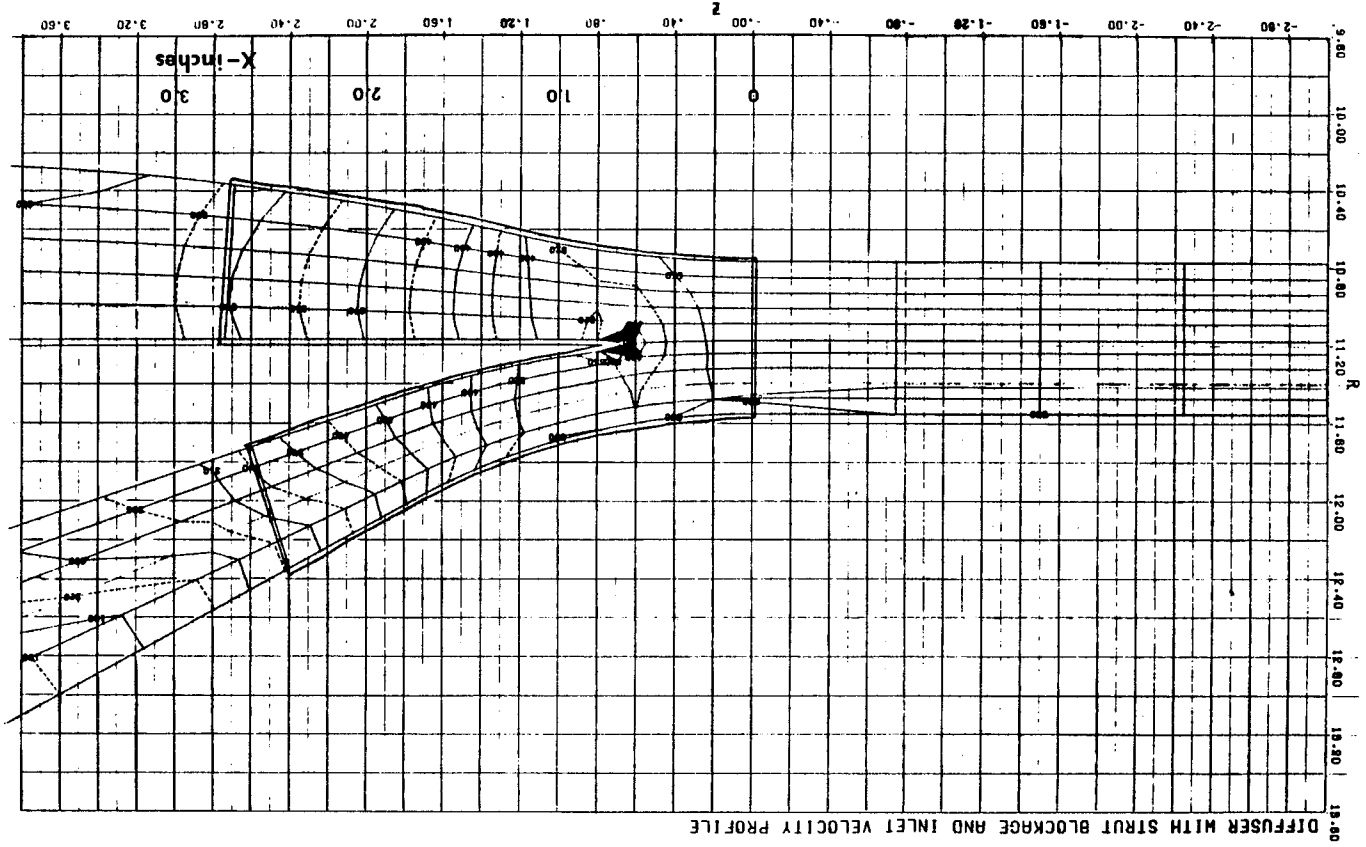


Figure 91. Inlet Diffuser Velocity Profile Streamline Plot.

station. Velocity distributions on the outer and inner prediffuser wall surfaces from the CAFD analysis are presented in Figure 92. These wall velocity distributions show the effects of the prediffuser wall curvature and the effects of the splitter vane and support strut blockages. The effective area ratio and length-to-inlet-height ratio of equivalent straight diffusers were determined directly from these velocity distributions and plotted on the Stanford diffuser flow regime correlations, as shown in Figure 93. The design level values for the equivalent straight diffusers fall below the line of no appreciable stall on the Stanford correlations.

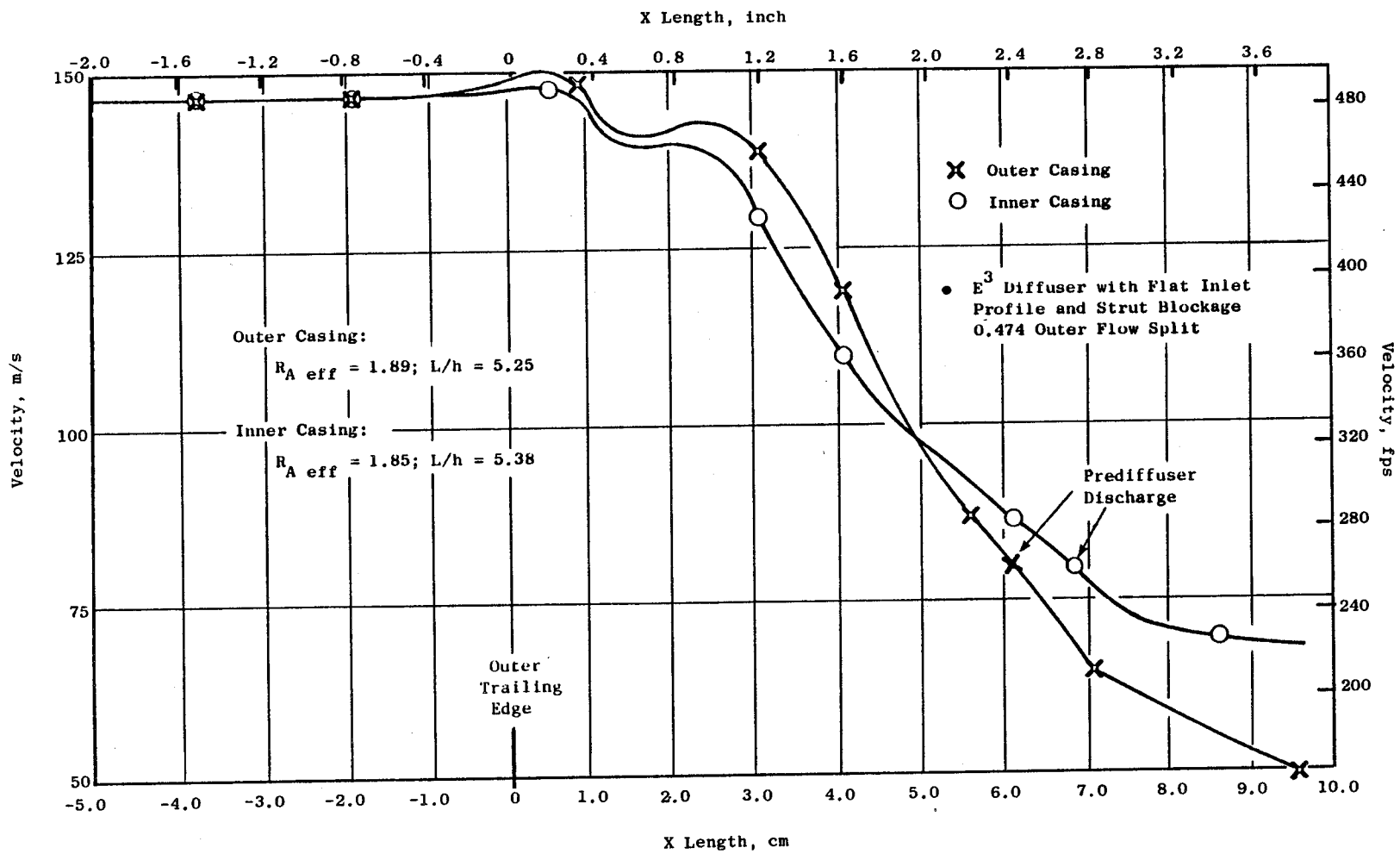
As a result of this analysis, the selected E³ diffuser design can be expected to have stable flow patterns with no regions of flow separation for a broad range of engine operating conditions.

Bleed airflow for turbine rotor cooling (about 6% of the total flow) is supplied through holes in the base region of the splitter vane. This airflow enters the hollow splitter vane structure, which serves as a plenum chamber for this flow, and passes through the 30-splitter vane support struts to the inner cavity of the engine to the first-stage turbine rotor. This bleed flow arrangement provides the turbine with cooling air that is taken from the center of the compressor exit flow. This core flow is considerably cooler than the flow near the casing walls of the compressor. Also, bleed flow from the base region of the splitter vane helps to stabilize the flow pattern in the dumping region downstream of the prediffuser.

6.1.1.3 Design Goals

The purpose of the combustor diffuser system is to deliver the high velocity airflow supplied by the compressor to the combustor and cooling flow to the turbine nozzle vanes with the smallest possible pressure loss.

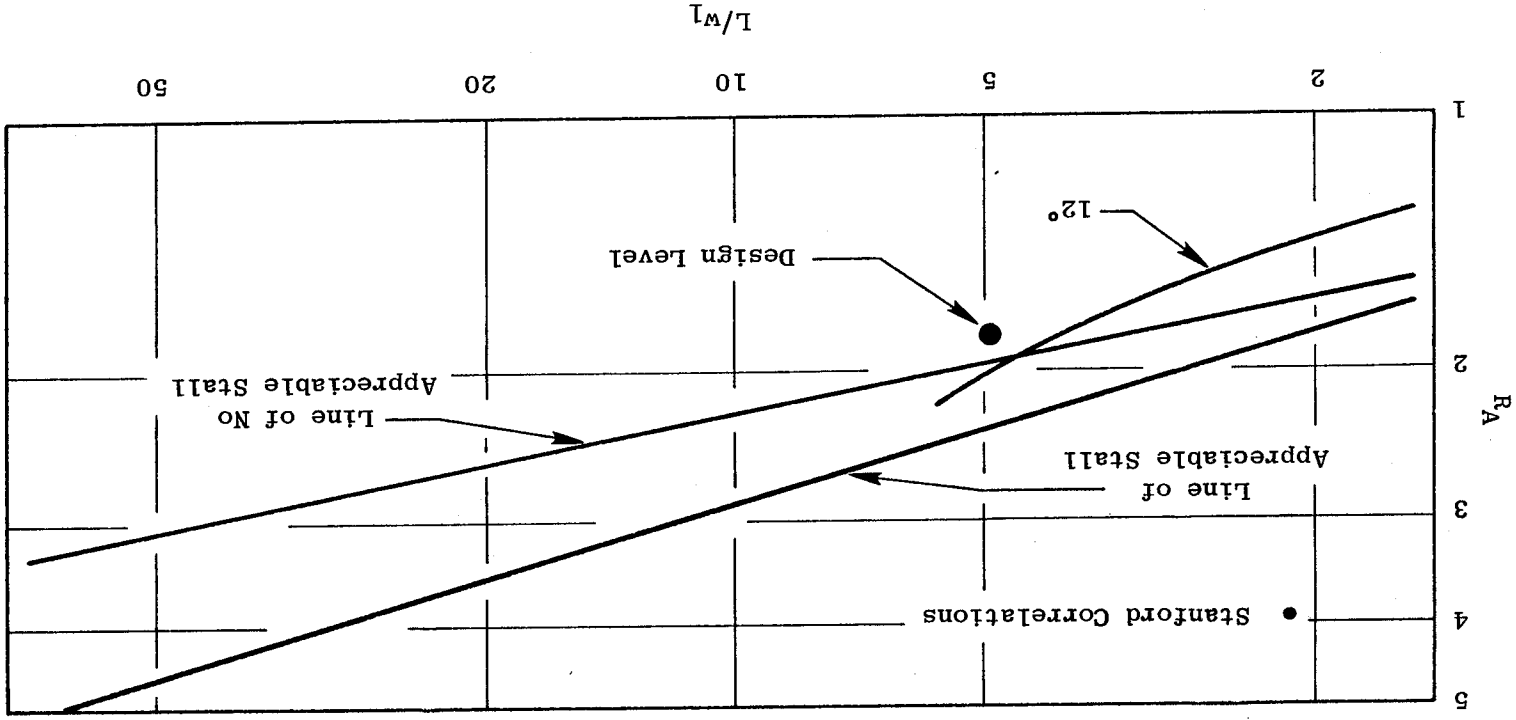
The overall pressure loss goal for the E³ combustion system is 5% of the inlet total pressure to the combustor and is measured from the OGV exit to the Stage 1 turbine nozzle inlet. This overall pressure loss is distributed throughout the combustion system.



ORIGINAL PAGE IS OF POOR QUALITY

Figure 92. Combustor Inlet Diffuser CAFD Analysis.

ORIGINAL PAGE IS
OF POOR QUALITY



$$RA = 1 - L/W_1 \text{ Tangent } \theta$$

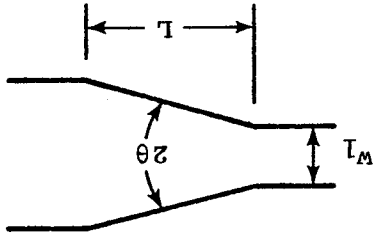


Figure 93. Split Duct Diffuser Flow Regimes.

A portion of the pressure loss is attributed to the prediffuser and the dumping loss due to the sudden expansion of the airflow streams as they discharge from the prediffuser. The remaining pressure loss is associated with the pressure drop required to flow the airflow through the fixed orifices of the combustor surfaces. The sum of these pressure losses, when mass weighted for the airflow in each of the combustor passage, comprises the overall combustion system pressure loss. Therefore, low diffuser pressure losses are important to provide the maximum available pressure loss to the combustor passages. The available pressure energy is a key parameter with respect to combustor and turbine performance. Therefore, keeping the losses in available pressure energy small is necessary to provide the desired combustor fuel/air mixing and gas temperature dilution to obtain the required combustor exit temperature distribution into the turbine. In addition, adequate pressure must be maintained in the passages which supply cooling air to the turbine nozzle to prevent hot combustion gases from being ingested into the turbine nozzle cooling circuits. This minimum level of pressure drop required is referred to as the turbine nozzle backflow margin. The goals for the diffuser system are shown in Table XXI in terms of pressure loss relative to the diffuser system inlet.

Table XXI. Diffuser Pressure Loss Goals.

	Outer Passage	Outer Dome	Center Passage	Inner Dome	Inner Passage	Mass-Weighted Average
Prediffuser $\Delta P/P$, %	1.1	-	-	-	1.1	-
Overall $\Delta P/P$, %	2.49	0.75	2.95	0.75	2.16	1.5
Turbine Backflow $\Delta P/P$, %	2.00	-	-	-	2.00	-

6.1.1.4 Water Table Model Tests

Preliminary diagnostic tests were conducted early in the program on a two-dimensional model of the diffuser using a water table. The test configuration was a three-times scale model of the fuel annular configuration which

simulated all of the key system features including prediffuser strut blockage and turbine cooling airflow extraction. The purpose of these tests was to identify any locations within the diffuser passages where regions of flow separation or instability might exist. These tests were conducted at very low Reynolds numbers compared to the engine. Therefore, the water table tests were used to obtain early diagnostic information as opposed to performance data.

The two-dimensional model of the E³ combustor passages tested on the water table is shown in Figure 94. The flow behavior around the cowl of the outer dome shows flow spillage from the dome region and flow entering the outer dome, center, and inner dome passages as visualized with dye injections and shown in Figure 95. The flow split in each of the channels was simulated by adjusting holes in a perforated plate that was inserted at the discharge of the channel. The flow rate in each channel was measured by observing the rate of movement of the injected dye with a stopwatch. The bleed flow was simulated with a plastic suction tube inserted into the hollow splitter vane. The total circulated flow was 120.7 l/min (31.9 gpm) and the bleed flow was 7.2 l/min (1.9 gpm) or 6% of the total flow.

For the initial test series on the water table, there was no evidence of flow separation or flow instability. However, considerable flow spillage from the combustor dome regions around the cowling leading edges was observed. Subsequent tests of the full-annular airflow model of the diffuser with the original cowling design indicated lower-than-expected static pressure recoveries in the outer and inner liner passages which were probably caused by the flow spillage from the cowlings. Therefore, modified versions of the cowling leading edges were tested on the water table. The outer and inner cowlings were extended to reduce the capture area of the openings. These modifications were made in two stages as illustrated in Figure 96. On the water table, the Mod I design eliminated the cowling flow spillage. Consequently, the airflow model cowling contours were changed to the Mod I design; and all of the following airflow testing was conducted with this design.

ORIGINAL PAGE IS
OF POOR QUALITY

ORIGINAL PAGE
BLACK AND WHITE PHOTOGRAPH

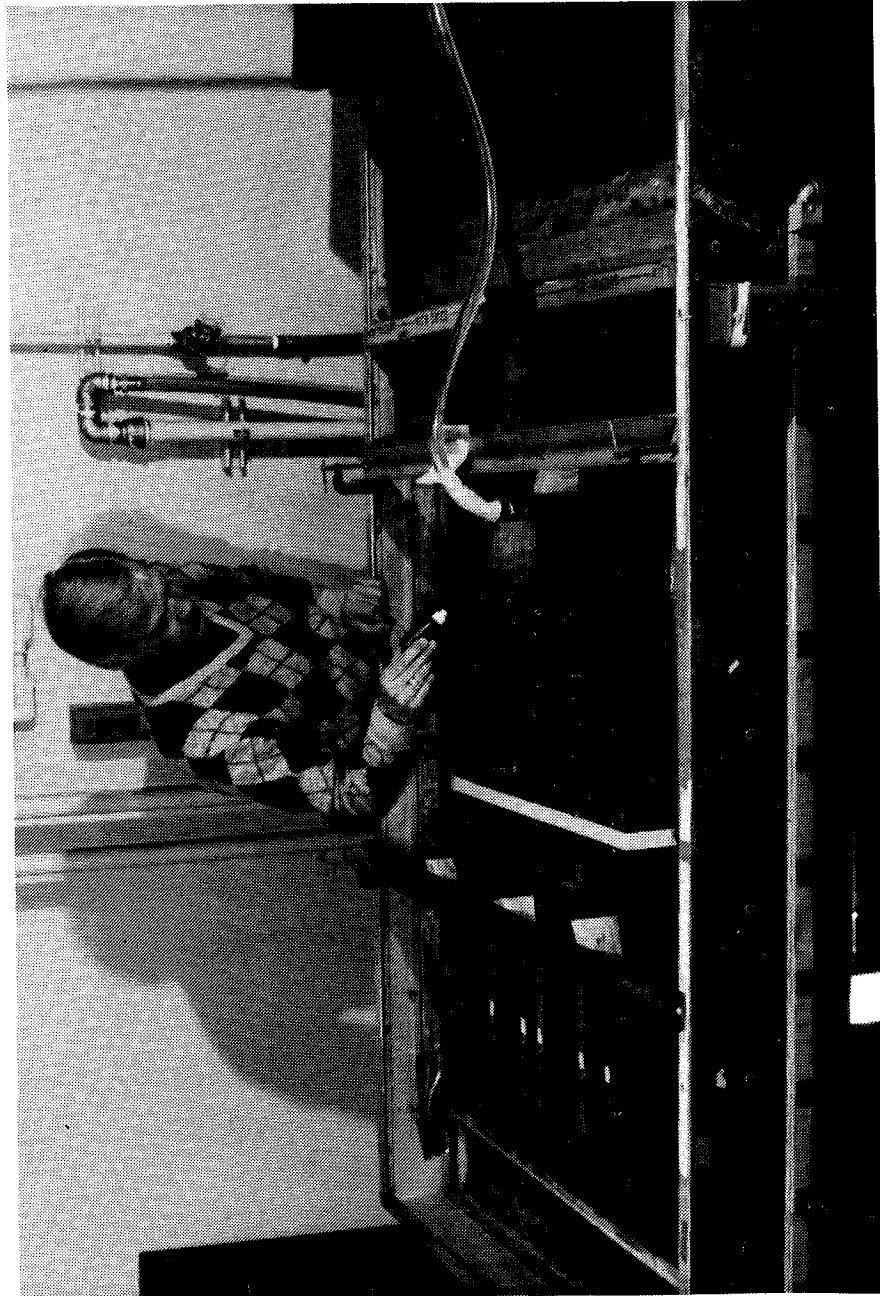


Figure 94. Diffuser Water Table Model.

ORIGINAL PAGE
BLACK AND WHITE PHOTOGRAPH

COPYING PERMITTED
BY THE AUTHOR

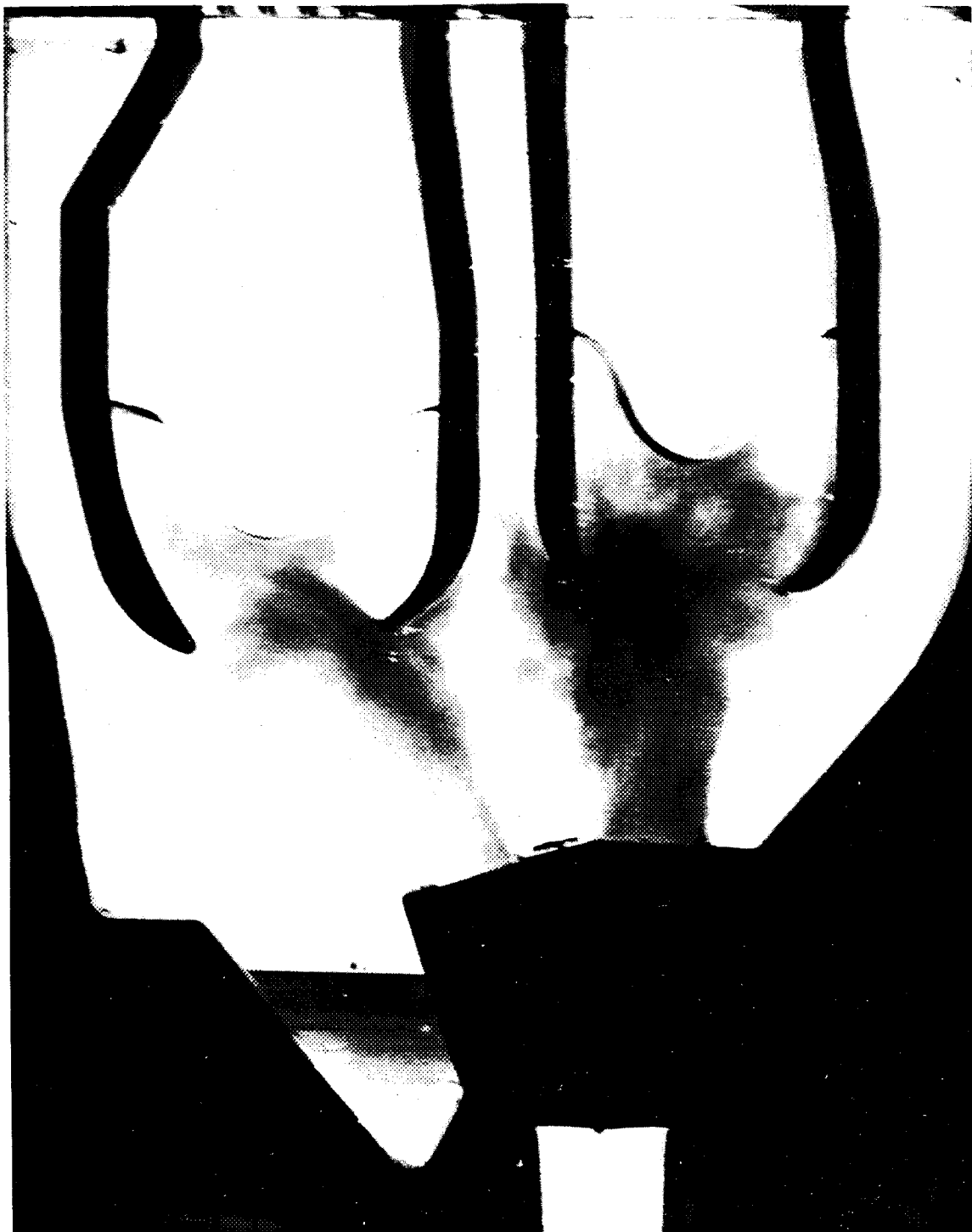


Figure 95. Split Duct Diffuser, 2-D Water Table Test.

ORIGINAL PAGE IS
OF POOR QUALITY

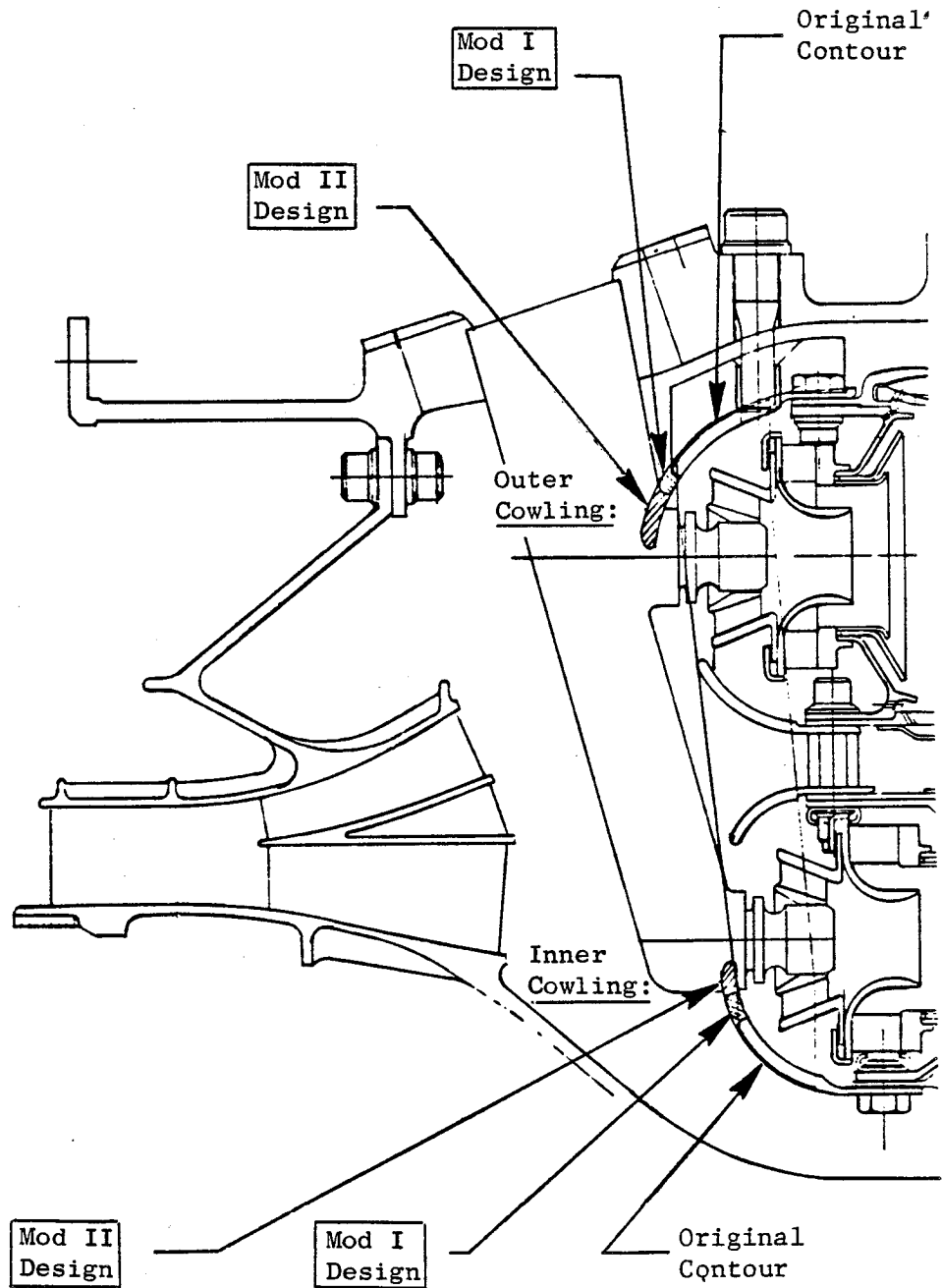


Figure 96. Combustor Cowling Modifications.

6.1.1.5 Annular Model Airflow Tests

The test facility used for the airflow testing is located in the Gas Dynamics Building at the K-1 site of GE/CR&DC. The air supply for this facility consists of four Fuller rotary vane-type air compressors. From the compressors, the air is ducted by means of 30.5 cm (12 inch) piping to a 116.8 cm (46 inch) diameter plenum chamber to which the model was attached. This chamber is equipped with screens and honeycomb to provide smooth, uniform flow to the model. The piping between the compressors and the plenum chamber is equipped with a metering section in which various size, sharp-edged orifices can be installed. This facility is capable of delivering approximately 5.23 kg/s (11.5 lb/s) of air at pressures up to 0.13 MPa (18.8 psi). (At reduced flow rates, higher pressures are available.)

For this test program, pressure measurements were made using a Scanivalve system and data logger. By automatic stepping of the Scanivalve pressure switches, the pressure from the various taps on the model were ducted to a single pressure transducer. The output of the transducer was fed to a digital voltmeter. At steady-state conditions, the data logger was automatically triggered. The output of the data logger was transmitted to a teletype readout and punched on paper tape. The paper tape was then fed to a computer for data reduction.

The E³ model assembled on its test pedestal is shown in Figure 97 and component sections of the model are shown in Figures 98 and 99.

Figure 98 shows the prediffuser discharge and strut assembly and Figure 99 shows the fuel nozzles, the combustion chamber outer passage, outer dome, center passage, inner dome, and the inner passage throttling plate with its perforated holes. This throttle plate provides the flexibility to independently vary the flow in each passage and thus determine the performance of each passage as a function of airflow quantity.

The operating conditions for the annular diffuser test were:

ORIGINAL PAGE
BLACK AND WHITE PHOTOGRAPH

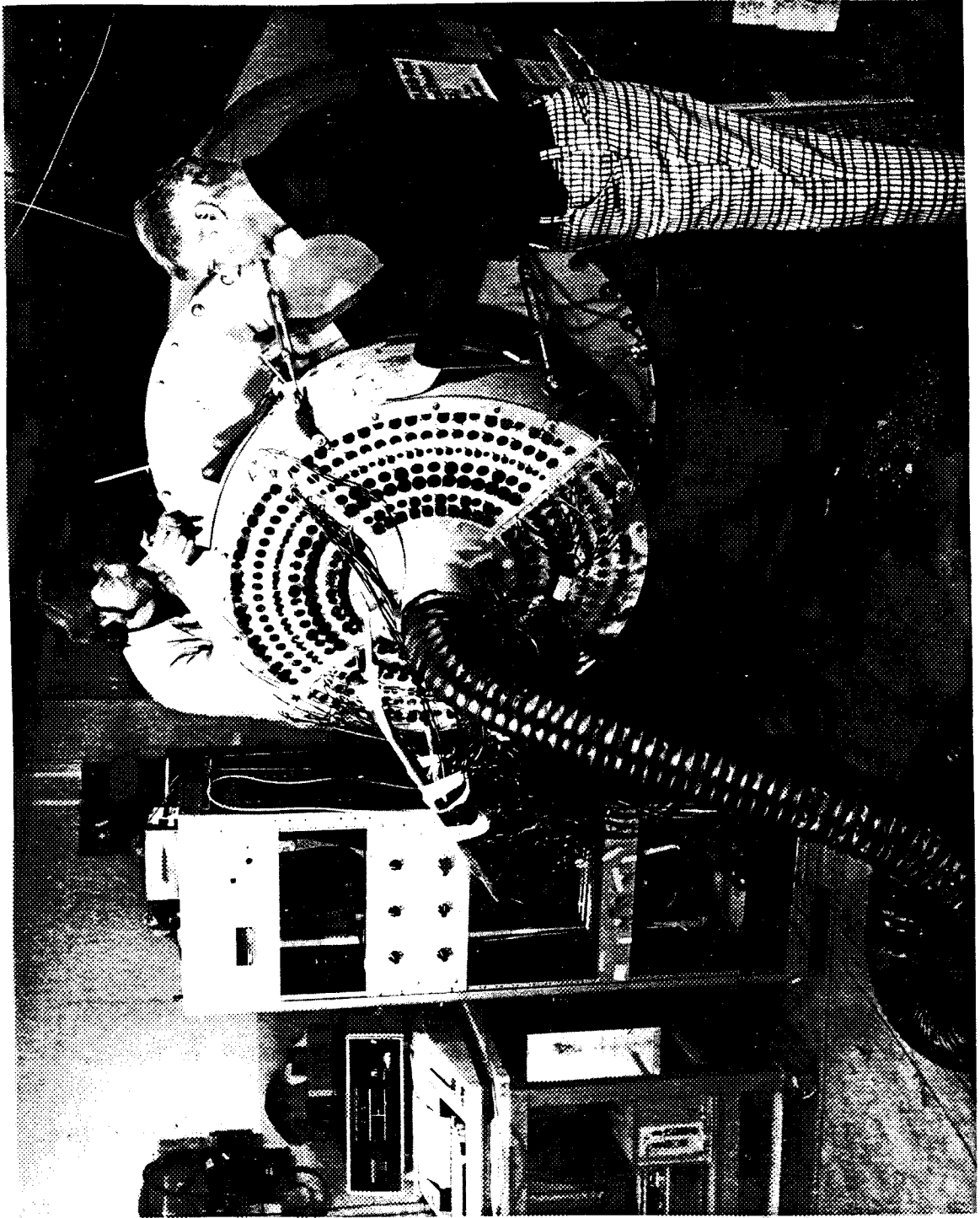


Figure 97. Diffuser Model in Test Cell.

ORIGINAL PAGE IS
OF POOR QUALITY

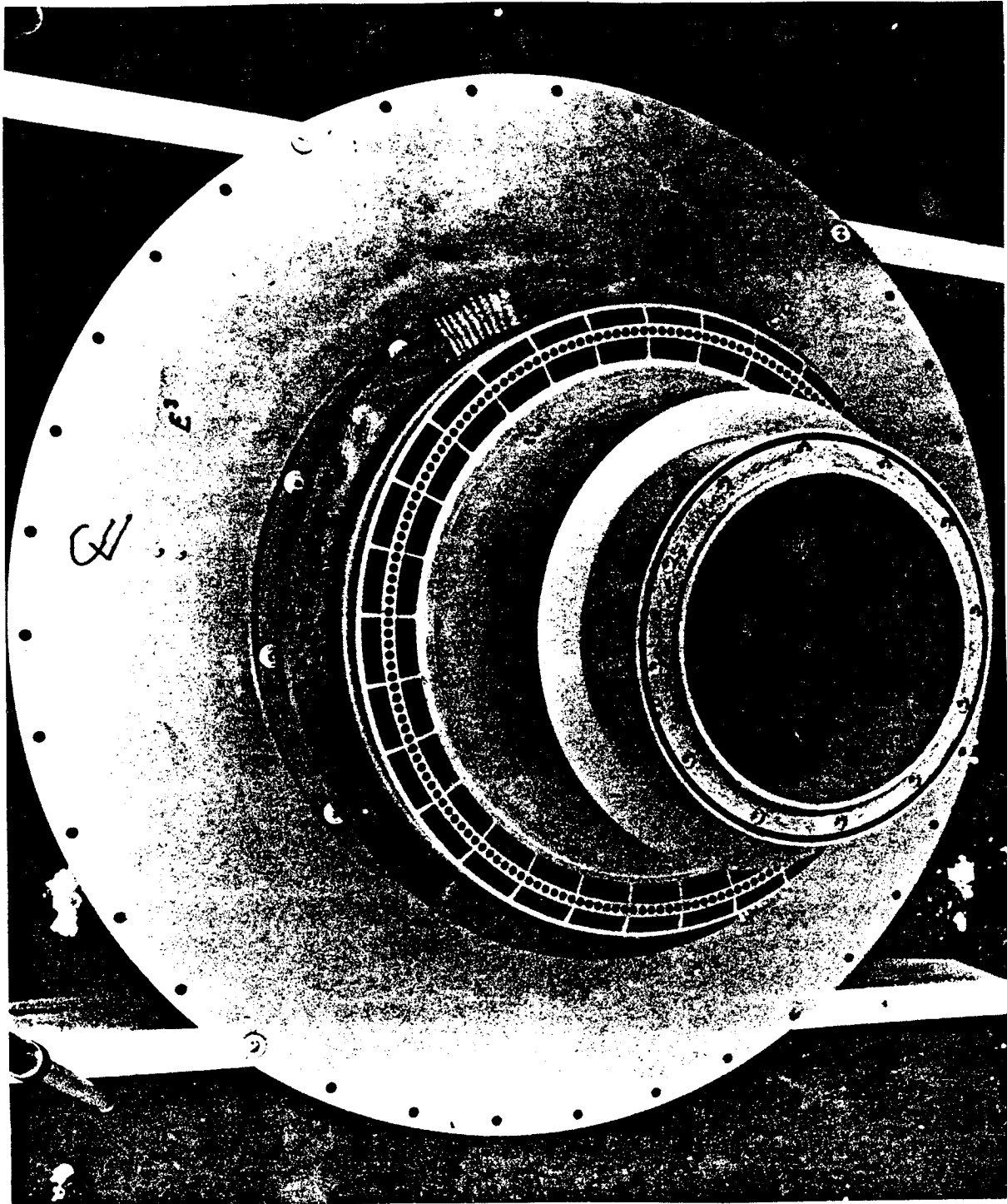


Figure 98. Diffuser Model, View Forward.

ORIGINAL PAGE IS
OF POOR QUALITY

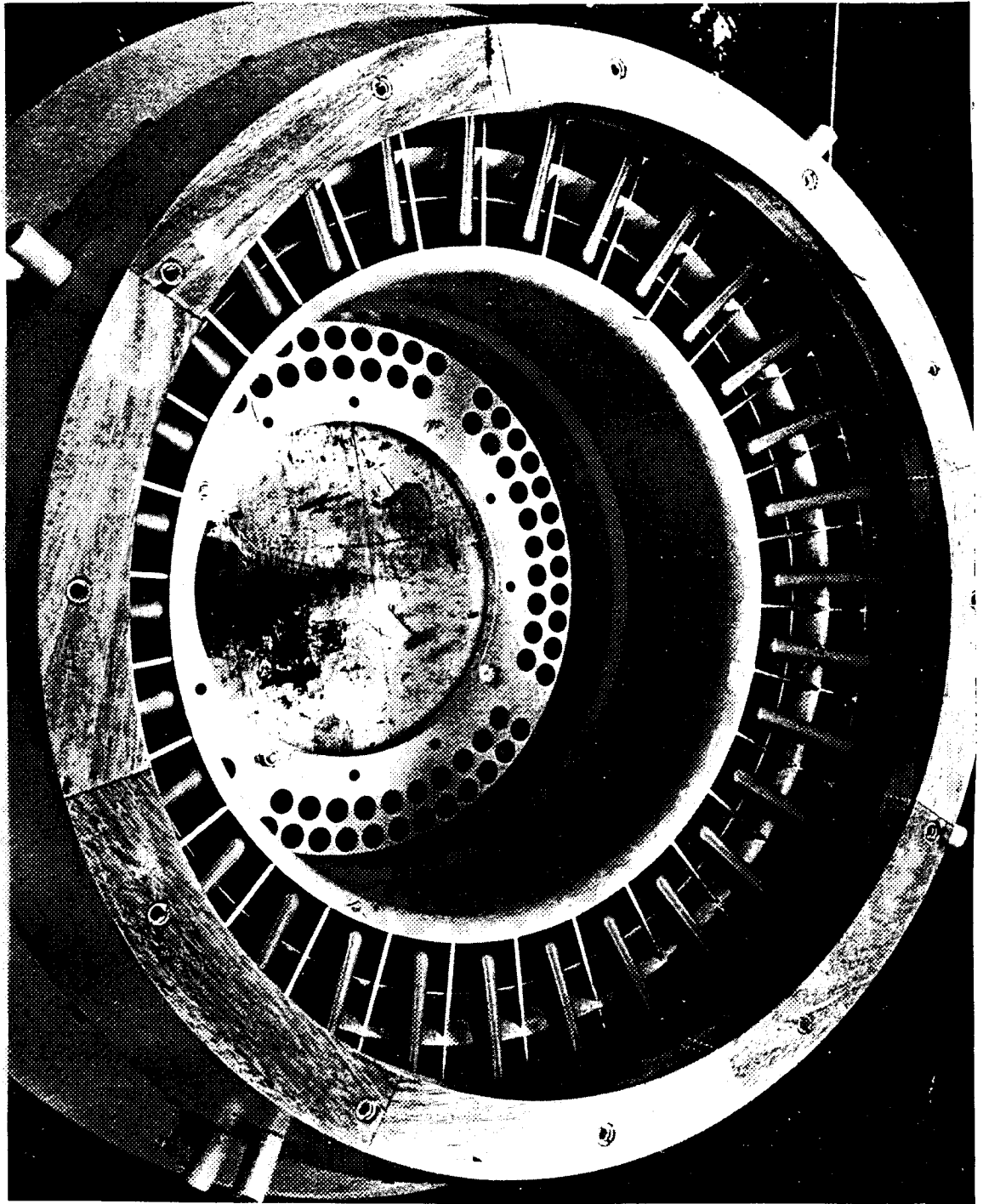


Figure 99. Diffuser Model, Aft View.

ORIGINAL PAGE
BLACK AND WHITE PHOTOGRAPH

- Airflow (W_3) = 4.5 kg/s (10 pps)
- Inlet Temperature (T_3) = Atmospheric
- Inlet Pressure (P_3) = Atmospheric
- Inlet Mach No. (M_3) = 0.30

A total of 132 static pressure taps were installed in the model. The location of these taps is shown in Figure 100, and the exact axial and circumferential positions are shown in Appendix A. The pressure taps located on the inner and outer surfaces of each of the passages were used to determine the static pressure recovery of each passage. The pressure taps located at the exit of each passage, when used in conjunction with the pressure taps located on the downstream side of the throttling plate, were used to determine passage airflow splits.

Kiel probes and hot film probes were employed to obtain the velocity profiles at the diffuser inlet plane and at the prediffuser discharge. The Kiel probe is a specially designed probe similar to that shown in Figure 101. This probe accurately measures the total pressure with minimum interference effects due to probe structure. The local velocity was calculated based on the measured total pressure and a measured wall static pressure. For the diffuser inlet profiler, a Kiel probe radial traverse was made at four equally spaced circumferential locations. The Kiel probe was traversed at nine radial stations to describe the radial velocity profile at these four circumferential locations. The hot film probe provides an indication of velocity directly based on calibration of the hot wire. The hot wire is less sensitive to flow direction than the Kiel probe, since it operates on an electrical resistance principle and essentially measures absolute velocity. However, it is sensitive to contamination from foreign substances which might be entrained in the air. Therefore, it was used only for the prediffuser discharge where measurement normal to the airflow would be difficult.

A series of calibration runs was made to calibrate each of the five passage exits to determine the variation of airflow with pressure drop across the orifice plate for several discharge orifice plate openings as represented by the different corking arrangements (that is, number of exit holes corked). The procedure used to perform these calibrations was to seal off four passage

ORIGINAL PHOTO OF
OF POOR QUALITY

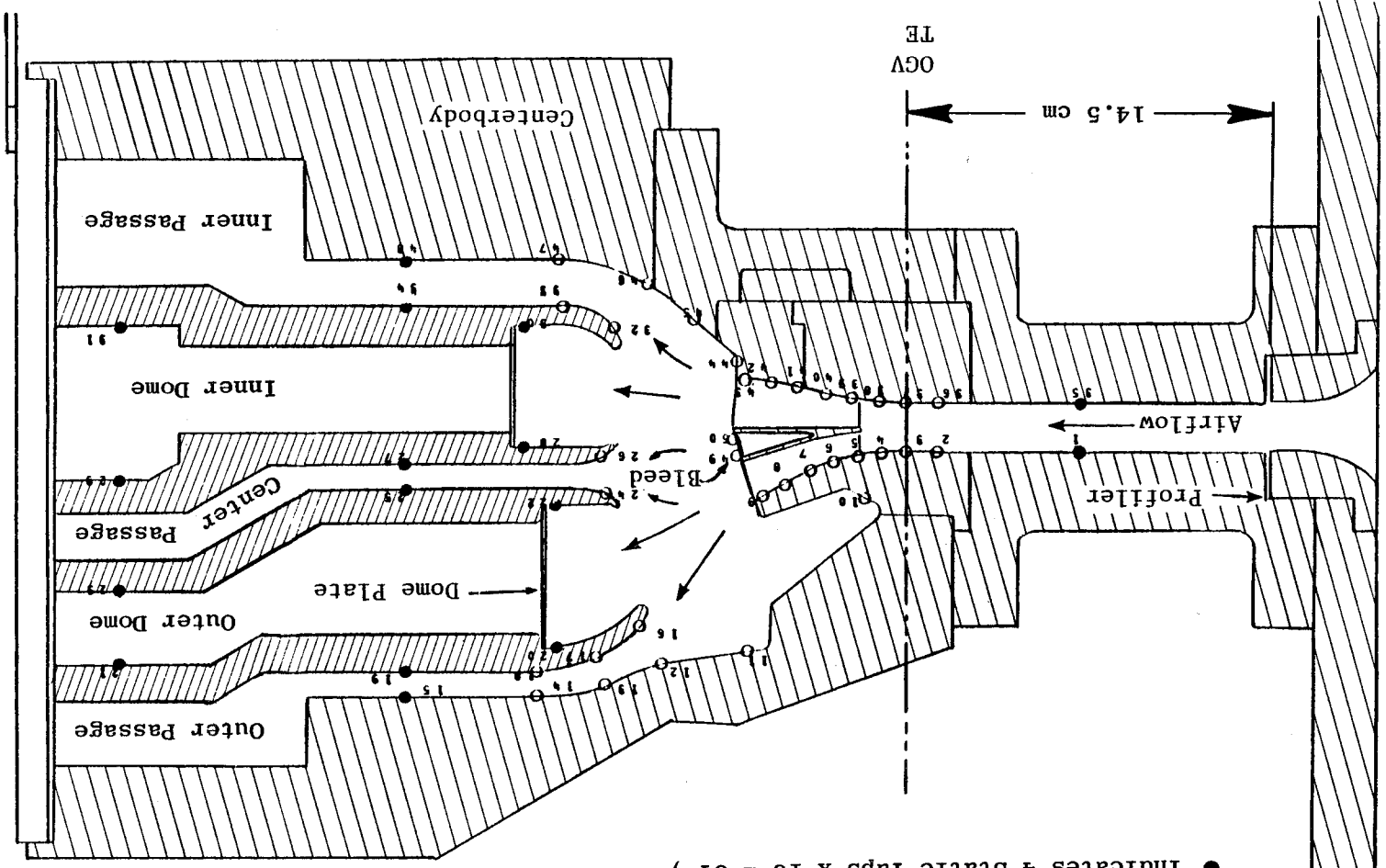
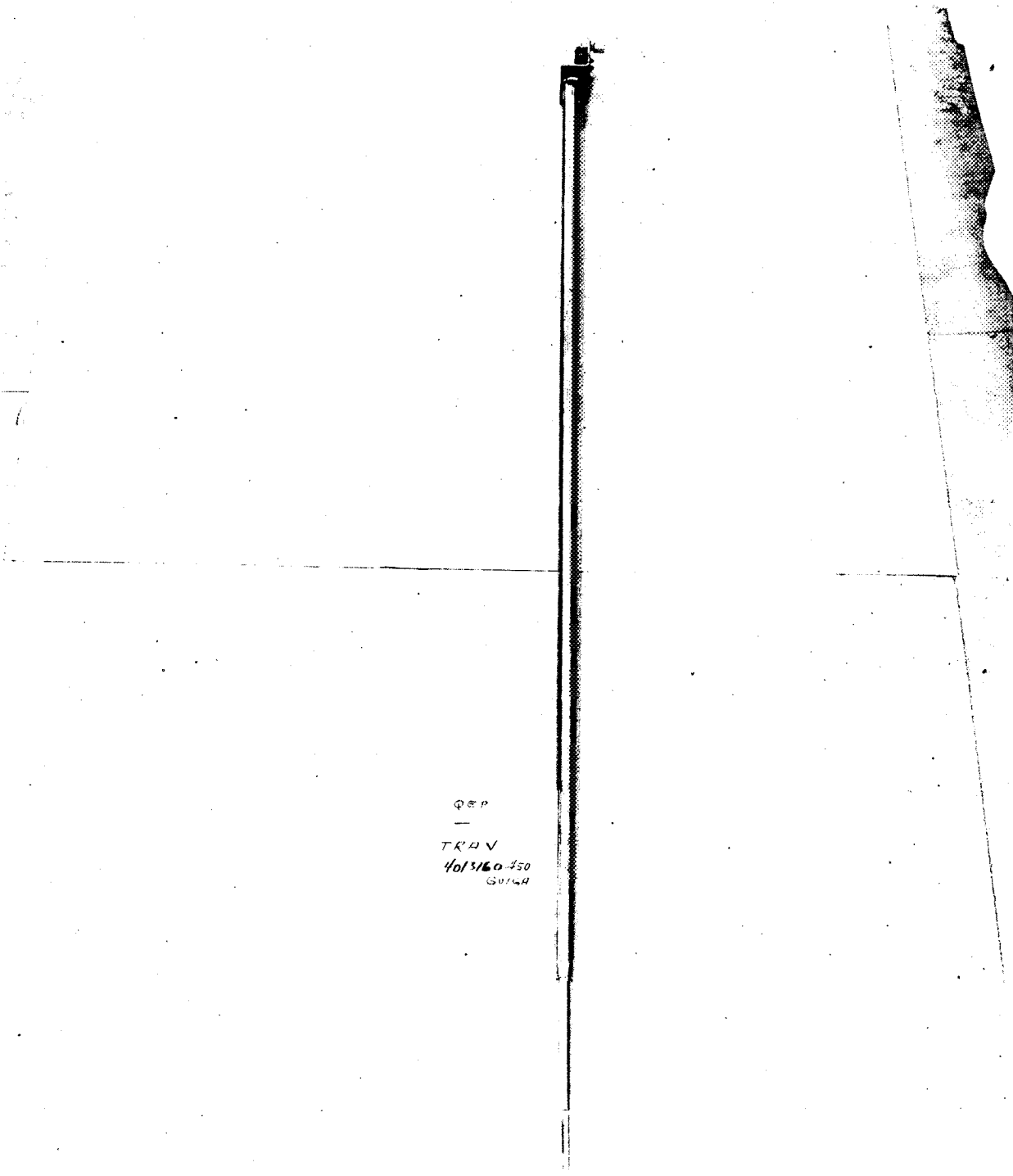


Figure 100. Annular Diffuser Model Instrumentation Layout.

○ Indicates 2 Static Taps x 34 = 68
● Indicates 4 Static Taps x 16 = 64
132 Taps Total

ORIGINAL PAGE IS
OF POOR QUALITY



QEP
—
TKAV
1015160-150
G0140

Figure 101. Keil Probe.

exits while calibrating the fifth. For each exit orifice place flow area, a discharge coefficient was computed as a function of airflow rate. These discharge coefficients were then plotted and a curve fit of the form

$$C_D = \alpha_1 \sqrt{\Delta P} + \alpha_0$$

was obtained, where

C_D is discharge coefficient

ΔP is pressure drop across orifice plate

α_1, α_0 are coefficient which best correlated the data.

Finally, the coefficients, α_1 and α_0 were plotted as a function of flow area and were fitted by a least squares polynomial curve fit. This procedure was followed for each of the five passages. The values obtained are shown in the tabulation below:

	<u>Outer Liner</u>	<u>Outer Dome</u>	<u>Centerbody</u>	<u>Inner Dome</u>	<u>Inner Liner</u>
α_0	0.0136	0.0176	0.00523	0.0208	0.0137
α_1	-0.0007	-0.000112	-0.0000485	-0.00015	-0.00006

The static pressure recovery of each of the five passages was based on the differential pressure between the average of the inner and outer surface of each of the passages and the prediffuser upstream static pressure. The flow split in the five passages was evaluated from the static pressure instrumentation located at each of the passage discharge stations and static pressure taps located just downstream of the orifice plate.

The pressure data recorded during the test of the E³ model were fed into a computerized data reduction program to obtain the performance characteristics. The performance characteristics computed fall into a number of basic categories as discussed below.

Based on the measured airflow to the model and the average inlet pressure, the average inlet velocity and Reynolds number were calculated. The

Reynolds number was based on the hydraulic diameter of the passage, that is, two annular passage heights. The amount of bleed flow was calculated from the air temperature and the measured pressures upstream and downstream of the 10.2 cm (4 inch) bleed flow orifice.

Flow split runs were made for each of the five passages of the E³ combustor diffuser model. The nominal flow splits selected for evaluation in the tests were evolved during the preliminary design phase of the combustor. These flow splits were selected based on design considerations including emissions, performance, and flowpath requirements. The design percentage flow split level for each passage is shown below:

	<u>% W₃</u>
Outer Channel	16.2
Outer Dome	24.4
Center Dome	9.15
Inner Dome	29.18
Inner Channel	15.25
Bleed Flow	5.82

The flow split level percentage was first obtained by varying the number of corks in the discharge orifice plate of each passage. The off-nominal flow setting of the outer channel was then varied while the flow areas at the discharge orifice plate of the other four channels was held fixed. This procedure was followed to obtain four off-nominal flow settings for the outer passage. In a similar manner, off-nominal settings for the other four passages were made. The sum of the five passage flows was added to the bleed flow, and the total airflow was then compared to that measured with the airflow supply upstream orifice plate to give an indication of the accuracy of the results. The airflow error for each test generally ranges from 2% to 3%.

One measure of the performance of the diffuser is provided by the surface static pressure coefficient distribution within the diffuser. This coefficient was determined for all pertinent wall static measurements and was defined as:

$$C_{PW} = \frac{P - P_{S_{inlet}}}{(1/2)\rho \bar{V}_{inlet}^2} = \frac{P - P_{S_{inlet}}}{\bar{q}_{inlet}}$$

where PS_{inlet} is the average of the inlet static pressures, P is the measured wall static pressure, and \bar{q} is the dynamic head based on the area-averaged inlet velocity.

An important measure of the performance of a diffuser passage is the degree of passage static pressure recovery. For this purpose, a passage static pressure recovery coefficient, C_{pp} , was defined using the same expression as used for the wall static pressure recovery:

$$C_{PP} = \frac{P - PS_{inlet}}{(1/2)\rho\bar{V}_{inlet}^2} = \frac{P - PS}{\bar{q}_{inlet}}$$

where in this definition P is the average of the static pressures measured at the point in the passage where the recovery is to be determined.

A measurement of the performance of the complete combustor diffuser is given by the mean total pressure loss coefficient, C_{pT} , defined as follows:

$$\begin{aligned} C_{pT} &= \frac{PT_{inlet} - PT}{\bar{q}_{inlet}} = \bar{w} \\ &= \frac{(PT_{inlet} - PS_{inlet}) - (PS - PS_{inlet}) - (PT - PS)}{\bar{q}_{inlet}} \\ &= (1 - C_p) - \frac{q}{\bar{q}_{inlet}} \end{aligned}$$

where PT and PS are the total and static pressures, respectively, in the passage where the pressure recovery was determined, q is the dynamic pressure at the same point and C_p is the static pressure recovery.

Since there are five passages (outer passage, outer dome, center passage, inner dome, and inner passage), the mean total pressure loss coefficient was calculated using the mass weighted average

$$C_{PT\ mean} = \frac{\sum_{n=1}^5 W_n C_{PT\ n}}{\sum_{n=1}^5 W_n}$$

where W_n is the flow rate in passage n and (C_{PT}) is the corresponding total pressure loss coefficient.

The full-annular airflow tests were conducted with three different inlet velocity profiles. These inlet velocity profiles were generated by profilers installed in the inlet passage. Schematics of the profiles used are shown in Figure 102. These velocity profiles, as illustrated in Figure 103, had peak velocities near the outer wall, in the center, and near the inner wall of the inlet section of the diffuser. Velocity profiles at the E³ compressor exit station are expected to be similar to the center peaked profile.

During the initial testing of the diffuser model, some very unexpected and disappointing results were obtained for the measured inlet velocity profiles and the diffuser performance. A posttest inspection of the diffuser model revealed a separation of the 30 struts from the outer flowpath (pilot stage) of the diffuser mode. Further investigation revealed the source of the strut failure and unexpected poor diffuser performance levels. The air loading on the test rig centerbody was of sufficient magnitude to deform the inlet plenum support struts and permit the test rig centerbody to move aft approximately 0.25 cm (0.098 inch). Not only did this result in prediffuser strut failure at the wall, it also resulted in an off-design prediffuser area ratio. The surprising outboard peaked velocity profiles obtained with the center peaked profiler were the result of the lower edge of the profiler shifting downstream directing the airflow toward the outer wall. The diffuser

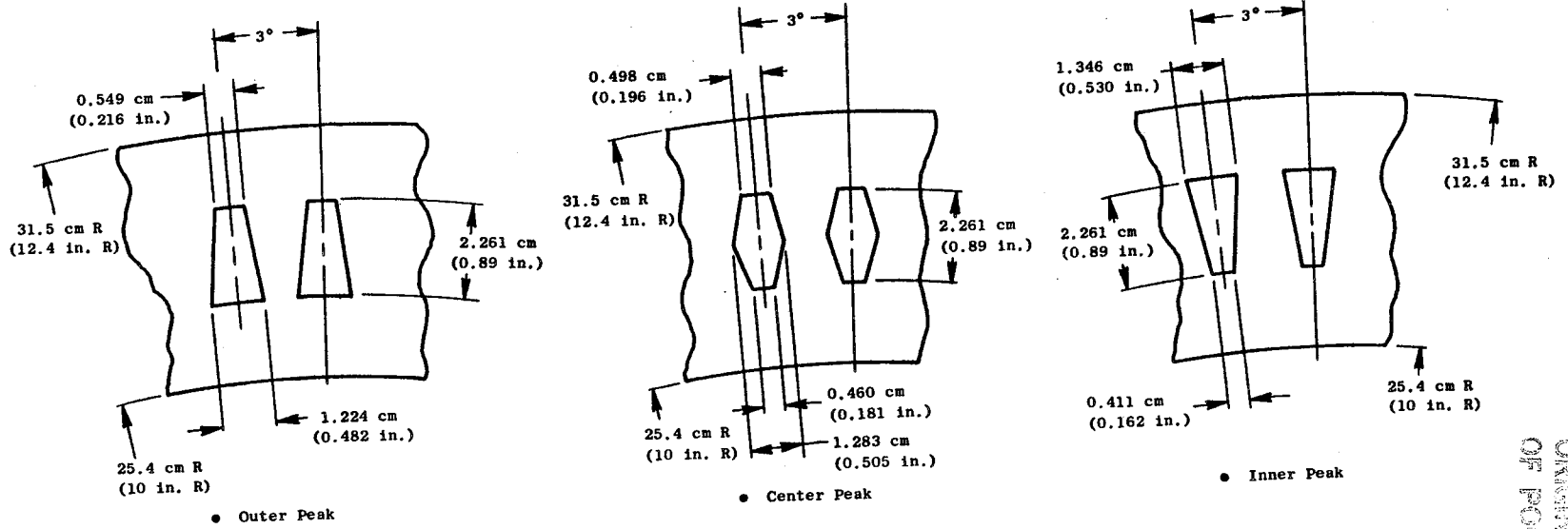


Figure 102. Diffuser Inlet Velocity Profiles.

ORIGINAL PAGE IS
OF POOR QUALITY

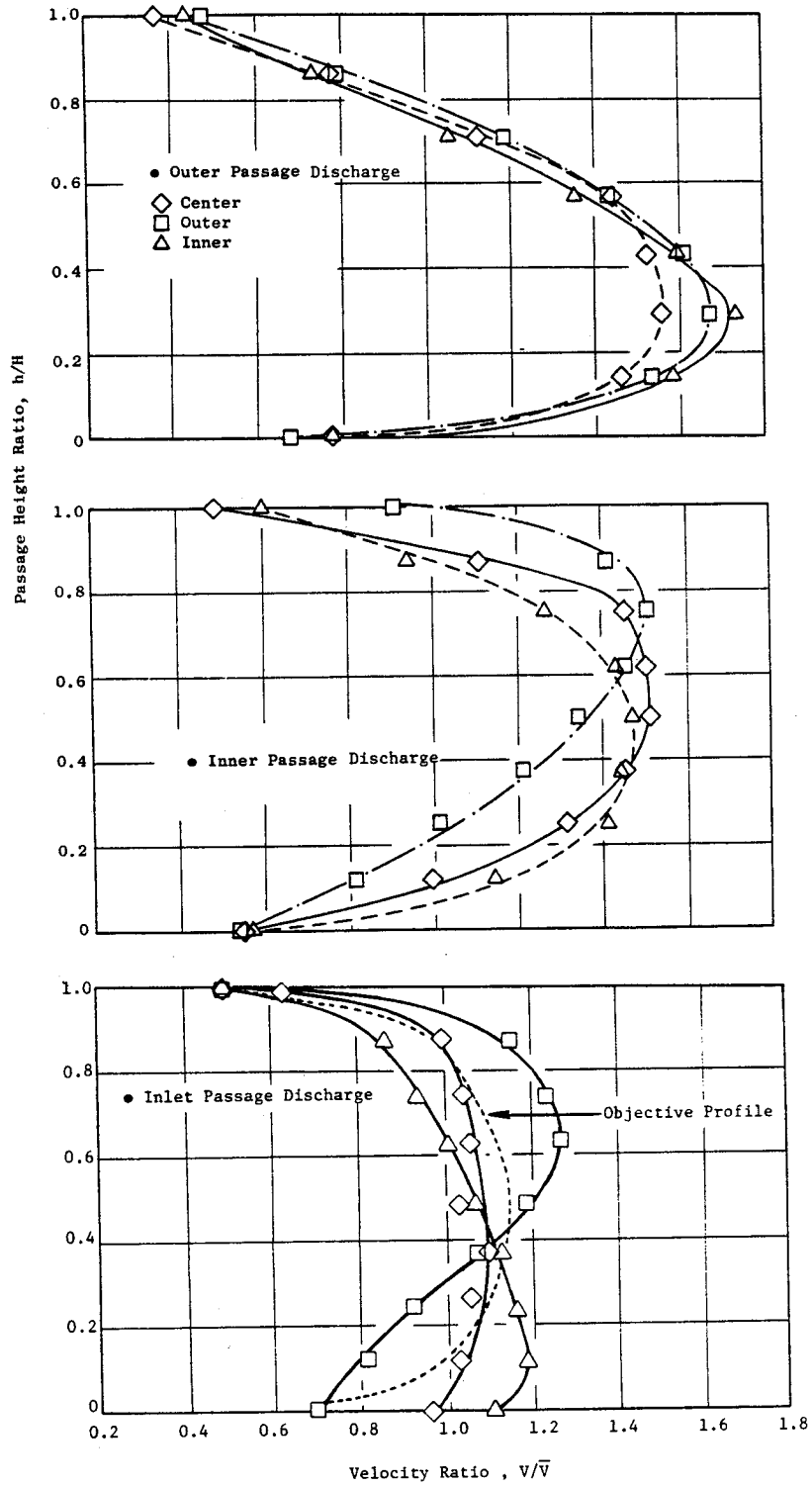


Figure 103. Prediffuser Velocity Profiles.

model was repaired and a method was incorporated to strengthen the test rig to prevent deflection of the inlet struts and retain the axial location of the centerbody. Testing with the refurbished diffuser model and reinforced test rig was then resumed.

Static pressure recovery levels in each of the five E^3 diffuser passages are presented in Figure 104 as a function of the flow level in the passage with the center peaked inlet velocity profile. Recovery levels with the outer peaked inlet velocity profile are presented in Figure 105 and recovery levels with the inner peaked inlet velocity profile are presented in Figure 106. Each of these sets of static pressure recovery curves represents a summary of all of the individual passage test runs. Static pressure recovery curves for each one of the individual passage test runs are included as Figures B-1 through B-15 in Appendix B.

As illustrated in Figure 104 for the center peaked profile, the static pressure recovery levels in all of the passages are very high at the design level flow conditions, although the outer passage recovery and the dome flow recoveries are not quite as high as anticipated. The dome recoveries were expected to be about 0.85 and the outer passage recovery was expected to be about 0.50. The inner passage recovery is very close to the expected value, and the center passage recovery is higher than the expected value. These results are similar to those of several previous diffuser test programs. The consistent results and the high recovery levels indicate that the flow in this diffuser is very stable and that the prediffuser does not have regions of flow separation.

With the outer peaked and inner peaked inlet velocity profiles, the recovery levels are higher than those with the center peaked profile. Recovery levels in the outer passage and outer dome region were considerably higher with the outer peaked profile, as anticipated. However, the recovery levels were higher in the inner passage, inner dome region, and in the center passage also. With the inner peaked profile, recovery levels were much higher in the inner passage and inner dome region as may be expected but were also higher in the outer passage and in the center passage. The most probable reasons for these high recovery levels are the high turbulence levels generated by the

● Center Peaked Profile

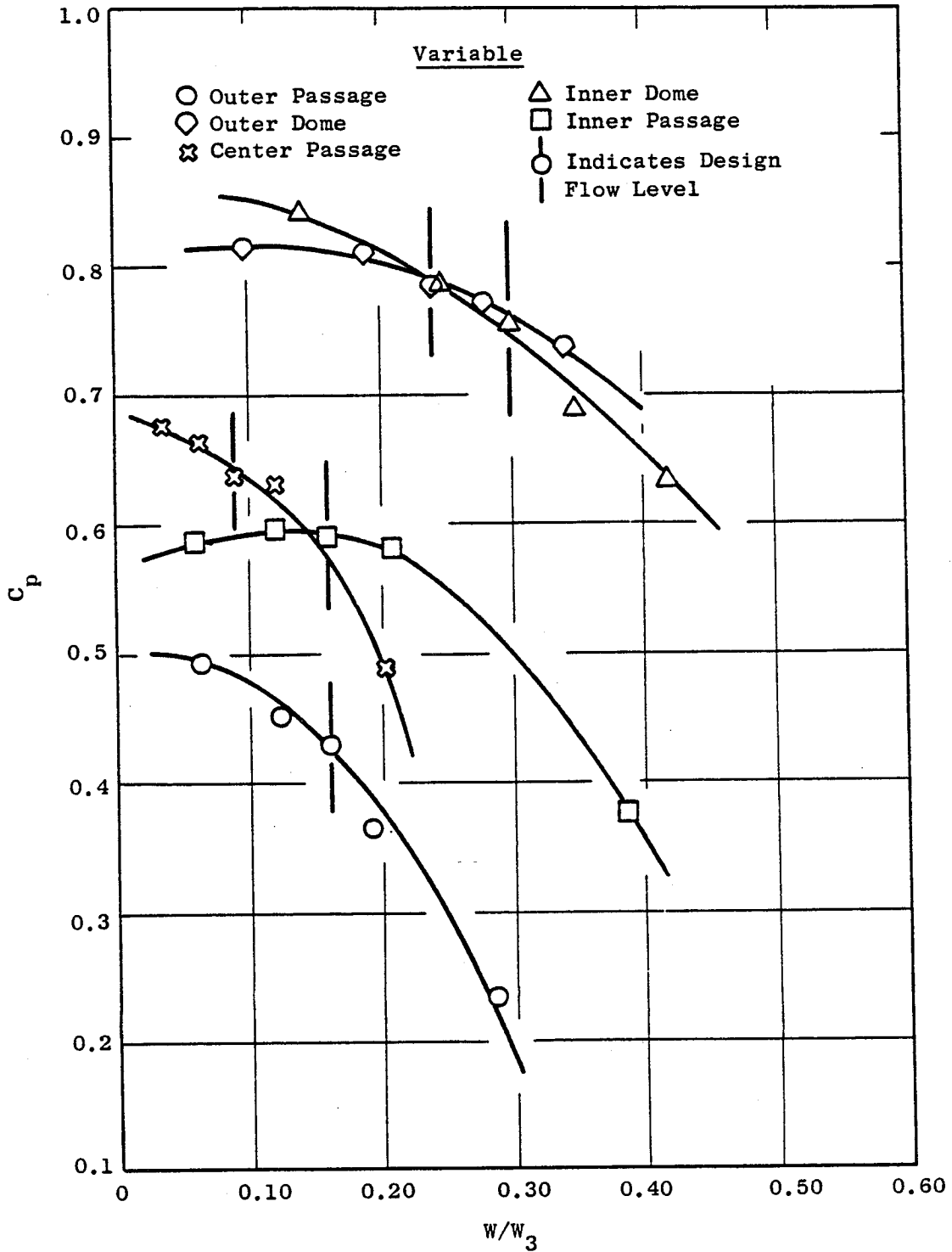


Figure 104. Static Pressure Recovery Levels, Center Peaked Profiles.

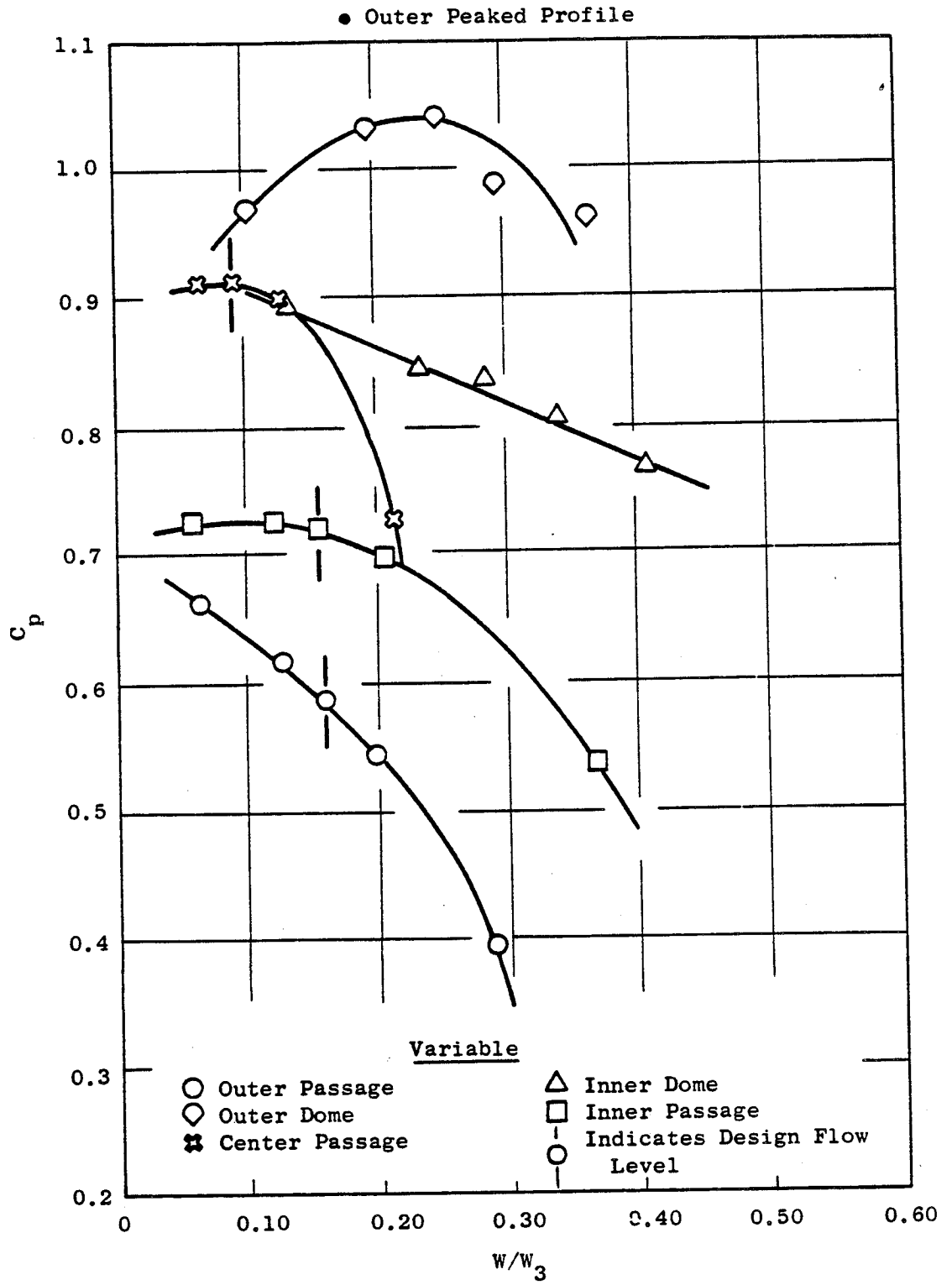


Figure 105. Static Pressure Recovery Levels, Outer Peaked Profile.

● Inner Peaked Profile

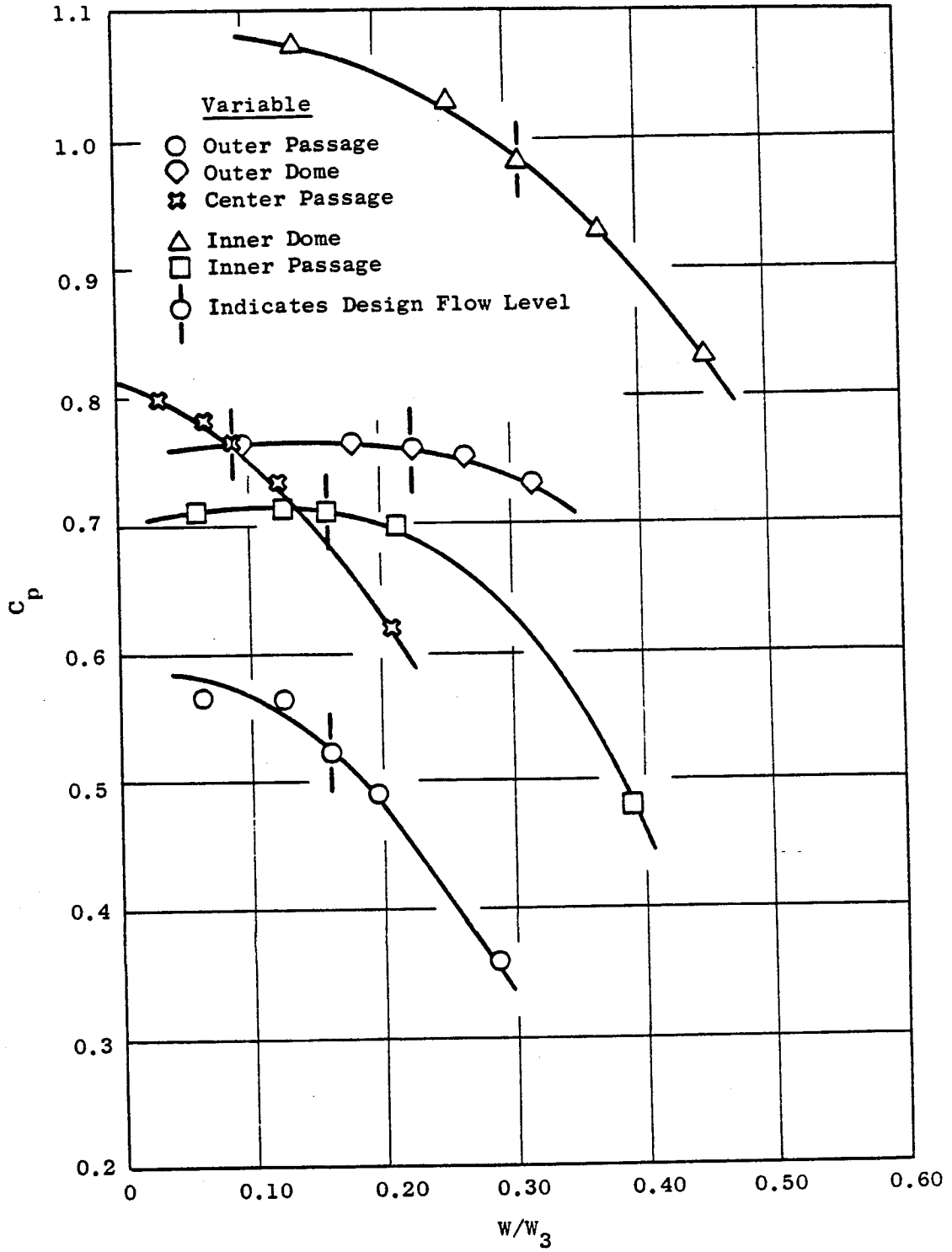


Figure 106. Static Pressure Recovery Levels, Inner Peaked Profile.

blockage elements of the inlet velocity profilers. Higher turbulence levels usually improve diffuser performance (References 5 and 6). The blockage elements of the outer and inner peaked profilers were larger than those for the center peaked profile and would generate larger scale turbulence.

All of the static pressure recovery curves have negative slopes at the design point flow conditions. This is an indication of a high degree of flow stability in the passages and low sensitivity to combustion system resonance effects.

Static pressure rise coefficients, measured with the pressure taps located along the outer and inner prediffuser and combustor casing walls, are presented in Figure 107 for design flow conditions with the center peaked inlet velocity profile. Similar curves for the outer peaked profile and for the inner peaked profile are presented in Figures 108 and 109, respectively. The initial reduction in static pressure, immediately downstream of the diffuser inlet, shows the effects of the diffuser wall curvature and the blockage of the strut and splitter vane leading edges. The static pressure increases strongly along the prediffuser walls to the end of the prediffuser. The pressure in the bluff base region of the splitter vane is somewhat higher than in the other base regions which may account for the higher-than-expected recovery levels in the center passage.

In the inner diffuser passage adjacent to the inner cowling, the static pressure continues to rise due to passage velocity profile mixing. In the outer passage, however, the static pressure drops sharply behind the fuel nozzle stems which is an indication of parasitic drag losses in this passage. The drag loss is probably caused by the fuel nozzle stems and the combustor mounting struts.

Total pressure loss coefficients for each of the five diffuser passages are presented in Figure 110 as a function of the flow levels in the passages. These curves are plotted for the center peaked velocity profile. The total pressure loss of any particular passage is the product of the total pressure loss coefficient for that passage and the diffuser inlet velocity head which, for the E^3 at sea level static conditions, is 5.78% of the compressor exit total pressure.

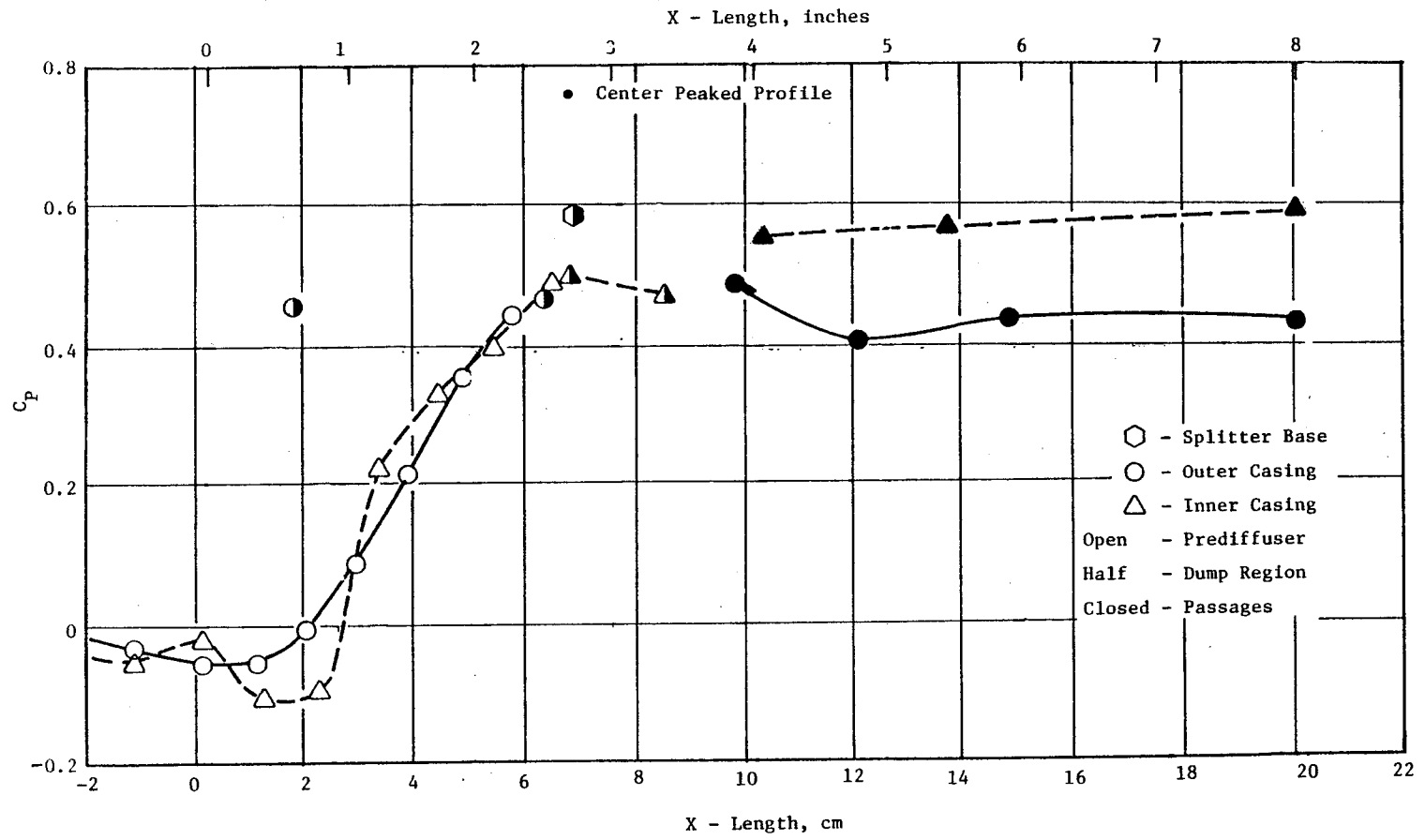


Figure 107. Static Pressure Rise Coefficients, Center Peaked Profile.

ORIGINAL PAGE IS OF POOR QUALITY

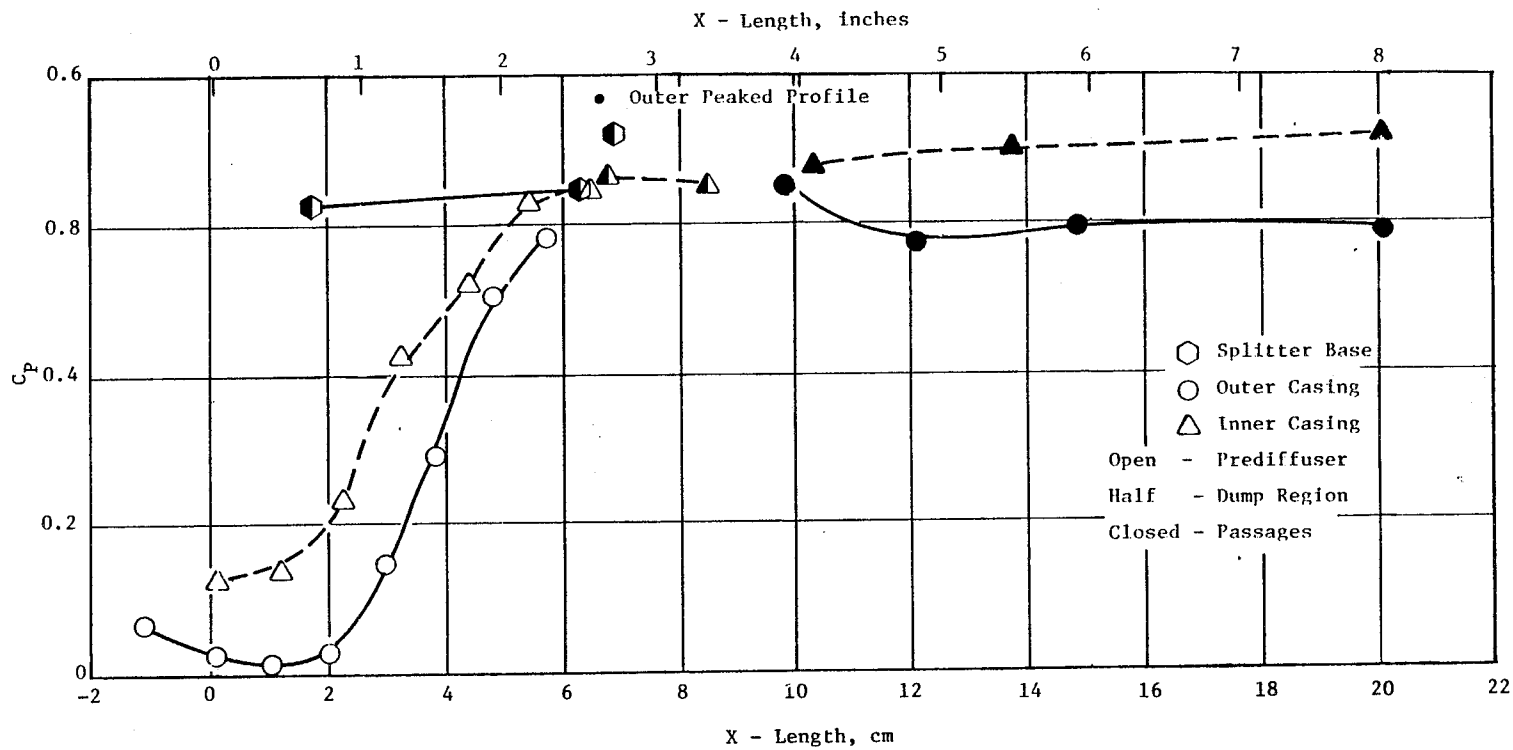


Figure 108. Static Pressure Rise Coefficients, Outer Peaked Profile.

ORIGINAL PAGE IS
OF POOR QUALITY

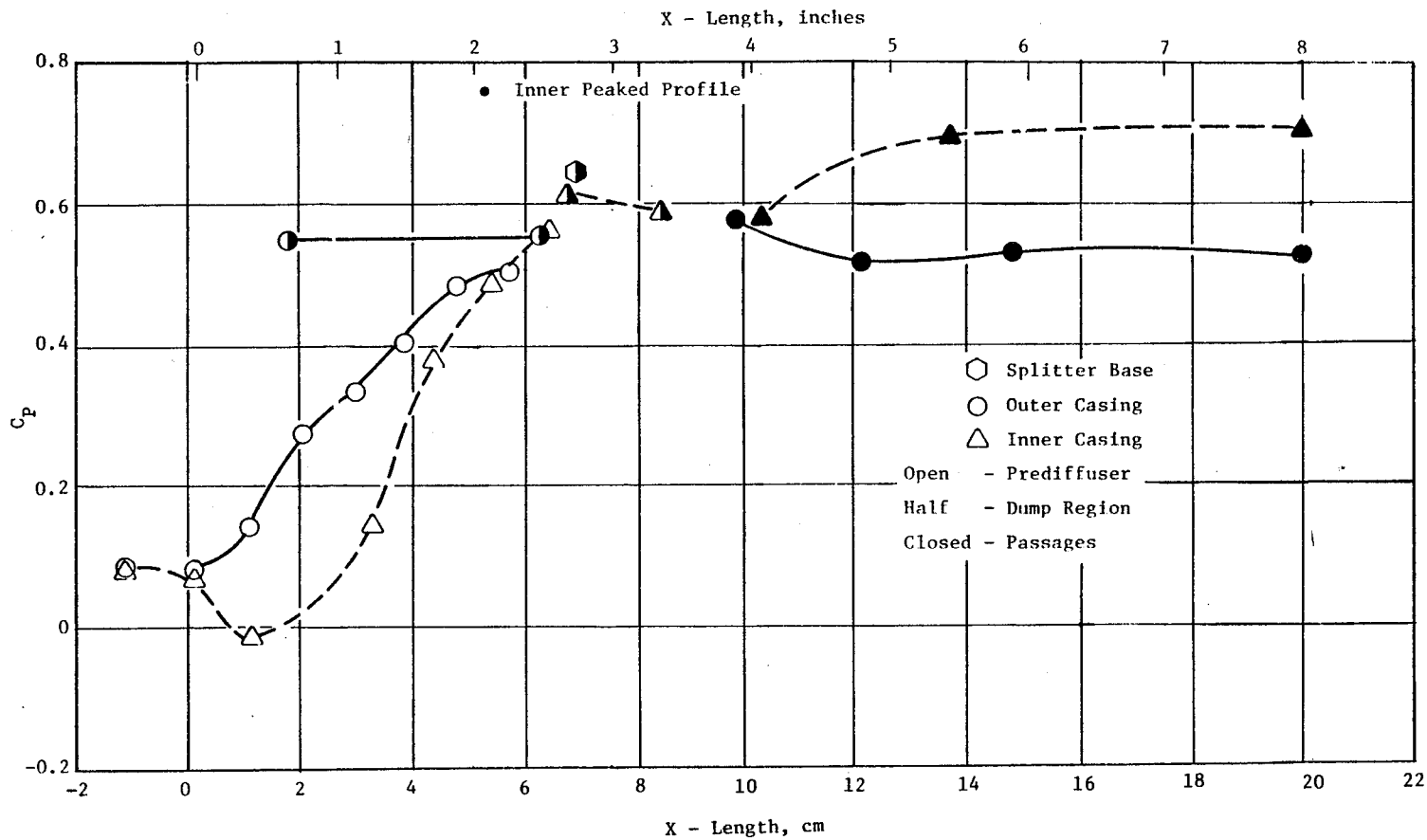


Figure 109. Static Pressure Rise Coefficients, Inner Peaked Profile.

ORIGINAL PAGE IS
OF POOR QUALITY

ORIGINAL PAGE IS
OF POOR QUALITY

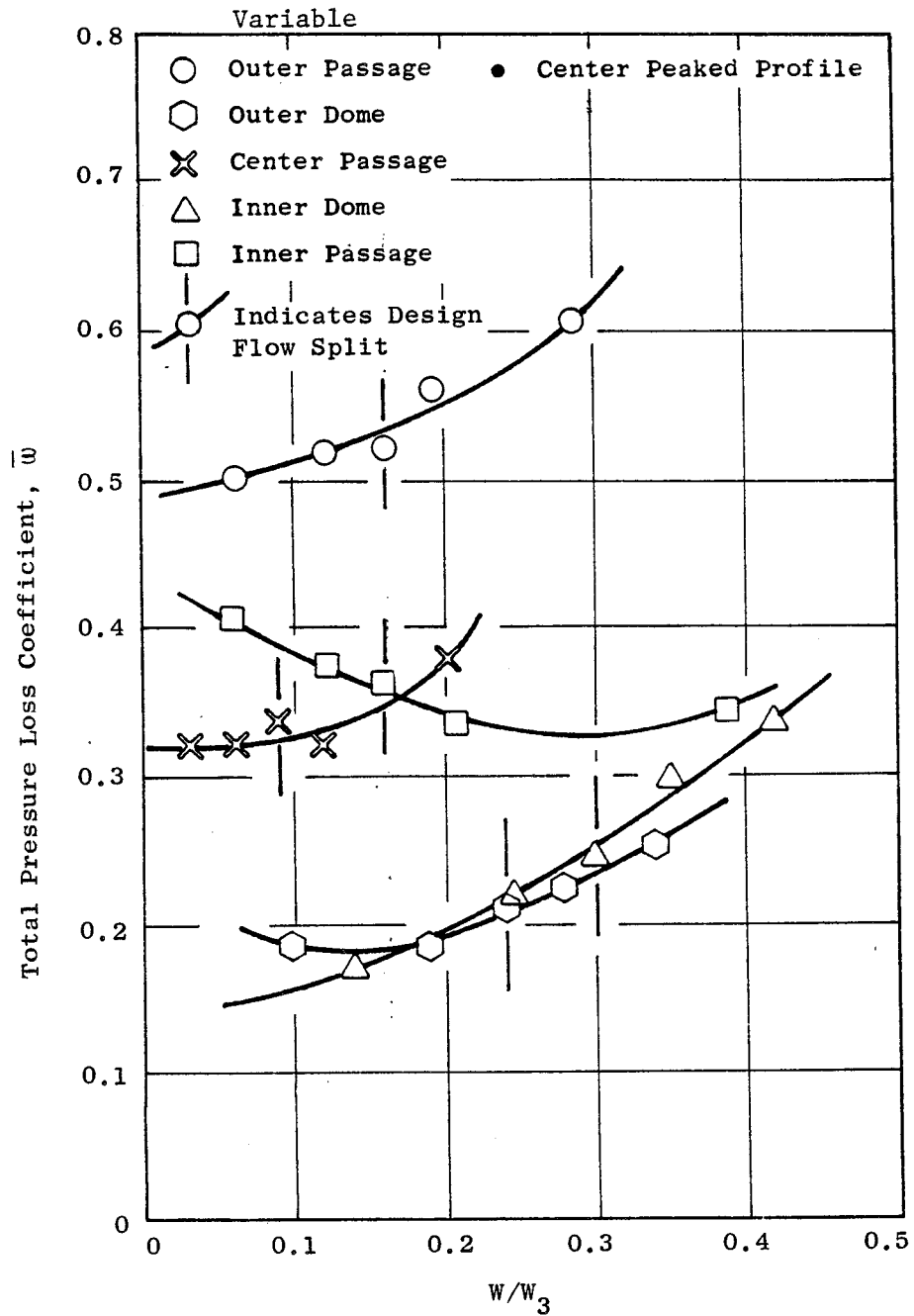


Figure 110. Total Pressure Loss Coefficients, Center Peaked Profile.

These curves also show the effects of parasitic drag losses in the outer diffuser passage. In the inner passage, as the flow is increased, the total pressure loss coefficient decreases because the effective dumping area ratio is reduced. However, in the outer passage, the pressure loss coefficient increases with increased flow, which is an indication of increased drag losses.

These total pressure loss coefficient curves were used to calculate the diffuser passage total pressure losses for the E³ at sea level static conditions. These values are presented in Table XXII where the measured diffuser pressure losses are compared to the values that were predicted prior to the test program. The overall mass-weighted loss is very close to the predicted value but the measured outer passage pressure loss is about 0.5% higher than the predicted value. This increment in total pressure loss is most likely associated with the higher-than-expected parasitic drag losses associated with the fuel nozzle bodies.

Table XXII. Diffuser Performance With Center, Outboard, and Inboard Peaked Profiles.

- Diffuser Bleed
- Ambient Test Conditions
- Nominal Flow Split

	Outer Passage	Outer Dome	Center Passage	Inner Dome	Inner Passage	Mass-Weighted Average	Inlet Velocity Profile
Passage $\Delta P/P$	3.06	1.21	1.88	1.44	2.08	1.81	Center Peaked
	2.47	1.43	1.21	0.08	1.44	1.17	Inner Peaked
	2.07	0.03	1.22	1.00	1.32	1.31	Outer Peaked
Goal	2.49	0.75	2.95	0.75	2.16	1.50	Center Peaked
Turbine $\Delta P/P^*$	1.60				2.55		Center Peaked
	2.10				3.20		Inner Peaked
	2.50				3.32		Outer Peaked
Goal	2.00				2.00		Center Peaked
*Backflow Margin							

Two other aspects of the diffuser performance were also investigated which related to off-design performance of the baseline diffuser configuration. First, the impact of the absence of diffuser bleed at the base of the splitter was evaluated. Second, the effect of a uniform, low level, turbulent inlet velocity was investigated by removing the profiler located upstream of the splitter vane. As expected, the absence of prediffuser bleed had very little effect on the diffuser performance. However, as shown in Table XXII, the uniform inlet velocity produced significantly poorer results than obtained with the nominal flow split design with a center peaked profiler in place. This performance deficiency is attributed to the very long undisturbed inlet passage which exists without the profiler. A very thick, low energy, laminar, boundary layer builds up in this passage which is easily separated from the walls as the passages diffuse. However, in the engine installation, the turbulence levels are expected to be much higher than experienced in the test rig due to the rotating machinery. Therefore, the turbulence levels in the rig with the profilers in place are more similar to what is expected in the engine application.

Table XXIII. Diffuser Model Performance Comparison.

- Nominal Flow Split
- Ambient Test Conditions
- Center Peaked Profile

	Outer Passage	Outer Dome	Center Passage	Inner Dome	Inner Passage	Mass-Weight Averaged
Baseline Configuration ($\Delta P/P$)						
● Bleed	2.97	1.19	1.90	1.27	2.09	1.74
● No Bleed	2.98	1.11	2.01	1.38	2.11	1.66
● No Profiler	3.98	1.16	2.75	1.47	3.03	2.07
Goal	2.49	0.75	2.95	0.75	2.16	1.50

6.1.1.6 Conclusions

Based on the results of the E³ diffuser model test program, it was concluded that:

1. The performance of the E³ combustor inlet diffuser design is satisfactory and meets the requirements of the E³.
2. The annular splitter vane used to design a short-length, high-area-ratio combustor inlet diffuser has good performance with stable, stall-free operation.
3. Combustor dome cowling designs must be carefully executed to provide high pressure recoveries with minimum flow spillage from the high pressure regions.
4. Lower-than-expected pressure recoveries in the outer liner passage of the E³ diffuser are probably due to higher-than-expected parasitic drag losses around the fuel nozzle stems and combustor liner support struts.
5. High inlet turbulence levels result in improved diffuser performance.
6. Elimination of diffuser bleed has no major impact on diffuser performance.

6.1.2 Swirl Cup Development Tests

6.1.2.1 Design and Development Approaches

The spray quality of fuel when introduced into the combustion zone has a major impact on the pollutant emissions levels, the ignition capabilities, and the life of a combustor. Fuel spray characteristics such as mass distribution, spray angle, and droplet size are of significant importance to the overall combustor performance and all are directly influenced by the swirl cup design characteristics, mainly, its recirculation zone. The spray angle has a direct effect on the flame stability. Wide fuel sprays tend to produce a bimodal fuel spray hence an unstable flame, while too narrow fuel sprays concentrate the fuel in the center region of the swirl cup producing an extended flame front inside the combustion chamber. The droplet size directly influences both ignition performance and emissions, and fuel mass distribution affects emissions as well as the life of the combustor liner.

The swirl cup and fuel spray visualization tests were conducted to determine the fuel spray characteristics of the pilot and main stage swirl cup design of the E³ double-annular combustor. The tests were also intended to identify an emission reduction sleeve configuration that will produce the desired spray quality and spray distribution. The effects of varying the fuel nozzle tip immersion and the primary swirler radial location relative to the assembly centerline (eccentricity) were also investigated.

The E³ swirl cup design featured an axial flow primary swirler coupled with a counterrotating radial inflow secondary swirler for both the pilot and main stage domes. Other swirl cup design features included an emissions reduction sleeve, a carbon preventing venturi, a primary-secondary swirler slip joint, and an overall simple mechanical design.

The swirl cup components tested were all E³ sector combustor test hardware installed in an F101 engine dome plate and splash plate modified to simulate the E³ dome. The cooling hole pattern for the dome plate was modified to provide 4.3% W_{comb} cooling air for the splash plate as specified for the E³ pilot dome design. Dome ring cooling was also added to the dome to better approximate the E³ dome aerodynamic and mechanical design. The fuel nozzle used in the tests was a simplex tip with 85° included spray angle rated at 20.5 kg/hr (45.2 lb/hr). The pilot dome and main dome swirl cup configurations for the E³ double-annular sector combustor were sized during these tests by selecting the appropriately sized secondary swirler to be used in the cup assembly and matching the primary to the secondary. A schematic of the test swirl cup/dome assembly used is shown in Figure 111.

Three different categories of tests were conducted on the E³ swirl cup assembly:

1. Fuel spray visualization tests
2. Fuel spray patternation tests
3. Recirculation zone survey tests

The spray visualization tests were conducted in the GE Building 302 Fuel Nozzle Laboratory. The apparatus used consisted of a box, used as a plenum,

ORIGINAL PAGE IS
OF POOR QUALITY.

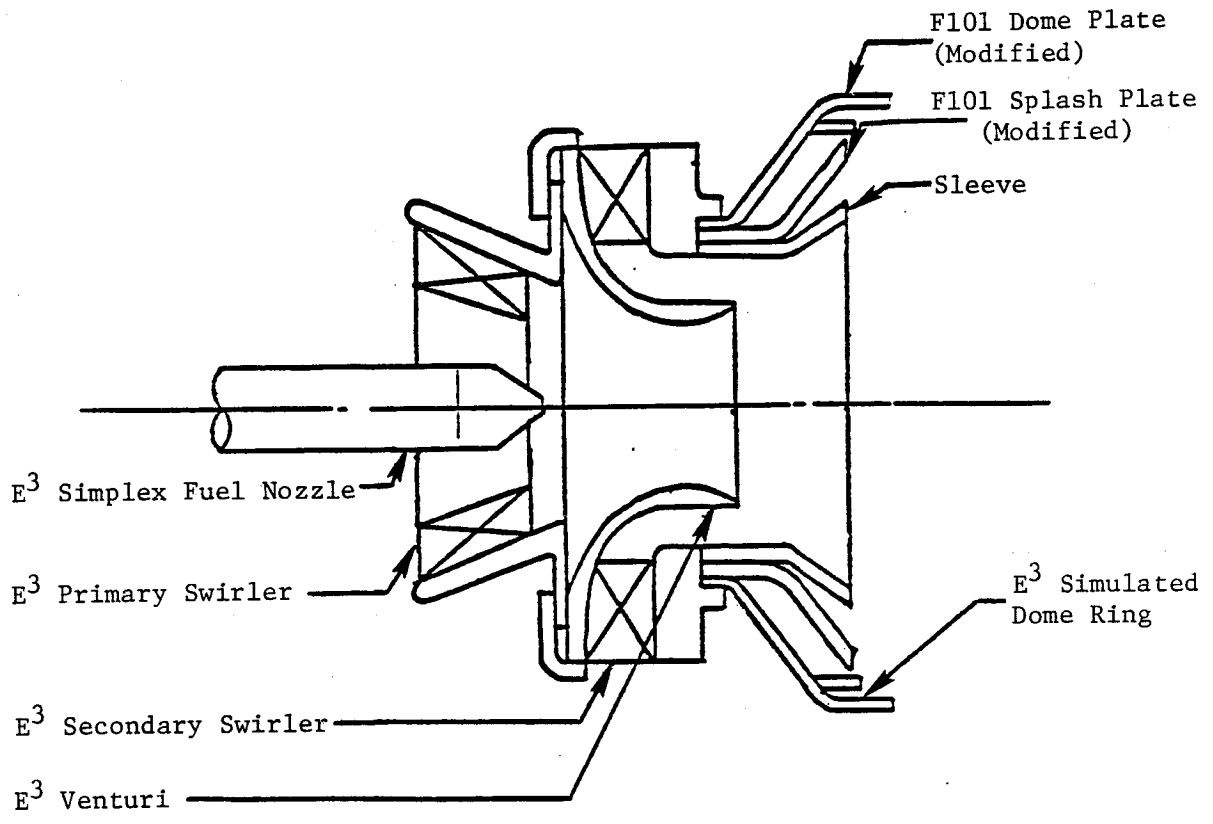


Figure 111. E³ Spray Characteristics Test Dome Assembly Cross Section.

and fuel and air supplies were piped into the box. The dome swirl cup assembly was mounted on one side of the box such that it discharged into a collector at ambient conditions. A schematic of the test setup is shown in Figure 112.

For the patternation tests, a similar apparatus to that of the visualization tests was used except that the discharged fuel was collected into an array of graduated tubes positioned in a semicircular arrangement. Each tube represented one radial location of a spray plane. The tubes were rotated to different plane locations and the fuel spray pattern was then determined.

The swirl cup recirculation zone tests were conducted in the GE Building 304 laboratory using the test stand shown schematically in Figure 113. The strength of the recirculation zone was determined by using a three-element aerodynamic probe to measure static and total pressures at the exit plane. The depth of the recirculation zone was obtained by the aid of a halogen detection device that was used to measure how far upstream halogen was able to recirculate when sprayed at the exit plane of the swirl cup.

The test conditions set for the visualization tests were those required to simulate the E³ key cycle conditions at the combustor inlet, Table XXIV. These conditions included ground start, ground idle, and sea level takeoff. For each of these full density conditions, three critical swirl cup parameters were simulated at one atmosphere - the dome pressure drop, the swirl cup velocity, and the fuel-to-air momentum ratio, by recalculating the dome pressure drop necessary to achieve each parameter individually.

The visualization test procedure requires setting the dome pressure drop and fuel flows, then visually inspecting the resulting fuel spray for its critical characteristics. A stable spray was defined as a single angle spray which could not be altered by any aerodynamic or mechanical disturbance. Photographs were taken at each point setting and used to compare the spray angle. The spray angle measurements were made to include the outermost boundary of the spray envelope and are considered to be only qualitative.

ORIGINAL PAGE IS
OF POOR QUALITY

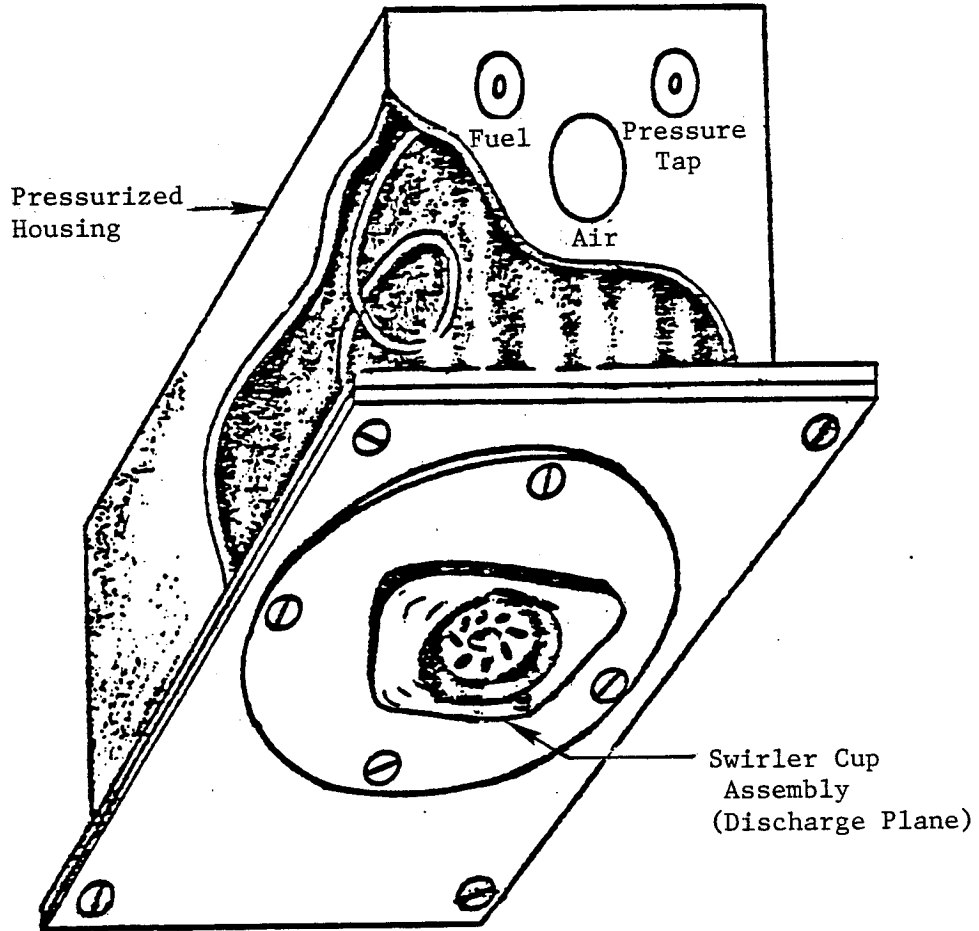


Figure 112. Visual Test Setup.

ORIGINAL PAGE IS
OF POOR QUALITY

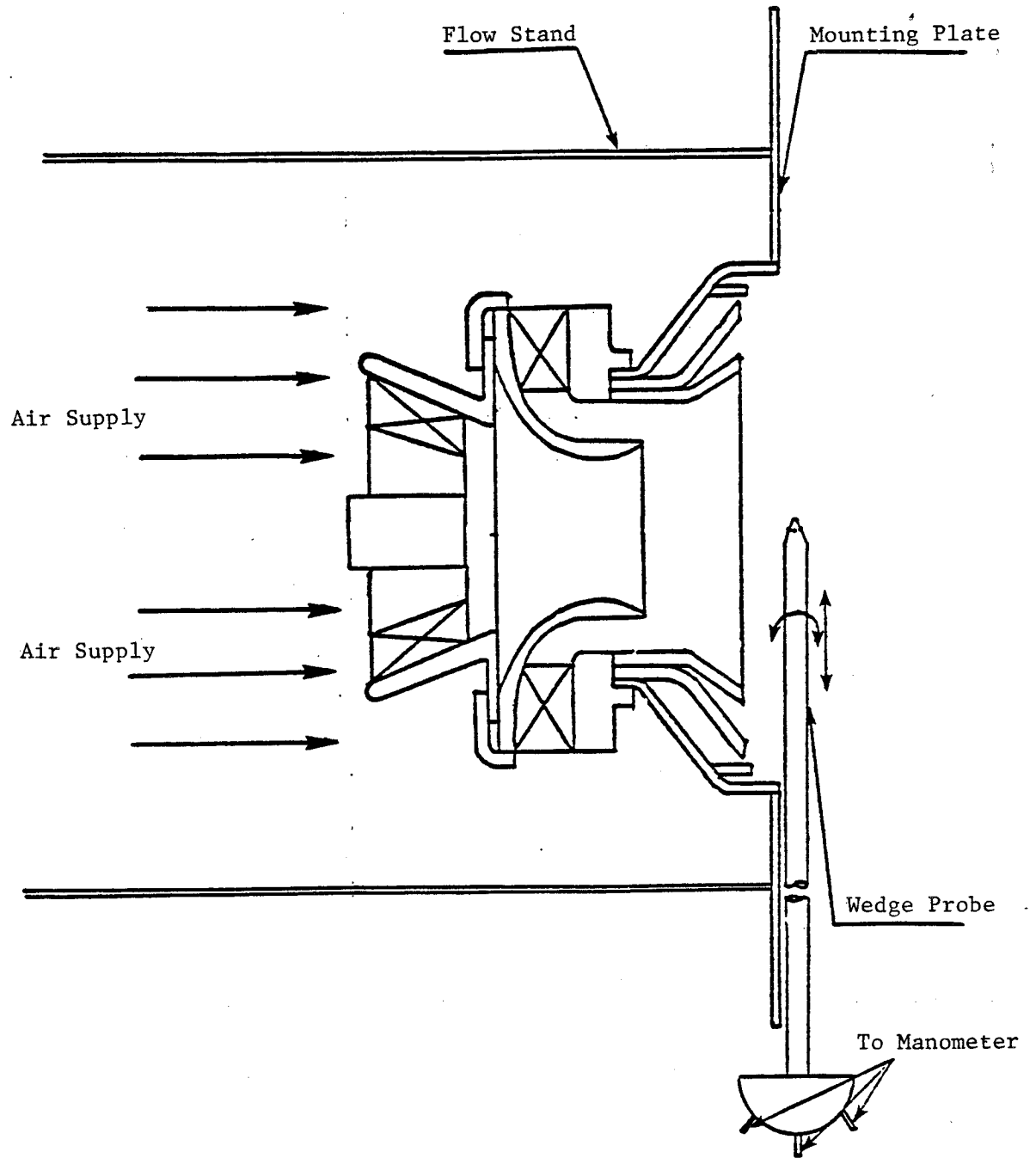


Figure 113. Wedge Probe Test Schematic, Flow Stand.

Table XXIV. Test Conditions for Fuel Spray Visualization Testing.

Cycle Condition	Swirl Cup Parameter Simulated	ΔP dome H ₂ O cm (inch)	Fuel Flow, kg/hr (pph)	Fuel/Air Ratio
Ground	ΔP Clip	6.1 (2.4)	11.34 (25)	5 x f/a (ss)
Start	Swirl Cup Velocity	7.1 (2.8)	11.79 (26)	5 x f/a (ss)
	Momentum Ratio	76.2 (30.0)	5.44 (12)	f/a (ss)
Ground	ΔP Cup	40.6 (16.0)	26.76 (59)	5 x f/a (ss)
Idle	Swirl Cup Velocity	68.1 (26.8)	27.67 (61)	4 x f/a (ss)
	Momentum Ratio	40.6 (16.0)	7.71 (17)	f/a (ss)
Sea Level	ΔP Cup	44.4 (17.5)	14.97 (33)	5 x f/a (ss)
Takeoff	Swirl Cup Velocity	127.0 (50.0)	12.25 (27)	2 x f/a (ss)
	Momentum Ratio	44.4 (17.5)	10.43 (23)	f/a (ss)

The same conditions used in the visualization tests were also used in the patternation tests. The discharged fuel was allowed to accumulate in the collecting tubes for 20 minutes at each test point. The volume of fuel collected in each tube was measured and used to establish the fuel flow mass distribution. Due to the length of time involved in these tests, only promising configurations from the visualization tests were tested on the patternation stand.

For the swirl cup recirculation zone tests, representative pressure drops across the dome were set to simulate the swirl cup aero conditions at ground idle and SLTO operation. Static and total pressure measurements were made along the horizontal cup centerline axis of the swirler assembly. The three-element probe used for the pressure measurement also had the capability of determining the direction of flow at each point by balancing the two static pressure elements in the probe tip. For the halogen detector testing, a small tube was inserted through a rubber plug inserted into the hole in the swirl cup which would normally house the fuel nozzle. The tube had a degree of freedom along the swirl cup axis. The upstream end of the tube was connected to

a detector that transmitted an audible signal when halogen was present. Freon gas was sprayed at the swirl cup exit with the detection tube tip in one position. If a signal was recorded, it was considered an indication that the recirculation zone extended at least to that particular tip location. The procedure was repeated with the tube moved to a new upstream position, until no further signal was transmitted by the detector. That location was then identified as the limit of the recirculation zone.

6.1.2.2 Test Results

Each of the E³ combustor pilot and main stage swirl cups was tested on the visual stand with several sleeve inserts with included angle which varied between 0° (cylindrical) and 90°. Although the quality of the fuel spray atomization and the spray angle for most sleeve configurations were acceptable, stable spray (that is, single angle) was obtained only with 45°, or less, included angle sleeves. The estimated spray angle obtained with the 45° sleeve was approximately 59° at inlet conditions simulating ground start conditions. Sleeves with included angles larger than 70° had very wide fuel sprays which tended to attach to the splash plate. This type of fuel spray was judged to be unsatisfactory because it tends to locate much of the fuel along the combustor liner wall, often resulting in high idle emissions and hot streaks on the combustor liners. Sleeves with angles between 50° and 70° initially produced stable fuel sprays; but when perturbed by an outside mechanical disturbance, the spray became attached to the splash plate. Table XXV and Figure 114 present a summary of spray stability results for the various sleeve configurations tested.

The patterning tests were conducted on the 45° sleeve, since it produced the most desirable fuel spray stability and spray angle. Configurations featuring this type of sleeve produced desirable, symmetrically double-peaked fuel mass distribution illustrated in Figure 115. As shown in Figure 116, 70° sleeve configuration also produced double-peaked distribution. However, the bulk of the fuel was concentrated at a very wide angle.

Varying the fuel nozzle tip immersion and/or eccentricity relative to the swirl cup centerline axis had no significant effect on the fuel spray stability. However, some slight effect on the fuel distribution symmetry was observed.

ORIGINAL SOURCE IS
OF POOR QUALITY

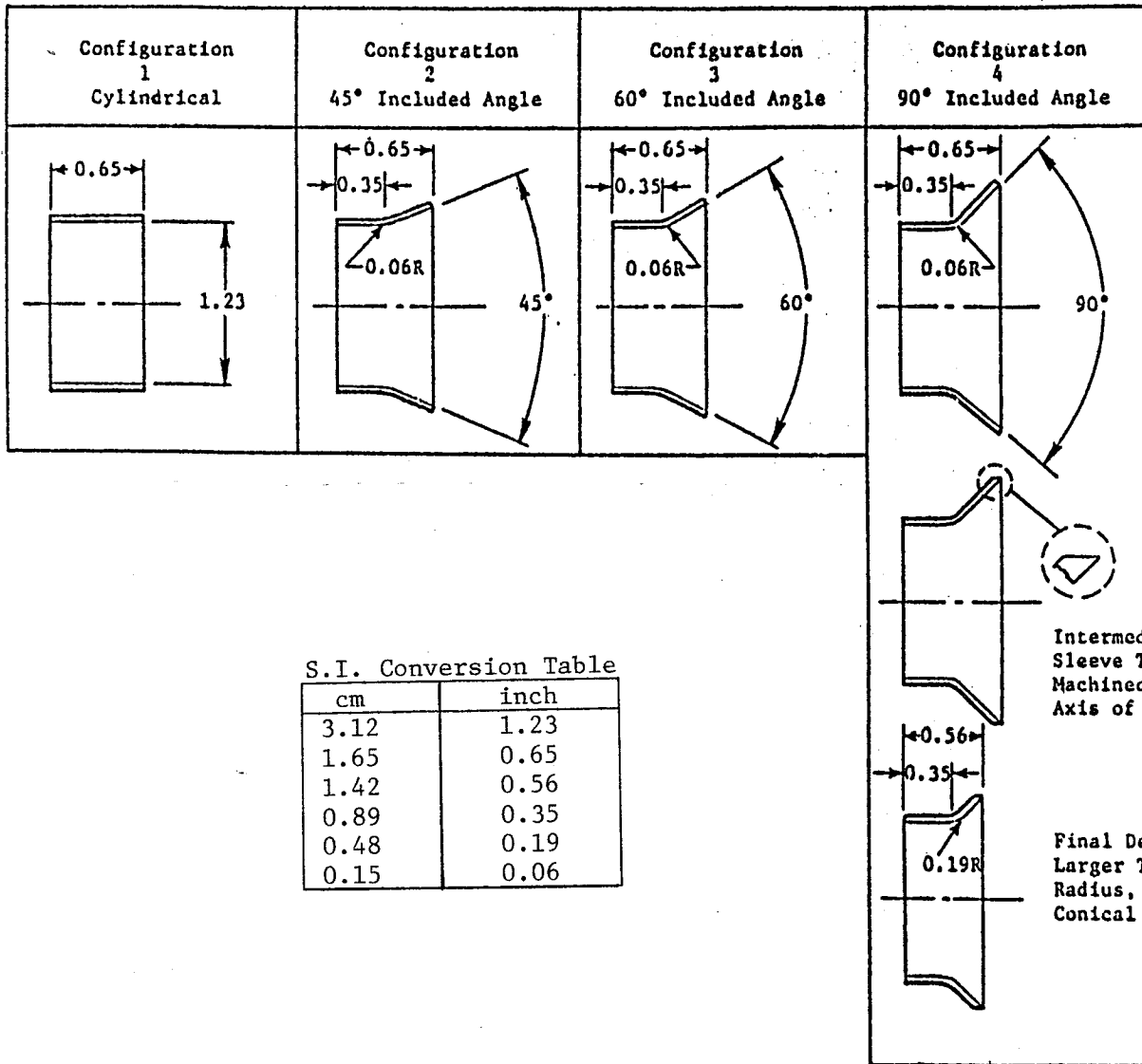


Figure 114. Development Swirl Cup Sleeve Configurations.

ORIGINAL PAGE IS
OF POOR QUALITY

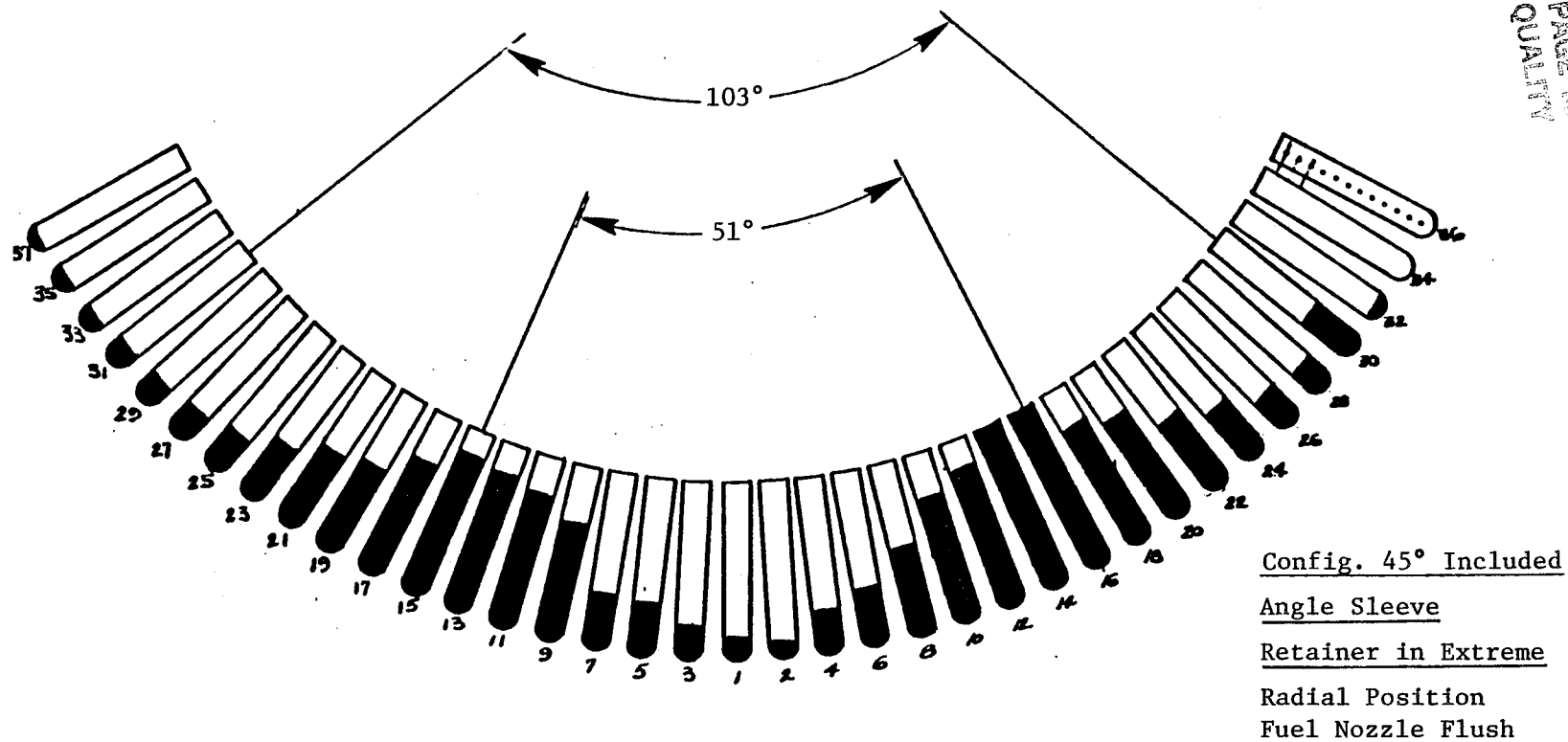


Figure 115. Fuel Spray Patternation Test Results, Pilot Stage Dome Cup.

ORIGINAL PAGE IS
OF POOR QUALITY

Config. 70° Included
Angle Sleeve
Retainer Centered
Fuel Nozzle Flush

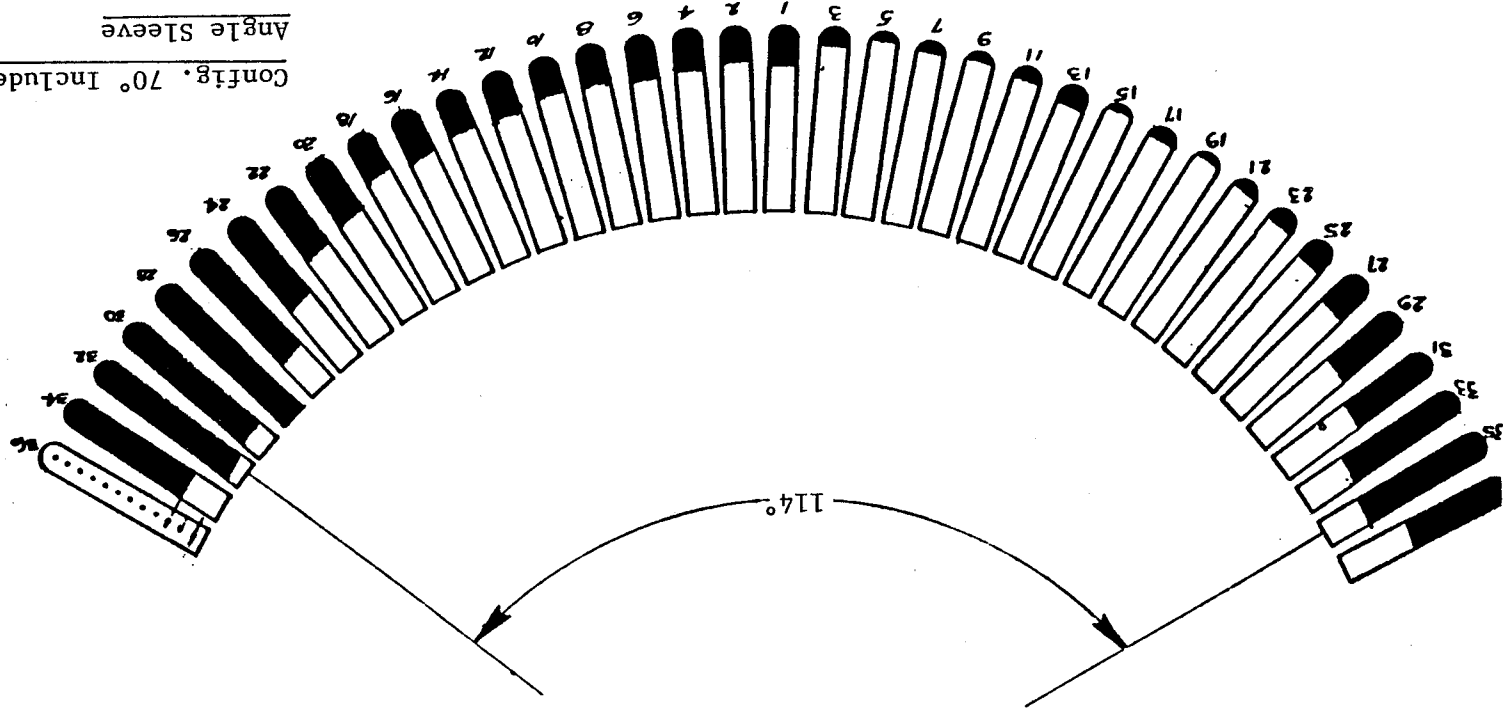
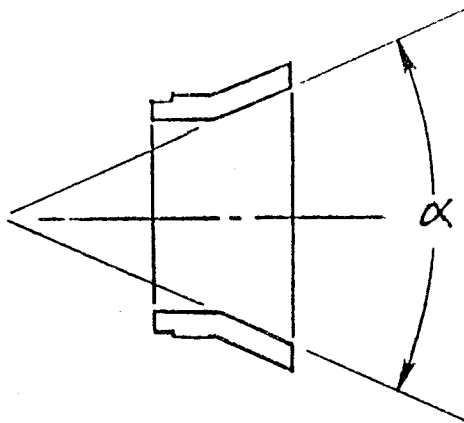


Figure 116. Fuel Spray Patternation Test Results, Main Stage Dome Cup.

Table XXV. E³ Combustor Swirl Cup Flow Visualization Test Results.



Emissions Sleeve Included Angle (α), degrees	Results
0 (cylindrical)	Stable - very narrow spray angle
15	Stable - very narrow spray angle
45	Stable - wider spray angle
50	Semistable - external disturbance
60	Unstable - no disturbance
70	Unstable - no disturbance
90	Unstable - no disturbance

The wedge probe surveys were conducted on the configuration with a 45° included angle sleeve to identify the velocity profile at the exit plane of the dome and to estimate the size and intensity of the recirculation zone. Similar surveys were conducted on the pilot and main stage swirl cups. The results of the surveys are presented as plots of axial velocity versus the radial distance from the centerline and are shown in Figures 117 and 118. The plots indicate that the diameter of the recirculation zone is approximately 2.3 cm (0.9 inch) for the pilot stage cup and 2.0 cm (0.8 inch) for the main stage cup at a plane flush with the mounting plate. The halogen detector tests indicated that the depth of the recirculation zone upstream of the mounting plate was found to equal 1.63 cm (0.65 inch) for the pilot stage and 1.55 cm (0.61 inch) for the main stage, Figure 119.

ORIGINAL PAGE IS
OF POOR QUALITY

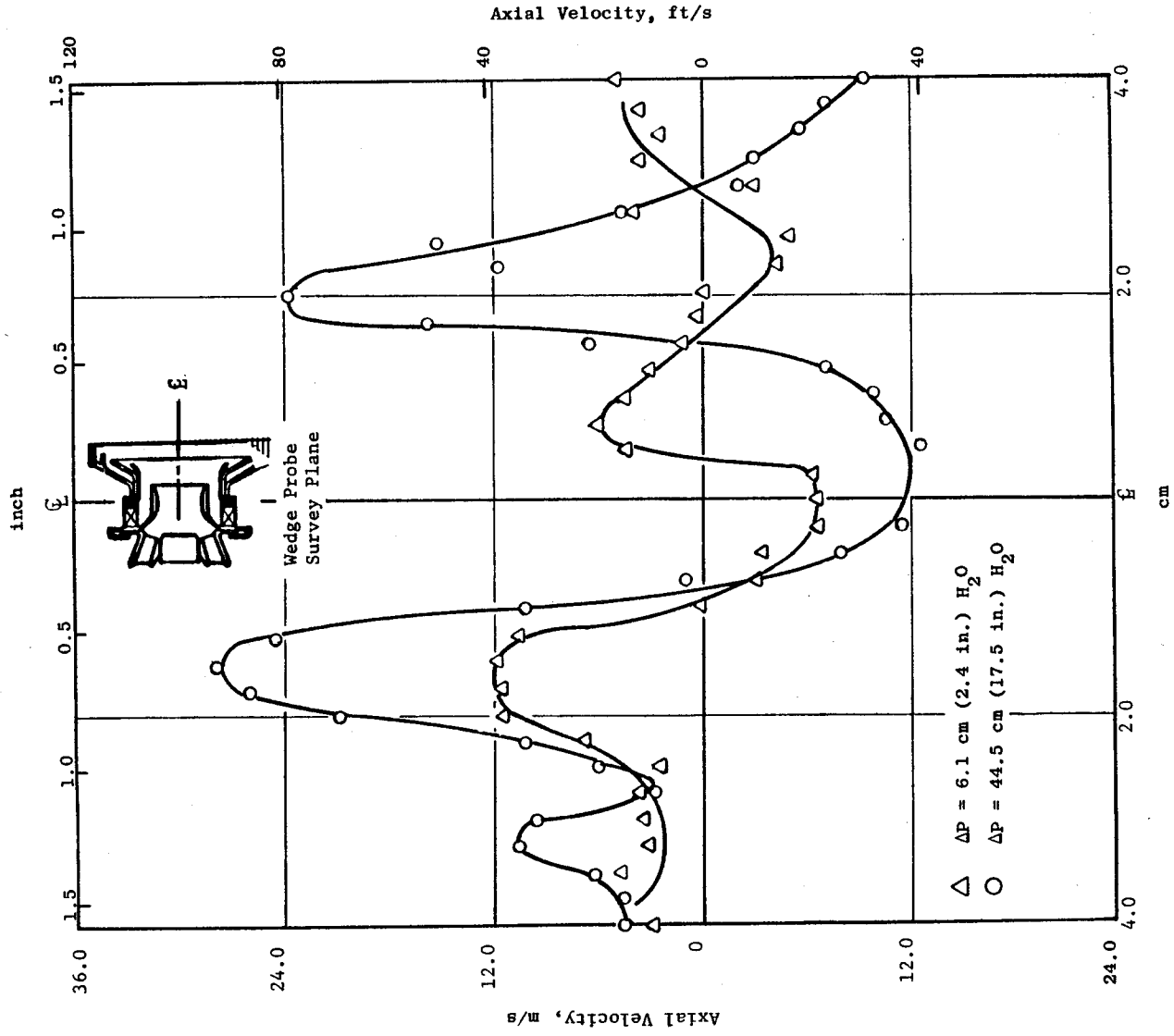


Figure 117. Swirl Cup Axial Velocity Profiles, Pilot Stage Cup.

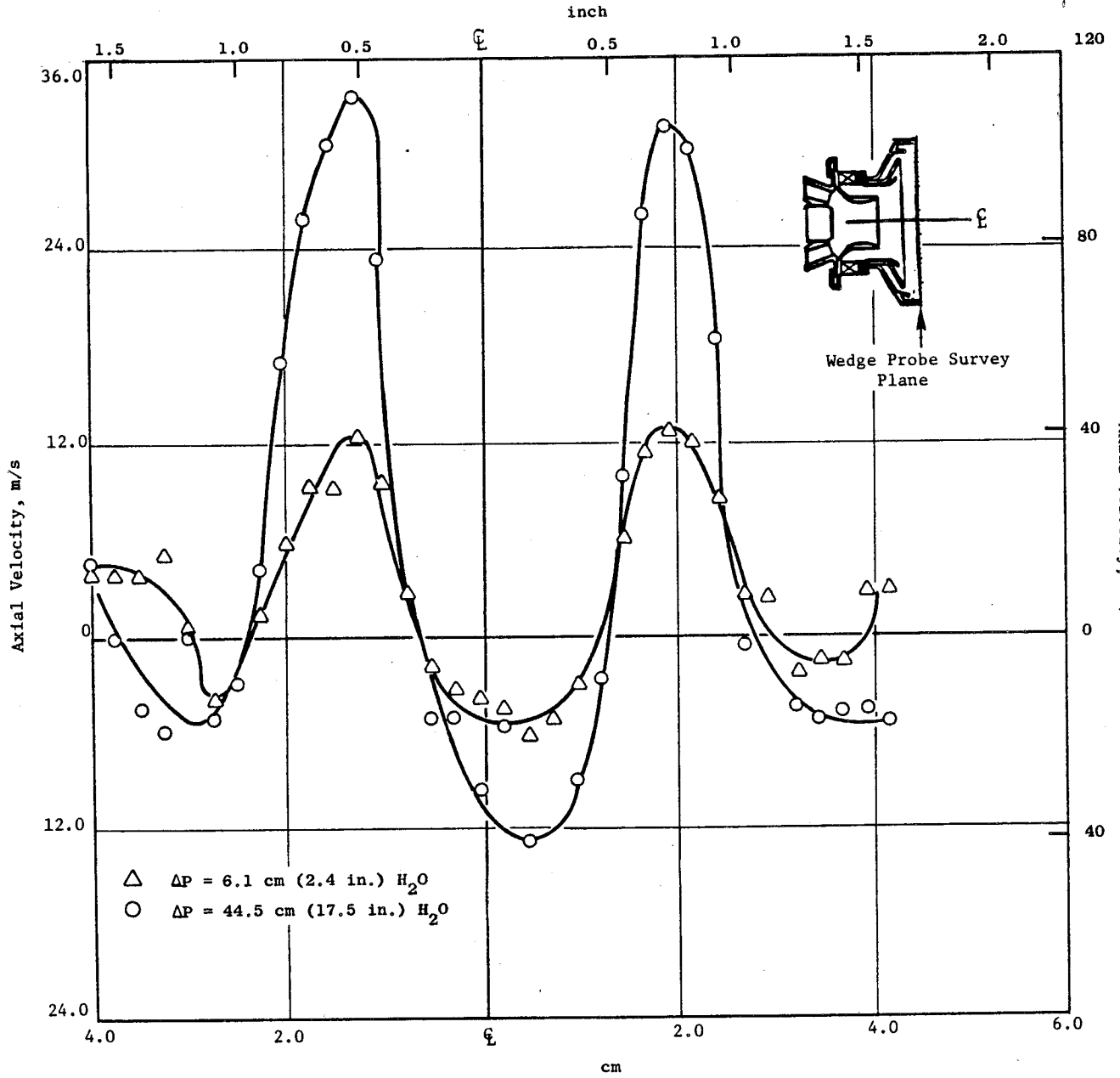


Figure 118. Swirl Cup Axial Velocity Profiles, Main Stage Cup.

ORIGINAL PAGE IS
OF POOR QUALITY

A = Depth of Recirculation Zone
A = 1.62 cm (0.64 in.) Pilot Stage
A = 1.55 cm (0.61 in.) Main Stage

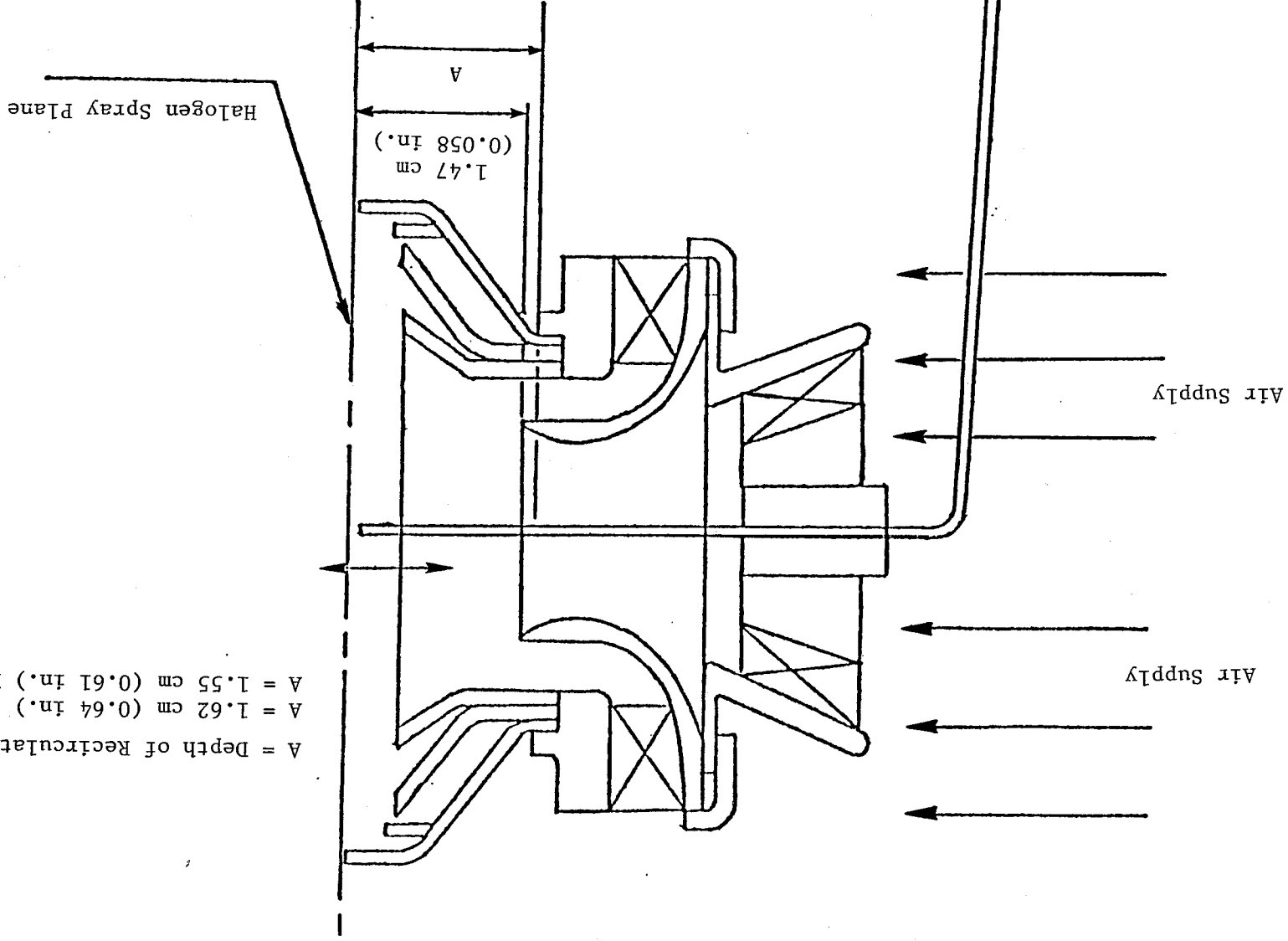


Figure 119. Recirculation Test Schematic (Halogen Detector).

To Halogen Detection Device

6.1.2.3.4 Concluding Remarks

The swirl cup test results indicated that the geometry of the emissions reduction sleeve has a significant effect on the spray stability and fuel distribution. Using a sleeve with a 45° included angle in either the pilot stage or main stage swirl cup designs of the E³ sector combustor produced the most desirable fuel spray characteristics necessary for reducing emissions levels. The baseline configuration pilot and main stage swirl cup recirculation zones were determined to be satisfactory in terms of strength and penetration. Based on these results, it was decided to use the 45° angle sleeves for the baseline configuration of the sector combustor.

6.1.3 Dome Metal Temperature Tests

6.1.3.1 Introduction

The initial E³ double-annular combustor design specified 4.3% of the combustor airflow for the pilot dome splash plate cooling. This level of cooling airflow was chosen because the surface area of the E³ pilot dome is smaller than for a conventional single-annular configuration, and low dome cooling flows result in lower CO and unburned HC emissions levels at ground idle operating conditions. However, splash plate cooling is strongly dependent on dome geometry; but the selected airflow level for the E³ pilot dome is relatively low when compared to those of existing GE combustors. Therefore, the adequacy of the splash plate cooling airflow selected for the E³ pilot dome design was questioned in light of past design practices.

The dome metal temperature tests were designed to determine the effectiveness of the pilot stage dome cooling and the impact of this unconventional low dome cooling airflow level on the life of the combustor hardware. The test rig availability also provided a good opportunity to investigate the effects of burning broad specification fuels on the dome metal temperatures in back-to-back tests.

6.1.3.2 Dome Design and Evaluation Approach

The approach chosen to conduct the dome metal tests was that of using a single cup setup to simulate the E³ dome design. Similar test configurations

have been used extensively for this purpose in other programs. The simulated E³ pilot stage dome was constructed from a combination of available E³ sector combustor swirl cup hardware and modified hardware from previous development programs. The dome assembly as tested consisted of the following hardware:

- F101-type dome plate modified in size, cooling hole pattern, and area to approximate the E³ pilot stage dome
- F101-type splash plate also modified to simulate the E³ pilot stage dome plate in size and shape
- NASA/Experimental Clean Combustor Program type primary swirler with an effective flow area approximately equal to the E³ primary swirler area
- F101-type emissions reduction sleeve with a 70° included angle
- E³ sector combustor pilot stage secondary swirler
- E³ sector combustor carbon preventing venturi
- F101-type simplex fuel nozzle tip.

A photograph of the various hardware items prior to assembly is shown in Figure 120.

The dome plate, splash plate, venturi, and sleeve were instrumented with thermocouples (T/C) at critical locations shown in Figure 121. To obtain accurate metal temperatures of the hardware close to the combustion gas, the splash plate T/C's, venturi T/C's, and the sleeve T/C's were embedded into the metal surface.

The assembled dome hardware was welded to a can-type liner and mounted inside a plenum in the test facility as shown schematically in Figure 122. The tests were conducted at the General Electric (Evendale) ACL Cell A5E test facility. This facility has capabilities for testing components at high pressure/high temperature conditions. An indirect gas-fired heater is utilized to heat the inlet air supplied to the test piece. Nominal facility limits are 840 K (1512° R), 18 atmospheres, and 5.5 kg/s (12.1 lb/s).

The test point schedule for the dome metal temperature tests is shown in Table XXVI. The test parameters shown in the table simulate actual E³ combustor

ORIGINAL PAGE
BLACK AND WHITE PHOTOGRAPH

ORIGINAL PAGE IS
OF POOR QUALITY

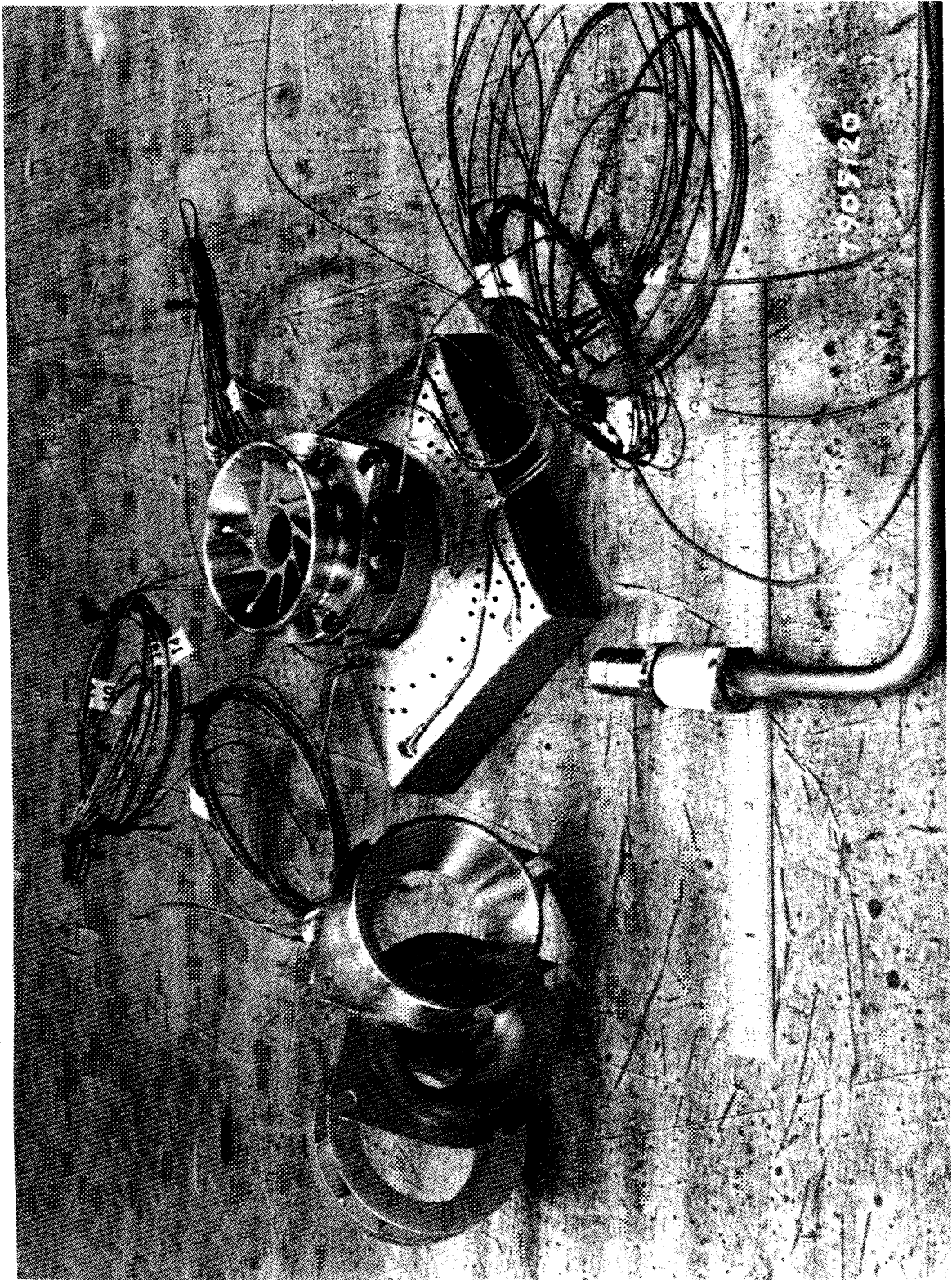
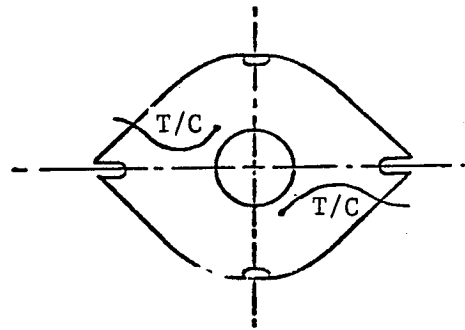
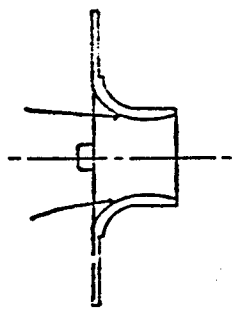
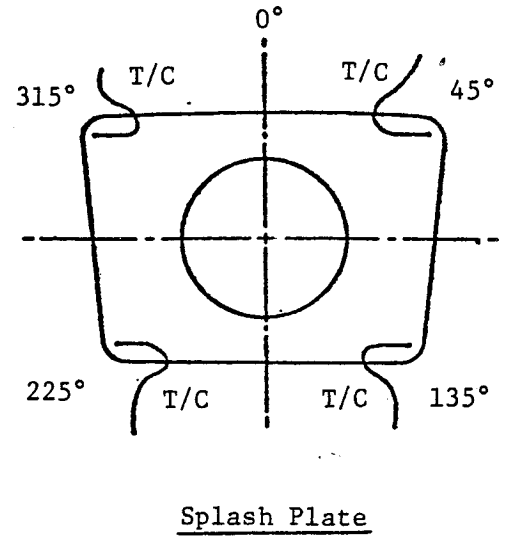
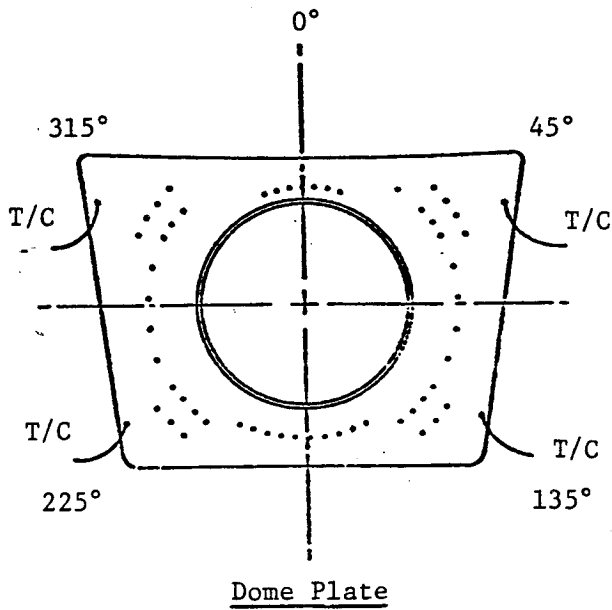
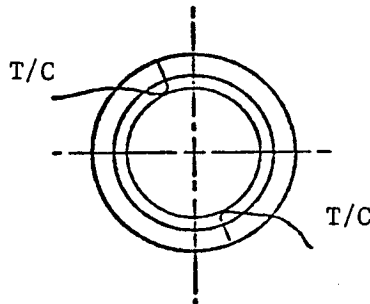
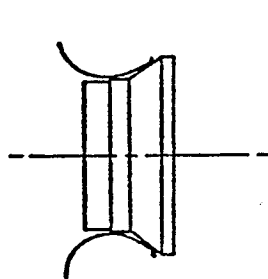


Figure 120. Dome Metal Temperature Test Hardware.

ORIGINAL PAGE IS
OF POOR QUALITY

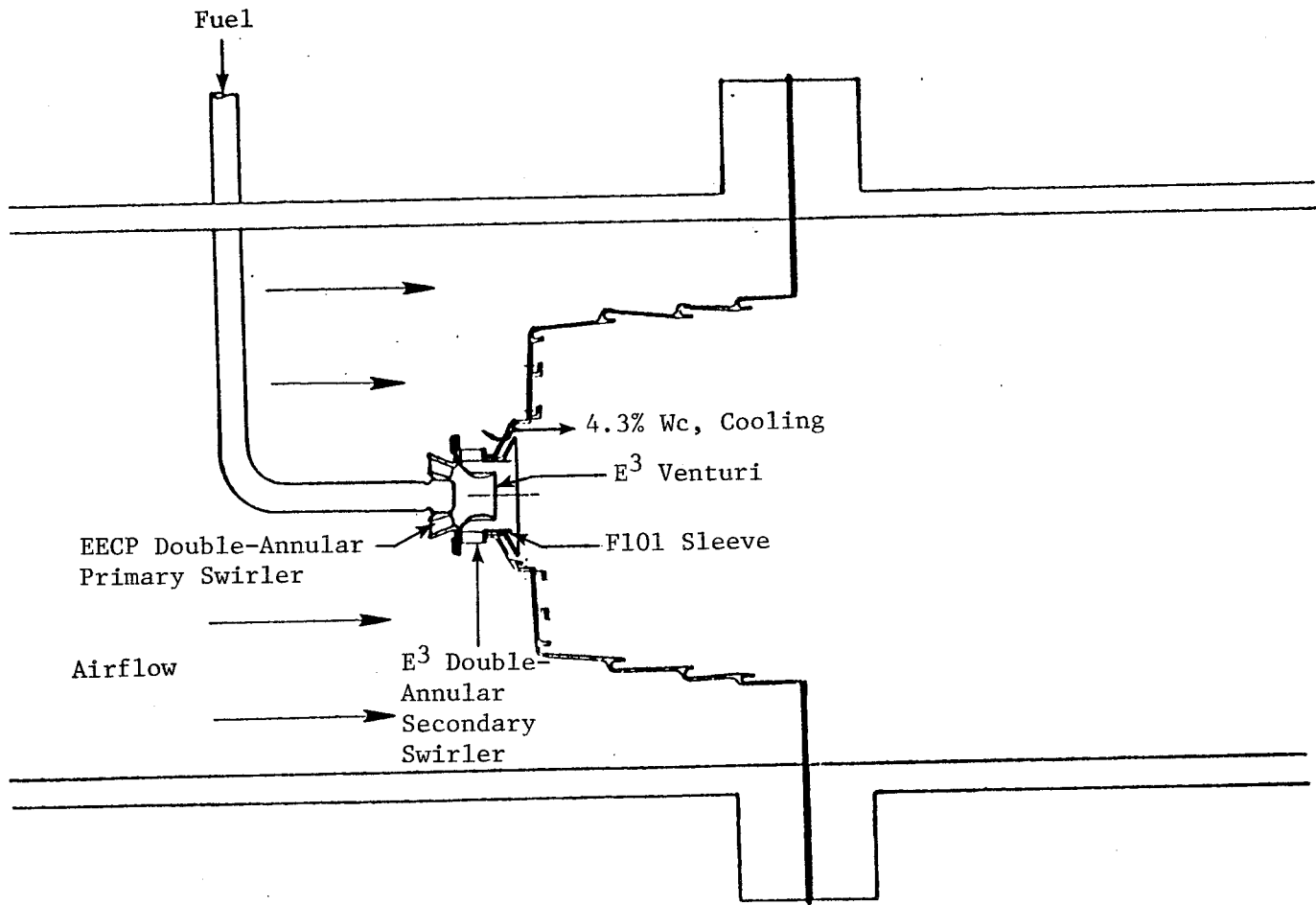


Venturi



Sleeve

Figure 121. Dome Metal Temperature Test Instrumentation.



ORIGINAL PAGE IS
OF POOR QUALITY

Figure 122. Dome Metal Temperature Test Rig.

Table XXVI. Dome Metal Temperature Test Point Schedule.

Point	Engine Condition Simulated	PT ₃ Atm.	T _{T3} , K, R	W _F , kg/hr (lb/hr)	ΔP Atm.	ΔP/P, %
1	Approach	11.84	667 (1200)	45.8 (101.0)	0.592	5.0
2	Approach	11.84	667 (1200)	76.7 (169.1)	0.592	5.0
3	Approach	11.84	667 (1200)	107.5 (234.0)	0.592	5.0
4	Approach	11.84	667 (1200)	45.4 (100.1)	0.415	3.5
5	Approach	11.84	667 (1200)	57.2 (126.1)	0.653	5.5
6	Cruise	12.86	782 (1408)	46.3 (102.1)	0.643	5.0
7	Cruise	12.86	782 (1408)	76.7 (169.1)	0.643	5.0
8	Cruise	12.86	782 (1408)	107.5 (234.0)	0.643	5.0
9	Cruise	12.86	782 (1408)	45.4 (100.1)	0.449	3.5
10	Cruise	12.86	782 (1408)	57.2 (126.1)	0.707	5.5
11	SLTO (derated)	19.05	814 (1465)	67.1 (147.9)	0.952	5.0
12	SLTO (derated)	19.05	814 (1465)	111.6 (246.0)	0.952	5.0
13	SLTO (derated)	19.05	814 (1465)	136.1 (300.0)	0.952	5.0
14	SLTO (derated)	19.05	814 (1465)	74.8 (164.9)	0.667	3.5
15	SLTO (derated)	19.05	814 (1465)	83.0 (183.0)	1.048	5.5

inlet conditions at key cycle operating points indicated. The airflow levels were approximated by setting similar pressure drops to those calculated in the cycle conditions. Fuel flows were selected to cover a wide range of fuel/air ratios including the design levels.

The test procedure consisted of setting the combustor inlet pressure, inlet temperature, combustor pressure drop, and combustor fuel flow for each test point in the test point schedule. Steady-state readings of all instrumentation was then recorded. Three complete test runs through the point schedule were made. The first run was conducted with Jet A fuel, the second with experimental referee broad specification-type (ERBS) fuel, and the third with marine diesel fuel. During the tests, a 1255 K (2260° R) limit was imposed on all thermocouple indicated temperatures to reduce instrumentation attrition and prevent hardware damage.

At the end of each test run, a flashback test was conducted to determine if burning could be detected upstream of the swirl cup venturi throat during a fuel flow chop. A flashback test consisted of resetting the combustor inlet conditions specified for test Point 12. These aero operating conditions were held constant while the fuel flow was rapidly decreased from 112 to 44 kg/hr (247 to 97 lb/hr). When a fuel flow of 44 kg/hr (97 lb/hr) was reached, the fuel flow was rapidly increased back to 112 kg/hr (247 lb/hr).

6.1.3.3 Experimental Test Results

To stay within the 1255 K (2260° R) limit on all of the thermocouple readings, the overall fuel/air ratio was limited to 0.021 corresponding to a dome fuel/air ratio of 0.101. This fuel/air is significantly higher than that which the pilot dome or the main dome would experience during normal operation of the engine.

For simulated sea level takeoff operation, peak metal temperatures recorded for the splash plate, dome plate, and sleeve were 1216 K (2189° R), 939 K (1690° R), and 1107 K (1993° R), respectively, at a dome fuel/air ratio of 0.088. Based on these results, peak metal temperatures of 983 K (1769° R) for the pilot stage and 1041 K (1874° R) for the main stage would be expected

at the FPS sea level takeoff operating conditions. The estimated increase in metal temperature to account for the derated pressure conditions is approximately 60 K (108° R).

The sea level takeoff conditions are the most severe conditions that the combustor will encounter under normal operating conditions. As expected, the recorded peak dome metal temperatures at approach and maximum cruise conditions were significantly lower than those obtained at SLTO conditions and, therefore, represent no threat to the dome hardware integrity. Figure 123 presents a plot of the splash plate metal temperatures recorded versus fuel/air ratio at all three engine operating conditions simulated. Table XXVII presents a summary of the expected dome metal temperatures for each of the conditions during full-annular combustor testing.

The results of the dome metal temperature tests using ERBS and marine diesel fuels were nearly identical to those obtained when using Jet A fuel. All dome metal temperatures followed a similar pattern and showed similar dependence on fuel/air ratios. When testing with marine diesel fuel at simulated sea level takeoff conditions and high fuel/air ratio (Point 13), an unstable condition was encountered with the splash plate and sleeve metal temperatures fluctuating widely. The explanation for the fluctuating temperatures was an unstable fuel spray. Fuel spray instability was caused by the combined effect of airflow and fuel flow momentums. However, since this condition was encountered only with diesel fuel, it is possible that the fuel properties were a contributing factor.

Hardware inspection at the conclusion of testing with marine diesel fuel revealed a thin film of carbon deposited on the splash plate surface. Since the test rig was not inspected between the ERBS and diesel fuels tests, it is uncertain as to which fuel caused the deposits. Inspection of hardware after the Jet A fuel tests revealed no carboning.

6.1.3.4 Concluding Remarks

The following conclusions were derived from the dome metal temperature tests:

ORIGINAL PAGE IS
OF POOR QUALITY

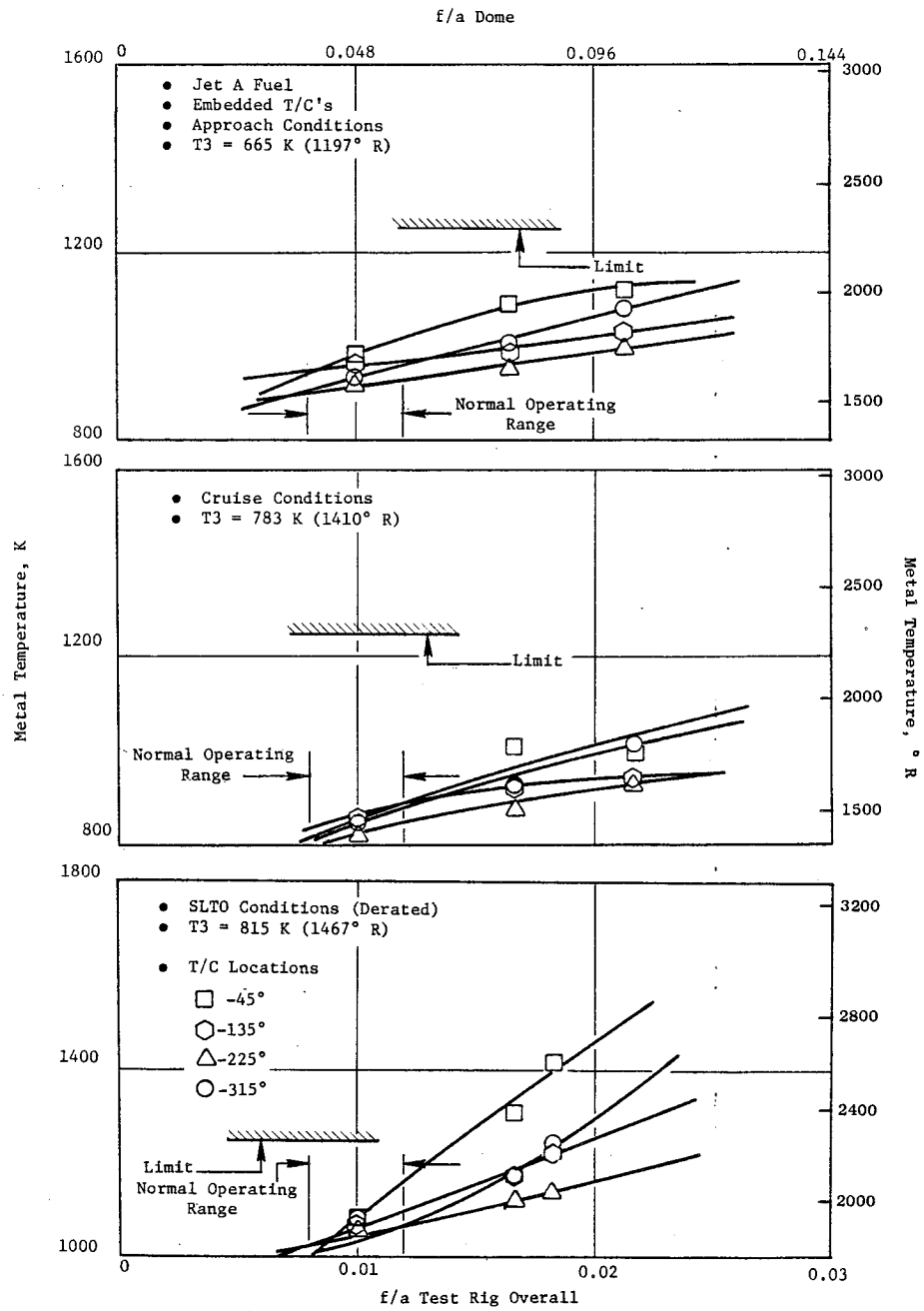


Figure 123. Dome Metal Temperature Test Results.

Table XXVII. Estimated Dome Metal Temperatures for Full-Annular Combustor Testing.

	Pilot Stage			Main Stage		
	Splash Plate Temp., K (° R)	Dome Plate Temp., K (° R)	Sleeve Temp., K (° R)	Splash Plate Temp., K (° R)	Dome Plate Temp., K (° R)	Sleeve Temp., K (° R)
Approach	722 (1300)	691 (1244)	761 (1370)	---	---	---
Maximum Cruise	811 (1460)	819 (1475)	877 (1580)	850 (1530)	825 (1485)	894 (1610)
SLTO	866 (1560)	889 (1600)	1044 (1880)	1044 (1880)	966 (1740)	1102 (1984)

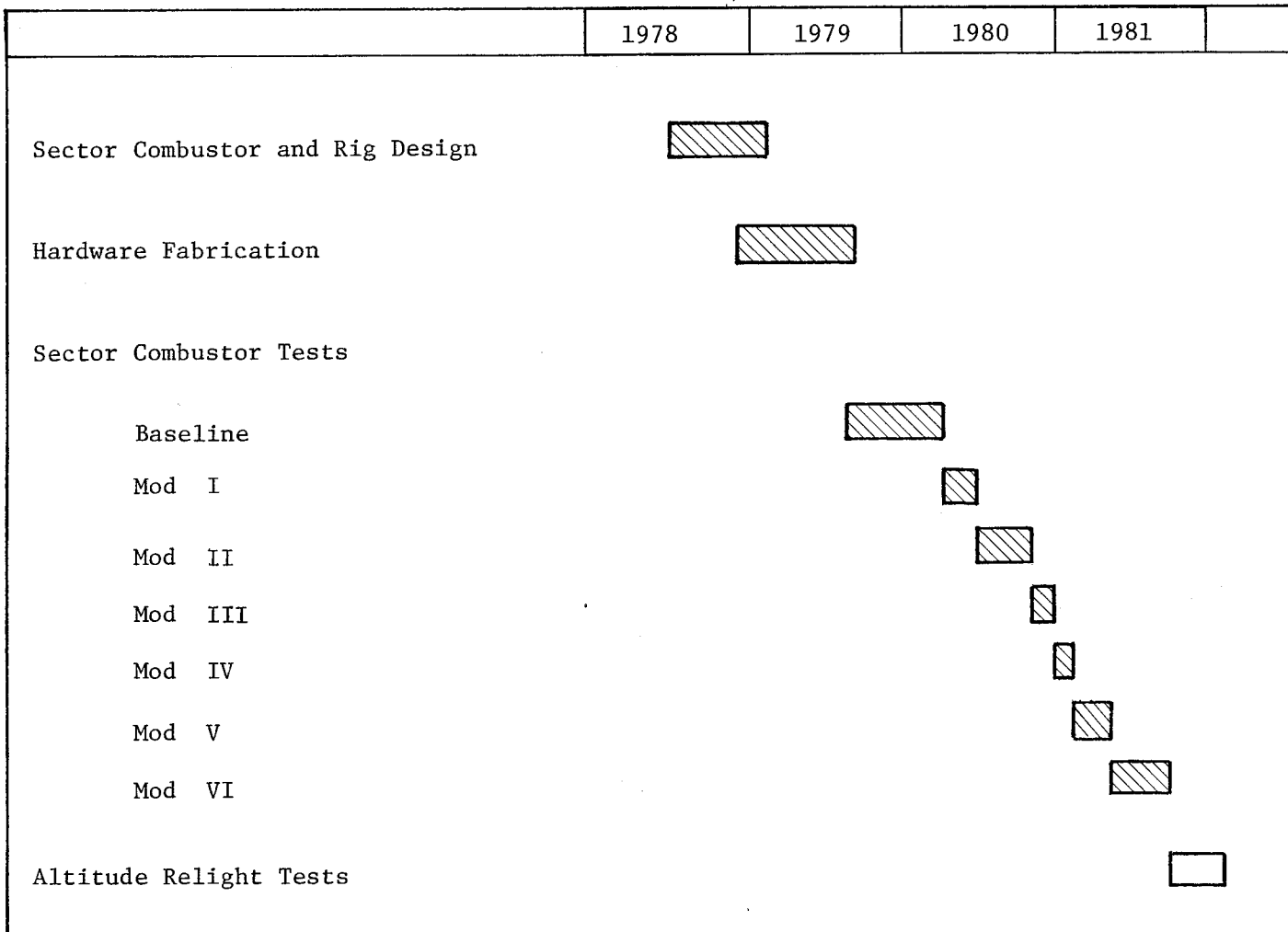
- The airflow levels selected for pilot stage dome splash plate cooling will be adequate in keeping the dome hardware metal temperatures at acceptable levels during the E³ Combustor Development Test Program. Specifically, the 4.3% of total combustor airflow selected for the pilot stage splash plate cooling is sufficient to maintain metal temperatures below 1100 K (1980° R) under the most severe combustor operating conditions expected. The main stage dome splash plate has a smaller surface area than that of the pilot stage; hence, an equal level of splash plate cooling airflow is expected to be at least as effective as in the pilot stage.
- The relatively cold fuel impinging on the inside of the venturi provides excellent cooling and maintains the venturi metal temperatures at levels near the combustor inlet air temperature levels.
- Dome metal temperatures measured from the tests closely agree with temperatures measured during similar single cup, high pressure tests previously conducted in other development programs, and no high metal temperatures were measured during flashback testing.
- The burning of broad specification fuels such as ERBS and marine diesel had only a very minor effect on dome metal temperatures. With the exception of a slight carbon deposition on the splash plate surface when using these fuels, the results from all tests were identical in terms of peak metal temperature location on hardware.
- There was no hardware damage noted at the conclusion of all the tests that were run.


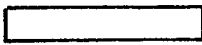
6.1.4 Sector Combustor Tests

6.1.4.1 Introduction

The sector combustor tests constituted the major part of the E³ Subcomponent Testing Program. They were intended to develop the E³ combustor performance characteristics including ignition, emissions exit temperature profiles, efficiency, and altitude relight. The sector combustor tests were planned to run parallel to the full-annular development program to permit refinement and investigation of any of these performance characteristics without interrupting the full-annular testing effort.

A total of seven basic sector combustor configurations were tested. Some of these configurations were subjected to more than one test with one or more of their features somewhat varied to investigate specific performance aspects. Figure 124 outlines the sector test schedule and progress within the schedule.



 - Work Completed
 - Work to be Done

ORIGINAL PAGE IS OF POOR QUALITY

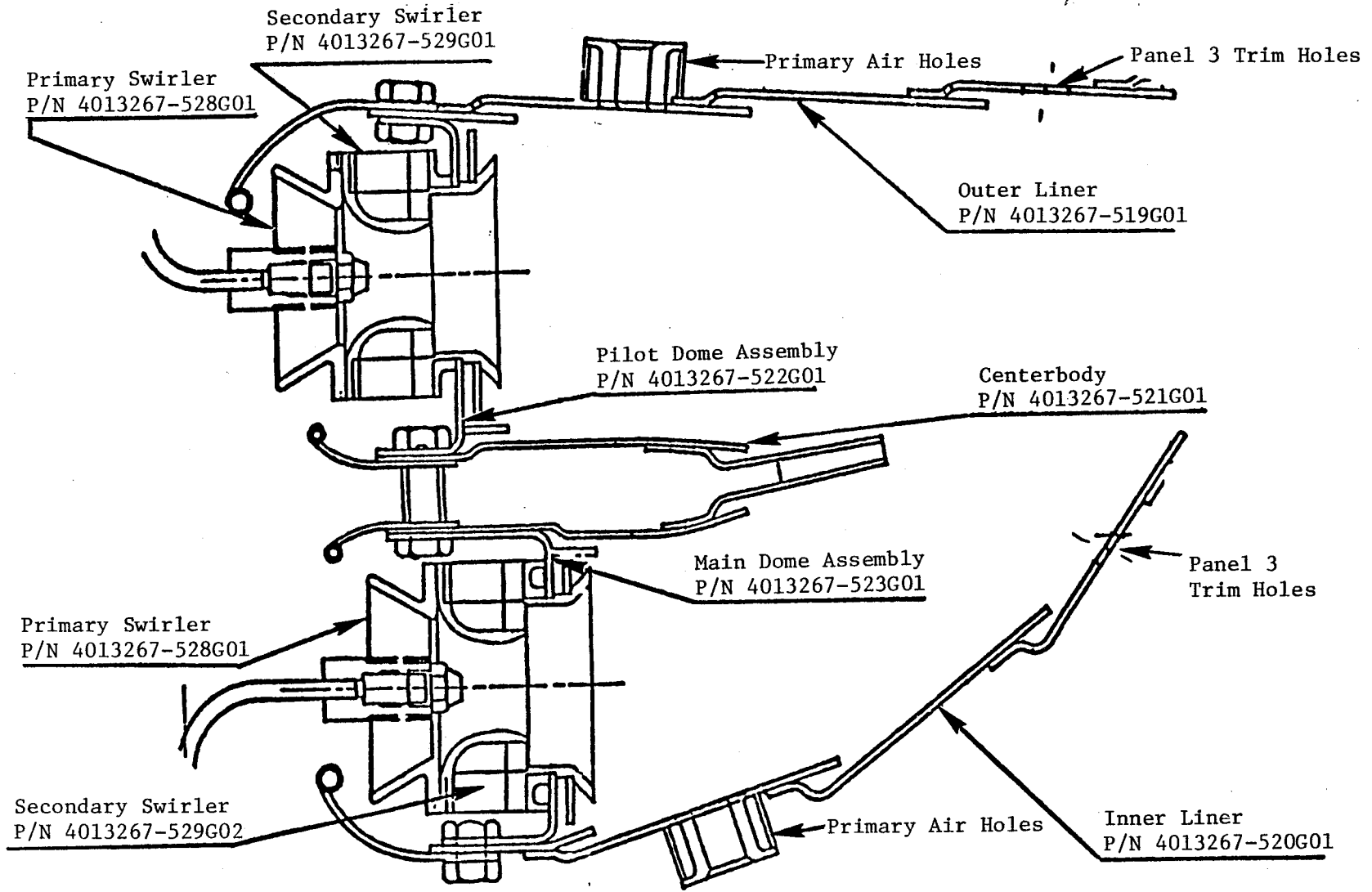
Figure 124. E³ Sector Combustor Test Schedule.

6.1.4.2 Design Approach

A five-cup, 60° annular sector combustor was selected as the test vehicle. This sector combustor was designed to duplicate the aerodynamic flowpath and physical dimensions of the baseline design of the E³ combustor. It was fabricated from prototype hardware because of the shorter manufacturing cycle. The prototype swirlers used were machined parts welded together, while the development swirlers were made from castings of the complete swirler unit. The sector combustor liners were fabricated from sheet metal panels that were spin formed into shape rather than brazed together, while the development combustor liners were machined from forgings. These differences in manufacture were not expected to result in any performance discrepancies.

The E³ sector combustor featured a double-annular dome design with an outer pilot stage and an inner main stage like the full-annular development combustor. Key design features of the E³ double-annular combustor included an axial primary, radial secondary counterrotating swirl cups, a carbon-preventing venturi, and an emissions reduction sleeve in both pilot and main stages. The original design called for 90° included angle sleeves; however, these were modified to 45° angle sleeves in the sector combustor baseline configuration based on the results of the swirl cup investigation. The combustor stages are separated by a film-cooled centerbody structure. Each of the combustor liners consisted of three panels, also film cooled. The baseline inner and outer liner design also featured Panel 2 primary dilution holes and Panel 3 trim dilution holes located in line with swirl cups. The primary dilution hole design was an extended dilution tube to simulate the thimble design featured on the engine combustor design. Figure 125 shows a cross section of the sector combustor and its key components. Figure 126 presents a photograph of the assembled sector combustor hardware. The flow area distribution for the baseline sector combustor is presented in Table XXVIII.

The sector combustor design included a split duct diffuser that also duplicated the design and flowpath of the full-annular combustor diffuser including diffuser bleed at the strut location.



ORIGINAL PAGE IS
OF POOR QUALITY

Figure 125. E³ Sector Combustor Cross Section.

ORIGINAL PAGE
BLACK AND WHITE PHOTOGRAPH

ORIGINAL PAGE IS
OF POOR QUALITY

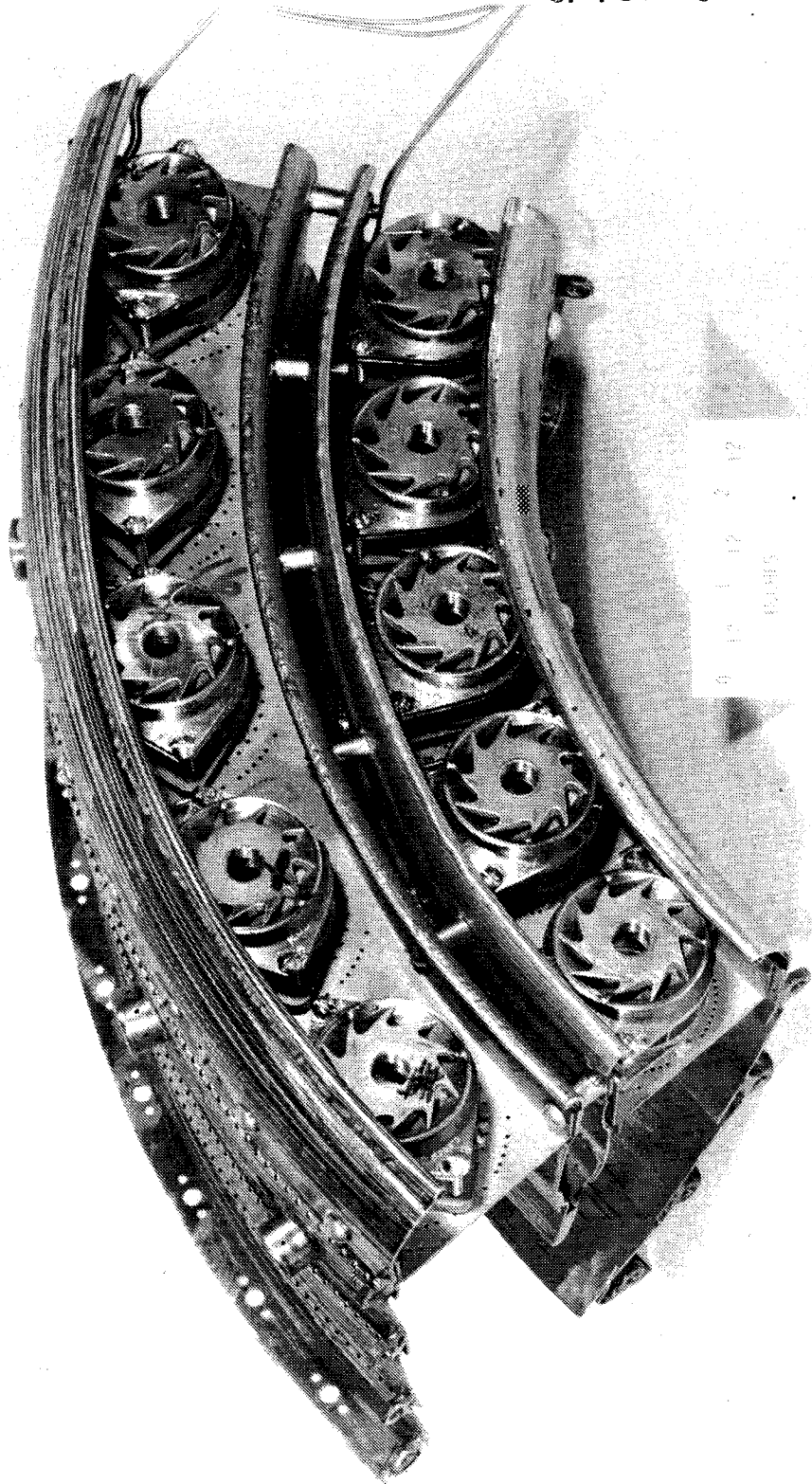


Figure 126. Sector Combustor Hardware.

Table XXVIII. Flow Area Distribution for Baseline Sector
Combustor Configuration.

<u>Outer Liner</u>	Area, cm ²	Total Area, %
Cooling Row 1 + Ring Cooling	1.84	3.55
Cooling Row 2	1.21	2.33
Cooling Row 3	1.07	2.07
Cooling Row 4	0.66	1.28
Primary Dilution	1.25	2.40
Trim Dilution	0.80	1.54
Total Outer Liner	6.83	13.18
<u>Inner Liner</u>		
Cooling Row 1 + Ring Cooling	1.86	3.60
Cooling Row 2	2.00	3.87
Cooling Row 3	1.47	2.84
Cooling Row 4	1.08	2.09
Primary Dilution	1.81	3.50
Trim Dilution	0.75	1.46
Total Inner Liner	8.03	15.49
<u>Centerbody</u>		
Outer Cooling Row 1 + Ring Cooling	0.72	1.38
Outer Dilution	1.64	3.16
Outer Cooling Row 2	0.37	0.72
Multijet	0.59	1.15
Inner Cooling Row 1 + Ring Cooling	1.16	2.24
Inner Dilution	1.82	3.51
Inner Cooling Row 2	0.59	1.15
Total Centerbody	6.90	13.93
<u>Pilot Dome</u>		
Swirl Cups	9.77	18.86
Splash Plate Cooling	3.94	7.61
Total Pilot Dome	13.71	26.41
<u>Main Dome</u>		
Swirl Cups	13.68	26.40
Splash Plate Cooling	2.66	5.13
Total Main Dome	16.34	31.53
Total Area	51.81	100.00

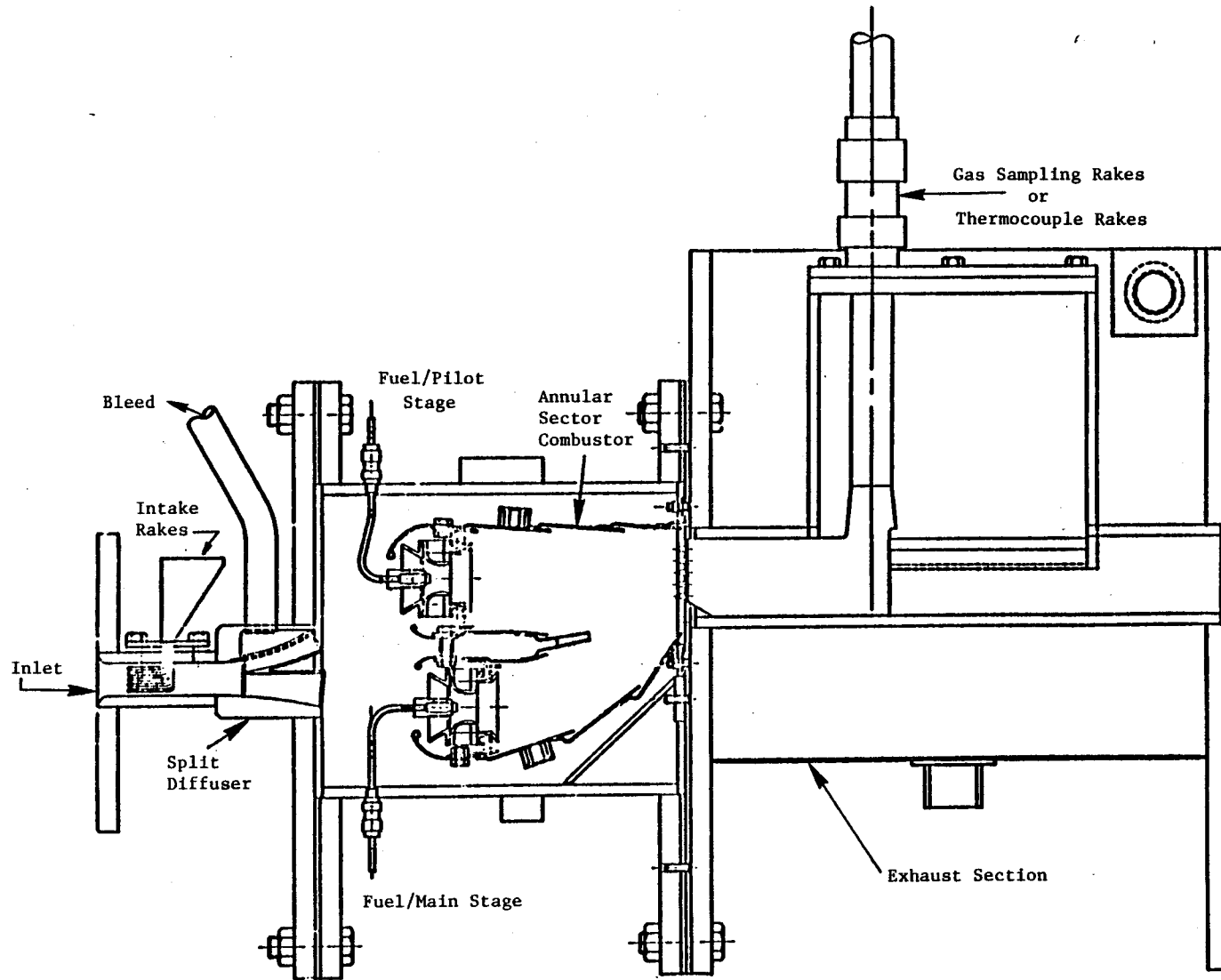
6.1.4.3 Test Rig and Instrumentation

A schematic of the E³ sector combustor test rig is shown in Figure 127. The test rig was designed to house the five-cup, 60° sector combustor and to operate at up to 4 atmospheres of pressure and 750 K (1350° R) of temperature at the combustor inlet. It consisted of the inlet plenum chamber, the diffuser section, the sector combustor section, and the combustor exit instrumentation section.

The inlet plenum chamber section of the test rig was attached to the test facility air supply. This plenum consisted of a large diameter pipe which served as a flow conditioner before the air entered the diffuser passage. The sector combustor diffuser was housed in another plenum just downstream of the inlet plenum. The diffuser was a single passage inlet with a split duct exit that provided the desired flow split between the two combustor stages. A photograph of the diffuser section (discharge) and housing is shown in Figure 128.

The combustor housing section was attached to the discharge of the diffuser and contained the fuel delivery system and the sector combustor. The fuel was supplied to the 10 fuel nozzles through a double manifold system. One manifold supplied the five pilot stage nozzles (outer annulus), and the other supplied the five main stage (inner annulus) nozzles. The fuel manifold systems could be operated independently. The instrumentation section of the test rig housed the rake assembly that was used to measure exhaust gas temperatures or to obtain gas samples for emissions measurements, depending on the type of rake installed.

Figure 129 shows the test rig instrumentation which includes various thermocouples and pressure probes in addition to the exhaust rake system. The thermocouples and pressure probes were used to obtain temperature and pressure data critical to the rig operation, combustor performance, and mechanical integrity. The pressure measurements included the diffuser inlet total and static pressures, diffuser exit total, and static pressures, dome upstream total and dome downstream static pressures, and liners' hot and cold side static pressures.



ORIGINAL PAGE IS
OF POOR QUALITY

Figure 127. E³ Sector Combustor Test Rig Schematic.

ORIGINAL PAGE
BLACK AND WHITE PHOTOGRAPH

ORIGINAL PAGE IS
OF POOR QUALITY

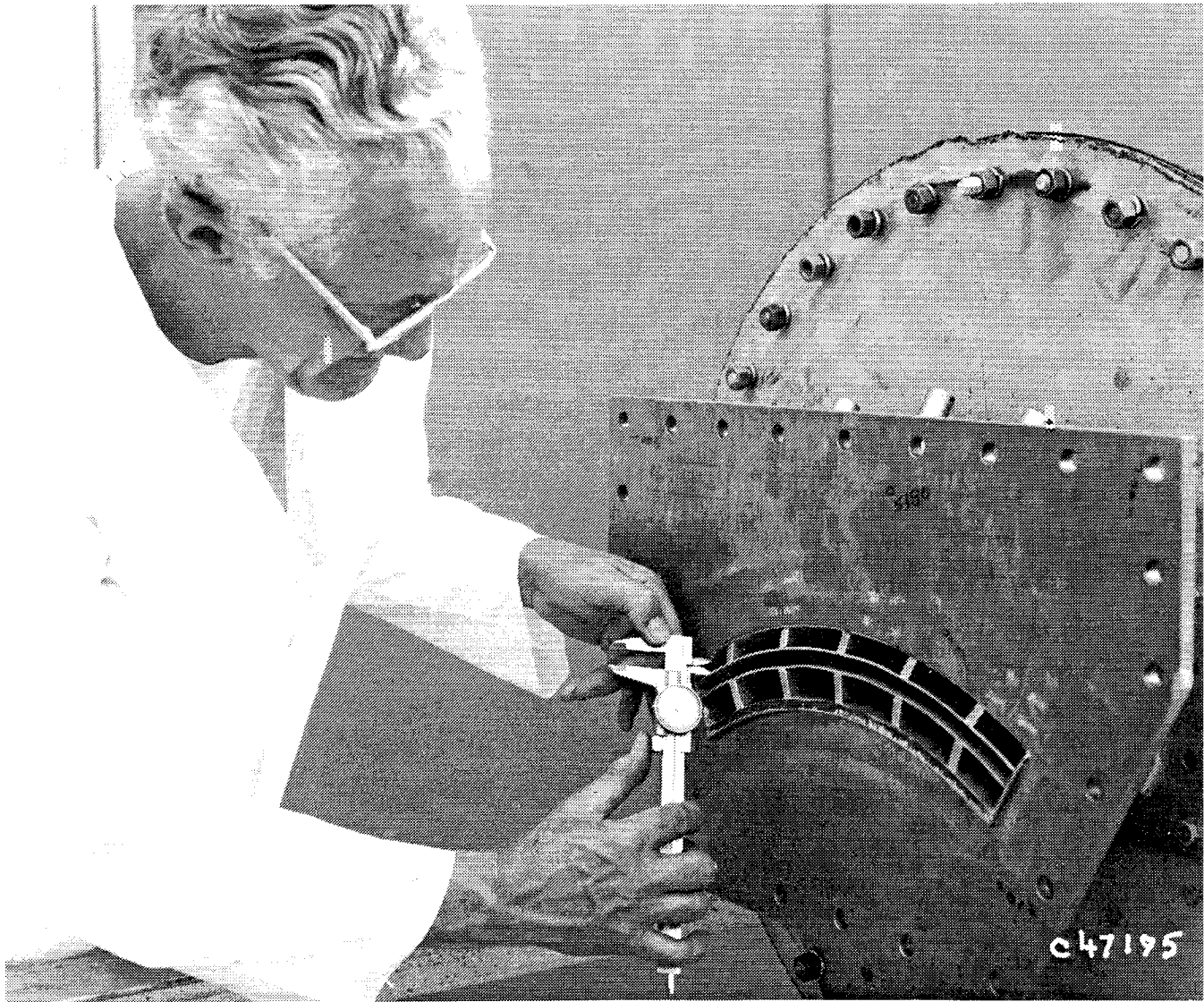


Figure 128. Sector Test Rig Inlet Diffuser.

ORIGINAL PAGE IS
OF POOR QUALITY

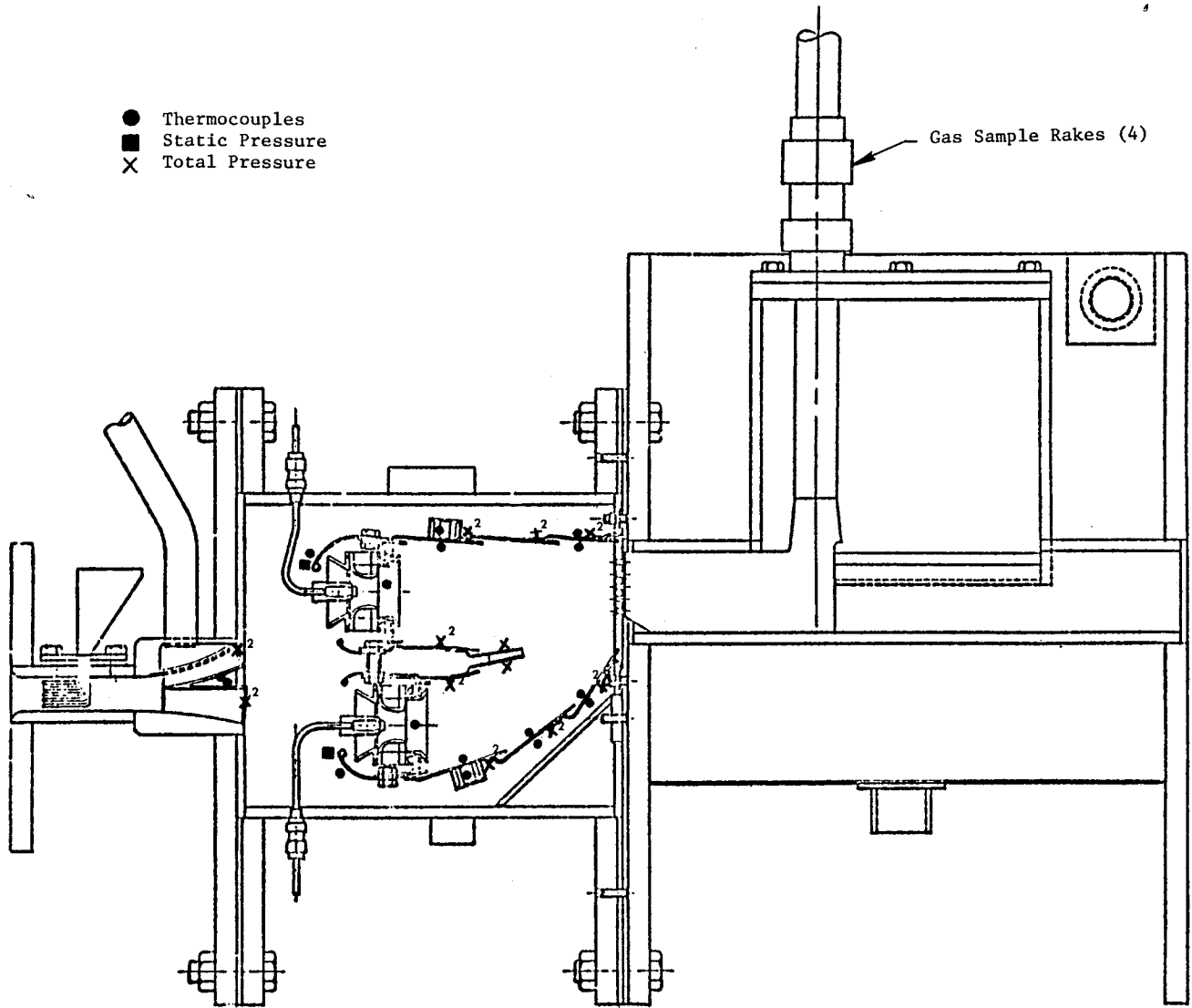


Figure 129. Test Rig and Instrumentation Emission Tests.

The total pressure at the combustor exit was measured using the gas sampling rake elements. These pressure measurements were employed in calculating combustor inlet velocity, pressure drops of the domes and liners, and overall combustor pressure drop.

Temperature measurements were made of the rig inlet airflow and on the inner and outer liner surfaces and the centerbody surfaces. The combustor exit temperature profiles were measured using four chromel-alumel thermocouple rakes installed in the instrumentation section of the test rig. Each of these exit rakes had seven thermocouples equally spaced on the leading edge of the rake and covered the entire sector combustor exit passage height. Several thermocouples were also located downstream of the instrumentation section in the facility exhaust system to monitor the facility operation.

The sector combustor exhaust gas samples were extracted from the exhaust flow by means of four gas sampling rakes installed, when required, in the instrumentation section of the test rig. Each of the gas sampling rakes had five sampling elements. The four rakes could be individually sampled or manifolded together to provide an average circumferential sample. Each of the five sampling elements was designed with a quick-quenching probe tip. In this design, the chemical reaction of the gas sample is quenched as soon as the sample enters the rake. Quenching is necessary to suppress any further chemical reaction of the gas sample within the sampling lines. Both water cooling of the rake body and steam heating of the gas sample lines within the rake were incorporated into the design. Water cooling of the rake body was required to protect the rake from damage due to the high temperature environment created at the combustor exit. Steam heating of the gas sampling lines was employed to prevent the condensation of hydrocarbon compounds and water vapor within the sampling lines. A photograph of a gas sampling rake is shown in Figure 130 and a schematic of a typical sampling element is shown in Figure 131.

6.1.4.4 Test Facility

All of the E³ sector combustor testing was conducted in the Advanced Combustion Laboratory facility, Building 306, located at the General Electric Evendale Plant. This facility is equipped with the inlet ducting, exhaust

ORIGINAL PAGE
BLACK AND WHITE PHOTOGRAPH

ORIGINAL PAGE IS
OF POOR QUALITY

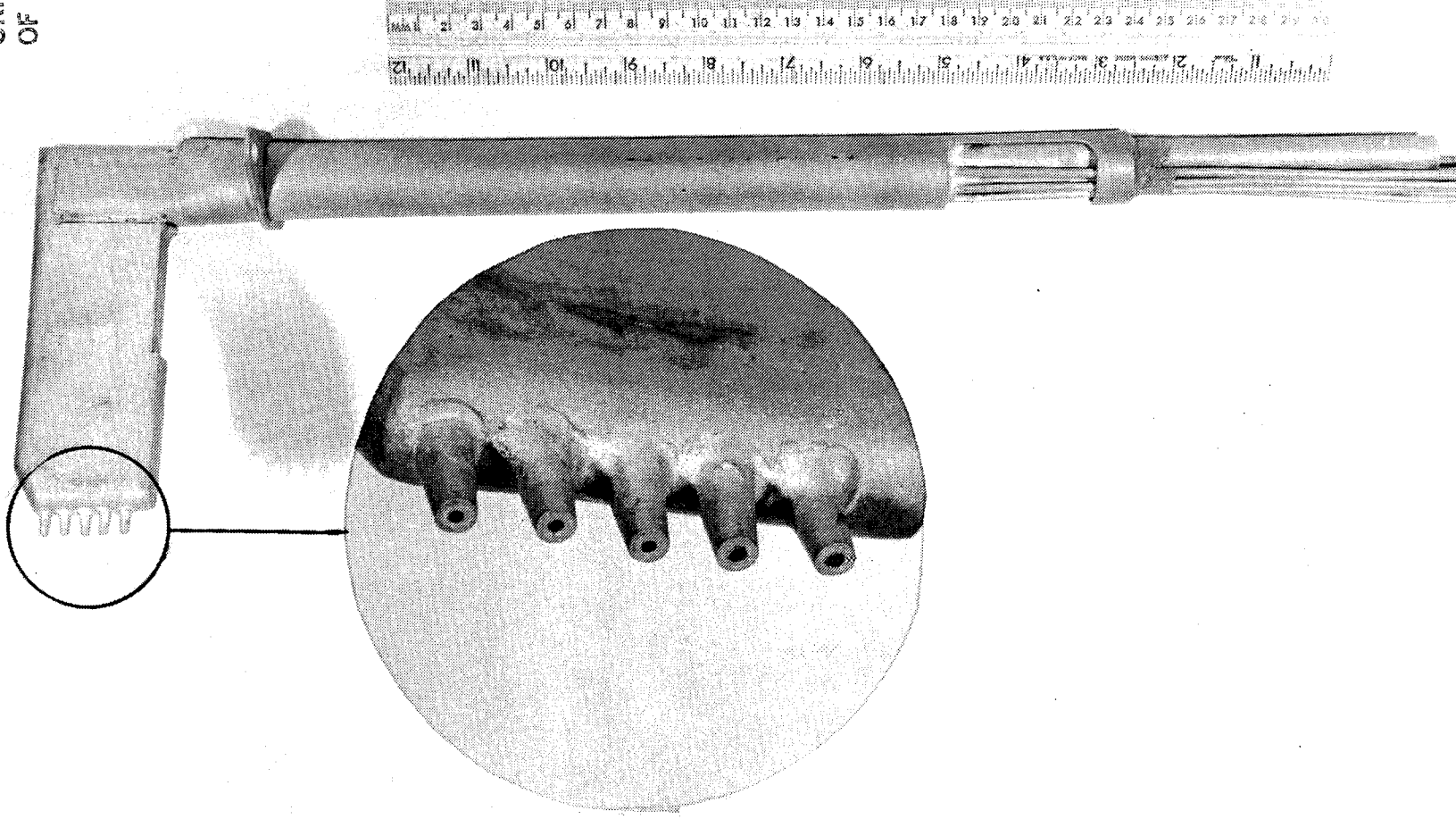


Figure 130. Sector Test Rig Gas Sampling Rake.

ORIGINAL PAGE IS
OF POOR QUALITY

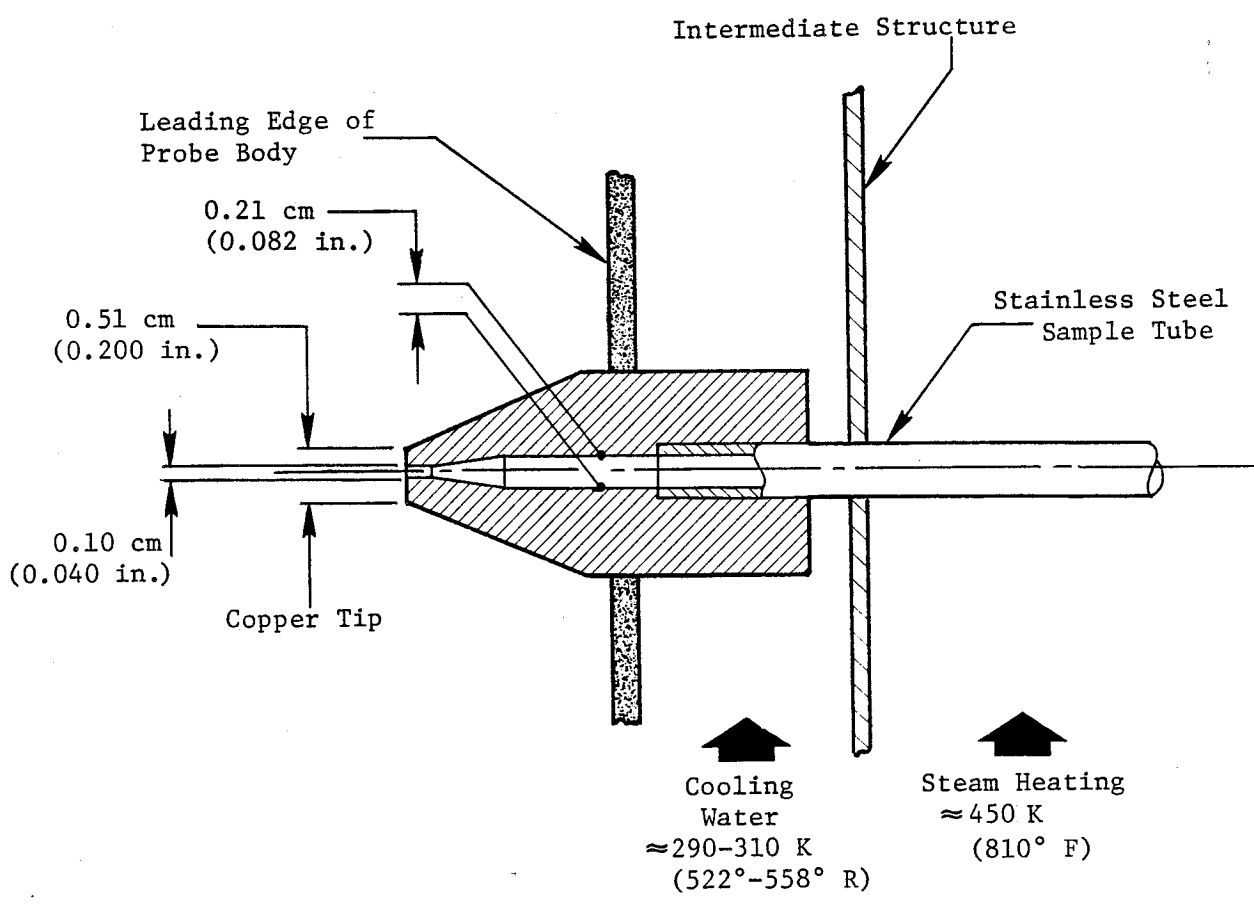


Figure 131. Schematic of Typical Rake Sampling Element.

ducting, controls, and instrumentation necessary for conducting sector combustor tests. The range of operating conditions obtainable in this facility is limited because of the airflow and heater capacity currently available. Airflow levels up to 2.8 kg/s (6.18 pps) can be supplied to the facility from a large compressor, plus an additional 1.8 kg/s (4 pps) can be supplied by the shop air system. Combustor inlet air temperatures above ambient are obtained using the facility liquid fueled, indirect-air preheater. The preheater has the capability to heat 1.35 kg/s (2.98 pps) airflow to 700 K (1260° R). Jet A fuel was supplied to the sector combustor test rig by a pipeline from storage tanks located adjacent to the facility. Instrumentation cooling and exhaust gas quenching was accomplished using the facility domestic water supply with pressure boost where necessary.

The facility also has the capability of simulating altitude conditions with the aid of a steam ejector system. This system allows the operator to reduce test rig pressure to 0.30 atmosphere. However, the facility does not have cold air or cold fuel capability. Therefore, all the altitude ignition testing was conducted at ambient air and fuel temperatures.

Test conditions were monitored using the facility instrumentation read-out equipment. Airflows were monitored by manometer readings of pressure drops across a standard ASME orifice in the air supply line. Fuel flows were metered by turbine-type flowmeters whose signal was input to an electronic frequency readout meter. Test rig pressures were monitored by either manometers or pressure gages, and thermocouple readings were obtained by self-balancing potentiometer recording instruments.

The sector combustor emissions were measured using the Contaminants Are Read On Line (CAROL) gas analysis system located in the test facility. This system consisted of the following instruments:

- Beckman Model 402 Total Hydrocarbon Analyzer (Flame Ionization Detector)
- Beckman Model 315-A Carbon Monoxide and Carbon Dioxide Analyzer (NDIR)
- Beckman Model 915 NO_x Analyzer (Chemiluminescence with converter, trap required).

Extracted exhaust gas samples were transmitted into this analysis equipment and the measured emissions levels were recorded on strip charts. An adequate supply of bottled calibration gases for the CAROL system was maintained throughout the emissions testing. A qualified technician calibrated and operated the CAROL system throughout the duration of data acquisition for each emissions test.

6.1.4.5 Test Procedures

The conditions selected for conducting the sector combustor ground start ignition tests simulated the E³ combustor inlet conditions at various core speeds from the E³ sea level standard day start model. The initial tests were conducted at atmospheric conditions with the instrumentation section of the test rig removed to allow for visual observation and monitoring of the ignition performance. The procedure for these tests entailed the following:

An airflow level and temperature simulating a set of conditions from within the E³ start model were set. The ignition source was activated and the pilot stage fuel flow was slowly increased. The fuel flow was recorded when at least one cup was lit. With the ignition source now deactivated, the fuel flow was further increased and recorded where each cup was lit until full propagation (all five cups) of the pilot stage was achieved. Then, the fuel flow was decreased and the level at which each cup extinguished was recorded.

The procedure was repeated until sufficient data repeatability was obtained.

In 1979, the engine startup procedure was revised to require operating the combustor on both stages up to idle speed at which point the main stage would be shut off. This required crossfiring the main stage as soon as the pilot stage was fully propagated. Hence, a major portion of the ground start ignition tests was devoted to developing crossfire performance. Once the pilot stage was fully propagated, the fuel flow was set at a level slightly above the pilot lean blowout limit; then, main stage fuel flow was introduced and increased slowly until one or more main stage cups were lit. The fuel flow was recorded, then recorded again when all cups were lit. Main stage

lean blowout fuel flow levels were also established in a procedure similar to that followed for the pilot stage.

For promising sector combustor configurations, a pressure ignition test was conducted with the instrumentation section of the test rig attached. These tests followed a similar procedure to the atmospheric ignition tests; except in this case, ignition was determined by monitoring thermocouples situated at the exit plane of the sector combustor downstream of each swirl cup. The actual pressures from the E³ start cycle were set for the pressure ignition tests. Table XXIX presents the test points and corresponding operating conditions for the ignition tests.

Table XXIX. Sector Combustor Ignition Test Point Schedule.

<ul style="list-style-type: none"> ● Based on E³ 9/27/79 Start Model ● Sector Combustor Flow Conditions (Annular Flow/6.0) 				
<u>Pressure Test</u>				
XNRH, %	P ₃ Atm.	T ₃ , K (° R)	W _c , kg/s (pps)	W _c √T ₃ /P ₃
21	1.020	295 (531)	0.21 (0.46)	3.54
58	1.837	383 (690)	0.57 (1.26)	6.07
70	2.463	427 (769)	0.79 (1.74)	6.63
<u>Atmospheric Test</u>				
21	1.0	295 (531)	0.20 (0.44)	3.54
32	1.0	314 (565)	0.25 (0.55)	4.43
46	1.0	344 (620)	0.28 (0.62)	5.19
58	1.0	383 (690)	0.31 (0.68)	6.07
70	1.0	427 (769)	0.32 (0.71)	6.63

The sector combustor performance evaluation tests consisted of conducting exit temperature surveys at ground start conditions for the calculation of combustion efficiencies, and at simulated SLTO conditions to establish exit temperature profiles. Other data obtained during these tests included pressure drops and metal temperatures. The temperature surveys were conducted using the four 7-element C/A thermocouple rakes located in the instrumentation section of the test rig. During the ground start efficiency tests, various core speeds, ranging from 46% to 77%, were evaluated with either pilot only or staged operation. The sea level takeoff temperature profile test conditions were limited by the available facility pressure level (approximately 4 atmospheres). The proper inlet temperatures, combustor fuel/air ratios, and Mach numbers were set in the test rig. The exit temperature profiles were then recorded for various pilot-to-main-stage fuel flow splits at a constant overall combustor fuel/air ratio.

All sector combustor instrumentation readings including static pressures, total pressures, and thermocouples were recorded throughout these tests. The recorded data were used in calculating dome and liner pressure drops, overall combustor pressure drops, and the conditions for and locations of highest metal temperatures.

The test conditions for the sector combustor emissions tests included low power as well as simulated high power operating conditions along the standard day, sea level static, E³ FPS operating cycle. The low power conditions included ground idle at 4% and 6% of sea level takeoff power with the only pilot stage fueled, and the EPA-defined 30% power (approach) operating conditions with both pilot only and staged combustor operation. The high power conditions tested simulated the 85% power (climbout) and sea level takeoff operating conditions in the staged combustor operating mode.

For the low power emissions tests, the true combustor operating conditions were duplicated in the sector combustor test rig. However, for the higher power emissions tests, the combustor flow function was simulated by derating the test rig inlet conditions to be consistent with the test facility limits. For all of the sector combustor test rig conditions, data were obtained over a range of combustor fuel/air ratios. A summary of the test point schedule for the emissions tests is presented in Table XXX.

Table XXX. Sector Combustor Emissions Test Point Schedule.

Cycle Condition	P ₃ Atm.	T ₃ , K (° R)	W ₃ , kg/s (pps)	W _{bled} kg/s (pps)	W _{F Pilot} , kg/hr (pph)	W _{F Total} , kg/hr (pph)	E/a Overall	W _{F Pilot}	
								W _{F Pilot}	W _{F Total}
4% Idle	3.40	466 (839)	1.45 (3.2)	0.11 (0.24)	48 (106)	0	0.010	1.0	1.0
	3.40	466 (839)	1.45 (3.2)	0.11 (0.24)	65 (143)	0	0.0135	1.0	1.0
	3.40	466 (839)	1.45 (3.2)	0.11 (0.24)	96 (212)	0	0.020	1.0	1.0
6% Idle	4.1	497 (895)	1.75 (3.86)	0.13 (0.29)	58 (128)	0	0.010	1.0	1.0
	4.1	497 (895)	1.75 (3.86)	0.13 (0.29)	71 (157)	0	0.0122	1.0	1.0
	4.1	497 (895)	1.75 (3.86)	0.13 (0.29)	93 (205)	0	0.0160	1.0	1.0
30% Approach	3.40	636 (1145)	1.33 (2.93)	0.10 (0.22)	63 (139)	0	0.0141	1.0	1.0
	3.40	636 (1145)	1.33 (2.93)	0.10 (0.22)	18 (40)	27 (60)	0.10	0.40	0.40
	3.40	636 (1145)	1.33 (2.93)	0.10 (0.22)	25 (55)	32 (71)	0.141	0.40	0.40
85% Climbout	3.40	700 (1260)	1.22 (2.69)	0.09 (0.20)	37 (81)	54 (119)	0.14	0.40	0.40
	3.40	700 (1260)	1.21 (2.68)	0.09 (0.20)	23 (51)	34 (75)	0.0140	0.40	0.40
	3.40	700 (1260)	1.21 (2.68)	0.09 (0.20)	29 (64)	44 (97)	0.0244	0.40	0.40
Sea Level Takeoff	3.40	700 (1260)	1.21 (2.68)	0.09 (0.20)	29 (64)	44 (97)	0.0244	0.40	0.40
	3.40	700 (1260)	1.21 (2.68)	0.09 (0.20)	45 (99)	68 (150)	0.0280	0.40	0.40
	3.40	700 (1260)	1.21 (2.68)	0.09 (0.20)	49 (108)	69 (152)	0.0244	0.30	0.50
3.40	700 (1260)	1.21 (2.68)	0.09 (0.20)	49 (108)	49 (108)	0.0244	0.40	0.40	
3.40	700 (1260)	1.21 (2.68)	0.09 (0.20)	47 (97)	65 (143)	0.0280	0.40	0.40	
3.40	700 (1260)	1.21 (2.68)	0.09 (0.20)	34 (75)	51 (112)	0.0220	0.40	0.40	
3.40	700 (1260)	1.21 (2.68)	0.09 (0.20)	22 (49)	34 (75)	0.0244	0.40	0.40	
3.40	700 (1260)	1.21 (2.68)	0.09 (0.20)	29 (64)	44 (97)	0.0244	0.40	0.40	

The combustor inlet conditions and corresponding fuel/air ratio for each point were set; then, the fixed combustor instrumentation readings were recorded. Exhaust gas samples were extracted using the gas sampling rakes and the pollutant emissions data from the gas analysis system were recorded. The normal procedure was to obtain a ganged sample from all four rakes simultaneously; however, for points of particular interest, individual samples from each rake were obtained and analyzed as well.

The altitude windmilling characteristics for the E³ were not defined prior to the testing; therefore, the CF6-50 engine windmilling map was used as a substitute to investigate the altitude relight capability of the E³ sector combustor. Actual pressures at altitude were set during these tests. However, ambient temperature inlet air and fuel were used. The tests consisted of determining the ignition and lean blowout limits over a selected range of windmilling conditions. The sector combustor inlet conditions were set, fuel flow initiated, and fuel flow levels at which each cup ignited were recorded. Then fuel flow is slowly decreased and levels were recorded at which each cup extinguished. For some conditions where ignition was unsuccessful, inlet pressure was slowly increased while holding a constant fuel flow until ignition was obtained.

6.1.4.6 Data Reduction Procedures

The recorded data of the ground start ignition tests and the altitude relight tests were simply reduced by calculating ignition and lean blowout fuel/air ratios for each test point and presenting the results as plots of fuel/air ratios versus either core speed or the combustor inlet conditions.

Exit temperature profiles were obtained from plots of the thermocouple rake data to which a radiation correction factor had been applied. Combustion efficiencies were also determined from rake data by calculating the ratio between the average of the exit temperatures measured and the theoretical gas temperature for the test fuel/air ratio.

The various sector combustor pressure drops and airflow distributions were calculated from the recorded test data and the known effective flow areas of the sector combustor hardware using a computer data reduction program.

Emissions data reduction was accomplished using two data reduction computer programs. One program performed curve fit calculations on the CAROL system calibration data obtained at the start of an emissions test. Calibration checks of the gas analysis system were performed before and after each emissions test run to prevent data drift. During a test, the measured emissions were recorded on chart recorders contained within the CAROL system. The emissions data were also recorded on test log sheets. Following the completion of each test run, the emissions data, along with the sector combustor performance data, were input into the other data reduction program where the reduction of the raw emissions data to emissions indices was performed. The calculation equations used in this program were basically those contained in SAE ARP 1256. In these calculations, the CO and CO₂ concentrations were corrected for the removal of water from the sample prior to its analysis. A fuel hydrogen-to-carbon atom ratio of 1.92, representing the Jet A fuel, was used in these calculations. Calculated combustion efficiency, sample fuel/air ratio, and an overall emissions index were also obtained from the data reduction program. The overall emission index represents a weighted average of the values obtained from each individual gas sampling rake and is defined as follows:

$$EI_j \text{ (Overall)} = \frac{\sum_{i=1}^N (EI_j)_i * (F/A \text{ Sampled})_i}{\sum_{i=1}^N (F/A \text{ Sampled})_i}$$

The (j) subscript refers to the identity of the gaseous pollutant, (CO, HC, or NO_x), and the (i) subscript refers to the individual rakes where (N) represents the total number of gas sampling rakes. Expressing the average of the emissions in this form reduces the influence of very lean combustion zones within the combustor where the concentrations of gaseous pollutants are low but where the calculated emissions indices are quite high. These weighted average emissions values are presented in the numerous data tables and figures of this report.

At the high power operating conditions where the combustor inlet pressure, temperature, and airflow were derated due to facility limitations, the measured emission levels were adjusted to reflect the actual engine cycle conditions. The adjustment relations used are defined in Appendix D.

6.1.4.7 Test Configurations

A total of seven basic configurations were tested during the E³ Sector Combustor Test Program. Some of these configurations were subjected to "piggyback" tests, with one or more of their features somewhat varied to investigate specific performance aspects. A brief description of each configuration features relative to the baseline configuration follows.

The following modifications to the baseline configuration design were incorporated for the Mod I configuration:

- The primary dilution holes in the outer and inner liners were relocated to "between swirl cups" from "in line with cups" in the baseline configuration. This modification was introduced in order to achieve a more uniform fuel/air mixture balance between the two zones.
- The 90° angle sleeves replaced the 45° angle sleeves that were featured in the baseline design. These wider angle sleeves were expected to produce a more dispersed fuel spray, and this was desired in spite of anticipated problems with spray instability. The 45° sleeve had been selected based on swirl cup investigation results. However, when installed in the sector combustor, these sleeves appeared to produce a somewhat more narrow spray angle than was desired, leading to a fuel rich zone in between cups. The wider angle sleeve did produce a more uniform primary zone fuel/air ratio distribution and did not have any observable instability problems.
- The pilot dome splash plate cooling was reduced by approximately 40% to bring it closer to the originally intended design level of 4.3% of the combustor airflow. This change was expected to help the CO emissions particularly at idle conditions.

The Mod II configuration featured the incorporation of the E³ full-annular, development combustor-type swirl cups to replace the prototype swirlers. This configuration also had a modified airflow distribution characterized by a reduction in the pilot stage swirl cup airflow and an increase in the main stage for the purpose of reducing NO_x emissions at high power conditions.

The Mod III configuration of the E³ sector combustor featured changes that were primarily directed at improving the ignition performance. The key changes included a substantially reduced main stage swirl cup airflow and the use of full-annular, development-type fuel nozzles in both stages in order to duplicate the full-annular, combustor fuel system design. In addition, a crossfire tube, similar in design to that of the full-annular combustor, was incorporated into the centerbody to provide an ignition source for the main stage. Up to this point, main stage ignition had been achieved by means of an auxiliary ignition system installed through the sector combustor sidewall. The 90° angle sleeves were retained in the Mod III because none of the anticipated fuel spray instability problems had occurred. In order to determine the effects of the fuel nozzle spray angle and the fuel nozzle shroud air on CO and HC emissions levels, several fuel nozzle configurations were tested in the Mod III configuration for emissions at the 6% ground idle conditions. There were three variations. Mod III-A differed from the Mod III by blocking off the fuel nozzle shroud air. Mod III-B featured the prototype simplex peanut fuel nozzles in place of the development nozzles, and Mod III-C utilized air-shrouded, development-type fuel nozzles rated at 23 kg/hr (50.7 pph).

For the Mod IV configuration, the pilot stage primary dilution airflow was increased to double the Mod III configuration level to provide more penetration and enhance mixing of the fuel and air to reduce idle emissions. Furthermore, the centerbody multijet length was shortened by approximately 1.78 cm (0.70 inch) for mechanical considerations. These two design changes were evaluated during the Mod IV configuration tests of the sector combustor with emphasis placed on evaluating whether a shorter centerbody would adversely affect the ignition and low power emissions performance.

The Mod V configuration of the E³ sector combustor featured a substantial increase in the main stage primary dilution effective area. This increase resulted in approximately a 7% increase in the total sector combustor effective flow area, and caused a reduction in the pilot stage swirl cup airflow as a percentage of total airflow. This reduction in swirl cup airflow was expected to further reduce idle CO and HC emissions, while the increase in the main stage primary dilution flow was expected to reduce NO_x emissions at high power combustor operating conditions.

The Mod VI configuration featured a simultaneous reduction in the swirl cup airflow level and an increase in the primary dilution airflow level of the sector combustor pilot stage. The swirl cup airflow was reduced by blocking three of the 12 vane passages for each of the secondary swirlers. This resulted in a reduction of approximately 20% of the pilot stage swirl cup airflow relative to the Mod V configuration. The pilot stage dilution airflow was increased by opening up the flow area of the dilution holes in the outer liner and the pilot stage side of the centerbody. In addition, 50% of the outer liner Row 1 and corresponding centerbody cooling holes, located in line with swirl cups, were closed off. All of these modifications were intended to produce a more uniform fuel/air distribution within the pilot stage dome of the sector combustor.

Five variations on the Mod VI configuration were tested in an effort to identify any quick design changes that could be implemented in the full-annular combustor design for the purpose of improving the main stage crossfire performance. In Mod VI-A, every other passage in the main stage primary swirler was blocked; and the main stage splash plate cooling flow was reduced by approximately 30%. This change was intended to enrich the main stage dome thereby improving the crossfire performance.

For Mod VI-B, the blockage from the pilot stage secondary swirler was removed to allow for a stronger recirculation zone and possibly force a larger flame through the crossfire tube into the main stage. In Mod VI-C, an extension was added to the main stage side of the crossfire tube. The purpose of the extension was to shelter the flame passing through the tube and prevent it from being swept downstream by the swirl cup flow. Another extension, added to the pilot stage side of the crossfire tube, made up the Mod VI-D configuration. The purpose of this extension was to capture the flame from the pilot stage and force it into the crossfire tube.

The crossfire tube geometry was again modified for the Mod VI-E configuration. The originally cylindrical tube was redesigned into a "D"-shaped cross section with an area equal to that of the circular design. The intent of this modification was to move the flow area of the crossfire tube as far forward on the centerbody as possible.

A summary of the test configurations, their features, their effectiveness, and estimated airflow distributions is provided in Appendix C.

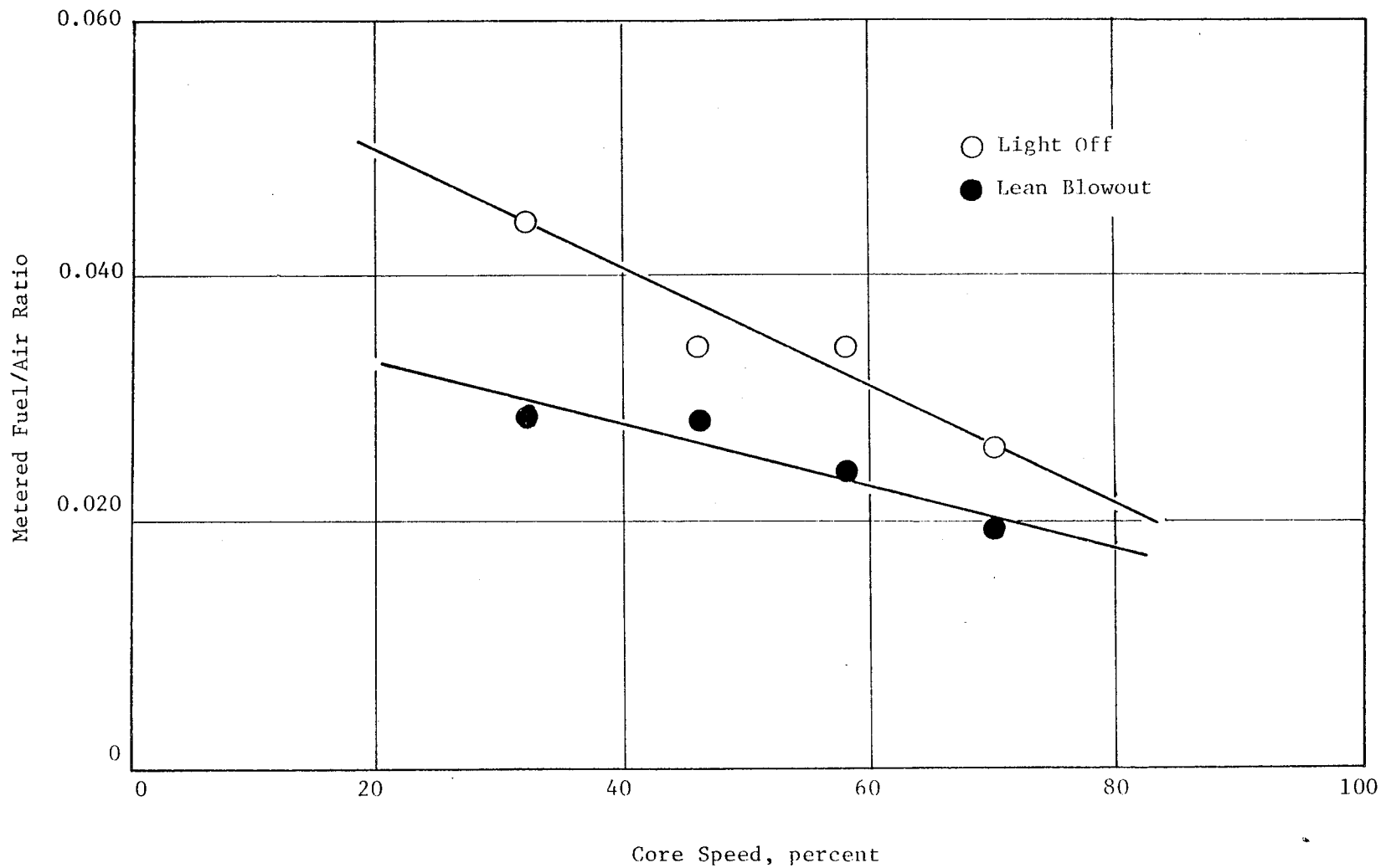
6.1.4.8 Ignition Test Results

The atmospheric ignition test results on the baseline configuration indicated that excessively high fuel/air ratios were required to light the pilot stage with ignition not attainable at the 21% core speed conditions. Full propagation was not possible for any of the test conditions in the E³ starting schedule. For those cups that did light, the fire appeared to be concentrated in between swirl cups rather than evenly distributed across the entire sector combustor. Figure 132 is a plot of the pilot stage lightoff and lean blowout fuel/air ratios versus percent core speed for the baseline configuration.

Attempts to crossfire the main stage during the baseline configuration tests were unsuccessful. However, the crossfire tube had not yet been incorporated into the centerbody design; therefore, crossfire had to occur around the tip of the centerbody.

As was the case for the baseline configuration tests, the initial Mod I ignition tests were conducted using a hydrogen torch as the ignition source. An improvement of approximately 20% in the pilot stage ignition performance was obtained in the Mod I configuration. Furthermore, full propagation was achieved at all test points and visual observation of the fire at the sector combustor exit indicated a more uniform flame. The pilot stage ignition test results for this configuration are shown in Figure 133. The improvement in the ignition performance was attributed to reducing the splash plate cooling airflow in the pilot stage and the wider angle sleeves. The flame uniformity, on the other hand, was attributed to relocating the primary dilution to between swirl cups.

Using a spark plug ignitor in place of the hydrogen torch in a subsequent test on the Mod I configuration resulted in approximately the same lightoff and lean blowout fuel/air ratio. Since the crossfire tube was still not incorporated into the design, no crossfire attempts were made on this configuration. However, the main stage ignition performance was investigated using



ORIGINAL PAGE IS
OF POOR QUALITY

Figure 132. Sector Combustor Baseline Ignition Results, Pilot Stage.

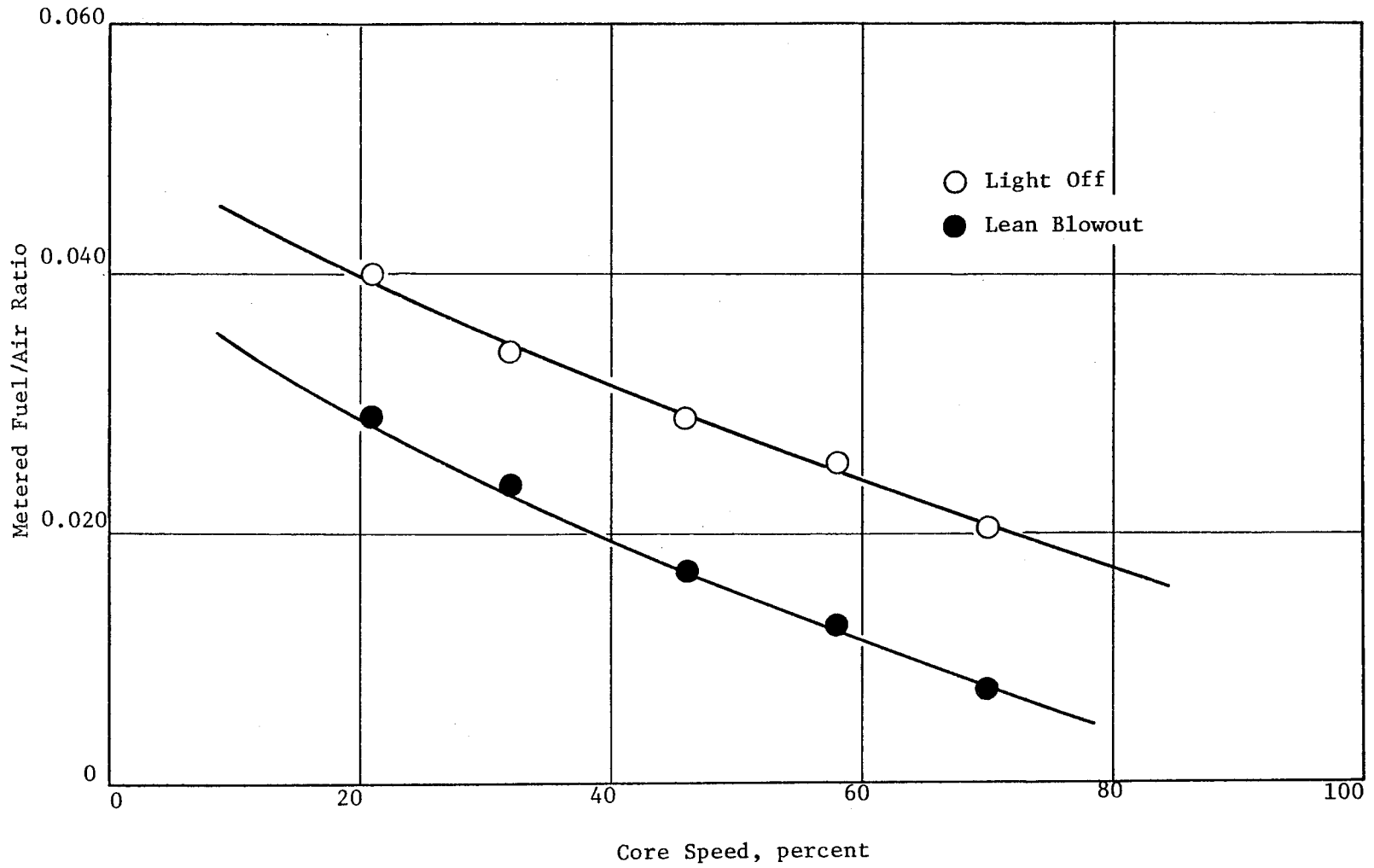


Figure 133. Sector Combustor Mod I Ignition Results, Pilot Stage.

ORIGINAL PAGE IS
OF POOR QUALITY

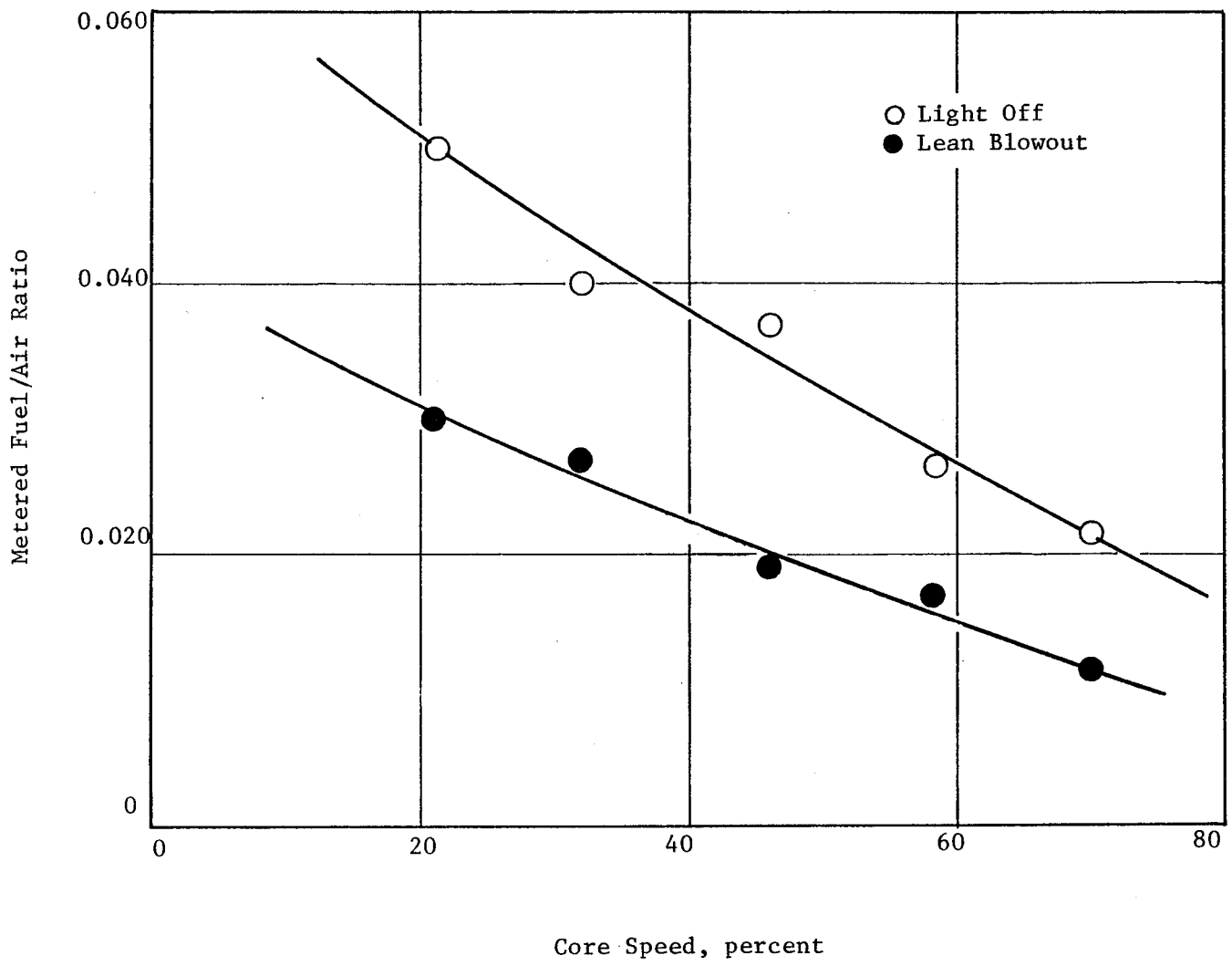
a hydrogen torch ignitor installed through the sector sidewall. The results are shown in Figure 134. Main stage lightoff fuel/air ratios were slightly higher than those of the pilot stage due to the higher velocities in the main stage dome.

Since the proposed E³ start sequence required obtaining ignition in both pilot and main stages at a selected core speed, it was necessary for the sum of the pilot stage lean blowout and main stage light-off fuel/air ratios to fall within the specified operating line at that core speed. Figure 135, which plots the results for the Mod I configuration, clearly indicated that further improvement was still required to satisfy this start requirement.

The Mod II configuration which featured development combustor-type swirl cups in both stages, produced disappointing ignition results. Lightoff and lean blowout fuel/air ratios obtained for the pilot as well as the main stage were higher than those obtained with the Mod I configuration. Visual observation of the fire at the sector exit indicated no signs of nonuniformity of the fuel spray. However, posttest fuel spray visualization tests of the swirl cup - fuel nozzle assembly revealed that the development combustor-type swirlers produced a significantly narrower fuel spray angle than that obtained with the prototype swirlers. This narrow fuel spray limited the ignition performance by causing the discharged fuel to be too far away from the ignition source.

The results of the Mod III ignition tests were much more encouraging than those of the Mod II results. Figure 136 shows a reduction of approximately 45% of the lightoff and lean blowout fuel/air ratios of the pilot stage was obtained. As expected, the main stage ignition performance approached the performance of the pilot stage due to the similarity in the swirl cup airflow levels. The improvement in the ignition performance of the pilot stage was largely attributed to the use of the development-type fuel nozzles instead of the prototype nozzles used in all earlier tests.

A crossfire tube was also installed in the sector combustor centerbody for the Mod III configuration and a crossfire test was conducted according to the test plan. Successful crossfire was obtained for each of the points



ORIGINAL PAGE IS
OF POOR QUALITY

Figure 134. Sector Combustor Mod I Ignition Results, Main Stage.

ORIGINAL PAGE IS
OF POOR QUALITY

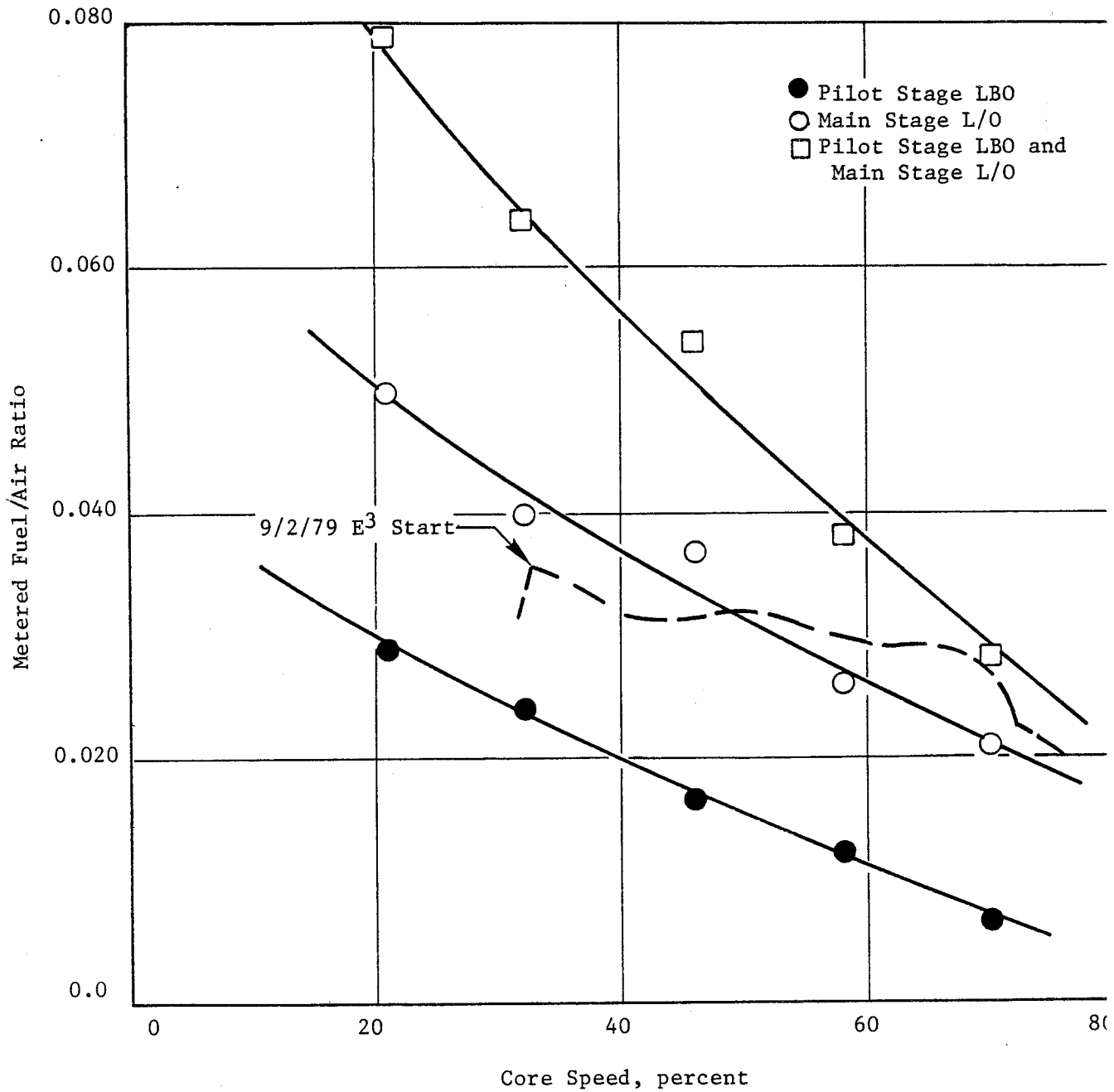


Figure 135. Sector Combustor Mod I Ignition Results Versus Cycle Requirement.

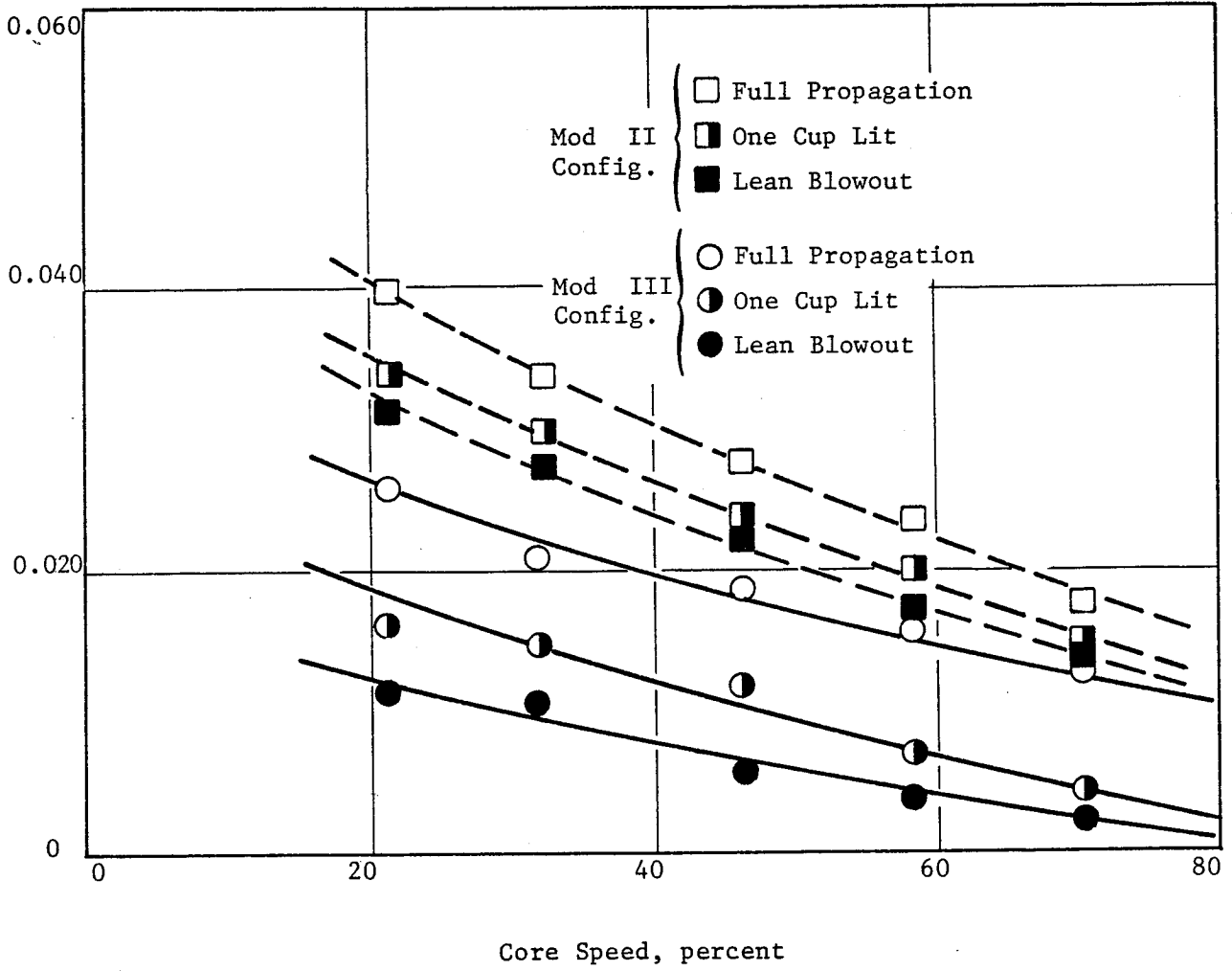


Figure 136. Sector Combustor Mod III Ignition Results.

in the ignition test point schedule. At low core speeds, the crossfire fuel/air ratios were somewhat higher than the full propagation fuel/air ratios obtained with the hydrogen torch ignitor for this configuration. However, at higher core speeds, the difference in the fuel/air for the two ignition sources was reduced significantly. This was attributed to the fact that at low core speeds, crossfire occurred across the centerbody trailing edge rather than through the crossfire hole at high core speeds. Figure 137 compares the crossfire fuel/air ratio to that obtained using a hydrogen torch ignition in both Mod II and III configurations.

A plot of the overall combustor fuel/air ratio, required to obtain main stage crossfire versus core speed along with the 9/2/79 E³ ground start fuel schedule for the Mod III configuration, is presented in Figure 138. The figure indicates that this sector combustor configuration meets the E³ start requirement at core speeds of 53% or higher.

A pressure ignition test, representing actual E³ conditions at the combustor inlet, was also conducted on the Mod III configuration. The results of this test showed a significant improvement over the atmospheric ignition test results in both pilot stage ignition and main stage crossfire performance. Figure 139 presents a plot of fuel/air ratio versus core speed for the Mod III pressure ignition results. The figure suggests that the E³ requirement will be met at core speeds of 38% or higher as compared to the 53% core speed level obtained from the atmospheric test results.

The ground start ignition test results of the Mod IV configuration were very similar to those of the Mod III configuration results. A shorter centerbody design did not have any adverse effects on the ignition performance of the sector combustor. The only other modification introduced to the Mod IV configuration was the increased primary dilution airflow and was intended for emission reduction purposes only.

The E³ sector combustor ignition performance was further improved in the Mod V configuration. The improvement was primarily in the main stage crossfire performance and was attributed to a decreased swirl cup airflow and an

ORIGINAL PAGE IS
OF POOR QUALITY

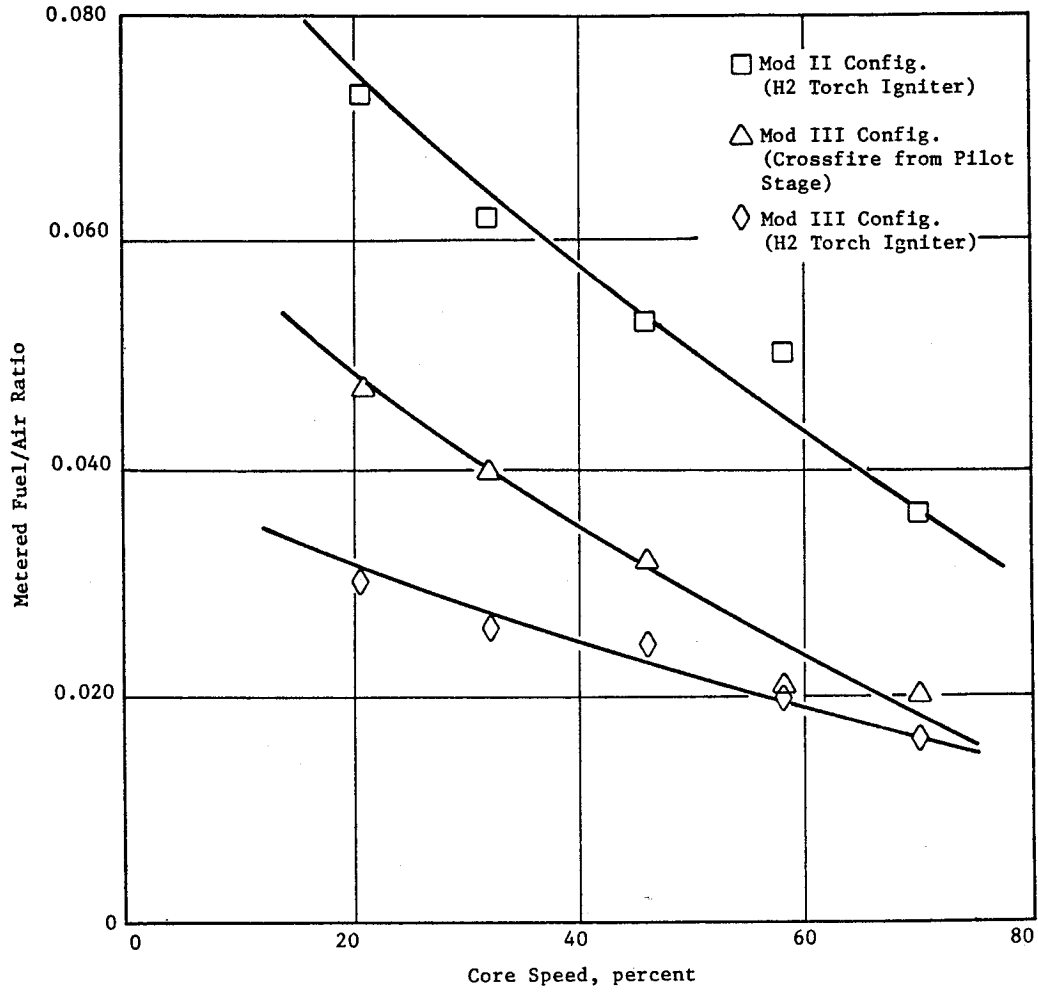


Figure 137. Sector Combustor Mod II and III Main Stage Ignition Results.

ORIGINAL PAGE IS
OF POOR QUALITY

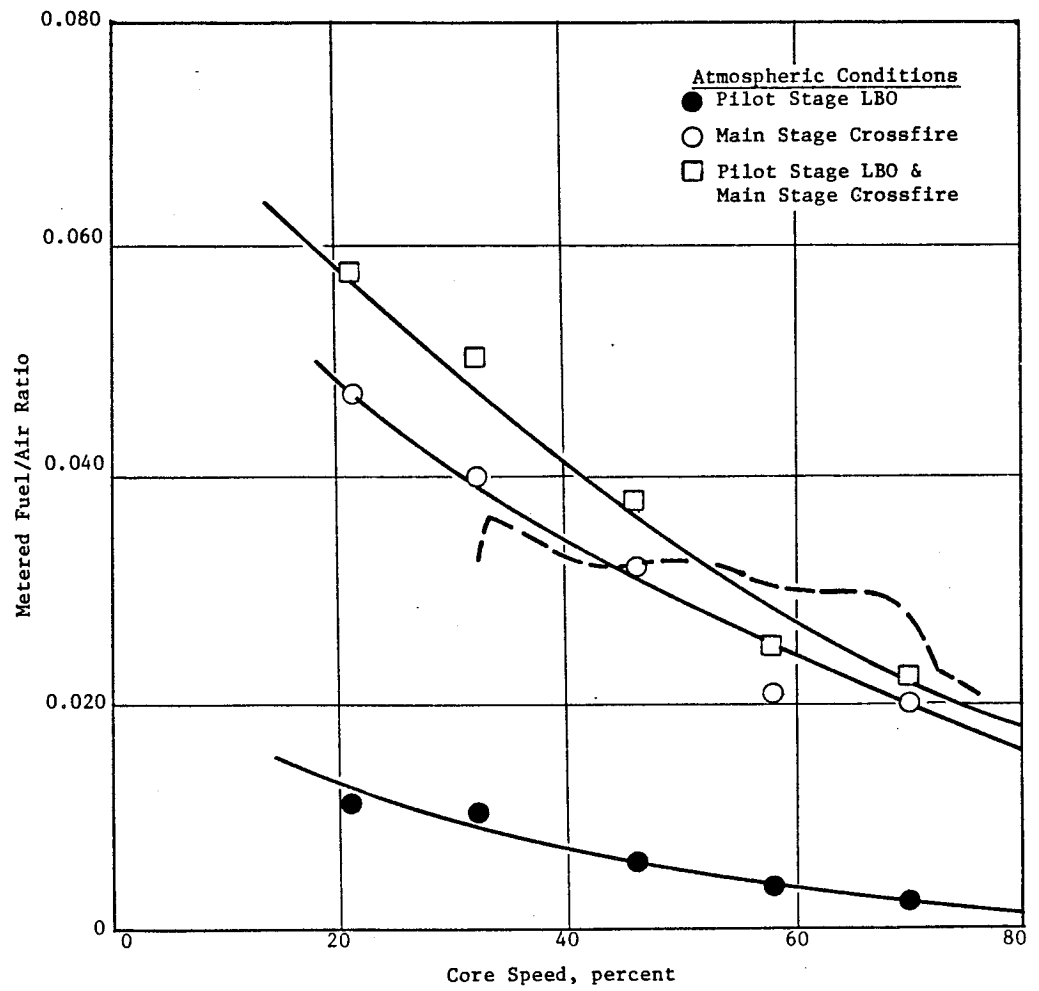


Figure 138. Sector Combustor Mod III Ignition Results Versus Cycle Requirement.

ORIGINAL PAGE IS
OF POOR QUALITY

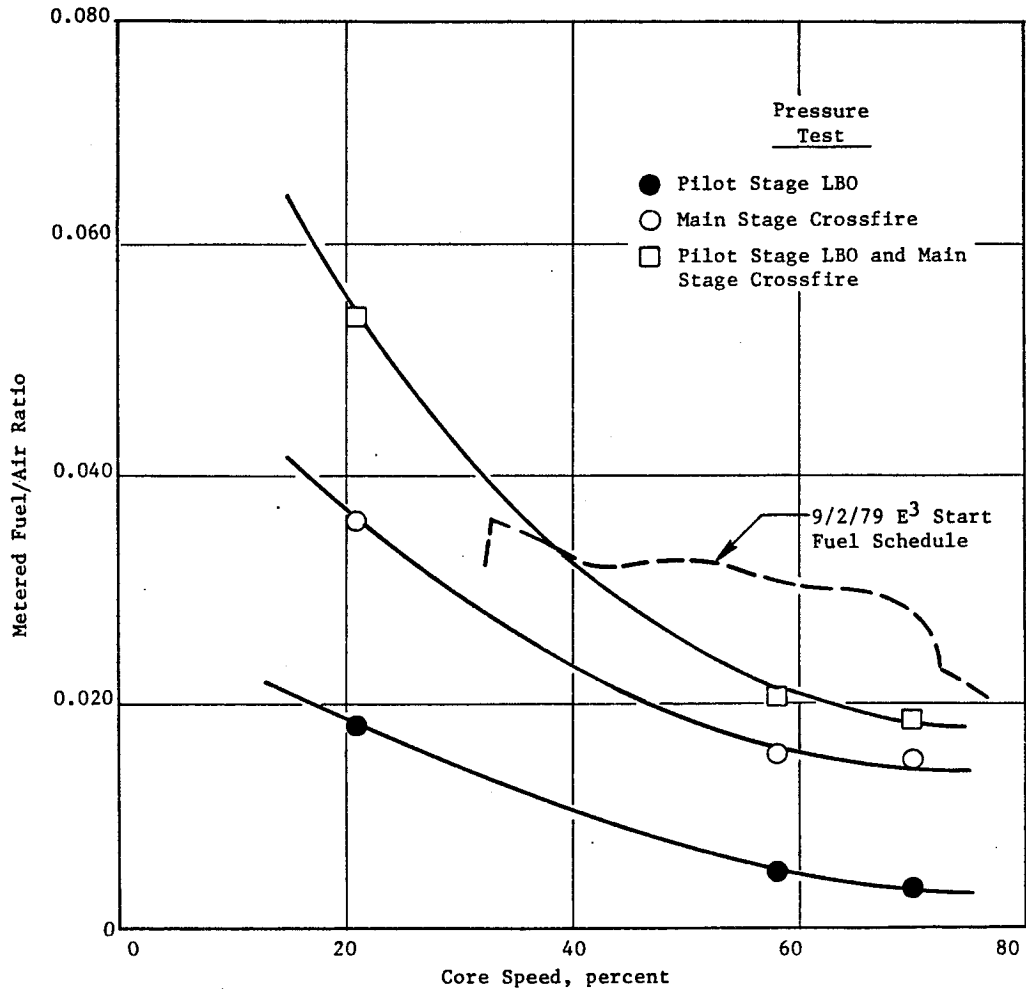


Figure 139. Sector Combustor Mod IV Ignition Results at Actual Inlet Pressure.

increased dilution airflow. Figure 140 shows the results of the pressure ignition test for this configuration, indicating that the E³ start requirement is met at 32% and higher core speeds.

No net gain in the sector combustor ignition performance was realized from the changes incorporated into the Mod VI configuration. The richer dome in the pilot stage which was expected to improve its ignition capability was offset by weaker recirculation due to a reduction in the secondary swirler airflow.

The hardware modifications that were later introduced to the Mod VI configuration (namely, reducing the main stage swirl cup airflow, adding extensions to the crossfire tube, and redesigning the crossfire hole geometry) were very effective in further improvement to the crossfire performance. However, concurrent with this stage of the sector combustor testing effort, a revised E³ SLS standard day ground start cycle was issued. This revised cycle eliminated the requirement of obtaining ignition in the main stage at subidle conditions. A pilot stage ignition test using the revised cycle conditions produced excellent results as shown in Figure 141. At 32% core speed where engine start is expected, the full propagation fuel/air ratio was approximately 0.0130 which was well below the 0.020 fuel/air ratio specified by the fuel schedule. Since the main stage ignition is required only above idle, no difficulty was anticipated in obtaining crossfire from the pilot stage to the main stage.

6.1.4.9 Exit Temperature Performance Test Results

Ground start efficiency tests and exit temperature profile tests were conducted only on the baseline configuration of the E³ sector combustor. Calculated combustion efficiencies at ground start conditions with the pilot stage only fueled ranged from 0.58 at 46% core speed to 0.98 at 77% core speed. As expected, average temperature profiles at these conditions were peaked outward, as shown in Figure 142. In the staged combustor operating mode for the same core speed with equal fuel flow in each dome, the temperature profiles are relatively flat as indicated in Figure 143. At simulated sea level takeoff conditions, the temperature profile and combustion efficiency were functions of the fuel flow split as illustrated in Figure 144.

ORIGINAL PAGE IS
OF POOR QUALITY

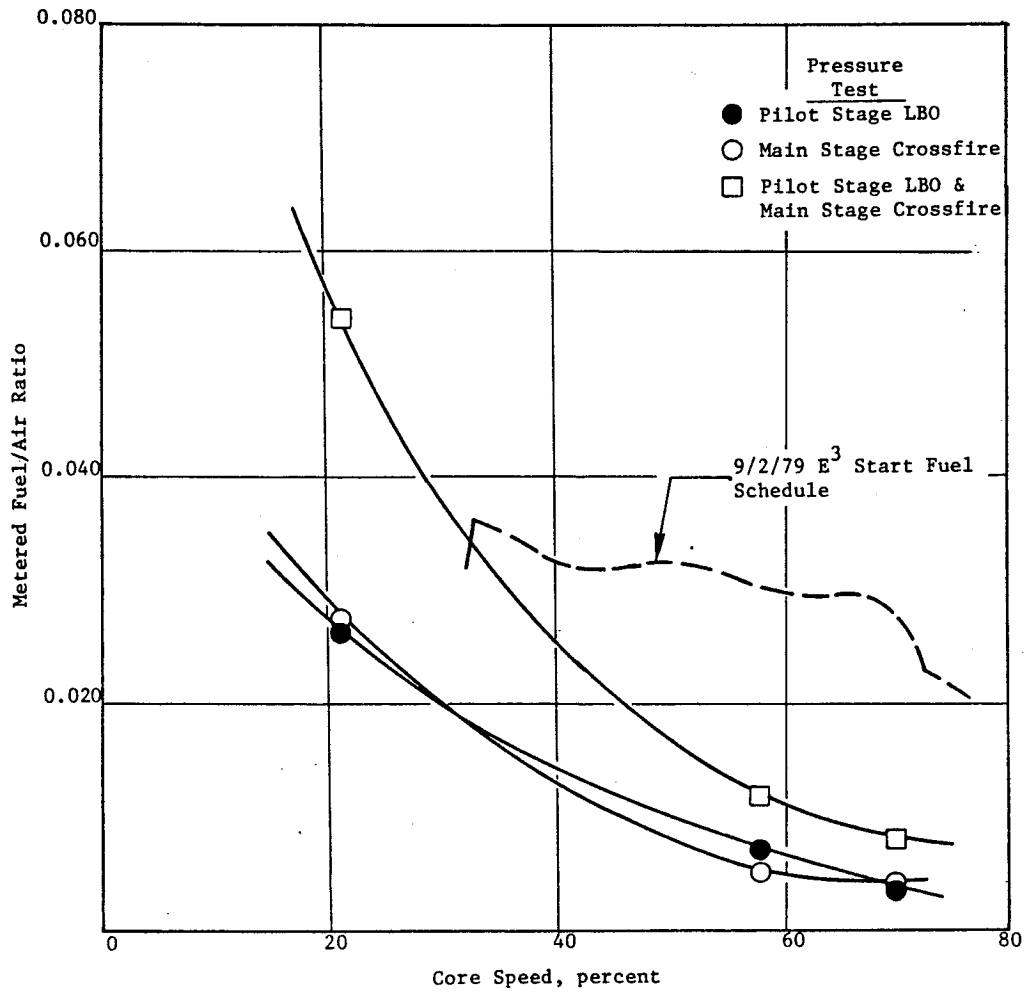
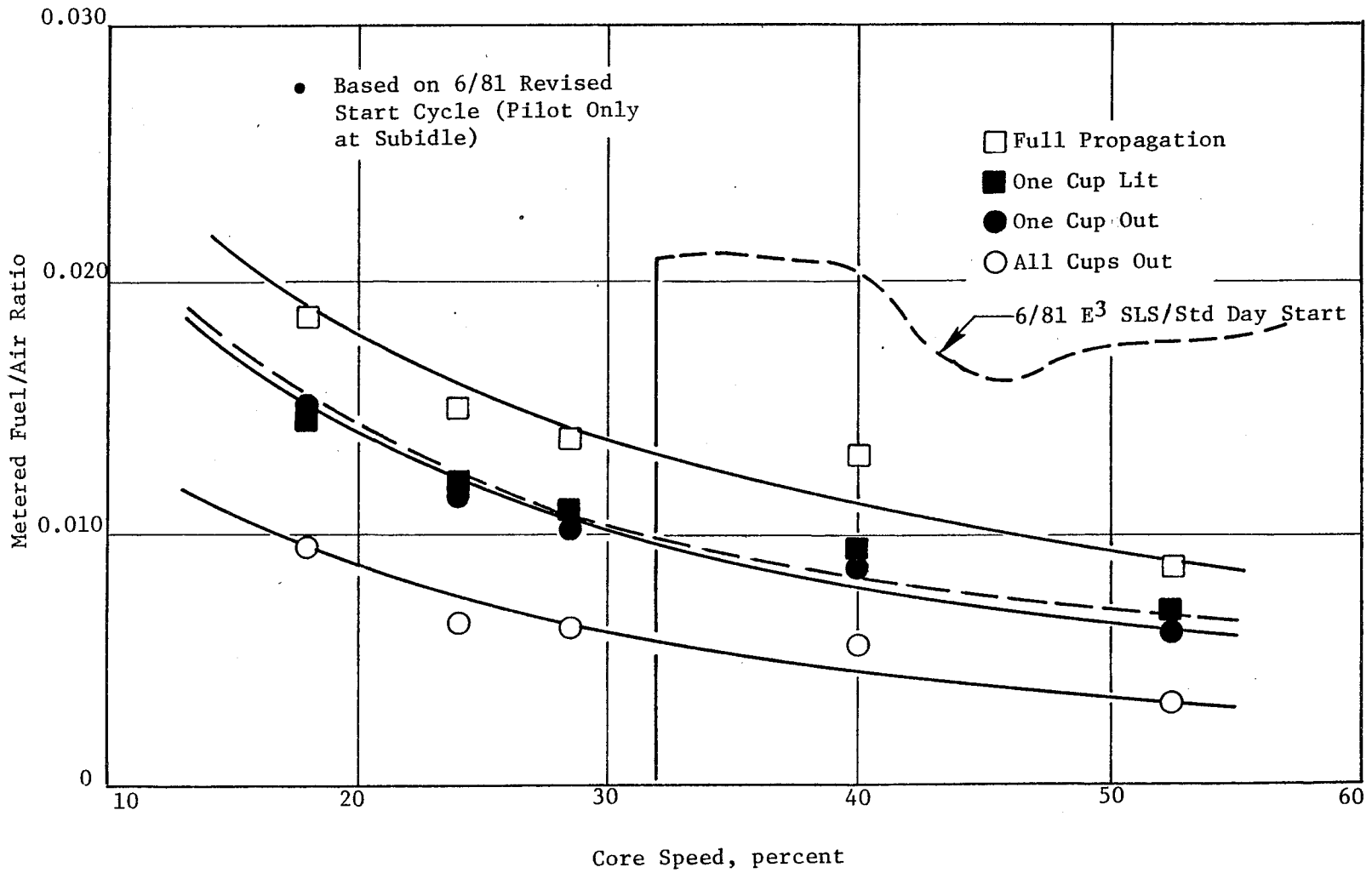


Figure 140. Sector Combustor Mod V Ignition Results at Actual Inlet Pressure.



ORIGINAL PAGE IS
 OF POOR QUALITY

Figure 141. Sector Combustor Mod VI Ignition Results.

ORIGINAL PAGE IS
OF POOR QUALITY

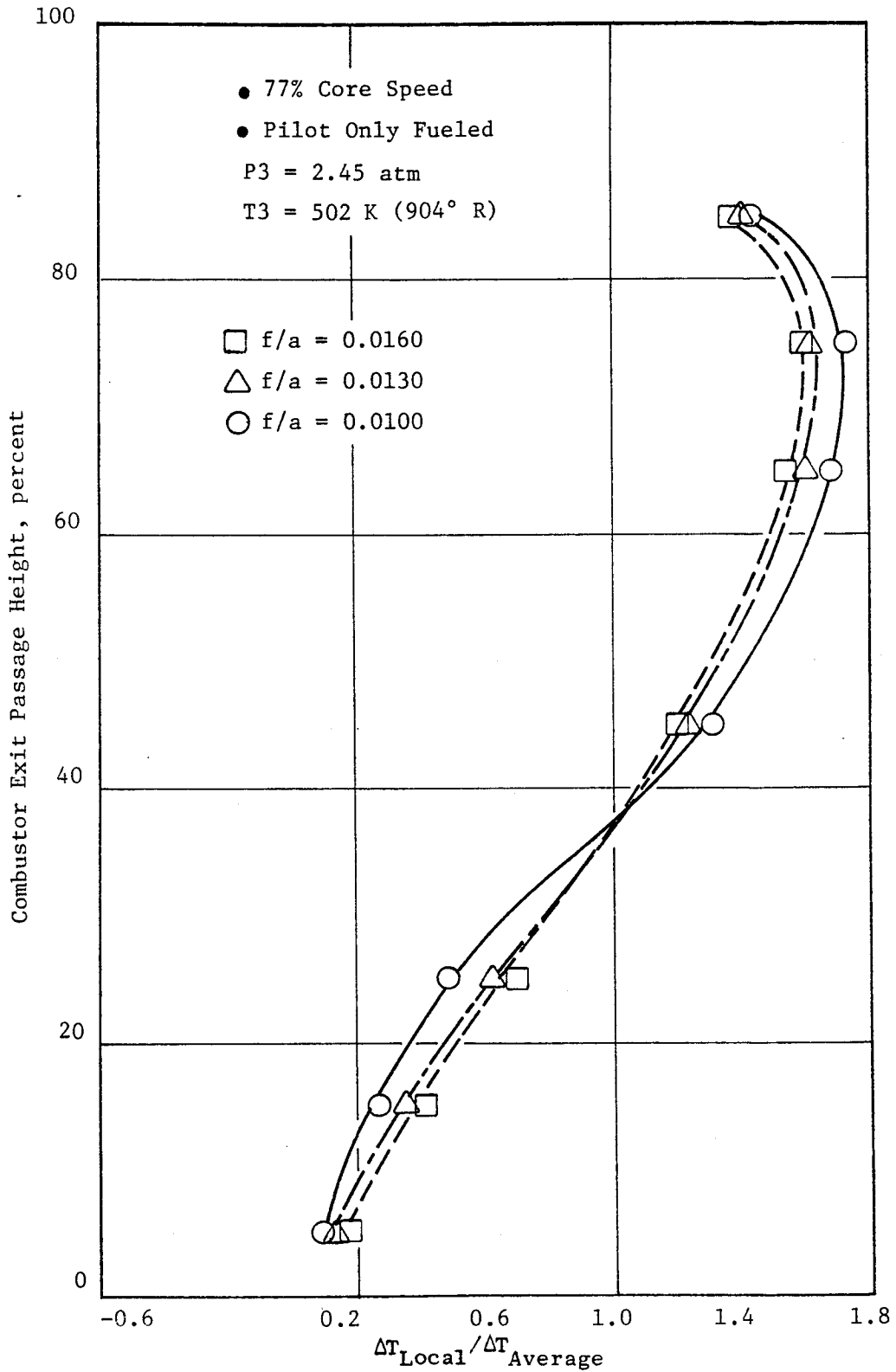


Figure 142. E^3 Sector Combustor Subidle EGT Profiles (Pilot Only).

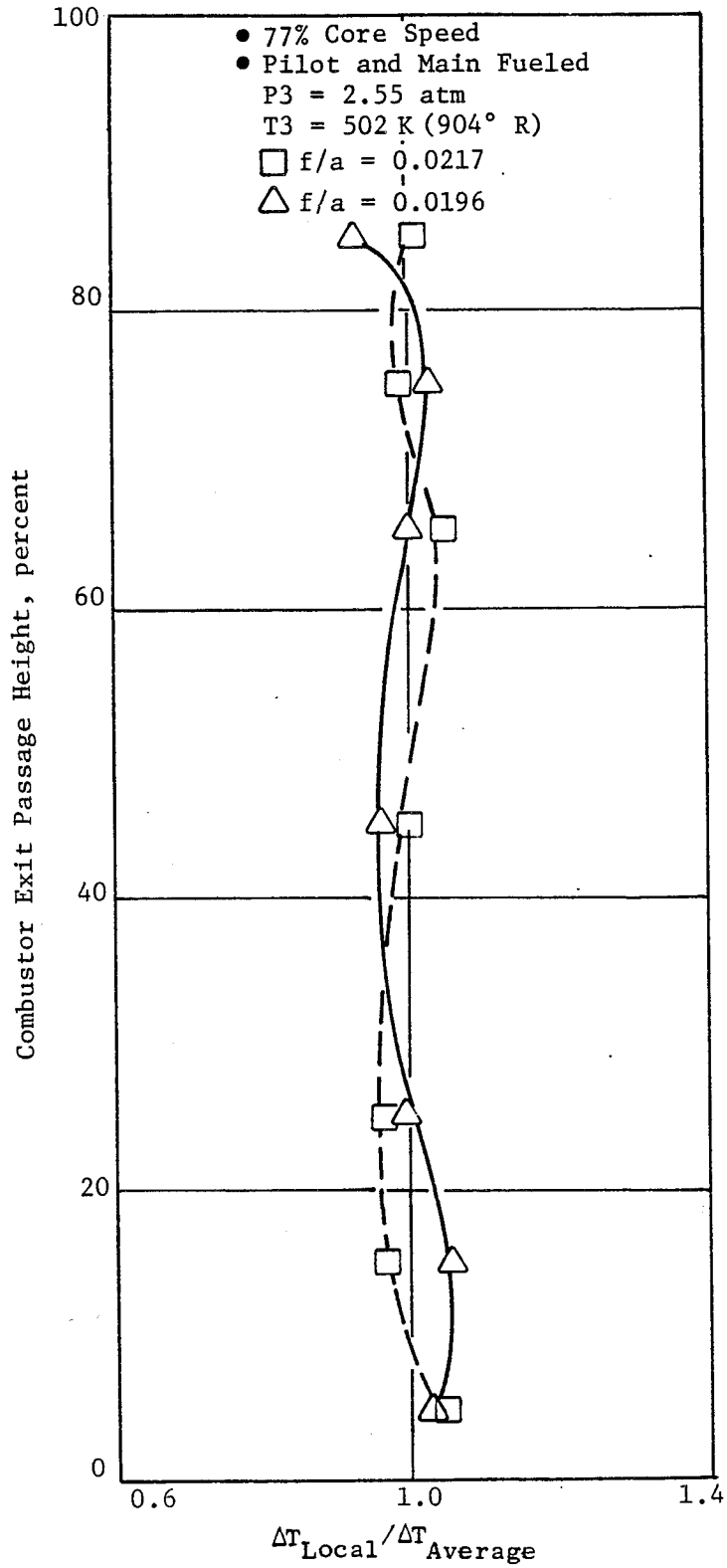


Figure 143. E^3 Sector Combustor Subidle EGT Profiles (Staged).

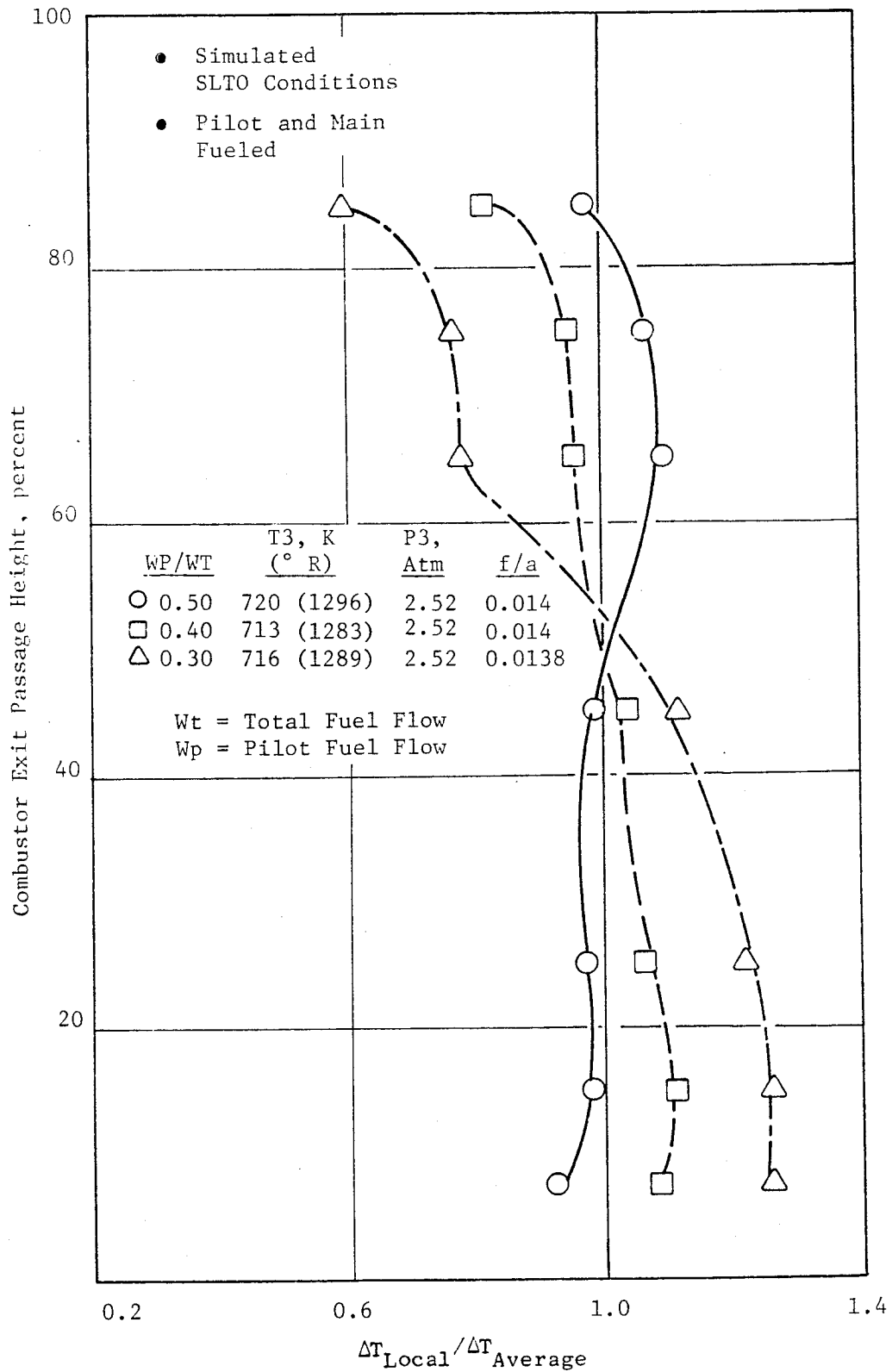


Figure 144. E³ Sector Combustor EGT Profiles at Simulated SLTO.

With a 50/50 fuel split, the temperature profile compares favorably with design limits; however, with a 30/70 pilot-to-main fuel split, the profile is peaked inboard at the design fuel/air ratio and considered unacceptable.

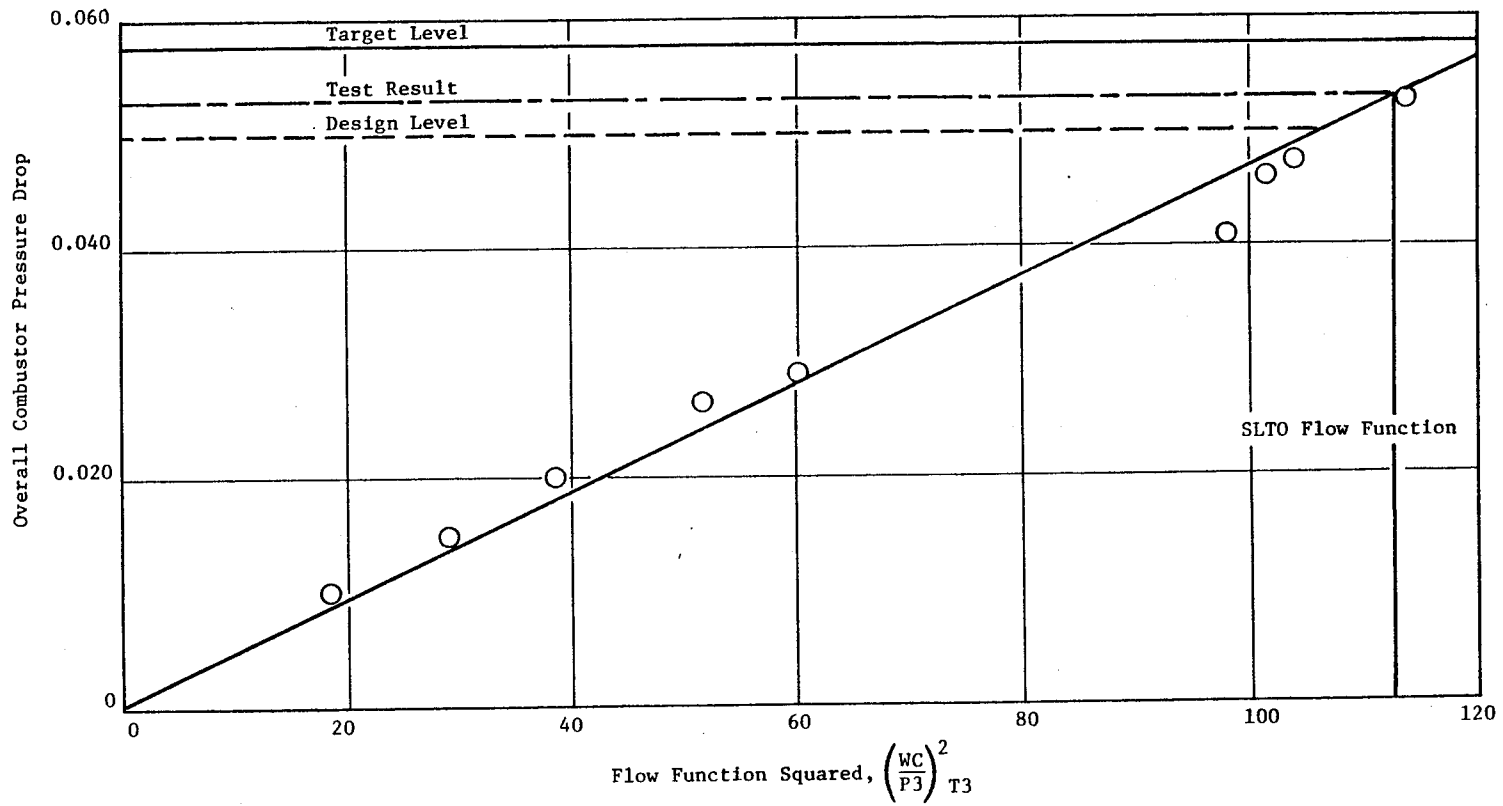
6.1.4.10 Pressure Drop Performance Results

Pressure measurements were obtained throughout the sector combustor test effort. Calculated pressure drops from these measurements varied slightly according to the effective areas of the configurations. However, overall combustor pressure drop generally compared very well with the design pressure drop level of 5%. Figure 145 is a plot of pressure drop versus combustor flow function for one of the configurations tested.

6.1.4.11 Emissions Test Results

Idle emissions test results for the baseline configuration are presented in Figure 146. At 6% ground idle conditions, which represent the actual E³ idle power setting, the measured CO and HC emissions were 40.0 g/kg (40.0 lbm/1000 lb) of fuel and 4.5 g/kg (4.5 lbm/1000 lb) of fuel, respectively. These levels significantly exceeded the target levels of 20.7 g/kg (20.7 lbm/1000 lb) of fuel for CO and 2.8 g/kg (2.8 lbm/1000 lb) of fuel for HC. However, they were considered extremely encouraging for the early stage of the combustor development. Comparison of individual rake samples indicated that the between-cup zones were significantly richer in fuel than the in-line cup zones. This observation led to the relocation of the primary dilution to between cups for the Mod I configuration in addition to using wider angle sleeves and reducing the pilot stage splash plate cooling. These modifications did result in a more uniform fuel/air distribution - consequently, a reduction of approximately 60% in CO and HC emissions to bring their levels very near the E³ Program target. A proportional improvement in emissions levels was also obtained at the 4% ground idle setting. The idle emissions results for the Mod I are shown in Figure 147.

The Mod II configuration, where major features were the development-type swirl cups and a reduction in the pilot stage swirl cup airflow, provided the design with the lowest idle emissions levels obtained during the entire sector



ORIGINAL PAGE IS OF POOR QUALITY

Figure 145. Sector Combustor Pressure Drop Versus Flow Function Parameter.

ORIGINAL PAGE IS
OF POOR QUALITY

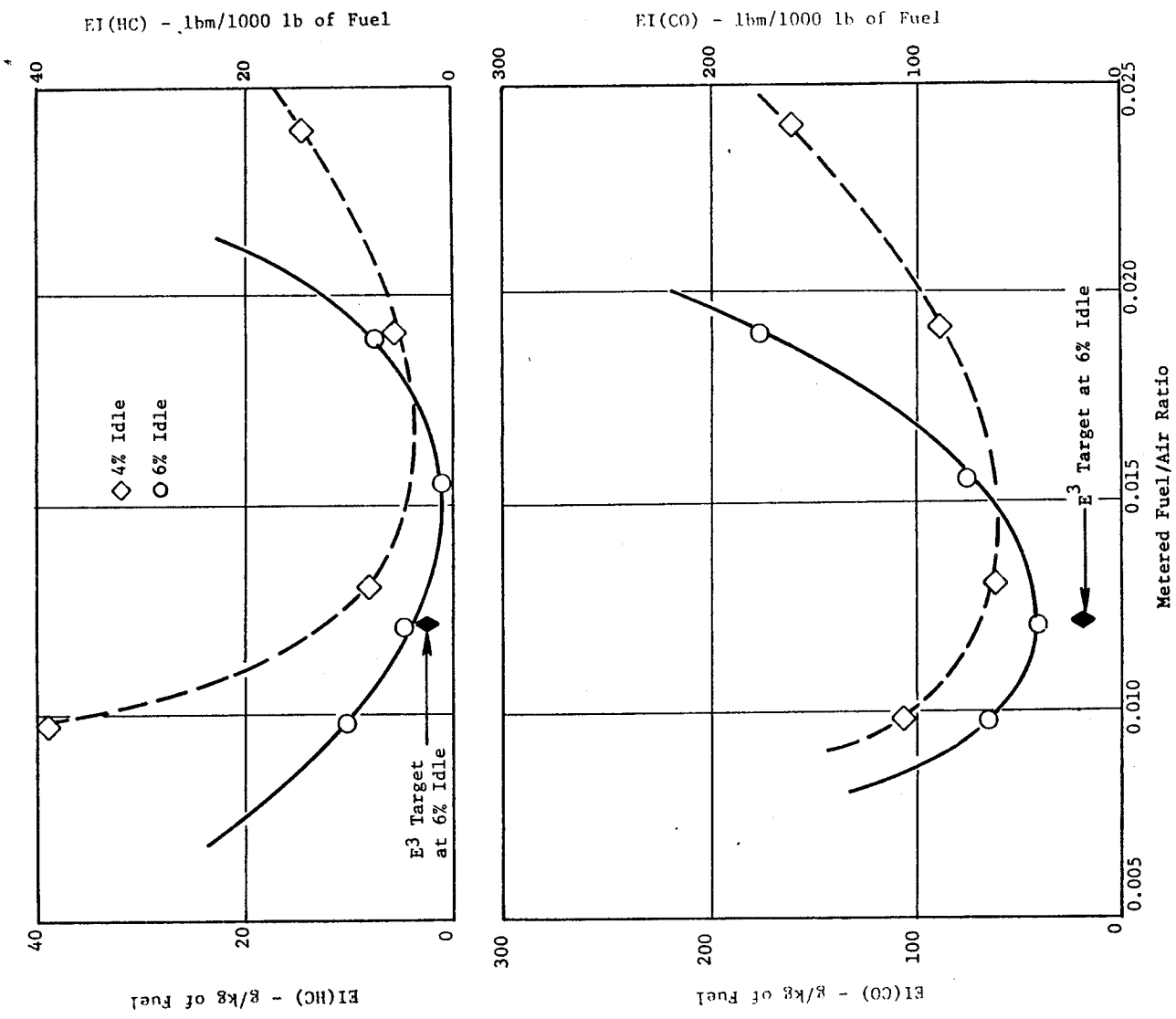


Figure 146. E³ Sector Combustor Emissions Results, Baseline Configuration.

ORIGINAL PAGE IS
OF POOR QUALITY

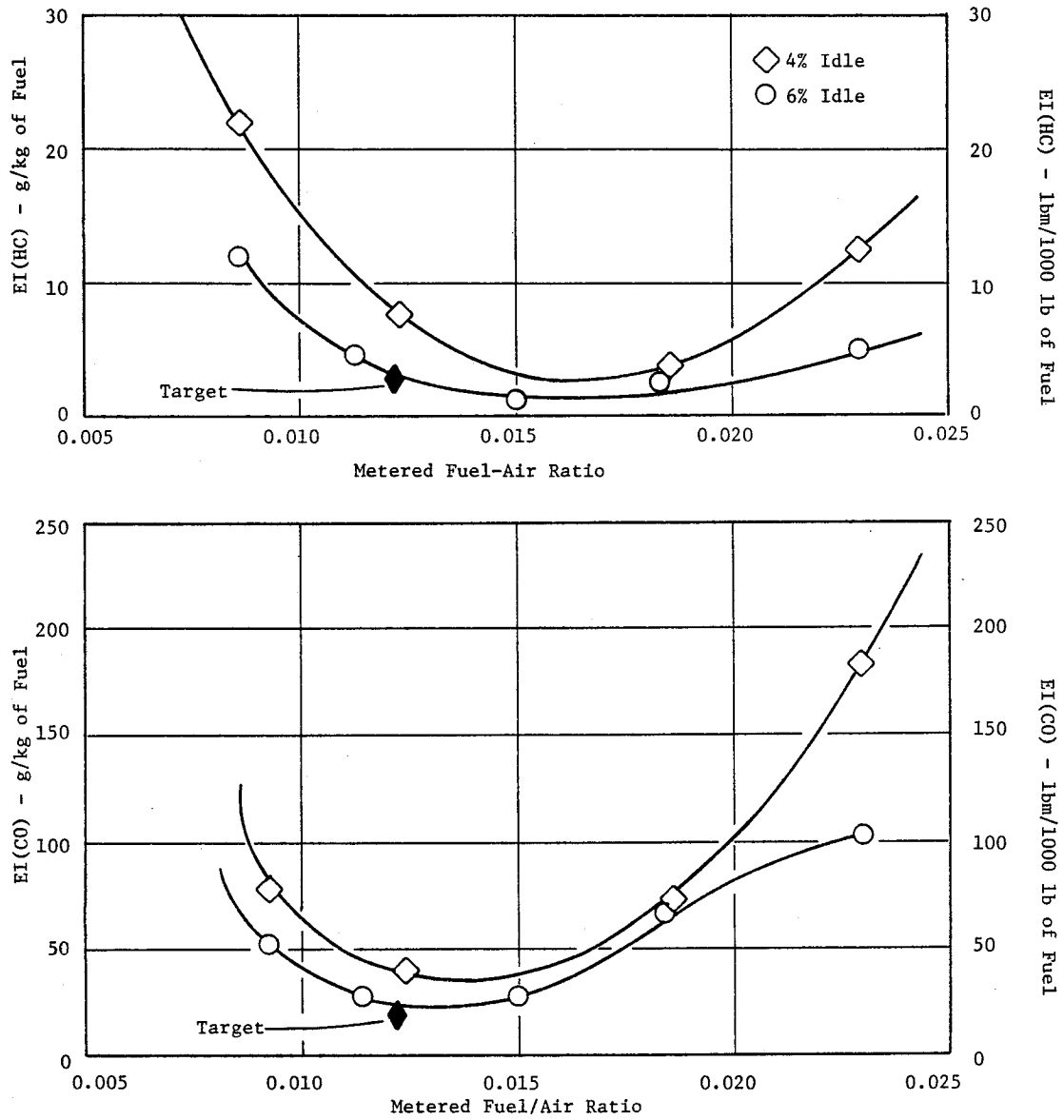


Figure 147. E3 Sector Combustor Emissions Results, Mod I Configuration.

combustor test effort. At 6% ground idle conditions, the CO and HC emission levels obtained were 15.0 g/kg (15.0 lbm/1000 lb) of fuel and 1.8 g/kg (1.8 lbm/1000 lb) of fuel, respectively, at the design fuel/air ratio of 0.0122. These levels met, with considerable margin, the E³ Program target levels for these two emissions categories. A plot of the CO and HC emissions versus the metered fuel/air ratio at 4% and 6% idle conditions for this configuration is shown in Figure 148.

Replacing the peanut-type fuel nozzles with development-type fuel nozzles in the Mod III configuration resulted in an increase of the idle emissions to approximately double the Mod II configuration levels as shown in Figure 149. The development-type fuel nozzles are air shrouded and are known to have a significantly more narrow spray angle than the prototype nozzles. The combination of this narrower spray angle and the shroud air was the primary cause of the increased CO and HC emissions levels. However, this same narrow spray angle was thought to be a strong contributor to the improved ignition performance of the Mod III configuration.

The effect of the fuel nozzle characteristics on idle emissions was further investigated in the Mod III configuration. Figure 150 shows a plot of the 6% idle emissions versus fuel/air ratio for the different types of nozzles investigated. The lowest CO and HC idle emissions were again obtained with the prototype peanut nozzles. Eliminating the air shroud from the development nozzles helped to reduce the idle emissions by approximately 13%; however, the air shroud prevents fuel nozzle plugging and carbon buildup on the venturi discharge surface.

Increasing the pilot stage primary dilution airflow in the Mod IV configuration resulted in only a modest reduction in the CO idle emissions as shown in Figure 151. However, this resulted in a slight increase in the HC emissions. As expected, shortening the centerbody did not appear to have a significant impact on idle emissions.

The Mod V configuration which featured an increased main stage dilution and, consequently, a richer pilot stage dome, resulted in a significant reduction in both CO and HC emissions at idle as shown in Figure 152. The measured

ORIGINAL PAGE IS
OF POOR QUALITY

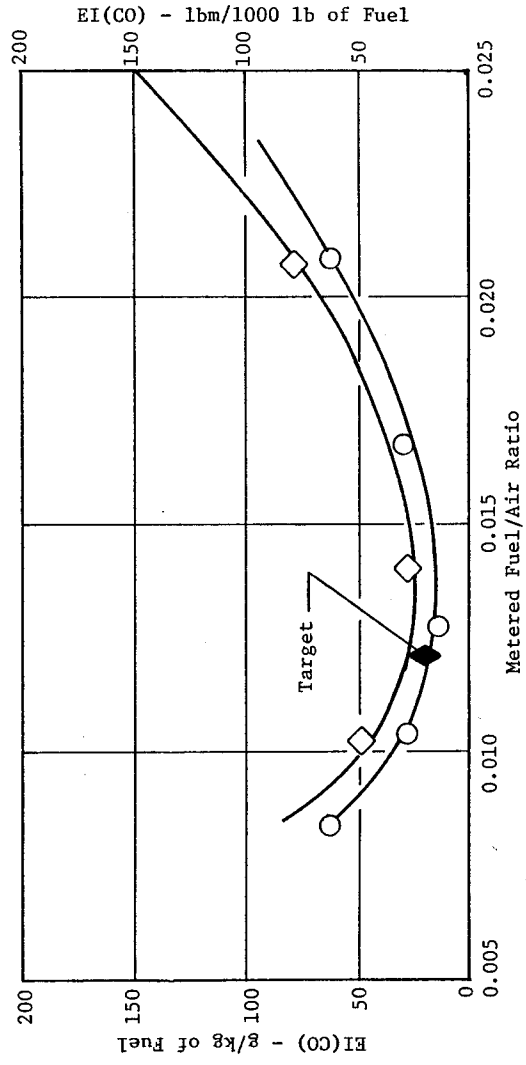
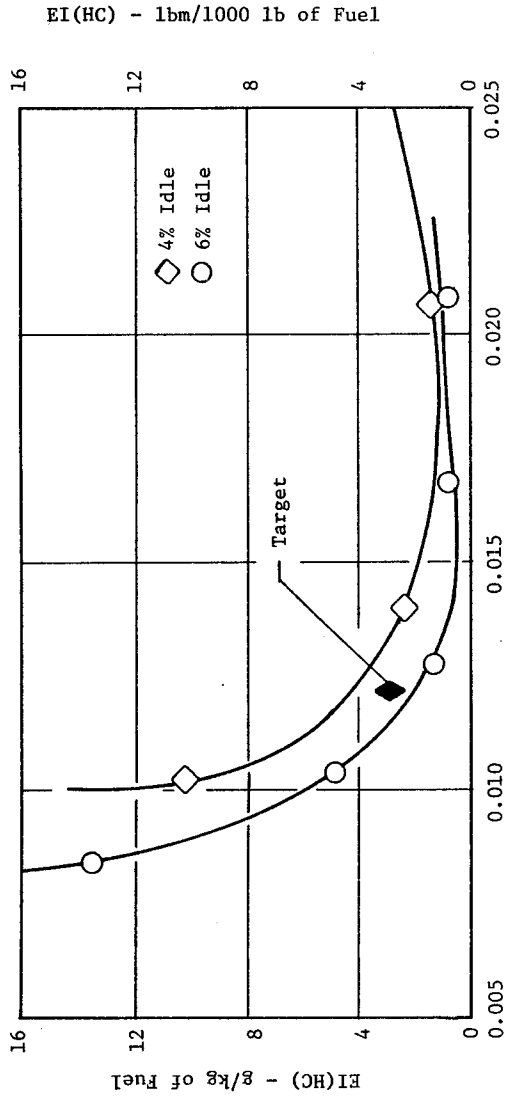


Figure 148. E₃ Sector Combustor Emissions Results, Mod II Configuration.

ORIGINAL PAGE IS
OF POOR QUALITY

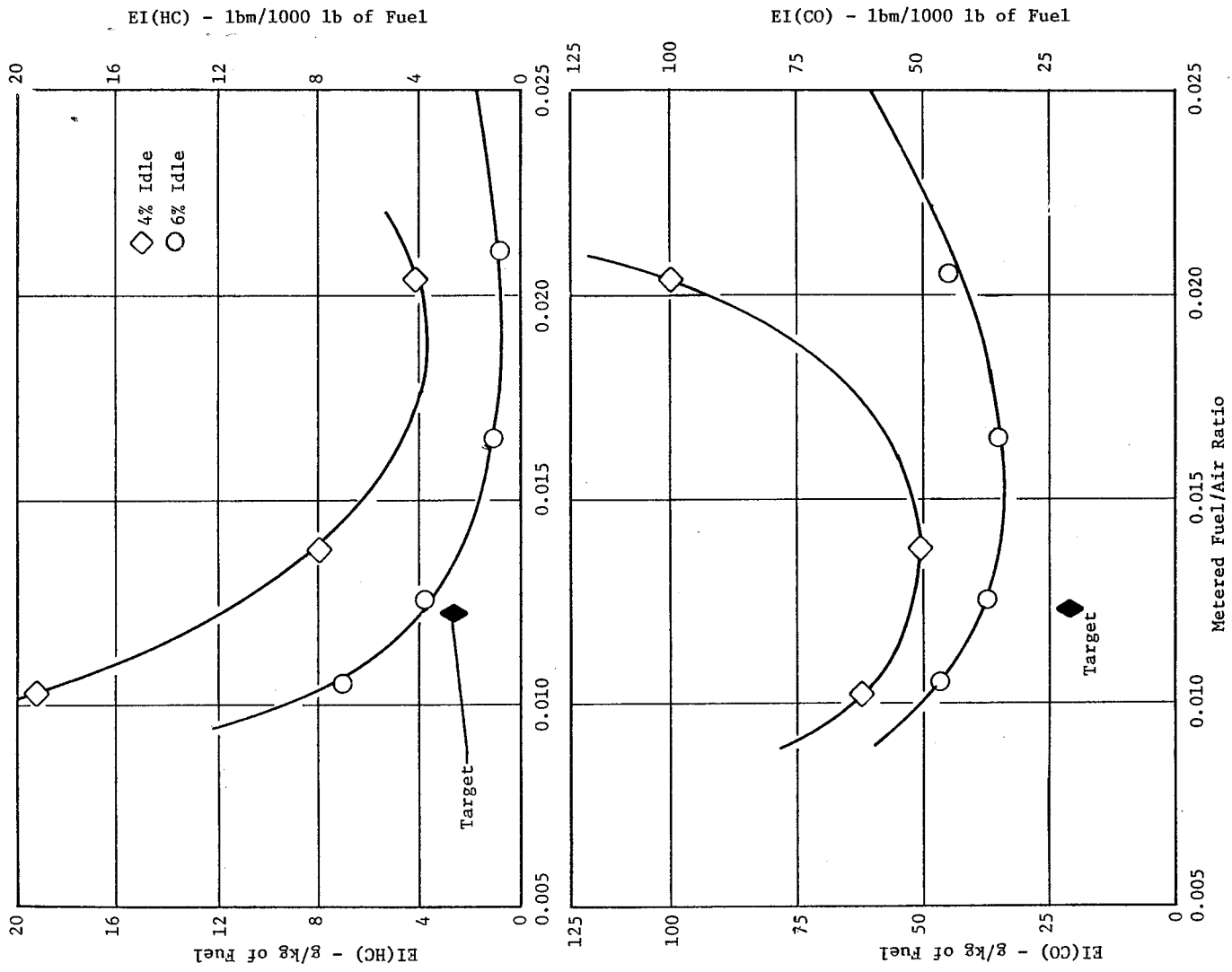


Figure 149. E³ Sector Combustor Emissions Results,
Mod III Configuration.

ORIGINAL PAGE IS
OF POOR QUALITY

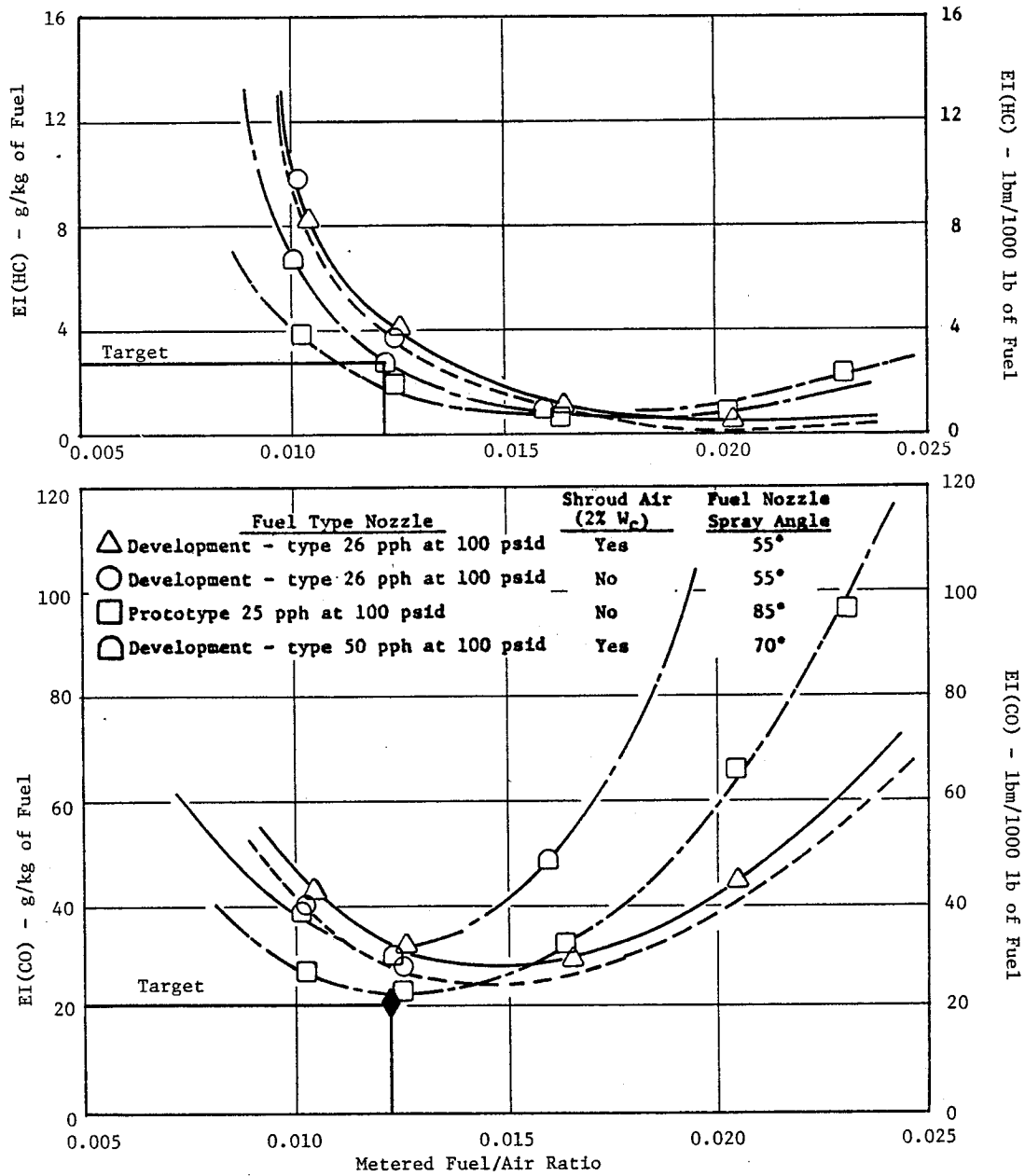


Figure 150. E³ Sector Combustor Emissions Results, Fuel Nozzle Type.

ORIGINAL PAGE IS
OF POOR QUALITY

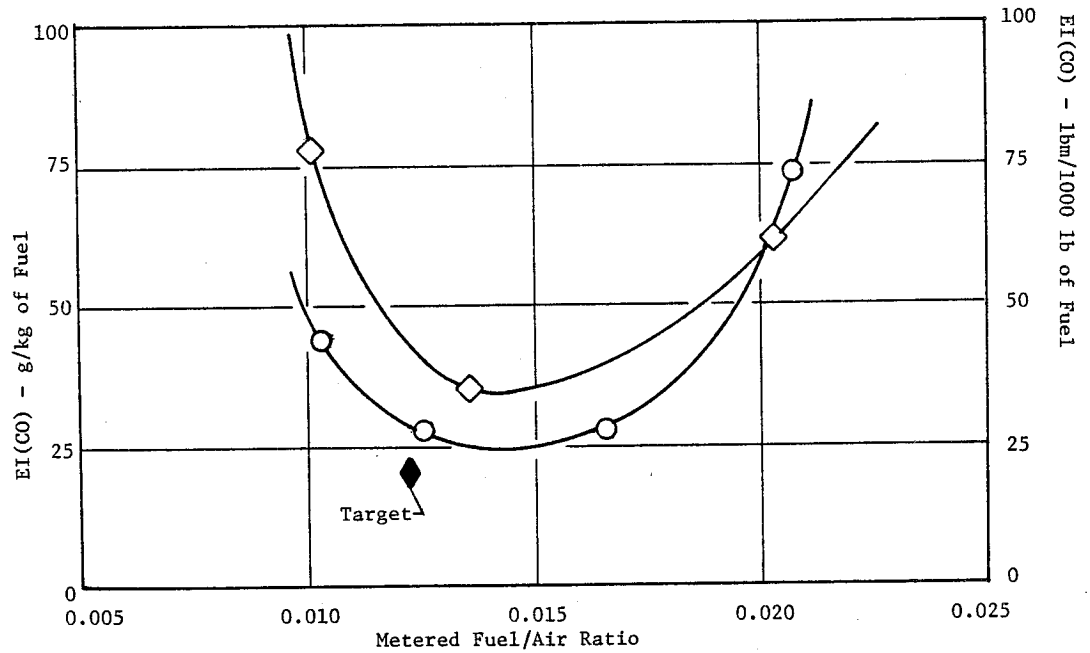
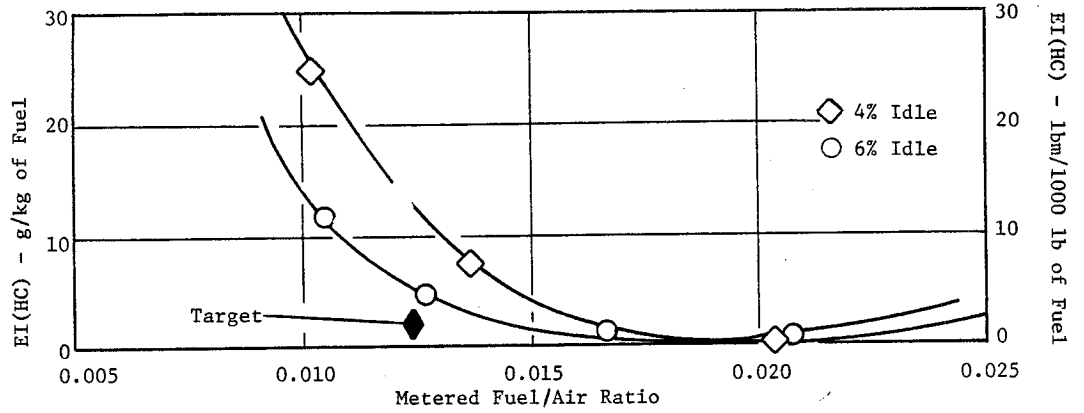


Figure 151. E³ Sector Combustor Emissions Results, Mod IV Configuration.

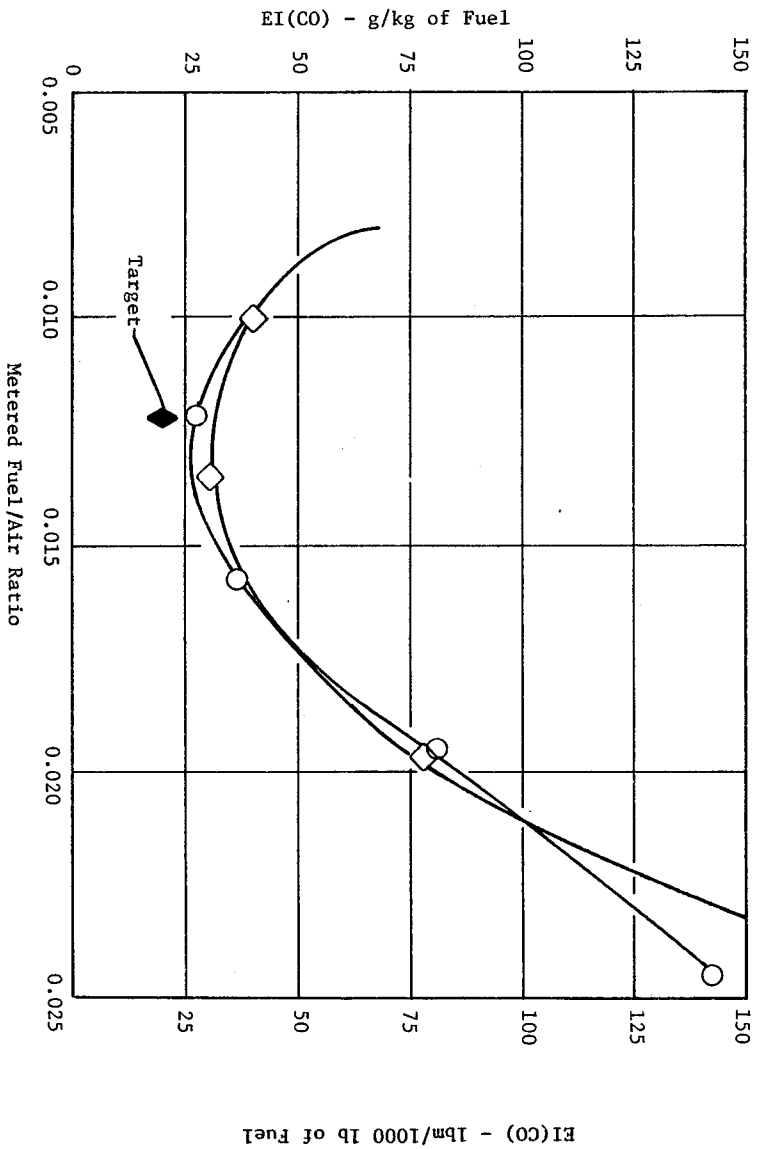
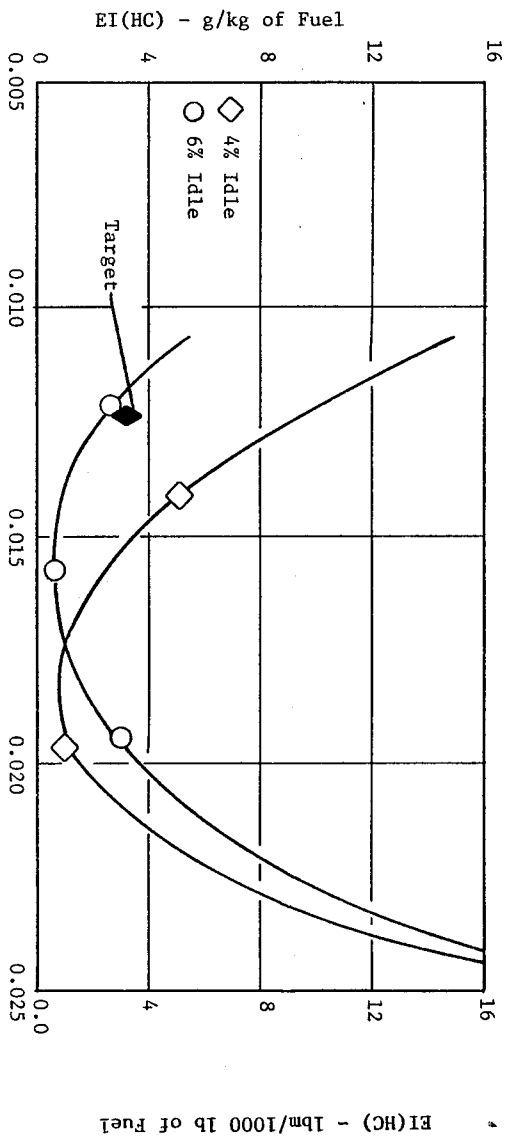


Figure 152. E3 Sector Combustor Emissions Results, Mod V Configuration.

levels for this configuration at 6% idle and the design fuel/air ratio were 26.0 g/kg (26.0 lbm/1000 lb) of fuel for CO and 2.6 g/kg (2.6 lbm/1000 lb) of fuel for HC emissions.

CO and HC emissions increased slightly in the Mod VI configuration as a result of a simultaneous reduction in the secondary swirler airflow level and an increase in the primary dilution airflow level of the pilot stage. Increased dilution alone caused a shift of the CO and HC emissions versus fuel/air ratio curves to the right. This resulted in a lower CO emission level and higher HC emission levels at the design fuel/air ratio for the 6% ground idle. The results for this configuration are shown in Figure 153.

CO and HC emissions were also measured at simulated EPA landing-takeoff approach conditions [30% $F_N(\text{SLTO})$] throughout the sector combustor tests. These emissions data were obtained with the pilot stage only operating mode and in the staged operating mode. In the pilot only mode at the approach power operating condition, CO emissions were generally low [<5.0 g/kg (5.0 lbm/1000 lb) of fuel], while HC emissions were practically nonexistent for all configurations tested. With both stages fueled, the CO and HC emissions varied with the configuration tested. The lowest levels, however, were obtained with the Mod V configuration which featured a significantly increased main stage dilution and somewhat richer dome regions in both stages.

The E^3 target levels for CO and HC emissions at approach power are a function of CO and HC emissions at idle conditions as shown in Figure 154. This dependency is a result of these two operating modes being the key contributors to CO and HC emissions in the EPA landing/takeoff cycle. This figure suggests that the HC emissions, on the other hand, fall short of meeting the target in either mode. The figure also indicates that the Mod II configuration CO and HC emissions levels, even though higher than those of the Mod V, will meet the target level due to the lower idle emissions.

NO_x emissions measurements at simulated sea level takeoff conditions were obtained only for the baseline, Mod I, Mod II, and Mod V configurations. NO_x emissions data were collected at idle and approach conditions for all configurations. From these low power data, NO_x emissions levels at sea level

ORIGINAL PAGE IN
OF POOR QUALITY

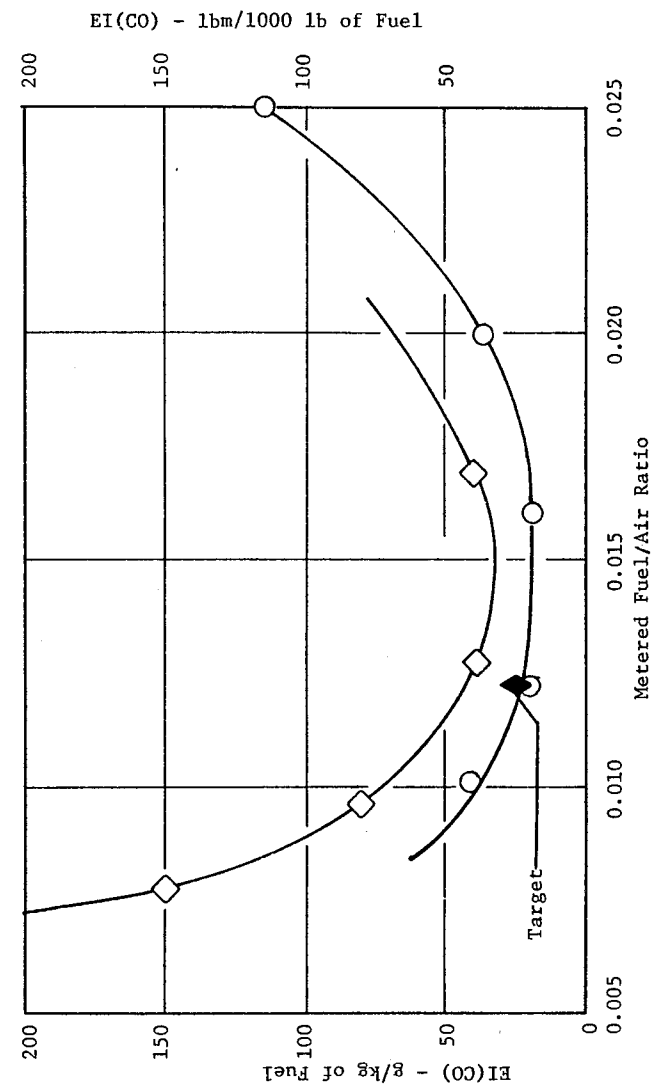
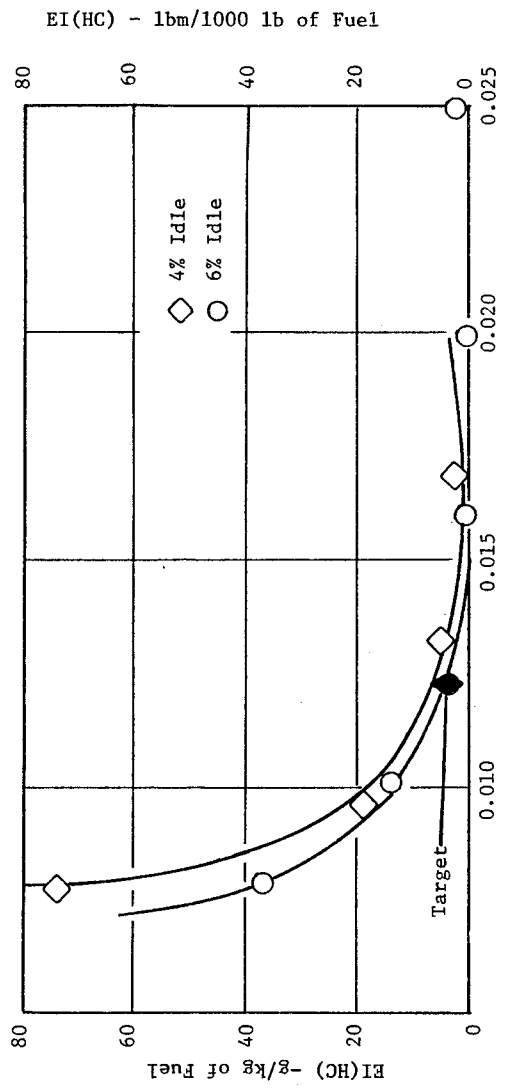


Figure 153. E³ Sector Combustor Emissions Results,
Mod VI Configuration.

ORIGINAL PAGE IS
OF POOR QUALITY.

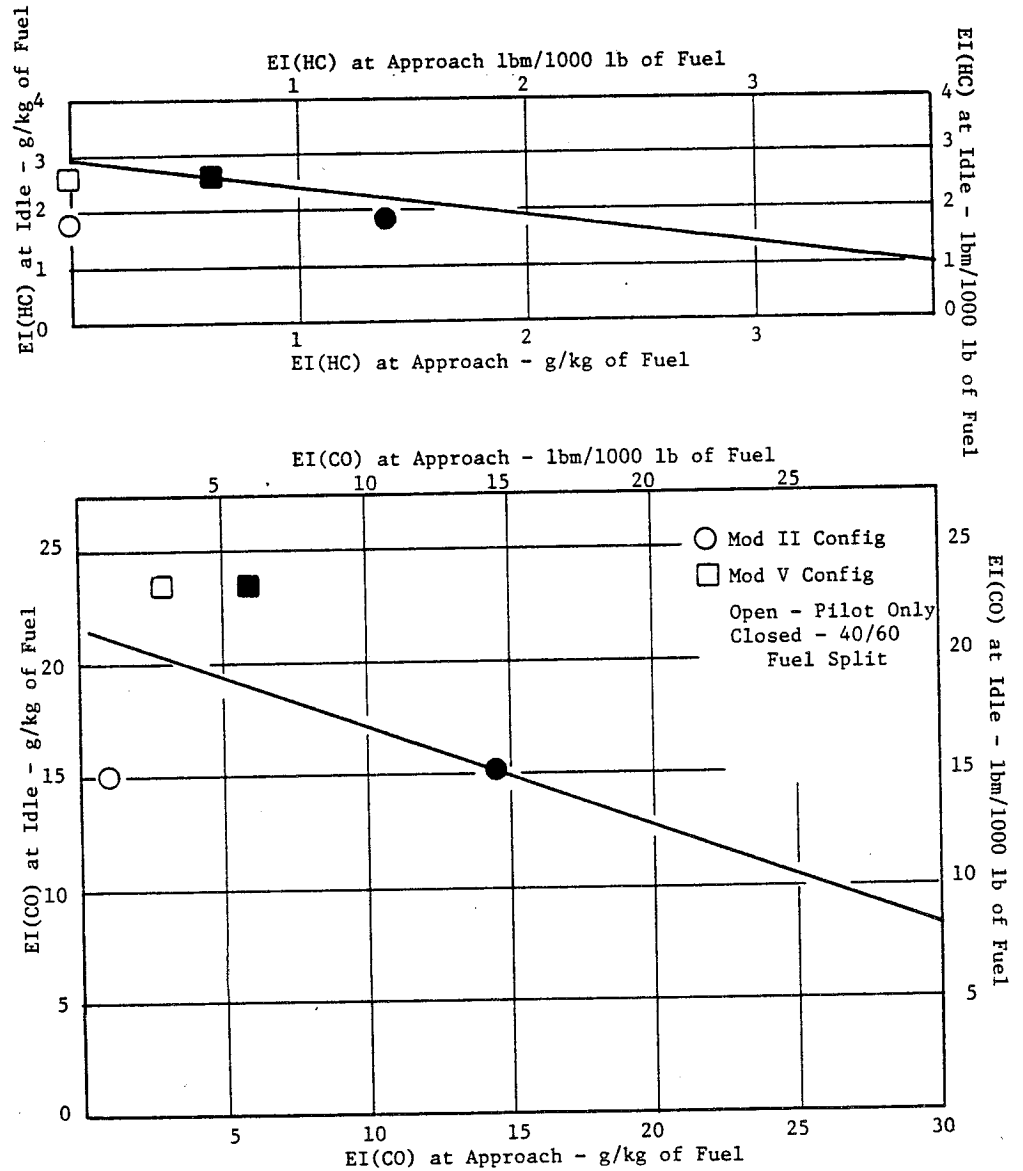


Figure 154. E³ Sector Combustor Emissions Results, Approach Conditions.

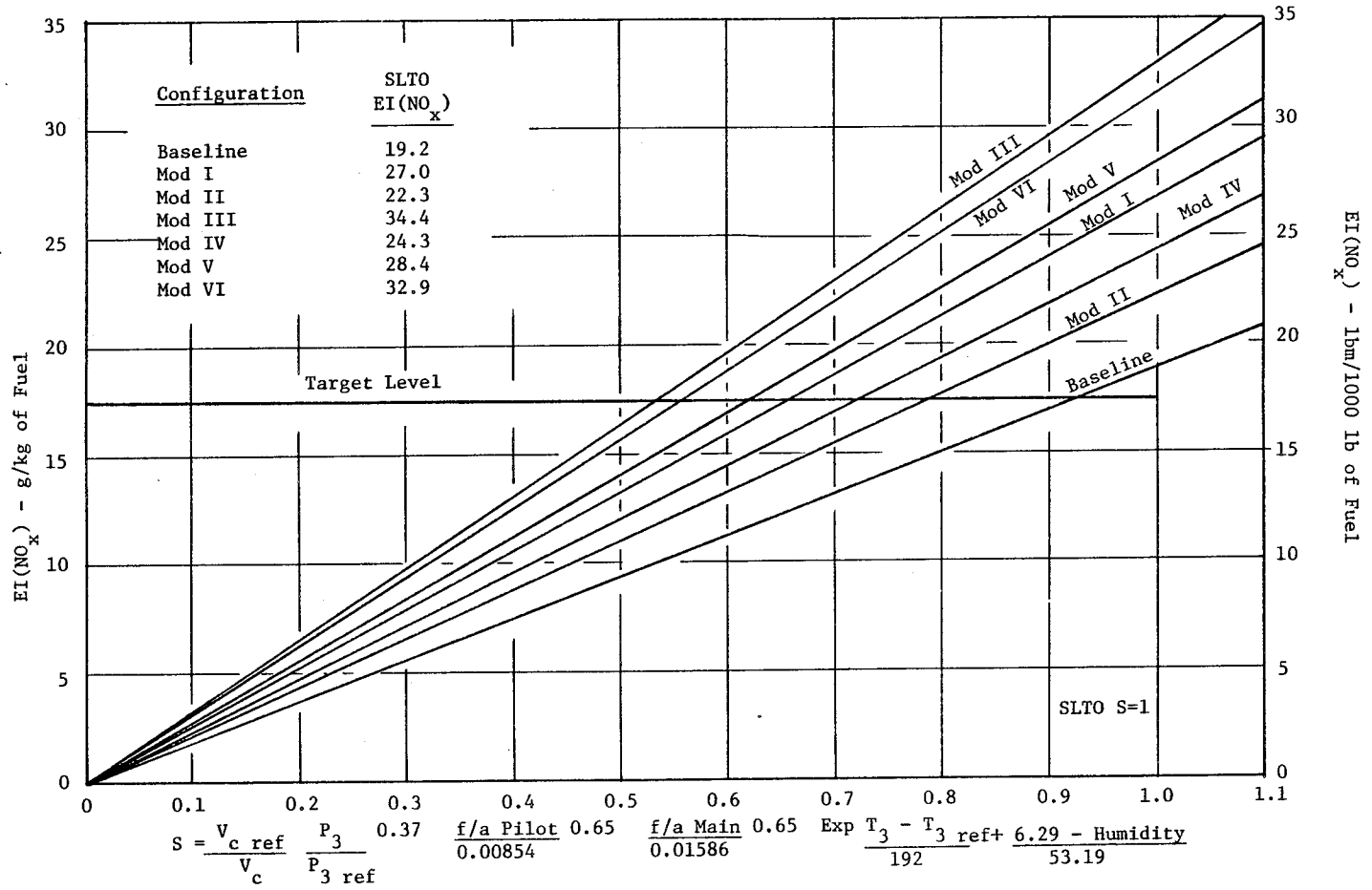
takeoff conditions were estimated with the use of a severity parameter linear correlation which takes into account the influence of pressure, temperature, humidity, fuel/air ratio, and fuel flow split between the pilot and main stages. The linear nature of the correlation allows for the extrapolation of NO_x results obtained at low power operating conditions to high power operating conditions. The results of the measured NO_x emissions correlation to this parameter are shown in Figure 155. The reference conditions represent the values at the actual FPS cycle sea level takeoff operating condition.

The baseline configuration produced the lowest NO_x emissions at a level of 19.2 g/kg (19.2 lbm/1000 lb) of fuel with a 40/60 pilot-stage-to-main-stage fuel flow split. The E³ target for NO_x emissions is 17.5 g/kg (17.5 lbm/1000 lb) of fuel. However, test experience indicated that the full-annular combustor generally produced lower NO_x emissions than the sector combustor with similar features.

The higher NO_x emissions obtained in all the subsequent configurations were primarily due to the higher flame temperatures resulting from higher combustion efficiencies associated with a more uniform dome stoichiometry. Furthermore, both pilot and main stage domes were enriched following the baseline configurations for ignition and idle emissions improvement purposes.

6.1.4.12 Altitude Relight Test Results

The altitude relight ignition performance of the E³ sector combustor was investigated only with the Mod VI configuration using the CF6-50 engine windmilling map. Successful relight was obtained only at test points simulating conditions in the lower left portion of the windmilling envelope as illustrated in Figure 156. This was thought to be caused by low pressure drop across the fuel nozzle tip due to the relatively large flow fuel nozzles used. Low fuel nozzle pressure drop usually results in poor fuel atomization. However, a repeat test with significantly smaller fuel nozzles seemed to have little effect on the number of successful relights even though the light-off fuel/air ratios for these successful relights dropped drastically. To verify that relight was not inhibited by a lack of fuel flow due to the small fuel nozzles, an intermediate set of nozzles was installed and the test was



ORIGINAL PAGE IS OF POOR QUALITY

Figure 155. E³ Sector Combustor Emissions Results, EI_{NO_x}.

ORIGINAL PAGE IS
OF POOR QUALITY

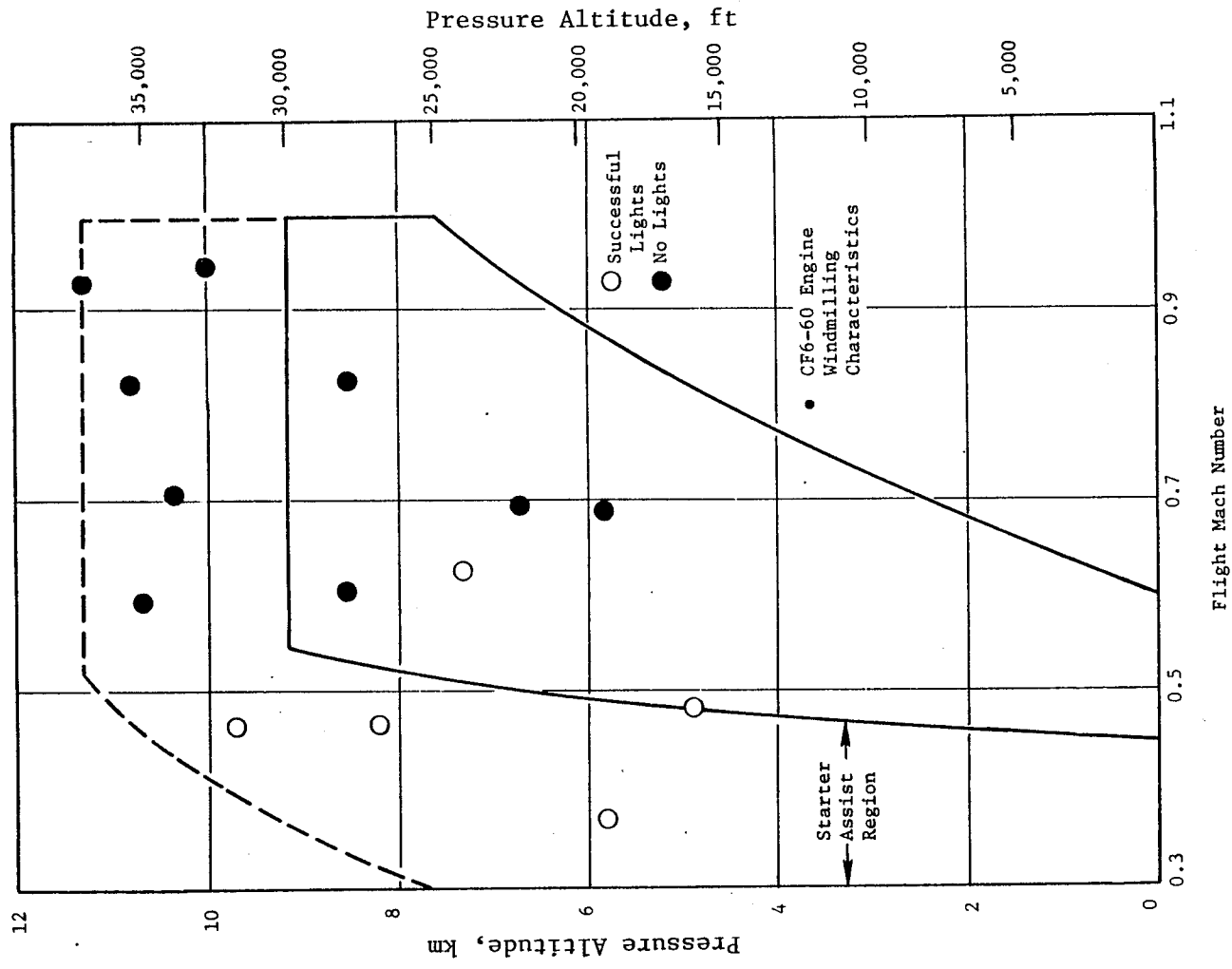


Figure 156. E³ Sector Combustor Altitude Relight Test Results,
Mod VI Configuration.

repeated. No additional points were added to the list of successful lights this time either, and the light-off fuel/air ratios were between those of the previous runs.

Additional altitude relight testing conducted with the pilot stage dilution blocked and prototype fuel nozzles indicated that no further improvements on the performance were attainable with the current configurations. The detailed results of all altitude ignition testing are summarized in Tables XXXI through XXXIV.

6.1.4.13 Concluding Remarks

Ignition Results

The sector combustor ignition performance was improved most effectively through the use of the air-shrouded, development-type fuel nozzles. These nozzles are known to have somewhat narrower spray angles and more effective fuel atomization than the prototype fuel nozzles. As expected, a fuel enriched dome region also enhanced the ignition performance. All the test results indicated that, in order for the main stage crossfire at subidle conditions to be reasonably attainable, the main stage swirl cup airflow had to be reduced to a level near that of the pilot stage swirl cup airflow. However, the latest E³ start cycle eliminated the requirement of starting the engine on both pilot and main stages. Consequently, the pilot stage ignition performance is expected to meet the revised E³ start schedule with considerable margin. No difficulty is anticipated with main stage crossfiring at conditions above idle. Table XXXV summarizes the sector ignition development testing.

Performance Results

Combustion efficiency and exit temperature profile measurements were only obtained for the baseline configuration of the E³ sector combustor. However, a basic conclusion can be made and considered applicable for all configurations tested. Due to the approximately equal airflow levels in the pilot and main stages, a fuel flow split of near 50/50 is required to obtain a uniform exit temperature profile.

Table XXXI. Altitude Ignition Testing Summary, Mod VI Configuration.

11.8 kg/hour (26.0 lb/hour) Development-Type Fuel Nozzles

W_c kg/s (lb/s)	P_3 atm	T_3 K(° F)	V_{ref} m/s (ft/s)	$\frac{W_c}{(P_3)^2} 2T_3$	$\Delta P/P$	ΔP_{fuel} at L/O atm	$\frac{PT}{V_{ref}}$	$\frac{PT \Delta P}{V_{ref} P}$	f/a 1 Cup Lit	f/a All Cups Lit	* 1 Cup Lit	† All Cups Lit
0.19 (0.42)	0.544	304 (87)	6.4 (21.0)	37.1	0.0285	0.796	25.8	0.752	0.0292	0.0342	2.4	2.8
0.07 (0.15)	0.476	293 (67)	2.6 (8.5)	6.4	0.010	0.395	53.6	0.546	0.0556	0.0570	4.5	4.6
0.07 (0.15)	0.408	295 (71)	3.0 (9.8)	8.7	0.011	0.592	40.1	0.442		0.068	-	5.5
0.07 (0.15)	0.340	296 (73)	3.7 (12.1)	12.6	0.0135	0.551	27.9	0.377	0.0655	0.084	5.3	6.8
0.05 (0.11)	0.272	296 (73)	3.0 (9.8)	8.6	0.0110	0.673	26.9	0.297	---	0.109	---	8.8
0.06 (0.13)	0.238	297 (75)	4.8 (15.7)	21.4	0.0191	---	15.0	0.288	0.0760	---	6.1	---
0.14 (0.31)	0.272	297 (75)	9.3 (30.5)	78.7	0.0559	---	8.9	0.498		No Light		
0.22 (0.49)	0.272	298 (76)	14.4 (47.2)	188.3	0.126	---	5.8	0.724		No Light		
0.29 (0.64)	0.272	306 (91)	19.1 (62.7)	325.6	0.213	---	4.5	0.951		No Light		
0.36 (0.79)	0.361	306 (91)	18.1 (59.4)	292.4	0.192	---	6.1	1.176		No Light		
0.36 (0.79)	0.544	306 (91)	12.0 (39.4)	128.0	0.087	1.05	14.1	1.231	---	0.0180	---	1.5
0.36 (0.79)	0.408	306 (91)	16.0 (52.5)	228.1	0.151	---	8.0	1.205		No Light		
0.36 (0.79)	0.544	306 (91)	12.1 (39.7)	131.3	0.089	1.53	13.9	1.244	---	0.0210	---	1.7
0.14 (0.31)	0.340	306 (91)	10.6 (34.8)	52.5	0.039	---	10.0	0.392	0.0370	---	3.1	---
0.22 (0.48)	0.408	306 (91)	13.4 (44.0)	83.6	0.059	1.01	9.5	0.550	0.0291	0.0355	2.3	2.9
0.33 (0.73)	0.476	306 (91)	12.5 (41.0)	138.6	0.094	---	11.9	1.11		No Light		

Table XXXII. Altitude Ignition Testing Summary, Mod VI Configuration.

2.3 kg/hour (5.1 lb/hour) Development-Type Fuel Nozzles

W_c kg/s (lb/s)	P_3 atm	T_3 K(° F)	V_{ref} m/s (ft/s)	$\frac{W_c}{(P_3)^2} 2T_3$	$\Delta P/P$	ΔP_{fuel} at L/O atm	$\frac{PT}{V_{ref}}$	$\frac{PT \Delta P}{V_{ref} P}$	f/a 1 Cup Lit	f/a All Cups Lit	* 1 Cup Lit	† All Cups Lit
0.19 (0.42)	0.544	296 (73)	6.3 (20.7)	36.1	0.0290	13.40	25.6	0.742	0.0187	0.0206	1.5	1.7
0.07 (0.15)	0.476	281 (46)	2.5 (8.2)	6.1	0.0093	3.27	53.5	0.498	0.0333	0.0333	2.7	2.7
0.07 (0.15)	0.408	288 (58)	2.9 (9.5)	8.5	0.0107	3.33	40.5	0.433	0.0342	0.0342	2.8	2.8
0.07 (0.15)	0.340	294 (69)	3.6 (11.8)	12.5	0.0131	4.08	27.8	0.364	0.0370	0.0370	3.0	3.0
0.05 (0.11)	0.272	294 (69)	3.1 (10.2)	9.9	0.0111	3.47	25.8	0.286	0.0516	0.0516	4.2	4.2
0.07 (0.15)	0.245	294 (69)	4.8 (15.7)	24.0	0.0190	3.20	15.0	0.285	0.0439	---	3.5	---
0.14 (0.31)	0.286	285 (53)	8.5 (27.9)	68.3	0.0500	---	9.6	0.480		No Light		
0.22 (0.48)	0.272	277 (39)	13.0 (42.6)	181.2	0.1120	---	5.8	0.650		No Light		
0.38 (0.84)	0.408	276 (37)	15.1 (49.5)	239.4	0.1470	---	7.5	1.103		No Light		

* ϕ , Dome Stoichiometry,

$$\frac{f_{dome}}{f_{stoich}}$$

Table XXXIII. Altitude Ignition Testing Summary, Mod VI Configuration.

2.3 kg/hour (5.1 lb/hour) and Development-Type Fuel Nozzles
(Pilot Stage Primary Dilution Closed Off)

W_c kg/s (lb/s)	P_3 atm	T_3 K(° F)	V_{ref} m/s (ft/s)	$(\frac{W_c}{P_3})^2 T_3$	$\Delta P/P$	ΔP_{fuel} at L/O atm	$\frac{PT}{V_{ref}}$	$\frac{PT \Delta P}{V_{ref} P}$	f/a l Cup Lit	f/a All Cups Lit	* ♦ l Cup Lit	♦ All Cups Lit
0.20 (0.44)	0.574	289 (60)	6.3 (20.7)	35.1	0.032	6.19	26.3	0.842	0.0122	0.0122	0.98	0.98
0.07 (0.15)	0.476	289 (60)	2.5 (8.2)	6.3	0.0095	3.61	55.0	0.523	0.0261	0.0261	2.1	2.1
0.07 (0.15)	0.408	291 (64)	2.9 (9.5)	8.6	0.0110	3.27	40.9	0.450	0.0258	0.0258	2.1	2.1
0.07 (0.15)	0.340	294 (69)	3.5 (11.5)	12.5	0.0136	3.67	28.6	0.389	0.0272	0.0272	2.2	2.2
0.04 (0.09)	0.272	279 (42)	2.5 (8.2)	6.0	0.0098	4.83	30.4	0.298	0.0491	0.0491	4.0	4.0
0.07 (0.15)	0.245	278 (40)	4.5 (14.8)	22.7	0.0202	4.42	15.1	0.305	0.0303	0.0302	2.4	2.4
0.15 (0.33)	0.265	278 (40)	9.5 (31.2)	89.1	0.0723	---	7.8	0.564			No Light	
0.21 (0.46)	0.279	277 (39)	12.4 (40.7)	156.9	0.1206	---	6.2	0.748			No Light	
0.28 (0.62)	0.272	273 (31)	16.6 (54.5)	289.3	0.2132	---	4.5	0.594			No Light	
0.14 (0.31)	0.347	284 (51)	6.8 (22.3)	46.2	0.0388	5.85	14.5	0.563	0.0167	0.0167	1.3	1.3
0.21 (0.46)	0.408	284 (51)	8.4 (27.6)	75.2	0.0581	24.45	13.8	0.802	0.0228	0.0228	1.8	1.8
0.32 (0.70)	0.476	277 (39)	10.9 (35.8)	125.2	0.1778	22.65	12.1	2.151	0.0145	0.0188	1.2	1.5
0.15 (0.33)	0.340	277 (39)	7.4 (24.3)	53.9	0.0460	---	12.7	0.584	0.0246	0.0281	2.0	2.3
0.21 (0.46)	0.524	278 (40)	6.6 (21.7)	44.6	0.0378	---	22.1	0.835	0.0178	0.0194	1.4	1.6
0.28 (0.62)	0.766	273 (31)	5.9 (19.4)	36.5	0.0314	---	35.4	1.111	0.0145	0.0171	1.2	1.4

Table XXXIV. Altitude Ignition Testing Summary, Mod VI Configuration.

11.3 kg/hour (24.9 lb/hour) Prototype Fuel Nozzles

W_c kg/s (lb/s)	P_3 atm	T_3 K(° F)	V_{ref} m/s (ft/s)	$(\frac{W_c}{P_3})^2 T_3$	$\Delta P/P$	ΔP_{fuel} at L/O atm	$\frac{PT}{V_{ref}}$	$\frac{PT \Delta P}{V_{ref} P}$	f/a l Cup Lit	f/a All Cups Lit	* ♦ l Cup Lit	♦ All Cups Lit
0.19 (0.42)	0.539	293 (67)	6.2 (20.3)	36.4	0.0326	1.430	25.5	0.831	0.0377	0.0377	3.0	3.0
0.07 (0.15)	0.471	294 (69)	2.6 (8.5)	6.5	0.0097	0.612	53.3	0.517	0.0683	0.0683	5.5	5.5
0.07 (0.15)	0.404	293 (67)	2.9 (9.5)	8.8	0.0111	0.748	40.8	0.453	0.0761	0.0761	6.1	6.1
0.07 (0.15)	0.337	293 (67)	3.5 (11.5)	12.6	0.0137	0.748	28.2	0.386	0.0777	0.0777	6.3	6.3
0.04 (0.09)	0.271	294 (69)	2.7 (8.8)	6.4	0.0101	1.020	29.5	0.298	0.1480	0.1480	12.0	12.0
0.07 (0.15)	0.244	294 (69)	4.8 (15.7)	24.2	0.0216	0.748	14.9	0.322	0.0777	0.0777	6.3	6.3
0.16 (0.35)	0.265	294 (69)	10.3 (33.8)	107.2	0.0788	---	7.6	0.599			No Light	
0.14 (0.31)	0.344	295 (71)	7.1 (23.3)	48.9	0.0410	1.293	14.3	0.586	0.0490	0.0490	4.0	4.0
0.21 (0.46)	0.408	295 (71)	9.0 (29.5)	78.2	0.0621	2.177	13.4	0.832	0.0429	0.0429	3.5	3.5

* ϕ , Dome Stoichiometry,

258 $\frac{f_{dome}}{f_{stoich}}$

Table XXXV. Sector Combustor Ignition Test Results.

	Pilot Stage, f/a	Target, f/a	Main Stage, f/a	Target, f/a
Baseline	0.045	0.032 at 32 PCNHR	No Light	0.022 at 35% PCNHR
Mod I	0.037	0.032 at 32 PCNHR	0.041	0.022 at 35% PCNHR
Mod II	0.030	0.032 at 32 PCNHR	0.041	0.022 at 35% PCNHR
Mod III	0.021	0.032 at 32 PCNHR	0.038	0.022 at 35% PCNHR
Mod IV	0.023 (0.021)	0.032 at 32 PCNHR	0.036 (0.026)	0.022 at 35% PCNHR
Mod V	0.022 (0.021)	0.032 at 32 PCNHR	0.031 (0.016)	0.022 at 35% PCNHR
Mod VI	0.022	0.032 at 32 PCNHR	0.032	0.022 at 35% PCNHR
New Start Cycle	0.013	0.015 at 32 PCNHR	No. reqt.	No. reqt.

Blocked numbers indicate requirements met.

The sector combustor pressure drop agrees very well with the design target of 5%.

Emissions Results

CO idle emissions met the E³ target level of 20.7 g/kg (20.7 lbm/1000 lb) of fuel for only two of the seven configurations tested - Mod II and Mod VI. One of these two configurations, Mod VI, featured the prototype fuel nozzles which were found to be detrimental for the sector combustor ignition performance. The HC emissions target level of 2.8 g/kg (2.8 lbm/1000 lb) of fuel was substantially exceeded in the other configuration, Mod II. The air-flow distribution of the Mod V configuration resulted in the best overall idle emissions performance with the HC emissions target met and the CO emissions target exceeded by 14%.

NO_x emissions at simulated sea level takeoff conditions are estimated to have exceeded the target level of 17.5 g/kg (17.5 lbm/1000 lb) of fuel for all configurations tested for this emissions category. The NO_x emissions

target was considered to be the most challenging of all the pollutant emissions targets. However, the E³ full-annular combustor test experiences have demonstrated that generally higher NO_x emissions were produced in the sector combustor than the full-annular combustor for similar configurations.

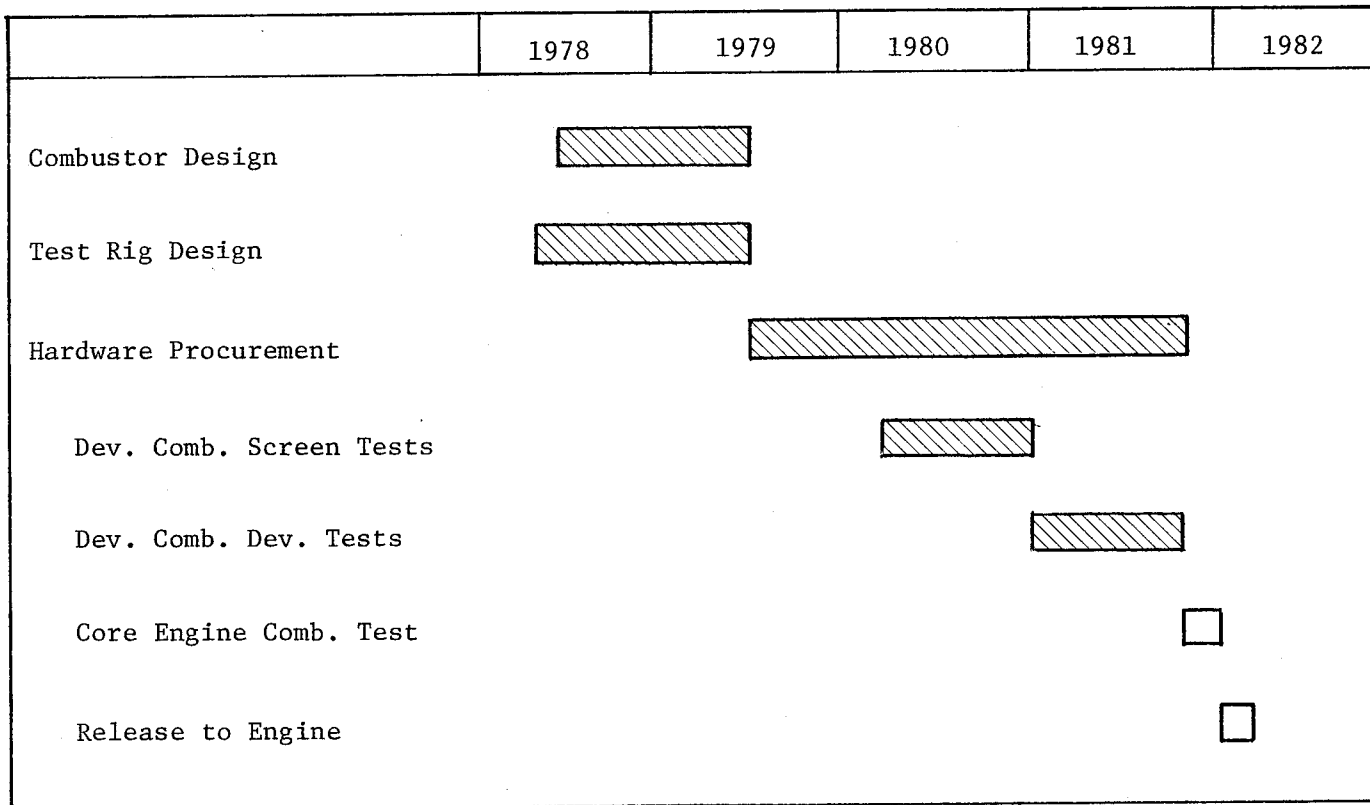
Altitude Relight Results


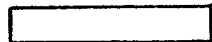
The sector combustor exhibited a limited success in altitude relight performance. Ignition was not attainable at speeds higher than Mach 0.6 and altitudes higher than 9.0 km (29,500 feet). Further investigation was required for any effort to improve the altitude relight performance; however, such effort was not planned in the E³ Sector Development Program scope.

6.2 FULL-ANNULAR TEST

Full-annular combustor component development testing of the E³ combustor involved two major combustor designs: lean main stage designs and rich main stage designs. The primary development effort involved the lean main stage designs and was directed toward evolving a combustor design capable of satisfying all of the design objectives established in the E³ combustor development program. In this effort, the baseline and Mods I, VI, and VII were evaluated for ground start ignition, exit temperature performance, and emissions. The secondary development effort involved the rich main stage designs and was directed toward evolving a combustor design capable of staged combustion during ground start operation. The Mod II through Mod V combustor configurations were evaluated for ground start ignition and exit temperature performance as part of this effort. These testing efforts were broken into two sections - screening tests and development tests. The overall annular test program schedule is shown in Figure 157.

In support of each design philosophy, promising design concepts which evolved from the various subcomponent testing efforts conducted as part of the E³ combustor development program were considered for incorporation into the full-annular combustor designs. Other promising design concepts considered were identified through analysis of test results obtained from previously tested, full-annular configurations. Many of these design concepts were



 - Work Completed
 - Work to be Done

ORIGINAL PAGE IS
 OF POOR QUALITY

Figure 157. Full-Annular Test Schedule.

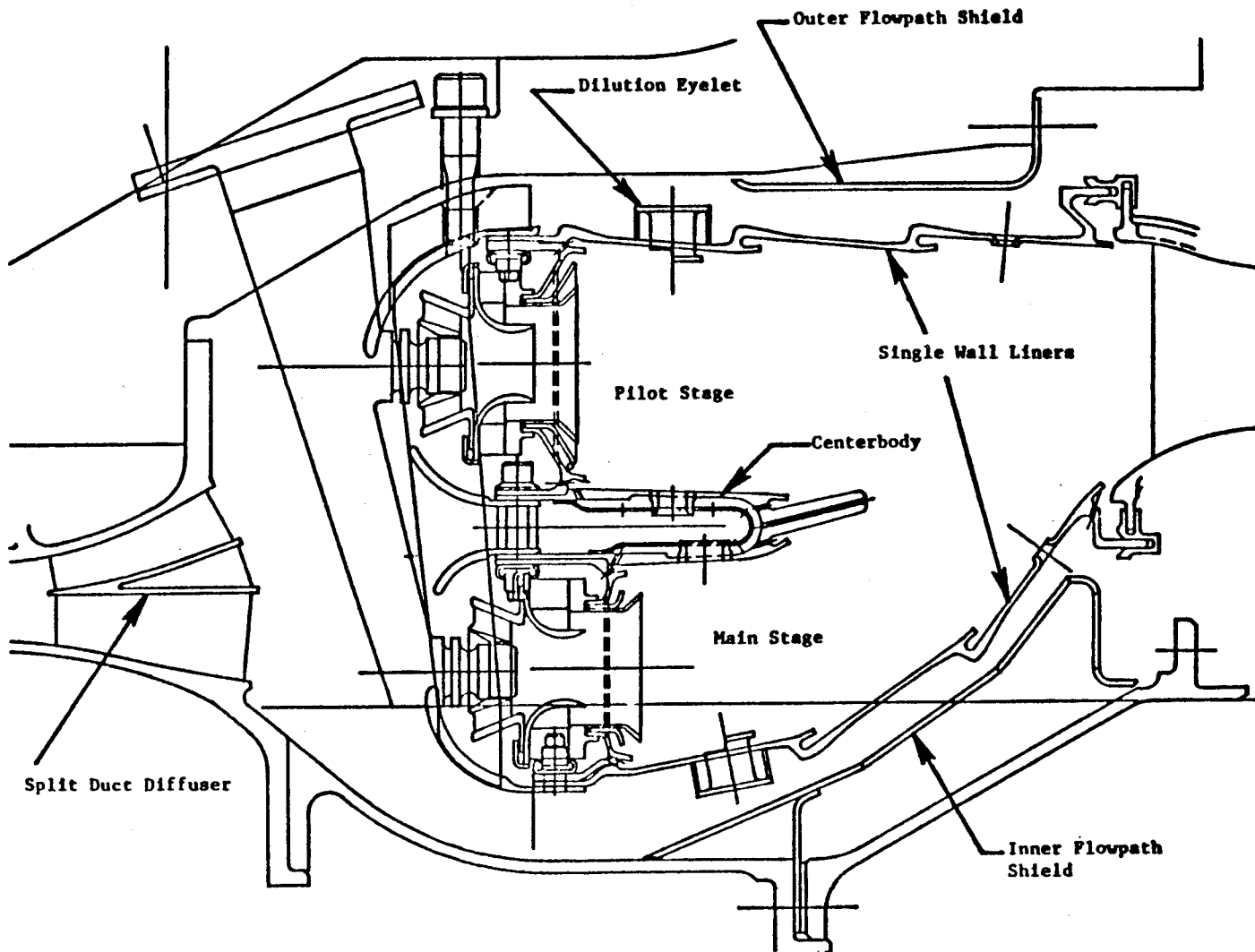
incorporated into the full-annular combustor for detailed evaluation. This procedure resulted in a very successful full-annular test program.

6.2.1 Test Hardware Description

6.2.1.1 Double-Annular Development Test Combustor

The E³ double-annular dome development test combustor was designed to provide an accurate simulation of the engine combustor flowpath. An illustration of the E³ development combustor and key features is shown in Figure 158. The development combustor consisted of a double-annular dome assembly separated by a centerbody. Each dome has 30 equally spaced swirl cup assemblies. The liners contain 30 equally spaced primary airholes and 60 equally spaced secondary trim air dilution holes. The primary holes are eyelet-type designs with a coannular clearance gap which provides a close simulation of the engine double-wall liner airhole aerodynamics. The liners are attached to the dome assembly by bolts which permitted assembling the liners with the primary airholes directly in line with the swirl cups or between the swirl cups. The centerbody structure, which is also bolted to the dome assembly, provides a sheltered region between the pilot stage outer dome annulus and the main stage inner dome annulus. The centerbody structure contains two crossfire tubes to permit propagation of hot gases from one burning dome annulus into the other for the purpose of ignition. There are also 30 equally spaced primary airholes which penetrate the outer dome annulus and 30 equally spaced primary airholes which penetrate the inner dome annulus. The centerbody can also be positioned so that the primary holes are either directly in line with the swirl cups or between the swirl cups.

The development combustor liners are a conventionally machined, ring film-cooled design. The inner surface of the development combustor liners match the engine combustor flowpath. However, because there is no impingement cooling liner, the outer surfaces of the liners do not match the engine combustor flowpath. In order to simulate the same inner and outer flow passage velocities and pressures, flowpath inserts were installed into the test rig combustor housing section, also shown in Figure 158. Plunged-type holes are used for the secondary trim dilution for both the inner and outer liners. Eight



ORIGINAL PAGE IS
OF POOR QUALITY

Figure 158. E³ Full-Annular Development Combustor Design.

major configurations of the E³ development combustor were built and evaluated in this testing effort. Table XXXVI provides a summary of these configurations, their purpose, and the testing accomplished.

The development combustor fuel injector assembly, shown in Figure 159, consists of a single body with two fuel passages and two simplex-type fuel nozzle tips to supply fuel to the outer dome annulus and inner dome annulus. The envelope of the development nozzle body duplicates that of the engine nozzle but has less complicated internal hydraulics. Both nozzles of each injector can be removed and replaced with simplex-type nozzle tips of different flow rates and spray characteristics. A schematic of a typical nozzle tip is also shown in the figure. A large assortment of these tips was purchased for use in the various kinds of testing to be performed.

6.2.1.2 Full-Annular Test Rig Description

The E³ double-annular dome development combustor evaluation were conducted in a full-annular, high pressure test rig specifically designed to house the E³ combustor. This full-annular combustor test rig exactly duplicates the engine combustor aerodynamic flowpath and envelope dimensions. The test rig consists of four major subassemblies: the inlet duct, diffuser flowpath transition section, combustor housing, and instrumentation section for gas sample data acquisition or atmospheric performance data acquisition. A detailed illustration of the test rig (P/N 4013186-466) is presented in Figure 160.

The inlet duct assembly is attached to the test facility air supply system (not shown) at a specially designed pipe flange of 95.4 cm (37.5 inch) diameter. The inlet duct assembly, in addition to providing the interface with the test facility air supply, also has provisions for transferring combustor bleed air and test rig cooling air in and out of the test rig. These ancillary airflow systems are connected to test facility control and measurement systems.

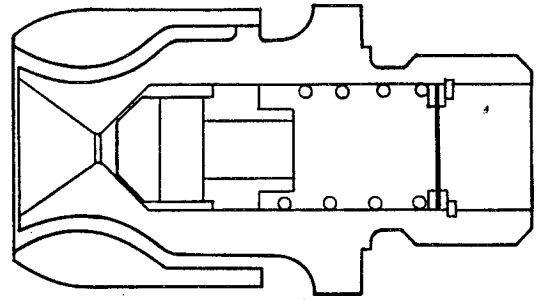
The outer shell of the inlet duct attaches to the transition section, which converges to form the outer wall of the prediffuser inlet. Six radial

Table XXXVI. Combustor Test Matrix.

Configuration	Purpose	Ignition at 1.0 Atmosphere	Ignition at Pressure	Exit Temp. Perf.	Low Power Emissions	High Power Emissions
Baseline	Evaluate Preliminary Design	X		X	X	X
Mod I	Improve Low Power Emissions and Main Stage Ignition	X	X	X	X	X
Mod II	Improve Main Stage Ignition with Rich Dome	X				
Mod III	Improve Main Stage Ignition with Rich Dome	X		X		
Mod IV	Improve Main Stage Ignition with Rich Dome	X				
Mod V	Improve Main Stage Ignition with Rich Dome	X		X		
Mod VI	Revert Back to Original Lean Dome Concept	X		X		
Mod VII	Improve Combustor Pattern Factor and Evolve Final Air Distribution	X	X	X	X	
Core	Evaluate Selected Aero Design for Core Engine Test	X	X	X	X	X

ORIGINAL PAGE IS
OF POOR QUALITY

ORIGINAL PAGE IS
OF POOR QUALITY



Typical Fuel Nozzle Tip

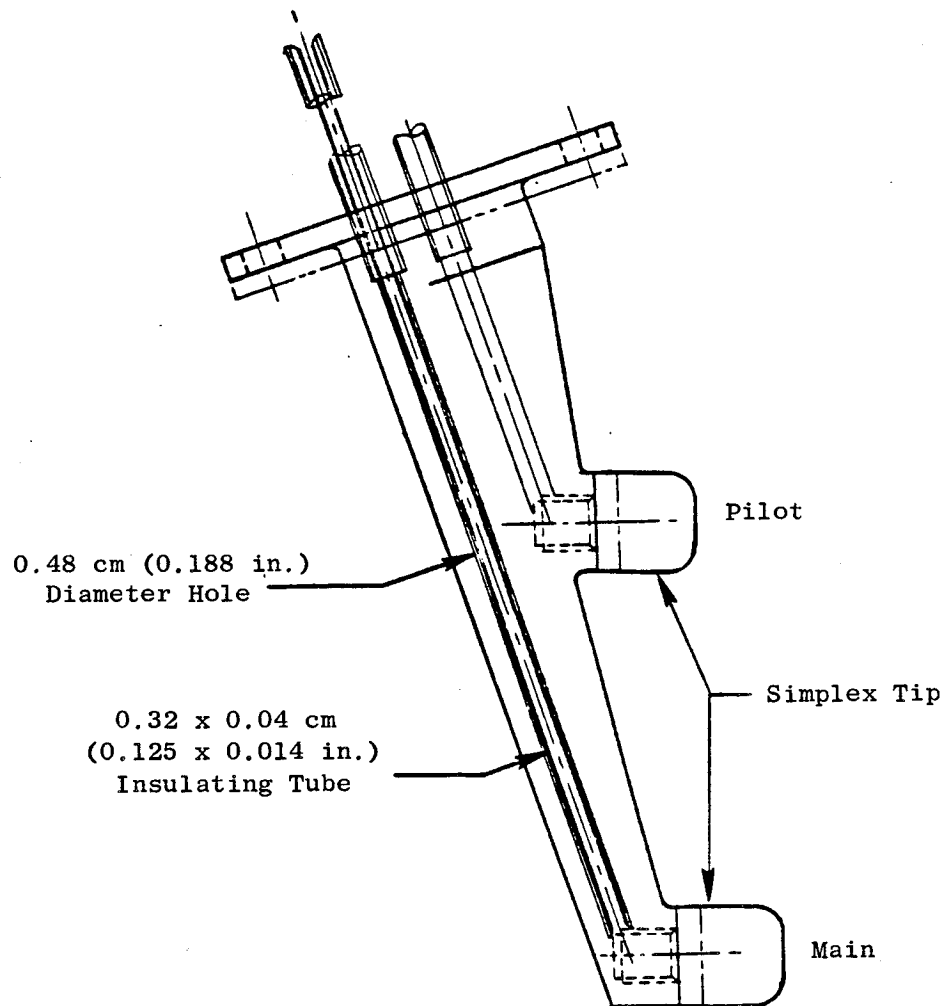


Figure 159. E³ Test Rig Fuel Nozzle Assembly.

ORIGINAL PAGE IS
OF POOR QUALITY

ORIGINAL PAGE IS
OF POOR QUALITY

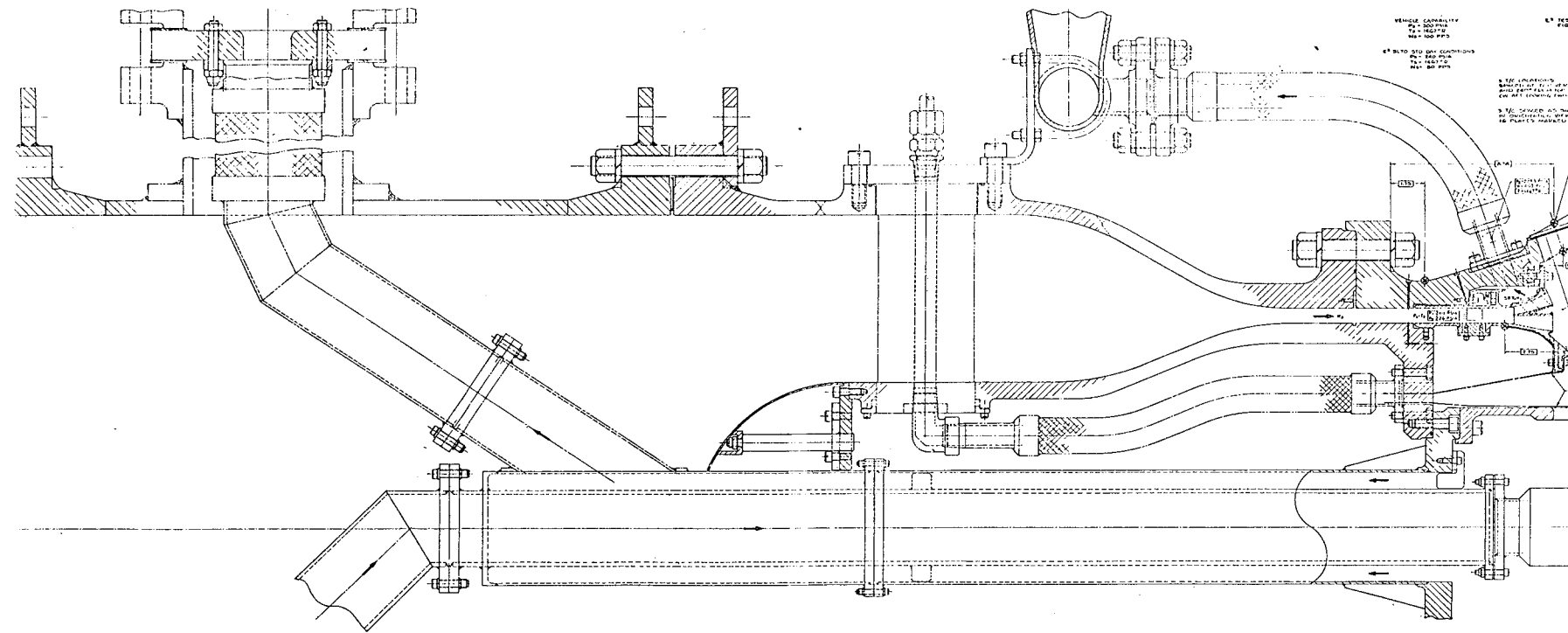
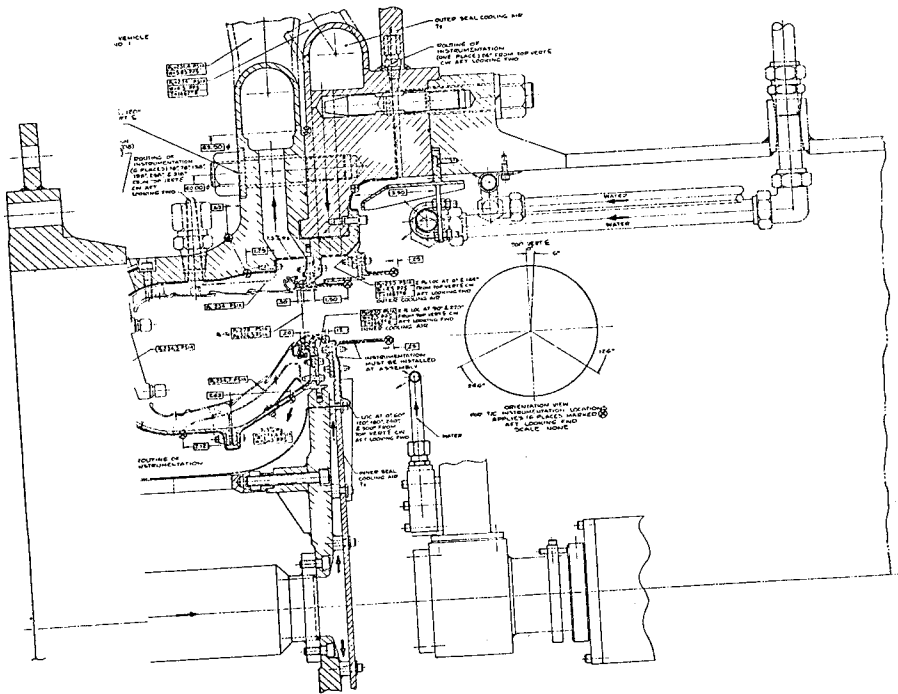


Figure 160. E³ Full-Annular Combustor Component Test Rig.

FOLDOUT FRAME

2 FOLDOUT FRAME

ORIGINAL PAGE IS
OF POOR QUALITY



267

3 FOLDOUT FRAME

struts support the bulletnose centerbody which transitions to the inner flowpath contour of the prediffuser inlet to duplicate the annular passage that exists at the compressor discharge plane. The centerbody provides an internal flowpath for transmitting the cooling and bleed airflows, as well as instrumentation. Leadouts go through passages in the radial struts.

The annular passage which simulates the compressor discharge exit connects to the prediffuser assembly located within the combustor housing. This annular passage splits into two separate annular passages with inner and outer walls conforming to the exact contours of the engine split prediffuser. The split prediffuser passages are supported by streamlined struts similar to those in the engine. Airflow can be extracted at the trailing edge of the prediffuser, in the cavity formed by the splitter vane walls, through ten 2.06 cm (0.81 inch) diameter bleed ports equally spaced around the circumference. The airflow extracted through these bleed ports is routed through piping in the support struts spanning the outer prediffuser passage, to a common manifold, then radially out of the rig through hoses to a bleed manifold which is connected to a standard ASME orifice run to meter the blow. A detailed schematic of this bleed system is shown in Figure 161. This prediffuser bleed system was designed to have the capability of varying the amount of bleed flow extracted from the combustor airflow to evaluate the effects of engine bleeding.

The outer pressure vessel housing is equipped with ports and bosses to accommodate 30 equally spaced, dual-nozzle fuel injector assemblies; two ignitors, and allow for borescope inspection and instrumentation leadout. Fuel is supplied to the fuel injectors through connecting tubes between the dual manifolded fuel supply and the pilot or main stage fuel inlet port in the injector body.

At the aft end of the outer flowpath, airflow can be extracted through thirty 3.0 cm (1.81 inch) diameter bleed ports equally spaced around the circumference to simulate turbine nozzle cooling flow from the combustor outer flowpath. The flow extracted from each bleed port is routed into a collector manifold then out of the test rig. At the aft end of the inner flowpath, airflow can be extracted through nine 3.5 cm (1.38 inch) diameter bleed ports

COPYRIGHT, MADE IN
OF POOR QUALITY

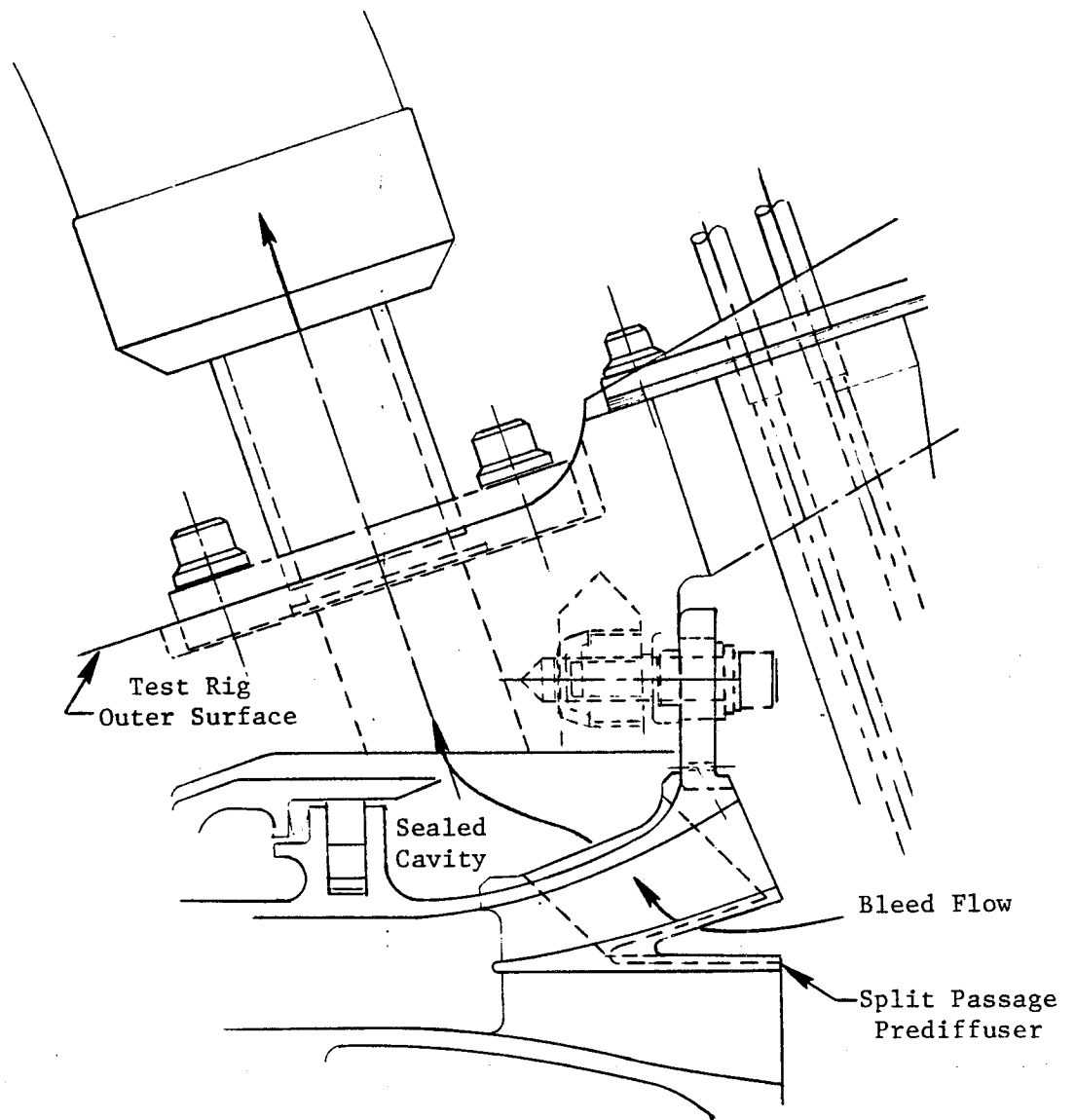


Figure 161. Test Rig Bleed Simulation System.

equally spaced around the circumference to simulated turbine nozzle cooling flow from the combustor inner flowpath. The flow extracted from each of these bleed ports is routed into a plenum cavity at the center of the test rig, then out through an annular pipe along the centerline of the centerbody assembly. Both the inner and outer passage bleed systems have standard ASME orifice runs to meter and measure the bleed flow. These bleed ports, together with the pre-diffuser bleed ports, provide the capability to accurately simulate and evaluate the effect of engine turbine cooling flows expected during engine operation.

The combustor mounting system used in the test rig is identical to that designed for the engine. The combustor is supported at the front end by engine mounting pins and is supported at the aft end by floating seals similar to those of the engine design.

The aft end of the combustor housing is connected to an adapter flange which provides cooling air to the aft outer combustor flowpath. This adapter has a single manifold cavity which feeds cooling air through twenty-two 2.5 cm (1 inch radial holes to the aft tail piece. In addition, the mounting provisions for the instrument spools are located in this adapter.

The instrumentation spool features a rotating internal shaft supported by six radial struts: three forward and three aft. A cross section of the rotating spool piece is shown in Figure 162. The end of the rotating shaft, which is supported by two bearings, has 10 mounting pads. The gas sample rakes and/or thermocouple rakes are mounted to these pads in locations and quantities as desired during test. Cooling of the shaft assembly and struts is accomplished by circulating water through the struts and along the shaft. A portion of the cooling water is directed to the rake mounting pads where it supplies an auxiliary water manifold and to the gas sample rakes for rake body cooling. The rake cooling water is discharged from the rake bodies into the duct. Additional structural cooling is accomplished by water discharged from spraybars and ring manifolds mounted near the duct walls.

Rotation of the center shaft is accomplished by a drive motor located outside the instrument spool duct wall. This motor drives a radial shaft supported in a strut that is connected to a helical gear set by a spherical gear

ORIGINAL PAGE IS
OF POOR QUALITY

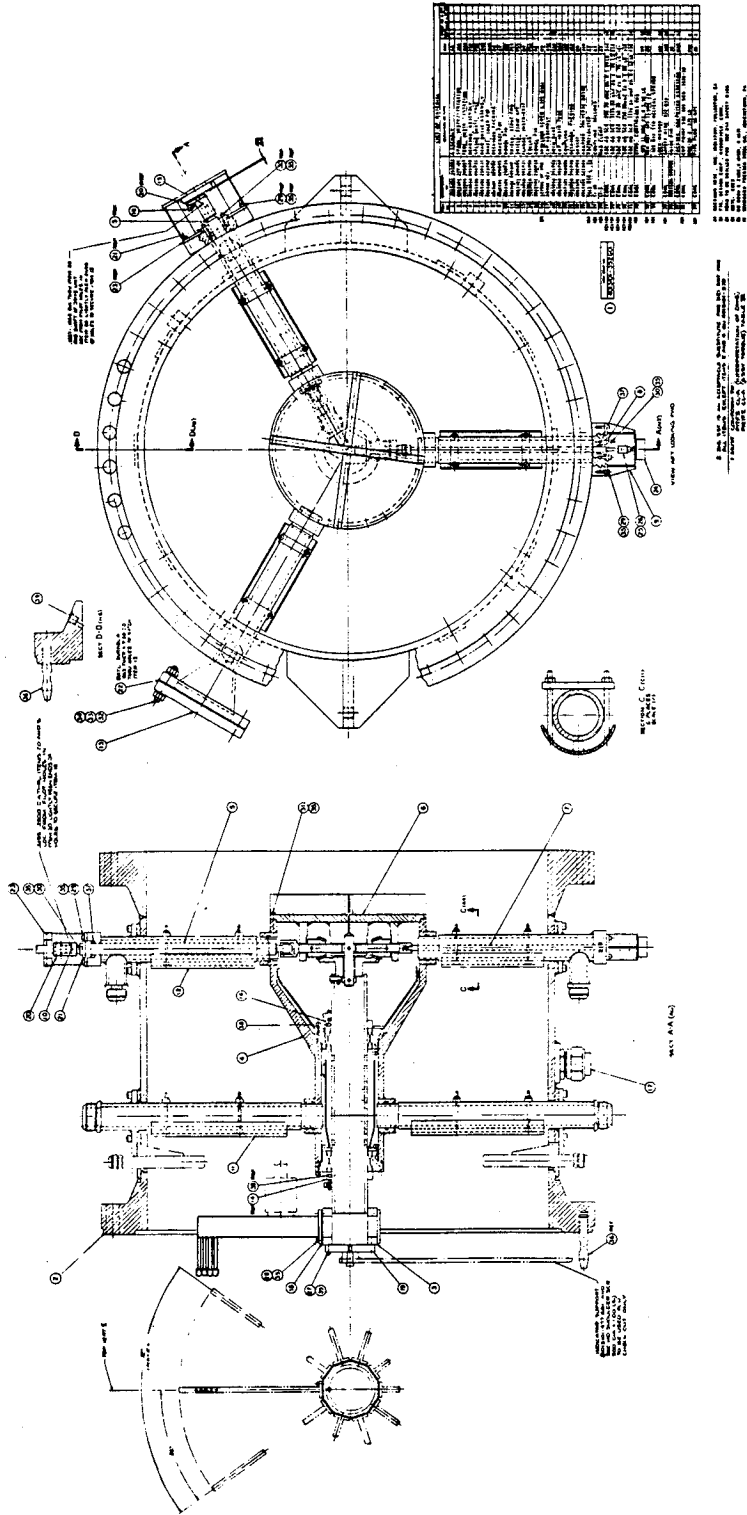


Figure 162. Test Rig Instrumentation Spool.

coupling. The spherical gear coupling permits rotation even with some shaft misalignment. The portion of the helical gear, which is aligned with the rake mounting shaft, contains a lug. This lug engages a slot in the shaft and can rotate the shaft a total of about 36° clockwise and counterclockwise for a total of nearly 72° rotation. The input coupling has a mechanical stop to prevent excessive travel. The drive shaft is equipped with shear pins to prevent damage to the gear mechanism in the event of hangup or overtravel.

The Atmospheric Combustion Test Stand (ACTS) system is used to obtain detailed temperature measurements at the combustor exit. The system adapts to the aft end of the combustor test rig housing as shown in Figure 163. Thermocouple rakes and/or pressure rakes are attached to the traverse ring and are guided by the roller system and track. The traverse ring is motor-driven and will rotate 90° clockwise or counterclockwise in increments as small as 1.5°. The thermocouple rakes are equipped with seven chromel alumel (C/A) elements. The thermocouple elements are led to a chromel alumel thermocouple system (CATS) block which transients the electronic signals to the data acquisition system. The exit temperature data, along with the fixed test rig and combustor instrumentation, are automatically processed by the data acquisition system and presented in a finished format of prescribed combustor performance parameters and operating conditions.

6.2.1.3 Test Methods

Atmospheric Tests

Ground start ignition, crossfire, and exit temperature performance characteristics of the E³ development combustor were evaluated at atmospheric inlet conditions. In this testing configuration, the test rig was discharged "open end" into the surrounding test cell ambient environment. This permitted useful visual observations of the combustor in operation. During these atmospheric tests, the combustor inlet temperatures duplicated the level of the desired operating cycle test point. However, the combustor airflows were scaled down to levels which simulated the combustor velocities while operating at atmospheric inlet pressure. This technique provides an inexpensive testing approach that will develop satisfactory ground start ignition and exit temperature performance characteristics while providing accurately simulated combustor operating conditions.

ORIGINAL PAGE IS
OF POOR QUALITY

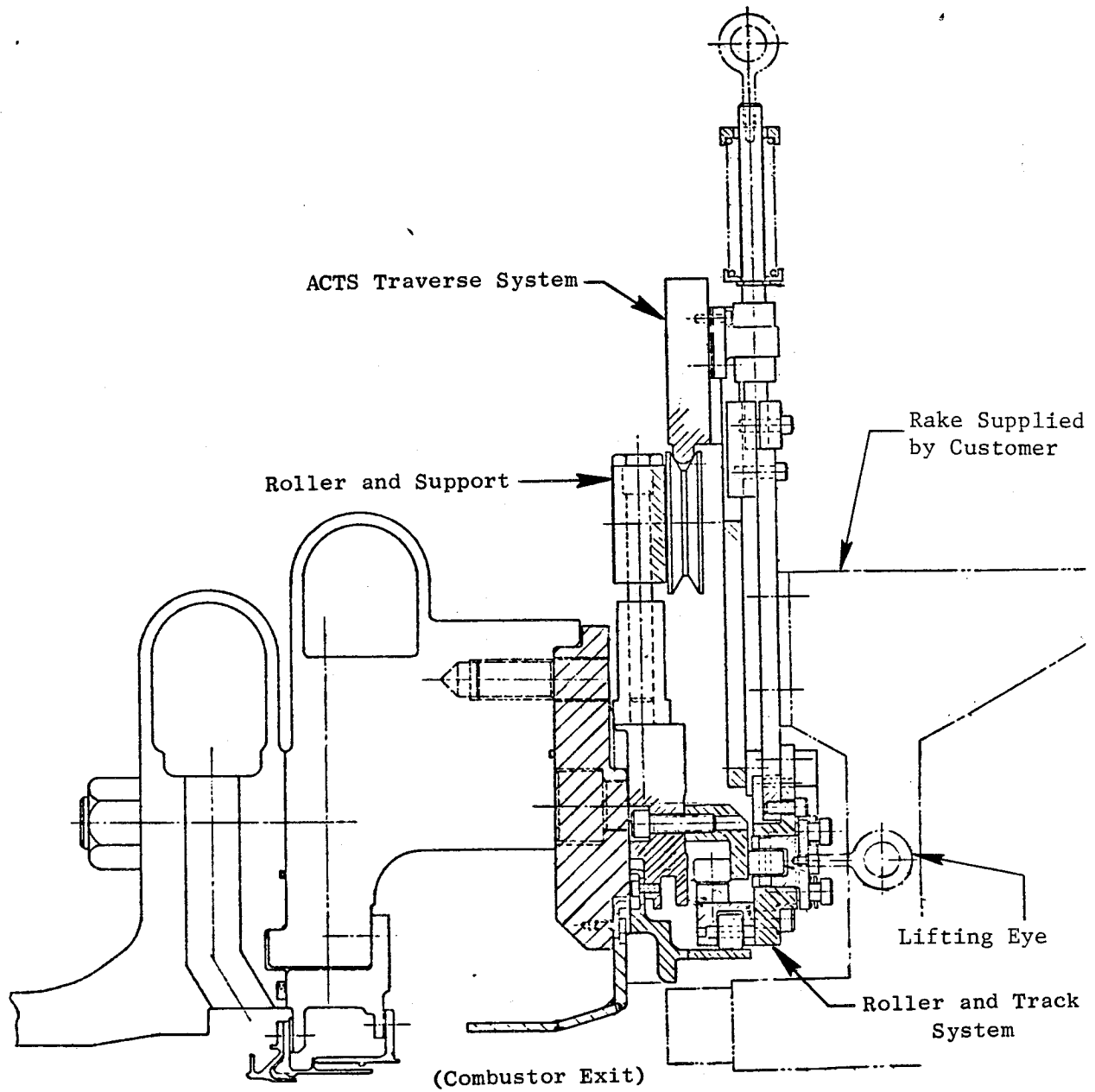


Figure 163. ACTS Traverse System.

Ground start ignition testing was conducted using the standard GE23 ignition system. This system consists of ignitor plug, exciter unit, and ignitor lead. This ignition system has an energy-delivered rating of 2 J with a firing rate of 2 sparks per second. The ignitor was positioned in outer liner Panel 1 at 240° CW aft looking forward (ALF). The ignition immersion was flush with the inside surface of the liner panel wall. To further simplify this testing, no bleed flows were set during the ignition evaluations. Past experience has shown that the effects of bleed flows on the ground start ignition characteristics are insignificant. The basic testing procedure used is as follows:

1. Set the combustor operating conditions corresponding to the selected steady-state test point.
2. Activate the ignition system.
3. Supply fuel to the pilot stage fuel nozzles. Continue to increase this fuel flow until the ignitor swirl cup has ignited. Deactivate the ignition system, and record the operating conditions and fuel flow level.
4. Continue to increase the fuel flow until full pilot stage propagation is achieved. Record the operating conditions and fuel flow level.
5. Reduce the fuel flow rate slowly until one pilot stage swirl cup extinguishes. Record the operating conditions and fuel flow level.
6. Continue to decrease the fuel flow rate until total lean blowout is obtained. Record the operating conditions and fuel flow level.
7. Repeat Steps 2 through 4; then, reduce the pilot stage fuel flow to a level 10% above the level recorded at one cup extinguished.
8. Holding the pilot stage fuel flow level steady, supply fuel to the stage fuel nozzles. Continue to increase the main stage fuel flow until the crossfire cup or cups ignite. Record the operating conditions and fuel flow levels.
9. Continue to increase the main stage fuel flow until full propagation is achieved. Record the operating conditions and fuel flow levels.
10. Reduce the main stage fuel flow slowly until total main stage lean blowout is obtained. Record the operating conditions and fuel flow levels. Then, shut off the main stage fuel flow.

11. Reduce the pilot stage fuel flow slowly until total pilot stage lean blowout is obtained. Record the operating conditions and fuel flow levels.
12. Shut off all combustor fuel flow; then, proceed to set the operating conditions corresponding to the next selected test point.

Throughout this procedure, visual observations were used to determine ignition, propagation, and lean blowout.

Atmospheric exit temperature performance testing was conducted using the ACTS system. Four E³ exit temperature rakes were mounted onto the traverse ring of the ACTS system, equally spaced around the circumference. These rakes, shown in Figure 164, contained seven chromel alumel thermocouple elements and were especially designed for use with the E³ combustor test rig. During atmospheric performance, testing only the prediffuser bleed flow was simulated. At all primary performance test points, exit temperature traverse data was obtained every 1.5° of the total 90° traverse. This provided temperature radial profile measurements at 240 circumferential positions for a total of 1680 individual temperature measurements. At off-design or secondary test points, data were obtained every 3° around the circumference in order to save time. All combustor test rig instrumentation and exit temperature performance data were recorded on the facility data acquisition system. This information was then automatically processed through a computer data reduction program to calculate the combustor operating conditions, the average and peak radial temperature profiles, and the pattern factor and profile factor using these relations:

$$\text{Pattern Factor} = \frac{T4 \text{ (max)} - T4 \text{ (avg)}}{T4 \text{ (avg)} - T3}$$

$$\text{Profile Factor} = \frac{T4 \text{ immersion avg (max)} - T4 \text{ (avg)}}{T4 \text{ (avg)} - T3}$$

Pressure Tests

Emissions characteristics of the E³ development combustors were evaluated at elevated inlet pressure. Several combustor configurations were also evaluated for ground start ignition and crossfire characteristics at elevated pressure as part of an emissions test. For this testing, the test rig was assembled to a gated exhaust system for inlet pressure controls. Since visual

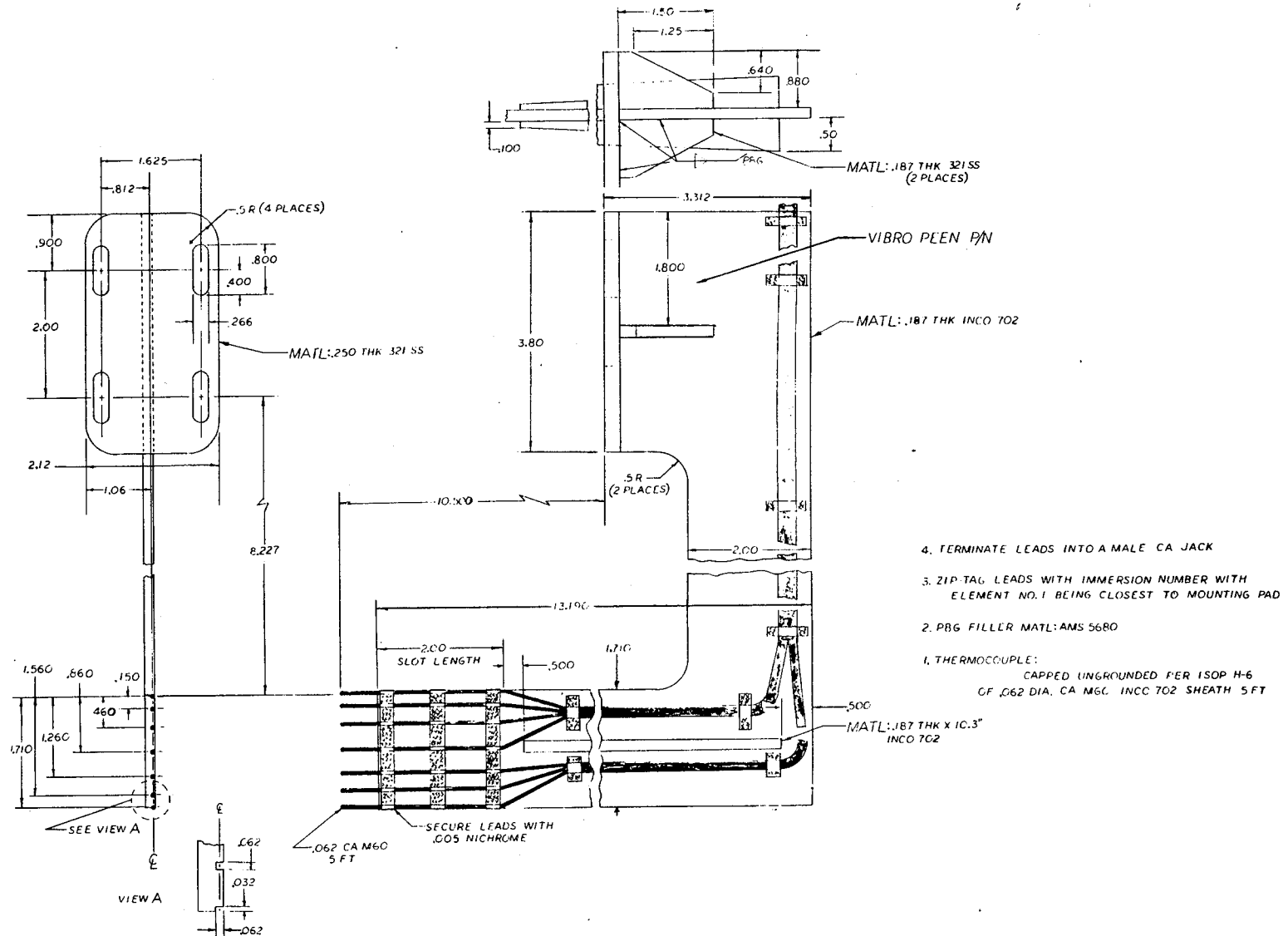


Figure 164. E³ Full-Annular Combustor EGT Thermocouple Rakes.

ORIGINAL DRAWING
OF POOR QUALITY

observations were not possible, monitoring the combustor operation was accomplished by using the available test rig and combustor pressure and temperature instrumentation.

Air was supplied to the test rig from the facility high pressure, high flow capacity system. With this system, combustor operating conditions in the test rig exactly duplicating the E³ FPS cycle conditions could be achieved up to 30% of sea level takeoff power. Above this power level, combustor airflow and inlet pressure were limited by the maximum capacity of the facility. At these high power operating points, test conditions were simulated by setting proper Mach numbers in the test rig. The combustor inlet temperature was set to the exact engine cycle level. The maximum available test section total pressure was approximately 1.655 MPa (240 psia). This compares to the 3.025 MPa (439 psia) level associated with the FPS sea level takeoff operating condition.

All CO, HC, and NO_x emissions levels measured at the simulated high power operating conditions were adjusted to reflect levels that would be obtained if measured under true engine cycle operating conditions. These adjustments were made using the relations presented in Appendix D.

Gas samples were extracted from the combustor discharge stream using the E³ gas sample rakes as shown in Figure 165. Five rakes were used, each with four sampling elements. For the purpose of ground start ignition testing, two chromel alumel-type thermocouples were strapped onto the outermost and innermost sampling elements of each of the five gas sampling rakes. This arrangement is illustrated in Figure 166. These thermocouples were connected to a "Metroscope" visual display system within the facility control room and were used in determining ignition, crossfire, and lean extinction in the pilot stage and main stage of the combustor.

For gas sampling purposes, all four elements of each gas rake were individually connected to the valving in the gas sampling equipment. This approach provided the flexibility to close off individual rake elements from the rake sample if problems would arise in any of the four elements. The five gas sampling rakes were equally spaced around the test rig instrumentation

ORIGINAL PAGE IS
OF POOR QUALITY

ORIGINAL PAGE
BLACK AND WHITE PHOTOGRAPH

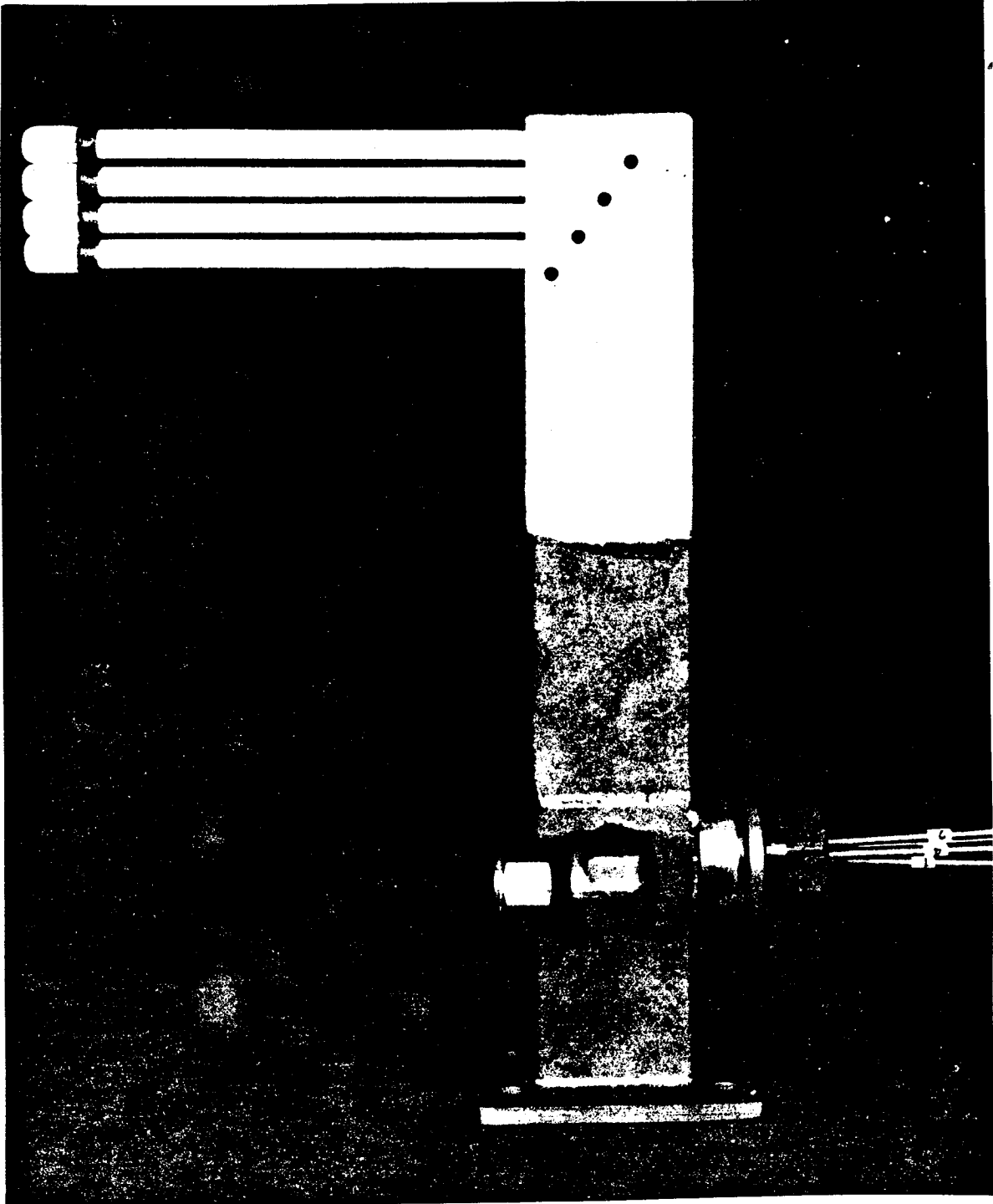


Figure 165. E^3 Full-Annular Combustor Gas Sampling Rakes.

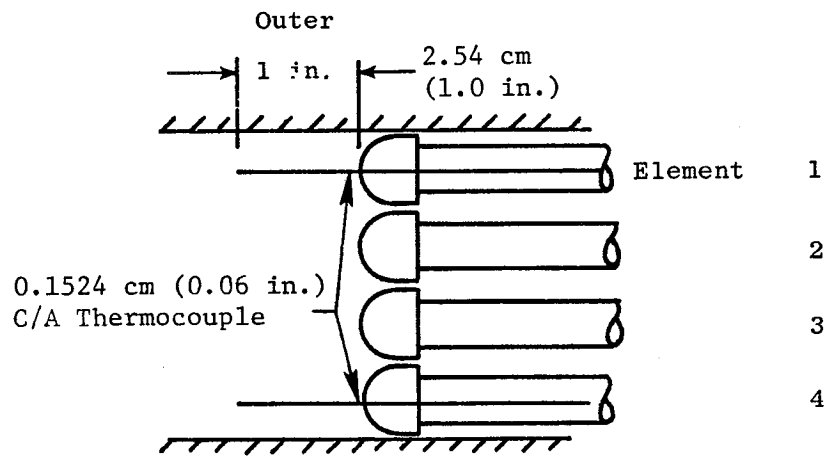
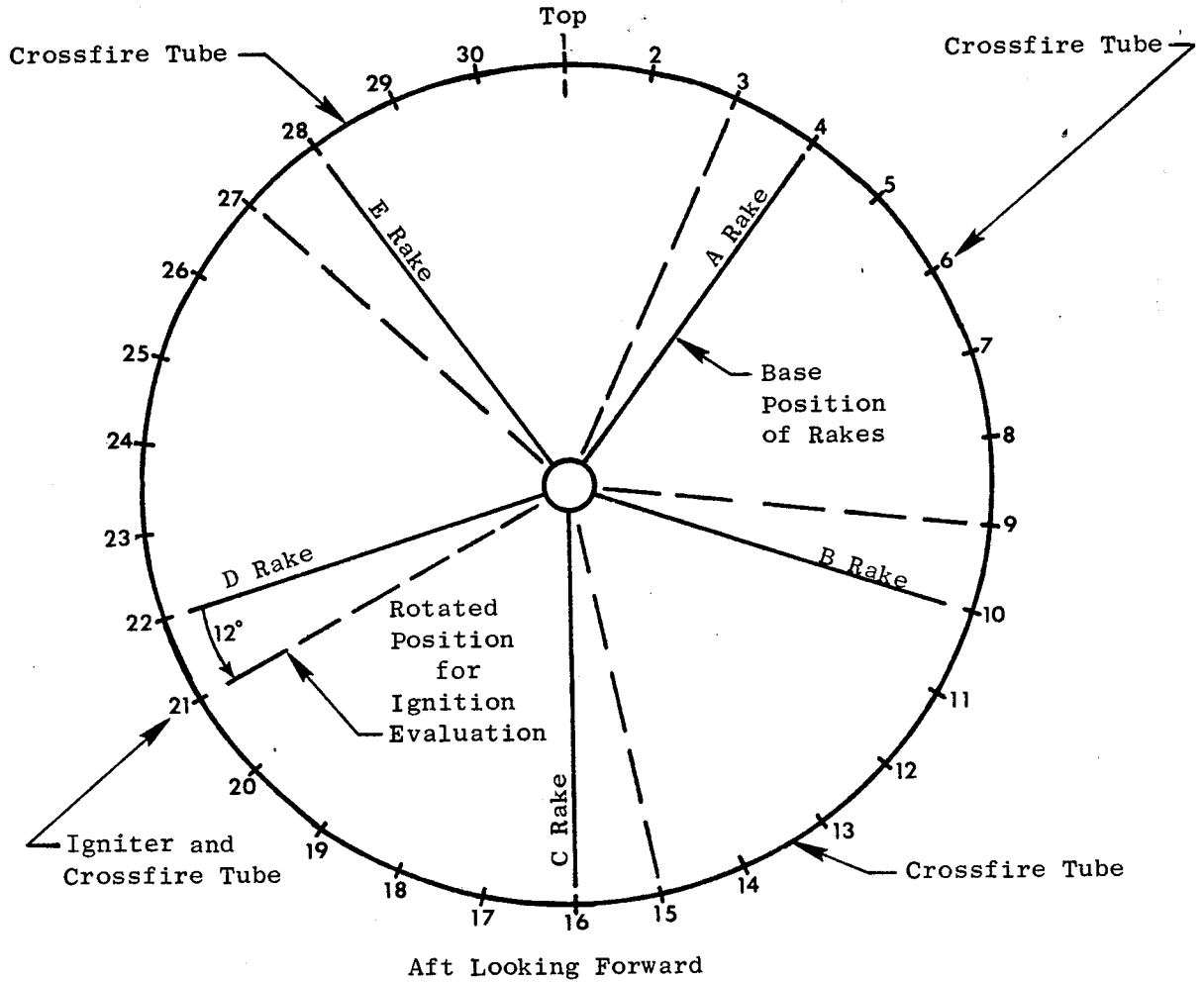


Figure 166. Gas Sampling Rake Instrumentation for Ignition Testing.

spool. Unheated water was used to cool the rakes during testing. The decision to use unheated water as the cooling medium was determined from results obtained during the emissions evaluation of the baseline development combustor.⁴ These results, shown in Figure 167, showed that the use of unheated cooling water had only a very minor impact on idle emissions.

During gas sampling, the rakes were traversed through 66° at 6° increments enabling gas samples to be obtained in line with and between all 30 swirl cups. For ignition and blowout evaluation, the gas sampling rakes were positioned so that one rake was located at 240° CW ALF, placing that rake with its two thermocouple elements directly downstream of the pilot stage ignitor cup and one of the two pilot-stage-to-main-stage crossfire tubes.

Gas samples were analyzed using the CAROL II analysis system located at the test facility. Instruments featured in this system include:

- Beckman Model 402 total hydrocarbon analyzer (flame ionization detector)
- Beckman Model 315-B carbon monoxide and carbon dioxide analyzer (NIDR)
- Beckman Model 915-H NO_x analyzer (heater chemiluminescence with converter).

Sample flow was passed through a refrigerated trap to remove excess water from the sample before entering the gas analysis instruments. Prior to testing, the CAROL II system was calibrated using a set of calibration gases. These gases and their GE constituent analysis are listed in Table XXXVII. During testing, calibration spot checks of the instruments, and any necessary adjustments, were made to assure that this equipment was in good working order at all times. Inlet air humidity was measured using an EG&G Model 440 dew point meter.

Smoke samples were taken only at designated key combustor operating points in the test schedule. Smoke samples were extracted from the exhaust gases using two of the five gas sampling rakes valved in a manner which provided a single sample. At those test points where smoke samples were taken,

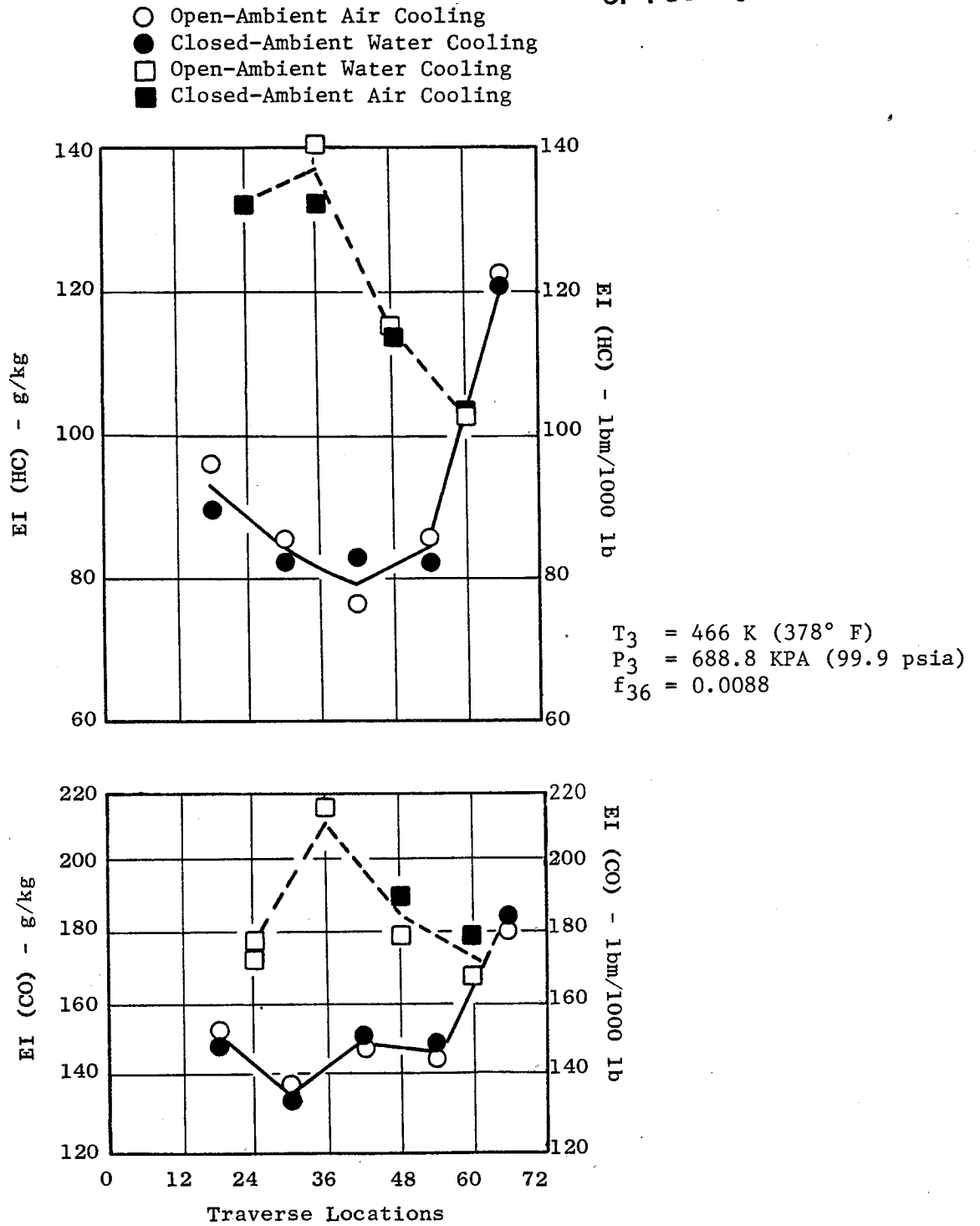


Figure 167. Effect of Gas Rake Cooling Medium on CO and HC Emissions.

the rakes were initially positioned in line with the swirl cups, then rotated 6° to between swirl cups. At each of these two positions, several smoke samples, each 0.0057 m³ (0.2 ft³) in volume, were obtained using a standard GE smoke console located in the cell control room.

Table XXXVII. CAROL Calibration Gases.

	Span 1	Span 2	Span 3	Span 4
Bottle S/N, CO, kg/m (ppm)	261131-227 (500)	2960095-468 (1032)	6742-1085 (2392)	49244-2350 (5181)
Bottle S/N, CO ₂ (%)	261131(1.27)	2960095(2.54)	6742(4.94)	49244(8.03)
Bottle S/N, HC, kg/m (ppm)	1317746-74.3 (164)	49301-143 (315)	127885-569 (1254)	49110-1328 (2928)
Bottle S/NM, NO _x , kg/m (ppm)	12553-29.1 (64)	12548-69.8 (154)	10766-234 (516)	3976-543 (1197)

All emissions and instrumentation data acquisition were automatically handled by the Cell A3 medium speed digital data acquisition system. From this system, data were processed through a computer data reduction program which performed calculations to compute the various emissions indices, combustor operating parameters, and convert digital signals from all pressure and temperature instrumentation to engineering units. All smoke samples were obtained on Wattman 4 filter paper. Following completion of testing, the smoke samples obtained were analyzed on a Densichron to determine the optical density used to compute the SAE smoke number.

6.2.2 Screening Combustor Test Results

6.2.2.1 Atmospheric Ground Start Ignition Test

The first test of the E³ double-annular dome development combustor and test rig was conducted on February 7, 1980, in the General Electric Aero Component Lab-Cell A3W test facility. The purpose of this test was to evaluate the baseline combustor configuration for ground start ignition, pilot-to-main stage crossfire, and the pilot and main stage lean blowout characteristics at

atmospheric inlet pressure along the E³ (9/79), ground start operating line. Test points and corresponding operating conditions are shown in Table XXXVIII.

Table XXXVIII. Baseline Atmospheric Ignition Test Point Schedule.

Point	Start Time (s)	XNRH (%)	T ₃ , K (° R)	P ₃ (atm.)	W ₃₆ [*] , kg/s (pps)
1	10	21.0	289 (520)	1.00	1.25 (2.75)
2	15	28.0	289 (520)	1.00	1.69 (3.62)
3	18	32.0	314 (565)	1.00	1.55 (3.42)
4	30	46.0	344 (619)	1.00	1.65 (3.64)
5	40	58.0	383 (689)	1.00	1.86 (4.10)
6	50	70.0	428 (770)	1.00	1.94 (4.28)
7	55	77.0	503 (905)	1.00	2.33 (5.14)

*If inlet air temperature cannot be set at the prescribed level, the airflow will be changed to maintain the $W_{36}\sqrt{T_3}/P_3$ value.

The baseline combustor configuration featured most of the mechanical and aerothermo characteristics evolved during the design phase of the combustor development program. The only significant difference from the proposed design was in the pilot dome splash plate cooling flow level. The combustor was designed to have approximately 4.3% of the total combustor flow for the pilot dome splash plate cooling. However, the hardware was fabricated to have approximately 2.5 times the design flow level to provide the ability to easily increase the splash plate cooling flow level if necessary. It was intended to block off a percentage of this flow to achieve the intended design levels if baseline testing indicated sufficiently low dome metal temperatures. The estimated airflow distribution for the baseline development combustor is available in Appendix E. The fuel nozzle assemblies used featured the E³ test rig fuel

nozzle bodies with simplex nozzle tips rated at 2.3 kg/hr (5 pph) at 689.5 KPa (100 psid) in the inner dome, and simplex nozzle tips rated at 12.0 kg/hr (26.5 pph) at 689.5 KPa (100 psid) in the outer dome. Both of these nozzle tips had fuel spray angles of approximately 50°.

It had been intended to use the GE23 ignition system to obtain the pilot stage ignition characteristics. However, problems were encountered at the onset of testing due to a failure in one of the components of the GE23 ignition system provided. As a result, a hydrogen torch ignition system was substituted and testing proceeded. Accurate pilot stage ignition data generally cannot be obtained with a hydrogen torch system due to its high specific energy output. However, pilot stage propagation, pilot-to-main-stage cross-fire, and pilot and main stage lean blowout data were obtained. By the time the last test point had been set, another GE23 ignition system had been obtained. This system was installed into the test rig with the intent of obtaining pilot stage ignition data starting at the last test point and working back toward the initial test point. Following the completion of ignition at Test Points 7, 6, and 5, another failure in the electrical ignition system occurred and testing was terminated. The failures involved the ignitor lead.

Test results obtained from the atmospheric ground start ignition evaluation of the E³ development combustor baseline configuration are presented in Figure 168. A detailed summary of the test data is provided in Appendix E. Ignition of the pilot stage ignitor cup using the hydrogen torch proceeded without difficulty at each test point evaluated. However, once ignition occurred, a substantial increase in the pilot stage fuel flow was required to obtain a full propagation of the fire. As observed from this figure, the pilot stage ignition characteristics were within the E³ start cycle requirements.

The three test points evaluated with the GE23 ignition system show excellent agreement with the results obtained with the hydrogen torch ignition system. Past experience has generally shown that as the combustor operating conditions become more severe for ignition, greater difficulty arises in achieving ignition with electrical systems than with the hydrogen torch systems. Therefore, it was expected that pilot stage ignition results obtained with the

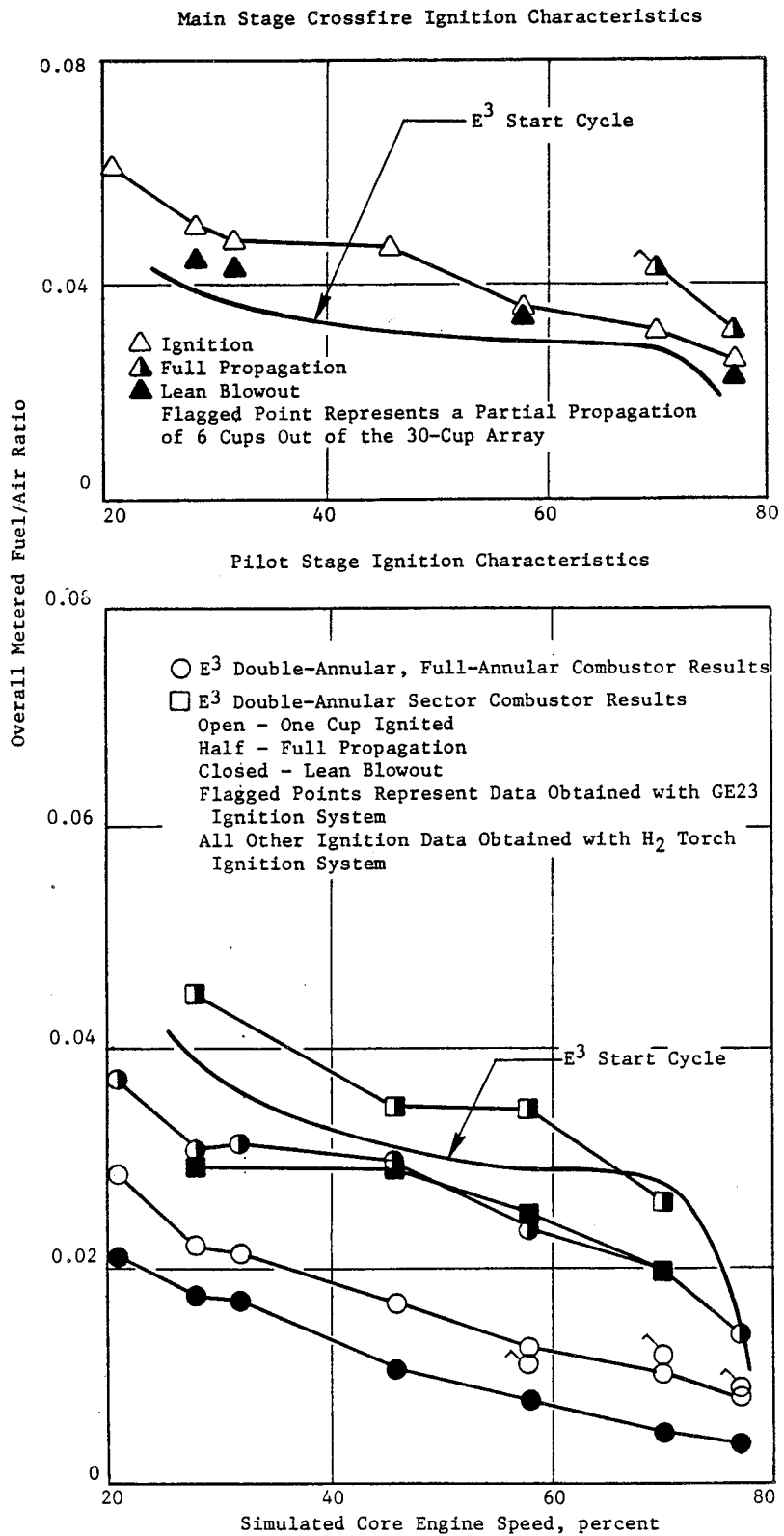


Figure 168. Development Combustor Baseline Atmospheric Ignition Test Results.

GE23 ignition system at the simulated lower speed points would be somewhat poorer than the results obtained with the hydrogen torch system but still within the start cycle requirements. The pilot stage demonstrated an acceptable lean blowout margin of about 30% along the entire start cycle operating line.

Ignition of the main stage was attempted at each test point. In all cases, this was accomplished by hot gases from the burning pilot stage passing through the two centerbody crossfire tubes located at 60° and 240° clockwise, aft looking forward. However, propagation of the fire in the main stage was only achieved at the simulated higher speed points. The low flow fuel nozzle tips used in the main stage limited the maximum fuel flow to approximately 160 kg/hr (350 pph) at the maximum fuel pressure that the facility could supply. A partial propagation (six cups) in the main stage was achieved at conditions representing the 70% engine speed point, while full propagation was achieved at conditions representing the 77% engine speed point. The combustor operating conditions at these points were favorable enough to offset the adverse effects of the lean main stage dome stoichiometry. Insufficient data were obtained to make a good assessment of the main stage lean blowout characteristics.

6.2.2.2 Atmospheric Exit Temperature Performance Test

Performance testing of the E³ combustor baseline configuration was then conducted. The purpose of this test was to evaluate the profile and pattern factor at simulated sea level takeoff conditions with variations in the pilot and main dome fuel staging. The test schedule and corresponding combustor operating conditions are presented in Table XXXIX.

Exit temperature data were obtained at simulated sea level takeoff inlet conditions, and overall fuel/air ratios of 0.020, the design level of 0.0244, and 0.0260. Fuel staging modes representing pilot-to-total fuel flow splits of 0.5, 0.4, and 0.3 were evaluated at the 0.020 and 0.0244 overall fuel/air ratio conditions. Pilot-to-total fuel flow splits of 0.4 and 0.3 were evaluated at the 0.0260 overall fuel/air condition.

Table XXXIX. Baseline Atmospheric EGT Performance Test Point Schedule.

Test Point	T ₃ , K (° R)	P ₃ , Atm.	W ₃ , kg/s (lb/s)	W _{Bleed} , kg/s (lb/s)	W _{Comb} , kg/s (lb/s)	f/a	W _f Total, kg/hr (lb/hr)	Pilot Total	W _f Pilot, kg/hr (pph)	W _f Main kg/hr (lb/hr)
1	495 (891)	1.00	2.67 (5.87)	0.19 (0.41)	2.48 (5.46)	0.0123	110 (242)	1.0	110 (242)	0 (0)
2	815 (1467)	1.00	2.41 (5.31)	0.15 (0.34)	2.26 (4.97)	0.0200	163 (358)	0.50	81 (179)	81 (179)
3	815 (1467)	1.00	2.41 (5.31)	0.15 (0.34)	2.26 (4.97)	0.0200	163 (358)	0.40	65 (143)	98 (215)
4	815 (1467)	1.00	2.41 (5.31)	0.15 (0.34)	2.26 (4.97)	0.0200	163 (358)	0.30	49 (107)	114 (251)
5	815 (1467)	1.00	2.41 (5.31)	0.15 (0.34)	2.26 (4.97)	0.0244	199 (437)	0.50	100 (219)	100 (219)
6	815 (1467)	1.00	2.41 (5.31)	0.15 (0.34)	2.26 (4.97)	0.0244	199 (437)	0.40	80 (175)	119 (262)
7	815 (1467)	1.00	2.41 (5.31)	0.15 (0.34)	2.26 (4.97)	0.0244	199 (437)	0.30	60 (131)	139 (306)
8	815 (1467)	1.00	2.41 (5.31)	0.15 (0.34)	2.26 (4.97)	0.0275	224 (492)	0.50	112 (246)	112 (246)
9	815 (1467)	1.00	2.41 (5.31)	0.15 (0.34)	2.26 (4.97)	0.0275	224 (492)	0.40	90 (197)	134 (295)
10	815 (1467)	1.00	2.41 (5.31)	0.15 (0.34)	2.26 (4.97)	0.0275	224 (492)	0.30	67 (148)	156 (344)

Performance results obtained at simulated 6% ground idle operating conditions are presented in Figure 169. In this operating mode with only the pilot stage fueled, the exit temperature profiles are sharply peaked outward. This is typical of double-annular combustor designs operating in this mode. Figure 170 shows the performance results obtained at the design fuel/air ratio. The maximum and average profiles illustrate the sensitivity of exit temperature profiles to pilot-main stage fuel split but are generally within established limits at the 0.50 pilot-to-total fuel flow split. Also, a pattern factor of 0.255 was obtained which is very close to the goal of 0.250.

A plot of the average circumferential exit distribution is presented in Figure 171. This temperature distribution represents data obtained at the simulated design cycle sea level takeoff operating condition with an 0.40 pilot-to-total fuel flow split. For this combustor operating mode, the peak temperatures generally occur in line with the swirl cups while the minimum temperatures occur between swirl cups. Cooler spots in the combustor appear to exit in the vicinity of swirl Cups 11 and 14. A posttest check of fuel nozzles revealed that the main stage nozzle tip in Cup 11 was approximately 5% below the average of all 30 main stage nozzle tips in fuel flow. The pilot stage nozzle tip in Cup 14 was approximately 17% below the average of all 30 pilot stage nozzle tips in fuel flow. These low fuel flow levels in the two swirl cups could have produced the cooler regions observed.

6.2.2.3 Emissions Test

Emissions testing of the E³ double-annular dome development combustor baseline configuration was conducted in the ACL Cell A3E test facility. This represented the first test in which the development combustor and test rig were operated at elevated pressure conditions. The purpose of this testing was to evaluate the baseline combustor design for emissions, pressure drop, and metal temperature characteristics at combustor operating conditions along the E³ FPS design operating cycle. Bleed flows from the split duct diffuser and the outer and inner flowpaths were extracted at levels simulating the actual engine combustor operation at all test points. Test points and corresponding operating conditions evaluated in this test are presented in Table XL. During the limited phase of testing, simplex-type fuel nozzles rated

ORIGINAL PAGE IS
OF POOR QUALITY

- 6% Idle (Pilot Only)
- Atmospheric Pressure
- Corrected Temperatures

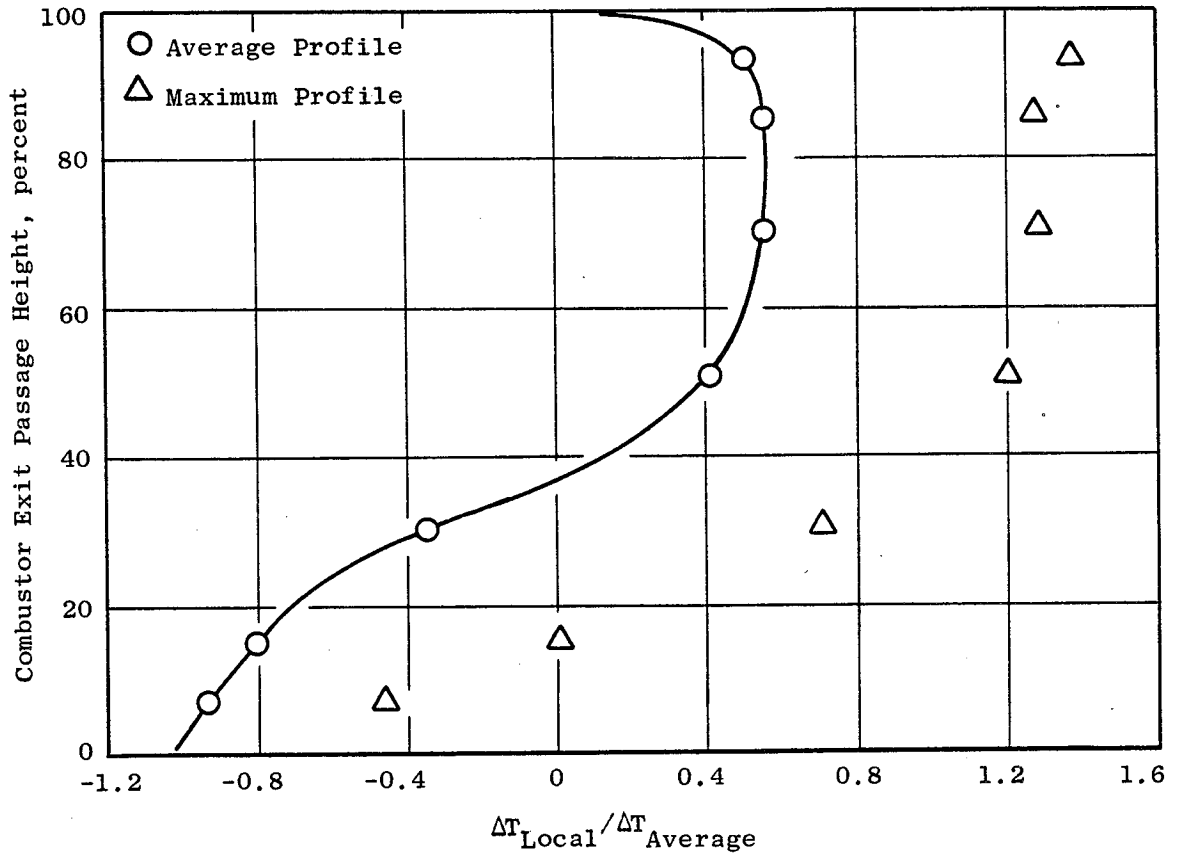


Figure 169. Development Combustor Baseline EGT Performance Test Results, Idle.

equally spaced around the circumference to simulated turbine nozzle cooling flow from the combustor inner flowpath. The flow extracted from each of these bleed ports is routed into a plenum cavity at the center of the test rig, then out through an annular pipe along the centerline of the centerbody assembly. Both the inner and outer passage bleed systems have standard ASME orifice runs to meter and measure the bleed flow. These bleed ports, together with the pre-diffuser bleed ports, provide the capability to accurately simulate and evaluate the effect of engine turbine cooling flows expected during engine operation.

The combustor mounting system used in the test rig is identical to that designed for the engine. The combustor is supported at the front end by engine mounting pins and is supported at the aft end by floating seals similar to those of the engine design.

The aft end of the combustor housing is connected to an adapter flange which provides cooling air to the aft outer combustor flowpath. This adapter has a single manifold cavity which feeds cooling air through twenty-two 2.5 cm (1 inch radial holes to the aft tail piece. In addition, the mounting provisions for the instrument spools are located in this adapter.

The instrumentation spool features a rotating internal shaft supported by six radial struts: three forward and three aft. A cross section of the rotating spool piece is shown in Figure 162. The end of the rotating shaft, which is supported by two bearings, has 10 mounting pads. The gas sample rakes and/or thermocouple rakes are mounted to these pads in locations and quantities as desired during test. Cooling of the shaft assembly and struts is accomplished by circulating water through the struts and along the shaft. A portion of the cooling water is directed to the rake mounting pads where it supplies an auxiliary water manifold and to the gas sample rakes for rake body cooling. The rake cooling water is discharged from the rake bodies into the duct. Additional structural cooling is accomplished by water discharged from spraybars and ring manifolds mounted near the duct walls.

Rotation of the center shaft is accomplished by a drive motor located outside the instrument spool duct wall. This motor drives a radial shaft supported in a strut that is connected to a helical gear set by a spherical gear

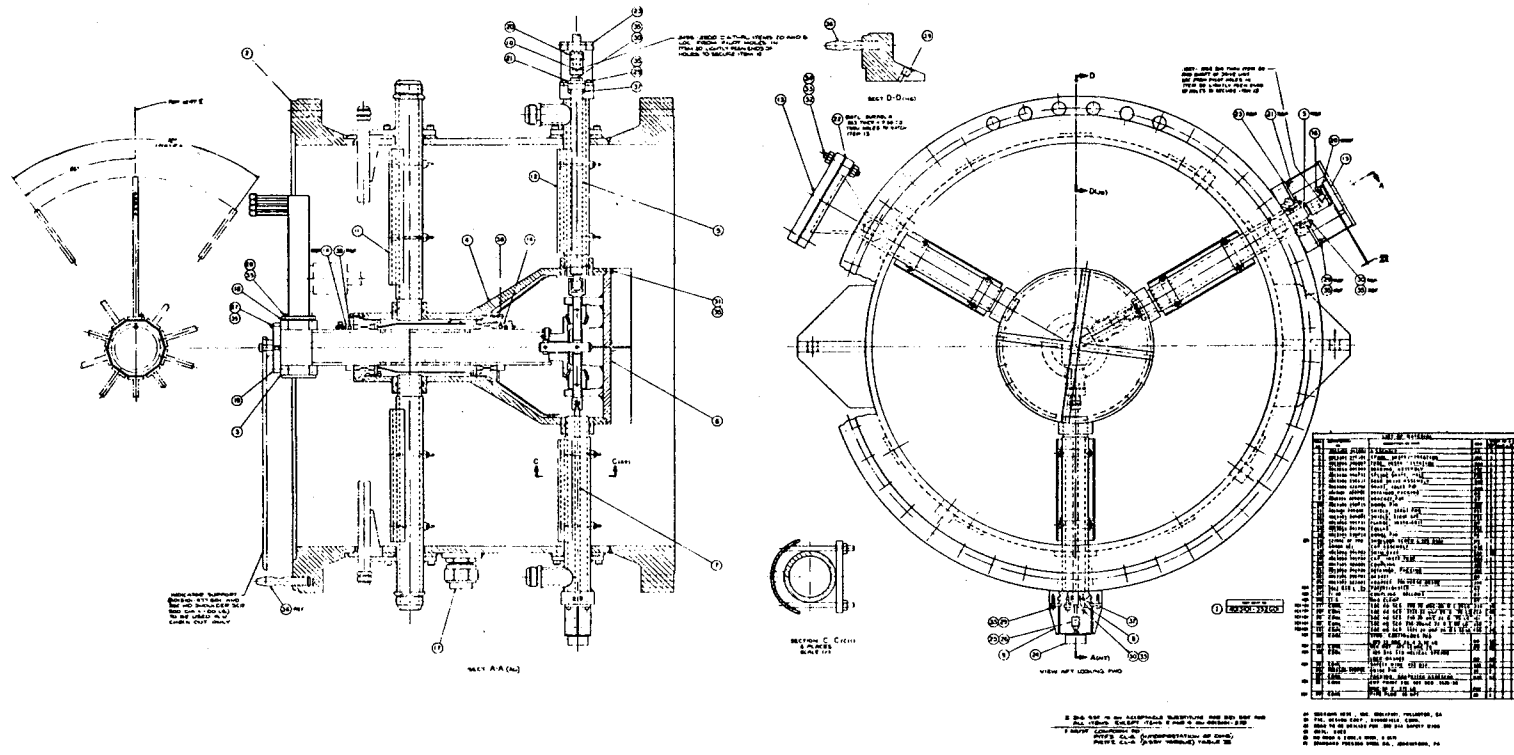


Figure 162. Test Rig Instrumentation Spool.

ORIGINAL PAGE IS
OF POOR QUALITY

coupling. The spherical gear coupling permits rotation even with some shaft misalignment. The portion of the helical gear, which is aligned with the rake mounting shaft, contains a lug. This lug engages a slot in the shaft and can rotate the shaft a total of about 36° clockwise and counterclockwise for a total of nearly 72° rotation. The input coupling has a mechanical stop to prevent excessive travel. The drive shaft is equipped with shear pins to prevent damage to the gear mechanism in the event of hangup or overtravel.

The Atmospheric Combustion Test Stand (ACTS) system is used to obtain detailed temperature measurements at the combustor exit. The system adapts to the aft end of the combustor test rig housing as shown in Figure 163. Thermocouple rakes and/or pressure rakes are attached to the traverse ring and are guided by the roller system and track. The traverse ring is motor-driven and will rotate 90° clockwise or counterclockwise in increments as small as 1.5°. The thermocouple rakes are equipped with seven chromel alumel (C/A) elements. The thermocouple elements are led to a chromel alumel thermocouple system (CATS) block which transients the electronic signals to the data acquisition system. The exit temperature data, along with the fixed test rig and combustor instrumentation, are automatically processed by the data acquisition system and presented in a finished format of prescribed combustor performance parameters and operating conditions.

6.2.1.3 Test Methods

Atmospheric Tests

Ground start ignition, crossfire, and exit temperature performance characteristics of the E³ development combustor were evaluated at atmospheric inlet conditions. In this testing configuration, the test rig was discharged "open end" into the surrounding test cell ambient environment. This permitted useful visual observations of the combustor in operation. During these atmospheric tests, the combustor inlet temperatures duplicated the level of the desired operating cycle test point. However, the combustor airflows were scaled down to levels which simulated the combustor velocities while operating at atmospheric inlet pressure. This technique provides an inexpensive testing approach that will develop satisfactory ground start ignition and exit temperature performance characteristics while providing accurately simulated combustor operating conditions.

ORIGINAL PAGE IS
OF POOR QUALITY

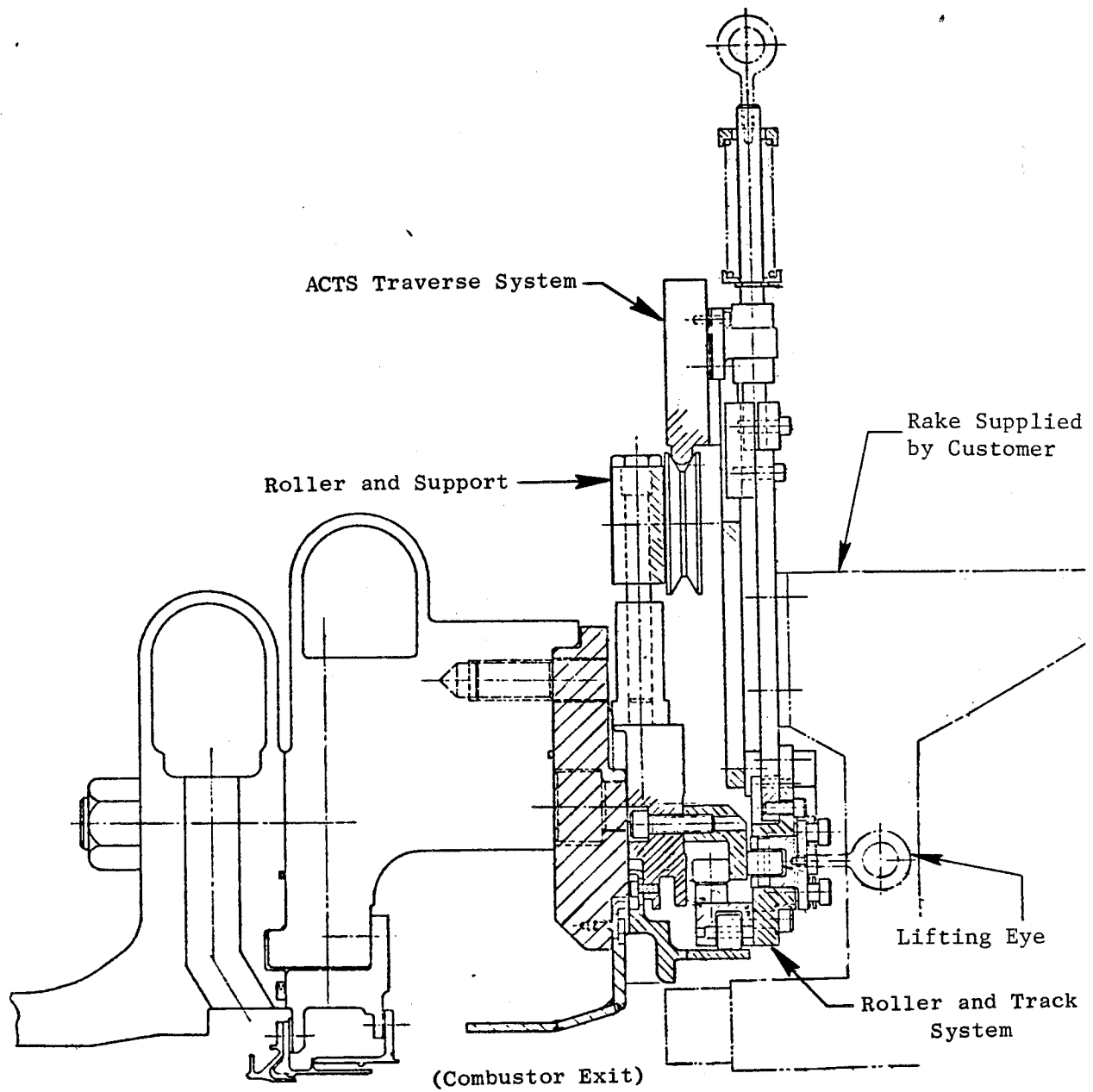


Figure 163. ACTS Traverse System.

Ground start ignition testing was conducted using the standard GE23 ignition system. This system consists of ignitor plug, exciter unit, and ignitor lead. This ignition system has an energy-delivered rating of 2 J with a firing rate of 2 sparks per second. The ignitor was positioned in outer liner Panel 1 at 240° CW aft looking forward (ALF). The ignition immersion was flush with the inside surface of the liner panel wall. To further simplify this testing, no bleed flows were set during the ignition evaluations. Past experience has shown that the effects of bleed flows on the ground start ignition characteristics are insignificant. The basic testing procedure used is as follows:

1. Set the combustor operating conditions corresponding to the selected steady-state test point.
2. Activate the ignition system.
3. Supply fuel to the pilot stage fuel nozzles. Continue to increase this fuel flow until the ignitor swirl cup has ignited. Deactivate the ignition system, and record the operating conditions and fuel flow level.
4. Continue to increase the fuel flow until full pilot stage propagation is achieved. Record the operating conditions and fuel flow level.
5. Reduce the fuel flow rate slowly until one pilot stage swirl cup extinguishes. Record the operating conditions and fuel flow level.
6. Continue to decrease the fuel flow rate until total lean blowout is obtained. Record the operating conditions and fuel flow level.
7. Repeat Steps 2 through 4; then, reduce the pilot stage fuel flow to a level 10% above the level recorded at one cup extinguished.
8. Holding the pilot stage fuel flow level steady, supply fuel to the stage fuel nozzles. Continue to increase the main stage fuel flow until the crossfire cup or cups ignite. Record the operating conditions and fuel flow levels.
9. Continue to increase the main stage fuel flow until full propagation is achieved. Record the operating conditions and fuel flow levels.
10. Reduce the main stage fuel flow slowly until total main stage lean blowout is obtained. Record the operating conditions and fuel flow levels. Then, shut off the main stage fuel flow.

11. Reduce the pilot stage fuel flow slowly until total pilot stage lean blowout is obtained. Record the operating conditions and fuel flow levels.
12. Shut off all combustor fuel flow; then, proceed to set the operating conditions corresponding to the next selected test point.

Throughout this procedure, visual observations were used to determine ignition, propagation, and lean blowout.

Atmospheric exit temperature performance testing was conducted using the ACTS system. Four E³ exit temperature rakes were mounted onto the traverse ring of the ACTS system, equally spaced around the circumference. These rakes, shown in Figure 164, contained seven chromel alumel thermocouple elements and were especially designed for use with the E³ combustor test rig. During atmospheric performance, testing only the prediffuser bleed flow was simulated. At all primary performance test points, exit temperature traverse data was obtained every 1.5° of the total 90° traverse. This provided temperature radial profile measurements at 240 circumferential positions for a total of 1680 individual temperature measurements. At off-design or secondary test points, data were obtained every 3° around the circumference in order to save time. All combustor test rig instrumentation and exit temperature performance data were recorded on the facility data acquisition system. This information was then automatically processed through a computer data reduction program to calculate the combustor operating conditions, the average and peak radial temperature profiles, and the pattern factor and profile factor using these relations:

$$\text{Pattern Factor} = \frac{T4 \text{ (max)} - T4 \text{ (avg)}}{T4 \text{ (avg)} - T3}$$

$$\text{Profile Factor} = \frac{T4 \text{ immersion avg (max)} - T4 \text{ (avg)}}{T4 \text{ (avg)} - T3}$$

Pressure Tests

Emissions characteristics of the E³ development combustors were evaluated at elevated inlet pressure. Several combustor configurations were also evaluated for ground start ignition and crossfire characteristics at elevated pressure as part of an emissions test. For this testing, the test rig was assembled to a gated exhaust system for inlet pressure controls. Since visual

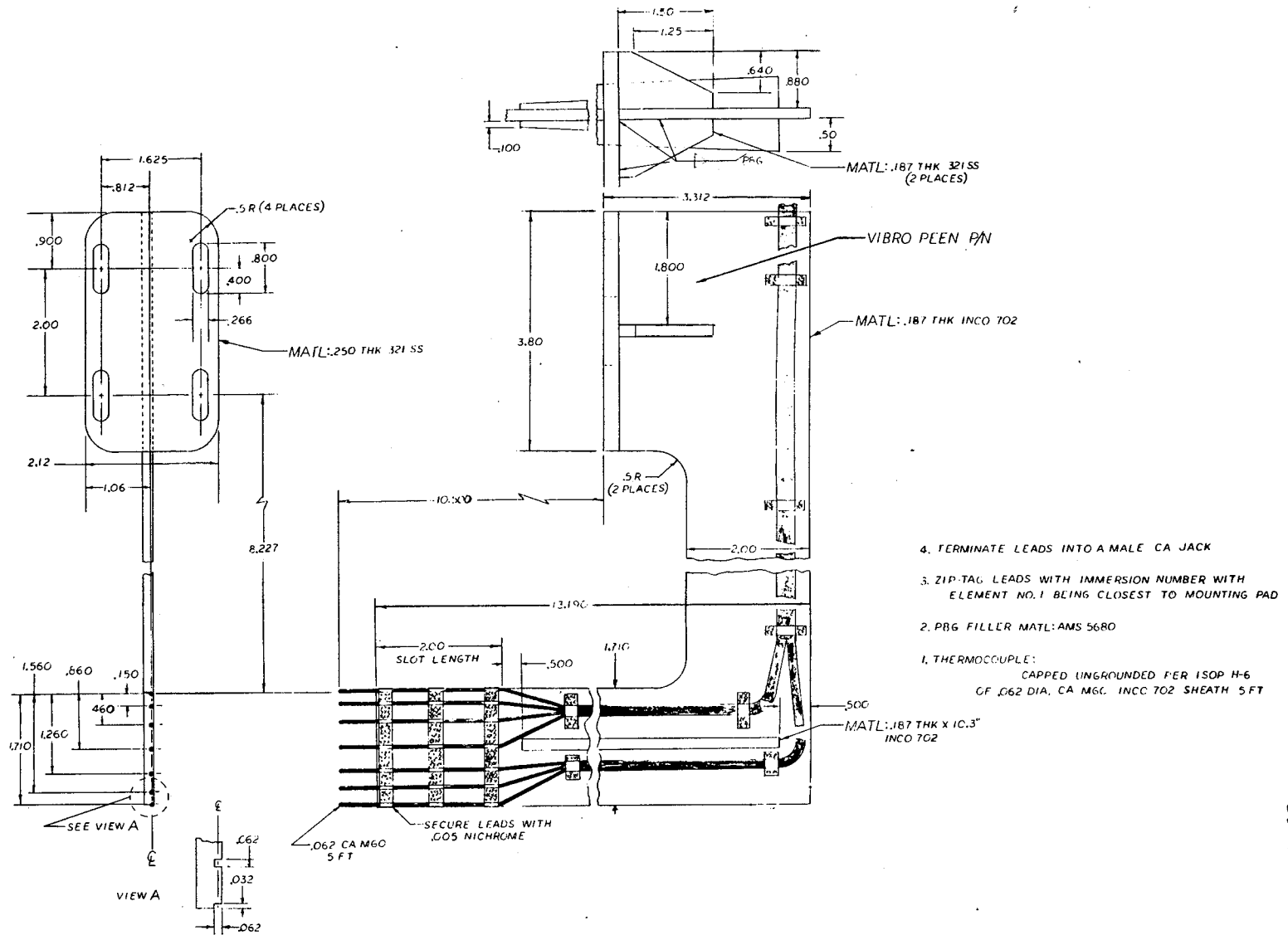


Figure 164. E³ Full-Annular Combustor EGT Thermocouple Rakes.

ORIGINAL PART OF POOR QUALITY

observations were not possible, monitoring the combustor operation was accomplished by using the available test rig and combustor pressure and temperature instrumentation.

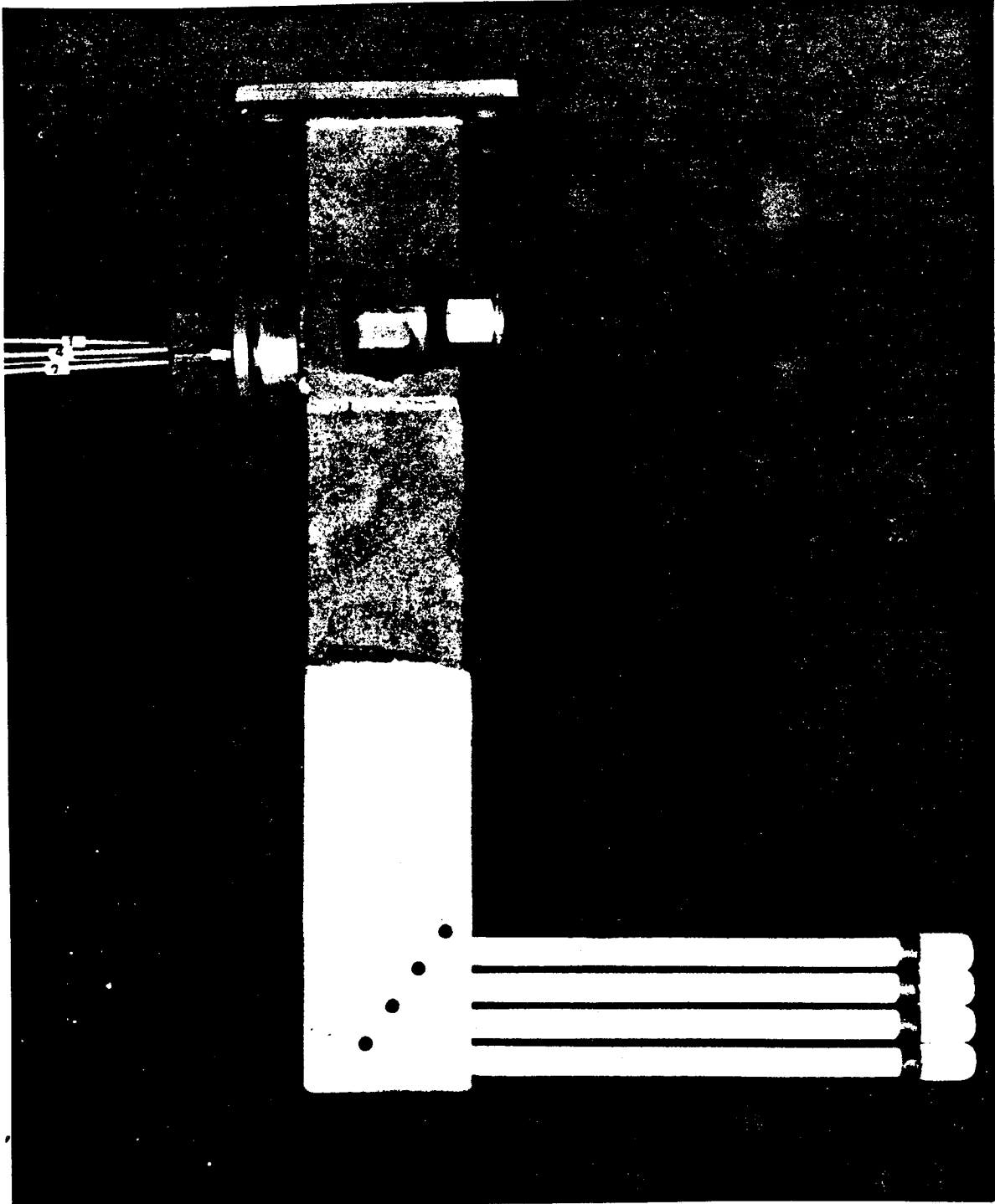
Air was supplied to the test rig from the facility high pressure, high flow capacity system. With this system, combustor operating conditions in the test rig exactly duplicating the E³ FPS cycle conditions could be achieved up to 30% of sea level takeoff power. Above this power level, combustor airflow and inlet pressure were limited by the maximum capacity of the facility. At these high power operating points, test conditions were simulated by setting proper Mach numbers in the test rig. The combustor inlet temperature was set to the exact engine cycle level. The maximum available test section total pressure was approximately 1.655 MPa (240 psia). This compares to the 3.025 MPa (439 psia) level associated with the FPS sea level takeoff operating condition.

All CO, HC, and NO_x emissions levels measured at the simulated high power operating conditions were adjusted to reflect levels that would be obtained if measured under true engine cycle operating conditions. These adjustments were made using the relations presented in Appendix D.

Gas samples were extracted from the combustor discharge stream using the E³ gas sample rakes as shown in Figure 165. Five rakes were used, each with four sampling elements. For the purpose of ground start ignition testing, two chromel alumel-type thermocouples were strapped onto the outermost and innermost sampling elements of each of the five gas sampling rakes. This arrangement is illustrated in Figure 166. These thermocouples were connected to a "Metroscope" visual display system within the facility control room and were used in determining ignition, crossfire, and lean extinction in the pilot stage and main stage of the combustor.

For gas sampling purposes, all four elements of each gas rake were individually connected to the valving in the gas sampling equipment. This approach provided the flexibility to close off individual rake elements from the rake sample if problems would arise in any of the four elements. The five gas sampling rakes were equally spaced around the test rig instrumentation

Figure 165. E³ Full-Annular Combustor Gas Sampling Rakes.



ORIGINAL PAGE IS
OF POOR QUALITY

ORIGINAL PAGE
BLACK AND WHITE PHOTOGRAPH

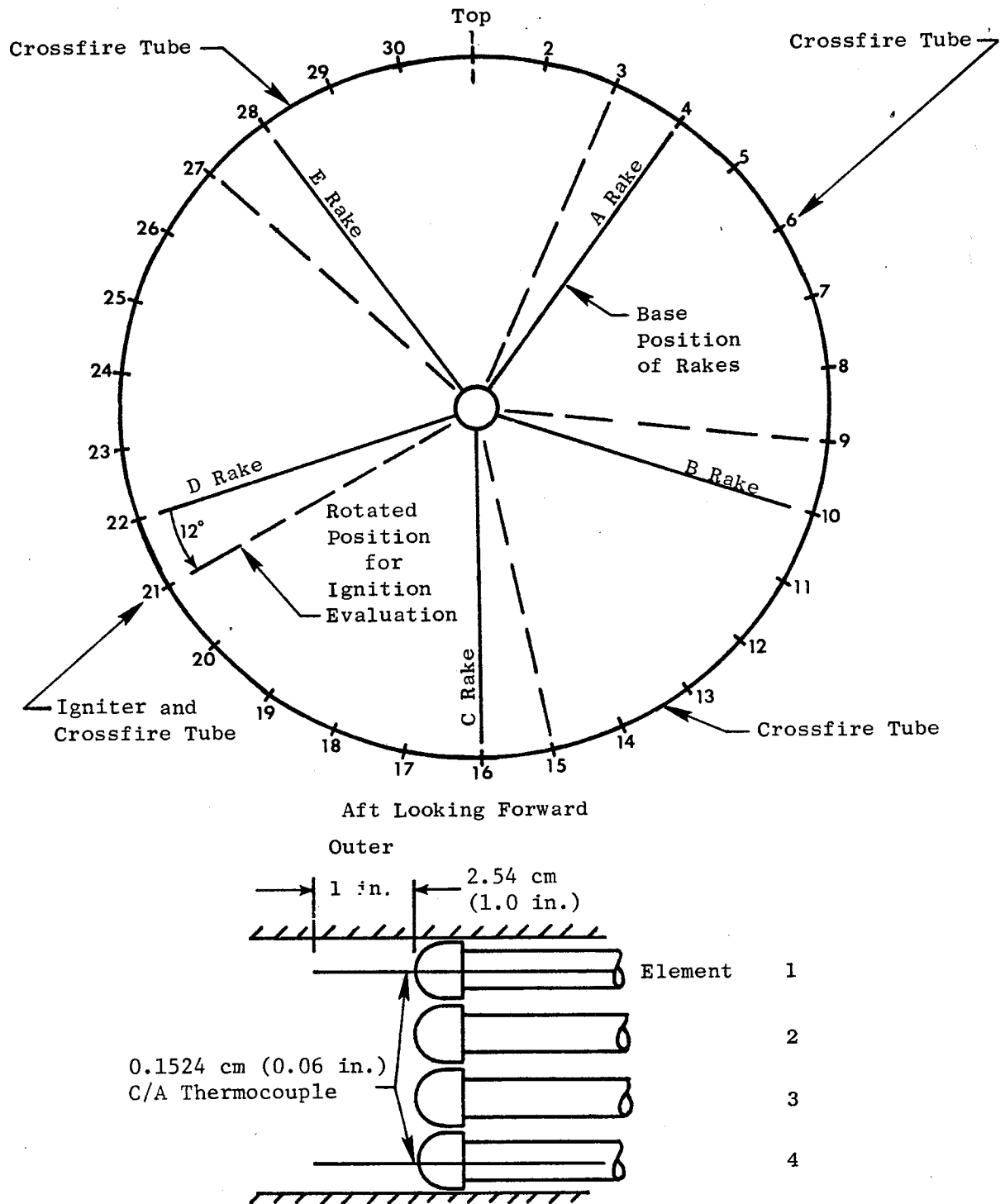


Figure 166. Gas Sampling Rake Instrumentation for Ignition Testing.

spool. Unheated water was used to cool the rakes during testing. The decision to use unheated water as the cooling medium was determined from results obtained during the emissions evaluation of the baseline development combustor.⁴ These results, shown in Figure 167, showed that the use of unheated cooling water had only a very minor impact on idle emissions.

During gas sampling, the rakes were traversed through 66° at 6° increments enabling gas samples to be obtained in line with and between all 30 swirl cups. For ignition and blowout evaluation, the gas sampling rakes were positioned so that one rake was located at 240° CW ALF, placing that rake with its two thermocouple elements directly downstream of the pilot stage ignitor cup and one of the two pilot-stage-to-main-stage crossfire tubes.

Gas samples were analyzed using the CAROL II analysis system located at the test facility. Instruments featured in this system include:

- Beckman Model 402 total hydrocarbon analyzer (flame ionization detector)
- Beckman Model 315-B carbon monoxide and carbon dioxide analyzer (NIDR)
- Beckman Model 915-H NO_x analyzer (heater chemiluminescence with converter).

Sample flow was passed through a refrigerated trap to remove excess water from the sample before entering the gas analysis instruments. Prior to testing, the CAROL II system was calibrated using a set of calibration gases. These gases and their GE constituent analysis are listed in Table XXXVII. During testing, calibration spot checks of the instruments, and any necessary adjustments, were made to assure that this equipment was in good working order at all times. Inlet air humidity was measured using an EG&G Model 440 dew point meter.

Smoke samples were taken only at designated key combustor operating points in the test schedule. Smoke samples were extracted from the exhaust gases using two of the five gas sampling rakes valved in a manner which provided a single sample. At those test points where smoke samples were taken,

ORIGINAL PAGE IS
OF POOR QUALITY

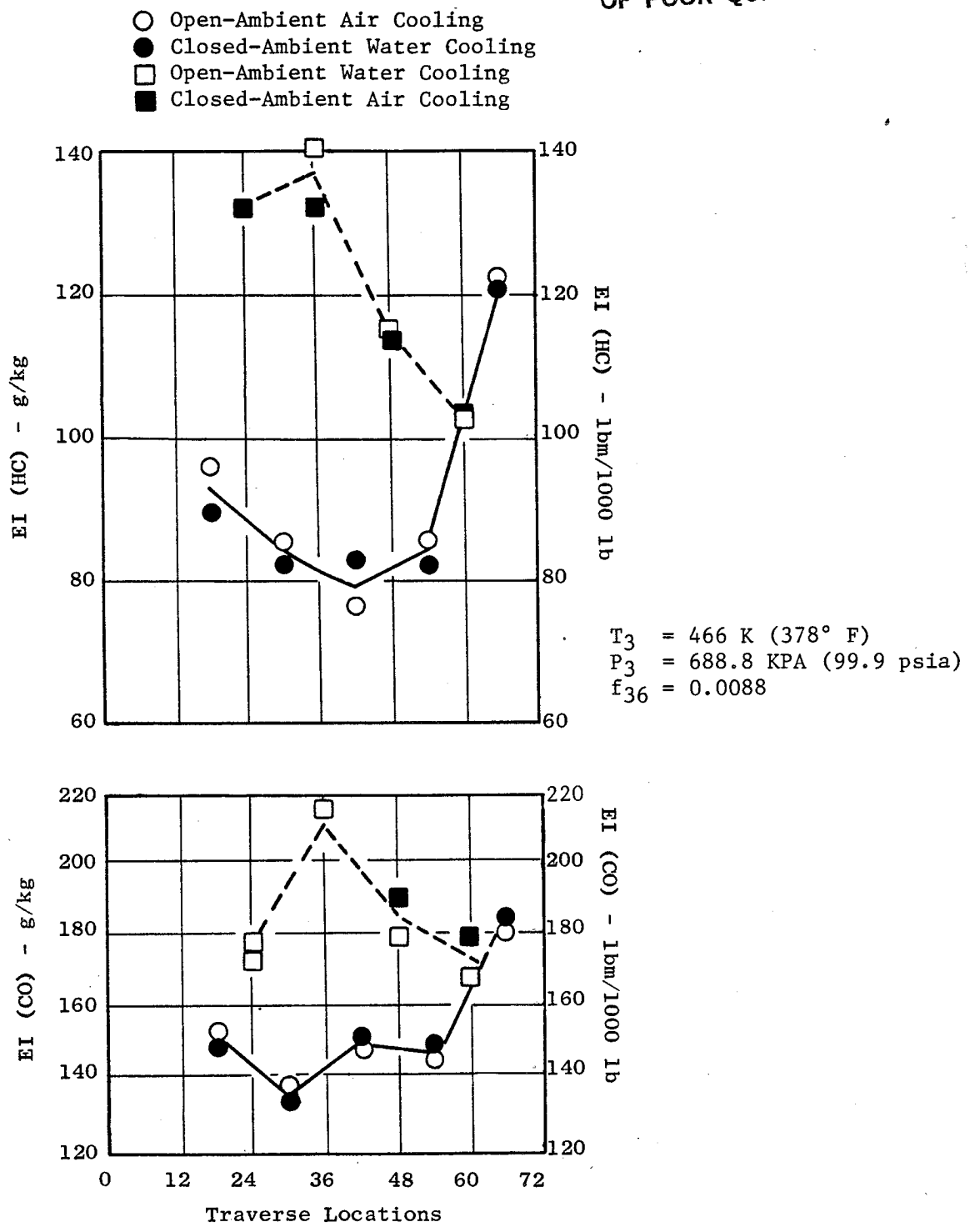


Figure 167. Effect of Gas Rake Cooling Medium on CO and HC Emissions.

the rakes were initially positioned in line with the swirl cups, then rotated 6° to between swirl cups. At each of these two positions, several smoke samples, each 0.0057 m³ (0.2 ft³) in volume, were obtained using a standard GE smoke console located in the cell control room.

Table XXXVII. CAROL Calibration Gases.

	Span 1	Span 2	Span 3	Span 4
Bottle S/N, CO, kg/m (ppm)	261131-227 (500)	2960095-468 (1032)	6742-1085 (2392)	49244-2350 (5181)
Bottle S/N, CO ₃ (%)	261131(1.27)	2960095(2.54)	6742(4.94)	49244(8.03)
Bottle S/N, HC, kg/m (ppm)	1317746-74.3 (164)	49301-143 (315)	127885-569 (1254)	49110-1328 (2928)
Bottle S/NM, NO _x , kg/m (ppm)	12553-29.1 (64)	12548-69.8 (154)	10766-234 (516)	3976-543 (1197)

All emissions and instrumentation data acquisition were automatically handled by the Cell A3 medium speed digital data acquisition system. From this system, data were processed through a computer data reduction program which performed calculations to compute the various emissions indices, combustor operating parameters, and convert digital signals from all pressure and temperature instrumentation to engineering units. All smoke samples were obtained on Wattman 4 filter paper. Following completion of testing, the smoke samples obtained were analyzed on a Densichron to determine the optical density used to compute the SAE smoke number.

6.2.2 Screening Combustor Test Results

6.2.2.1 Atmospheric Ground Start Ignition Test

The first test of the E³ double-annular dome development combustor and test rig was conducted on February 7, 1980, in the General Electric Aero Component Lab-Cell A3W test facility. The purpose of this test was to evaluate the baseline combustor configuration for ground start ignition, pilot-to-main stage crossfire, and the pilot and main stage lean blowout characteristics at

atmospheric inlet pressure along the E³ (9/79), ground start operating line. Test points and corresponding operating conditions are shown in Table XXXVIII.

Table XXXVIII. Baseline Atmospheric Ignition Test Point Schedule.

Point	Start Time (s)	XNRH (%)	T ₃ , K (° R)	P ₃ (atm.)	W ₃₆ [*] , kg/s (pps)
1	10	21.0	289 (520)	1.00	1.25 (2.75)
2	15	28.0	289 (520)	1.00	1.69 (3.62)
3	18	32.0	314 (565)	1.00	1.55 (3.42)
4	30	46.0	344 (619)	1.00	1.65 (3.64)
5	40	58.0	383 (689)	1.00	1.86 (4.10)
6	50	70.0	428 (770)	1.00	1.94 (4.28)
7	55	77.0	503 (905)	1.00	2.33 (5.14)

*If inlet air temperature cannot be set at the prescribed level, the airflow will be changed to maintain the $W_{36}\sqrt{T_3}/P_3$ value.

The baseline combustor configuration featured most of the mechanical and aerothermo characteristics evolved during the design phase of the combustor development program. The only significant difference from the proposed design was in the pilot dome splash plate cooling flow level. The combustor was designed to have approximately 4.3% of the total combustor flow for the pilot dome splash plate cooling. However, the hardware was fabricated to have approximately 2.5 times the design flow level to provide the ability to easily increase the splash plate cooling flow level if necessary. It was intended to block off a percentage of this flow to achieve the intended design levels if baseline testing indicated sufficiently low dome metal temperatures. The estimated airflow distribution for the baseline development combustor is available in Appendix E. The fuel nozzle assemblies used featured the E³ test rig fuel

nozzle bodies with simplex nozzle tips rated at 2.3 kg/hr (5 pph) at 689.5 KPa (100 psid) in the inner dome, and simplex nozzle tips rated at 12.0 kg/hr (26.5 pph) at 689.5 KPa (100 psid) in the outer dome. Both of these nozzle tips had fuel spray angles of approximately 50°.

It had been intended to use the GE23 ignition system to obtain the pilot stage ignition characteristics. However, problems were encountered at the onset of testing due to a failure in one of the components of the GE23 ignition system provided. As a result, a hydrogen torch ignition system was substituted and testing proceeded. Accurate pilot stage ignition data generally cannot be obtained with a hydrogen torch system due to its high specific energy output. However, pilot stage propagation, pilot-to-main-stage cross-fire, and pilot and main stage lean blowout data were obtained. By the time the last test point had been set, another GE23 ignition system had been obtained. This system was installed into the test rig with the intent of obtaining pilot stage ignition data starting at the last test point and working back toward the initial test point. Following the completion of ignition at Test Points 7, 6, and 5, another failure in the electrical ignition system occurred and testing was terminated. The failures involved the ignitor lead.

Test results obtained from the atmospheric ground start ignition evaluation of the E³ development combustor baseline configuration are presented in Figure 168. A detailed summary of the test data is provided in Appendix E. Ignition of the pilot stage ignitor cup using the hydrogen torch proceeded without difficulty at each test point evaluated. However, once ignition occurred, a substantial increase in the pilot stage fuel flow was required to obtain a full propagation of the fire. As observed from this figure, the pilot stage ignition characteristics were within the E³ start cycle requirements.

The three test points evaluated with the GE23 ignition system show excellent agreement with the results obtained with the hydrogen torch ignition system. Past experience has generally shown that as the combustor operating conditions become more severe for ignition, greater difficulty arises in achieving ignition with electrical systems than with the hydrogen torch systems. Therefore, it was expected that pilot stage ignition results obtained with the

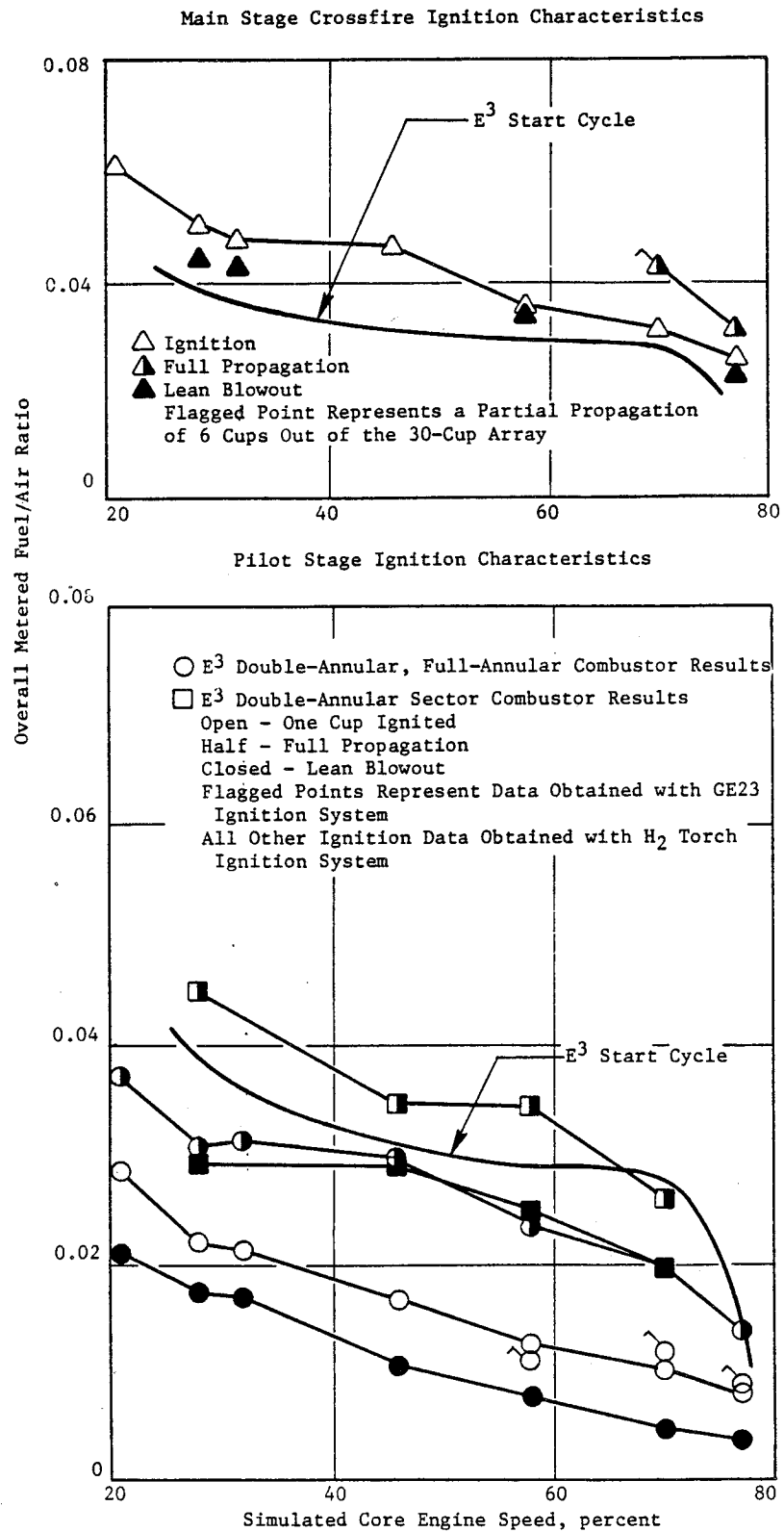


Figure 168. Development Combustor Baseline Atmospheric Ignition Test Results.

GE23 ignition system at the simulated lower speed points would be somewhat poorer than the results obtained with the hydrogen torch system but still within the start cycle requirements. The pilot stage demonstrated an acceptable lean blowout margin of about 30% along the entire start cycle operating line.

Ignition of the main stage was attempted at each test point. In all cases, this was accomplished by hot gases from the burning pilot stage passing through the two centerbody crossfire tubes located at 60° and 240° clockwise, aft looking forward. However, propagation of the fire in the main stage was only achieved at the simulated higher speed points. The low flow fuel nozzle tips used in the main stage limited the maximum fuel flow to approximately 160 kg/hr (350 pph) at the maximum fuel pressure that the facility could supply. A partial propagation (six cups) in the main stage was achieved at conditions representing the 70% engine speed point, while full propagation was achieved at conditions representing the 77% engine speed point. The combustor operating conditions at these points were favorable enough to offset the adverse effects of the lean main stage dome stoichiometry. Insufficient data were obtained to make a good assessment of the main stage lean blowout characteristics.

6.2.2.2 Atmospheric Exit Temperature Performance Test

Performance testing of the E³ combustor baseline configuration was then conducted. The purpose of this test was to evaluate the profile and pattern factor at simulated sea level takeoff conditions with variations in the pilot and main dome fuel staging. The test schedule and corresponding combustor operating conditions are presented in Table XXXIX.

Exit temperature data were obtained at simulated sea level takeoff inlet conditions, and overall fuel/air ratios of 0.020, the design level of 0.0244, and 0.0260. Fuel staging modes representing pilot-to-total fuel flow splits of 0.5, 0.4, and 0.3 were evaluated at the 0.020 and 0.0244 overall fuel/air ratio conditions. Pilot-to-total fuel flow splits of 0.4 and 0.3 were evaluated at the 0.0260 overall fuel/air condition.

Table XXXIX. Baseline Atmospheric EGT Performance Test Point Schedule.

Test Point	T ₃ , K (° R)	P ₃ , Atm.	W ₃ , kg/s (lb/s)	W _{Bleed} , kg/s (lb/s)	W _{Comb} , kg/s (lb/s)	f/a	W _f Total, kg/hr (lb/hr)	Pilot Total	W _f Pilot, kg/hr (pph)	W _f Main kg/hr (lb/hr)
1	495 (891)	1.00	2.67 (5.87)	0.19 (0.41)	2.48 (5.46)	0.0123	110 (242)	1.0	110 (242)	0 (0)
2	815 (1467)	1.00	2.41 (5.31)	0.15 (0.34)	2.26 (4.97)	0.0200	163 (358)	0.50	81 (179)	81 (179)
3	815 (1467)	1.00	2.41 (5.31)	0.15 (0.34)	2.26 (4.97)	0.0200	163 (358)	0.40	65 (143)	98 (215)
4	815 (1467)	1.00	2.41 (5.31)	0.15 (0.34)	2.26 (4.97)	0.0200	163 (358)	0.30	49 (107)	114 (251)
5	815 (1467)	1.00	2.41 (5.31)	0.15 (0.34)	2.26 (4.97)	0.0244	199 (437)	0.50	100 (219)	100 (219)
6	815 (1467)	1.00	2.41 (5.31)	0.15 (0.34)	2.26 (4.97)	0.0244	199 (437)	0.40	80 (175)	119 (262)
7	815 (1467)	1.00	2.41 (5.31)	0.15 (0.34)	2.26 (4.97)	0.0244	199 (437)	0.30	60 (131)	139 (306)
8	815 (1467)	1.00	2.41 (5.31)	0.15 (0.34)	2.26 (4.97)	0.0275	224 (492)	0.50	112 (246)	112 (246)
9	815 (1467)	1.00	2.41 (5.31)	0.15 (0.34)	2.26 (4.97)	0.0275	224 (492)	0.40	90 (197)	134 (295)
10	815 (1467)	1.00	2.41 (5.31)	0.15 (0.34)	2.26 (4.97)	0.0275	224 (492)	0.30	67 (148)	156 (344)

Performance results obtained at simulated 6% ground idle operating conditions are presented in Figure 169. In this operating mode with only the pilot stage fueled, the exit temperature profiles are sharply peaked outward. This is typical of double-annular combustor designs operating in this mode. Figure 170 shows the performance results obtained at the design fuel/air ratio. The maximum and average profiles illustrate the sensitivity of exit temperature profiles to pilot-main stage fuel split but are generally within established limits at the 0.50 pilot-to-total fuel flow split. Also, a pattern factor of 0.255 was obtained which is very close to the goal of 0.250.

A plot of the average circumferential exit distribution is presented in Figure 171. This temperature distribution represents data obtained at the simulated design cycle sea level takeoff operating condition with an 0.40 pilot-to-total fuel flow split. For this combustor operating mode, the peak temperatures generally occur in line with the swirl cups while the minimum temperatures occur between swirl cups. Cooler spots in the combustor appear to exit in the vicinity of swirl Cups 11 and 14. A posttest check of fuel nozzles revealed that the main stage nozzle tip in Cup 11 was approximately 5% below the average of all 30 main stage nozzle tips in fuel flow. The pilot stage nozzle tip in Cup 14 was approximately 17% below the average of all 30 pilot stage nozzle tips in fuel flow. These low fuel flow levels in the two swirl cups could have produced the cooler regions observed.

6.2.2.3 Emissions Test

Emissions testing of the E³ double-annular dome development combustor baseline configuration was conducted in the ACL Cell A3E test facility. This represented the first test in which the development combustor and test rig were operated at elevated pressure conditions. The purpose of this testing was to evaluate the baseline combustor design for emissions, pressure drop, and metal temperature characteristics at combustor operating conditions along the E³ FPS design operating cycle. Bleed flows from the split duct diffuser and the outer and inner flowpaths were extracted at levels simulating the actual engine combustor operation at all test points. Test points and corresponding operating conditions evaluated in this test are presented in Table XL. During the limited phase of testing, simplex-type fuel nozzles rated

ORIGINAL PAGE IS
OF POOR QUALITY

- 6% Idle (Pilot Only)
- Atmospheric Pressure
- Corrected Temperatures

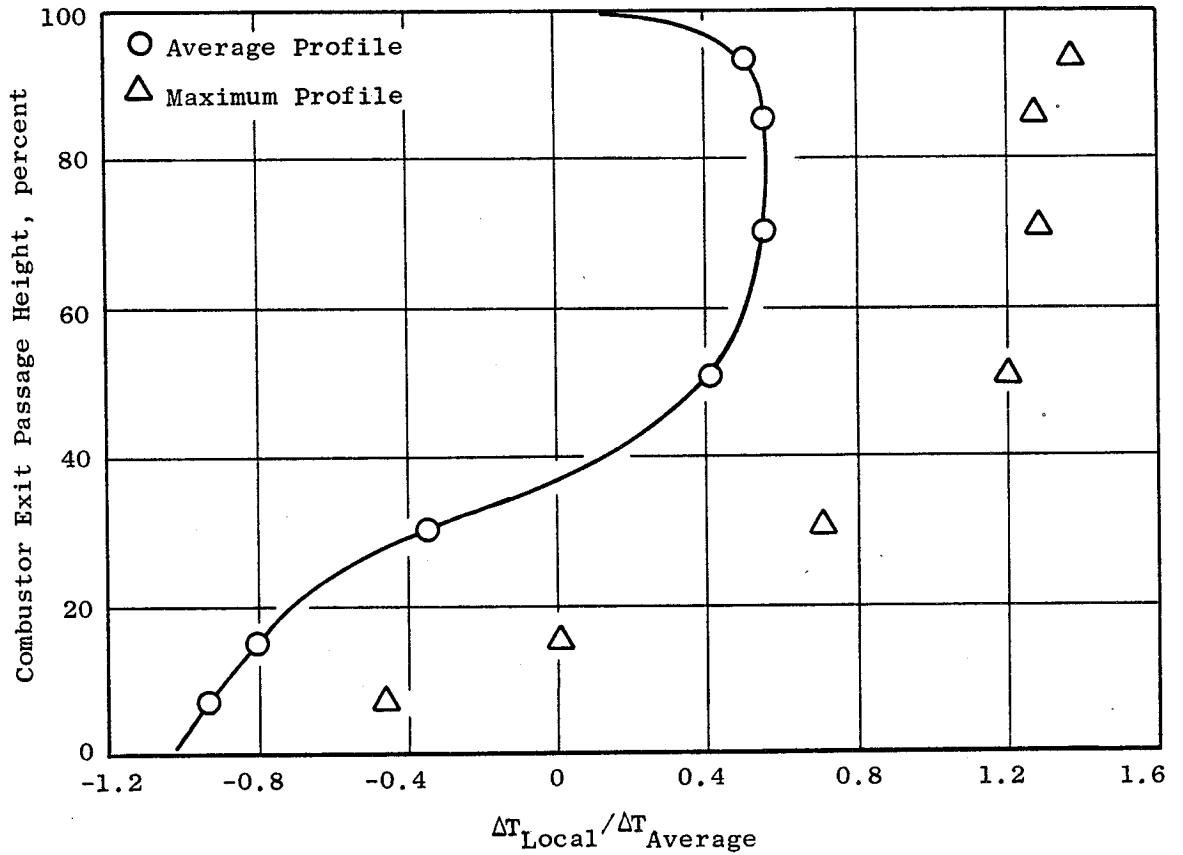
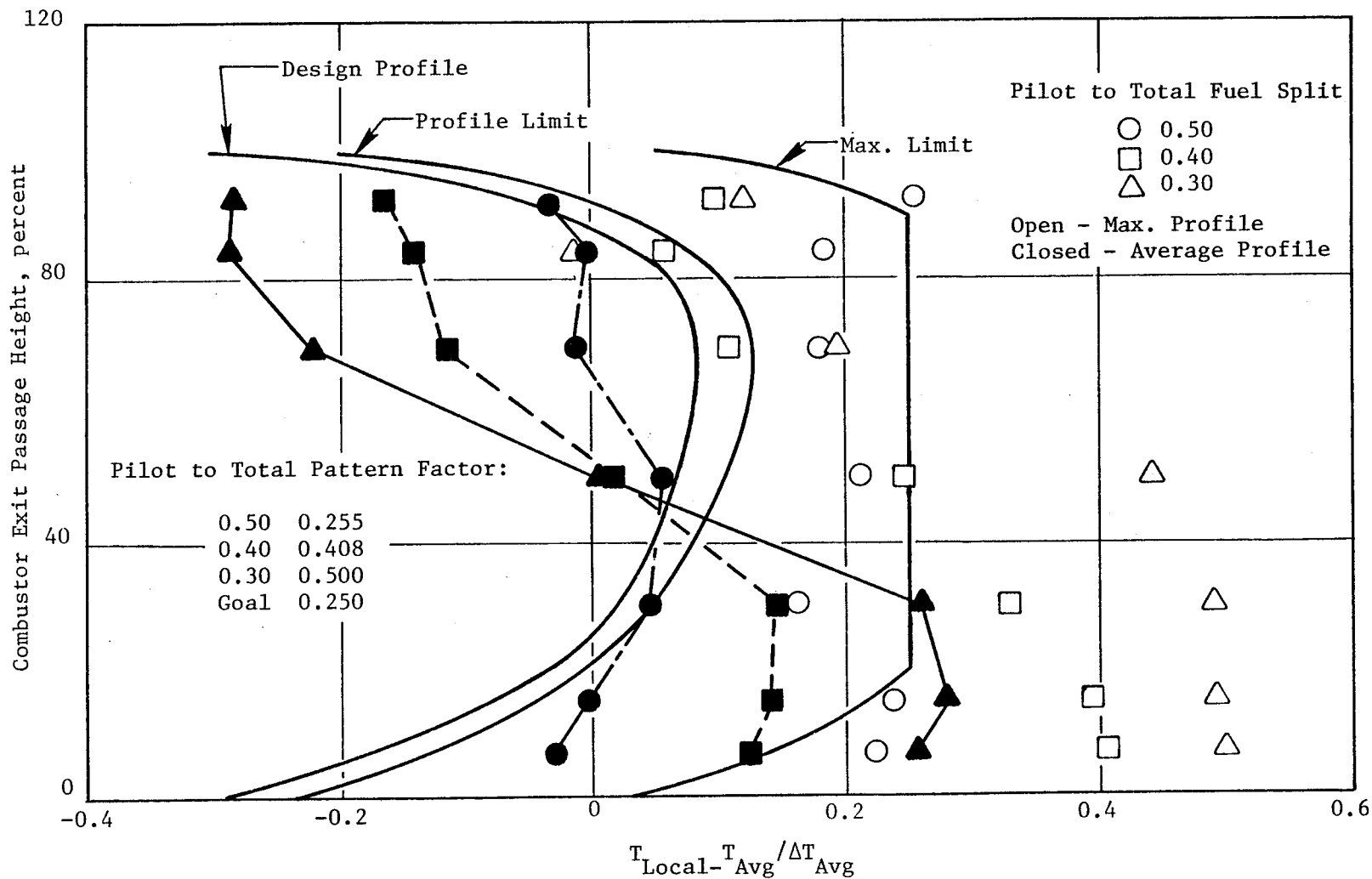


Figure 169. Development Combustor Baseline EGT Performance Test Results, Idle.

- Run No. 6
- Configuration: Baseline
- Simulated Sea Level Takeoff, $f/a = 0.0244$

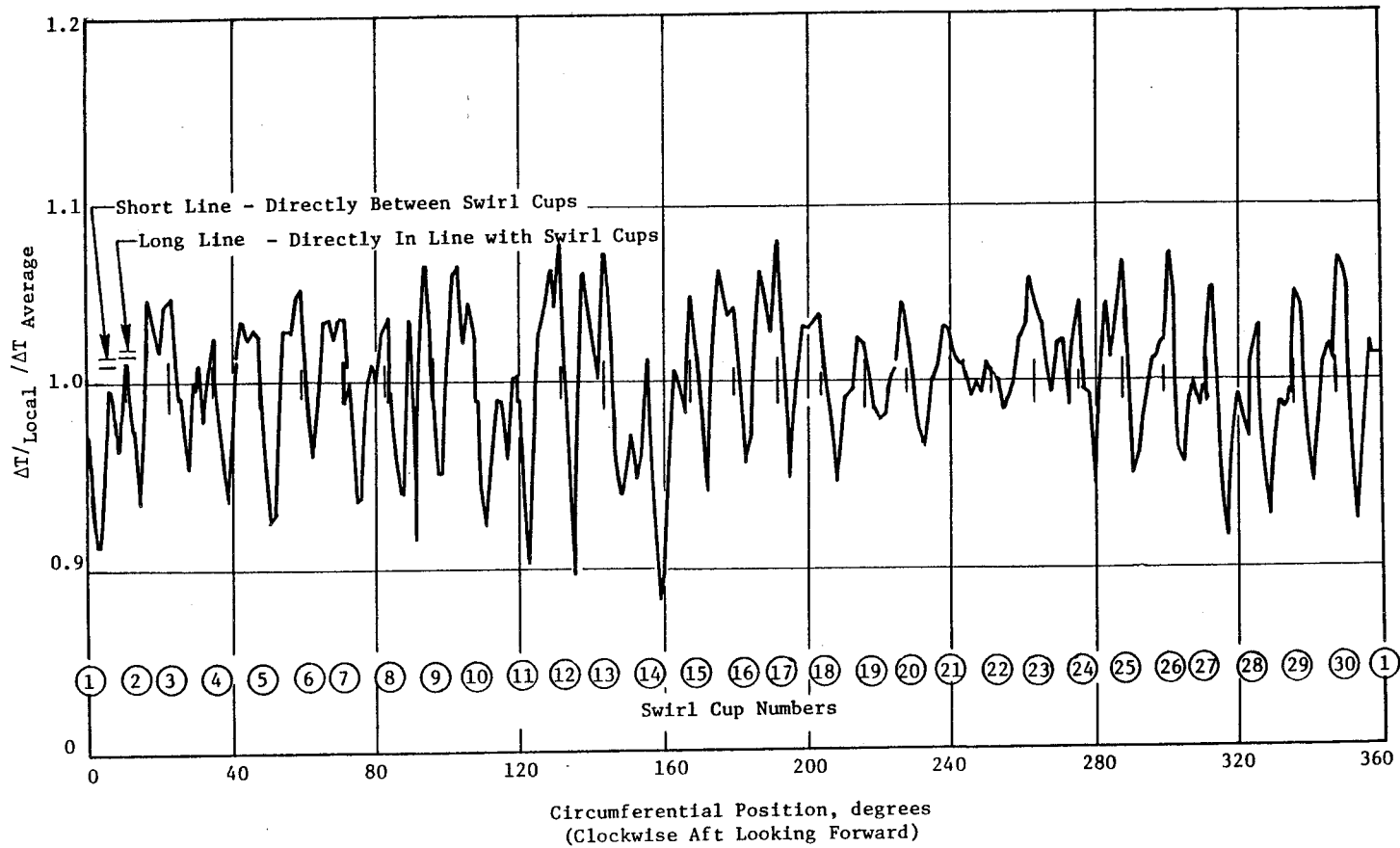


ORIGINAL PAGE IS OF POOR QUALITY

Figure 170. Development Combustor Baseline EGT Performance Test Results, SLTO.

Average Circumferential Exit Temperature Distribution

- Simulated Sea Level Takeoff $f/a = 0.0244$
- 0.40 Pilot-to-Total Fuel Split
- Corrected Thermocouples



ORIGINAL PAGE IS
OF POOR QUALITY

Figure 171. Development Combustor Baseline EGT Performance Test Results, Circumferential Temperatures.

Table XL. Baseline Emissions Test Point Schedule.

Test Point	Operating Condition, percent	K	T ₃ : A	T ₃ : MPa (psi)	W ₃ : kg/s (lb/s)	W _{bleed, Outer} : kg/s (lb/s)	W _{bleed, Inner} : kg/s (lb/s)	W _{bleed, Prediff} : kg/s (lb/s)	W _{comb} : kg/s (lb/s)	f/a Overall	W _g : kg/hr (lb/hr)	Pilot Total	W _g Pilot: kg/hr (lb/hr)	W _{happ} : kg/hr (pph)	Sampling Probe
1	4 Idle	466 (839)	0.339 (49.2)	9.55 (21.1)	0.55 (1.2)	0.50 (1.1)	0.61 (1.3)	7.86 (17.3)	0.0090	255 (562)	1.00	255 (562)	0 (0)	G	
2	4 Idle	466 (839)	0.339 (49.2)	9.55 (21.1)	0.55 (1.2)	0.50 (1.1)	0.61 (1.3)	7.86 (17.3)	0.0120	340 (750)	1.00	340 (750)	0 (0)	G	
3	4 Idle	466 (839)	0.339 (49.2)	9.55 (21.1)	0.55 (1.2)	0.50 (1.1)	0.61 (1.3)	7.86 (17.3)	0.0138	390 (860)	1.00	390 (860)	0 (0)	G, I, S	
4	4 Idle	466 (839)	0.339 (49.2)	9.55 (21.1)	0.55 (1.2)	0.50 (1.1)	0.61 (1.3)	7.86 (17.3)	0.0200	566 (1248)	1.00	566 (1248)	0 (0)	G	
5	4 Idle	466 (839)	0.339 (49.2)	9.55 (21.1)	0.55 (1.2)	0.50 (1.1)	0.61 (1.3)	7.86 (17.3)	0.0250	708 (1561)	1.00	708 (1561)	0 (0)	G	
6	6 Idle	495 (891)	0.436 (63.2)	12.32 (27.2)	0.71 (1.6)	0.65 (1.43)	0.78 (1.7)	10.18 (22.4)	0.0090	330 (728)	1.00	330 (728)	0 (0)	G	
7	6 Idle	495 (891)	0.436 (63.2)	12.32 (27.2)	0.71 (1.6)	0.65 (1.43)	0.78 (1.7)	10.18 (22.4)	0.1100	403 (888)	1.00	403 (888)	0 (0)	G	
8	6 Idle	495 (891)	0.436 (63.2)	12.32 (27.2)	0.71 (1.6)	0.65 (1.43)	0.78 (1.7)	10.18 (22.4)	0.0123	451 (994)	1.00	451 (994)	0 (0)	G, I, S	
9	6 Idle	495 (891)	0.436 (63.2)	12.32 (27.2)	0.71 (1.6)	0.65 (1.43)	0.78 (1.7)	10.18 (22.4)	0.0150	500 (1212)	1.00	550 (1212)	0 (0)	G	
10	6 Idle	495 (891)	0.436 (63.2)	12.32 (27.2)	0.71 (1.6)	0.65 (1.43)	0.78 (1.7)	10.18 (22.4)	0.0200	733 (1616)	1.00	733 (1616)	0 (0)	G	
11	30 Approach	637 (1147)	1.206 (174.9)	31.36 (69.1)	1.80 (4.0)	1.65 (3.66)	2.00 (4.4)	25.90 (56.0)	0.0143	1332 (2937)	1.00	1332 (2937)	0 (0)	G, I, S	
12	30 Approach	637 (1147)	1.206 (174.9)	31.36 (69.1)	1.80 (4.0)	1.65 (3.66)	2.00 (4.4)	25.90 (56.0)	0.0143	1332 (2937)	0.5	666 (1468)	666 (1468)	G	
13	30 Approach	637 (1147)	1.206 (174.9)	31.36 (69.1)	1.80 (4.0)	1.65 (3.66)	2.00 (4.4)	25.90 (56.0)	0.0143	1332 (2937)	0.4	533 (1175)	799 (1761)	G	
14	30 Approach	637 (1147)	1.206 (174.9)	31.36 (69.1)	1.80 (4.0)	1.65 (3.66)	2.00 (4.4)	25.90 (56.0)	0.0143	1332 (2937)	1.3	400 (882)	932 (2055)	G	
15	52 Power	700 (1260)	1.524 (221.0)	36.36 (80.1)	2.09 (4.5)	1.92 (4.2)	2.31 (5.1)	30.05 (66.2)	0.0173	1870 (4123)	0.4	748 (1650)	1122 (2473)	G	
16	70 Power	746 (1343)	1.655 (240.0)	37.68 (83.1)	2.16 (4.76)	1.99 (4.39)	2.40 (5.3)	31.14 (68.7)	0.0204	2284 (5035)	0.4	916 (2019)	1370 (3020)	G	
17	85 Climb	949 (1708)	1.655 (240.0)	37.41 (82.5)	2.15 (4.74)	1.97 (4.3)	2.38 (5.2)	30.91 (68.1)	0.0225	2500 (5511)	0.5	1250 (2756)	1250 (2755)	G	
18	85 Climb	949 (1708)	1.655 (240.0)	37.41 (82.5)	2.15 (4.74)	1.97 (4.3)	2.38 (5.2)	30.91 (68.1)	0.0225	2500 (5511)	0.35	875 (1929)	1625 (3582)	G, I, S	
19	85 Climb	949 (1708)	1.655 (240.0)	37.41 (82.5)	2.15 (4.74)	1.97 (4.3)	2.38 (5.2)	30.91 (68.1)	0.0225	2500 (5511)	0.20	500 (1102)	2000 (4409)	G	
20	93 Power	963 (1733)	1.655 (240.0)	36.27 (80.0)	2.08 (4.59)	1.91 (4.2)	2.81 (5.1)	29.95 (66.0)	0.0236	2541 (5602)	0.35	889 (1960)	1652 (3642)	G	
21	100 SLTD	1007 (1813)	1.655 (240.0)	36.27 (80.0)	2.08 (4.59)	1.91 (4.2)	2.81 (5.1)	29.95 (66.0)	0.0247	2664 (5873)	0.5	1332 (2936)	1332 (2937)	G	
22	100 SLTD	1007 (1813)	1.655 (240.0)	36.27 (80.0)	2.08 (4.59)	1.91 (4.2)	2.81 (5.1)	29.95 (66.0)	0.0247	2664 (5873)	0.35	932 (2055)	1732 (3818)	G, I, S	
23	100 SLTD	1007 (1813)	1.655 (240.0)	36.27 (80.0)	2.08 (4.59)	1.91 (4.2)	2.81 (5.1)	29.95 (66.0)	0.0247	2664 (5873)	0.20	533 (1175)	2131 (4698)	G	

Sampling Modes: C - Caged Sample
I - Individual Bake Sample
S - Smoke Sample

ORIGINAL PHOTO OF POOR QUALITY

at 12.0 kg/hr (26.5 pph) and 23 kg/hr (50.0 pph) were used in the pilot and main stage domes, respectively, to simulate the fuel spray atomization quality expected from the engine duplex-type fuel nozzles at the lower power operating condition. For the higher power operating conditions, simplex-type fuel nozzles rated at 23 kg/hr (50 pph) and 55 kg/hr (120 pph) were used, respectively, in the pilot and main stage domes to obtain the required fuel flows within the test facility fuel pump discharge pressure capacity.

The combustor instrumentation consisted of 26 static pressures and 49 grounded and capped chromel alumel thermocouples. This instrumentation provided important data concerning various combustor pressures and metal skin temperatures throughout the emissions test. The locations of this instrumentation on the combustor hardware are illustrated in Figures 172 through 175. The selected locations for the thermocouples were accomplished with the assistance of heat transfer personnel. Some of the thermocouples were located on the combustor liners at places which had been observed as "hot spots" during the previous exit temperature performance test of this combustor. A dynamic pressure probe was installed through a primary dilution hole in the outer liner of the combustor to monitor combustion frequencies and fluctuations. In addition, numerous pressure and temperature instrumentation was installed on the test rig vehicle. This instrumentation included upstream total pressure and air temperature rakes to measure the combustor inlet total pressure and temperature. Test rig flowpath wall static pressures provided important data concerning diffuser system performance while thermocouples were used to monitor the test rig to ensure the rig mechanical integrity. The location of the more important test rig instrumentation is illustrated in Figure 176.

All CO, HC, and NO_x emissions levels measured were adjusted to reflect emissions levels that would be obtained if measured at the actual E³ FPS design cycle operating conditions.

At the lower power operating conditions (4%, 6%, and 30%), these adjustments provided corrections which accounted for small discrepancies between the test conditions set in the cell, and the cycle conditions represented. At the higher power operating conditions, these adjustments primarily provided corrections for emissions levels measured at reduced inlet pressure and airflow conditions associated with the facility capacity to simulate the actual high

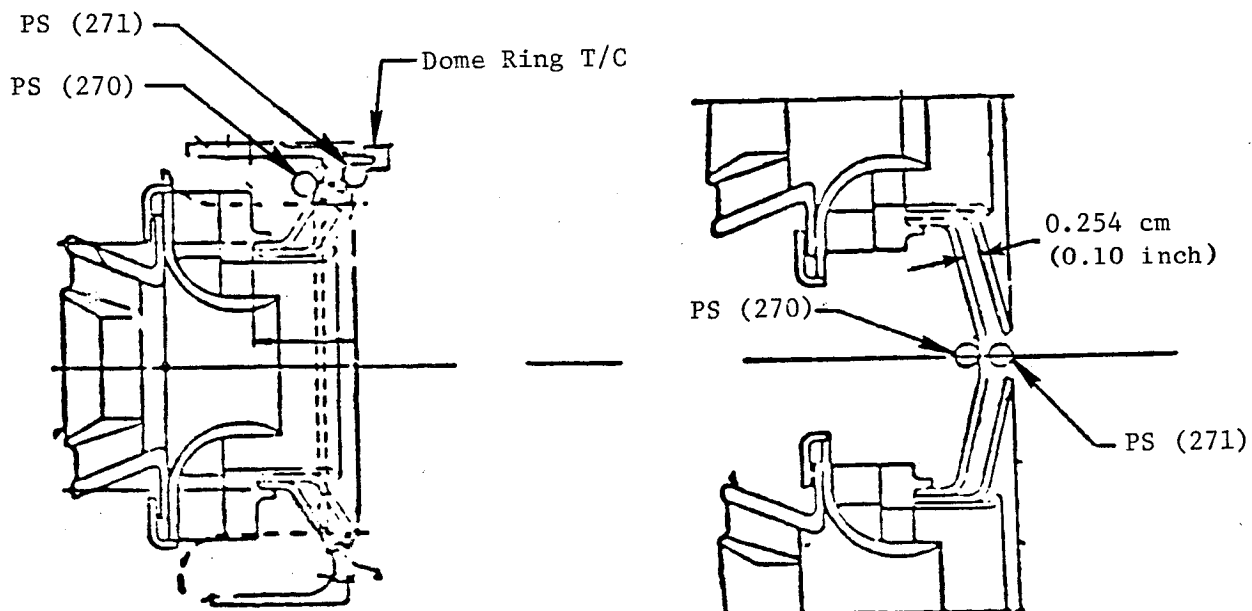
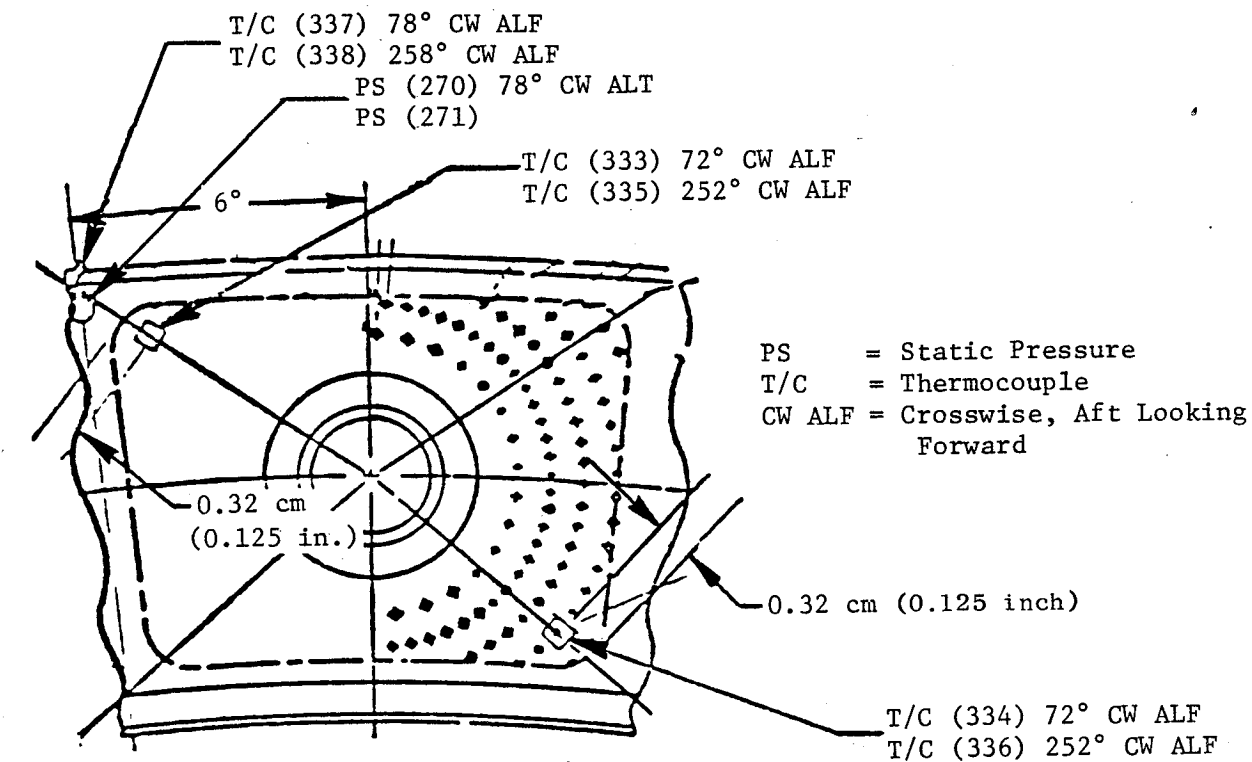
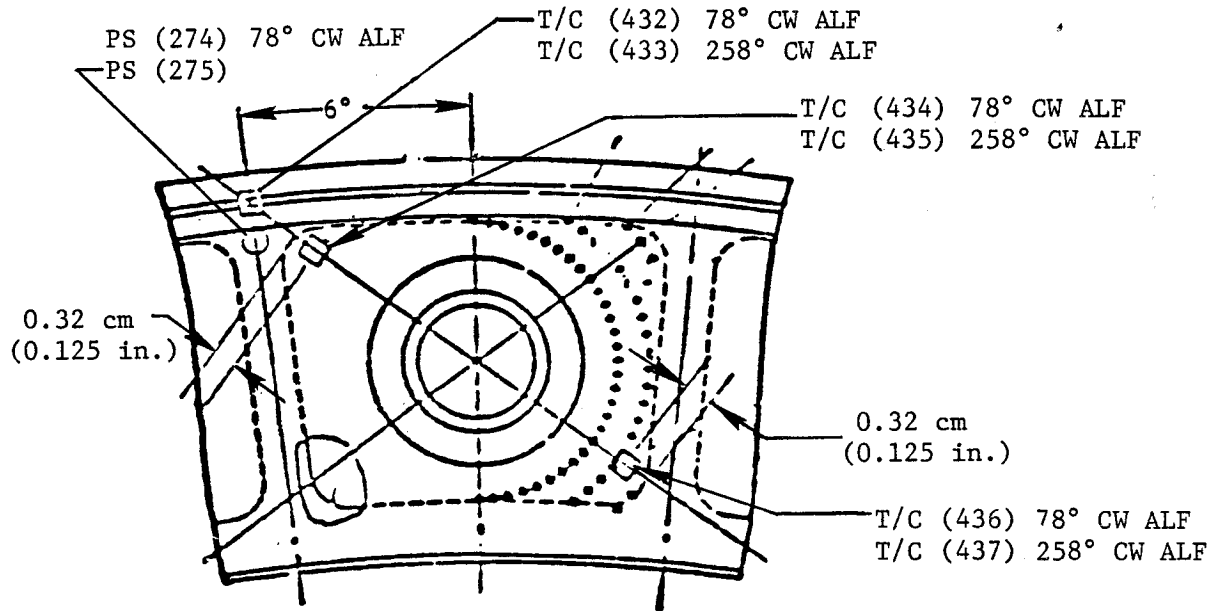


Figure 172. Baseline Combustor Instrumentation Layout, Pilot Stage.

ORIGINAL PAGE IS
OF POOR QUALITY



PS = Static Pressure
T/C = Thermocouple
CW ALF = Crosswise, Aft Looking Forward

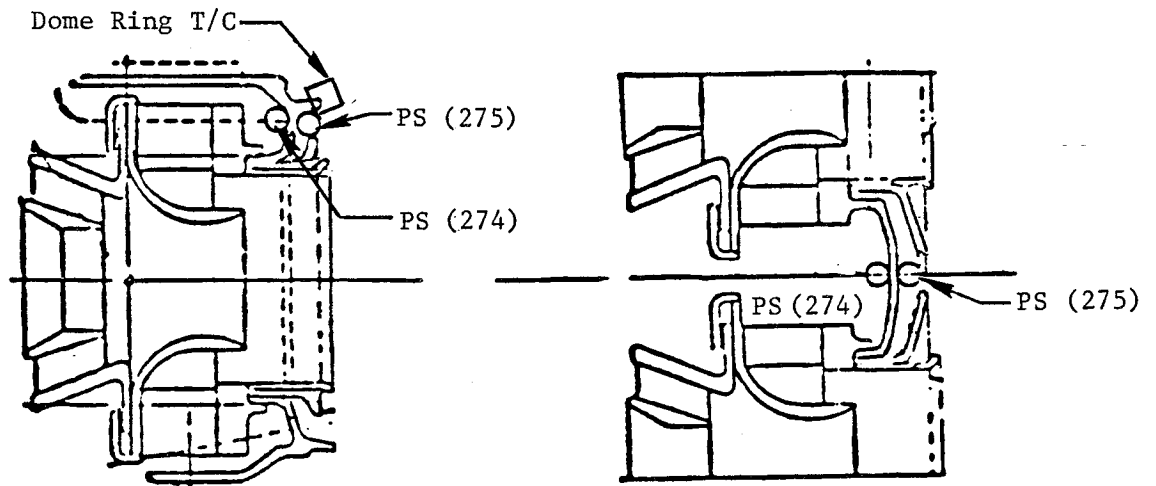
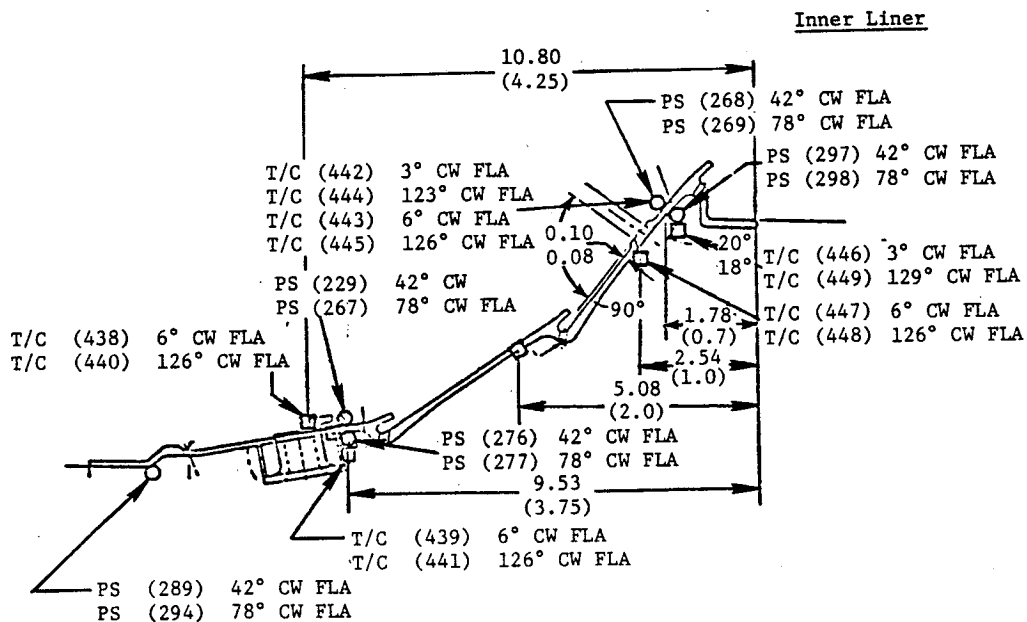
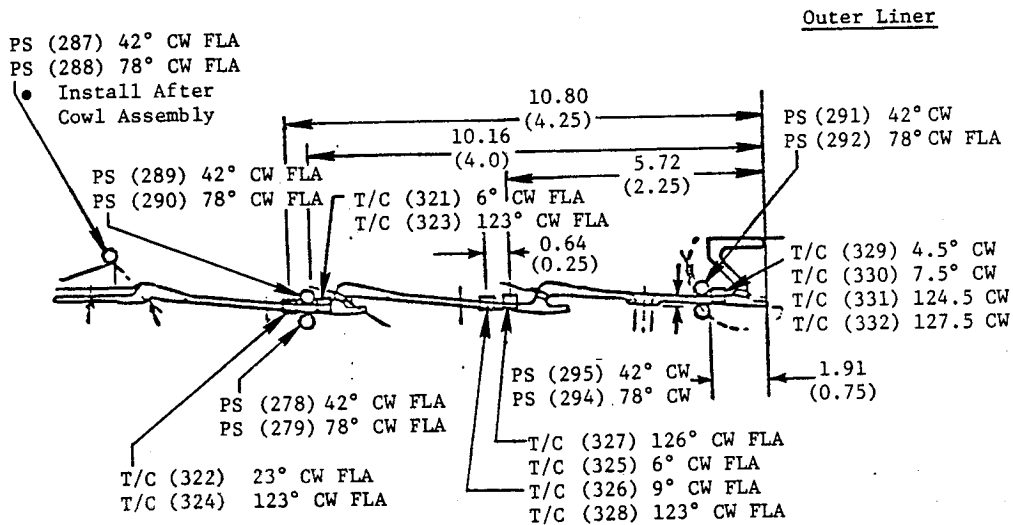


Figure 173. Baseline Combustor Instrumentation Layout, Main Stage.

ORIGINAL PAGE IS
OF POOR QUALITY



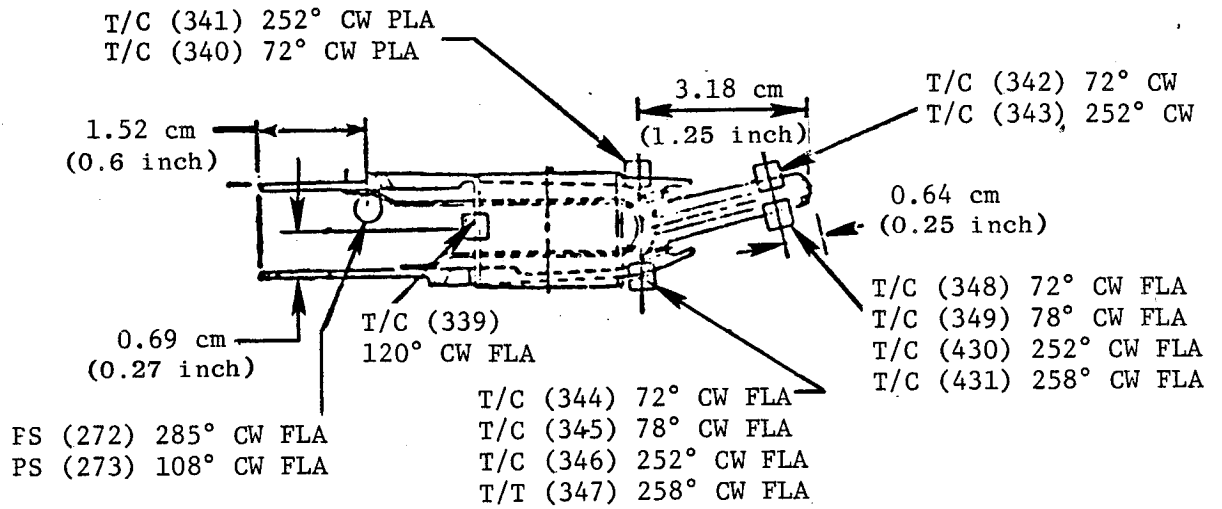
• All Dimensions in cm (in.)



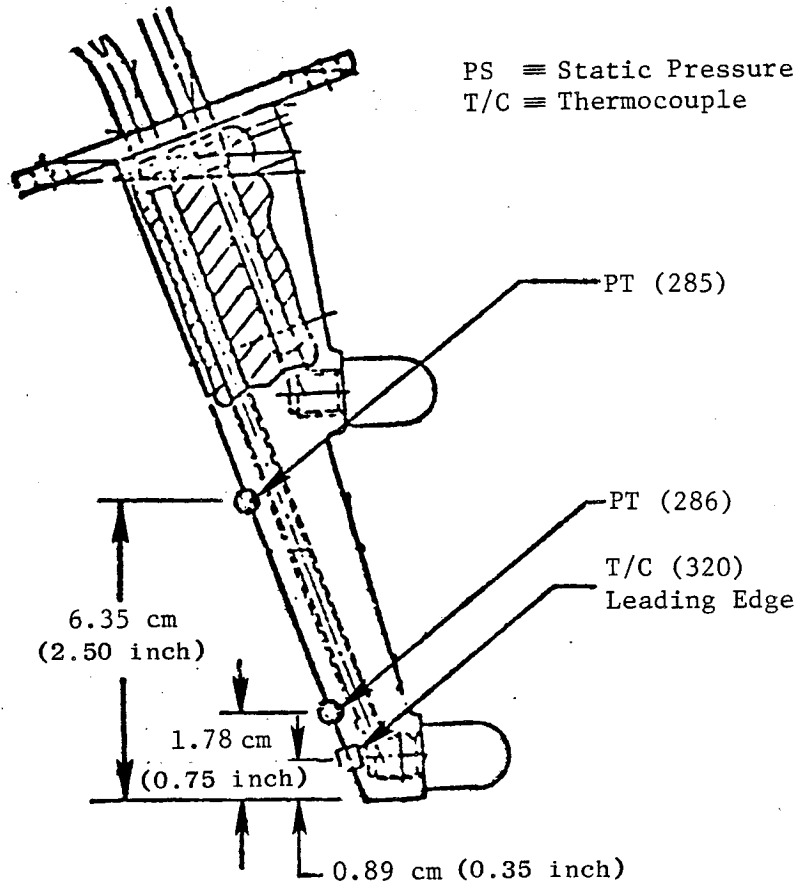
P/S ≡ Static Pressure
 T/C ≡ Thermocouple
 CW ALF = Crosswise, Aft Looking Forward

Figure 174. Baseline Combustor Instrumentation Layout, Liners.

ORIGINAL PAGE IS
OF POOR QUALITY



Centerbody Instrumentation



Fuel Nozzle Instrumentation (Cup No. 7 Nozzle)

Figure 175. Baseline Combustor Instrumentation Layout, Centerbody and Fuel Nozzles.

ORIGINAL PART IS
OF POOR QUALITY

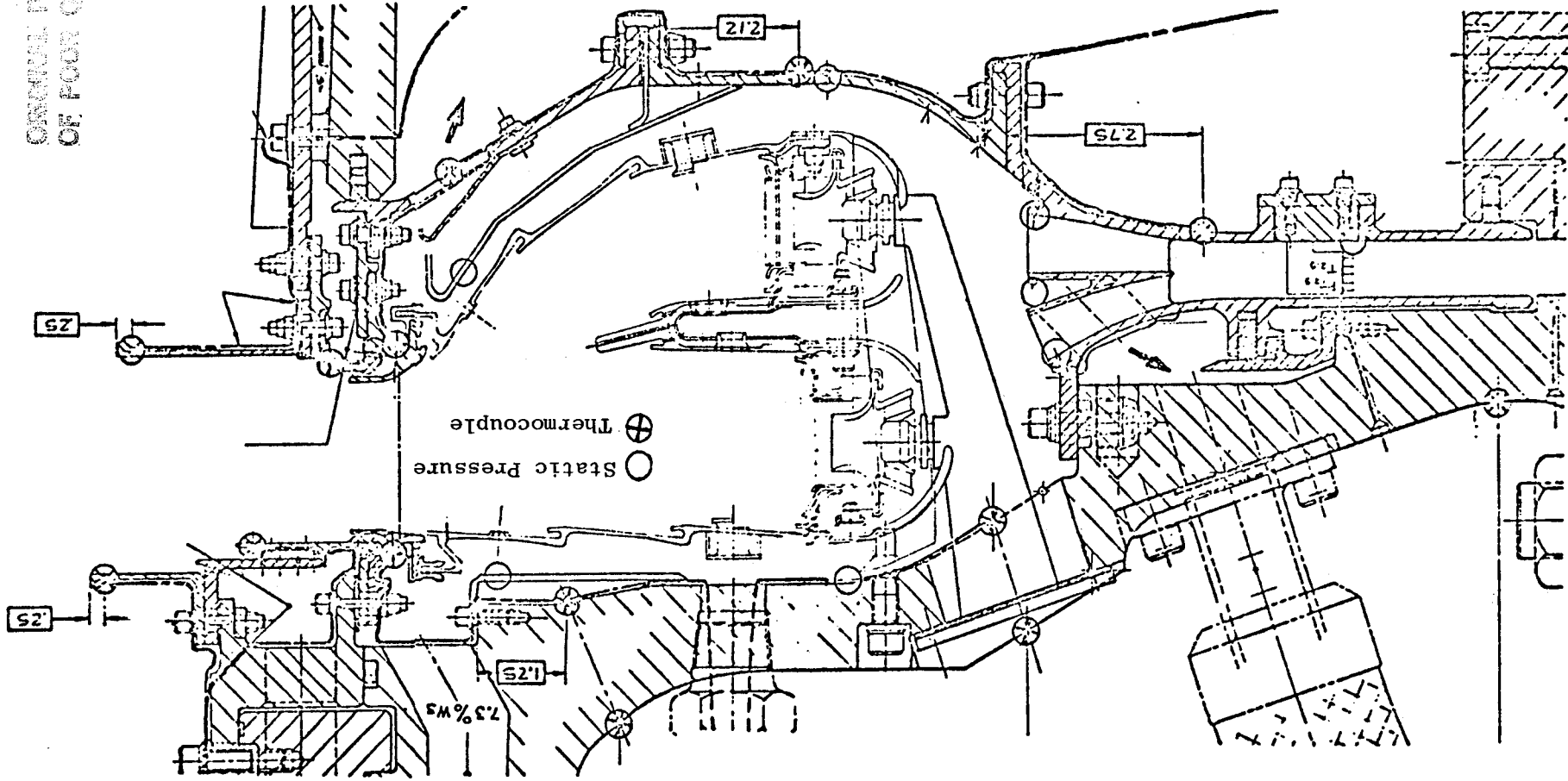


Figure 176. Combustor Test Rig Instrumentation.

power design operating conditions. The adjustment for the measured NO_x emission levels also includes a correction for inlet air humidity.

The results of the idle emissions testing of this baseline combustor configuration are presented in Figures 177 and 178. As observed from Figure 177, CO emissions levels of 59.5 g/kg (59.5 lbm/1000 lb) of fuel and 57.5 g/kg (57.5 lbm/1000 lb) of fuel were obtained, respectively, at the 4% and 6% ground idle design cycle operating conditions. It had been estimated that a CO emissions level of 20.7 g/kg (20.7 lbm/1000 lb) of fuel would be required at the 6% ground idle operating condition to satisfy the program CO emissions goal. The small reduction in the measured CO emissions level from the 4% to 6% ground idle test condition is related to the decrease in the design cycle fuel/air ratio which offsets the expected advantages of increased combustor inlet pressure and temperature. At the 6% ground idle condition, a minimum CO emissions level of 35 g/kg (35 lbm/1000 lb) of fuel was demonstrated at a metered overall fuel/air ratio of 0.0155. It is also observed from this figure that the CO emissions levels are sensitive to changes in the combustor fuel/air ratio. This characteristic is similar to that observed during earlier test programs conducted on double-annular dome combustor designs such as those developed for the NASA/GE ECCP and QCSEE program. This appears to be related to rapid pilot stage stoichiometry changes under conditions of pilot-only operation in which the addition of fuel occurs in a region containing only a portion of the total combustor dome airflow. HC emissions levels of 36 g/kg (36 lbm/1000 lb) of fuel and 22.5 g/kg (22.5 lbm/1000 lb) of fuel were obtained, respectively, at the 4% and 6% ground idle design cycle operating conditions. An HC emissions index of 3.0 g/kg (3.0 lbm/1000 lb) of fuel had been estimated as the required level at 6% ground idle to satisfy the program HC emission goal. HC emission levels at or below this target level were measured at metered overall fuel/air ratios greater than 0.0180.

Emissions were measured at the 30% power approach operating condition at pilot-only plus pilot-to-total fuel flow splits of 0.50, 0.40, and 0.30. The effects of these fuel staging modes on the measured CO, HC, and NO_x emissions are illustrated in Figure 179. As observed from this figure, the expected trend of low CO emissions levels with accompanying higher NO_x emissions levels at the pilot-only operating mode is evident. However, what was not expected

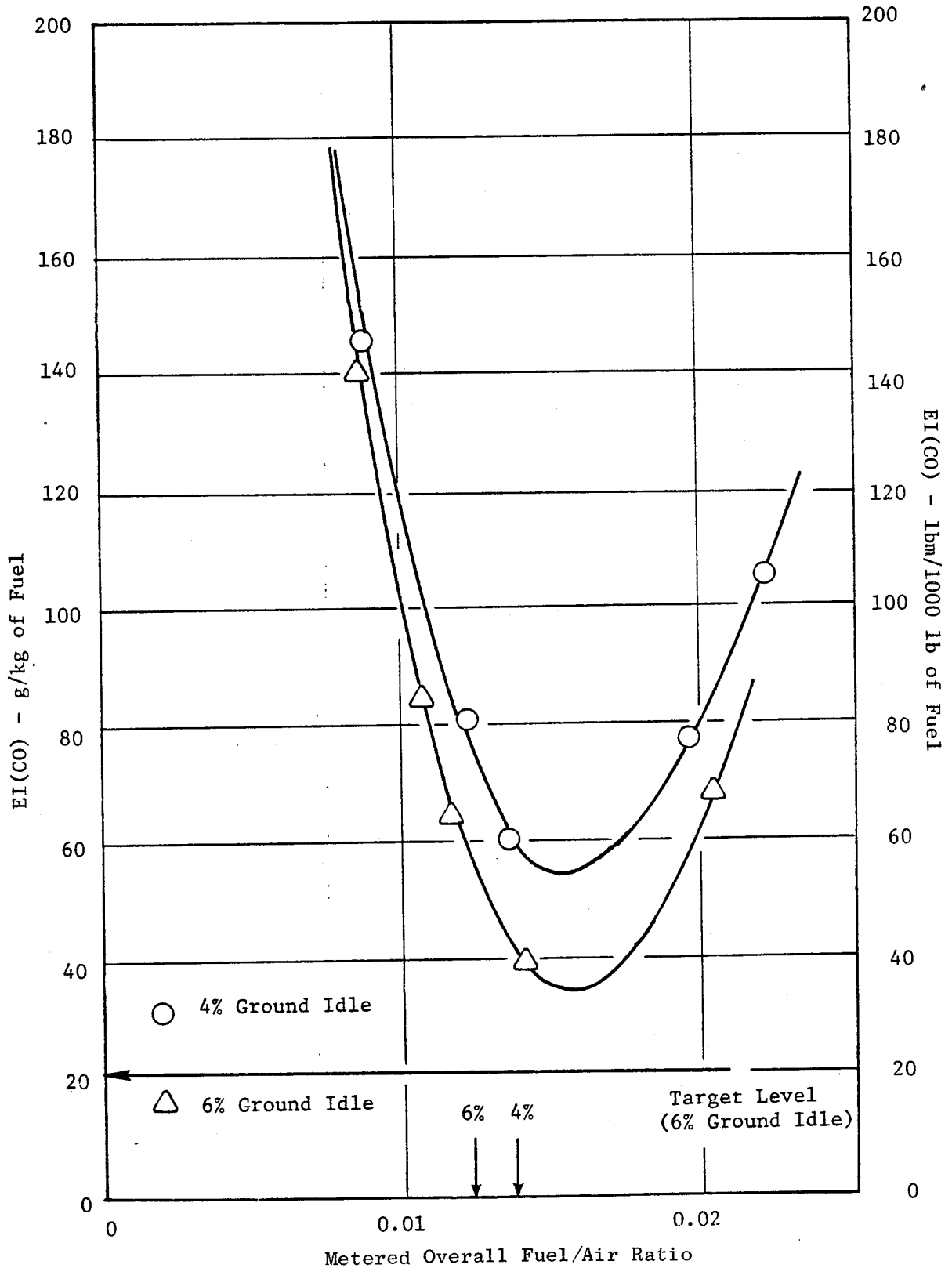


Figure 177. Baseline Combustor Emissions Results, Idle EI_{CO}.

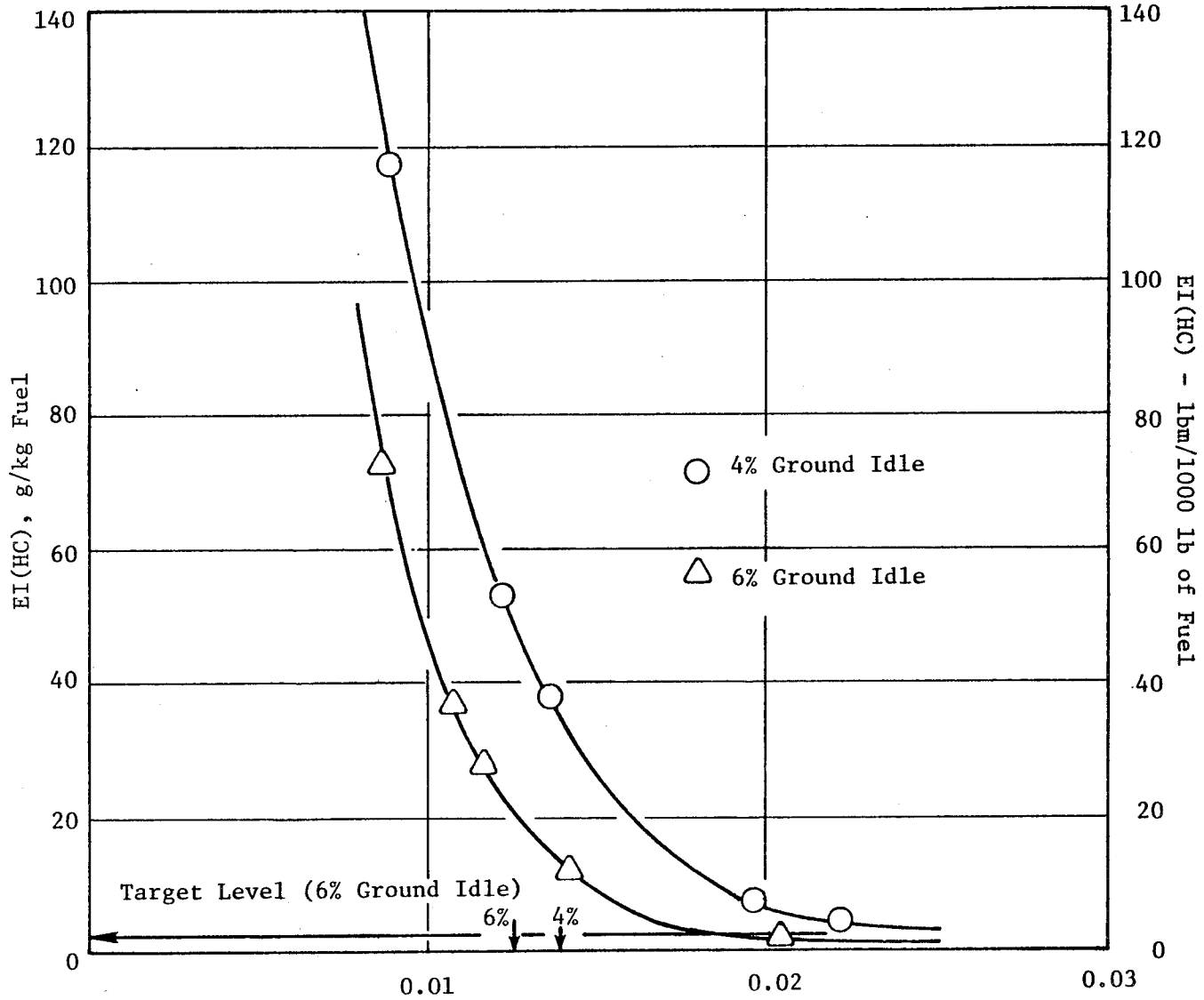


Figure 178. Baseline Combustor Emissions Results, Idle, EI_{HC} .

ORIGINAL PAGE IS
OF POOR QUALITY

ORIGINAL PAGE IS
OF POOR QUALITY.

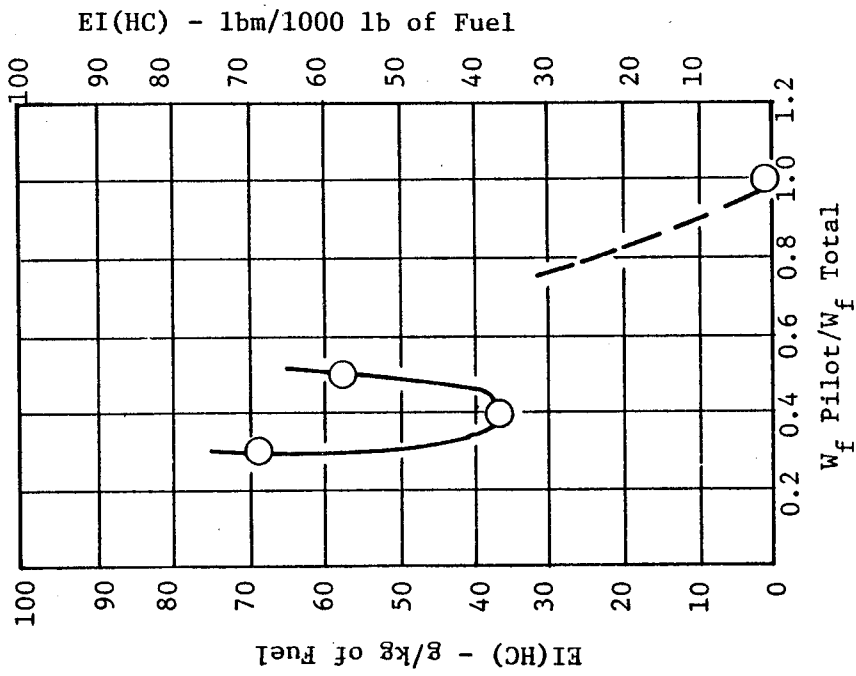
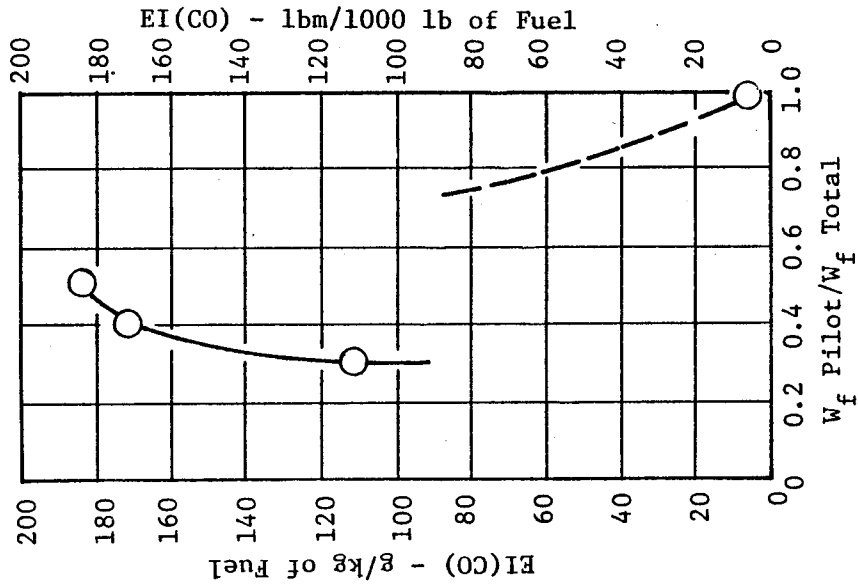
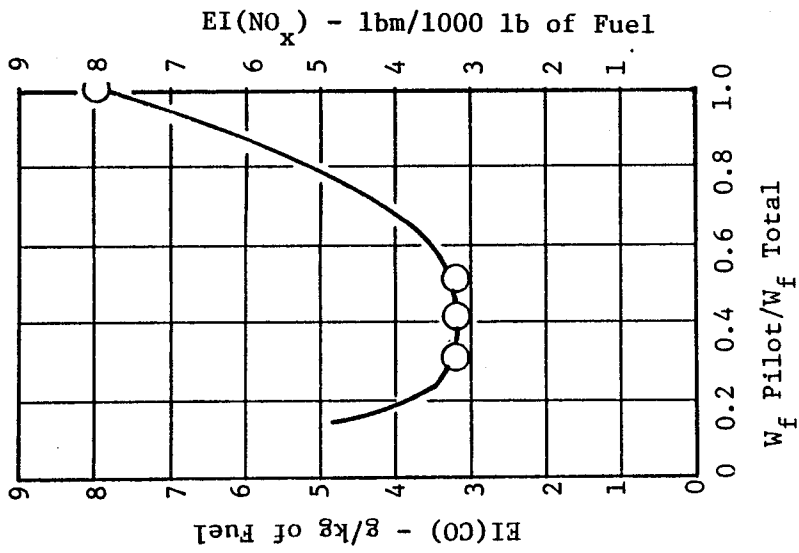


Figure 179. Baseline Combustor Emissions Results, 30% Power.

was the very high CO and HC emissions levels obtained with both the pilot and main stages fueled. The apparent cause results from poor combustion efficiency created by excessively lean fuel/air mixtures in both domes when the relatively low overall fuel/air ratio of 0.0140 at the 30% power condition is divided between the two stages. But, these lean conditions contributed to the very favorable NO_x emissions levels obtained.

The adjusted CO, HC, and NO_x emissions level obtained along the E³ FPS design cycle operating line are presented in Figures 180 and 181. Of particular interest are the NO_x emissions levels at the higher power operating conditions. As observed from Figure 181, sea level takeoff NO_x emissions levels from 16.8 g/kg (16.8 lbm/1000 lb) of fuel to 17.8 g/kg (17.8 lbm/1000 lb) of fuel were obtained. It was unfortunate that at these higher power operating conditions additional fuel splits, lower than those indicated, could not be evaluated because of excessively high metal temperatures measured on the inner liner. Thus insufficient data were obtained at these conditions to determine the fuel split which would produce the lowest NO_x emissions level. At the sea level takeoff condition, a NO_x emission level of 17.5 g/kg (17.5 lbm/1000 lb) of fuel had been estimated as necessary to satisfy the program NO_x emissions goal.

Using the emissions results from the baseline development combustor, EPA Parameter (EPAP) numbers, based on the EPA landing/takeoff cycle for CO, HC, and NO_x, were generated for several cases representing various combustor operating modes at the approach and sea level takeoff conditions. These EPAP results are compared with the E³ program goals in Table XLI. The E³ program emissions goals are identical to the EPA 1/81 standards for newly certified engines greater than 89-kN (20,000 lb) thrust. As observed from this table at all of the combustor operating modes investigated, the CO and HC emissions levels were significantly above the E³ program goals. However, the NO_x emissions levels satisfy the goal with at least 7% margin.

Smoke levels obtained are presented along with the combustor operating conditions at which they were measured in Table XLII. As observed, the smoke levels for this combustor are very low. Although somewhat higher levels would be expected at the actual design cycle conditions at high power, the smoke levels would be expected to be well below the E³ program smoke number goal of 20.

ORIGINAL PAGE IS
OF POOR QUALITY

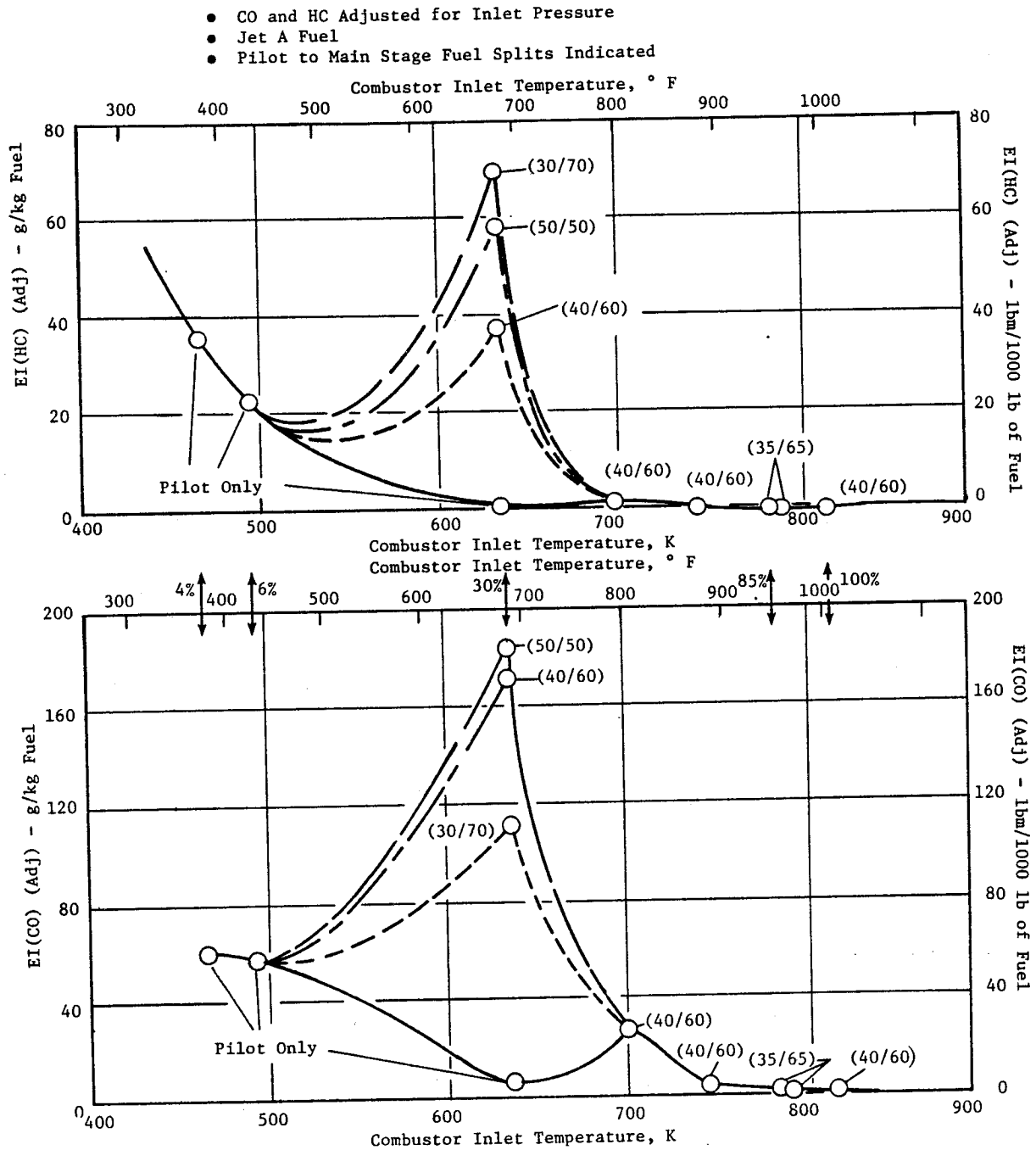


Figure 180. Baseline Combustor Emissions Results, at Staging.

ORIGINAL PAGE IS
OF POOR QUALITY

- NO_x Emissions Adjusted for (P_3 , T_3 , Velocity, Humidity)
- Jet A Fuel
- Pilot to Main Stage Fuel Splits Indicated

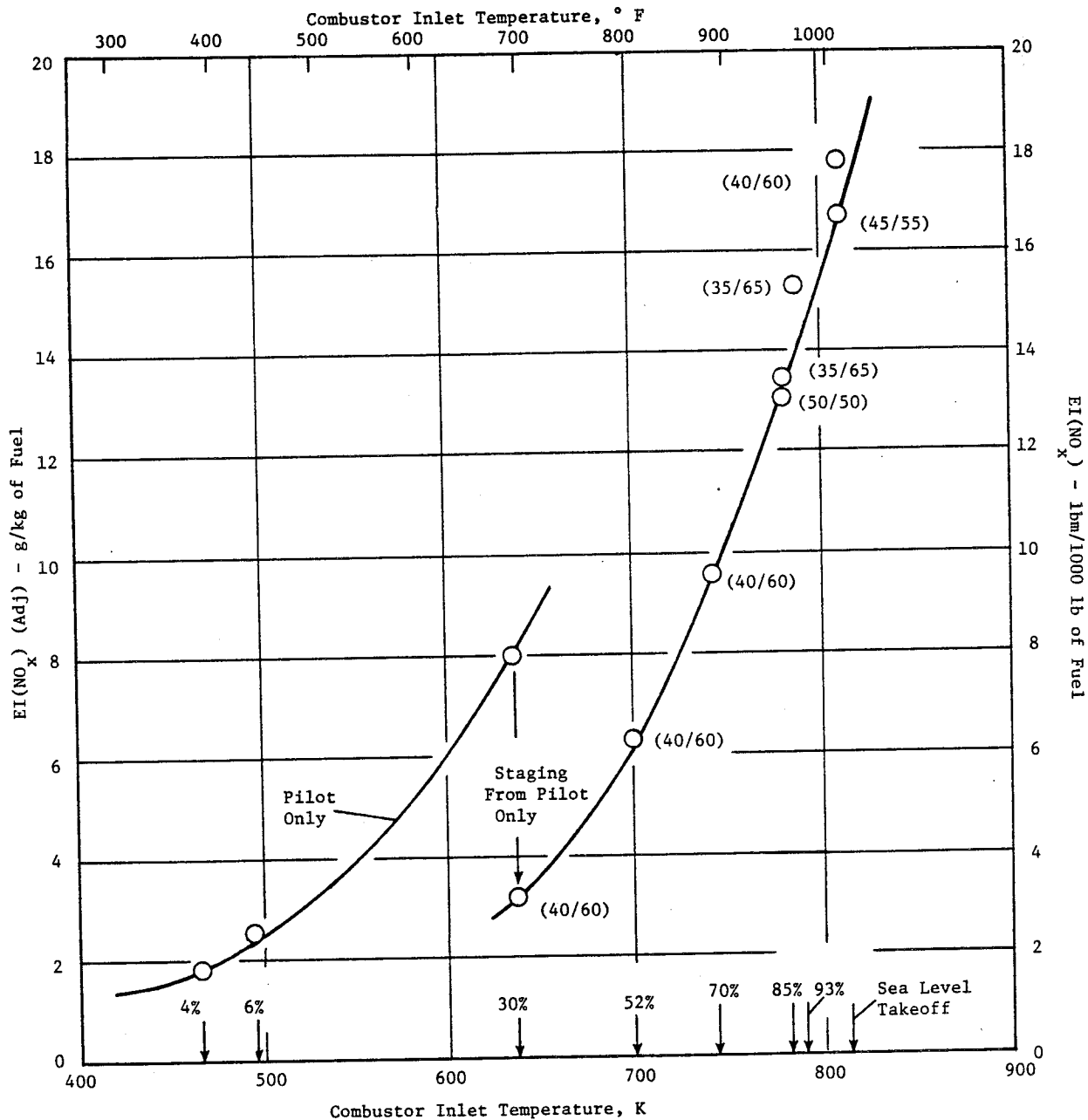


Figure 181. Baseline Combustor Emissions Results, EI_{NO_x} .

Table XLI. Baseline Combustor EPAP Results.

Mode of Operation	EPAP kg/450 kg (1b/1000 lb) Thrust-Hour-Cycle		
	CO	HC	NO _x
<ul style="list-style-type: none"> Pilot Only at Approach 40/60 Split at Climb 45/55 Split at SLTO 	3.69 (8.20)	1.36 (3.03)	1.35 (2.78)
<ul style="list-style-type: none"> Pilot Only at Approach 40/60 Split at Climb 40/60 Split at SLTO 	3.69 (8.20)	1.36 (3.03)	1.27 (2.82)
<ul style="list-style-type: none"> 40/60 Split at Approach 40/60 Split at Climb 45/55 Split at SLTO 	6.55 (14.55)	3.23 (7.17)	1.12 (2.49)
<ul style="list-style-type: none"> 40/60 Split at Approach 40/60 Split at Climb 40/60 Split at SLTO 	6.55 (14.55)	3.23 (7.17)	1.14 (2.53)
<ul style="list-style-type: none"> 30/70 Split at Approach 40/60 Split at Climb 45/55 Split at SLTO 	8.17 (18.16)	2.36 (5.25)	1.12 (2.49)
<ul style="list-style-type: none"> Goals (1981 Standards) 	1.35 (3.00)	0.18 (0.40)	1.35 (3.00)

Table XLII. Baseline Combustor Smoke Results.

<ul style="list-style-type: none"> Jet A Fuel Cell A3 Operating Conditions 						
P ₃ Atm.	T ₃ K (° R)	W _c kg/s (lb/s)	f/a	W _f Pilot/ W _f Total	Combustor SAE Smoke Number	Comments
3.36	466 (839)	7.88 (17.33)	0.0136	1.00	3.45	4% Ground Idle
4.27	493 (887)	10.79 (23.74)	0.0115	1.00	4.38	6% Ground Idle
11.91	634 (1141)	26.34 (57.94)	0.0140	1.00	0.94	30% Approach
16.38	782 (1407)	31.06 (68.33)	0.0223	0.35	2.24	Simulated 85%
16.43	814 (1465)	30.67 (67.48)	0.0246	0.40	2.16	Simulated 100%

At the simulated sea level takeoff operating condition, data from pressure instrumentation in the diffuser section of the test rig were used to calculate total pressure losses, providing a performance measurement of the split duct diffuser design. Total and static pressure upstream of the diffuser inlet were used to calculate the velocity profile in the test rig passage at the inlet of the diffuser. This profile in the form of the local-to-average Mach number ratio is shown in Figure 182. As observed, the profile is essentially flat, peaked only 2% above average slightly outward from the center of the passage. Calculated diffuser total pressure losses are presented in Table XLVIII. These values are compared with losses measured in the full-annular diffuser model subcomponent tests with center peaked and flat inlet velocity profiles. As observed from this comparison, the test rig diffuser performance generally agreed well with the annular diffuser subcomponent test results obtained with a flat velocity profile. The discrepancy in the outer dome loss is most likely related to erroneous outer dome pressure data obtained from the test rig. The comparison also shows that the test rig diffuser performance was considerably below that obtained in the diffuser subcomponent testing with the center peaked velocity profile. It is believed that the level of diffuser performance observed in the test rig is related to the low level of turbulence in the test rig flow upstream of the diffuser, which results from the absence of a velocity profiler. Improvement could be achieved by installing a profile with a center peaked characteristic into the E³ test rig.

Measured overall combustor pressure drops and pilot and main stage dome pressure drops are plotted against the square of the combustor inlet flow function parameter along the E³ FPS design cycle operating line in Figure 183. At sea level takeoff, an overall combustor pressure drop of 5.5% was obtained compared to the engine design value of 5.0%. Prior to the initial testing of this combustor configuration, it had been determined that the combustor total open hole flow area was about 2% less than design. Both the pilot and main stage dome pressure drops appear to be a little low. This is related to the higher-than-anticipated pressure losses measured in the rig diffuser resulting in low dome upstream total pressures. Pressure drops across the liners were between 2% and 3% while levels of 3% and 3.5% were measured across the centerbody structure.

ORIGINAL PAGE IS
OF POOR QUALITY

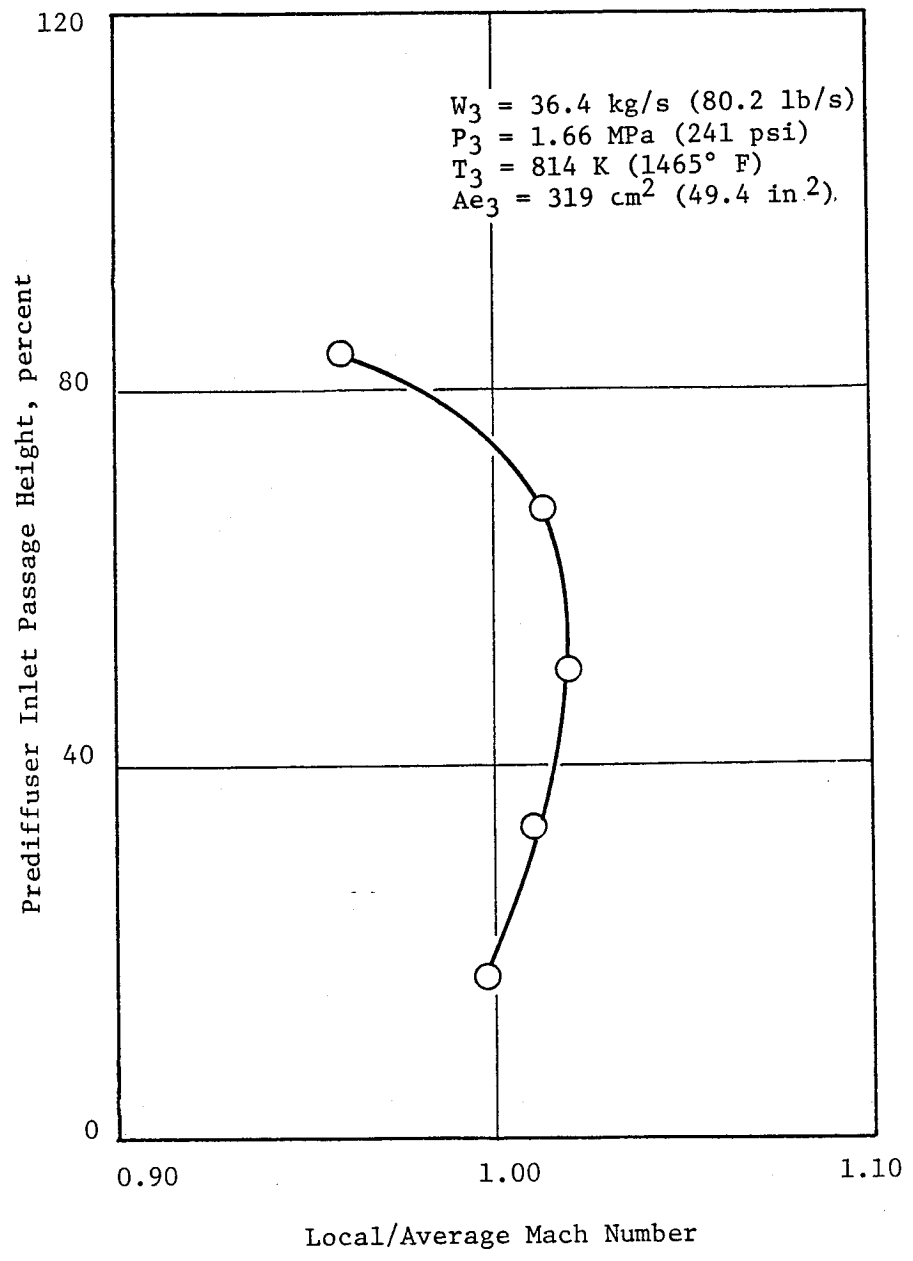


Figure 182. Diffuser Inlet Mach Number Profile (Baseline Test).

Table XLIII. Calculated Diffuser Performance for Baseline Test.

● Diffuser Total Pressure Losses			
Description	Results from Combustor Emissions Test, %	Diffuser Test Flat Profile	Diffuser Test Center Peaked Profile
Prediffuser Outer Passage	1.86	2.12	1.31
Outer Dump	1.83	1.92	1.66
Total Outer	3.69	4.04	2.97
Prediffuser Inner Passage	1.79	1.93	1.10
Inner Dump	0.99	1.12	0.99
Total Inner	2.78	3.05	2.09
Centerbody	2.30	2.77	1.90
Outer Dome	2.53	1.16	1.19
Inner Dome	1.72	1.47	1.27

ORIGINAL PAGE IS
OF POOR QUALITY

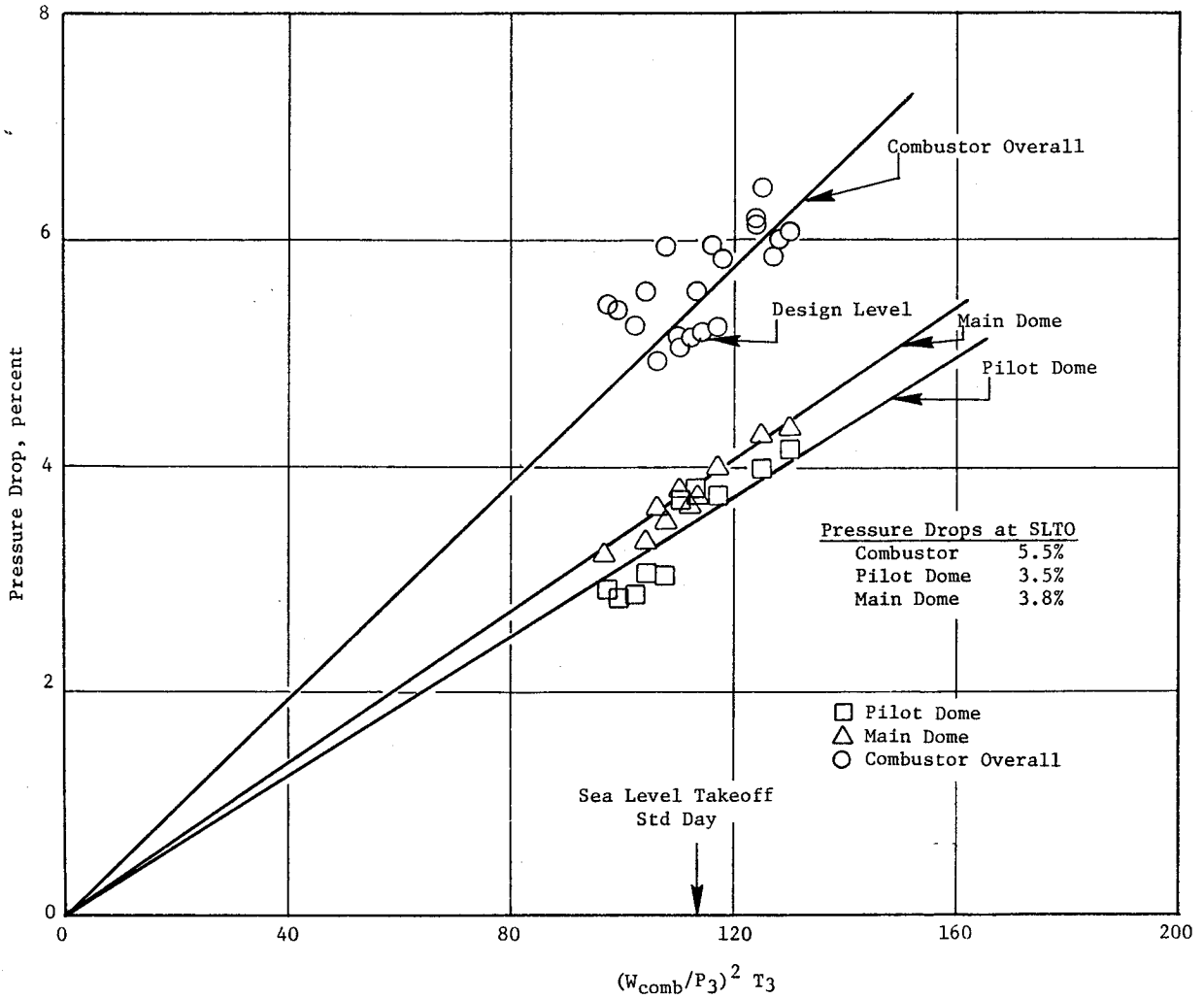


Figure 183. Measured Combustor Pressure Losses for Baseline.

Dynamic pressures were recorded on tape and later reduced to provide the absolute levels and frequencies. The reduced data indicated that the absolute dynamic pressure levels were below 6.895 kPa (1.0 psi) peak-to-peak at all operating conditions with no apparent dominant frequencies.

Combustor metal temperatures measured during testing are plotted against the combustor inlet temperature in Figures 184 through 192. To determine the locations of these indicated temperatures, match the item numbers on these figures with the item numbers shown on the instrumentation layout shown in Figures 172 through 175. A maximum outer liner temperature of 1232 K (2218° R) was observed on Panel 1 at the simulated sea level takeoff operating condition with a 0.45 pilot-to-total fuel flow split. A maximum inner liner temperature of 1259 K (2266° R) was observed on Panel 1 at the simulated sea level takeoff operating condition with a 0.40 pilot-to-total fuel flow split. These excessively high metal temperatures were experienced within a narrow range of fuel splits, and limited the ability to obtain emissions data over a wider range of fuel splits. The thermocouples that indicated these temperatures were located slightly aft and approximately 3° clockwise (aft looking forward) from the dilution thimble directly in line with the top swirl cup in each dome. Temperature paint applied to two sections of each liner indicated a repetitive pattern of these "hot spots" in the same relative location in the vicinity of each dilution thimble on both the outer and inner liners. Indicated metal temperatures on the centerbody structure were within acceptable limits. A maximum metal temperature of 1160 K (2088° R) was observed on the main stage side of the multijet cooling ring at the simulated sea level takeoff condition with a pilot-to-total stage fuel flow split of 0.40. Peak metal temperatures on the crossfire tubes through the centerbody structure between the pilot dome annulus and the main dome annulus remained below 1038 K (1860° R) at all test conditions. There had been some concern that the temperature of these parts might become excessive due to conducting hot gases from the pilot dome to the main dome for ignition of the main stage. Out of a total of six thermocouples located on the pilot dome, only two were reading during testing. One of these thermocouples, located on the splash plate surface in the lower right corner (aft looking forward), indicated a peak temperature of 894 K (1609 ° R). The other of these two thermocouples, located on the pilot dome spectacle plate directly between swirl cups, indicated a peak

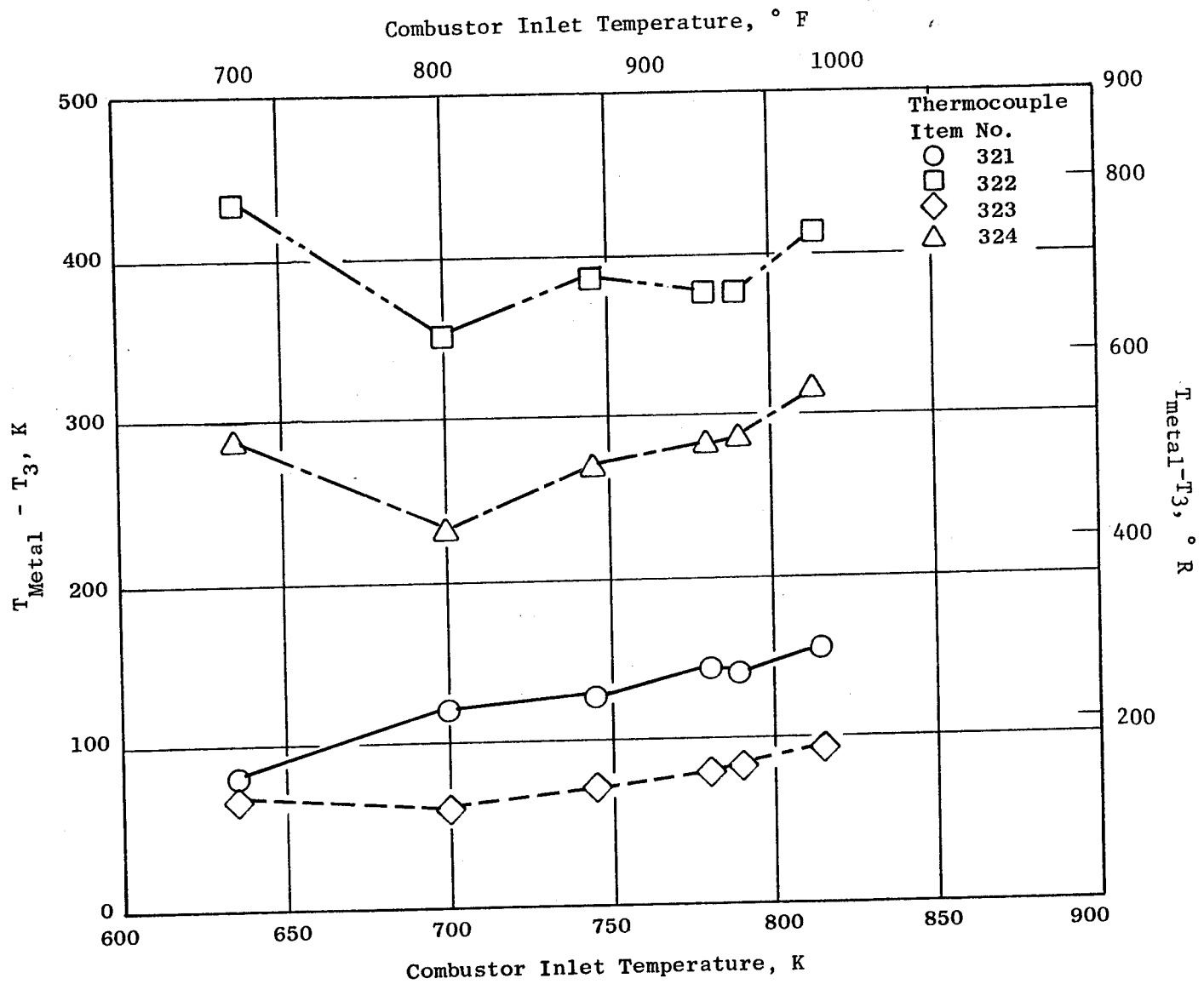


Figure 184. Measured Combustor Metal Temperatures for Baseline Test, Panel 1, Outer Liner.

ORIGINAL PARTIAL
OF POOR QUALITY

ORIGINAL PAGE IS
OF POOR QUALITY

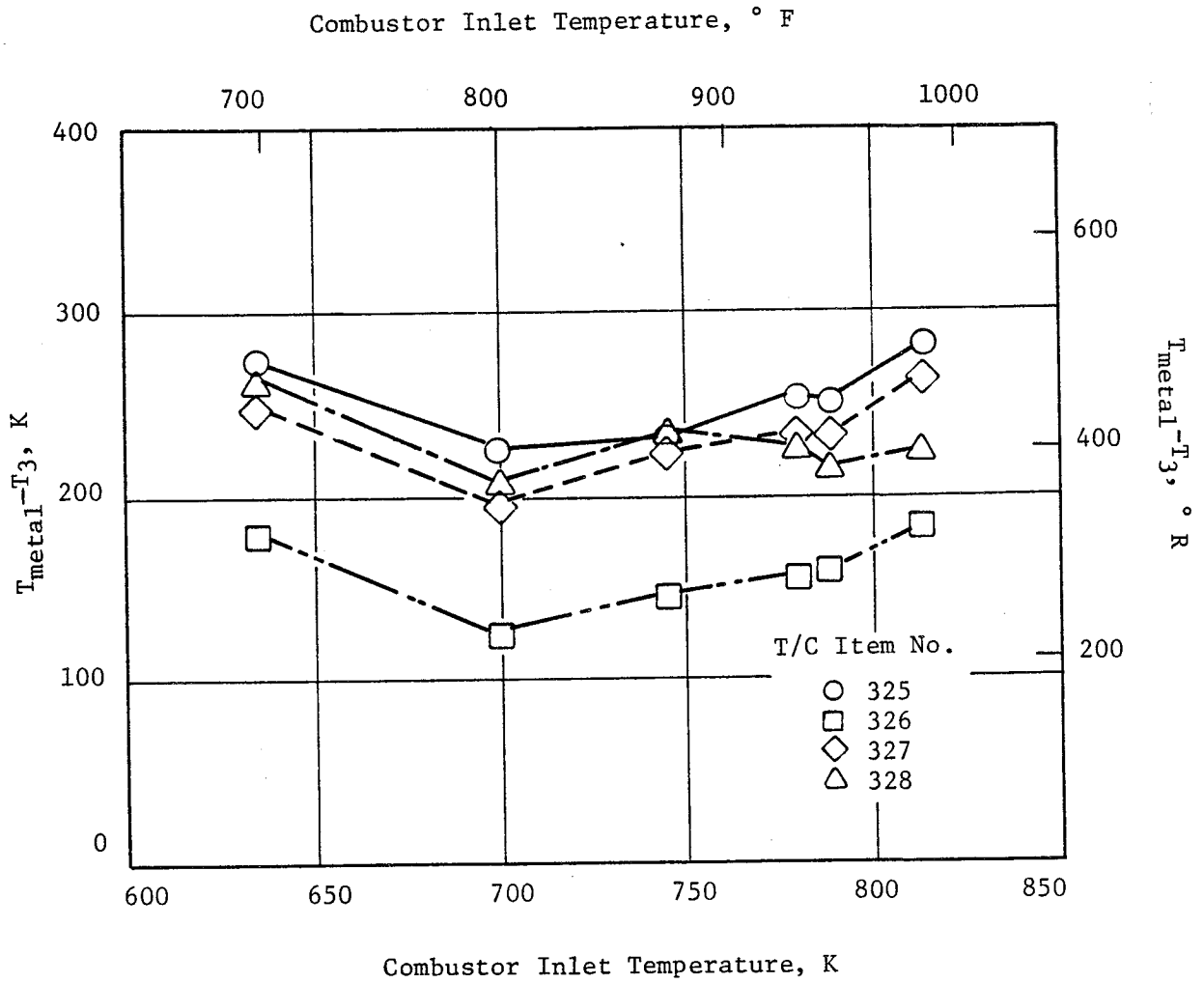


Figure 185. Measured Combustor Metal Temperatures for Baseline Test, Panel 2, Outer Liner.

ORIGINAL PAGE IS
OF POOR QUALITY

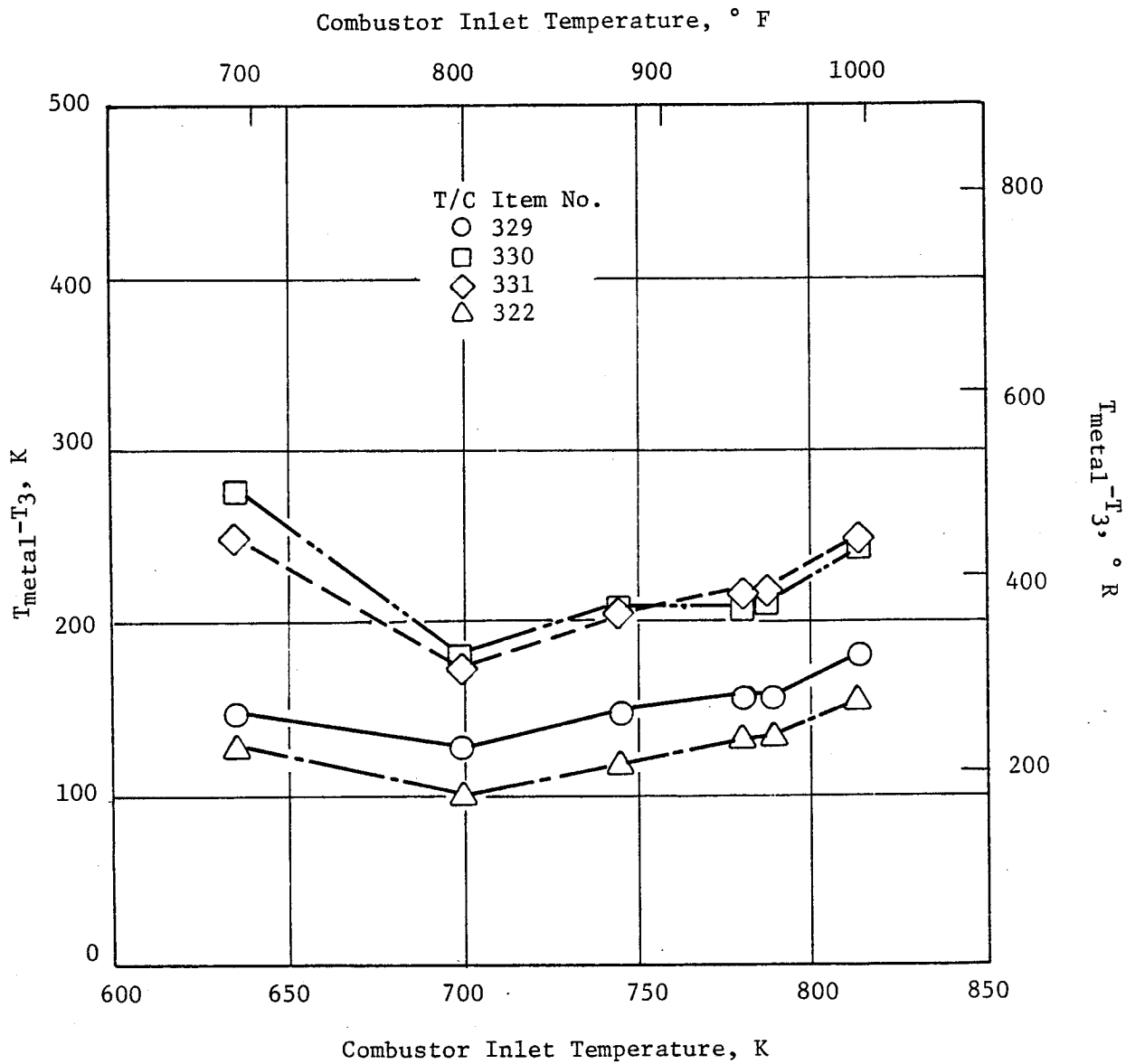


Figure 186. Measured Combustor Metal Temperatures for Baseline Test, Panel 3, Outer Liner.

ORIGINAL PAGE IS
OF POOR QUALITY

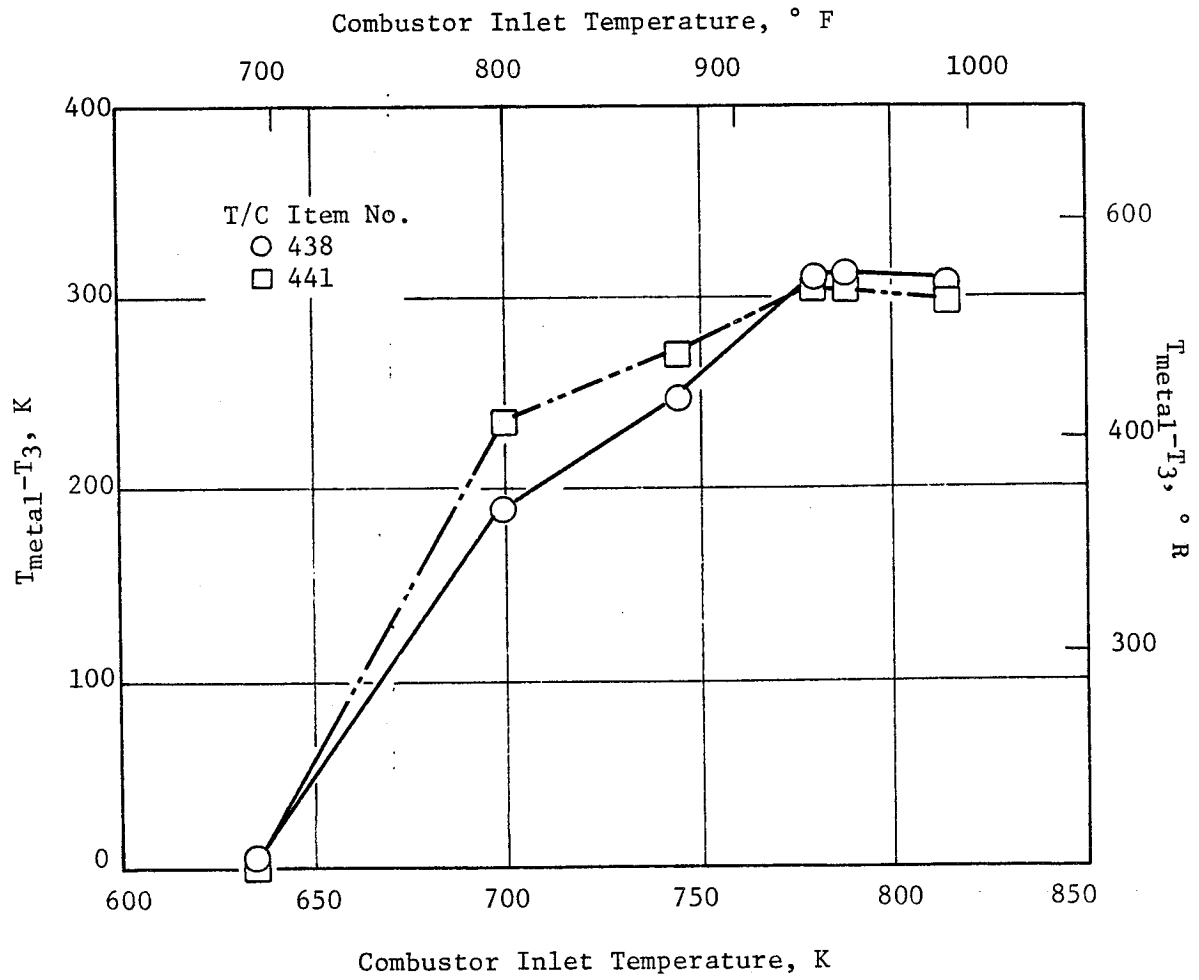


Figure 187. Measured Combustor Metal Temperatures for Baseline Test, Panel 1, Inner Liner.

ORIGINAL PAGE IS
OF POOR QUALITY

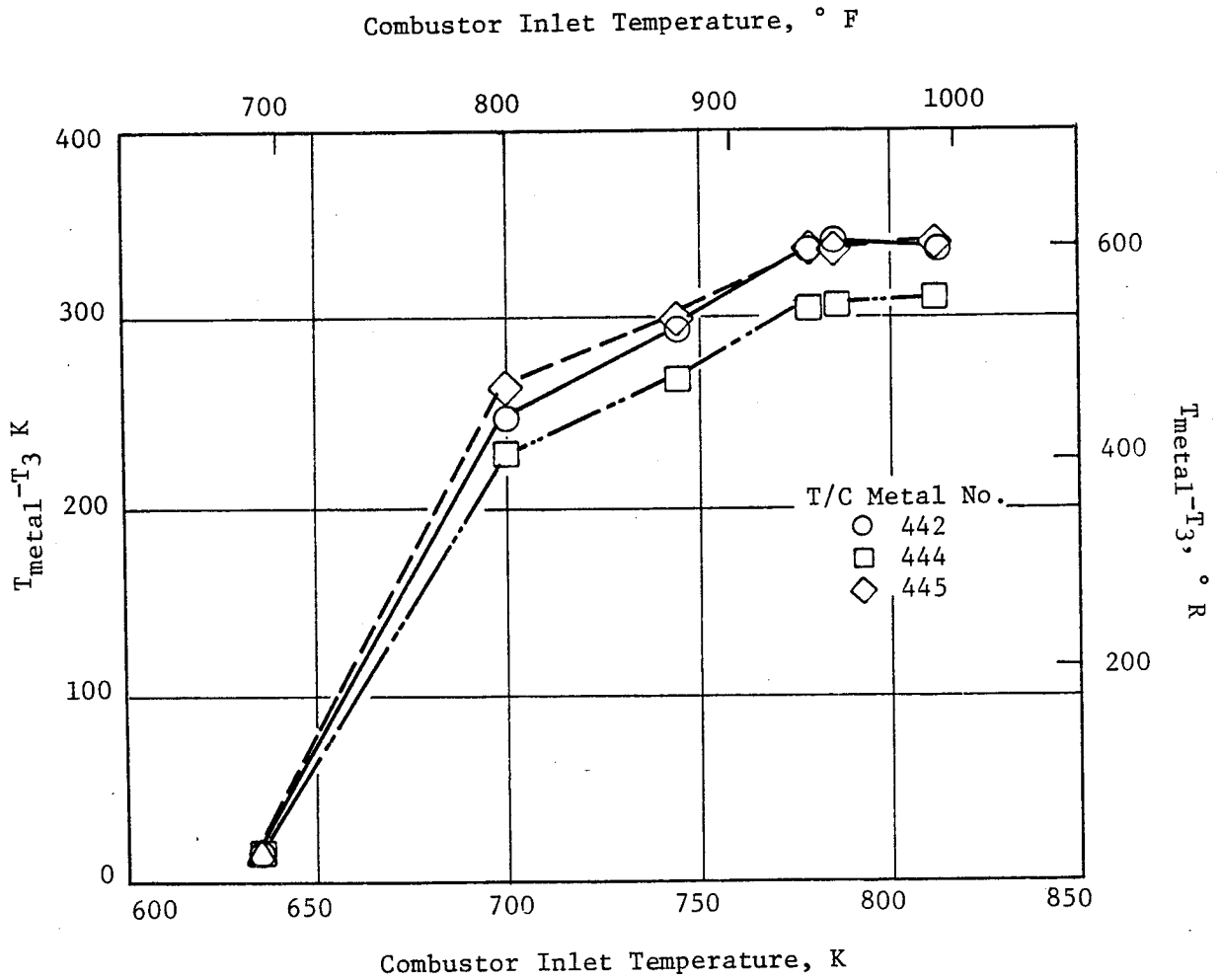


Figure 188. Measured Combustor Metal Temperatures for Baseline Test, Panel 2, Inner Liner.

ORIGINAL PAGE IS
OF POOR QUALITY

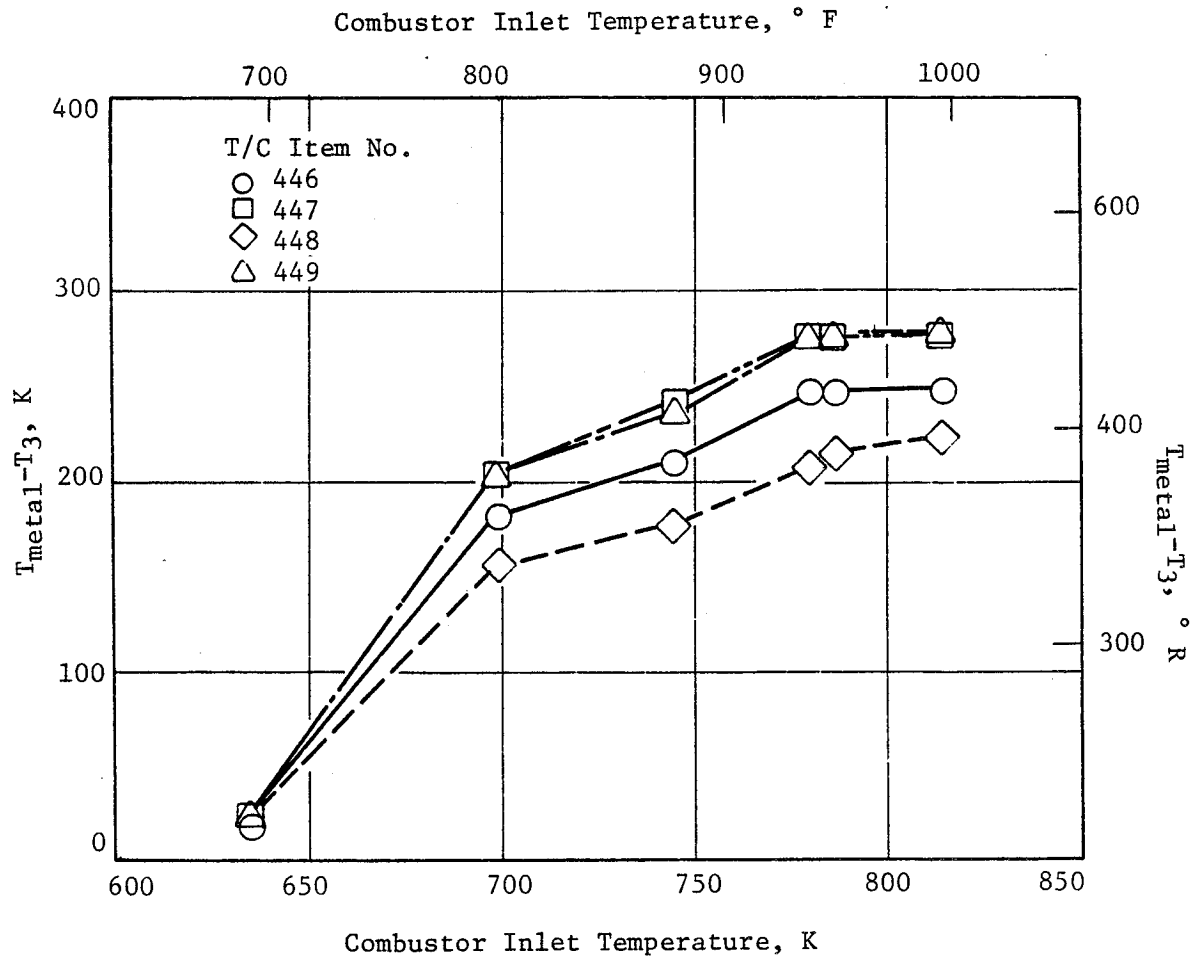


Figure 189. Measured Combustor Metal Temperatures for Baseline Test, Panel 3, Inner Liner.

ORIGINAL PAGE IS
OF POOR QUALITY

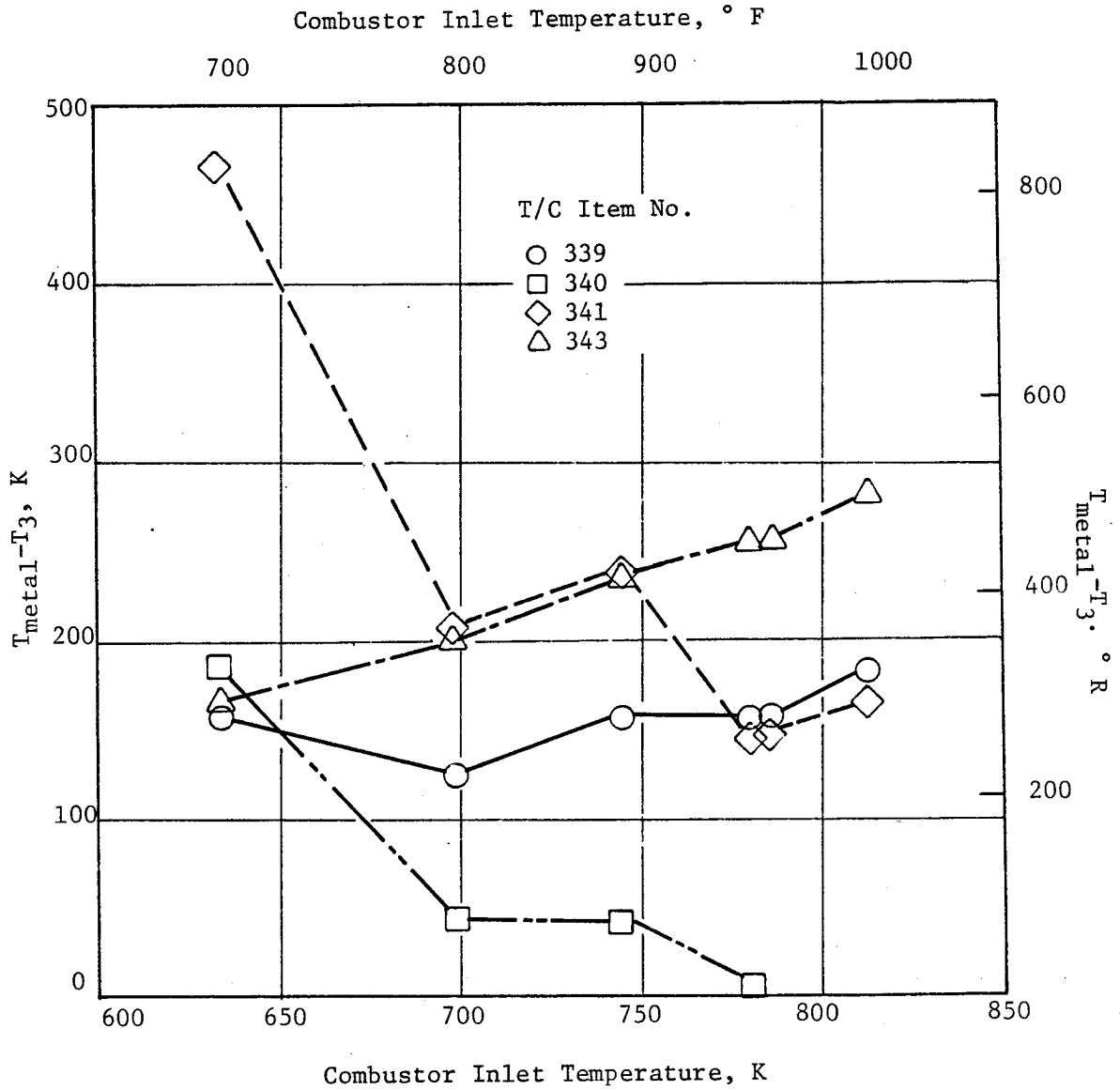


Figure 190. Measured Combustor Metal Temperatures
for Baseline Test, Centerbody, Pilot Side.

ORIGINAL PAGE IN
OF POOR QUALITY

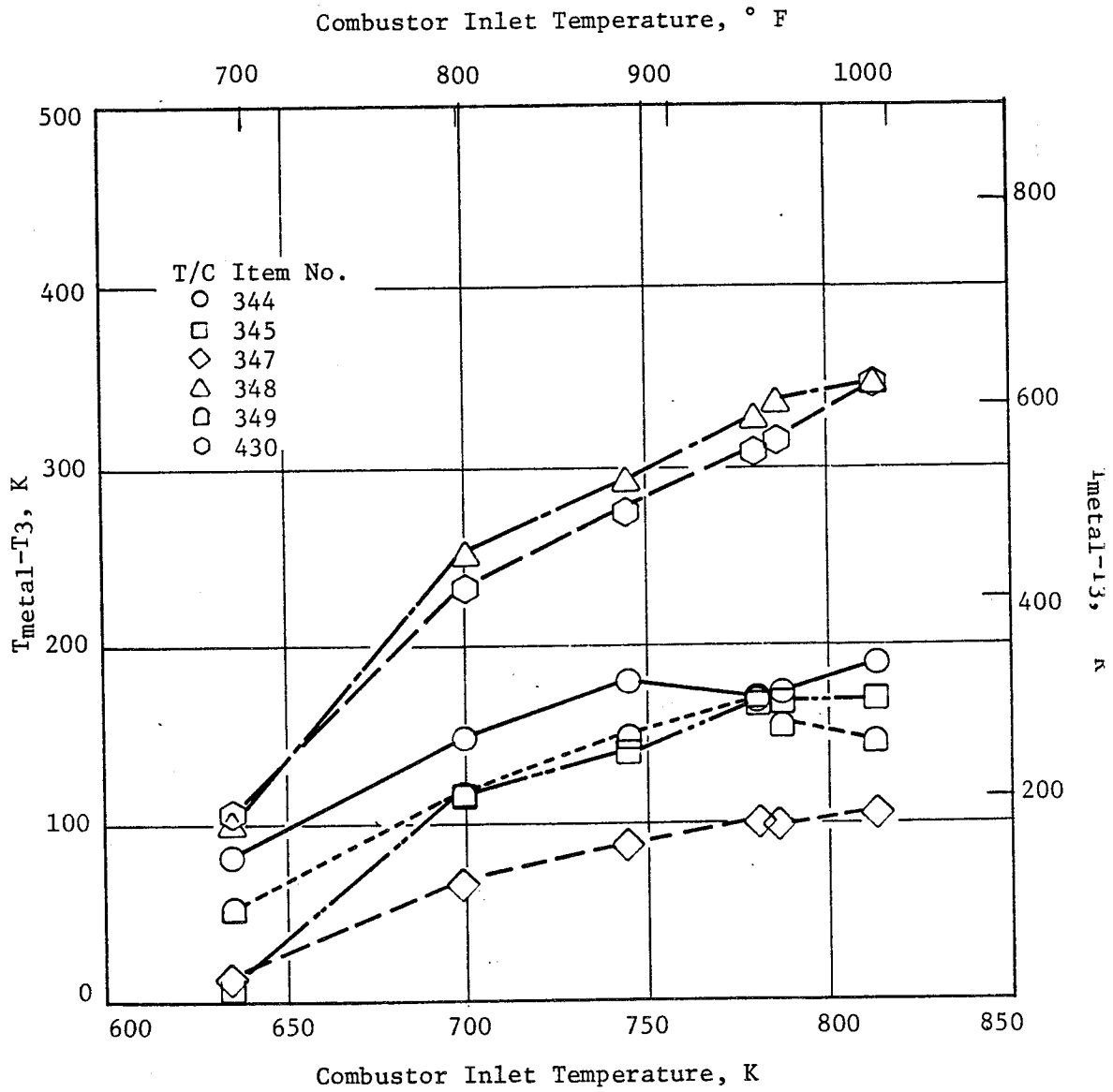


Figure 191. Measured Combustor Metal Temperatures for Baseline Test, Centerbody, Main Stage Side.

ORIGINAL PAGE IS
OF POOR QUALITY

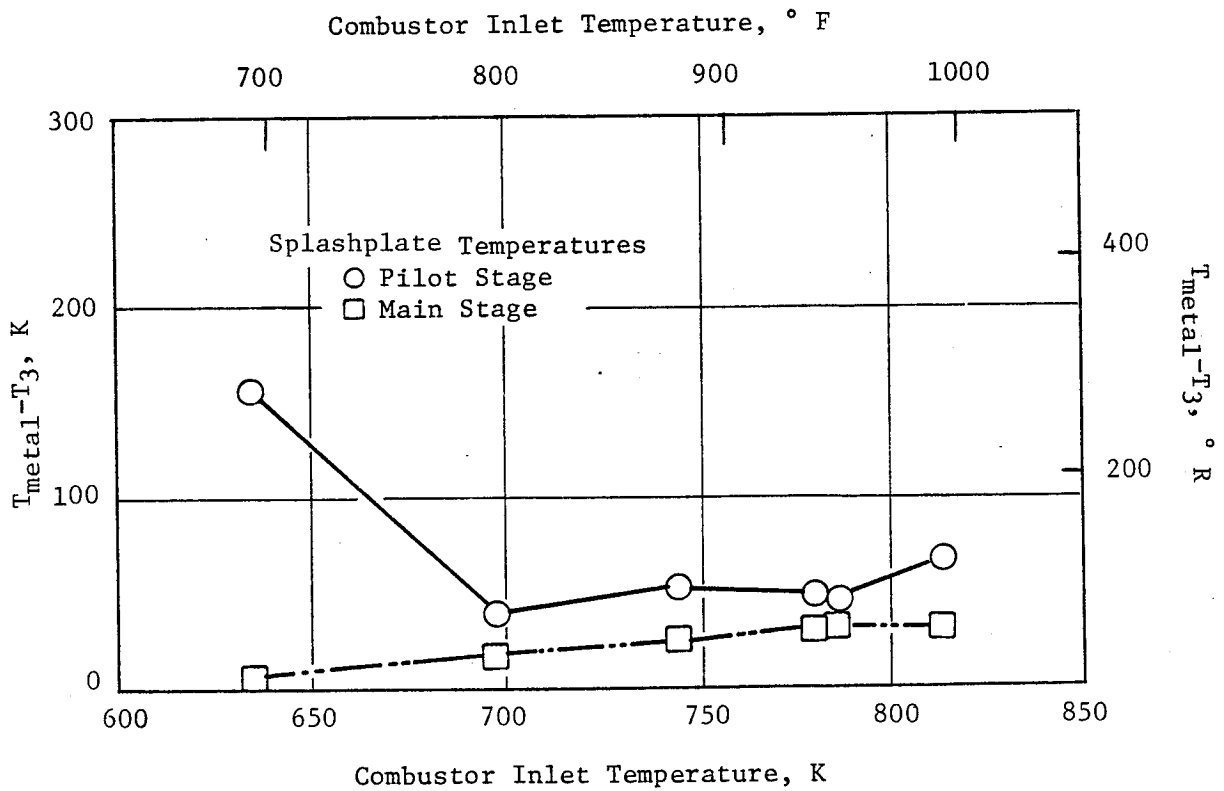


Figure 192. Measured Combustor Metal Temperatures for Baseline Test, Splash Plate.

metal temperature of 814 K (1465° R) at the sea level takeoff condition. Three out of six main dome skin thermocouples were active during testing. Two of these, located on the splash plate surface in the upper left and lower right corners (aft looking forward), indicated peak metal temperatures only about 28 K (50° R) above the inlet temperature of 814 K (1465° R) at the sea level takeoff condition. The other metal thermocouple, located on the main dome splash plate directly between swirl cups, indicated a peak metal temperature of 829 K (1492° R). These pilot and main stage dome temperatures are significantly below the maximum allowable metal temperature and provide strong evidence in support of a significant reduction in the cooling flow levels of each dome.

6.2.2.4 Concluding Remarks - Baseline Combustor

Testing results obtained from the ground start ignition, exit temperature performance, and emissions evaluations of the E³ baseline combustor were very encouraging, especially considering that this was the first test of this advanced combustor design. However, improvements in all three combustor performance areas were required in order to achieve all of the combustion system goals of the E³. Key problem areas identified from this test series included:

- Improving main stage crossfire and propagation
- Reducing the idle emissions
- Reducing the CO and HC emissions at the 30% power condition in the staged combustor operating mode.

Despite obtaining an exit temperature pattern factor which closely approaches the program goal, additional combustor development design optimization would be required to simultaneously satisfy the exit temperature performance and emissions goals.

Immediate attention was directed at identifying combustor design modifications that would provide significant reductions in the ground idle and staged approach emissions levels, plus provide reductions in the outer and inner liner Panel 1 metal temperatures. This would be accomplished by providing added Panel 1 cooling, enriching the pilot stage primary combustion zone to produce more favorable conditions for CO and HC consumption, providing

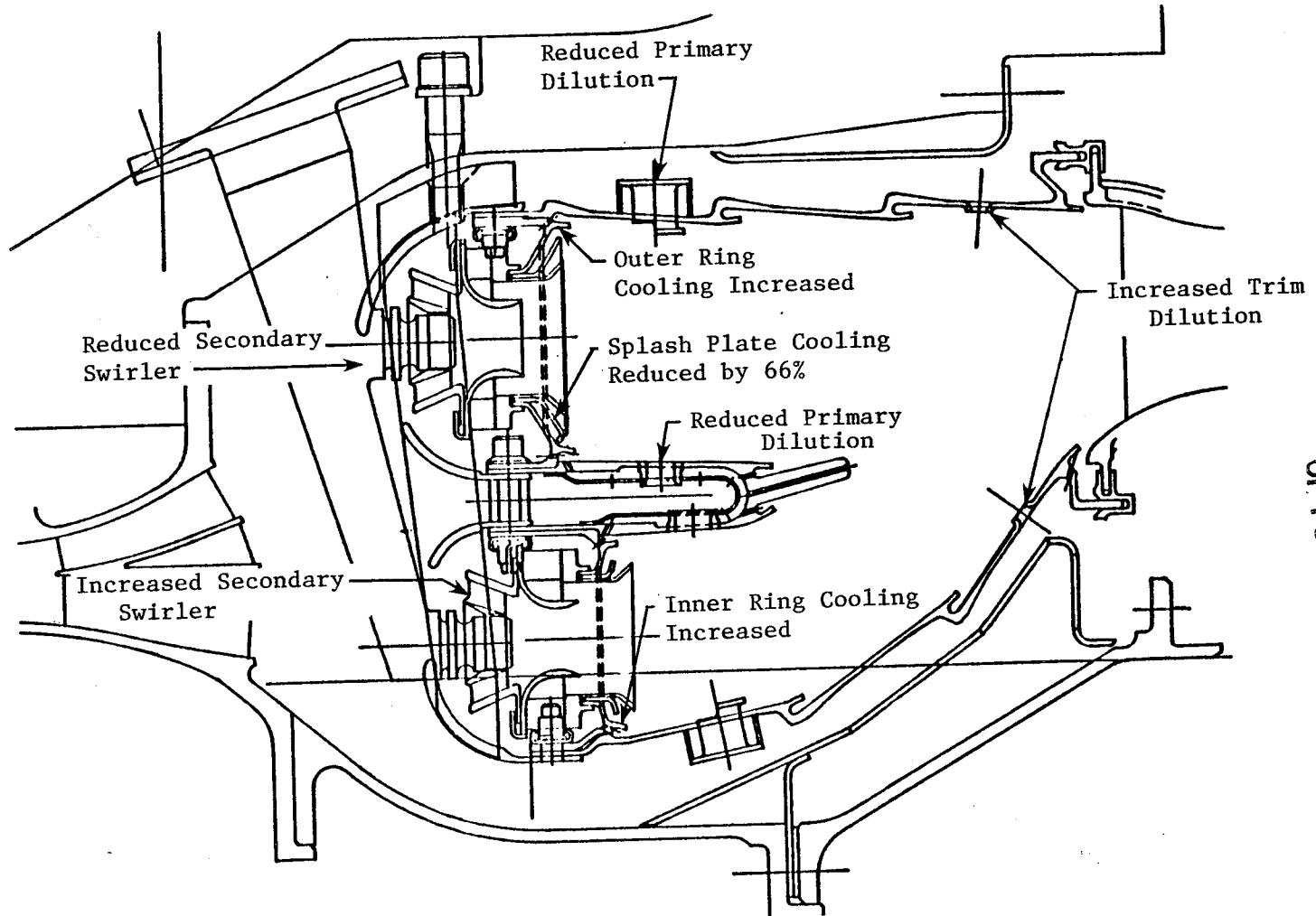
a leaner main stage primary combustion zone to achieve further reductions in the NO_x emissions levels at high power operating conditions, modifying dilution air to provide improvement to the exit temperature performance, and maintaining the combustor overall pressure drop.

6.2.2.5 Mod I Combustor Test Results

The Mod I combustor featured an enriched pilot stage primary combustion zone. This was accomplished by reducing the pilot stage swirl cup flow, the pilot dome splash plate cooling flow, and the pilot stage primary dilution flow. The pilot dome outer ring cooling flow was increased to provide added film cooling for the forward panel of the outer liner. Outer liner trim dilution was also increased to provide attenuation for the exit temperature radial profile resulting from pilot only operation. This combustion configuration also was redesigned with a leaner main stage primary zone accomplished by an increase in the main stage swirl cup flow. The main dome inner ring cooling flow was increased to provide added film cooling flow for the forward panel of the inner liner. Inner liner trim dilution was also increased to provide improvement in the exit temperature performance at high power operating conditions. In addition, the outer liner, centerbody, and inner liner assemblies were rotated 6° clockwise, aft looking forward, with respect to the dome relocating the pilot stage and main stage primary holes from in-line to between the swirl cups. With the rotation of the centerbody, the two pilot-to-main stage crossfire tubes became located between swirl cups. The decision to change to "between cup" primary airholes was based on sector combustor subcomponent tests. Results from this testing had demonstrated that significant reductions in idle emissions could be obtained by adopting the between-cup orientation. The design modifications featured in the Mod I combustor configuration are illustrated in Figure 193. The resultant changes in the combustor airflow distribution are presented in Appendix E.

6.2.2.6 Atmospheric Ground Start Ignition Test

Atmospheric ground start ignition testing of the Mod I combustor was initiated on July 16, 1980. Test points simulated combustor inlet conditions along the E³ (September 1979) ground start operating line and are presented in Table LXIV.



ORIGINAL PAGE IS
OF POOR QUALITY

Figure 193. Mod I Combustor Hardware Modifications.

Table LXIV. Combustor Mod I Atmospheric Ignition Test Point Schedule.

XNRH, %	K	T ₃ , (°R)	P ₃ Atm.	W ₃₆ , kg/s	(lb/s)
21	289	(520)	1.0	1.25	(2.75)
28	289	(520)	1.0	1.69	(3.71)
32	314	(565)	1.0	1.55	(3.40)
46	344	(619)	1.0	1.65	(3.64)
58	383	(690)	1.0	1.86	(4.09)
70	429	(772)	1.0	1.94	(4.26)
77	503	(905)	1.0	2.33	(5.13)

The fuel nozzle assemblies used had the E³ test rig fuel nozzle bodies. The nozzle tips installed in the pilot dome were rated at 12 kg/hr (26.4 lb/hr), while those installed in the main dome were rated at 4.5 kg/hr (9.92 lb/hr). Shutoff-type valves were installed into every other main stage fuel line pigtail to allow evaluating the main stage crossfire and propagation characteristics using a uniform 15 on - 15 off fuel nozzle operating mode.

During the initial test run, pilot stage ignition and propagation proceeded without difficulty at all points of the test schedule. However, main stage crossfire was not achieved at any of the test conditions evaluated. Excessive test facility exhaust plenum temperature limited the main stage fuel flow level to 272.2 kg/hr (600 pph) with the pilot stage fueled and burning. Visual observations indicated that fire from the pilot stage swirl cups, now between the two crossfire tubes, was not penetrating into the main stage dome annulus through the crossfire tubes. Without conduction of hot pilot stage gases into the main stage dome to provide an ignition source, the ignition of the main stage was unsuccessful. During ground start ignition evaluation of the baseline combustor configuration, it was observed that main stage ignition was obtained from hot pilot gas penetrating into the main stage dome annulus through the crossfire tubes located directly in line with swirl cups No. 6 and 21. The inability to successfully crossfire the main stage in the Mod I configuration was concluded to be the result of the between-cup

location of the existing crossfire tubes. It was decided to remove the combustor from the test rig to incorporate two additional crossfire tubes in the centerbody structure. These additional crossfire tubes were located 180° apart and perpendicular to the alignment of the existing crossfire tubes. Upon reassembly of the combustor, the new crossfire tubes were located directly in line with cup No. 6 and the ignitor cup No. 21. After completion of the rework, the combustor was installed back into the test rig to resume the ground start ignition evaluation. Through the duration of the atmospheric ground start ignition testing, main stage crossfire was achieved.

Test results obtained from this ground start ignition evaluation of the E³ development combustor Mod I configuration are presented in Figures 194 and 195.

As observed from Figure 194, significant improvement in pilot ignition, propagation, and total blowout was achieved compared with the results of the baseline configuration. The Mod I configuration demonstrated full propagation of the pilot stage with between 50% and 100% fuel margin compared to the E³ ground start cycle combustor fuel/air ratio operating line with a minimum of 40% blowout margin. These observed improvements reflected the benefit of the enriched pilot stage stoichiometry of this configuration. Ignition of the main stage was investigated for two fueling modes. In one mode, fuel was supplied to all 30 main stage nozzles. In the second mode, all main stage nozzles in even numbered cups were shut off. The main stage cup in line with the ignitor and crossfire tube (cup No. 21) was fueled. In general, the main stage ignition characteristics of the Mod I configuration were no better than those demonstrated in the baseline configuration. In the 30-nozzle mode, overall fuel/air ratios exceeding the E³ September 1979 ground start cycle operating line were required to ignite the two main stage swirl cups in line with the crossfire tubes. Full propagation of the main stage was demonstrated only at the simulated 77% core engine speed operating condition. However, the propagation fuel/air ratio required was well above the required fuel schedule operating line. Partial propagations were obtained at 48%, 58%, and 70% simulated core engine speed operating conditions. These also occurred at fuel/air ratios well above the requirement. Some benefit in the ignition characteristics of the main stage was obtained using the 15 on - 15 off nozzle operating

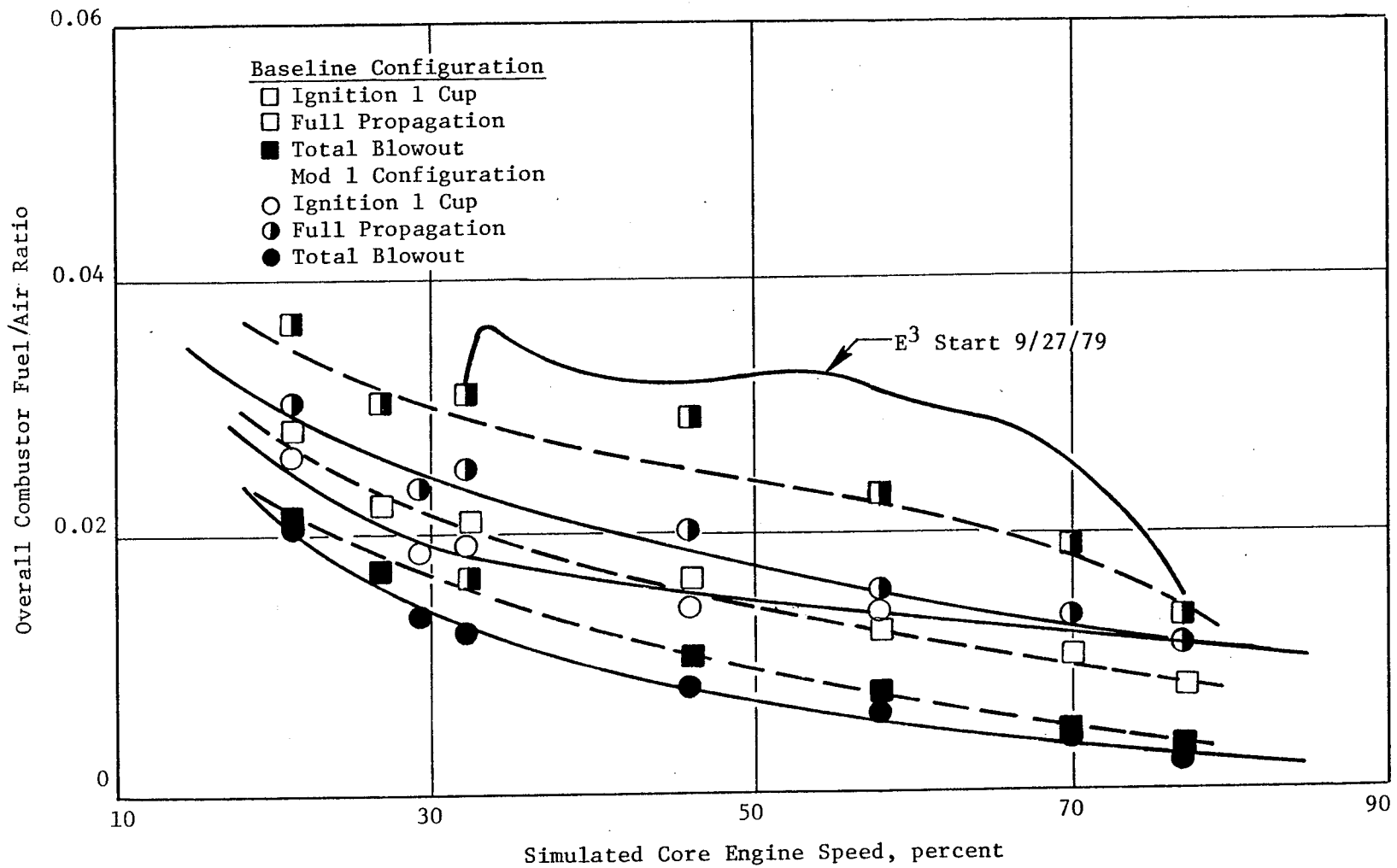


Figure 194. Mod I Atmospheric Ignition Test Results, Pilot Stage.

ORIGINAL PAGE IS
OF POOR QUALITY

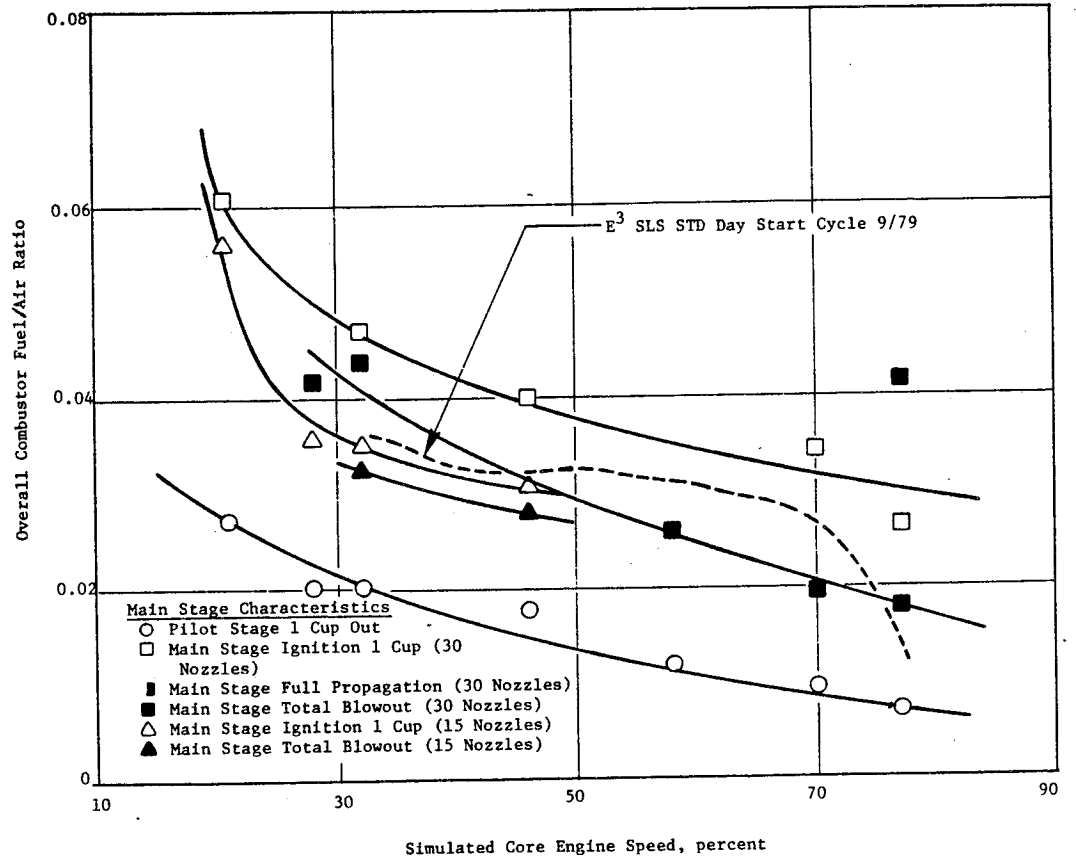


Figure 195. Mod I Atmospheric Ignition Test Results, Main Stage.

mode. However, full or partial propagations were not obtained in this mode. The adverse effects of the greater effective swirl cup spacing eliminated the benefit of locally richer conditions in the vicinity of the fueled swirl cups.⁴ It was observed that the flame in the main stage annulus had difficulty holding position. This flame instability appears to result from the lean stoichiometry and high dome velocities produced from the increased main stage airfoil of this configuration. The main stage swirl cups in the Mod I configuration have approximately a 12% increase in airflow. Overall main stage primary zone airflow is up by 14% compared to levels calculated for the baseline configuration.

6.2.2.7 Atmospheric Exit Temperature Performance Test

Performance testing of the Mod I configuration was also conducted. The purpose of this test was to evaluate the Mod I combustor configuration for profile and pattern factor at simulated sea level takeoff conditions at various pilot and main dome fuel flow ratios. In addition, data were also obtained at both conditions simulating 46% and 58% core engine speed along the E³ September 1979 ground start operating line and at simulated 6% ground idle operating conditions with the pilot stage only fueled. Fuel/air ratios set at both subidle operating conditions were limited to 0.0255 because of the facility fuel pump discharge limitations using the nozzle tips selected for this test. The E³ September 1979 start cycle defines fuel/air ratios of 0.031 and 0.028, respectively, for the 46% and 58% core speed operating conditions. The test point schedule and corresponding combustor operating conditions are presented in Table XLV.

The E³ test rig fuel nozzle assemblies were used for featured nozzle tips rated at 2.3 kg/hr (5 pph) in the pilot stage, and nozzle tips rated at 4.5 kg/hr (10 pph) in the main stage.

Test results obtained at the subidle operating conditions and at the 6% ground idle operating condition are presented in Figure 196. As anticipated with the pilot stage only fueled, the average and maximum profiles are sharply peaked outward. The anticipated attenuation in these outer peaked profiles did not occur. It was interesting to note that the average and maximum profiles at the 6% ground idle condition were more severe than those

Table XLV. Combustor Mod I Atmospheric EGC

Test Point	T_3 , K ($^{\circ}$ R)	P_3 (Atm.)	W_3 , kg/s (pps)	W_{Bleed} kg/s (pps)	W_c , kg/s (pps)	f/a	Pilot Total	W_{fPilot} kg/hr (pph)	W_{fMain} kg/hr (pph)
1	344 (619)	1.00	1.78 (3.92)	0.13 (0.28)	1.65 (3.69)	0.031	1.0	184 (406)	0 0
2	383 (690)	1.00	2.00 (4.40)	0.14 (0.31)	1.86 (4.09)	0.028	1.0	187 (412)	0 0
3	495 (891)	1.00	2.55 (5.60)	0.18 (0.40)	2.36 (5.20)	0.0123	1.0	105 (230)	0 0
4	815 (1467)	1.00	2.41 (5.31)	0.15 (0.34)	2.26 (4.97)	0.0244	0.5	100 (219)	100 (219)
5	815 (1467)	1.00	2.41 (5.31)	0.15 (0.34)	2.26 (4.97)	0.0244	0.4	80 (175)	119 (262)
6	815 (1467)	1.00	2.41 (5.31)	0.15 (0.34)	2.26 (4.97)	0.0244	0.3	60 (131)	139 (306)

ORIGINAL PAGE IS
OF POOR QUALITY

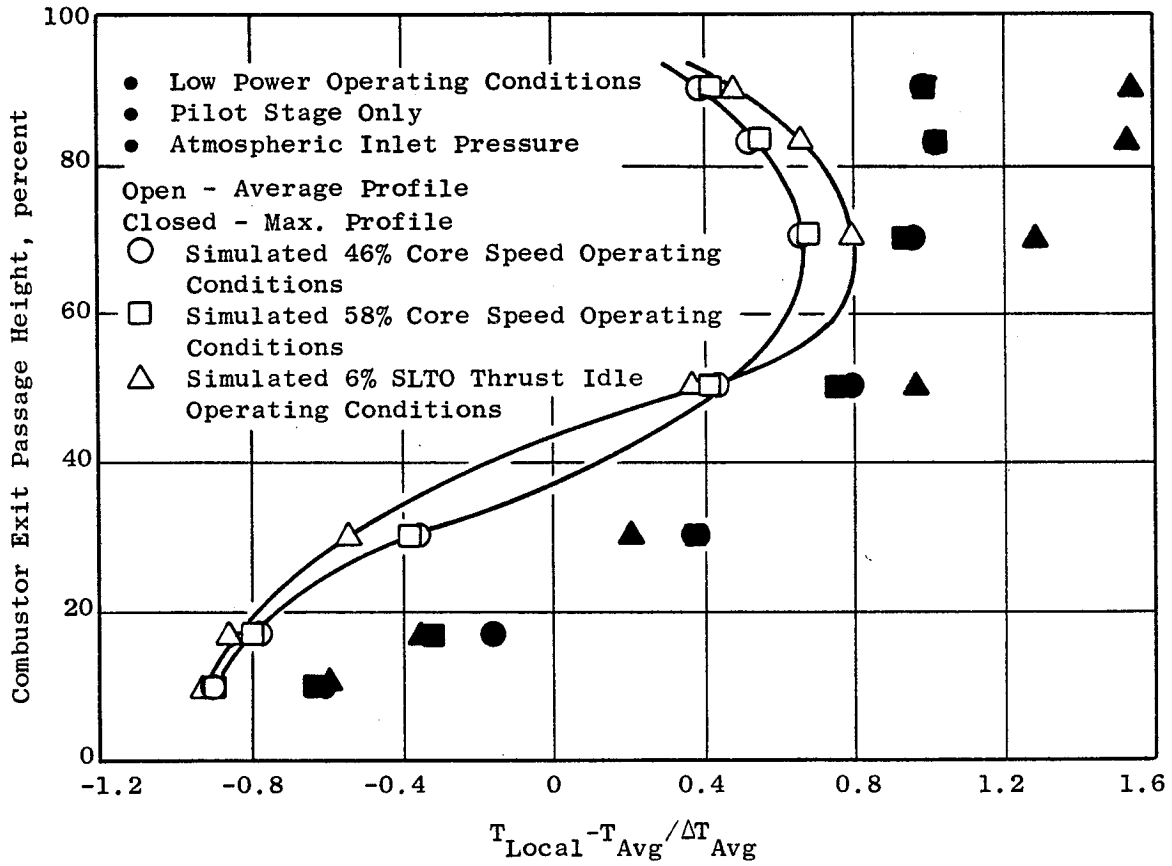


Figure 196. Mod I EGT Performance Test Results, Pilot Only.

obtained at the subidle conditions. This is relative to the lower average gas temperature rise, and high maximum gas temperatures associated with the lower fuel/air ratio (0.0123 as compared to 0.0255) and higher combustion efficiency at the 6% ground idle condition. At all three low power conditions, pattern factors in excess of 1.00 were obtained.

At the simulated SLTO operating conditions, exit gas temperature data were obtained at pilot-to-total fuel splits of 0.5, 0.4, and 0.3. At each fuel split evaluated, full propagation of the fire within the main stage could not be achieved. It was observed that several main stage cups were not burning, while others appeared to be unstable. Attempts to achieve full propagation of the main stage by increasing main stage fuel flow were not successful. As a result, temperature traverse data were obtained at the design fuel/air ratio (0.0244) with a partially burning main stage annulus. An analysis was conducted to explain why full propagation of the main stage could not be achieved. The results indicated that equivalence ratios in the main stage swirl cup were near or below the lean stability limit, as determined from the results of the ground start ignition test.

The exit temperature data that was obtained indicated that a 60° section of the combustor between Cups 9 and 14 had stable main stage combustion at all three fuel splits evaluated. The data obtained from this combustor annulus section was used to determine the average and maximum profiles presented in Figures 197 through 199. At a pilot-to-total fuel flow split of 0.5, the average and maximum profiles are within the limits. A pattern factor of 0.243 was obtained at 90% of the passage height compared to the target value of 0.250. A maximum profile within the required limit was also obtained at a pilot-to-total fuel flow split of 0.4. At this condition, a pattern factor of 0.244 was obtained at 30% of the passage height. However, the average profile exceeded the required limit below 40% of the passage height. At a pilot-to-total fuel flow split of 0.3, both the average and maximum profiles are peaked inward, exceeding the required limits by a considerable amount. At this fuel split, a pattern factor of 0.396 was obtained. The average and maximum profiles obtained from the Mod I combustor configuration show significant improvement in the inner region of the exit passage over the baseline combustor configurations. This probably reflects the large increase in the inner liner trim dilution featured in the Mod I combustor.

ORIGINAL PAGE IS
OF POOR QUALITY

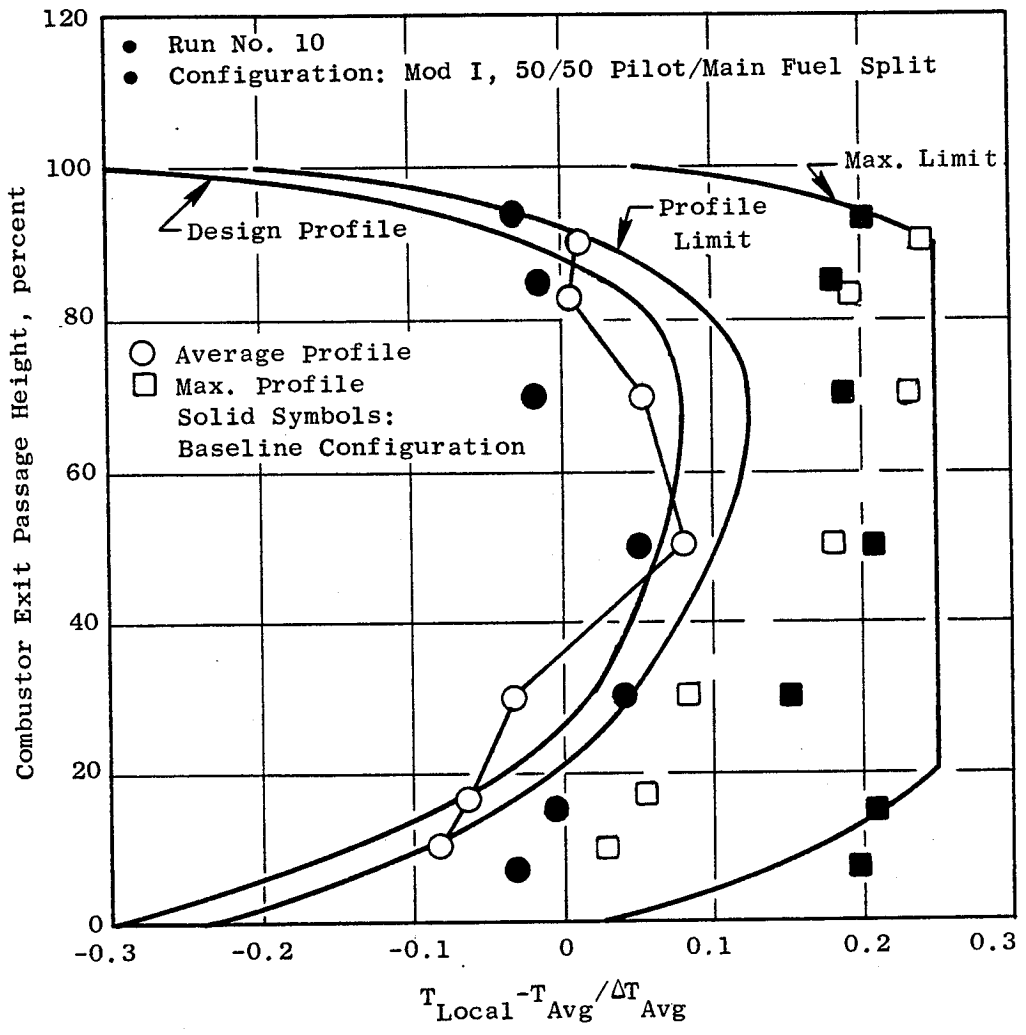


Figure 197. Mod I EGT Performance Test Results, 50/50 Fuel Flow Split.

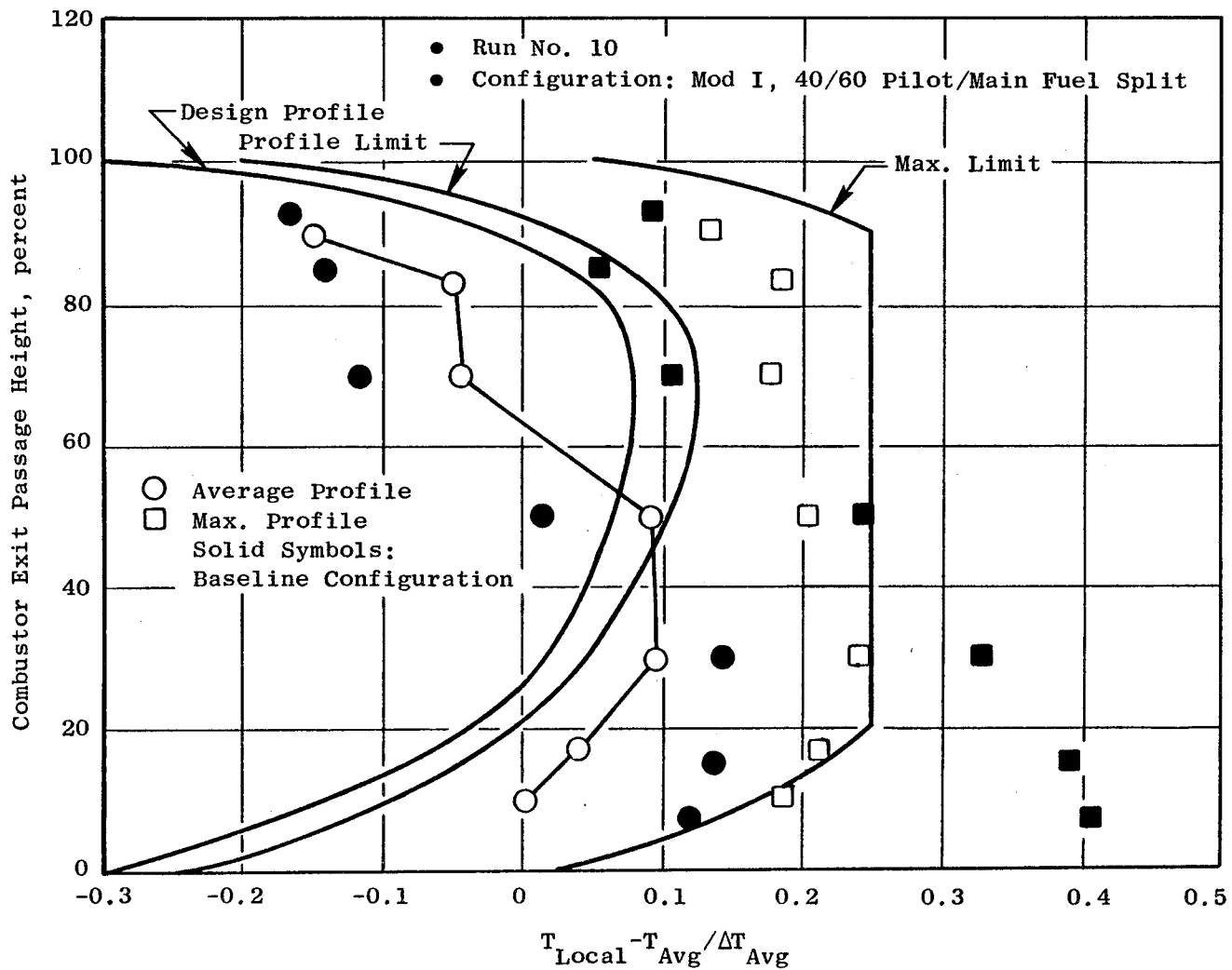


Figure 198. Mod I EGT Performance Test Results, 40/60 Fuel Flow Split.

ORIGINAL PAGE IS
OF POOR QUALITY

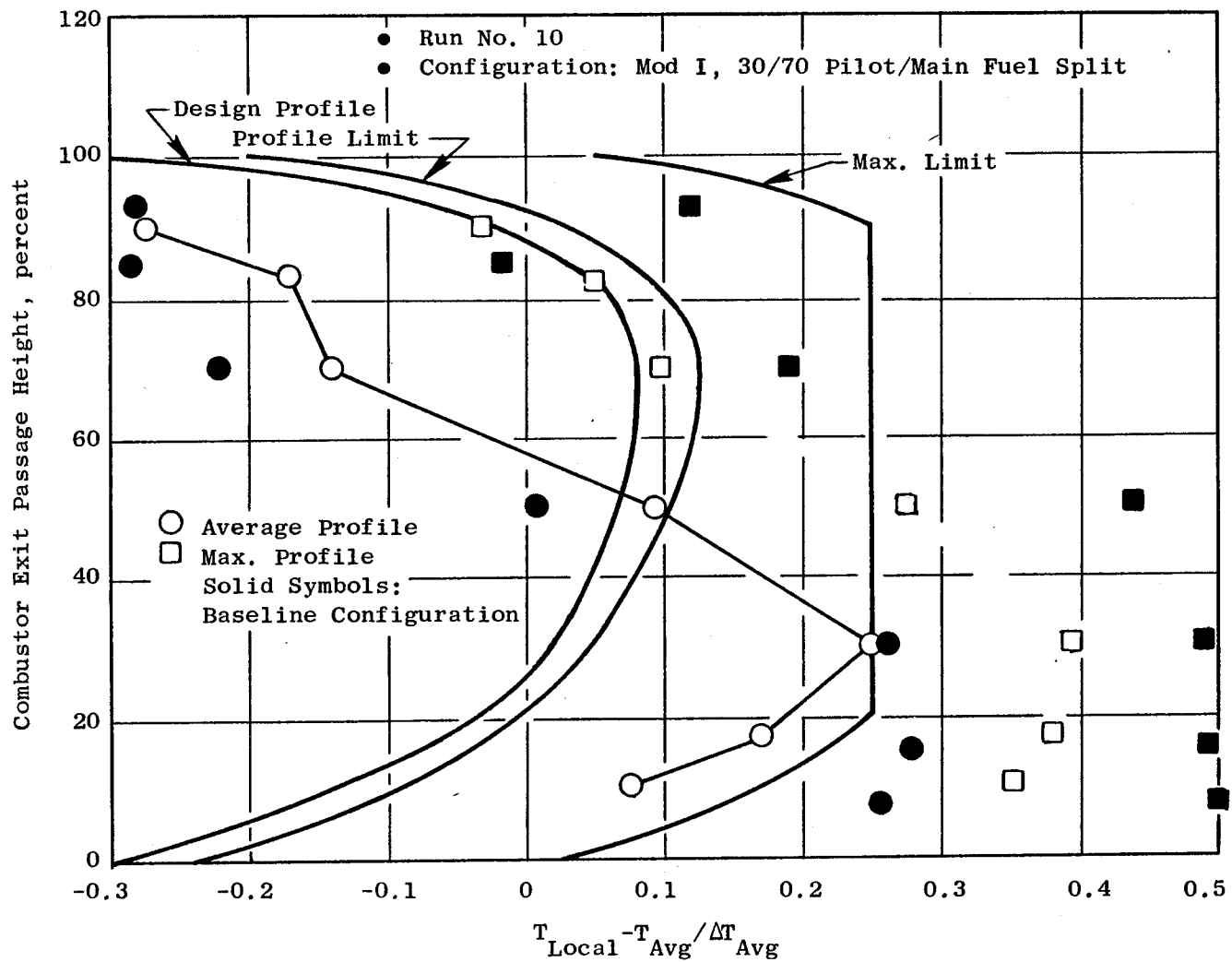


Figure 199. Mod I EGT Performance Test Results, 30/70 Fuel Flow Split.

ORIGINAL PAGE IS
 OF POOR QUALITY

6.2.2.8 Emissions Test

As part of the emissions testing of the Mod I combustor configuration, additional ground start ignition testing was conducted at the actual ground start cycle inlet pressures. Ignition, propagation, and blowout of the pilot and main stages were determined from thermocouples mounted onto the five equally spaced gas sampling rakes located in the test rig instrumentation spool.

The E³ test rig fuel nozzle assemblies were used for this test. Nozzle tips rated at 12 kg/hr (26.5 pph) were installed in the pilot stage. Nozzle tips rated at 23 kg/hr (50.7 pph) were installed in the main stage. These nozzle tips were also used for the low power emissions testing.

The pilot and main stage ignition, propagation, and blowout characteristics obtained at actual ground start cycle combustor inlet pressure conditions are shown in Figure 200. Main stage data presented in this figure are based on the pilot stage operating at a fuel flow level at which full pilot stage propagation was achieved. These data, therefore, represent a worst case statement for the overall fuel/air ratios at which the main stage ignition, propagation, and lean blowout were obtained. In reality, the pilot stage would operate at the lowest fuel flow level at which all 30 swirl cups remained burning. However, since it would be difficult to determine this level in the pressure rig, the above approach was selected. It was observed that the ignition and propagation characteristics of the combustor improve substantially when operated at true cycle pressure conditions, as compared to atmospheric operation. However, little, if any, impact was demonstrated on the blowout characteristics. Even with the pressure performance improvement, the ground start ignition, propagation, and blowout characteristics of the main stage were not adequate to meet the September 1979 engine ground start requirement.

Emissions testing of the Mod I configuration was conducted to evaluate this combustor design for emissions, pressure drop, and metal temperature characteristics at combustor operating conditions along the E³ FPS operating line. The test was conducted in two phases. The first phase involved evaluation at 4% and 6% ground idle conditions. The second phase of the

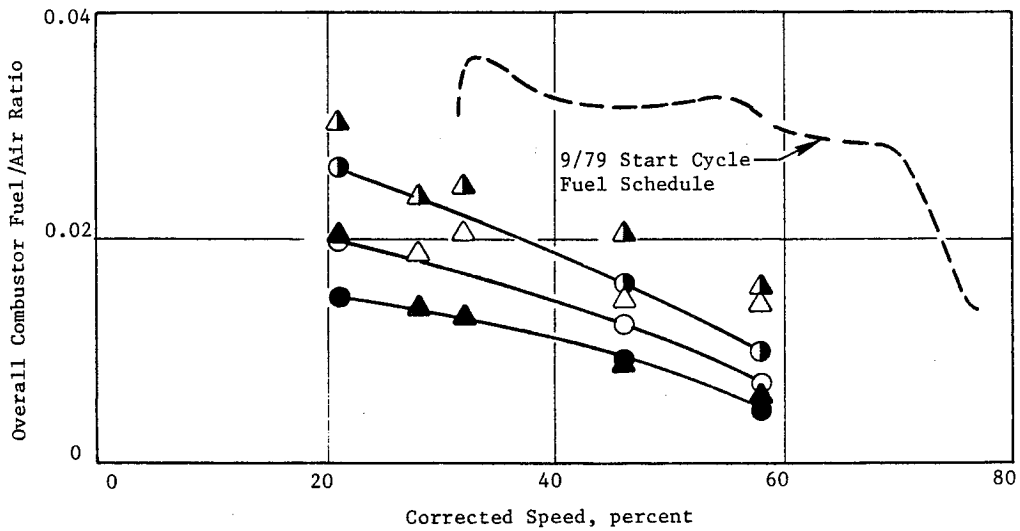
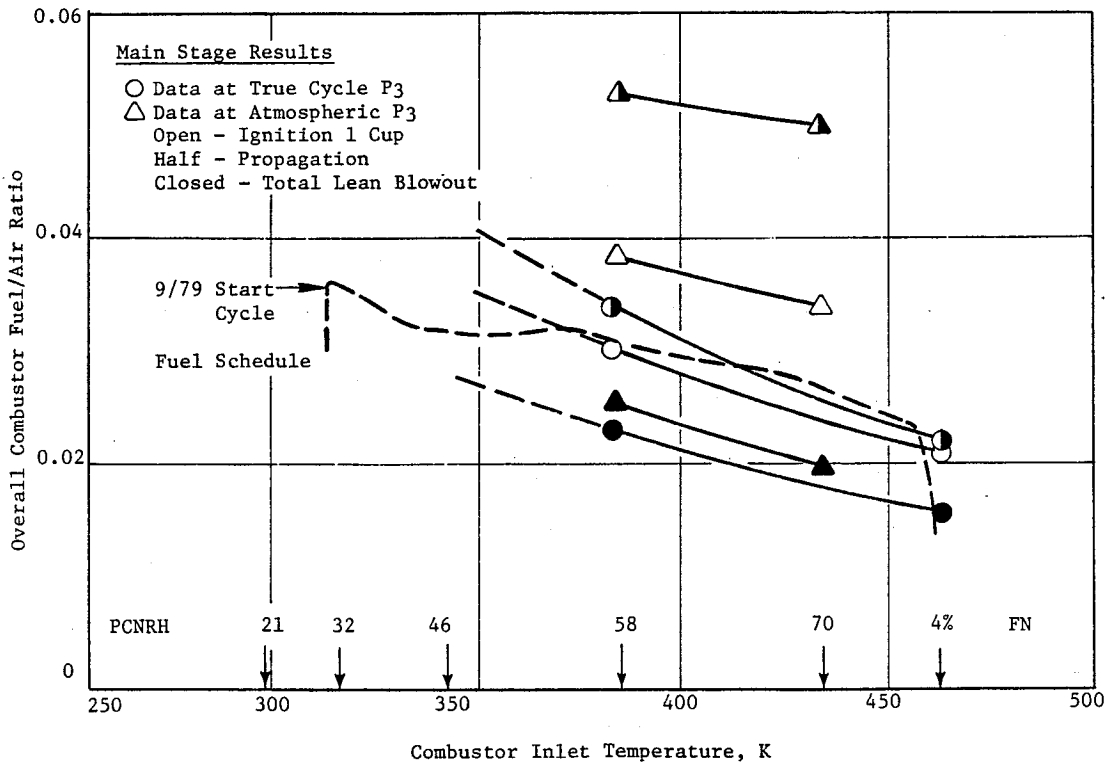


Figure 200. Mod I Ignition Results at True Cycle Conditions.

test was directed at evaluation at higher power operating conditions. This pause in testing was necessary to allow for a change in the fuel nozzle tip sizes in each dome. In the second phase of the test, nozzle tips rated at 23 kg/hr (50 pph) were installed into the pilot stage, while nozzle tips rated at 55 kg/hr (120 pph) were installed into the main stage. It had been intended to evaluate the combustor at 30% approach conditions and at simulated SLTO conditions. However, problems with the facility operation resulted in a severe test schedule time restriction. This time problem coupled with indications of excessively high centerbody metal temperatures prevented the acquisition of all of the desired data. As a result, only a limited amount of high power emissions data was obtained at combustor operating conditions that deviated from the E³ FPS design cycle. Test points and corresponding operating conditions evaluated in this test are presented in Table XLVI.

Combustor instrumentation consisted of 15 static pressures and 27 grounded and capped chromel alumel thermocouples. The locations of this instrumentation on the combustor hardware are illustrated in Figures 201 through 204. In addition, data from numerous pressure and temperature instrumentation affixed to the test rig vehicle were also obtained. This instrumentation included upstream total pressure and air temperature rakes to measure the combustor inlet total pressure and temperatures. Test rig flowpath wall static pressures provided data concerning diffuser system performance while thermocouples were used to monitor the test rig to assure the rig mechanical integrity.

The results of the idle emissions testing on the Mod I combustor configuration are presented in Figures 205 and 206. As observed from Figure 205, CO emission levels of 48 g/kg (48 lbm/1000 lb) of fuel and 30 g/kg (30 lbm/1000 lb) of fuel were obtained, respectively, at the 4% and 6% ground idle design cycle operating conditions. These compare to levels of 59.9 g/kg (59.9 lbm/1000 lb) of fuel and 57.5 g/kg (57.5 lbm/1000 lb) of fuel demonstrated during evaluation of the baseline configuration. At 6% ground idle, the minimum CO emission level occurred at the design cycle fuel/air ratio. It has been estimated that a CO emission level of 20.7 g/kg (20.7 lbm/1000 lb) of fuel at the 6% ground idle operating condition would satisfy the E³ Program CO emission goal. HC emission levels of 5.5 g/kg (5.5 lbm/1000 lb) of fuel and 4.0 g/kg (4.0 lbm/1000 lb) of fuel were obtained, respectively, at the 4% and

Table XLVI. Combustor Mod I Emissions Test Point Schedule.

Operating Condition	P ₃ , MPa (psia)	T ₃ , K (°R)	W ₃ , kg/s (pps)	W _{Bleed} Outer, kg/s (pps)	W _{Bleed} Inner, kg/s (pps)	W _{Bleed} Prediff, kg/s (pps)	W _c , kg/s (pps)	f/a, Overall	Pilot Total	W _{fPilot} kg/hr (pph)	W _{fMain} kg/hr (pph)
4% Idle	0.344 (49.9)	466 (839)	9.55 (21.0)	0.55 (1.2)	0.50 (1.1)	0.59 (1.3)	7.86 (17.3)	0.009	1.0	255 (561)	0
4% Idle	0.344 (49.9)	466 (839)	9.55 (21.0)	0.55 (1.2)	0.50 (1.1)	0.59 (1.3)	7.86 (17.3)	0.0120	1.0	340 (747)	0
4% Idle	0.344 (49.9)	466 (839)	9.55 (21.0)	0.55 (1.2)	0.50 (1.1)	0.59 (1.3)	7.86 (17.3)	0.0138	1.0	390 (858)	0
4% Idle	0.344 (49.9)	466 (839)	9.55 (21.0)	0.55 (1.2)	0.50 (1.1)	0.59 (1.3)	7.86 (17.3)	0.0200	1.0	566 (1246)	0
6% Idle	0.436 (63.3)	495 (891)	12.32 (27.1)	0.73 (1.6)	0.64 (1.4)	0.77 (1.7)	10.18 (22.4)	0.009	1.0	330 (726)	0
6% Idle	0.436 (63.3)	495 (891)	12.32 (27.1)	0.73 (1.6)	0.64 (1.4)	0.77 (1.7)	10.18 (22.4)	0.0110	1.0	403 (887)	0
6% Idle	0.436 (63.3)	495 (891)	12.32 (27.1)	0.73 (1.6)	0.64 (1.4)	0.77 (1.7)	10.18 (22.4)	0.0123	1.0	451 (992)	0
6% Idle	0.436 (63.3)	495 (891)	12.32 (27.1)	0.73 (1.6)	0.64 (1.4)	0.77 (1.7)	10.18 (22.4)	0.0150	1.0	550 (1210)	0
6% Idle	0.436 (63.3)	495 (891)	12.32 (27.1)	0.73 (1.6)	0.64 (1.4)	0.77 (1.7)	10.18 (22.4)	0.0200	1.0	733 (1613)	0
High Power	1.664 (241.3)	702(1264)	34.82 (76.6)	1.64 (3.6)	1.55 (3.4)	3.45 (7.6)	28.14 (61.9)	0.0197	0.4	785 (728)	1205 (2652)
High Power	1.667 (241.7)	698(1256)	34.77 (76.5)	1.82 (4.0)	1.68 (3.7)	3.05 (6.7)	28.23 (62.1)	0.0226	0.4	873 (1920)	1423 (3130)

ORIGINAL PAGE IS
OF POOR QUALITY

ORIGINAL PAGE IS
OF POOR QUALITY

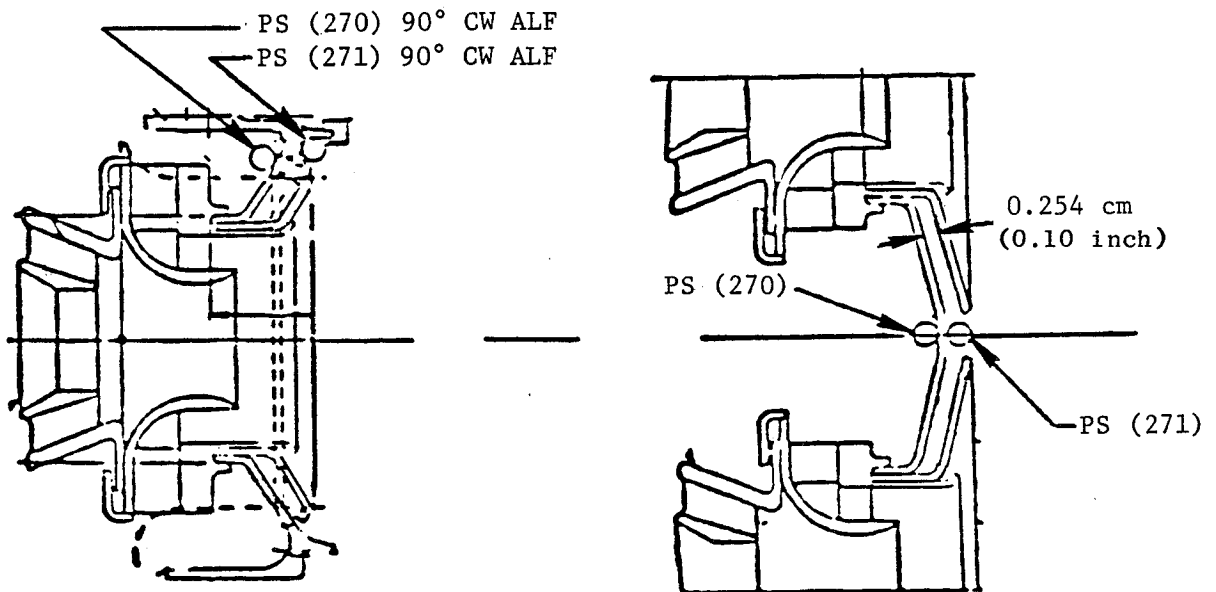
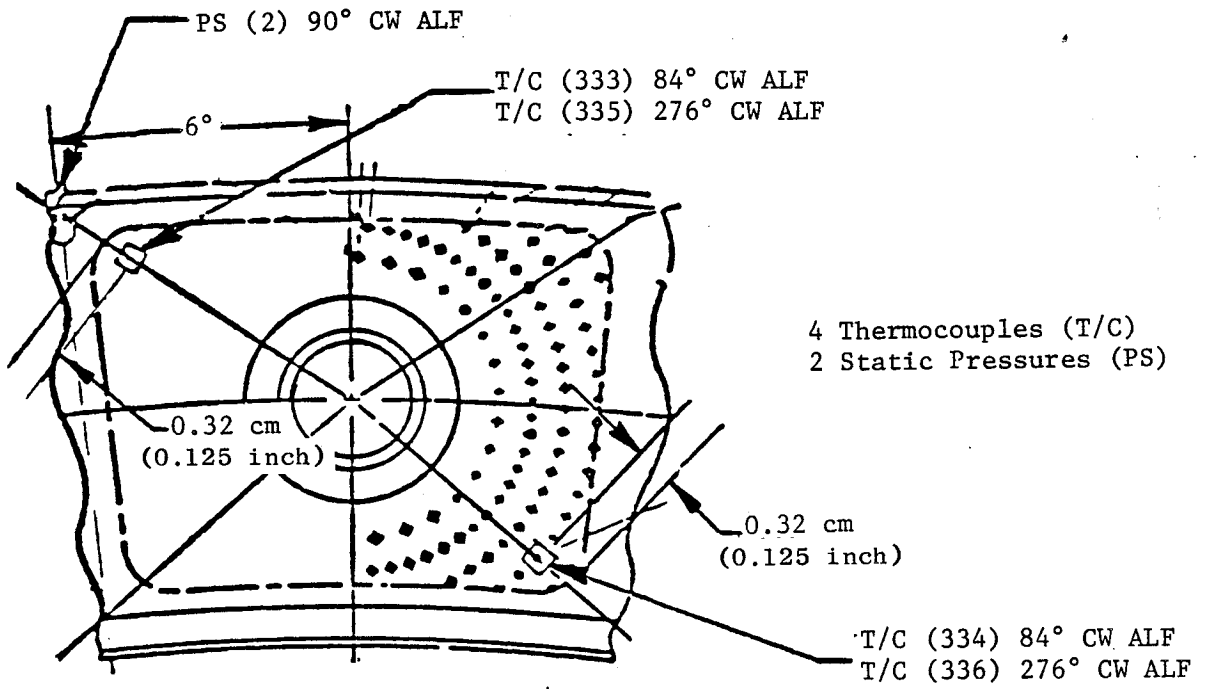
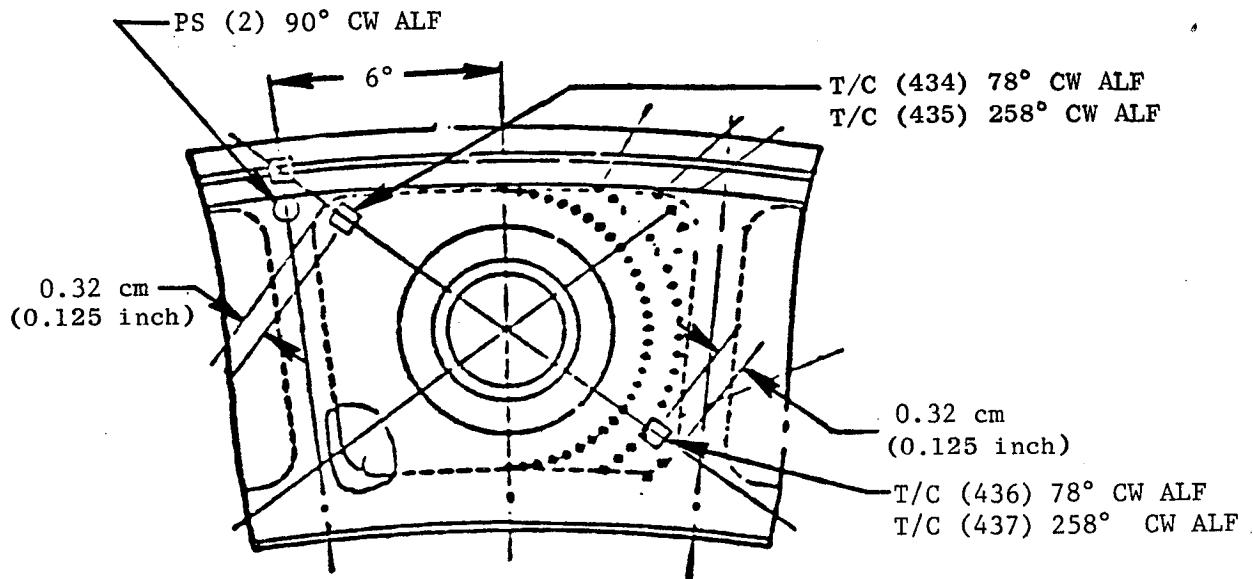


Figure 201. Mod I Combustor Instrumentation Layout,
Pilot Stage.

ORIGINAL PAGE IS
OF POOR QUALITY



4 Thermocouples (T/C)
2 Static Pressures (PS)

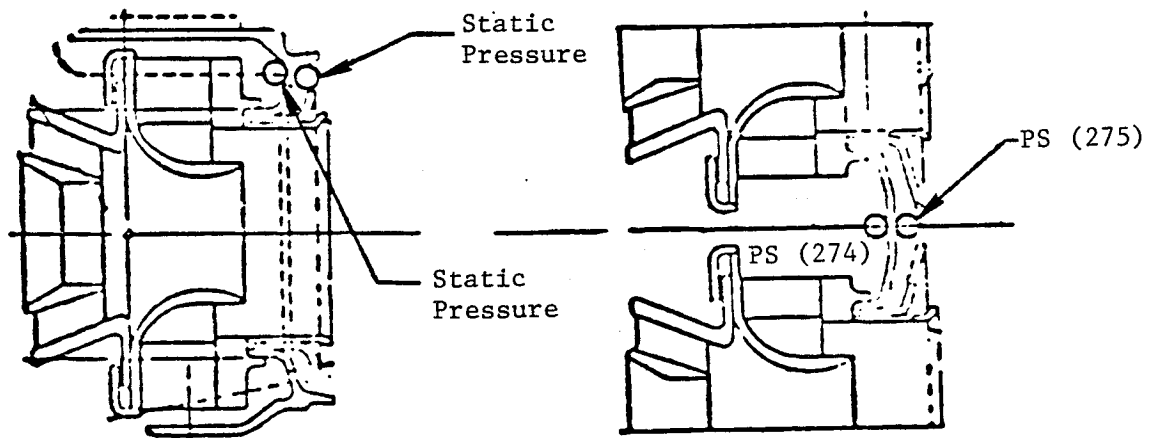


Figure 202. Mod I Combustor Instrumentation Layout, Main Stage.

ORIGINAL PAGE IS
OF POOR QUALITY

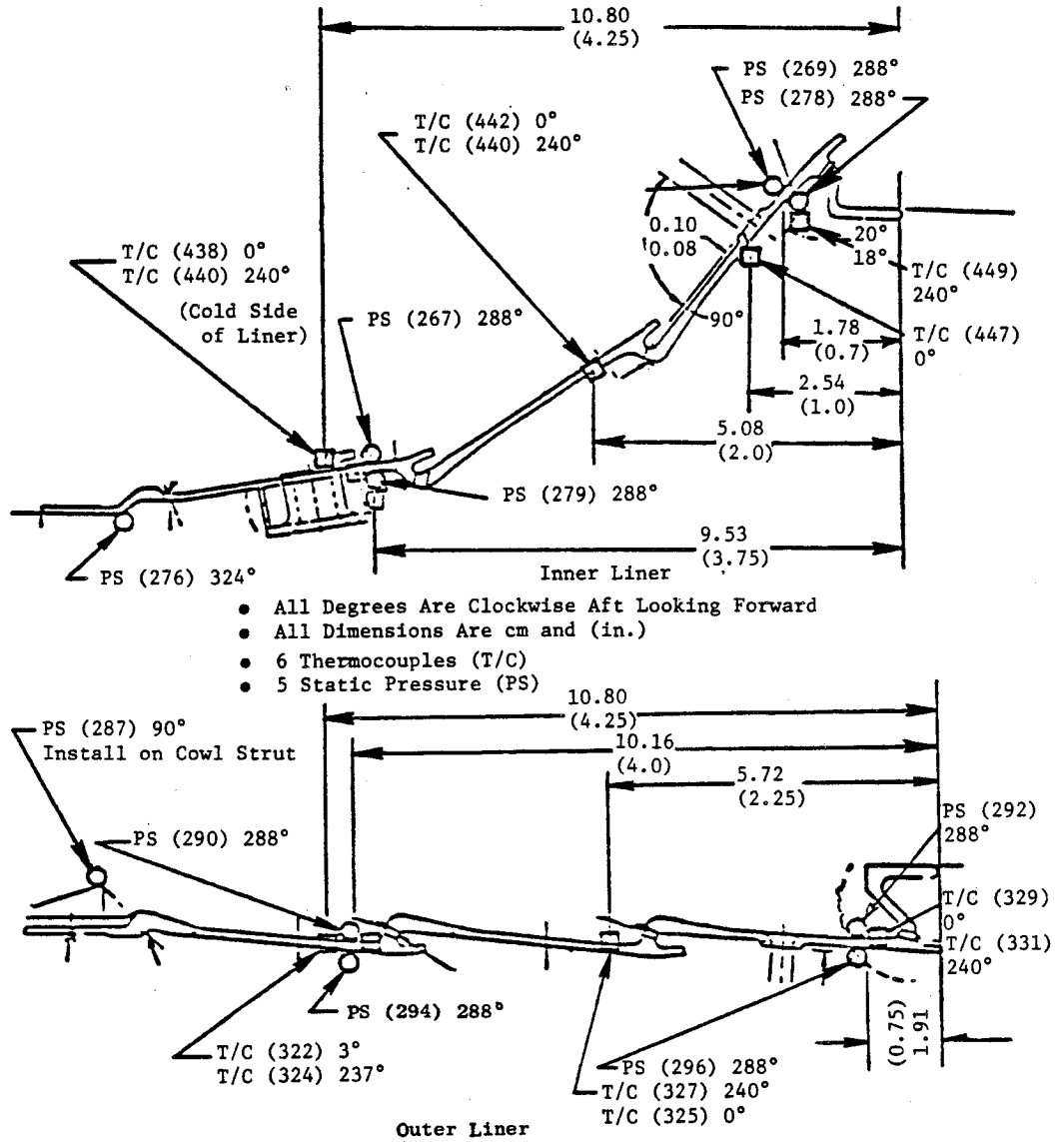


Figure 203. Mod I Combustor Instrumentation Layout, Outer and Inner Liners.

ORIGINAL PAGE IS
OF POOR QUALITY

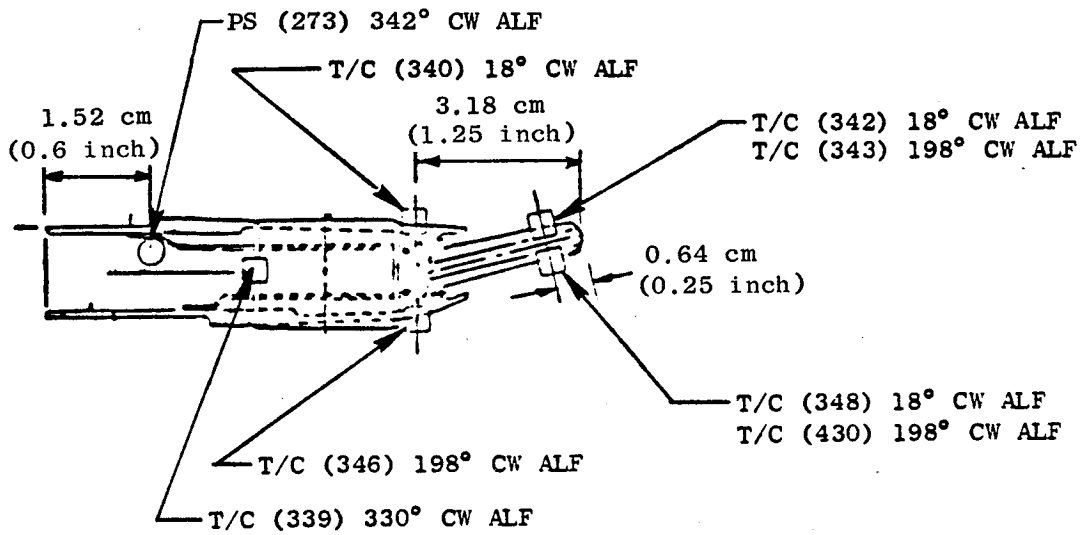


Figure 204. Mod I Combustor Instrumentation Layout,
Centerbody.

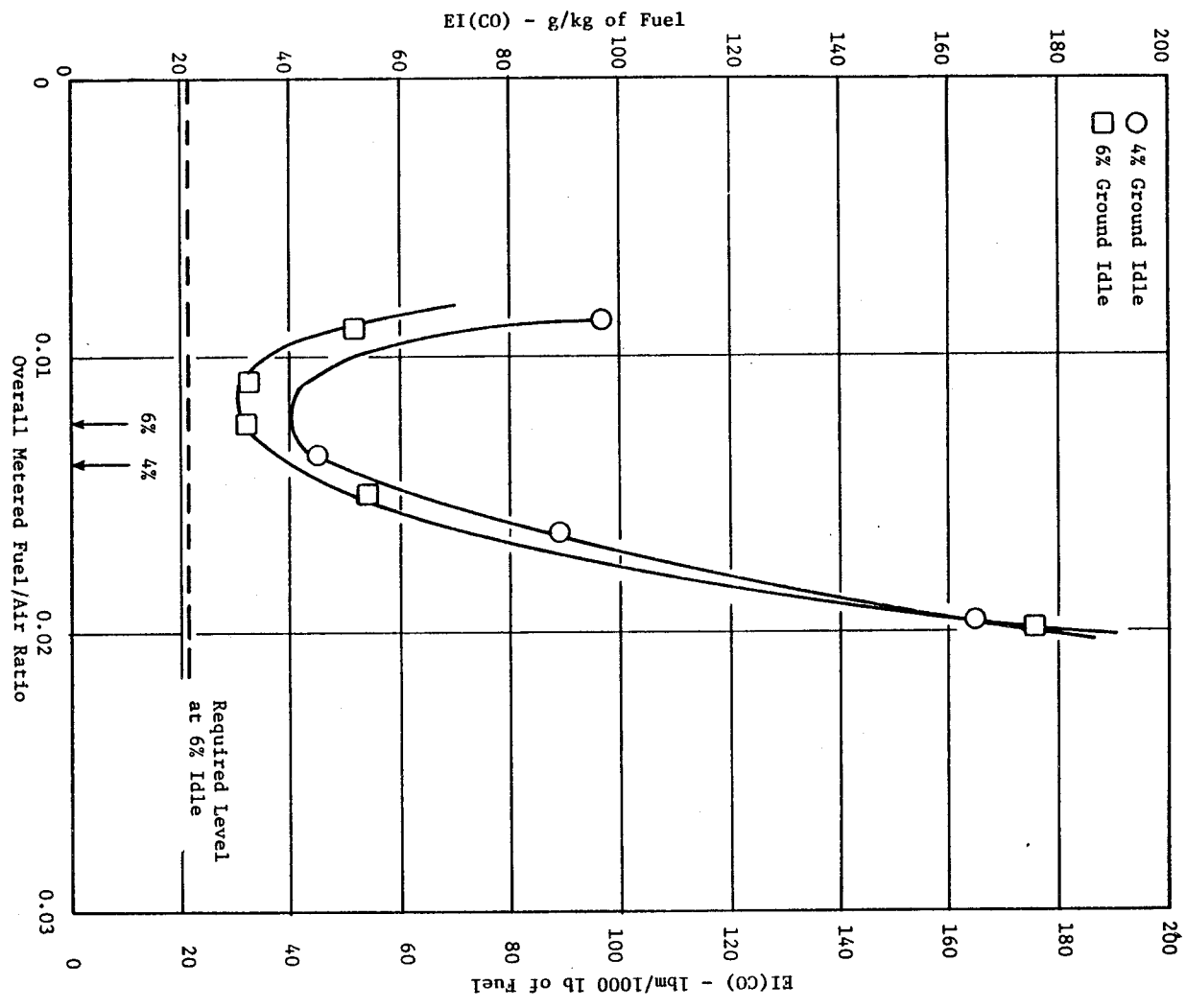


Figure 205. Mod I Emissions Test Results,
EI(CO) at Idle.

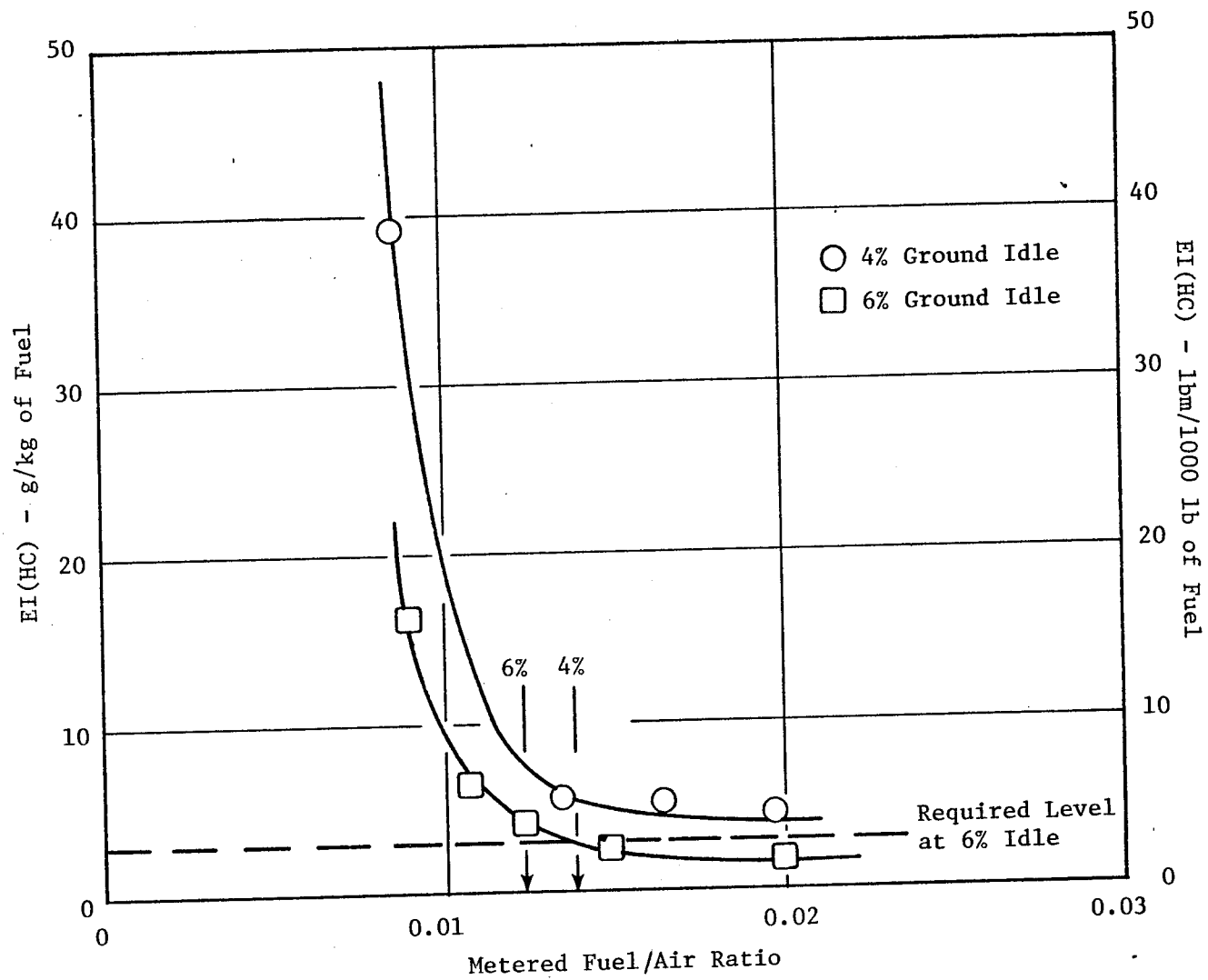


Figure 206. Mod I Emissions Test Results, EI_{HC} at Idle.

ORIGINAL PAGE IS
 OF POOR QUALITY

6% ground idle design cycle operating conditions. Levels of 36 g/kg (36 lbm/1000 lb) of fuel and 22.5 g/kg (22.5 lbm/1000 lb) of fuel were demonstrated during evaluation of the baseline configuration. A HC emission index of 3.0 g/kg (3.0 lbm/1000 lb) of fuel has been estimated as the required level of 6% ground idle to satisfy the program HC emission goal. HC levels at or below this target goal were demonstrated at 6% ground idle operating conditions at metered overall fuel/air ratios greater than 0.014.

Prior to testing, each element of the five gas sampling rakes was flowed to determine if all elements of each rake were open and flowing freely. The results of this check indicated that, in general, the flow from the elements of each rake was unbalanced. Elements sampling the inner region of the combustor exit annulus flowed more than those in the outer region. Attempts were made to clear restrictions in the elements and obtain better uniformity. Although these efforts improved the situation, partial restrictions remained in some outer elements of the rakes. During the low power emissions testing, gas sampling problems were experienced. It was evident that as time progressed, the sampling problem became more severe, as illustrated in Figures 207. By the conclusion of the low power emissions testing, one rake became almost totally restricted, while the others obtained samples which biased the unfueled inner annulus region. This problem lends suspicion to the quality of the emissions data obtained.

Time restrictions and facility-related problems experienced during the high power emissions evaluation prevented the acquisition of data at 30% approach operating conditions. While attempting to establish the simulated SLTO operating conditions, indications of excessively high centerbody metal temperatures were observed. It was decided to obtain emissions and performance data at the combustor operating conditions existing at the time and not continue the test in order to prevent possible damage to the combustor hardware. These combustor operating conditions were not representative of the E³ FPS design cycle. NO_x emission data obtained at these conditions were plotted against the E³ design cycle severity parameter. This yields a linear relation that can be used for extrapolating to the high power operating conditions. The resulting NO_x emission characteristics, shown in Figure 208, yields a NO_x emission index of 17.7 g/kg (17.7 lbm/1000 lb) of fuel at the E³ SLTO condition.

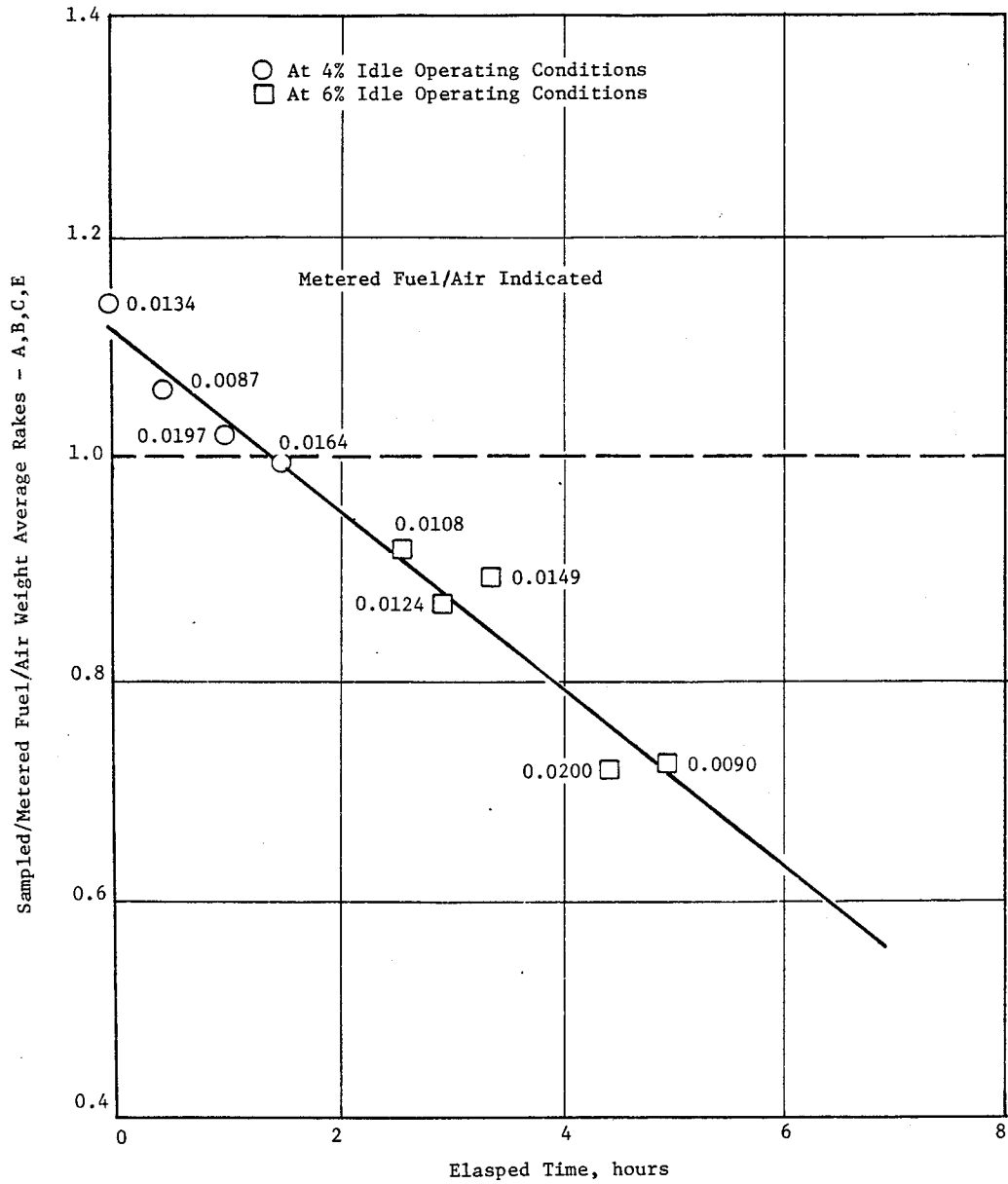


Figure 207. Rake Gas Sample Level at Idle.

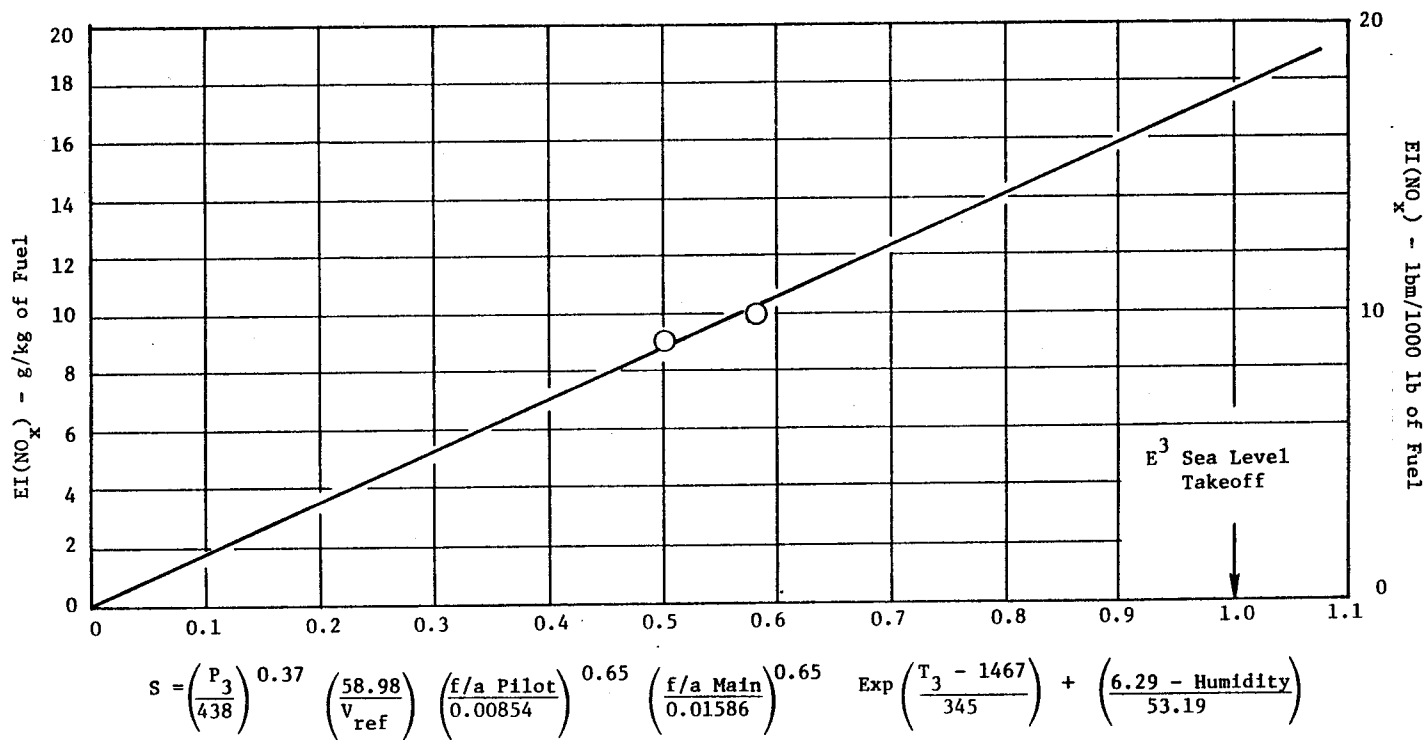


Figure 208. Mod I Emissions Test Results,
EI_{NO_x}.

This is nearly identical to the NO_x emissions levels obtained with the baseline configuration. At the SLTO condition, a NO_x emission level of 17.5 g/kg (17.5 lbm/1000 lb) of fuel had been estimated as required to satisfy the E³ Program NO_x emission goal. Unfortunately, at the high power condition evaluated, additional fuel splits could not be evaluated. Thus insufficient data were obtained to determine what fuel split would produce the lowest NO_x emission level.

Prior to conducting the high power emissions test, the gas sampling rakes were flow checked and cleaned out as much as possible. As before, this procedure failed to achieved a satisfactory rake element flow distribution. Thus emissions data obtained at the high power conditions reflected similar sampling problems as experienced during low power emissions testing. At the conclusion of the high power emissions testing, it was observed that two outer elements of one gas sampling rake and a single outer element of another rake had been burned away. This problem was determined to be related to insufficient water cooling caused by setting water pressure levels too low for the size water hose used in the test rig instrumentation spool.

EPA parameter numbers, based on the EPA landing/takeoff cycle for CO, HC, and NO_x were generated for combustor operation at 6% ground idle and pilot only at approach. Because of the lack of data at the approach and climb operating conditions, results obtained with the baseline combustor configuration at these conditions were used. These EPAP results are compared against those determined for the baseline configuration and the E³ Program goals in Table XLVII.

Table XLVII. Mod I Combustor EPAP Results.

<ul style="list-style-type: none"> ● 6% Ground Idle ● Pilot Only at Approach ● Jet A Fuel ● FPS Design Cycle 			
	EPAP* CO	EPAP* HC	EPAP* NO _x
Mod I	4.55	0.57	2.81
Baseline	8.22	3.10	2.81
E ³ Program Goals	3.0	0.40	3.0
*lb/1000 lb thrust-hour/cycle			

This table shows that significant improvements in CO and HC emissions were achieved compared to the baseline configuration. CO and HC emissions closely approached their respective goals. The NO_x emission levels demonstrated would meet the goal.

At the 6% ground idle design cycle operating condition, data from pressure taps located in the diffuser section of the test rig were used to calculate total pressure losses, thus providing a measurement of the performance of the split duct diffuser. An insufficient amount of usable data was obtained at the high power condition to make an assessment of the diffuser performance at these test conditions. Total and static pressures upstream of the diffuser inlet were used to calculate the velocity profile in the test rig passage at the inlet of the diffuser. This profile in the form of the local-to-average Mach number ratio is shown in Figure 209. The profile is flat, peaked only 1.6% above average, slightly inward from the center of the passage. Calculated diffuser total pressure losses are presented in Table XLVIII. These values are compared with losses calculated from measured data obtained from evaluation of the baseline combustor configuration at simulated SLTO operating conditions, and to losses measured in the full-annular diffuser model subcomponent tests with a flat inlet velocity profile and passage flow splits similar to those calculated for the Mod I combustion system. In general, the test rig diffuser performance calculated from the Mod I test data agrees well with the performance calculated for the baseline combustor test and the diffuser model test. However, the Mod I data shows a sharp increase in the inner dome loss. This was probably due to instrumentation problems. Because of damaged instrumentation, pressure losses for the centerbody and the outer dome flow streams could not be determined.

Table XLVIII. Calculated Diffuser Performance for Mod I Test.

$\Delta P/P, \%$	Mod I Configuration	Baseline Configuration	Diffuser Test Flat Profile
Total Outer	3.78	3.69	4.04
Total Inner	3.14	2.78	3.05
Centerbody	No Data	2.30	2.77
Outer Dome	No Data	2.53	1.16
Inner Dome	2.57	1.72	1.47

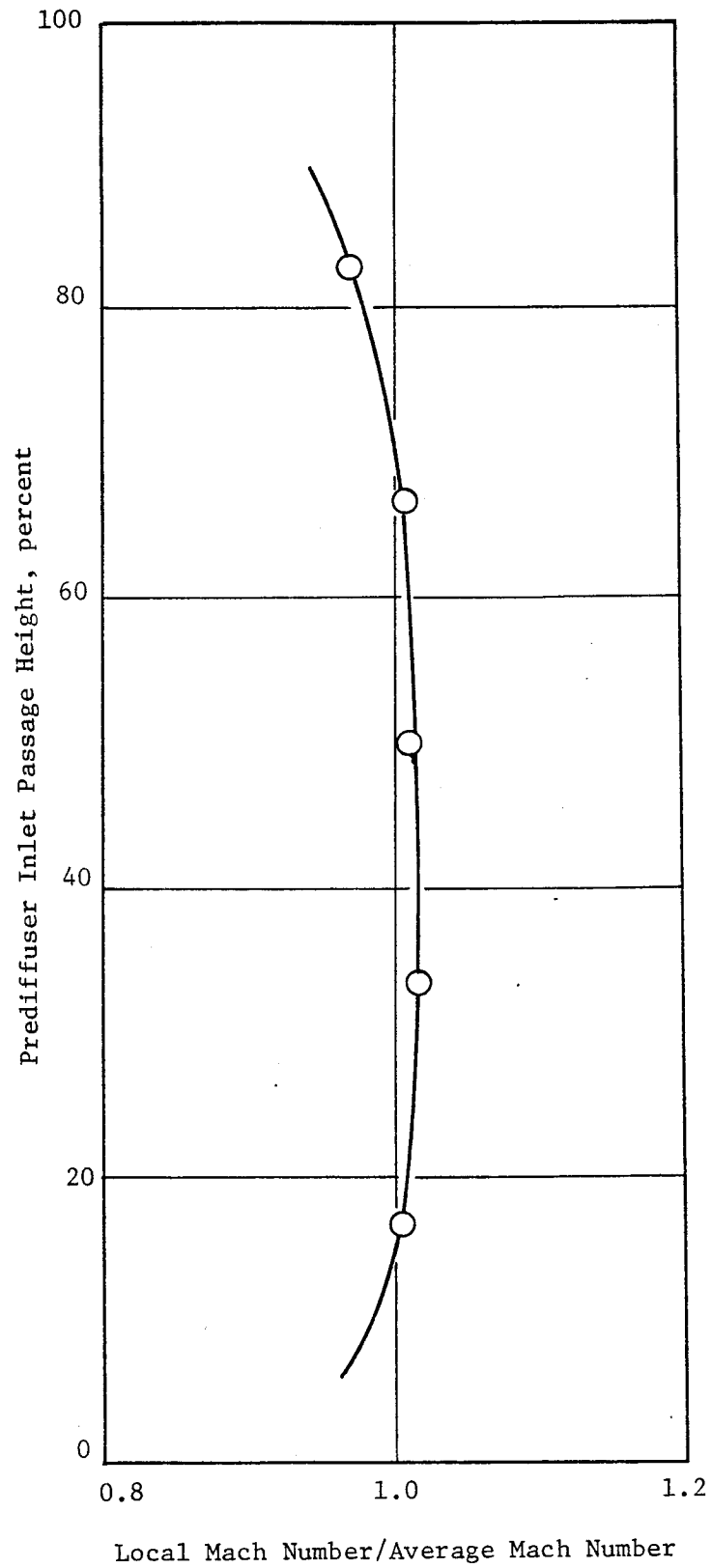
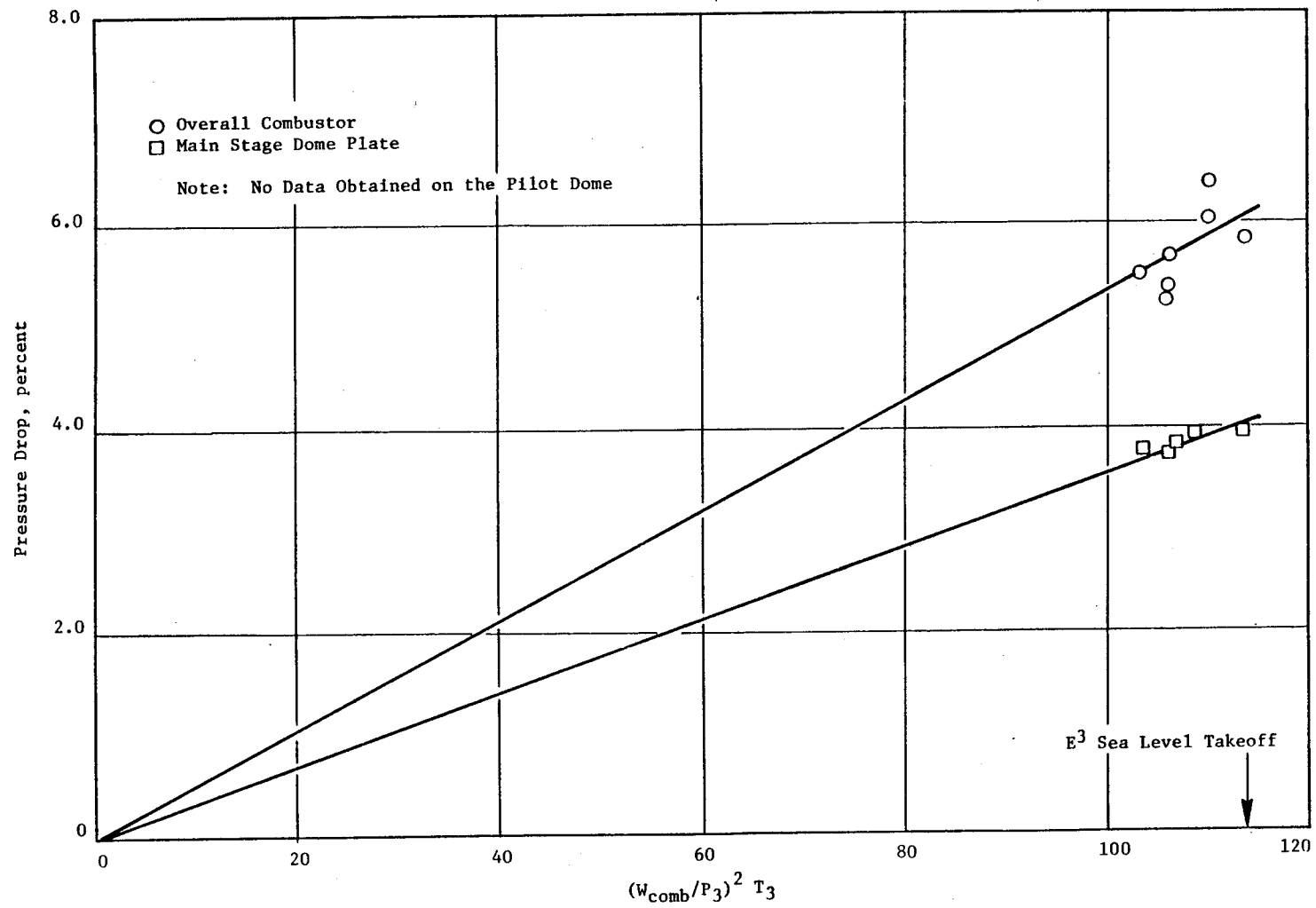


Figure 209. Diffuser Inlet Mach Number Profile (Mod I Test).

Measured overall combustor pressure drops and main stage pressure drops were plotted against the square of the combustor inlet flow function parameter along the E³ FPS design cycle operating line in Figure 210. The pilot stage dome pressure drop characteristics could not be obtained because of the damaged upstream pressure instrumentation. At SLTO operating conditions, an overall combustor pressure drop of 6% is estimated. This compared to a value of 5.5% measured in the baseline combustor test and the engine combustor design value of 5.0%. The measured total combustor flow area of the Mod I configuration was nearly identical to the baseline configuration. The higher-than-anticipated overall total pressure loss was related to the difficulty that appeared to be associated with facility hookup problems. Since the gas sampling rakes were used to measure exit total pressure, the sample line restrictions evident during testing also contributed. Pressure drops across the liners were between 2% and 3%. Because of damaged instrumentation, pressure drops across the centerbody structure could not be determined.

Combustor metal temperatures measured during emissions testing are plotted against the combustor inlet temperature in Figures 211 through 220. The locations of these temperatures can be obtained by locating the specific thermocouple item number on the combustor instrument layout presented in Figures 201 through 204. As discussed earlier, excessively high metal temperatures indicated on the centerbody structure contributed to the premature termination of high power emissions testing. It was later determined that five of the six thermocouples located on the centerbody had secondary junctions exposed to the hot gas stream. Thus the validity of indicated temperatures from these thermocouples is highly questionable. This is supported by detailed inspection of the centerbody hardware, which did not reveal any indication of high metal temperatures. Thermocouple Item 340 on the pilot side of the centerbody had no indications of secondary junctions. Pilot dome splash plate temperatures 139 K (250° R) above the combustor inlet temperature were indicated, an increase of approximately 83 K (150° F) over temperatures measured on the baseline combustor configuration. This change was less than anticipated based on the large reduction in the pilot stage splash plate cooling flow featured in the Mod I combustor configuration. With the exception of outer liner Panel 2, indicated liner metal temperatures generally decreased, compared to the baseline levels. The decrease was more substantially along the inner liner. It



ORIGINAL PAGE IS
 OF POOR QUALITY

Figure 210. Measured Pressure Losses for Mod I Combustor.

ORIGINAL PAGE IS
OF POOR QUALITY

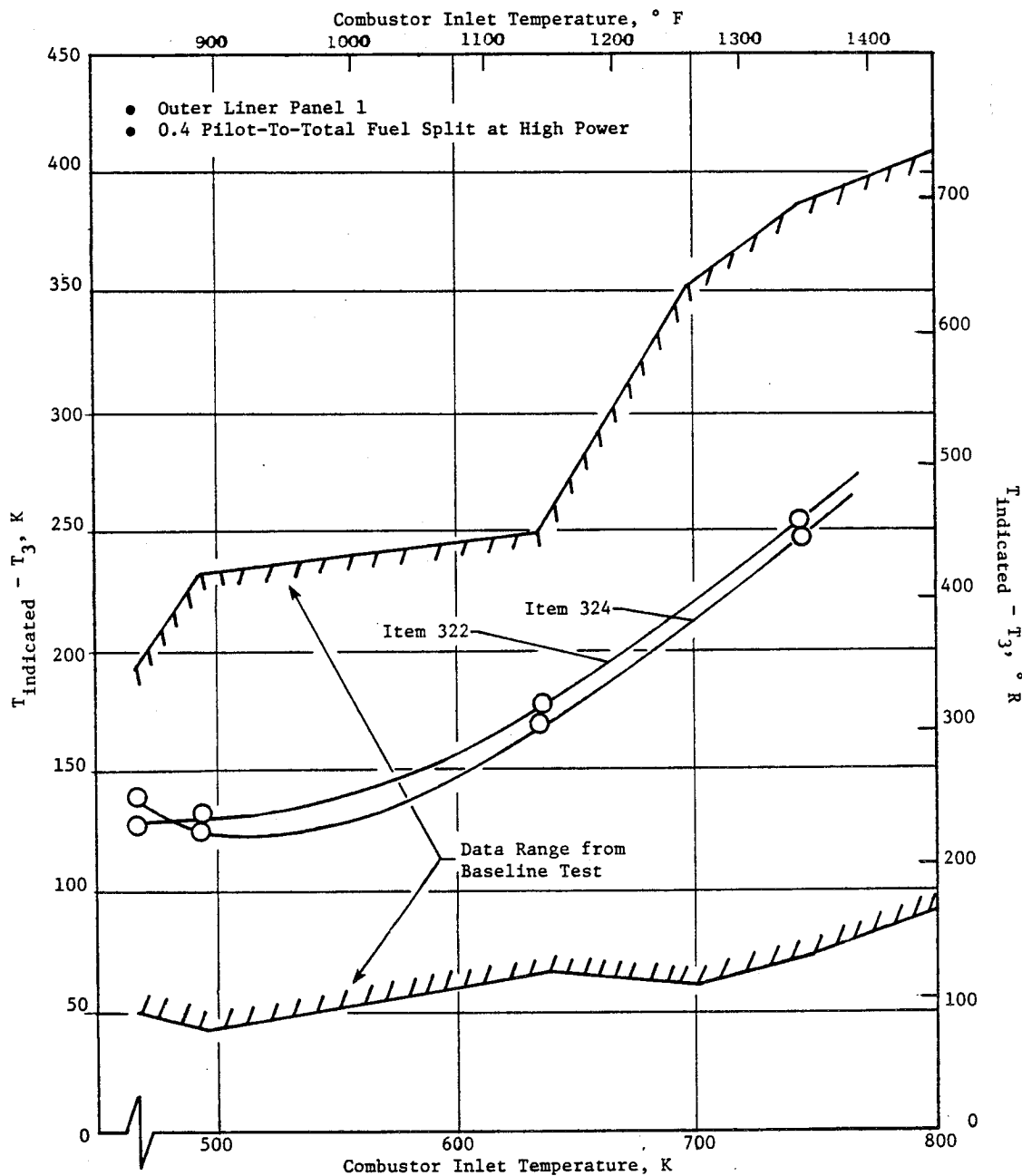


Figure 211. Measured Combustor Metal Temperatures for Mod I Test, Panel 1, Outer Liner.

ORIGINAL PAGE IS
OF POOR QUALITY

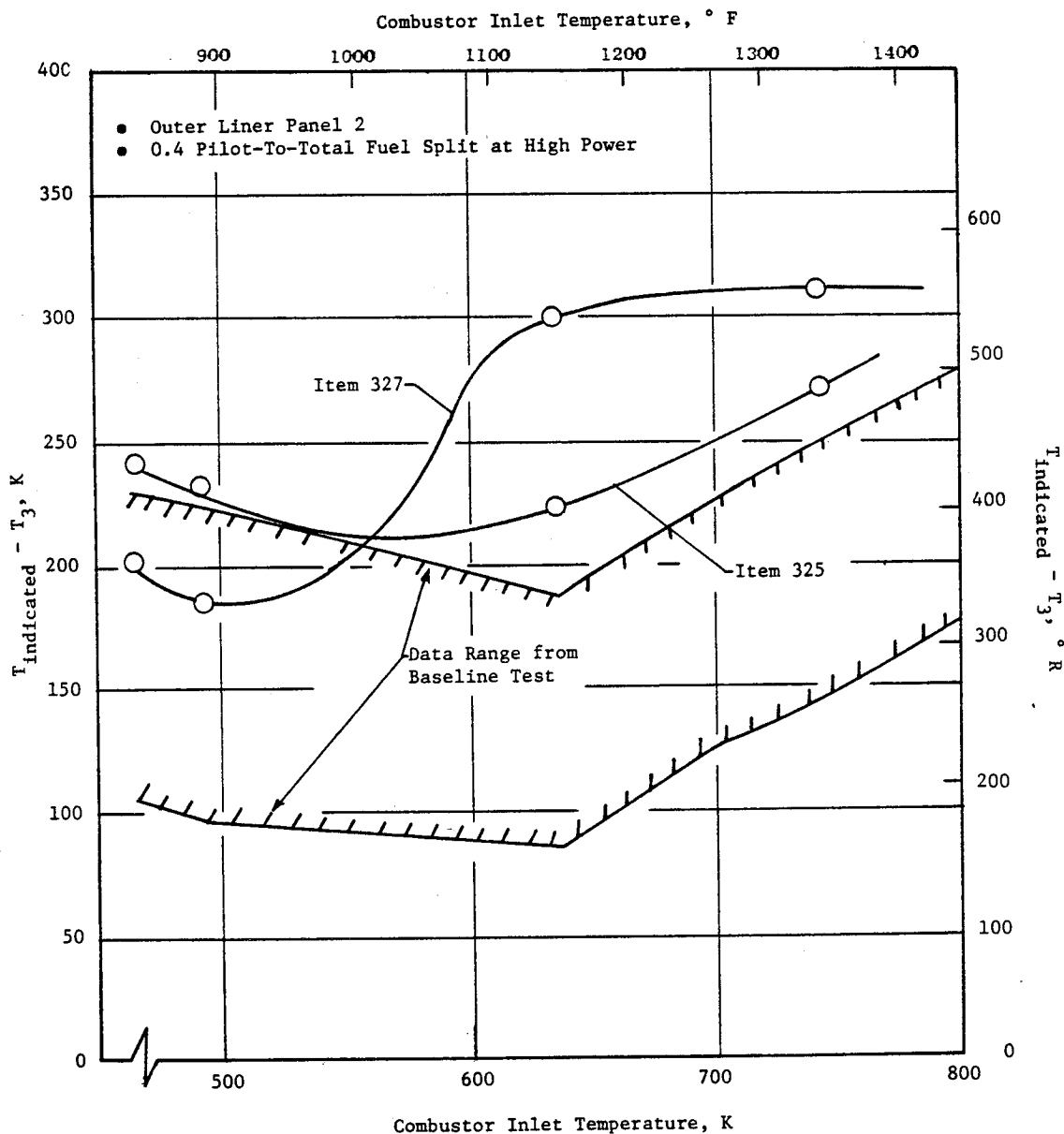


Figure 212. Measured Combustor Metal Temperatures for Mod I Test, Panel 2, Outer Liner.

ORIGINAL PAGE IS
OF POOR QUALITY

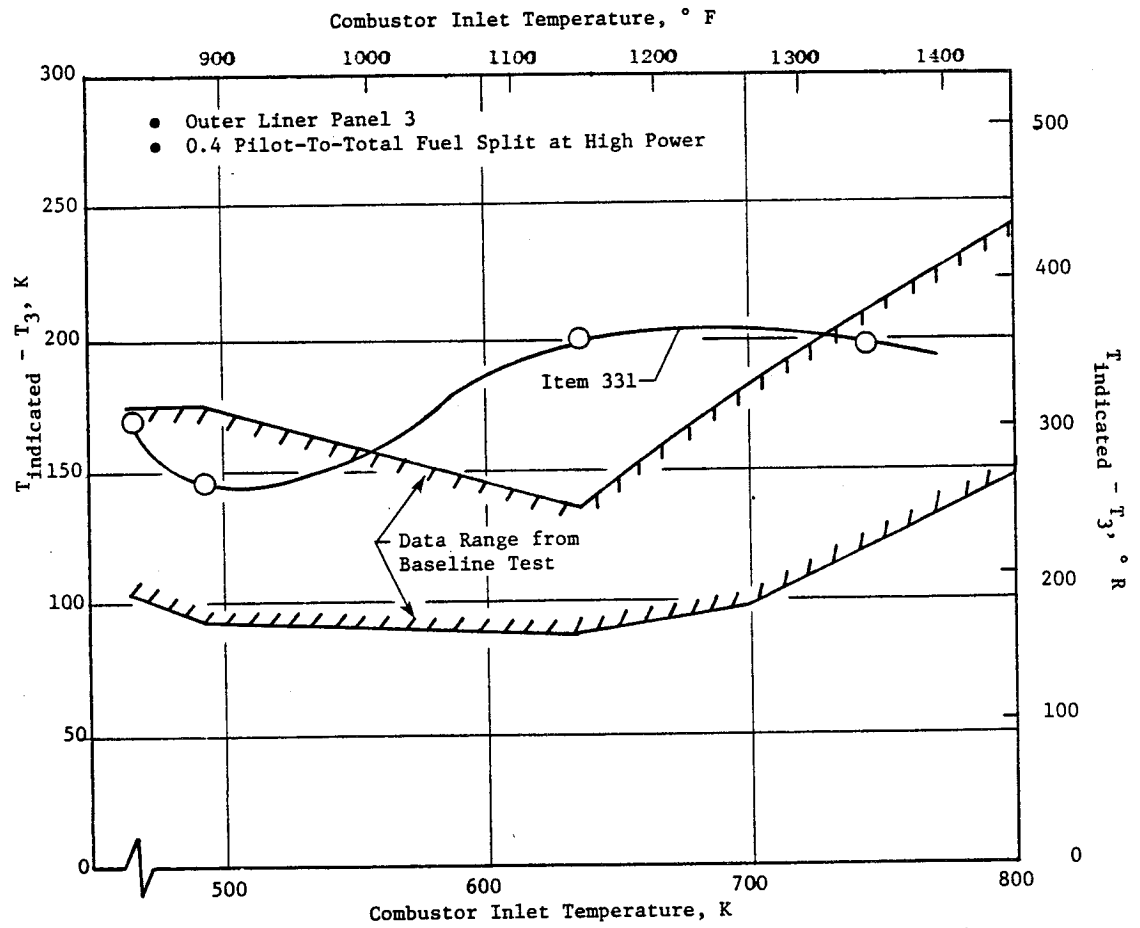


Figure 213. Measured Combustor Metal Temperatures for Mod I Test, Panel 3, Outer Liner.

ORIGINAL DRAWING
OF POOR QUALITY

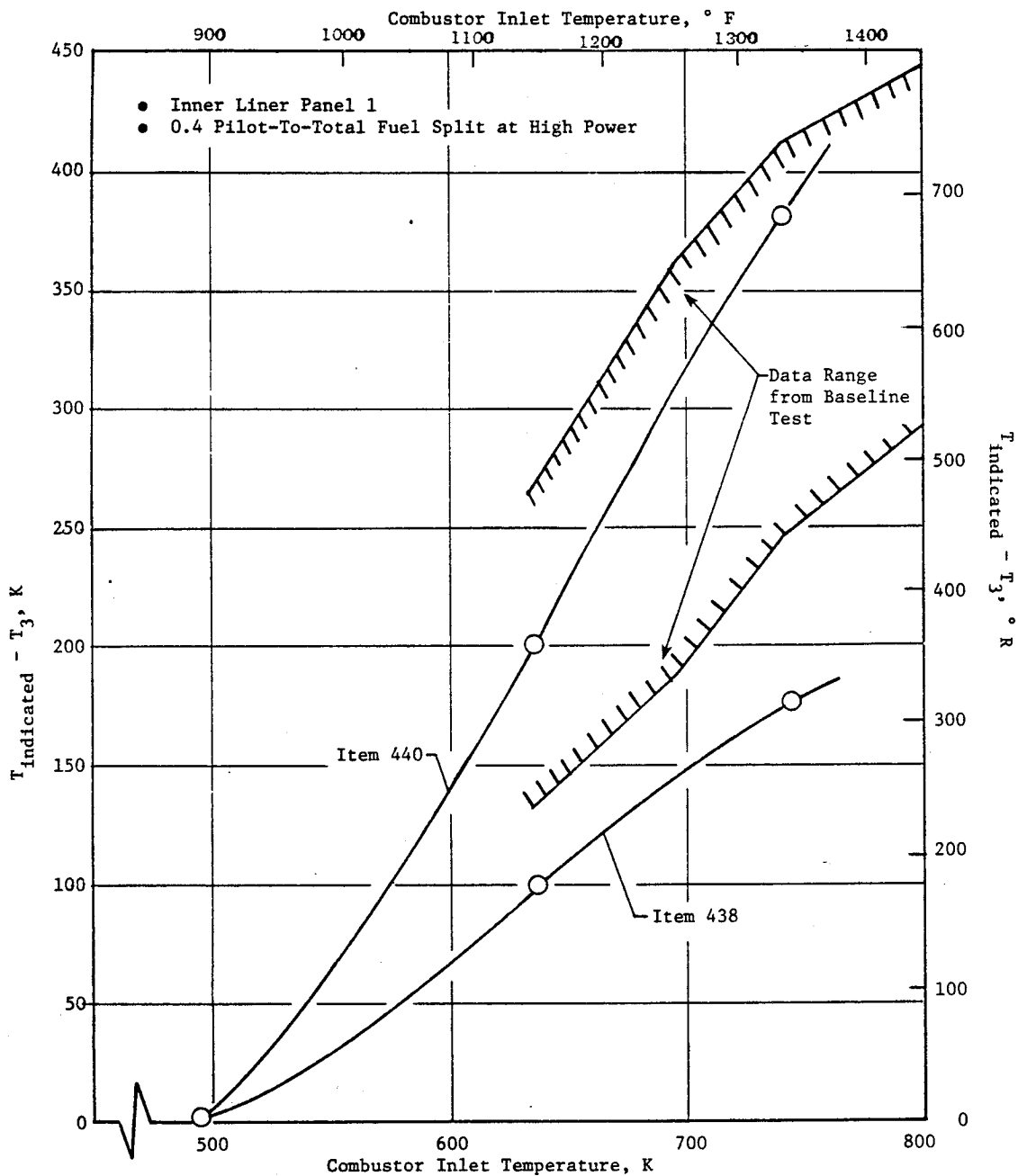


Figure 214. Measured Combustor Metal Temperatures for Mod I Test, Panel 1, Inner Liner.

ORIGINAL PAGE IS
OF POOR QUALITY

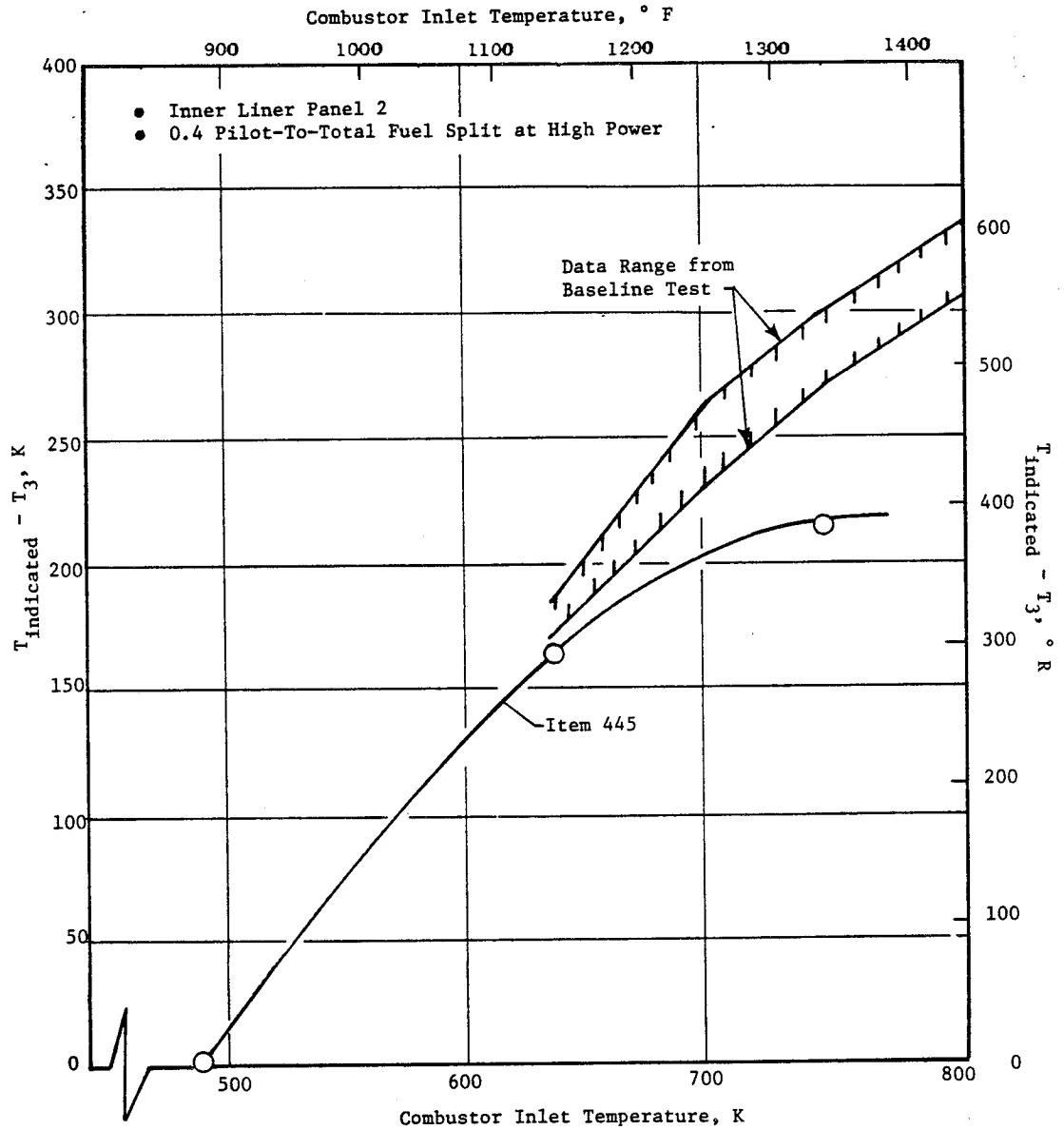


Figure 215. Measured Combustor Metal Temperatures for Mod I Test, Panel 2, Inner Liner.

ORIGINAL PAGE IS
OF POOR QUALITY

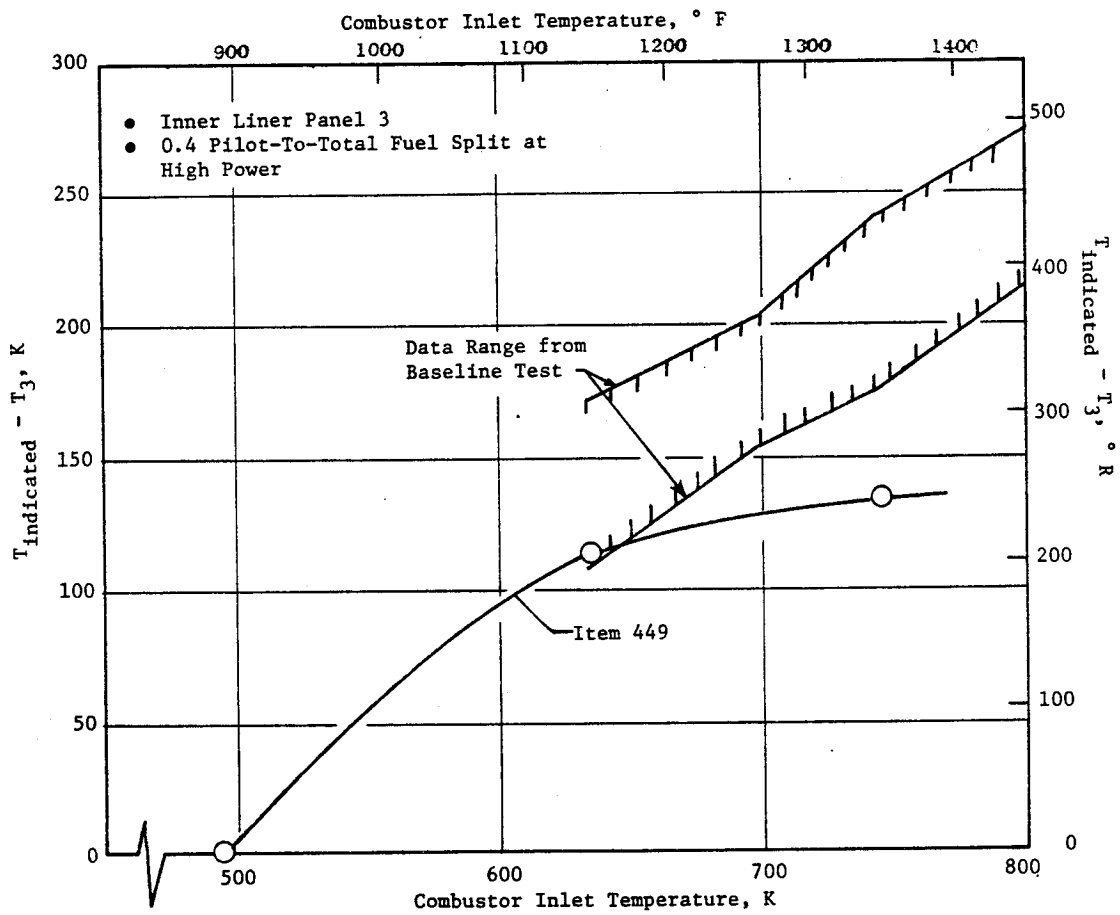


Figure 216. Measured Combustor Metal Temperatures for Mod I Test, Panel 3, Inner Liner.

ORIGINAL PAGE IS
OF POOR QUALITY

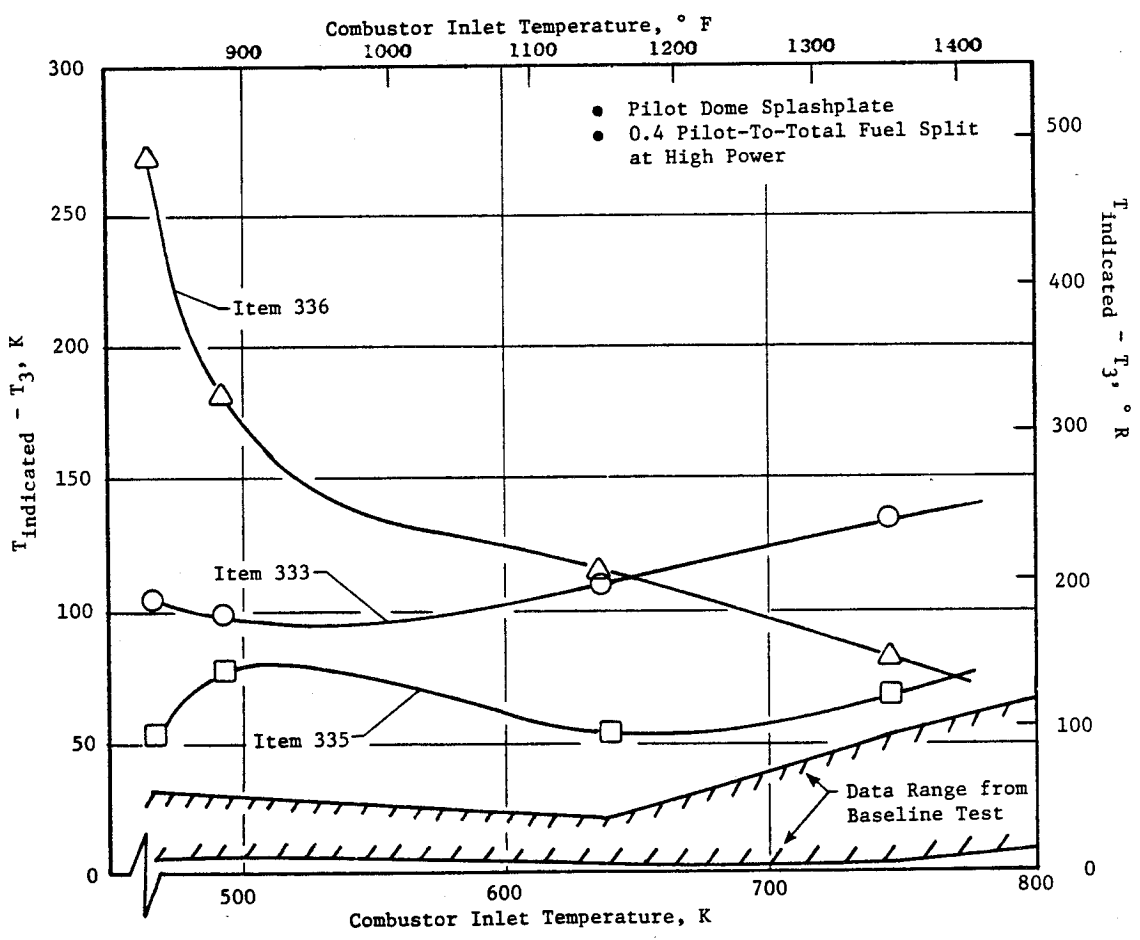


Figure 217. Measured Combustor Metal Temperatures for Mod I Test, Splash Plate, Pilot.

ORIGINAL PAGE IS
OF POOR QUALITY

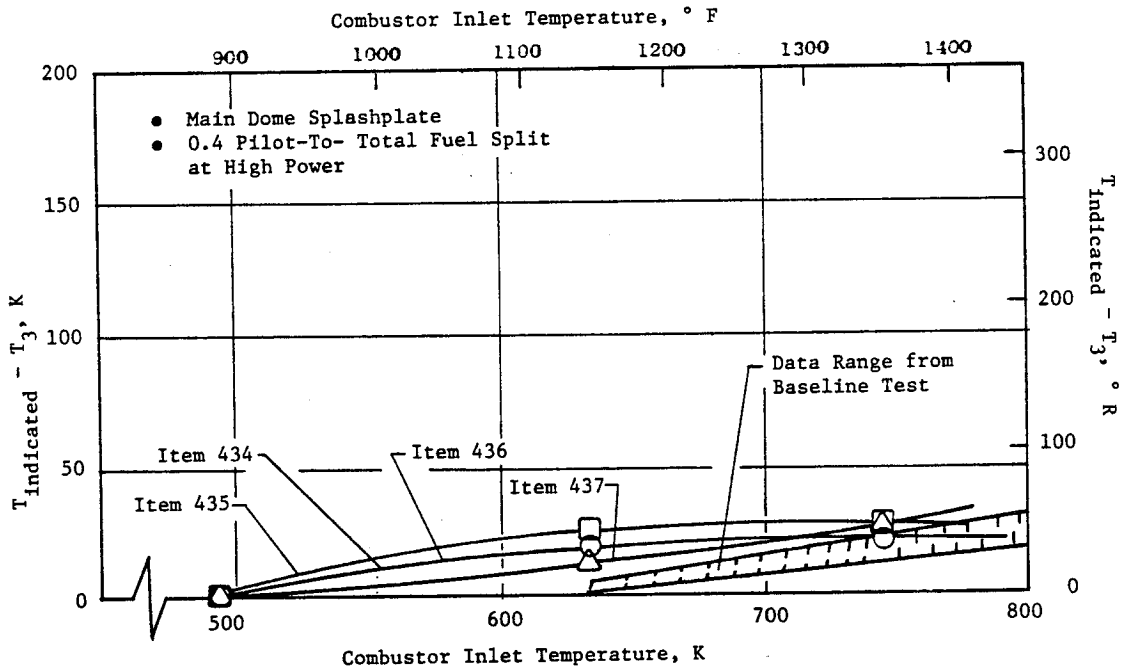


Figure 218. Measured Combustor Metal Temperatures for Mod I Test, Splash Plate, Main.

ORIGINAL PAGE IS
OF POOR QUALITY

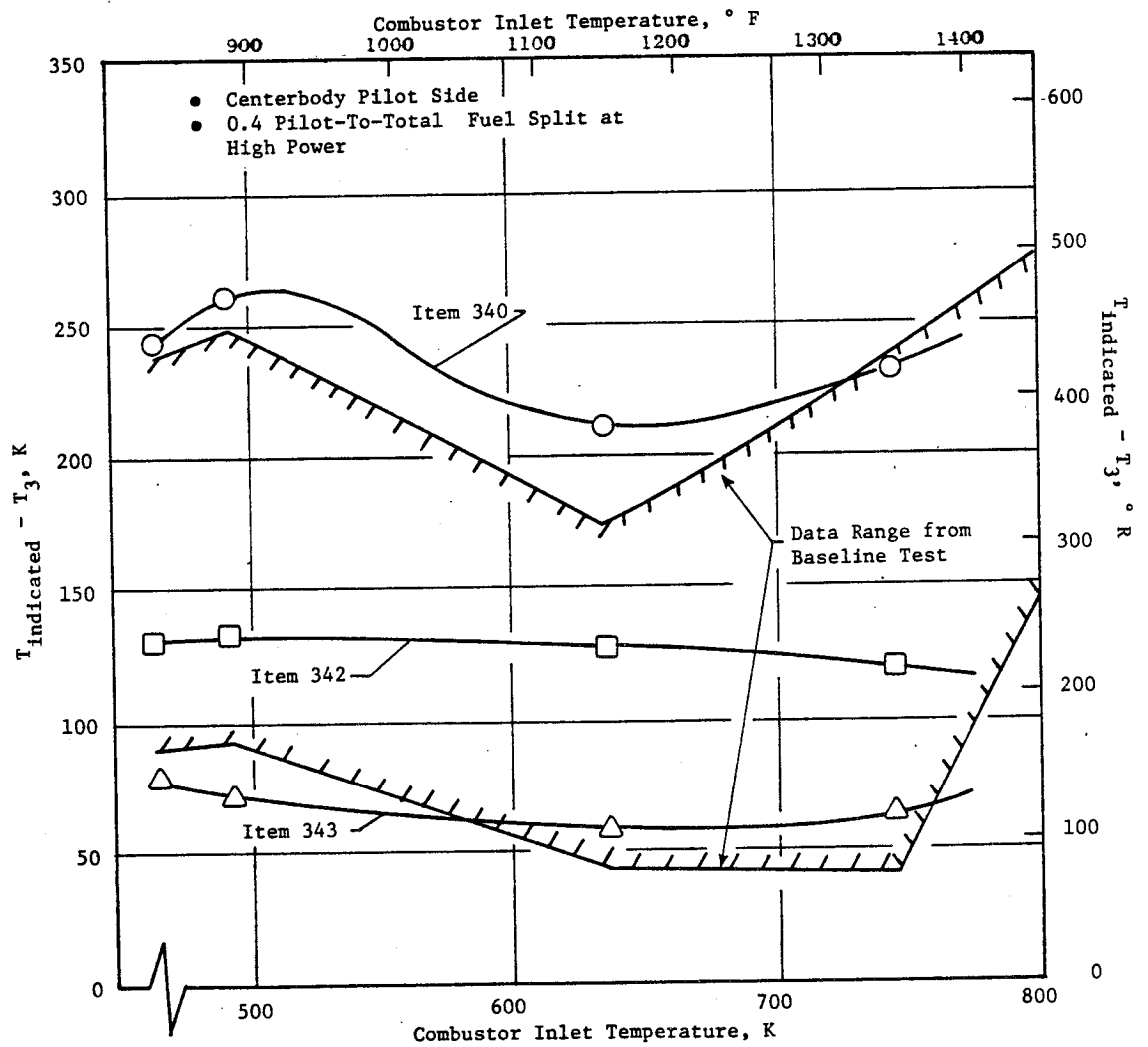


Figure 219. Measured Combustor Metal Temperatures for Mod I Test, Centerbody, Pilot Side.

ORIGINAL PAGE IS
OF POOR QUALITY

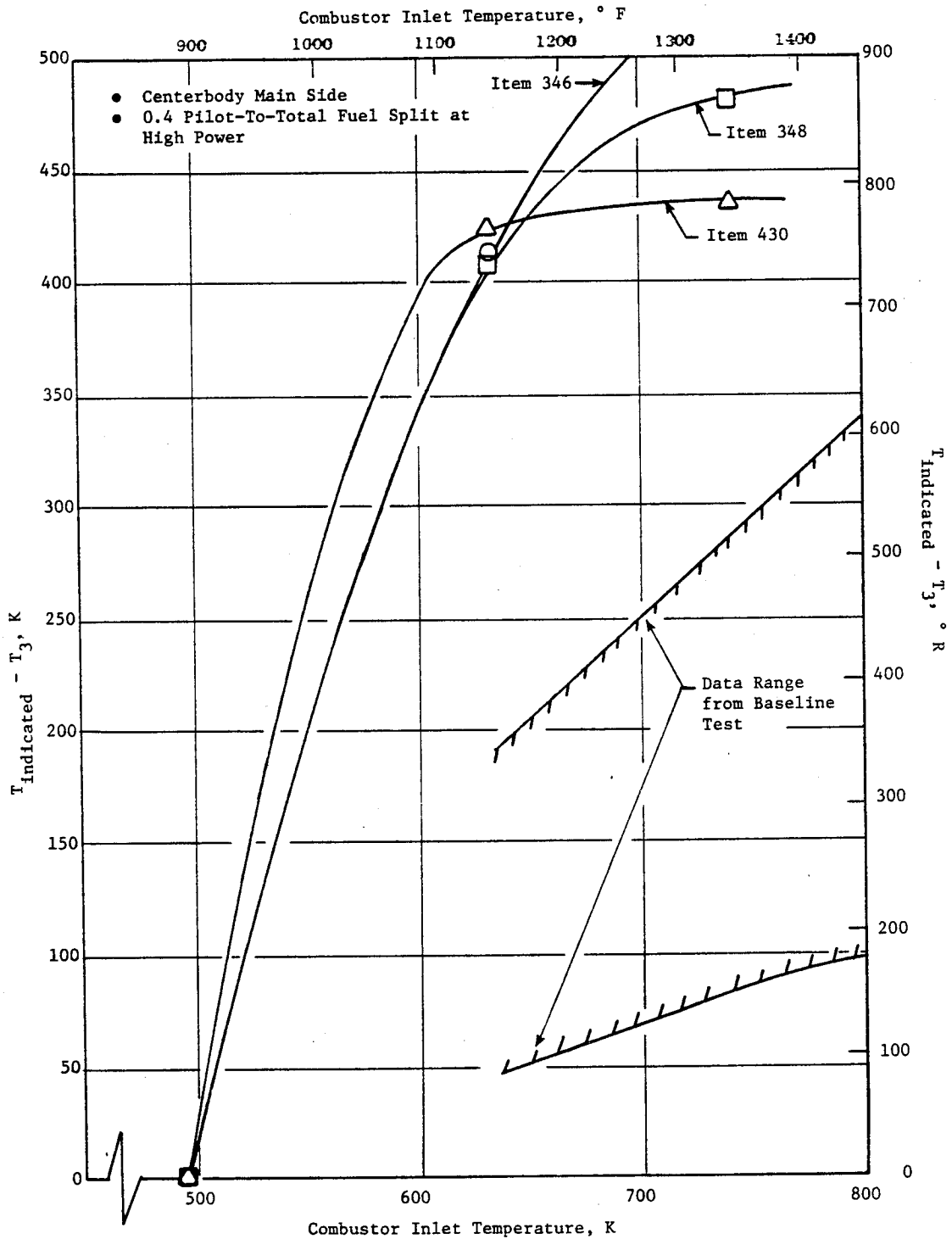


Figure 220. Measured Combustor Metal Temperatures for Mod I Test, Centerbody, Main Side.

is interesting to note that the highest indicated metal temperature along the inner liner was located across from a pilot-to-main stage crossfire tube. This same area on the inner liner was the hottest spot indicated along the inner liner in the baseline combustor evaluation. No explanation linking the hot spot location with the crossfire tube was established.

6.2.2.9 Concluding Remarks - Mod I Combustor

The results of evaluating the Mod I combustor showed significant reductions in ground idle emissions levels with little effect on the high power NO_x emissions level. Significant improvements in pilot stage ground start ignition characteristics, as well as exit temperature performance, were also demonstrated. However, further improvements in all of these performance areas were necessary to evolve a combustor design capable of demonstrating all of the combustion system goals for the E³. A major problem identified involved the poor ignition and propagation characteristics of the main stage. Substantial improvement would be required to achieve main stage crossfire and propagation during ground start operation within the fuel schedule defined in the E³ (September 1979) ground start cycle.

To address the improvement needs identified, attention was directed to defining further combustor design modifications. These modifications included: redistributing the air in the pilot stage primary zone to provide further reductions in ground idle emissions; significantly enriching the main stage primary zone to provide better ignition and propagation; and additional main stage trim dilution to further improve the exit temperature performance. In addition, increased cooling flow would be supplied to the centerbody structure as a precaution against exceeding metal temperature limitations.

6.2.3 Development Testing

6.2.3.1 Mod II and III Development Combustor Test Results

Engine starting studies were performed by Systems Engineering using the existing E³ cycle model and the E³ September 1979 ground start operating cycle. The fuel schedule generated from these studies along with combustor exit

gas temperature profiles measured in the pilot-only mode of operation was used as inputs to conduct a heat transfer analysis of the high pressure and low pressure turbine systems. The results of this analysis indicated that high combustor fuel/air ratios of "pilot stage only" operation generated sharply outward peaked temperature profiles for the September 1979 ground start operating line which produced excessively high blade metal temperatures in both the high pressure and low pressure turbine systems. To reduce the effects of these high gas temperatures in the subidle region, it was decided to start the E³ with both domes of the combustor burning. The original design intent of the combustor main stage dome was to provide a lean primary zone with high velocities and low residence times to reduce high power pollutant emissions such as NO_x.

However, the high dome velocity, coupled with the small dome height of the original main stage configuration, adversely affected the ignition capability, particularly in the very severe ignition environment associated with operation in the subidle region. To enhance the ignition performance of the main stage dome at ground start conditions, various hardware modifications were evaluated in several development combustor configurations.

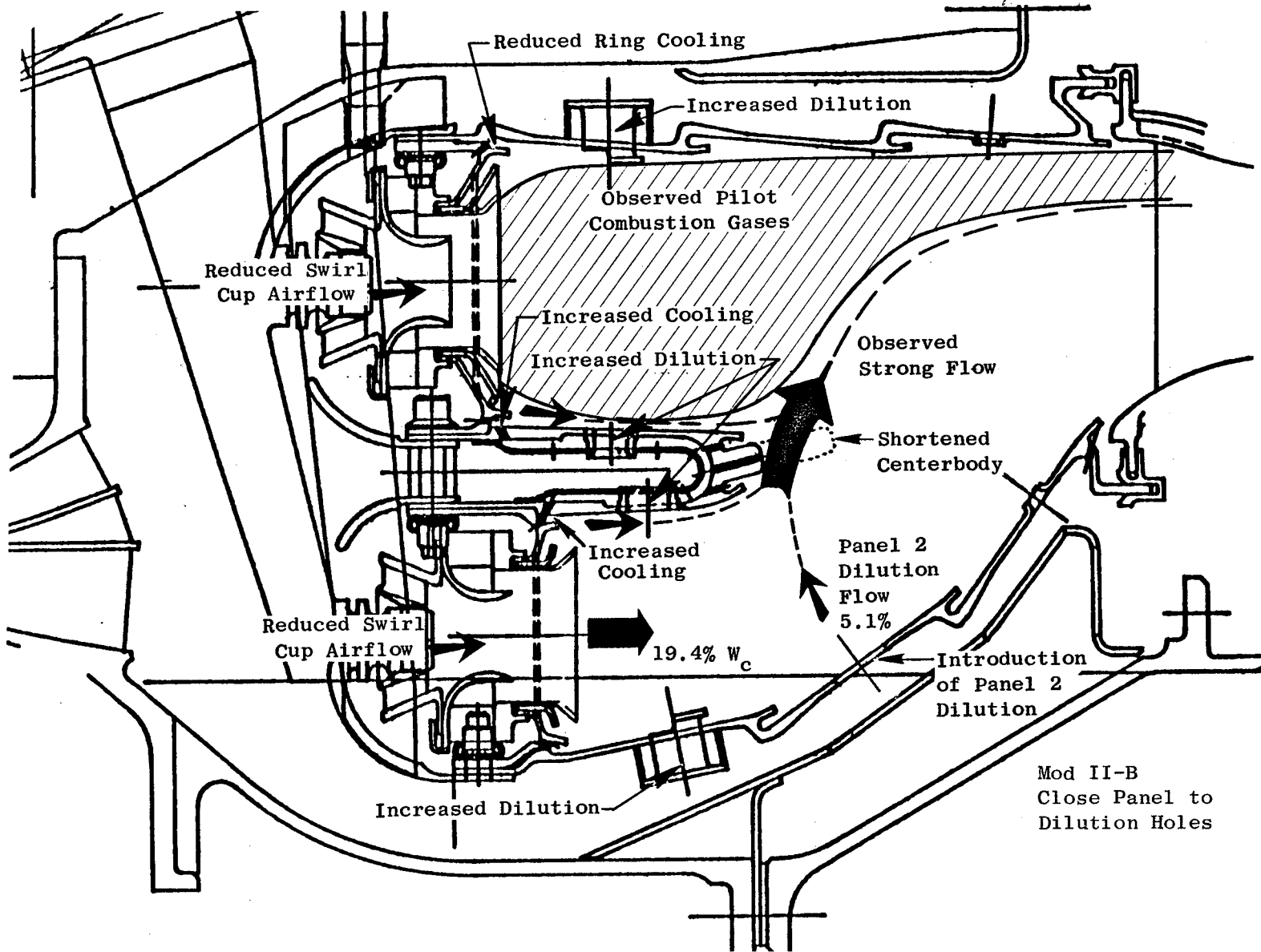
In the Mod IIA combustor configuration, the pilot stage swirl cup airflow was decreased by reducing the area of the secondary swirler. The pilot stage primary dilution was increased to a level similar to the baseline configuration. Outer liner Ring 1 cooling flow was reduced by closing off every fifth cooling hole in both the outer liner cooling Ring 1 and the pilot dome outer cooling ring. Both features feed the first cooling slot. The pilot side centerbody forward cooling flow was increased by the enlargement of the cooling holes. Main stage swirl cup airflow was decreased by significantly reducing the secondary swirler area. The main stage primary air was increased approximately 4% W_C by increasing the thimble hole diameter. The main side centerbody forward cooling flow level was increased by the enlargement of the cooling holes. Inner liner Panel 2 dilution holes were introduced. The pattern featured 60 holes equally spaced around the circumference directly in line with and between all swirl cups. In addition to these modifications, the trailing edge of the centerbody structure was shortened by 1.78 cm (0.70 inch). These design modifications were intended to improve idle emissions, improve

main stage ignition characteristics, provide better cooling of the centerbody structure, and reduce the trailing edge mass of the centerbody structure. The reduction in the centerbody length was an engine combustor design consideration incorporated into the development combustor.

The Mod II-B combustor configuration modifications involved blocking off all inner liner Panel 2 dilution holes. Observations of the Mod II-A test clearly indicated that the presence of this dilution flow was very detrimental to the main stage ignition.

In the Mod III-A combustor configuration, the main stage swirl cup airflow was further reduced by blocking off every other primary swirler vane passage. Main stage splash plate cooling flow was reduced by closing off 46 of 112 holes per splash plate. The main stage dome outer cooling ring flow was reduced by closing off every other hole in the ring plus six additional holes in line with the crossfire tubes. This provided a sheltered region of 11 consecutive blocked off cooling holes in line with the crossfire tubes. These reductions in main stage dome flow were intended to further enrich the main stage dome, plus reduce the main stage dome velocity to levels similar to those in the pilot stage dome. The outer liner and inner liner aft dilution was increased to maintain the overall combustor pressure drop. The crossfire tubes were replaced with new tubes which featured extended lengths along the upstream surface. The extended length was intended to provide additional shelter for the combustion gases passing through the crossfire tubes allowing them to penetrate deeper into the main stage dome annulus.

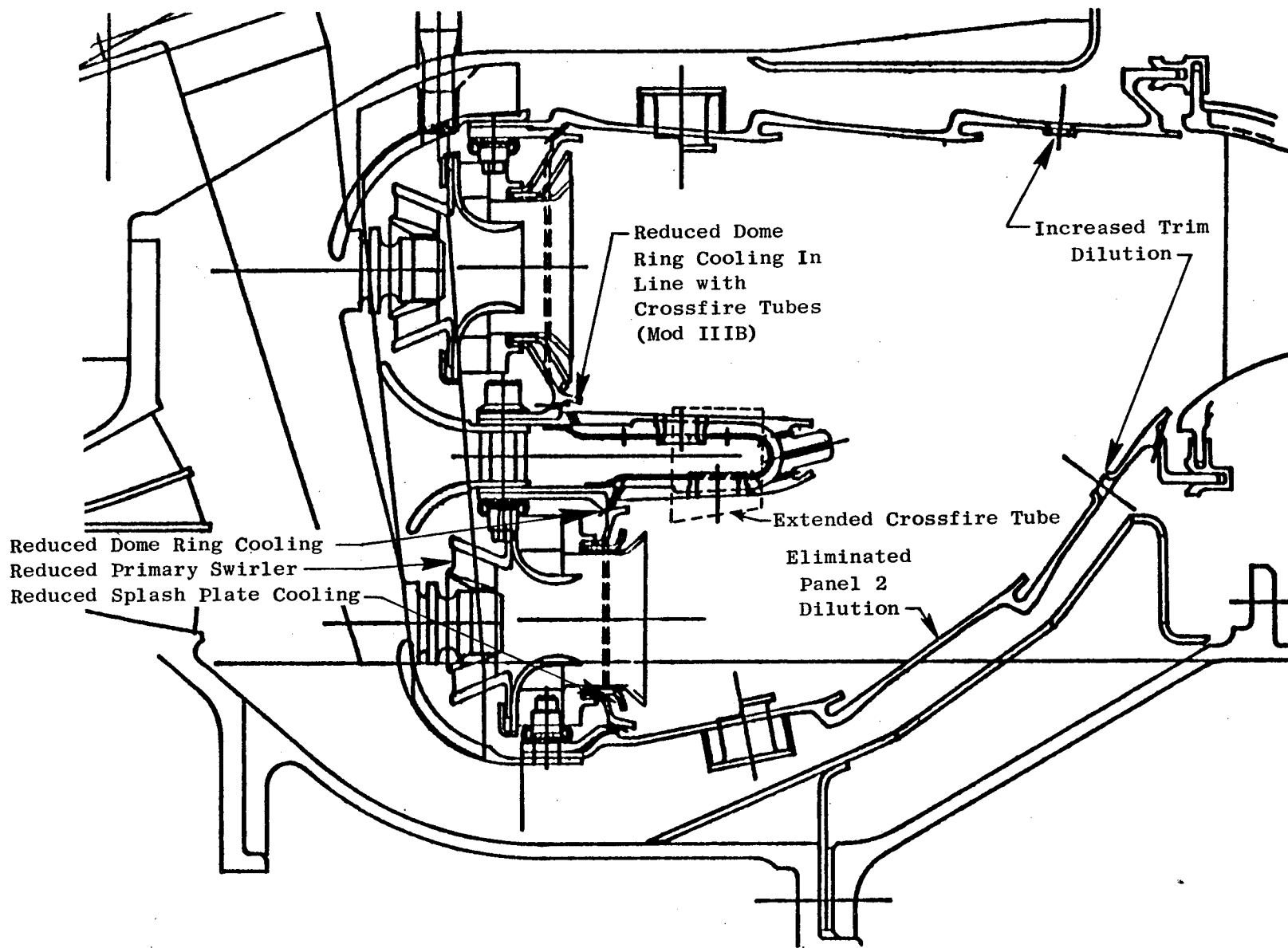
In the Mod III-B configuration, modification involved only blocking off pilot side centerbody forward cooling flow in line with the crossfire tubes. This was to eliminate the film of cooling air which passes over the crossfire tubes enabling the pilot stage combustion gases to more easily pass through the crossfire tubes into the main stage annulus. Illustrations of the hardware modifications featured in these four combustor configurations are presented in Figures 221 and 222. Estimated combustor airflow distributions for each configuration is contained in Appendix E.



ORIGINAL PAGE IS OF POOR QUALITY

Mod II-B
Close Panel to
Dilution Holes

Figure 221. Mod II-A Combustor Hardware Modification.



ORIGINAL WORK IS
OF POOR QUALITY

Figure 222. Mod III-A Combustor Hardware Modification.

6.2.3.2 Atmospheric Ground Start Ignition Test

All four combustor configurations were tested for ground start characteristics using nozzle tips rated at 12 kg/hr (26.5 lb/hr) installed in both the pilot and main stage swirl cups. The purpose of this series of tests was to evolve combustor design features that would result in main stage ignition and lean extinction characteristics within the fuel schedule requirements of the E³ September 1979 ground start cycle operating line. To investigate the effect of high combustor airflows on ignition, additional testing was conducted on the Mod III-B configuration in which combustor airflows were increased 15% and 30% above the cycle level at the 32%, 46%, and 77% corrected core engine speed points. Without heavy bleeding of the compressor, engine combustor air-flow levels in the start region could be significantly greater than currently estimated in the ground start cycle. Prediffuser and combustor aft bleed flows were not used in this test series. Test points and corresponding operating conditions are presented in Table XLIX.

Test results obtained from ground start ignition evaluation of the Mod II-A combustor configuration are presented in Appendix F. The light-off characteristics of the pilot stage swirl cup in line with the igniter were similar to the Mod I combustor configuration. Full propagation of the pilot stage was considerably more difficult to achieve. The main stage crossfire and propagation characteristics were very poor. Full main stage propagation was achieved only at the simulated 77% corrected core speed test point. Observations made during the test revealed an unusually strong flow of air passing along the main side of the centerbody trailing edge and penetrating deeply into the pilot combustion gas stream. This strong flow appeared to quench a considerable amount of the pilot combustion gases as they passed downstream beyond the centerbody trailing edge. This sudden quenching appeared to be responsible for the difficulty in obtaining full pilot stage propagation and main stage ignition. Combustion gases passing through the crossfire tubes into the main stage annulus became entrained in this flow along the centerbody and were swept downstream before penetrating sufficiently into the main stage annulus to provide a good ignition source. The existence of this strong flow of air appeared related to three of the hardware modifications featured in the

Table XLIX. Mod II and III Atmospheric Ignition Test Point Schedule.

% PCNHR Test Point	Combustor Inlet Conditions			
	W_{comb} , kg/s (lb/s)	P_3 , Atm.	T_3 , K (°R)	
21	1.25 (2.76)	1.00	289 (520)	} Standard Airflow Conditions
28	1.69 (3.73)	1.00	289 (520)	
32	1.55 (3.42)	1.00	314 (565)	
46	1.65 (3.64)	1.00	344 (619)	
58	1.86 (4.10)	1.00	383 (689)	
70	1.94 (4.28)	1.00	429 (772)	
77	2.33 (5.13)	1.00	503 (905)	
32	1.70 (3.75)	1.00	314 (565)	} High Airflow Conditions, Mod III-B Only
32	1.94 (4.28)	1.00	314 (565)	
46	1.82 (4.01)	1.00	344 (619)	
46	2.06 (4.54)	1.00	344 (619)	
77	2.54 (5.59)	1.00	503 (905)	
77	2.89 (6.37)	1.00	503 (905)	

Actual Engine Cycle Combustor Inlet Pressures		
% PCNHR	P_3 MPa	(psi)
21	0.103	(15.0)
28	0.105	(15.2)
32	0.119	(17.3)
46	0.144	(20.9)
58	0.187	(27.1)
70	0.248	(36.0)
77	0.428	(62.0)



Mod II-A combustor configuration: the shortening of the centerbody, the introduction of inner liner Panel 2 dilution, and the increased centerbody main side cooling flow (Figure 221). Because of the quantity of the inner liner Panel 2 dilution (approximately 5.1% W_{comb}), it was suspected that this had the strongest impact of the three.

Test results for the Mod II-B combustor configuration are presented in Appendix F. In comparison to the Mod II-A configuration, no significant improvement in the pilot stage ignition was obtained. Some improvement in the main stage full propagation and lean extinction characteristics was demonstrated, especially at the lower speed operating conditions.

Test results obtained for the Mod III-A combustor configuration are presented in Appendix F. The implementation of the combustor hardware modifications featured in this configuration proved very effective in achieving significant improvement in the main stage ignition characteristics. Successful ignition and full propagation of the main stage were obtained at simulated corrected core speeds as low as 32%. A partial propagation was obtained at 28% PCNHR. These ignition data were adjusted to true engine cycle combustor inlet pressure conditions using pressure effect characteristics determined from sector subcomponent and Mod I development combustor ignition testing at pressure. As shown in Figure 223, when adjusted for the combustor inlet pressure, the Mod III-A combustor configuration was estimated to achieve full main stage propagation within the ground start fuel schedule at corrected core speeds at or above 45%. During testing of this configuration, several observations were made. At the lower simulated core speed operating points, hot combustion gases passing through the crossfire tubes were still being swept downstream upon discharging into the main stage annulus. Main stage ignition and initial flame stabilization appeared to occur in the plane of the main stage liner primary air introduction. As the fuel/air mixture in the main stage leaned out, the flame front propagated upstream into the recirculating zone established by the swirl cup. At test conditions where main stage ignition occurred, the main dome swirl cup equivalence ratios were around 3.0 above the rich stability limit. At the plane of the liner primary air introduction, the equivalence ratios were near 1.0, considered ideal for ignition.

ORIGINAL PART OF
OF PCOR CLAW

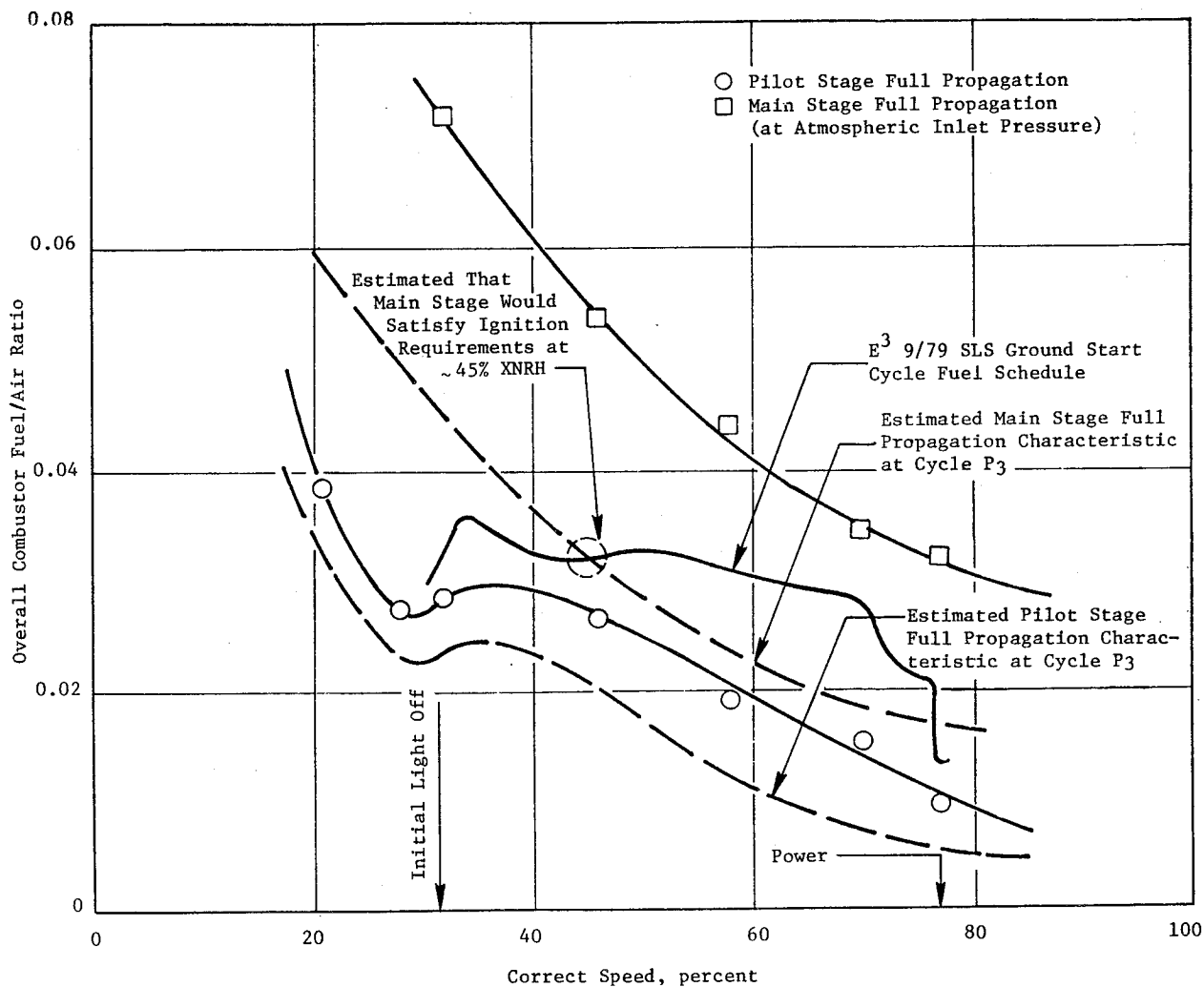


Figure 223. Mod III-A Atmospheric Ignition Test Results.

C-5

It appeared that a substantial improvement in the main stage ignition characteristics could be obtained by reducing the equivalence ratio in the main stage dome, and moving the crossfire tubes (ignition source) closer to the main stage swirl cup. Because of the design of the centerbody, moving the crossfire tubes upstream any significant amount was not possible.

Test results obtained for the Mod III-B combustor configuration are presented in Appendix F. From these results, it can be concluded that, in general, the hardware modification incorporated into this configuration produced no significant change in the ignition and lean extinction characteristics of the Mod III-A combustor configuration. However, one significant result did emerge. Substantial improvements were achieved in both the pilot and main stage ignition and lean extinction characteristics at test points where the effect of increased combustor airflow was evaluated. This result may have been associated with better fuel atomization and fuel/air mixing created from higher swirl cup airflows and pressure drops, offsetting the adverse effects of higher dome velocities. Estimated main stage ignition performance at actual engine combustor inlet pressure is presented for the standard and high flow operating conditions in Figure 224. These results indicate that without compressor bleed during ground startup, the main stage could be successfully crossfired at corrected core engine speeds below 40%.

6.2.3.3 Concluding Remarks - Mod II and III Combustors

In summary, the development effort represented in this ignition testing series evolved a promising combustor configuration capable of demonstrating satisfactory pilot and main stage ignition and lean extinction characteristics that would meet the E³ September 1979 ground start cycle requirements. It was further demonstrated that additional improvements in the combustor ignition and lean extinction characteristics would result if the requirement for large amounts of compressor bleed during ground startup were eliminated.

Despite these encouraging results, it was decided to apply additional development effort into the rich main stage design concept to achieve further improvements in ground start ignition characteristics, while demonstrating acceptable exit temperature performance. Modifications in the outer and inner

ORIGINAL PAGE IS
OF POOR QUALITY

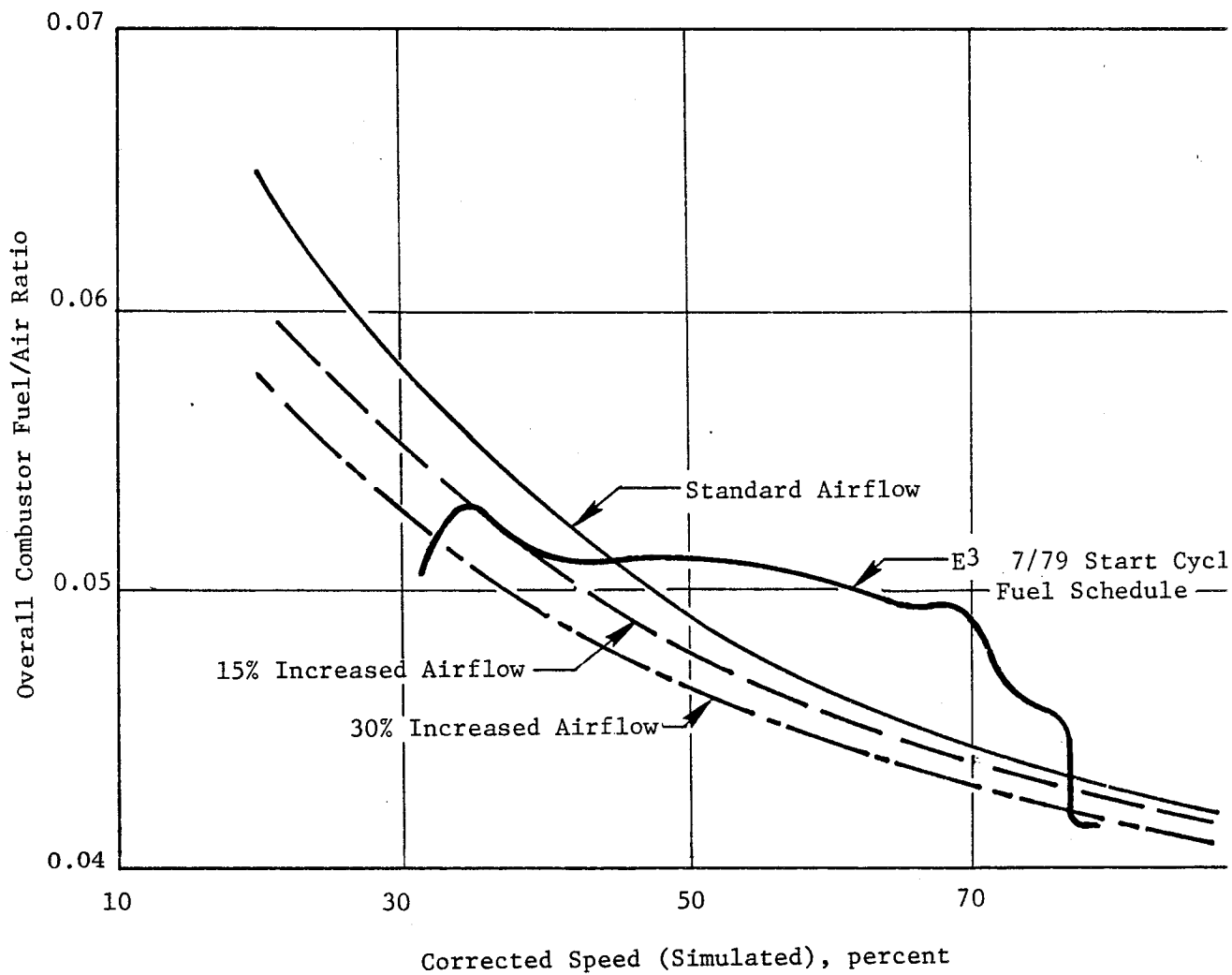


Figure 224. Mod III-B Atmospheric Ignition Test Results.

liner trim dilution were considered to investigate their impact on these two combustor operating performance characteristics.

6.2.3.4 Mod IV and V Development Combustor Test Results

The Mod IV combustor configuration hardware modifications involved reducing the inner liner panel trim dilution holes while introducing holes in inner liner Panel 2. The dilution hole arrangement in Panel 2 liner was the same pattern featured in the Mod II-A combustor configuration, but the holes were smaller. With this arrangement, Panel 2 and 3 dilution holes were staggered providing for the introduction of dilution air every 3° around the combustor inner annulus. These dilution modifications had two intentions: to add mixing length by introducing some of the inner trim dilution air further upstream, and to investigate the impact of a small quantity of Panel 2 dilution on the main stage ignition.

The Mod V combustor configuration hardware modifications involved reducing the size of the main stage inner side and centerbody side primary dilution thimble holes. In addition, 60 equally spaced dilution holes were pierced into Panel 2 of the outer liner. These holes were staggered with respect to the outer liner Panel 3 dilution hole arrangement. These modifications were intended to further enrich the main stage dome to improve the ignition characteristics and attenuate the exit gas temperature profiles, especially in the pilot only mode of operation. Illustrations of the combustor hardware modifications featured in each configuration are presented in Figures 225 and 226.

The resultant changes in the combustor airflow distribution for each of these configurations are presented in Appendix E.

6.2.3.5 Atmospheric Ground Start Ignition Test

Ground start ignition testing was performed on both the Mod IV and V development combustor configurations. The test points investigated were the same as those investigated with the Mod II and III configurations.

ORIGINAL PAGE IS
OF POOR QUALITY

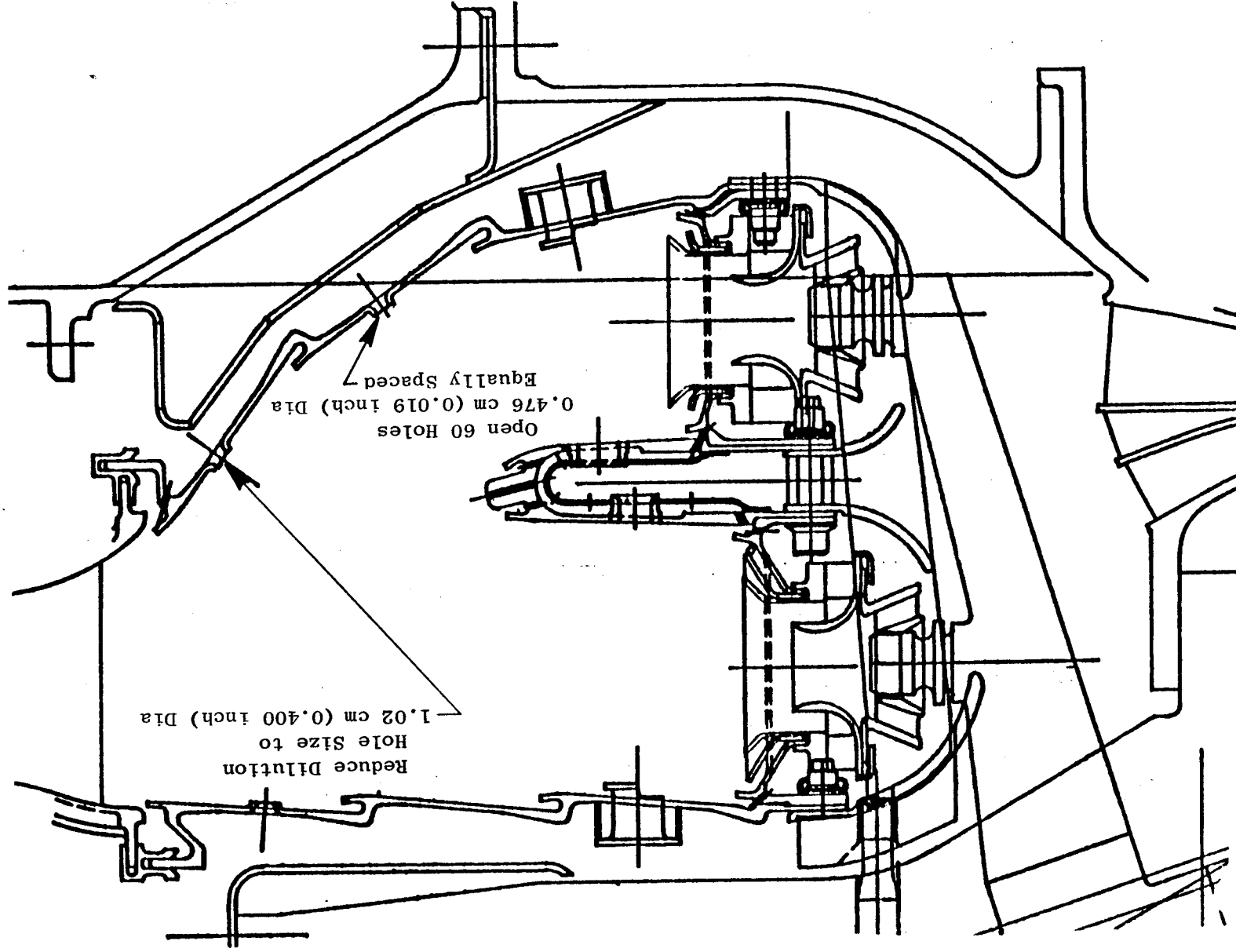
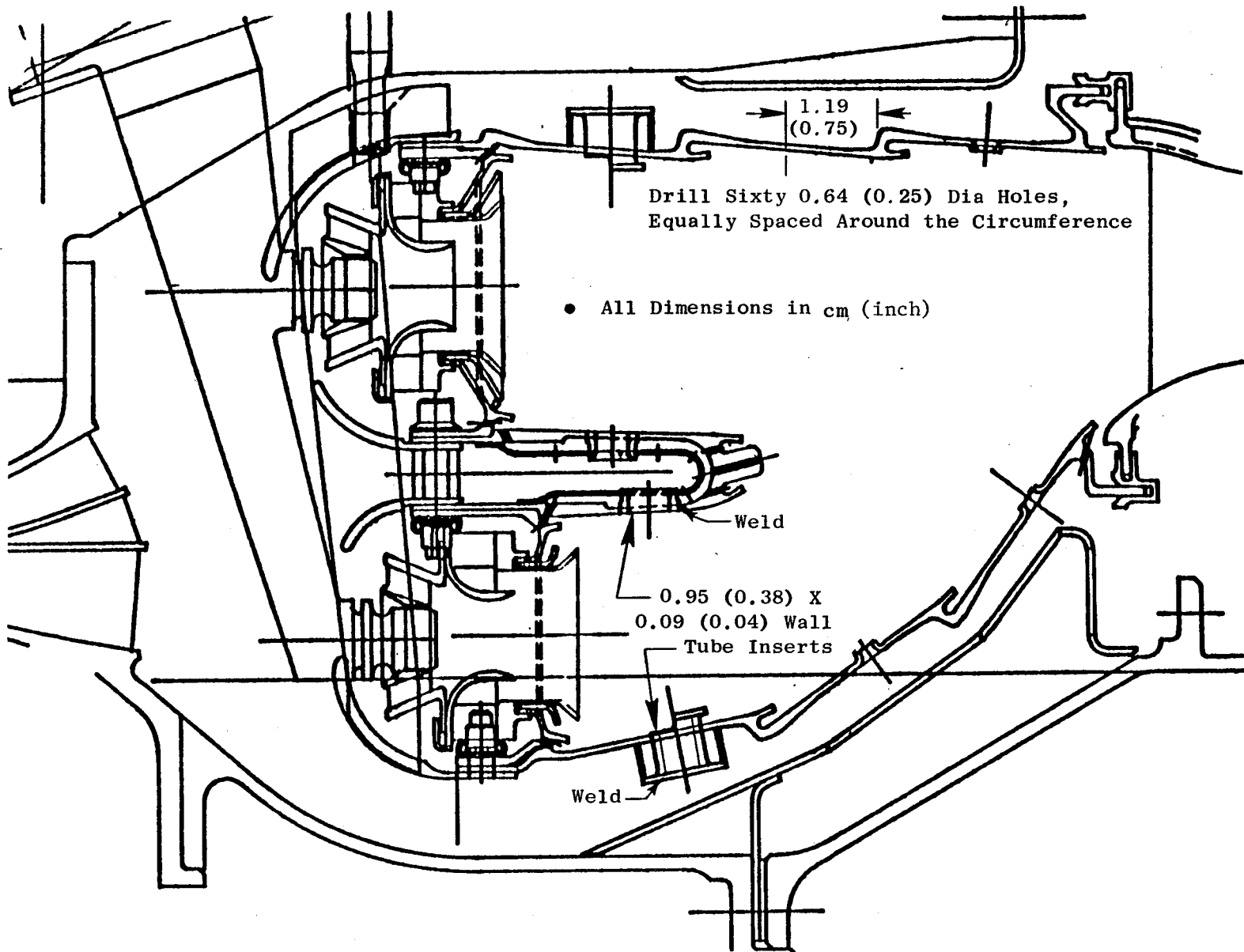


Figure 225. Mod IV Combustor Hardware Modification.



ORIGINAL PAGE IS
OF POOR QUALITY

Figure 226. Mod V Combustor Hardware Modification.

For this ground start ignition test series, the E³ test rig fuel nozzle assemblies were used. Nozzle tips rated at 12 kg/hr (26.5 pph) were installed in both combustor stages.

Ground start ignition test results for the Mod IV combustor configuration are compared with the results obtained from the Mod III-A configuration in Figure 227. A tabulation of the data is presented in Appendix F. The Mod III-A configuration had demonstrated marginally acceptable main stage subidle ignition characteristics. As observed from this figure, the pilot stage full propagation and one cup out characteristics remained unchanged. This was expected as there were no hardware modifications made to the pilot stage dome. However, some deterioration in main stage full propagation and one cup out characteristics did result. Overall combustor fuel/air ratios approximately 10% greater than in the Mod III-A configuration were required to obtain full propagation of the main stage. Some reduction in the lean stability margin was also observed. Despite the fact that some deterioration in the main stage ignition characteristics did occur, the Mod IV results indicated that small amounts of inner liner Panel 2 dilution did not seriously impact main stage ignition.

Ground start ignition test results for the Mod V combustor configuration are presented as a comparison with the results of the Mod III-A and IV ignition test results in Figure 228. As observed from the figure, some minor improvements in main stage ignition characteristics over those demonstrated with the Mod IV configuration were obtained. However, the main stage ignition performance is not quite as good as that demonstrated with the Mod III-A configuration. From these results and estimates of the expected improvements resulting from operation at actual engine cycle combustor inlet pressures, it is estimated that full propagation of the main stage could be achieved at a corrected core engine speed of 50%. This compares to a speed of 45% identified for core engine starting. Despite the introduction of some outer liner Panel 2 dilution, the pilot stage ignition characteristics remained unchanged.

6.2.3.6 Atmospheric Exit Temperature Performance Test

The Mod V development combustor configuration was evaluated for exit temperature performance. Operating conditions simulated sea level takeoff

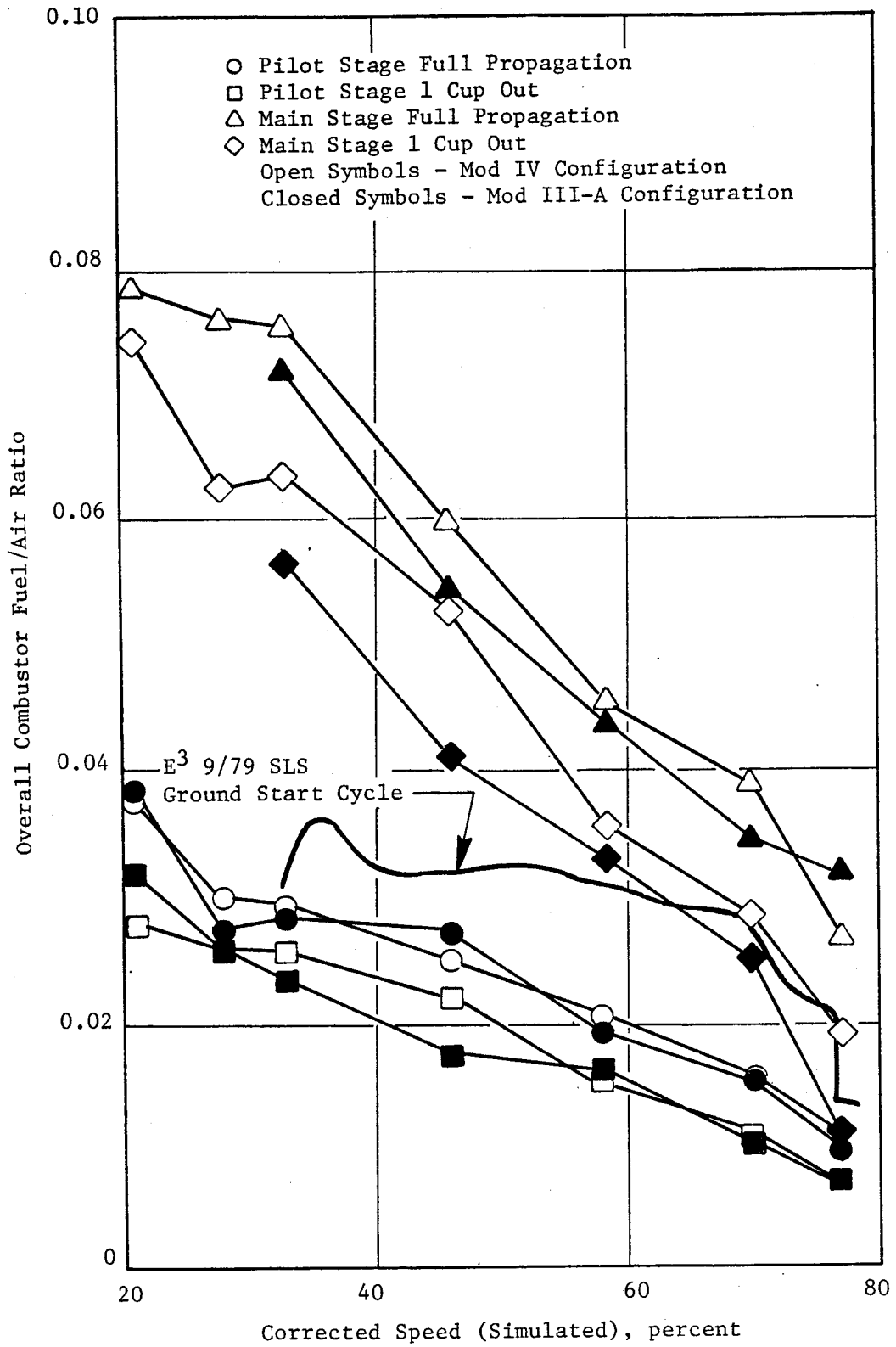


Figure 227. Mod IV Atmospheric Ignition Test Results.

ORIGINAL PAGE IS
OF POOR QUALITY

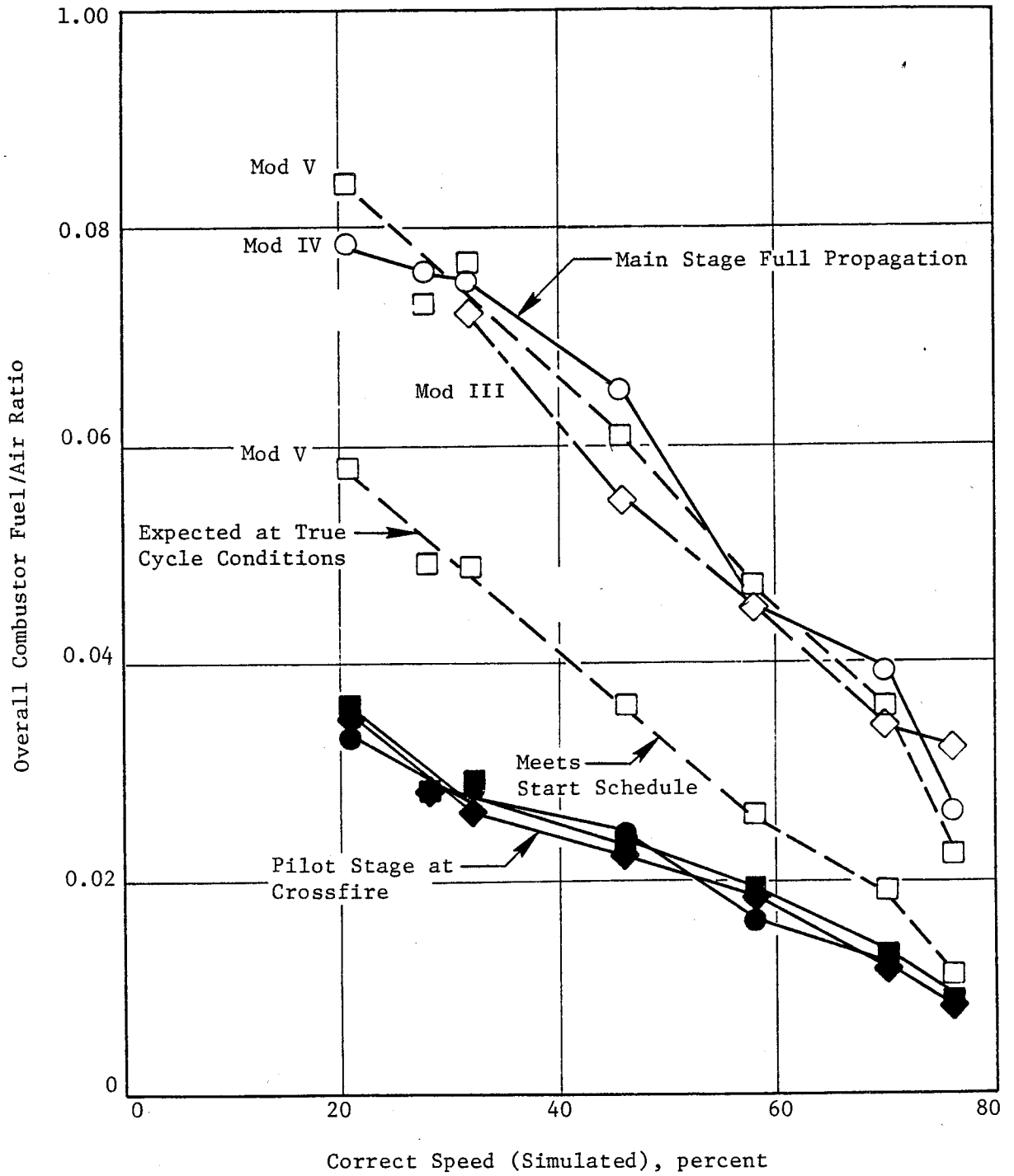


Figure 228. Mod V Atmospheric Ignition Test Results.

power with pilot-to-total fuel splits of 0.5, 0.4, and 0.3. Data were also taken at operating conditions simulating 77%, 58%, and 46% corrected core engine speeds as defined in the E³ September 1979 ground start cycle. Pilot-to-total fuel splits of 1.0, 0.5, and 0.4 were evaluated at 77 PCNHR, while the pilot only operating mode was evaluated at 58 and 46 PCNHR. At the sub-idle test points, fuel/air ratios 30% lower than cycle conditions were set because of fuel nozzle flow limitations. Test points and corresponding combustor conditions are presented in Table L.

Nozzle tips rated at 2.3 kg/hr (5 pph) were installed in the pilot stage. In the main stage, a set of slightly modified nozzle tips was used. These tips originally were rated at 3.2 kg/hr (7 pph). The modifications increased their flow rate to approximately 6.8 kg/hr (15 pph) at the same fuel pressure. Some variance in fuel flow levels ($\pm 10\%$) between these 30 modified nozzle tips was evident from the pretest fuel flow calibration. The variation was attributed to the fact that the modifications were done manually.

Results from the performance test of the Mod V combustor configuration are presented in Figure 229. The average profile at the 50/50 fuel split is generally within the established limit and reasonably flat. However, as fuel is biased to the main stage, unacceptable profiles result. The maximum profiles are sharply peaked inward and exceed the established limit by a considerable amount. In Figure 230, the performance results for pilot only operation at the simulated subidle conditions are presented. Data obtained at the simulated 77 PCNHR condition with the pilot-to-total fuel splits of 0.5 and 0.4 were of extremely poor quality and not considered worth processing. It is observed from Figure 230 that maximum profiles less than 1.0 were obtained at all of the pilot only subidle operating conditions investigated. These levels are significantly lower than levels measured during performance testing of the Mod I configuration at the same operating conditions. This improvement is attributed to the outer liner Panel 2 dilution features in the Mod V configuration. The significance of this result relates to the concern over the effects on turbine hardware survival when subjected to sharply peaked temperature profiles resulting from pilot only operation. Any attenuation in these profiles would be very beneficial to turbine life.

Table L. Mod V Atmospheric EGT Performance Test Point Schedule.

Test Point	T ₃ , K (°F)	P ₃ , Atm.	W ₃ , kg/s (pps)	W _{bleed} , kg/s (pps)	W _c , kg/s (pps)	f/a	W _{fPilot} / W _{fTotal}	W _{fPilot} , kg/hr (pph)	W _{fMain} , kg/hr (pph)	Traverse Positions	Traverse Increments, degrees
1	815 (1007)	AMB	2.41 (5.31)	0.15 (0.34)	2.26 (4.97)	0.0244	0.50	99 (218)	99 (218)	120	1.5
2	815 (1007)	AMB	2.41 (5.31)	0.15 (0.34)	2.26 (4.97)	0.0244	0.40	80 (175)	119 (262)	120	1.5
3	815 (1007)	AMB	2.41 (5.31)	0.15 (0.34)	2.26 (4.97)	0.0244	0.30	60 (131)	139 (306)	120	1.5
4	314 (105)	AMB	1.55 (3.40)	0	1.55 (3.40)	*	1.0	*	0	60	1.5
5	344 (160)	AMB	1.65 (3.64)	0	1.65 (3.64)	*	1.0	*	0	60	1.5
6	344 (160)	AMB	1.90 (4.19)	0	1.90 (4.19)	*	1.0	**	0	60	1.5
7	383 (230)	AMB	1.86 (4.09)	0	1.86 (4.09)	*	1.0	*	0	60	1.5
8	495 (432)	AMB	2.33 (5.13)	0	2.33 (5.13)	*	1.0	*	0	60	1.5
9	495 (432)	AMB	2.33 (5.13)	0	2.33 (5.13)	*	0.5	*	0	60	1.5
10	495 (432)	AMB	2.33 (5.13)	0	2.33 (5.13)	*	0.4	*	0	60	1.5

* Set minimum pilot stage fuel flow at which all 30 cups are burning
 ** Set same fuel flow in pilot stage as was set in test Point 5

ORIGINAL FROM THE
OF POOR QUALITY

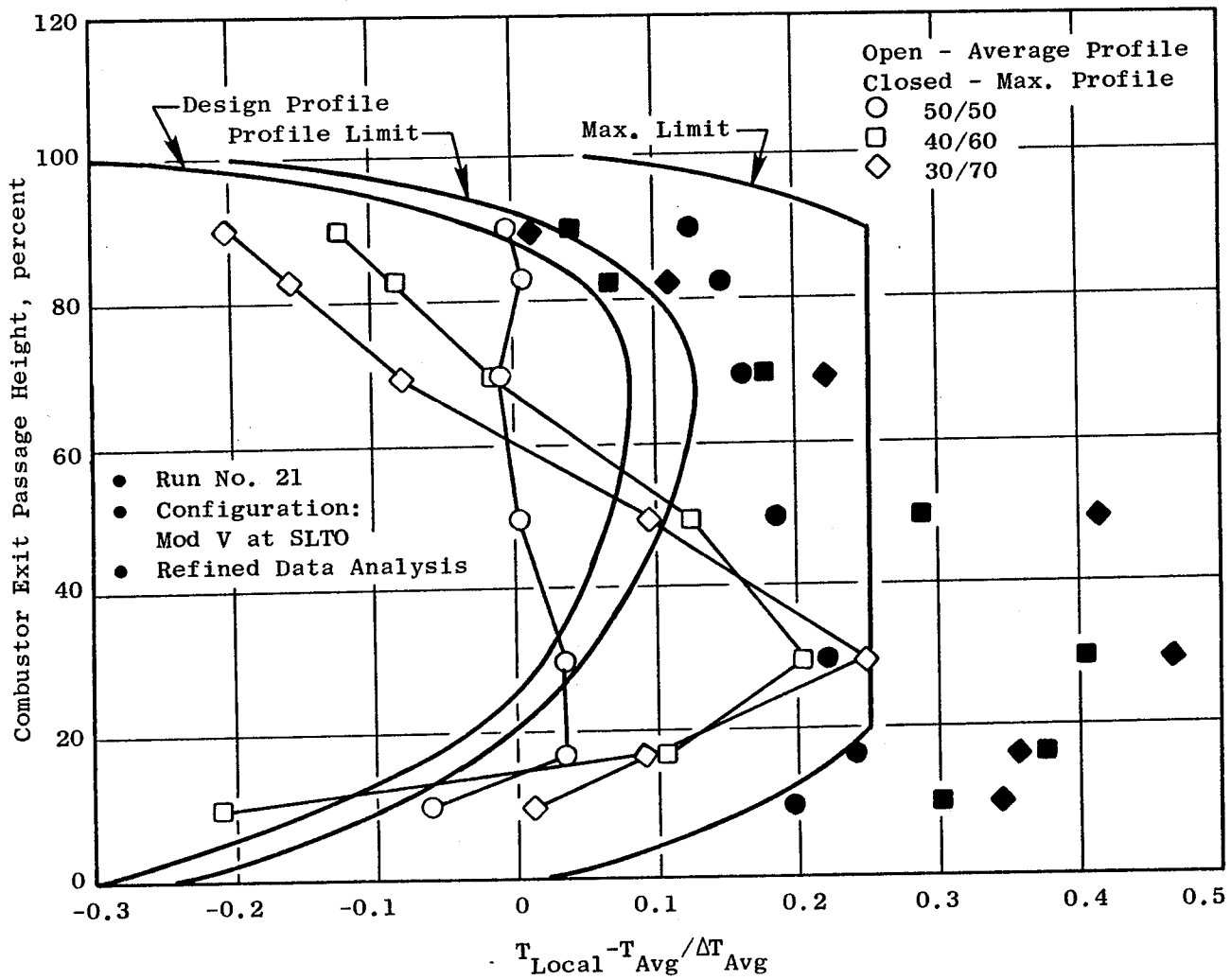


Figure 229. Mod V EGT Performance Test Results.

ORIGINAL PAGE IS
OF POOR QUALITY

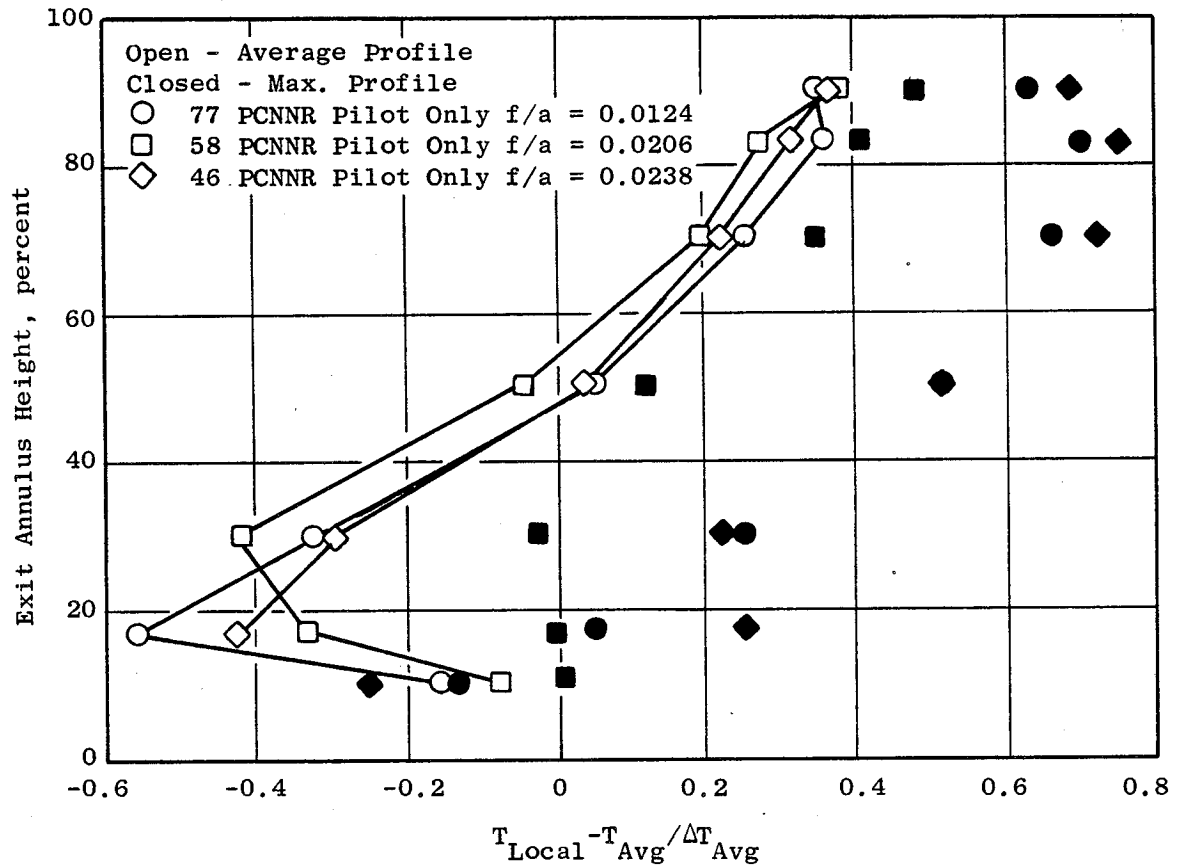


Figure 230. Mod V EGT Performance Test Results.

6.2.3.7 Concluding Remarks - Mod IV and V Combustors

The combustor hardware modifications featured in the Mod IV and V configurations failed to provide any improvement in the ground start ignition characteristics. However, the results did show that small amounts of inner liner Panel 2 dilution could be incorporated into the design without significantly affecting the main stage ignition characteristics.

Exit temperature performance results obtained from the Mod V configuration revealed excessively high pattern factor levels, despite the large quantities of trim dilution air featured in this rich main stage combustor design. Such results suggest that the short length of the E³ combustor does not provide sufficient length in which to effectively mix large quantities of trim dilution with the combustion gases. A more uniformly mixed combustor could be achieved by introducing most of the combustor air in the primary zones. Here, the air and fuel are subjected to intense mixing phenomena and have greater physical length in which to further mix before discharging from the combustor. This design philosophy is supported by making a comparison of the Mod I and V development combustors. In the Mod I combustor, 80% of the combustor air was introduced into the primary zone, while only 5% of the air was introduced as trim dilution. This configuration demonstrated acceptable exit temperature performance levels. In the Mod V combustor, only 64% of the combustor air was introduced into the primary zones with 21% of the air introduced as trim dilution. This configuration demonstrated poor exit temperature performance levels.

From testing performed on the Mod II, III, IV, and V combustor configurations, design changes involving significant reductions in the main stage primary zone airflow were necessary to evolve the desired main stage ignition characteristics. The large quantities in trim dilution air in these designs were necessary to compensate for the reduced dome flows in order to maintain the combustor overall total pressure drop. All of this suggested that it will be extremely difficult to evolve a rich main stage design of this short length combustor that will demonstrate the desired main stage ignition characteristics as well as exit temperature performance levels within the E³ goals. Considerably more development effort would be necessary to resolve this problem.

6.2.3.8 Mod VI and VII Development Combustor Test Results

The Mod VI and VII combustor configurations featured hardware modifications intended to revert the combustor design from the rich main stage dome designs featured in configurations Mod II through V, back to the original lean main stage design concept.

The decision to revert back to the original design intent was based on the results of an updated starting study of the E³ system conducted by Systems Engineering. In this study, measured performance data from the major components were incorporated into the E³ dynamic start model. Based on this component test data, the measured performance of the compressor and high pressure turbine components was considerably better in the low speed operating range than had originally been projected. Therefore, it would be possible to start the engine within the specified time requirements with a considerably lower T₄ level, significantly reducing the risk of overtemperating the turbine from the high levels of combustor exit temperature pattern factor associated with the pilot only mode of operation.

All of the hardware modifications required to revert back to the original design intent were identified by tracing the development history of the combustor. The combustor hardware modifications featured in the Mod VI configuration are provided below:

- Open all holes currently welded closed in the outer dome outer cooling ring and the outer liner cooling Ring 1.
- Open all holes in the outer dome inner cooling ring that are in line with the two crossfire tubes.
- Close off all outer liner Panel 2 dilution holes.
- Reduce the size of all outer liner Panel 3 dilution holes.
- Return the main stage swirl cup primary swirlers to standard configuration by removing the nichrome patches used in the Mod V combustor to block off every other vane passage. Also, replace the main stage secondary swirlers with larger size swirlers, originally used in the baseline combustor main stage.
- Restore the main stage splash plate cooling to standard level by opening all holes closed off in the Mod V combustor.
- Reopen all holes closed in the inner dome outer cooling ring.

- Reduce the size of all inner liner Panel 3 dilution holes.

It would have been preferred to incorporate even larger secondary swirlers in the main stage. However, this would have required machining another set of castings leaving an insufficient supply for the core engine combustor.

The Mod VII configuration, like the Mod VI configuration, featured a lean main stage design. The combustor was completely disassembled and refurbished to improve the hardware quality. New dome sleeves were installed in both the pilot stage and main stage swirl cups. The new main stage sleeves featured a shortened, overall length with the same trailing edge diameter. In addition, a small amount of inner liner Panel 3 trim dilution was moved upstream into Panel 2. Estimates of the airflow distribution of these configurations are presented in Appendix E.

6.2.3.9 Atmospheric Ground Start Ignition Test

Ground start ignition evaluation of the E³ development combustor Mod VI configuration was conducted in the ACL Cell A3W facility on June 25, 1981. The purpose of this test was to evaluate the ignition, crossfire, and lean extinction characteristics of this combustor configuration at selected steady-state operating points along the E³ (June 1981) ground start design cycle. For the purposes of main stage crossfire, data was also obtained at simulated steady-state operating conditions representing 4%, 6%, 10%, and 30% of sea level takeoff power along the E³ FPS-II design operating cycle. Test points and corresponding operating conditions are presented in Table LI.

Ground start ignition test results for the Mod VI combustor configuration are presented in Figure 231. As observed, the pilot stage ignition characteristics satisfy the fuel schedule requirements defined in the revised (June 1981) start cycle with and without compressor bleed. Taking into consideration the improvement in ignition characteristics anticipated at actual cycle inlet pressures, the pilot stage would demonstrate considerable ignition margin along the revised start cycle. Also observed from this figure are the main stage crossfire and lean extinction characteristics. Overall combustor fuel/air ratios of 0.030 or higher were required to successfully crossfire and fully

Table LI. Mod VI and VII Atmospheric Ignition Test Point Schedule.

<ul style="list-style-type: none"> • Subidle conditions from 6/81 start cycle • Higher power condition from FPS-II cycle • Standard day • Atmospheric inlet pressure • 44.19 cm² (6.85 in.²) 					
Test Point	PCNHR	P ₃ , Atm.	T ₃ , K (° R)	W ₃₆ , kg/s (pps)	Comments
1*	21.0	1.00	304 (547)	2.19 (4.82)	Simulated No Bleed 6/81
2*	21.0	1.00	304 (547)	2.10 (4.61)	Simulated Bleed 6/81
3*	24.5	1.00	310 (558)	2.50 (5.50)	Simulated No Bleed 6/81
4*	24.5	1.00	310 (558)	2.38 (5.24)	Simulated Bleed 6/81
5* **	30.0	1.00	322 (580)	2.86 (6.30)	Simulated No Bleed 6/81
6* **	30.0	1.00	322 (580)	2.75 (6.06)	Simulated Bleed 6/81
7*	36.9	1.00	339 (610)	3.20 (7.05)	Simulated No Bleed 6/81
8*	36.9	1.00	339 (610)	3.12 (6.87)	Simulated Bleed 6/81
9**	4% FN	1.00	466 (839)	2.40 (5.29)	FPS-II Cycle
10**	64.3	1.00	483 (870)	2.29 (5.03)	6/81 Cycle
11**	6% FN	1.00	495 (892)	2.44 (5.36)	FPS-II Cycle
12**	10% FN	1.00	539 (970)	2.42 (5.33)	FPS-II Cycle
13**	30% FN	1.00	637 (1147)	2.25 (4.94)	FPS-II Cycle
<p>Note: * = Core engine motoring combustor inlet conditions (no fuel) ** = Ignition characteristics of main stage to be investigated</p>					

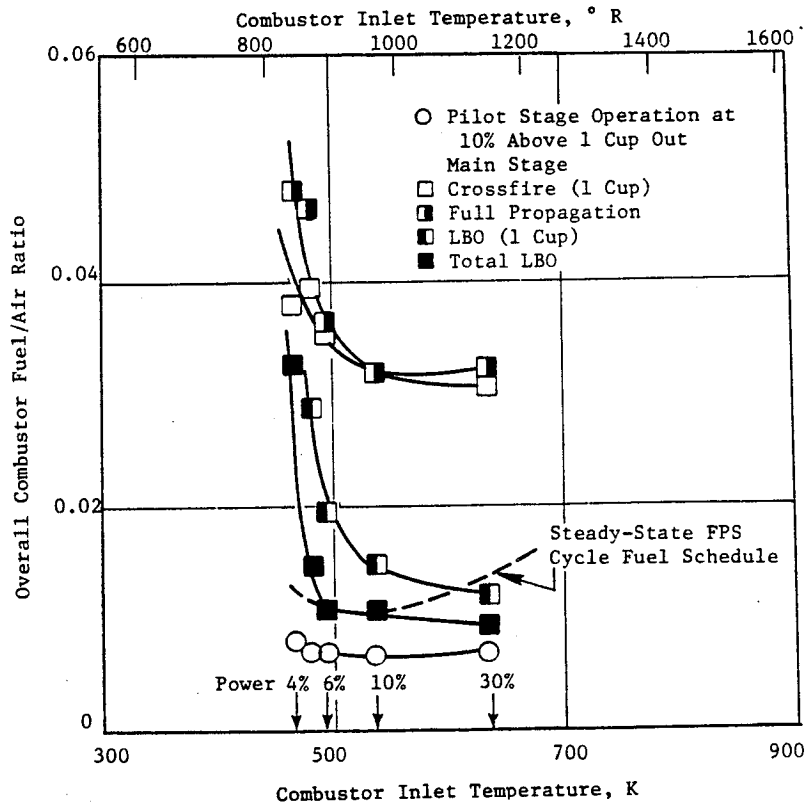
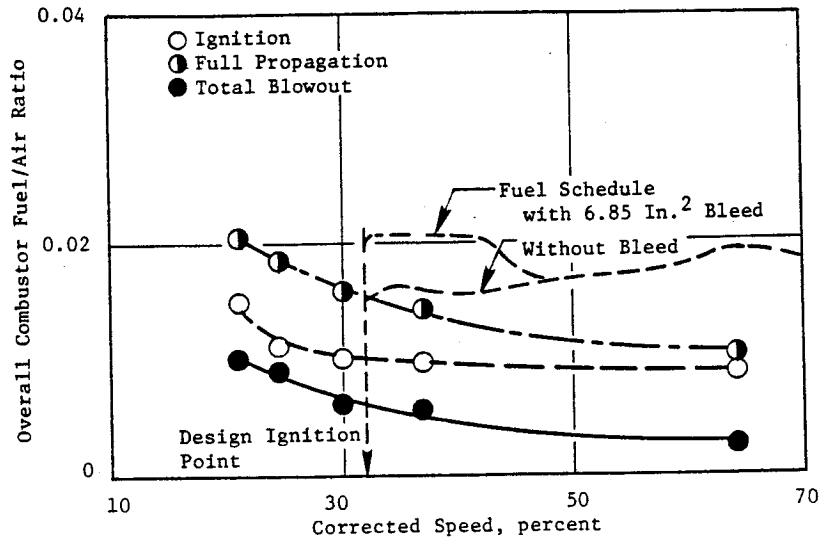


Figure 231. Mod VI Atmospheric Ignition Test Results.

propagate the main stage. These levels are well above the fuel schedule in the 4% to 30% power range as defined in the FPS design cycle and are typical of levels previously demonstrated by other configurations featuring lean main stage dome designs (baseline and Mod I configurations). As with the pilot stage, a significant amount of improvement in the main stage crossfire characteristics would be expected at actual engine cycle inlet pressures. However, it is doubted that the amount of improvement would be enough to achieve full main stage propagation below 6% power. The main stage did demonstrate sufficient blowout margin to assure that once fully propagated it would remain fully propagated at actual cycle operating conditions as low as 4% power.

Since the combustor modifications featured in the Mod VII configuration did not involve aerodynamic changes to the pilot stage, no change in the pilot stage ground start ignition characteristics was anticipated. Some slight change in the main stage ignition characteristics could be anticipated due to the modifications. Because the pilot only operating mode was once again the approach selected for engine ground start, it was felt that no new information of any significance would be obtained by evaluating the Mod VII combustor for ground start ignition characteristics. Thus this configuration was not tested for this purpose.

6.2.3.10 Atmospheric Exit Temperature Performance Test

Exit gas temperature performance testing of the E³ double-annular dome development combustor Mod VI configuration was conducted on June 29, 1981, in the ACL Cell A3W facility. The purpose of this test was to evaluate this lean main stage dome design for exit gas temperature performance at operating conditions simulating SLTO, 30% thrust, and 6% thrust along the E³ FPS-II design cycle. At simulated SLTO operating conditions, performance data were obtained at pilot-to-total fuel splits of 0.5, 0.4, and 0.3. At the simulated 30% thrust and 4% thrust operating conditions, performance data were obtained in the pilot only mode. Test points and corresponding combustor operating conditions are presented in Table LII. E³ test rig nozzle assemblies incorporating nozzle tips rated at 2.3 kg/hr (5 pph) in the pilot stage, and nozzle tips rated at 6.4 kg/hr (14 pph) in the main stage were used.

Table LII. Mod VI Atmospheric EGT Performance Test Point Schedule.

Test Point	T ₃ , K (° R)	P ₃ Atm.	W ₃ , kg/s (pps)	W _{Bleed} kg/s (pps)	W _{Comb} kg/s (pps)	f/a	W _F Pilot/ W _F Total	W _{fPilot} kg/hr (pph)	W _{fMain} kg/hr (pph)
1	1007 (1813)	1	2.41 (5.31)	0.15 (0.34)	2.26 (4.97)	0.0245	0.50	99 (218)	99 (218)
2	1007 (1813)	1	2.41 (5.31)	0.15 (0.34)	2.26 (4.97)	0.0245	0.40	80 (175)	119 (262)
3	1007 (1813)	1	2.41 (5.31)	0.15 (0.34)	2.26 (4.97)	0.0245	0.30	60 (131)	139 (306)
4	687 (1237)	1	2.58 (5.68)	0.16 (0.36)	2.42 (5.32)	0.0143	1.00	125 (274)	0
5	432 (778)	1	2.55 (5.60)	0.18 (0.40)	2.37 (5.20)	0.0123	1.00	105 (230)	0

The exit temperature performance results for the Mod VI configuration were disappointing. As observed from Figure 232, a pattern factor of 0.36 was obtained at the simulated SLTO operating condition at a pilot-to-total fuel split of 0.4. Even higher pattern factor levels were obtained at the other fuel splits investigated at this operating condition. The pattern factor goal established for this combustor development program is a level of 0.25. At a pilot-to-total fuel split of 0.5, the average profile is center peaked and generally within the design limit. However, at the 0.4 and 0.3 fuel splits, the average profile is inner peaked, and exceeds the design limit in the hub region by a considerable amount. Visual observations of the combustor during testing revealed the existence of streaks in the flame pattern at several positions around the circumference, verifying the poor performance characteristics measured. The most notable streak appeared to originate in the pilot stage in the vicinity of Cup 7. It was later discovered that an undersized pilot stage primary dilution hole existed in the vicinity of this swirl cup lending suspicion to it being the probable cause. Data obtained at the 30% thrust and 6% thrust operating conditions in the pilot only mode are presented in Figure 233. As observed from this figure, the profiles are sharply outward peaked as expected. The pattern factor levels are higher than had been anticipated with a level of 1.35 at simulated 30% thrust conditions, and a level of 1.60 at simulated 6% thrust conditions.

The combustor was removed for a detailed hardware inspection. This inspection revealed numerous hardware quality problems, many of which could be directly linked to the poor performance levels measured. Some of these problems are discussed below:

- Domes - Many of the emissions reduction sleeves were out-of-round or not concentric to the primary venturi. In addition, many sleeves had nicks and dents where they have been impacted during assembly. The emissions sleeves in the main stage also appeared to be too long compared to the design intent.
- Liners - Most of the dilution thimbles were cocked so that the conical gap was closed on one side. Many dilution holes had burrs on the hole trailing edge.
- Centerbody - The primary holes on the pilot side had burrs resulting from the use of an installation tool. The primary holes on the main side had weld beads protruding into the hole where an insert was added.

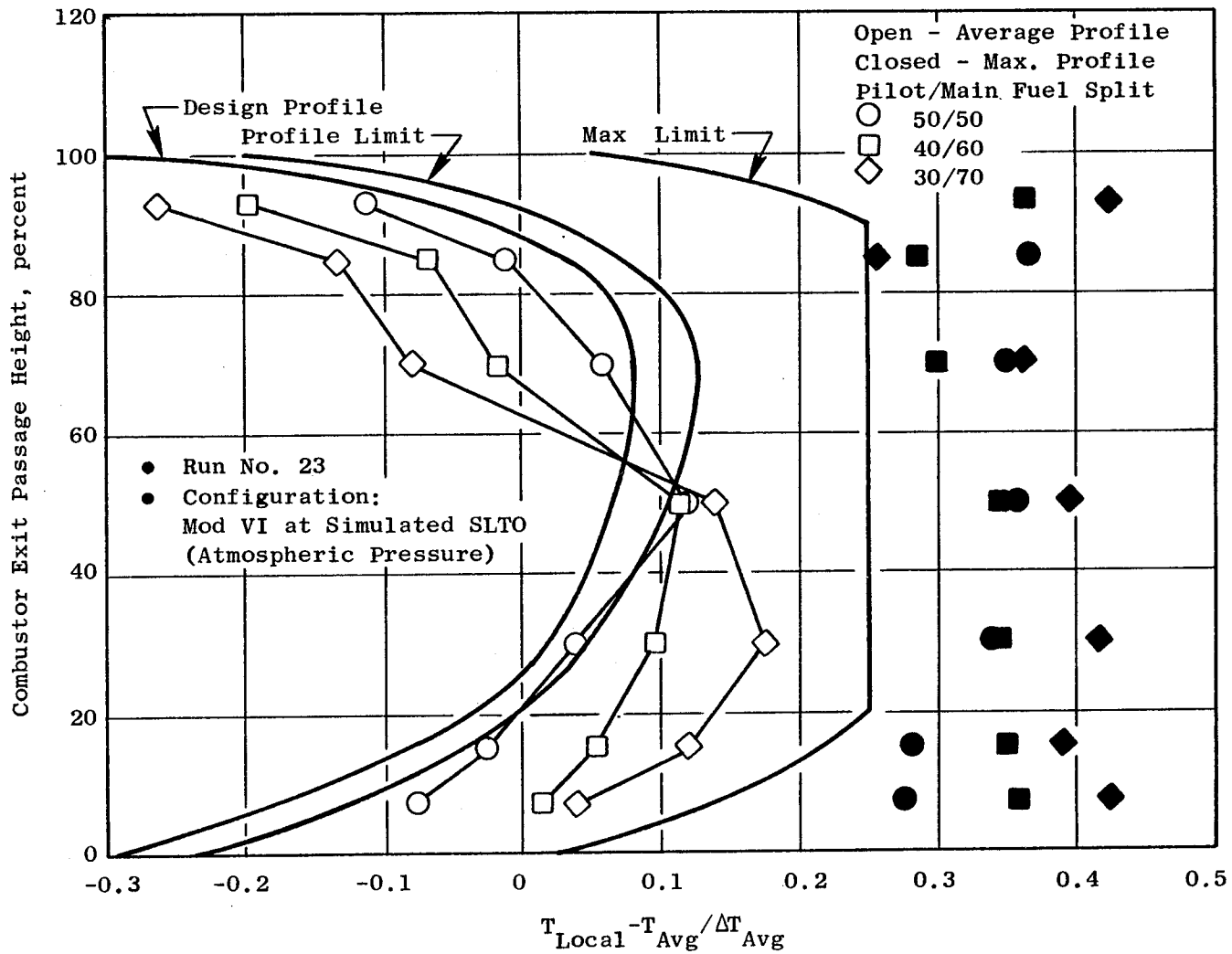


Figure 232. Mod VI EGT Performance Test Results, SLTO.

ORIGINAL PAGE IS
OF POOR QUALITY

ORIGINAL PAGE IS
OF POOR QUALITY

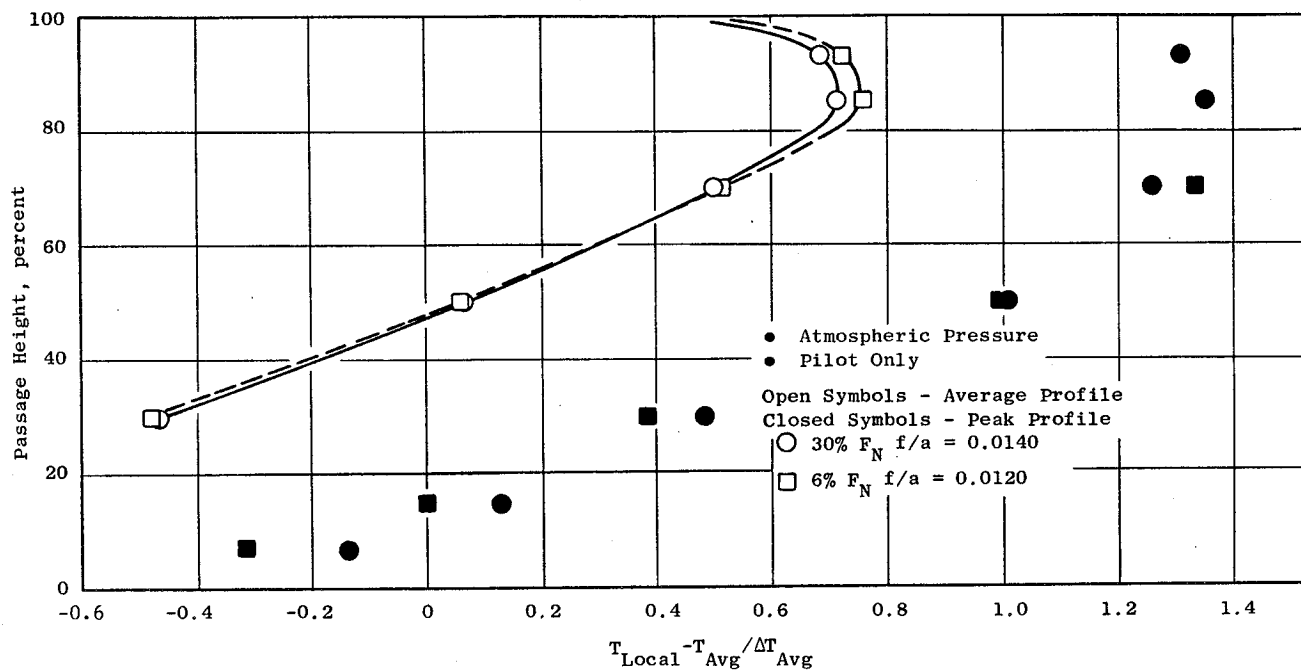


Figure 233. Mod VI EGT Performance Test Results,
Pilot Only.

The crossfire tubes extended above the centerbody surface 0.05-0.155 cm (0.020-0.060 inch). As was previously mentioned, it was also discovered that the outer liner primary dilution hole between pilot Cups 7 and 8 was considerably undersized. This particular set of combustor hardware had been subjected to six major hardware modifications with many extensive design changes implemented. Because of the hardware quality problems, the results from the exit gas temperature performance test of this combustor configuration were not considered representative of the design. The combustor hardware was reworked to improve the quality. It was then retested for exit temperature performance as the Mod VII combustor configuration.

Performance testing of the Mod VII configuration was conducted on August 21, 1981. New simplex fuel nozzles rated at 6.4 kg/hr (14.0 pph) were used in the pilot stage and main stage. Exit temperature performance evaluation of this combustor was conducted at simulated sea level takeoff operating conditions with pilot-to-total fuel splits of 0.5, 0.4, and 0.3. Data were also taken at operating conditions simulating 30% thrust at pilot-to-total fuel splits of 1.0, 0.5, and 0.4, and at simulated 4% ground idle at pilot-to-total fuel splits of 1.0 and 0.5. Test points and corresponding combustor operating conditions are presented in Table LIII.

At the simulated SLTO operating conditions, overall combustor fuel/air ratios approximately 10% above design levels were established. At the simulated lower power operating conditions with staged combustion, an overall combustor fuel/air ratio of 0.024 was established. This compared to the design level of 0.014 at the 30% approach power condition and 0.0125 at the 4% ground idle condition. The higher fuel/air ratios were necessary to achieve and maintain main stage propagation at atmospheric operating conditions.

Despite operating the combustor at higher fuel/air ratios, it was observed that several main stage cups failed to light at the simulated SLTO and 30% approach operating conditions. The problem was considerable at the simulated 4% ground idle operating condition where approximately half of the main stage cups failed to light. Throughout the development testing effort, this had been a recurring problem related to the main stage swirl cup dome design as opposed to a problem with the type of fuel nozzles used.

Table LIII. Mod VII Atmospheric EGT Performance Test Point Schedule.

Test Point	T ₃ , K (° R)	P ₃ , Atm.	W ₃ , kg/s (pps)	W _{Bleed} , kg/s (pps)	W ₃₆ , kg/s (pps)	f/a	W _f Pilot/ W _f Total	W _f Pilot kg/hr (pph)	W _f Main kg/hr (pph)	No. of Traverse Positions	Simulated Condition
1	817 (1471)	1.0	2.27 (5.00)	0.15 (0.34)	2.12 (4.66)	0.0242	0.5	92 (203)	92 (203)	120	SLTO
2	817 (1471)	1.0	2.27 (5.00)	0.15 (0.34)	2.12 (4.66)	0.0242	0.4	74 (162)	111 (244)	120	SLTO
3	817 (1471)	1.0	2.27 (5.00)	0.15 (0.34)	2.12 (4.66)	0.0242	0.3	55 (122)	129 (284)	120	SLTO
4	640 (1152)	1.0	2.69 (5.91)	0.17 (0.37)	2.52 (5.54)	0.0140	1.0	127 (279)	0	60	30% F _N
5	640 (1152)	1.0	2.69 (5.91)	0.17 (0.37)	2.52 (5.54)	0.0140	0.5	63 (139)	63 (140)	60	30% F _N
6	640 (1152)	1.0	2.69 (5.91)	0.17 (0.37)	2.52 (5.54)	0.0140	0.4	51 (112)	76 (167)	60	30% F _N
7	466 (839)	1.0	2.95 (6.48)	0.19 (0.41)	2.76 (6.07)	0.0127	1.0	126 (278)	0	60	4% F _N
8	466 (839)	1.0	2.95 (6.48)	0.19 (0.41)	2.76 (6.07)	0.0127	0.5	63 (139)	63 (139)	60	4% F _N

Average and peak profiles determined at the simulated sea level takeoff operating conditions are presented in Figure 234. As observed from this figure, the design average profile was closely approached at a 50/50 fuel split. The minimum peak profile occurred at a 40/60 fuel split with a pattern factor of 0.275. This compared to a minimum pattern factor of 0.36 obtained for the Mod VI configuration demonstrating the degree of improvement achieved by better quality. Despite the improvement, the pattern factor still exceeded the design goal of 0.250 by 10%. At the 40/60 fuel split, the average profile had a center peaked characteristic slightly exceeding the design limit at the hub. Average and peak profiles determined at the simulated lower operating conditions are presented in Figure 235. It is observed from this figure that pattern factors of 1.25 would be expected from operation of this combustor design in the pilot-only mode. A pattern factor level of 1.50 had been previously demonstrated by the baseline and Mod I combustor configurations at similar operating conditions.

The hardware modifications and refurbishment incorporated into the Mod VII combustor configuration produced significant reductions in pattern factor when compared to results from the Mod VI configuration. Although the results fell slightly short of the design goal, no further hardware modifications intended to provide additional reductions in pattern factor were made. Instead, it was decided to proceed to evaluate this development combustor configuration at true cycle operating conditions for ground start ignition performance and low power emissions at true engine cycle operating conditions.

6.2.3.11 Emissions Testing

Ignition and emissions testing of the development combustor Mod VII configuration was conducted on September 15, 1981 in the ACL Cell A3E test facility. The purpose of this test was to evaluate this combustor design for ground start ignition, crossfire from pilot-to-main-stage domes, and low power emissions characteristics at true engine operating conditions for selected points along the revised (June 1981) E³ start cycle operating line and the E³ FPS design cycle operating line. It had been intended to evaluate the combustor for emissions at 30% F_N approach power conditions at slightly derated operating conditions with pilot-to-total fuel splits of 1.0, 0.4, and

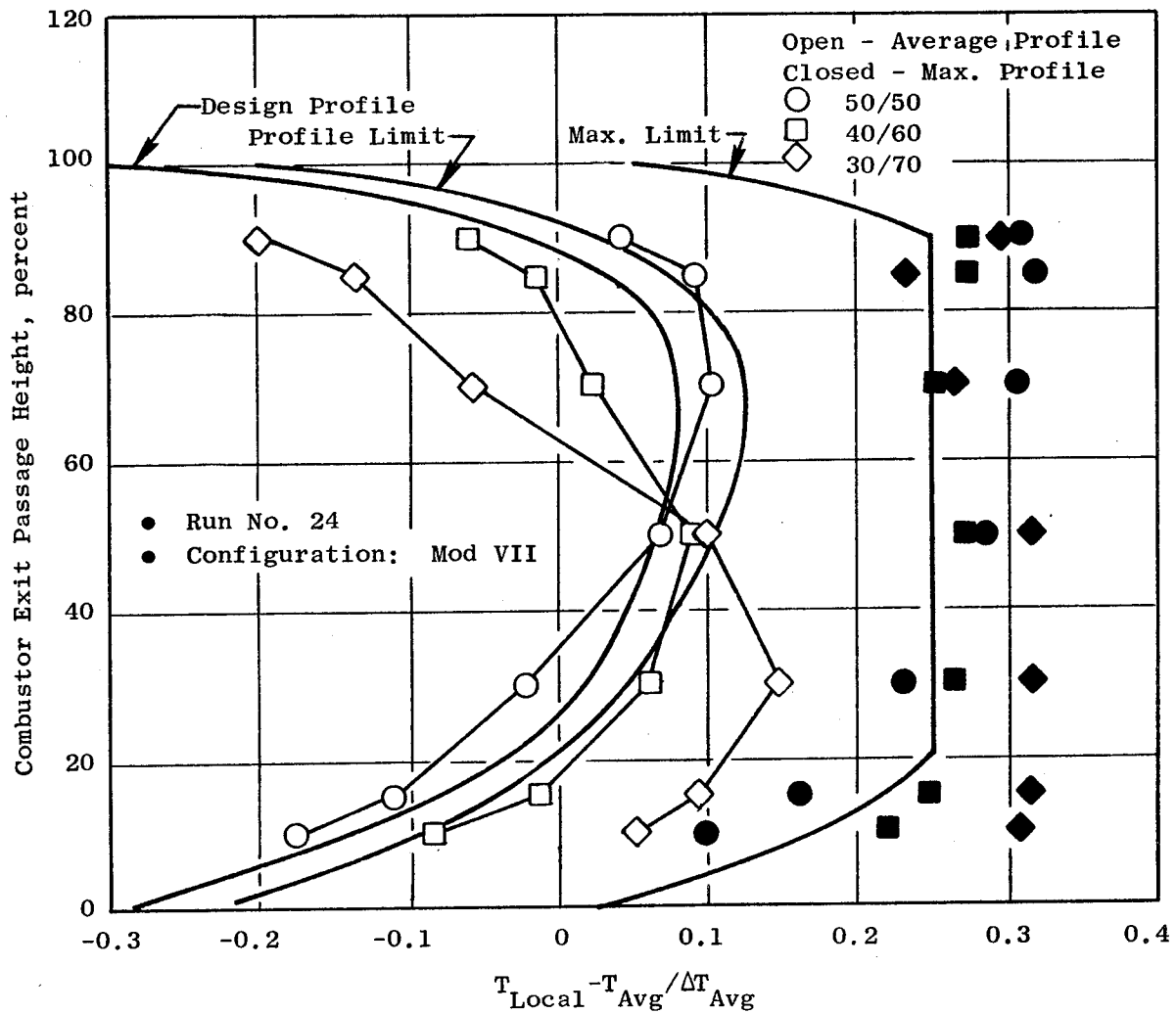


Figure 234. Mod VII EGT Performance Test Results, SLTO.

ORIGINAL PAGE IS
 OF POOR QUALITY

ORIGINAL PAGE IS
OF POOR QUALITY

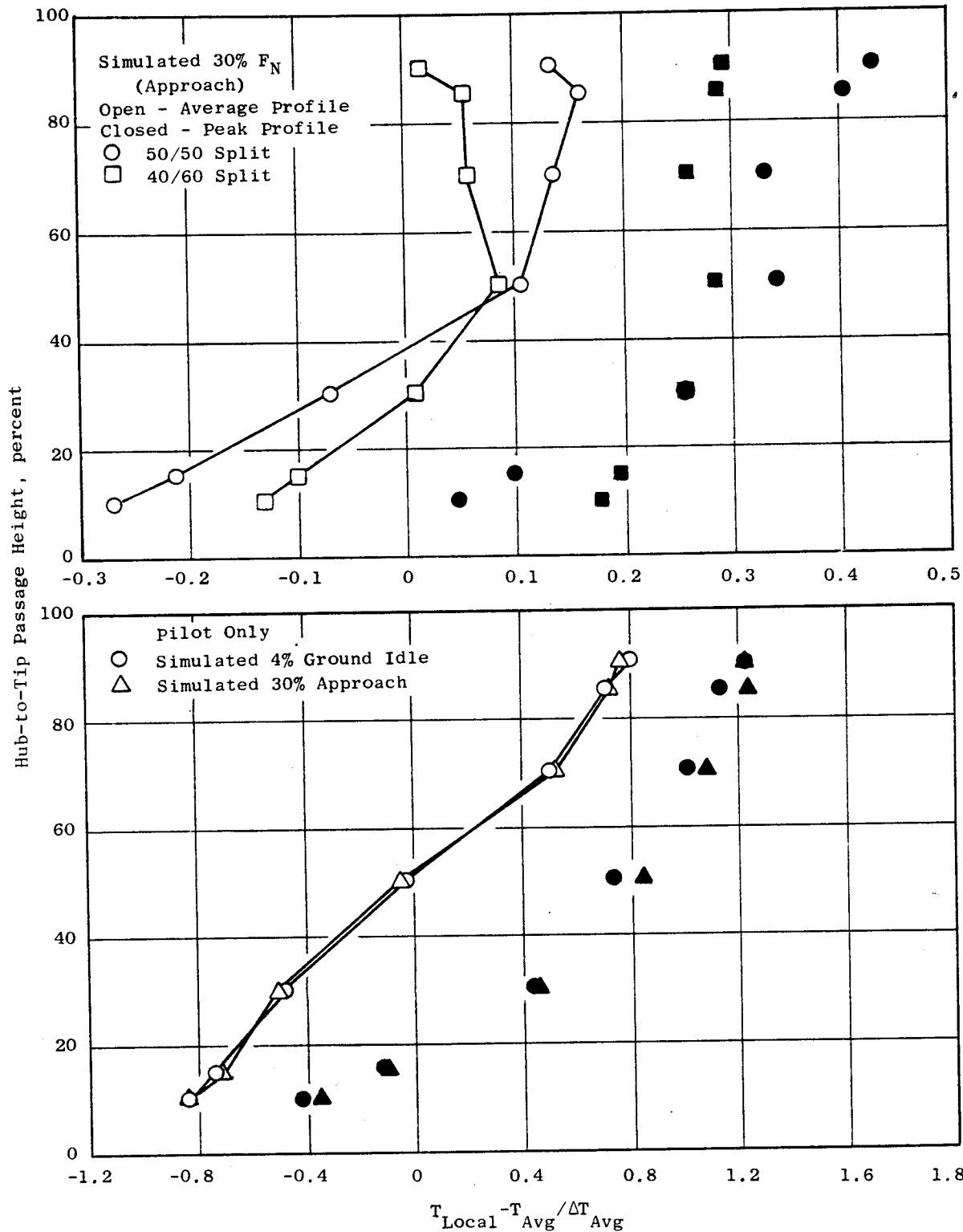


Figure 235. Mod VII EGT Performance Test Results, Low Power.

0.3. This was required to achieve the desired combustor fuel/air ratio in the pilot only mode of operation using the simplex fuel nozzles selected for use in the outer dome. However, because of problems with the facility operation, it was necessary to further derate the approach power test conditions to a maximum inlet total pressure of 0.69 MPa (100 psi) compared to the desired value of 0.90 MPa (130 psi). The engine cycle combustor inlet pressure at this operating condition is 1.21 MPa (175 psi). Test points and corresponding operating conditions are presented in Table LIV.

Simplex-type fuel nozzles rated at 12 kg/hr (26.5 pph) were used in both the pilot and main stage domes. Because this test was conducted at low power operating conditions, no combustor instrumentation was used.

As anticipated, significant improvement in both the pilot stage ignition and main stage crossfire characteristics was demonstrated at true cycle operating pressures as compared to previous atmospheric test results obtained with the Mod VI configuration. As observed from Figure 236, the pilot stage ignition satisfies the E³ (June 1981) start cycle fuel schedule with considerable margin at corrected core speeds above 30%. However, it appears unlikely that crossfire and full propagation of the main stage would be accomplished within the start cycle fuel schedule at subidle operating conditions. The main stage did demonstrate sufficient lean blowout margin to assure that, once fully propagated, the main stage would remain fully propagated at subidle operating conditions.

The results of the idle emissions testing of the Mod VII combustor configuration are presented in Figure 237. Measured emissions data obtained in the vicinity of swirl cup No. 28 (324° CW ALF) showed signs of poor combustion, yielding high levels of CO and HC emissions. A posttest inspection of the fuel nozzles revealed the presence of leaks in both the pilot and main stage nozzle tips that were located at the cup No. 28 position. The leaks appeared related to deteriorated seal rings between the nozzle tips and the mounting stems. Emissions data measured in this vicinity were factored out of the results.

Table LIV. Mod VII Emissions Test Point Schedule.

Test Point	Operating Condition	T ₃ , K (* R)	P ₃ , MPa (psi)	W ₃ , kg/s (pps)	W, kg/s (pps)	W, kg/s (pps)	W, kg/s (pps)	W _{comb} , kg/s (pps)	f/a Overall	W _f Total (pph)	W _{fPilot} / W _{fTotal}	W _{fPilot} kg/hr (pph)	W _{fMain} kg/h (pph)	Sampling Mode
1	2l	304 (547)	0.112 (16.9)	2.36 (5.2)	0	0	0	2.36 (5.2)						Ignition
2		310 (558)	0.117 (16.9)	2.81 (6.2)	0	0	0	2.81 (6.2)						Ignition
3		322 (580)	0.125 (18.1)	3.45 (7.6)	0	0	0	3.45 (7.6)						Ignition
4		351 (632)	0.161 (23.3)	3.73 (8.6)	0	0	0	3.73 (8.2)						Ignition
5	4% Idle	466 (839)	0.346 (50.2)	8.18 (18.0)	0	0	0	8.18 (18.6)						Ignition
6	6% Idle	402 (886)	0.436 (63.2)	10.41 (22.9)	0	0	0	10.41 (22.9)						Ignition
7	10% Idle	533 (960)	0.596 (86.4)	14.09 (31.0)	0	0	0	14.09 (31.0)						Ignition
8	4% Idle	466 (839)	0.346 (50.2)	9.86 (21.7)	0.57 (1.23)	0.52 (1.15)	0.63 (1.38)	8.14 (19.9)	0.0090	264 (581)	1.0	264 (581)	0	G
9		466 (839)	0.346 (50.2)	9.86 (21.7)	0.57 (1.23)	0.52 (1.15)	0.63 (1.38)	8.14 (19.9)	0.0110	323 (710)	1.0	323 (710)	0	G
10		466 (839)	0.346 (50.2)	9.86 (21.7)	0.57 (1.23)	0.52 (1.15)	0.63 (1.38)	8.14 (19.9)	0.0127	372 (819)	1.0	372 (819)	0	G,I
11		466 (839)	0.346 (50.2)	9.86 (21.7)	0.57 (1.23)	0.52 (1.15)	0.63 (1.38)	8.14 (19.9)	0.15	440 (968)	1.0	440 (968)	0	G
12		466 (839)	0.346 (50.2)	9.86 (21.7)	0.57 (1.23)	0.52 (1.15)	0.63 (1.38)	8.14 (19.9)	0.02	586 (1290)	1.0	586 (1290)	0	G
13	6% Idle	492 (887)	0.436 (63.2)	12.5 (27.5)	0.72 (1.58)	0.66 (1.45)	0.80 (1.75)	10.32 (22.7)	0.008	297 (654)	1.0	297 (654)	0	G
14		492 (887)	0.436 (63.2)	12.5 (27.5)	0.72 (1.58)	0.66 (1.45)	0.80 (1.75)	10.32 (22.7)	0.01	371 (817)	1.0	371 (817)	0	G
15		492 (887)	0.436 (63.2)	12.5 (27.5)	0.72 (1.58)	0.66 (1.45)	0.80 (1.75)	10.32 (22.7)	0.0116	431 (948)	1.0	431 (948)	0	G,I
16		492 (887)	0.436 (63.2)	12.5 (27.5)	0.72 (1.58)	0.66 (1.45)	0.80 (1.75)	10.32 (22.7)	0.015	557 (1226)	1.0	557 (1226)	0	G
17		492 (887)	0.436 (63.2)	12.5 (27.5)	0.72 (1.58)	0.66 (1.45)	0.80 (1.75)	10.32 (22.7)	0.02	743 (1634)	1.0	743 (1634)	0	G
18	30%	640 (1152)	0.896 (130.0)	23.45 (51.6)	1.37 (2.94)	1.23 (2.71)	1.48 (3.26)	19.41 (42.7)	0.014	978 (2156)	1.0	978 (2156)	0	G
19		640 (1152)	0.896 (130.0)	23.45 (51.6)	1.37 (2.94)	1.23 (2.71)	1.48 (3.26)	19.41 (42.7)	0.014	978 (2156)	0.4	391 (861)	587 (1291)	G
20		640 (1152)	0.896 (130.0)	23.45 (51.6)	1.37 (2.94)	1.23 (2.71)	1.48 (3.26)	19.41 (42.7)	0.014	978 (2156)	0.8	294 (646)	685 (1506)	G

ORIGINAL FROM IS OF POOR QUALITY

ORIGINAL PAGE IS
OF POOR QUALITY

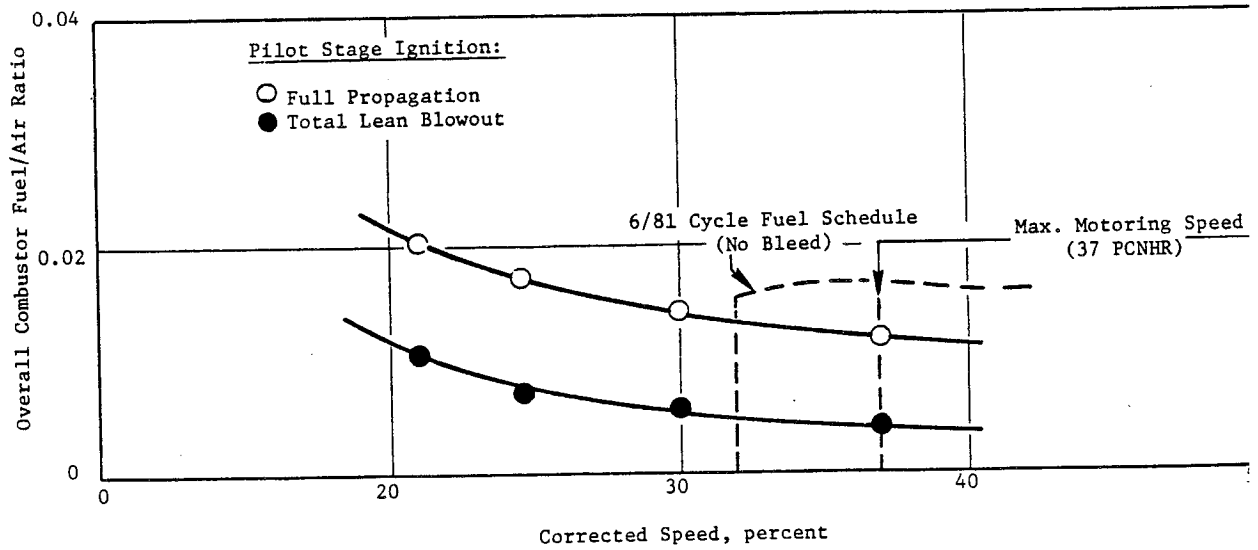
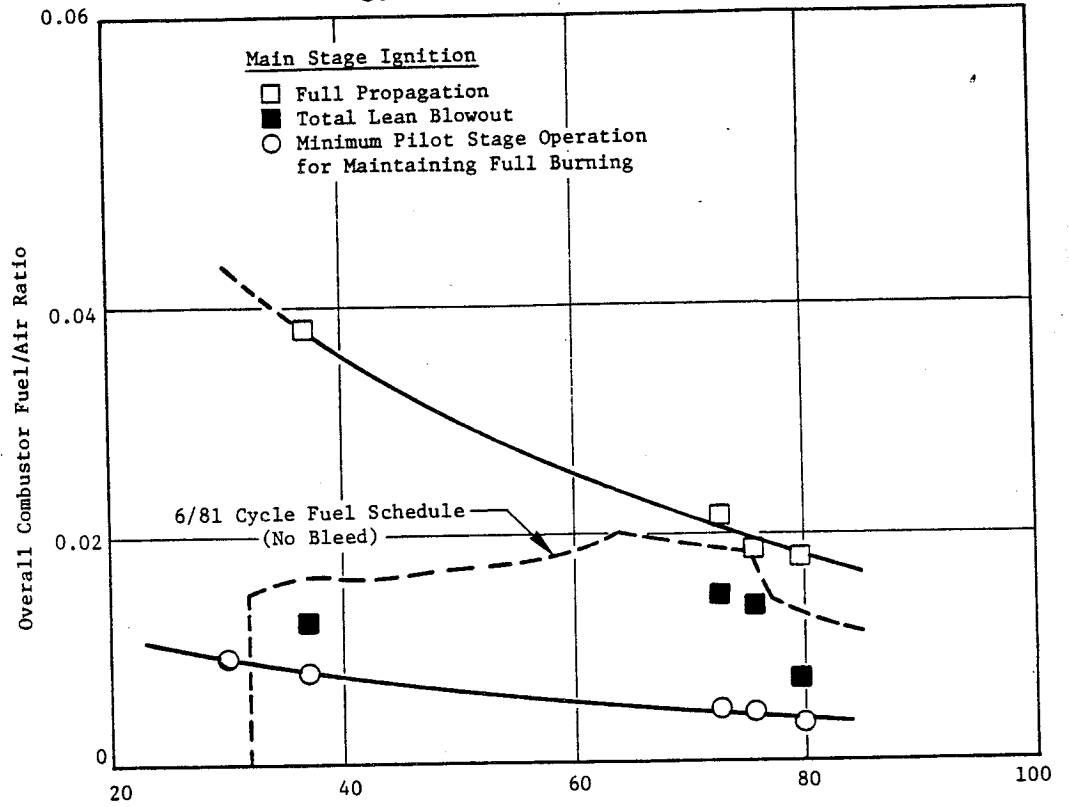


Figure 236. Mod VII Ignition Results at True Cycle Conditions.

As observed from Figure 237, significant reductions in CO emissions were achieved compared to levels previously demonstrated with the Mod I configuration. At the 6% design idle operating condition, a CO level of 23.3 g/kg (23.3 lbm/1000 lb) of fuel was obtained. This closely approached the program target level of 20.7 g/kg (20.7 lbm/1000 lb) of fuel. A minimum level of 20 g/kg (20 lbm/1000 lb) of fuel was achieved at a slightly off-design combustor fuel/air ratio of 0.0129 compared to the design cycle fuel/air ratio of 0.0116. Hydrocarbon emissions were nearly identical to levels previously demonstrated with the Mod I configuration. A HC emissions level of 4.3 g/kg (4.3 lbm/1000 lb) of fuel was obtained at the 6% design idle operating condition. The program target level at this operating condition is a level of 2.8 g/kg (2.8 lbm/1000 lb) of fuel. HC levels at or below this target level were demonstrated at 6% ground idle operating conditions at overall fuel/air ratios greater than 0.015. CO and HC emissions data obtained at the derated approach power operating condition (30% F_N) were adjusted to correct for the low inlet total pressures. The results presented in Table LV show that very low levels of CO and HC emissions were demonstrated in the pilot only operating mode. However, significantly higher levels resulted for the staged operating modes. These results are similar to those previously obtained for the baseline and Mod I development combustor configurations evaluated at similar conditions. As previously suggested, the reason for the high CO and HC emissions levels is related to the low design cycle fuel/air ratio of 0.014 at this operating condition which produces two very lean domes in the staged operating mode.

Table LV. Mod VII Emissions Results at Approach Power.

Combustor Operation Mode	Emission Index, g/kg fuel (lbm/1000 lb)		
	CO	HC	NO _x
Pilot only	2.9 (2.9)	0.4 (0.4)	10.7 (10.7)
40/60 Split	54.0 (54.0)	22.9 (22.9)	2.7 (2.7)
30/70 Split	56.0 (56.0)	40.7 (40.7)	2.2 (2.2)

ORIGINAL PAGE IS
OF POOR QUALITY

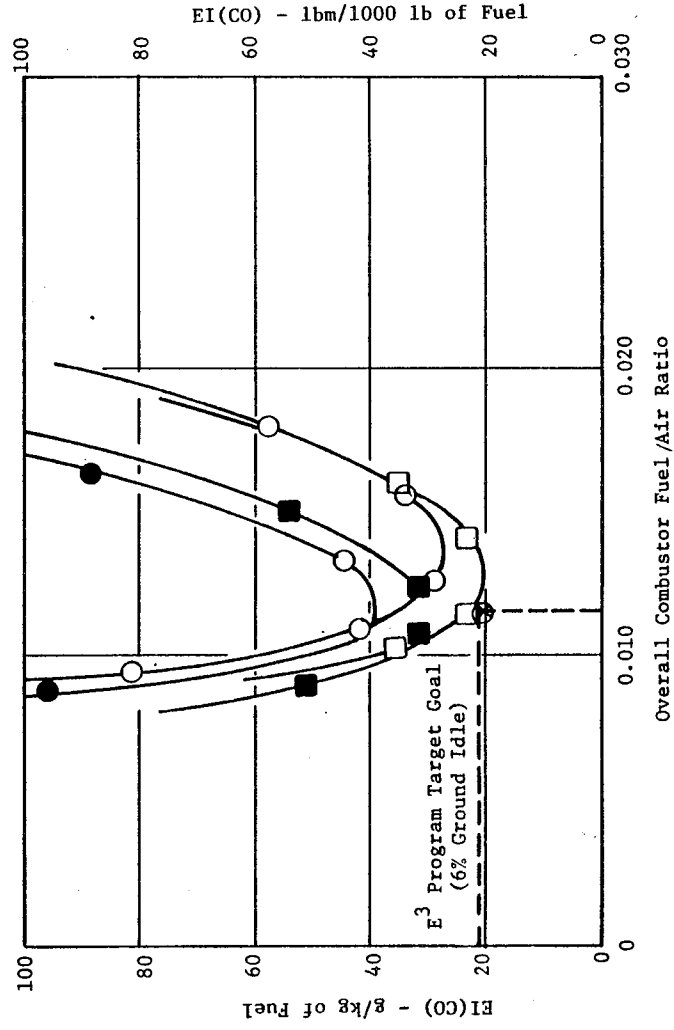
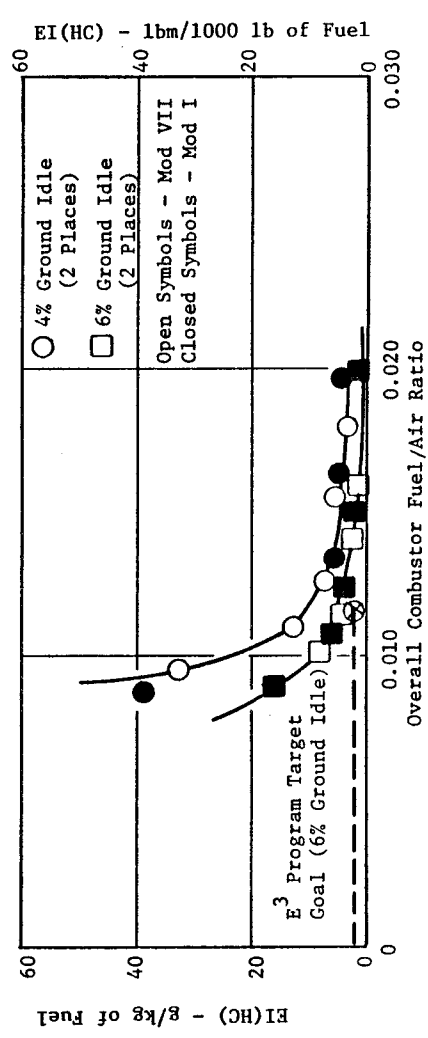


Figure 237. Mod VII Emissions Test Results, Idle Conditions.

NO_x emission data obtained at the derated approach power operating conditions were also adjusted to the correct operating conditions. The results for the three pilot-to-total fuel splits are also presented in Table LIII. As would be expected, the lean combustion conditions associated with fuel staging yields very low levels of NO_x, while the pilot only operating mode yields levels considerably higher. In Figure 238, the measured NO_x emission levels obtained in the staged operating mode are plotted against the E³ design cycle severity parameter. Also shown in this figure are measured data obtained from the baseline and Mod I combustor configurations. It is observed from this figure that the NO_x emission characteristic of the Mod VII configuration appears to be very similar to the characteristics demonstrated by the other configurations. Therefore, NO_x emission levels at sea level takeoff operating conditions similar to the other two configurations would be anticipated. Both the baseline and Mod I combustors demonstrated NO_x levels which satisfied the E³ Program goal.

EPA parameter numbers, based on the EPA landing-takeoff cycle for CO, HC, and NO_x, were generated for combustor operation at 6% ground idle and pilot-to-total fuel splits of 1.0 and 0.35 at the approach power operating condition. The results are presented in Table LVI and compared to the E³ Program goals for the three emissions categories. As observed from this table, the NO_x emission levels satisfy the program goal with pilot only or staging at the approach power operating condition. However, both the CO and HC emissions levels fail to meet the respective program goals with either operating mode. With the pilot only operating mode, the CO emissions closely approach the goal, while reductions greater than 30% are required for the HC emissions. Significantly greater reductions in both CO and HC emissions are required to satisfy the program target goals for staged combustor operation at approach.

Table LVI. Mod VII EPAP Results.

	Pilot Only at Approach	35/65 Split at Approach	E ³ Program Goals
	lb Emission/1000 lb Thrust-Hr-Cycle		
Carbon Monoxide	3.27	6.40	3.00
Hydrocarbons	0.58	2.48	0.40
Oxides of nitrogen	2.96	2.51	3.00

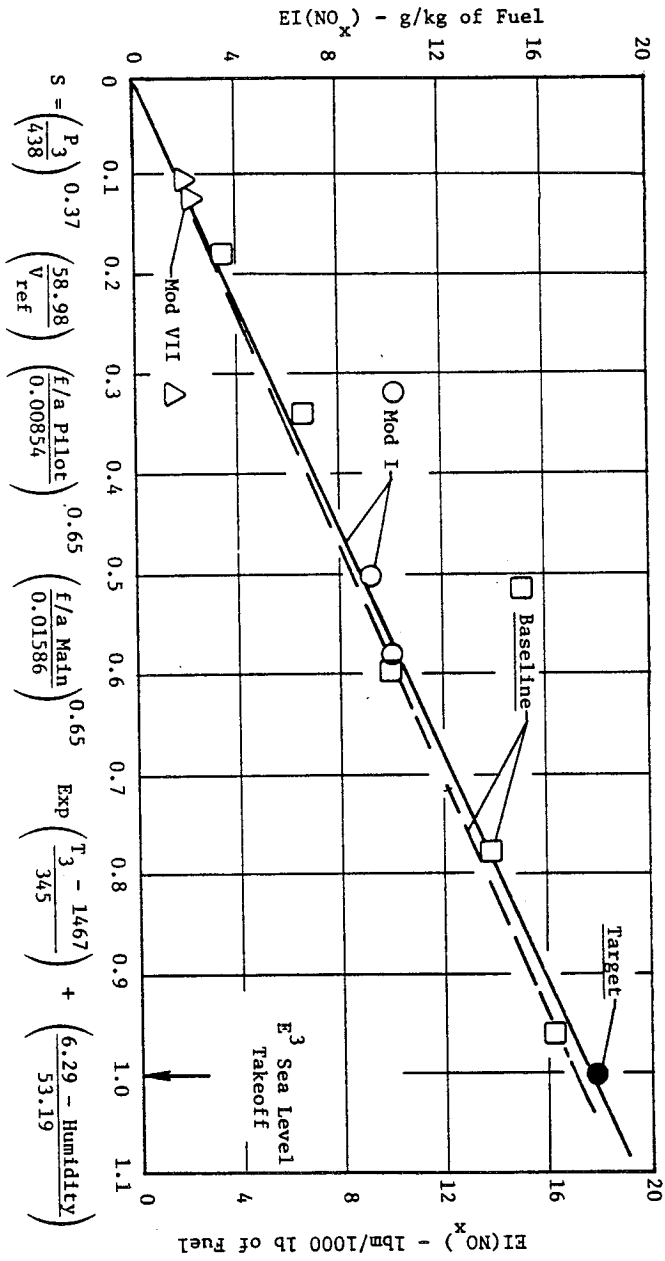


Figure 238. Mod VII Emissions Test Results, EI_{NO_x}

ORIGINAL DOCUMENT
OF POOR QUALITY

As part of the emissions test, combustor pressure drop data were measured. The Mod VII combustor meets the E³ goal level of 5.0% at sea level takeoff as shown in Figure 239. The current data represent an improvement with respect to data incurred on the baseline and Mod I combustors shown in Figure 239.

6.2.3.12 Concluding Remarks - Mod VI and VII Combustors

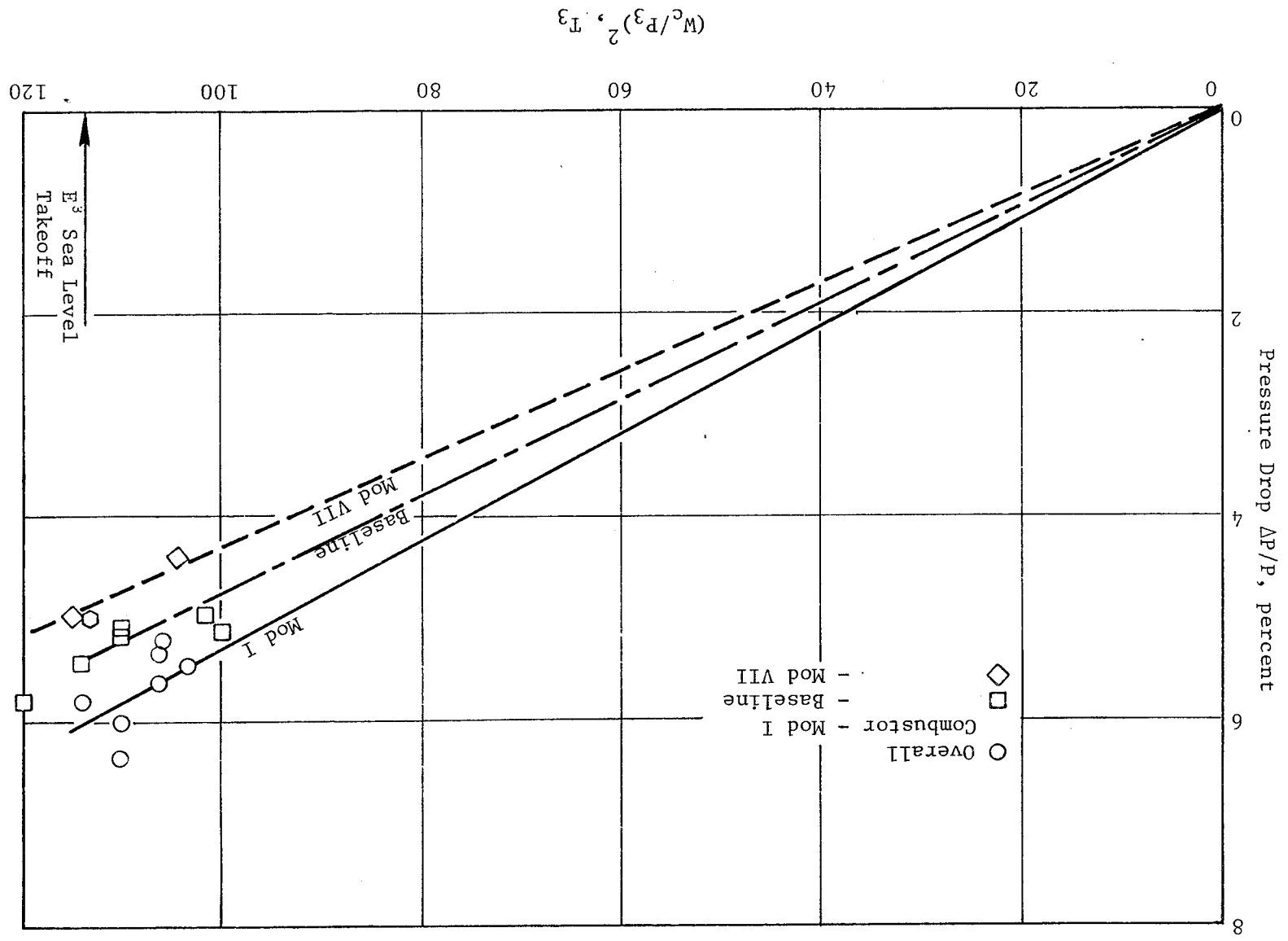
The Mod VII combustor configuration evolved from this test series represented the final E³ development combustor design configuration. This configuration succeeded in demonstrating excellent pilot stage ignition characteristics, acceptable exit temperature performance, and emissions which meet (NO_x) or closely approach (CO and HC) the combustor development program emissions goals. Like earlier lean main stage designs evaluated in this development program, the main stage ignition characteristics are not good enough to allow staging at subidle operating conditions. However, this should pose no problem in actual engine operation since modifications in the ground start operating cycle permit tolerable starts to idle power with the pilot only staging mode.

Studies conducted on E³ swirl cup hardware have indicated the potential to achieve improvement in the main stage ignition characteristics by adjusting the secondary-to-primary swirler area ratio. Other studies conducted as part of the E³ sector combustor subcomponent testing have demonstrated a significant impact of fuel nozzle design on emissions performance. Using fuel nozzles with wider spray angles and better atomization than obtained with the development combustor fuel nozzles produced significant reductions in CO and HC emissions at idle operating conditions. Thus improvements in swirl cup and fuel nozzle design have the potential to provide improvement in the CO and HC emissions to levels sufficient to satisfy the program goals.

6.2.3.13 Conclusion - Summary

During the E³ full-annular combustor component testing effort, a total of 25 test runs were conducted. These test runs represented ground start ignition, exit temperature performance, and emissions evaluations of 10 development combustor configurations (six rich main stage designs and four lean main stage

OVERALL PRESSURE LOSS
OF POOR QUALITY



$(W_c/P_3)^2, T_3$

Pressure Drop $\Delta P/P$, percent

- Overall
- Combustor - Mod I
- Baseline
- Mod VII

E^3 Sea Level Takeoff

designs). Summaries of these design configurations and their evaluation results are presented in Tables LVII and LVIII.

Results of the ground start ignition testing are summarized in Table LIX. Development combustor Mod VII meets the ignition requirement for pilot stage only fueled.

The emissions results for the lean dome combustor designs are summarized in Table LX. Development combustor Mod VII meets the requirement for NO_x and closely approaches the CO and HC goal levels with pilot only fueled at approach power. The smoke level goal was demonstrated with slight margin.

Combustor pressure loss meets the goal level, and measured efficiency levels are satisfactory above idle.

The results of pattern factor and profile shape are outlined in Table LXI. Development combustor Mod VII meets the profile requirement but needs root trim and is 10% high of the pattern factor goal.

Peak metal temperatures measured should pose no problems during engine operations.

Table LVIII. Summary of Full-Annular Combustor Configurations.

Combustor	Pilot Dome	Main Dome	Centerbody	Outer Liner	Inner Liner
Mod I	<ul style="list-style-type: none"> ● Swirl cup flow reduced ● Cooling reduced 	Increased swirl cup flow	Reduced pilot dilution	Increased <ul style="list-style-type: none"> ● Primary dilution ● Trim dilution ● Ring 1 cooling 	Increased <ul style="list-style-type: none"> ● Trim dilution ● Ring 1 cooling
Mod II	Reduced swirl cup flow	Reduced swirl cup flow	<ul style="list-style-type: none"> ● Increased -Pilot and main dilution ● Increased pilot and main cooling ● Shortened 	<ul style="list-style-type: none"> ● Increased primary dilution ● Reduced Ring 1 cooling 	<ul style="list-style-type: none"> ● Increased primary dilution ● Added Pannel 2 dilution
Mod III	Pilot dome cooling reduced	<ul style="list-style-type: none"> ● Swirl cup flow reduced ● Dome cooling reduced 	Extended cross-fire tube	Aft dilution increased	<ul style="list-style-type: none"> ● Aft dilution increased ● Eliminated Panel 2 dilution
Mod IV	Same	Same	Same	Same	<ul style="list-style-type: none"> ● Aft dilution reduced ● Panel 2 dilution added
Mod V	Same	Same	Reduced primary dilution thimble	Added Panel 2 dilution	Reduced primary dilution thimble
Mod VI	Same	Swirl cup flow increased	Original cross-fire tube	<ul style="list-style-type: none"> ● Panel 2 removed ● Aft dilution reduced 	Aft dilution reduced
Mod VII	Same	Same	Same	Same	Panel 2 dilution increased

Table LVIII. Summary of Full-Annular Combustor Test Results.

Config.	Ground Start Igniton Performance	EGT Performance	Emissions Performance EPAP			Comments
			CO	HC	NOx	
Mod II-A	<ul style="list-style-type: none"> ● Pilot stage ignition characteristics not as good as Mod I, but acceptable. ● Main stage ignition characteristics not as good as Mod I. 	No data obtained.	No data obtained.			Strong airflow currents produced from combined effects of inner Panel 2 dilution and C/B cooling flow appears to prevent fire from pilot stage from penetrating into main stage annulus through crossfire tubes for ignition.
Mod II-B	<ul style="list-style-type: none"> ● No change in pilot stage ignition characteristics. ● Main stage ignition characteristics improved but still not good enough to permit staging at subidle operating conditions. 	No data obtained.	No data obtained.			Combustion gases from pilot stage do not penetrate into main stage annulus through crossfire tubes.
Mod III-A	<ul style="list-style-type: none"> ● No significant change in pilot stage ignition characteristics. ● Significant improvement in main stage ignition characteristics. At true cycle inlet pressures, staging can occur down to 45% core speed. 	No data obtained.	No data obtained.			Crossfire tube needs to be moved forward to bring ignition source closer to main stage dome.
Mod III-B	Slight improvement in main stage ignition characteristics. At true cycle inlet pressures, staging can take place at 40% core speed with little or no compressor bleed.	A pattern factor of 0.45 demonstrated at 40/60 fuel split.	No data obtained.			Too much inner trim dilution. Mixing distance too short to allow that much air to mix with combustion gases to provide better uniformity.
Mod IV	<ul style="list-style-type: none"> ● Pilot stage ignition characteristics unchanged. ● Main stage ignition characteristics deteriorated. 	No data obtained.	No data obtained			Introduction of inner liner Panel 2 dilution is detrimental to main stage ignition characteristics.
Mod V	<ul style="list-style-type: none"> ● Pilot stage ignition characteristics unchanged. ● Main stage ignition improved slightly. At true cycle inlet pressures, staging can take place at 50% core speed. 	<ul style="list-style-type: none"> ● A pattern factor of 0.50 demonstrated at 40/60 fuel split. ● Average profile inward peaked and exceeds the design limit by a considerable amount. 	No data obtained			<p>Removing airflow from primary zone of main stage to enrichen for ignition improvements is detrimental to EGT performance of this length combustor.</p> <p>In conclusion, to evolve a rich dome main stage combustor configuration with acceptable ignition and EGT performance will require substantial additional development.</p>

ORIGINAL PAGE IS
OF POOR QUALITY

Table LVIII. Summary of Full-Annular Combustor Test Results (Concluded).

Config.	Ground Start Igniton Performance	EGT Performance	Emissions Performance EPAP			Comments
			CO	HC	NOx	
Baseline	<ul style="list-style-type: none"> • Marginal pilot stage ignition characteristics. • Poor main stage ignition characteristics in subidle operating range. 	<ul style="list-style-type: none"> • Pattern factor of 0.41 at 40/60 fuel split. • Pattern factor of 0.26 at 50/50 fuel split. 	8.20	3.03	2.78	<ul style="list-style-type: none"> • Main stage not required to ignite at subidle conditions. • Minimum CO and HC emissions occurred at f/a above design cycle conditions.
Mod I	<ul style="list-style-type: none"> • Significantly improved pilot stage ignition characteristics. • Satisfies goal with margin. • Main stage ignition characteristics not as good as baseline configurations. 	<ul style="list-style-type: none"> • Pattern factor of 0.24 at 40/60 fuel split. • Average temperature profile beyond limit in hub region. 	4.55	0.47	2.81	Minimum CO and HC emissions occurred near design cycle f/a.
Mod VI	<ul style="list-style-type: none"> • Pilot stage ignition characteristics satisfy 6/81 start cycle with margin. • Could not achieve main stage full propagation at subidle conditions. 	<ul style="list-style-type: none"> • Pattern factor of 0.36 at 40/60 fuel split. • Average temperature profile beyond limit in hub region. 	No data obtained.			Poor combustor quality believed related to poor EGT performance.
Mod VII	<ul style="list-style-type: none"> • Ignition characteristics of pilot and main stage similar to Mod 6. 	<ul style="list-style-type: none"> • Pattern factor of 0.27 at 40/60 fuel split. • Average profile only slightly beyond limit in hub region. 	3.27	0.58	2.96	Main stage will ignite at operating condition above 10% power.

ORIGINAL PAGE IS
OF POOR QUALITY

Table LIX. Subidle Ignition Test Results.

	Pilot Stage	Target	Main Stage	Target
Baseline	0.031	0.032 at 32% PCNHR	No reqt.	No reqt.
Mod I	0.025 (0.021)	0.032 at 32% PCNHR	No reqt.	No reqt.
Mod II	0.031	0.032 at 32% PCNHR	No light	0.022 at 35% PCNHR
Mod III	0.026	0.032 at 32% PCNHR	0.064	0.022 at 35% PCNHR
Mod IV	0.029	0.032 at 32% PCNHR	0.070	0.022 at 35% PCNHR
Mod V	0.029	0.032 at 32% PCNHR	0.070	0.022 at 35% PCNHR
Mod VI	0.015	0.0155 at 32% PCNHR	No reqt.	No reqt.
Mod VII	0.013	0.0155 at 32% PCNHR	No reqt.	No reqt.
Boxed-in numbers meet requirements.				

ORIGINAL PAGE IS
OF POOR QUALITY

Table LX. Combustor Emissions Summary.

<ul style="list-style-type: none"> ● 6% Ground Idle ● Pilot Only at Approach ● Jet A Fuel ● FPS Design Cycle 			
Configuration	lb/1000 lb Thrust- hr/Cycle		
	EPAP CO	EPAP HC	EPAP NO _x
Mod VII	3.3	0.58	2.96
Mod I	4.55	0.57	2.81
Baseline	8.22	3.10	2.81
E ³ Program Goals	3.0	0.40	3.0

Table LXI. E³ Development Combustor Exit Temperature Distribution Results.

<ul style="list-style-type: none"> ● Atmospheric Test ● Pilot-to-Total Flow Split = 0.40 			
Configuration	Pattern Factor	Profile Factor	Main Dome Design
Baseline	0.41	0.14	Lean
Mod I	0.25	0.10	Lean
Mod II	N/A	N/A	Rich
Mod III	0.56	0.04	Rich
Mod IV	N/A	N/A	Rich
Mod V	0.40	0.20	Rich
Mod VI	0.36	0.12	Lean
Mod VII	0.27	0.09	Lean
Goal	0.25	0.125	

7.0 CONCLUDING REMARKS

The NASA/GE E³ combustor development program has been a very successful component development effort. Technology derived from design studies and development testing efforts were used to design an engine combustion system. Despite the successes, several performance areas stand out as requiring further development to evolve the design into one which would be totally acceptable for use in advanced aircraft engine applications.

These areas involve improving the main stage crossfire characteristics to permit combustor staging at ground idle operation, improving combustion efficiency at the 30% approach power conditions while operating the combustor in the staged mode, and further reducing the high power NO_x emissions.

Significantly better performance levels were predicted for the engine diffuser system than those demonstrated with the combustor component test rig diffuser. Therefore, the high NO_x levels demonstrated in the component (test rig) evaluation of the engine combustion system are not considered representative of the E³ FPS design. From knowledge of the flow characteristics of the combustor and engine diffuser performance predictions, the E³ FPS combustion system will satisfy the E³ Program NO_x emission goal as well as the CO and HC goals. Estimates of the E³ FPS emissions are presented in terms of the EPA parameter in Table LXII.

Table LXII. E³ FPS Emissions Predictions.

<ul style="list-style-type: none"> • EPAP lb/1000 lb - Thrust-Hour-Cycle • E³ FPS Sea Level Static Standard Day Operating Cycle • Pilot Only at Approach Power 					
	Program Goal	Ground Idle at 4% FN		Ground Idle at 6% FN	
		EPAP	Percent Margin	EPAP	Percent Margin
CO	3.00	2.45	23	1.58	90
HC	0.40	0.22	82	0.11	364
NO _x	3.00	2.98	1	2.80	7

In summary, at the close of this reporting period, the following has been accomplished:

- Combustor aeromechanical design complete
- Subcomponent tests complete except for inspection and flow check of the engine fuel nozzles
- Development combustor tests complete:
 - Satisfactory ignition
 - Pattern factor very close to goal
 - NO_x emissions meet goal
 - CO and HC emissions closely approach goal for pilot only at approach
- Core engine combustor component tests imminent.

APPENDIX - TABLE OF CONTENTS

Appendix	Title
A	Location and Numbering of E ³ Annular Rig Instrumentation
B	Performance Curves of E ₃ Combustor Split Duct Diffuser as Obtained from Full-Scale Model Testing at Schenectady CR&D Center
C	Summary and Description of Component Sector Rig Test Configurations and Results
D	Emissions Correction and Correlation Equation
E	Estimated Airflow Distributions for E ³ Annular Combustor Configurations During Development Program
F	Data Summary Tables for E ³ Development Annular Combustor Tests

APPENDIX A
LOCATION AND NUMBERING OF E³ ANNULAR RIG INSTRUMENTATION

<u>Group No.</u>	<u>Quantity</u>	<u>Axial Location from Start of Diff.</u>	<u>Angular Position (degrees)</u>	<u>Tap No.</u>	<u>Measurement Function</u>
1	4	-2.75	48, 132, 228, 312	101-104	Pressure Recovery
2	2	-0.50	48, 228	105-106	Pressure Recovery
3	2	0.	48, 228	107-108	Pressure Recovery
4	2	0.38	48, 228	109-110	Pressure Recovery
5	2	0.76	48, 228	111-112	Pressure Recovery
6	2	1.14	48, 228	113-114	Pressure Recovery
7	2	1.51	48, 228	115-116	Pressure Recovery
8	2	1.89	48, 228	117-118	Pressure Recovery
9	2	2.27	48, 228	119-120	Pressure Recovery
10	2	0.65	48, 228	121-122	Pressure Recovery
11	2	2.50	48, 228	123-124	Pressure Recovery
12	2	3.90	48, 228	125-126	Pressure Recovery
13	2	4.80	48, 228	127-128	Pressure Recovery
14	2	5.90	48, 228	129-130	Pressure Recovery
15	4	8.00	48, 132, 228, 312	131-134	Pressure Recovery and Flow Split
16	2	4.25	45, 225	201-202	
17	2	4.97	48, 228	203-204	
18	2	5.90	48, 228	205-206	

PRECEDING PAGE BLANK NOT FILMED

PRECEDING PAGE BLANK NOT FILMED

PAGE 4/6 INTENTIONALLY BLANK

<u>Group No.</u>	<u>Quantity</u>	<u>Axial Location from Start of Diff.</u>	<u>Angular Position (degrees)</u>	<u>Tap No.</u>	<u>Measurement Function</u>
19	4	8.00	48, 132, 228, 312	207-210	Pressure Recovery and Flow Split
20	4	5.60	45, 135, 225, 315	301-304	Pressure Recovery
21	4	8.00		305-308	Flow Split
22	4	5.60	45, 135, 225, 315	401-404	Pressure Recovery
23	4	8.00	48, 132, 228, 312	405-408	Flow Split
24	2	4.80	225	501-502	
25	4	8.00	45, 135, 225, 315	503-506	Pressure Recovery and Flow Split
26	2	4.85	45, 225	601-602	
27	4	8.00	45, 135, 225, 315	603-606	Pressure Recovery and Flow Split
28	4	6.10	45, 135, 225, 315	701-704	Pressure Recovery
29	4	8.00	48, 132, 228, 312	705-708	Flow Split
30	4	6.10	45, 135, 225, 315	801-804	Pressure Recovery
31	4	8.00		805-808	Flow Split
32	2	4.65	45, 225	901-902	
33	2	5.45	45, 225	903-904	
34	4	8.00	48, 132, 228, 312	905-908	Pressure Recovery and Flow Split

<u>Group No.</u>	<u>Quantity</u>	<u>Axial Location from Start of Diff.</u>	<u>Angular Position (degrees)</u>	<u>Tap No.</u>	<u>Measurement Function</u>
35	4	-2.75	48, 132, 228, 312	1001-1004	
36	2	-0.50	48, 228	1005-1006	
37	2	0.	48, 228	1007-1008	
38	2	0.43	48, 228	1009-1010	
39	2	0.85	48, 228	1011-1012	
40	2	1.28	48, 228	1013-1014	
41	2	1.71	48, 228	1015-1016	
42	2	2.14	48, 228	1017-1018	
43	2	2.56	48, 228	1019-1020	
44	2	2.689	48, 228	1021-1022	
45	2	3.38	48, 228	1023-1024	
46	2	4.10	48, 228	1025-1026	
47	2	5.45	48, 228	1027-1028	
48	4	8.00	48, 132, 228, 312	1029-1032	Pressure Recovery and Flow Split
49	2	Prediffuser	48, 228	1101-1102	
50	2	Discharge	48, 228	1103-1104	

APPENDIX B

PERFORMANCE CURVES OF E³ COMBUSTOR SPLIT DUCT DIFFUSER AS OBTAINED
FROM FULL-SCALE MODEL TESTING AT SCHENECTADY CR&D CENTER

This Appendix presents static pressure recovery curves for each of the individual passage test runs with the three inlet velocity profiles for the E³ combustor inlet diffuser as shown in Figures 1B through 15B.

ORIGINAL SOURCE
OF FOUR QUARTERS

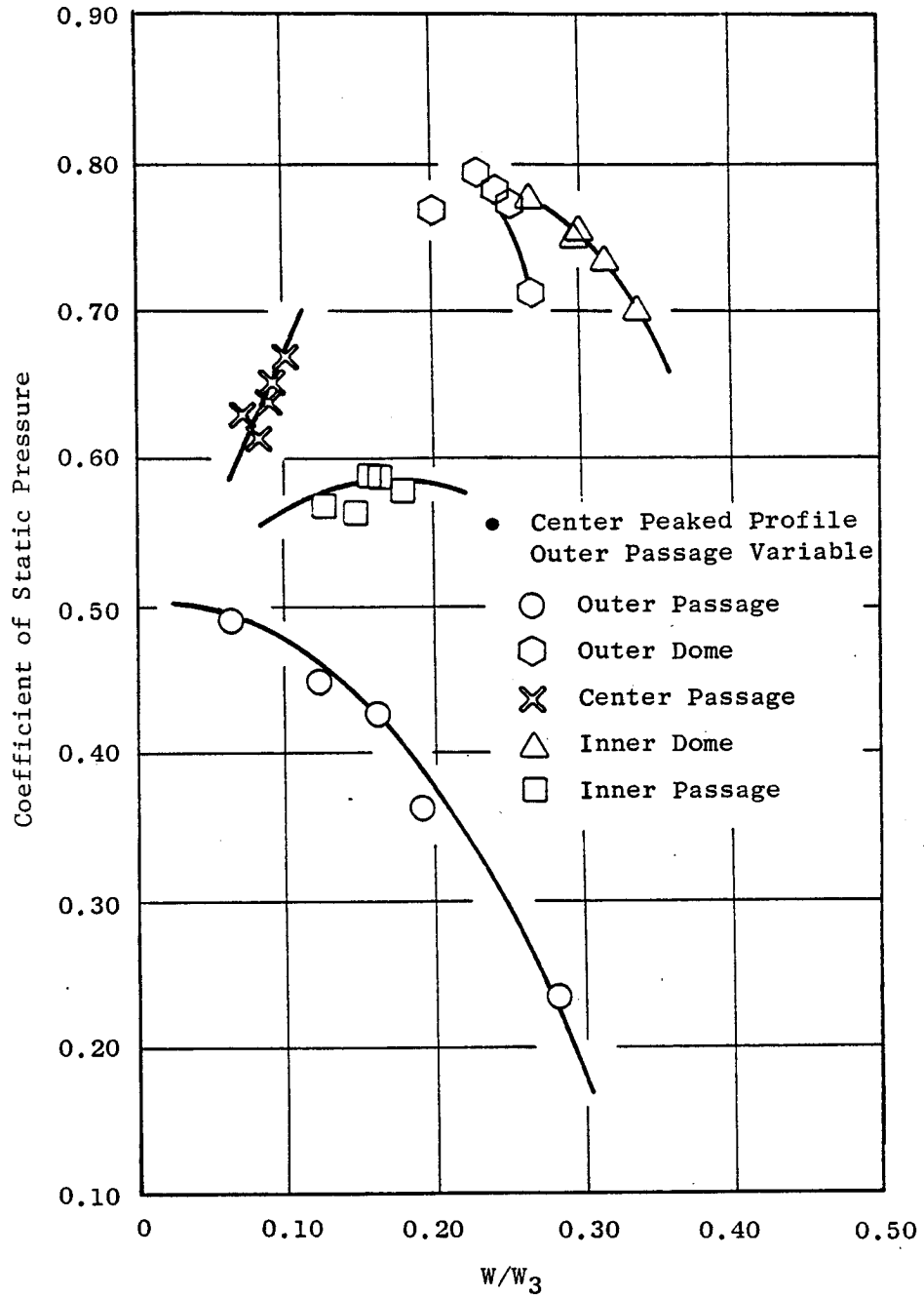


Figure 1B. E³ Combustor Inlet Diffuser CR&D Model Test Data.

ORIGINAL PAGE IS
OF POOR QUALITY

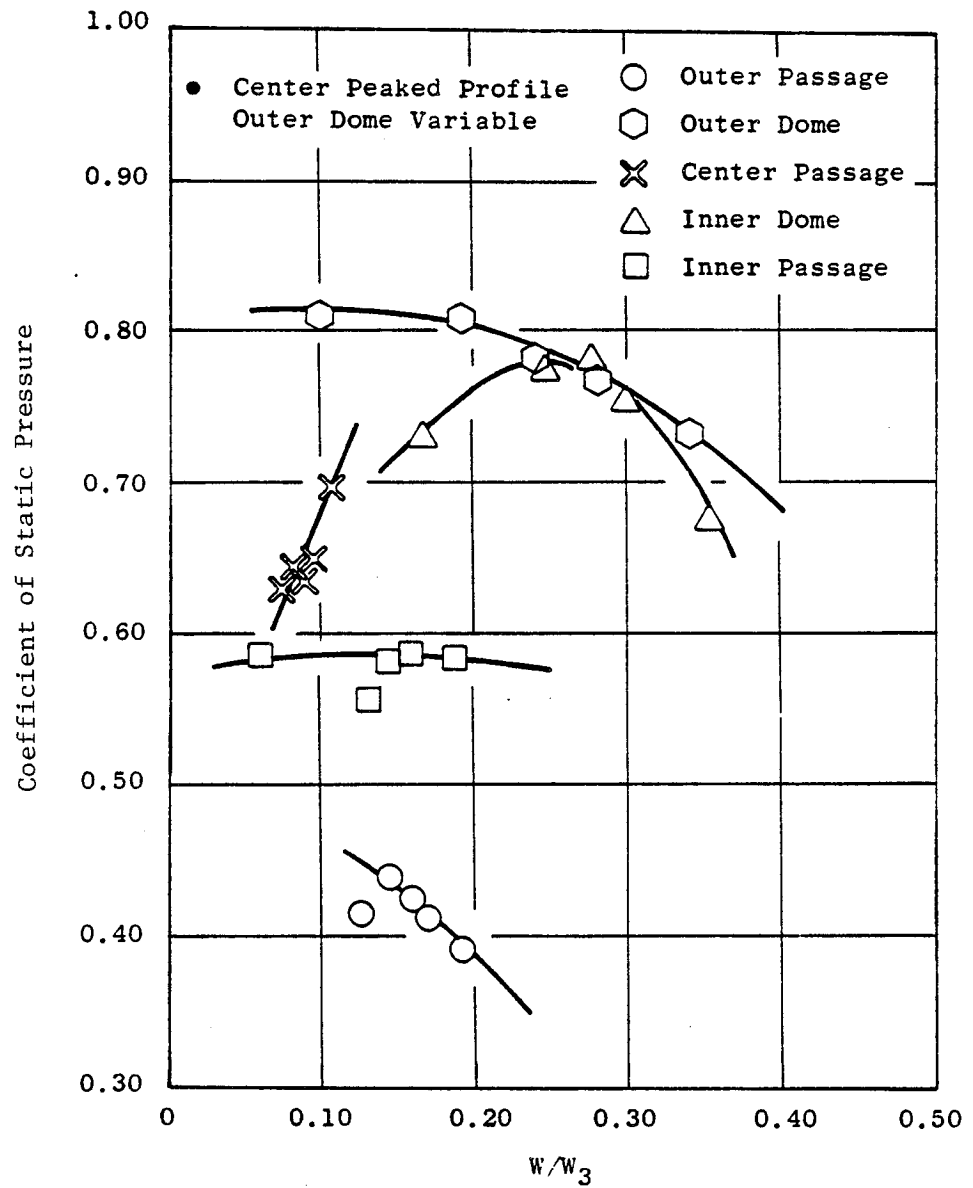


Figure 2B. E³ Combustor Inlet Diffuser CR&D Model Test Data.

ORIGINAL PAGE IS
OF POOR QUALITY

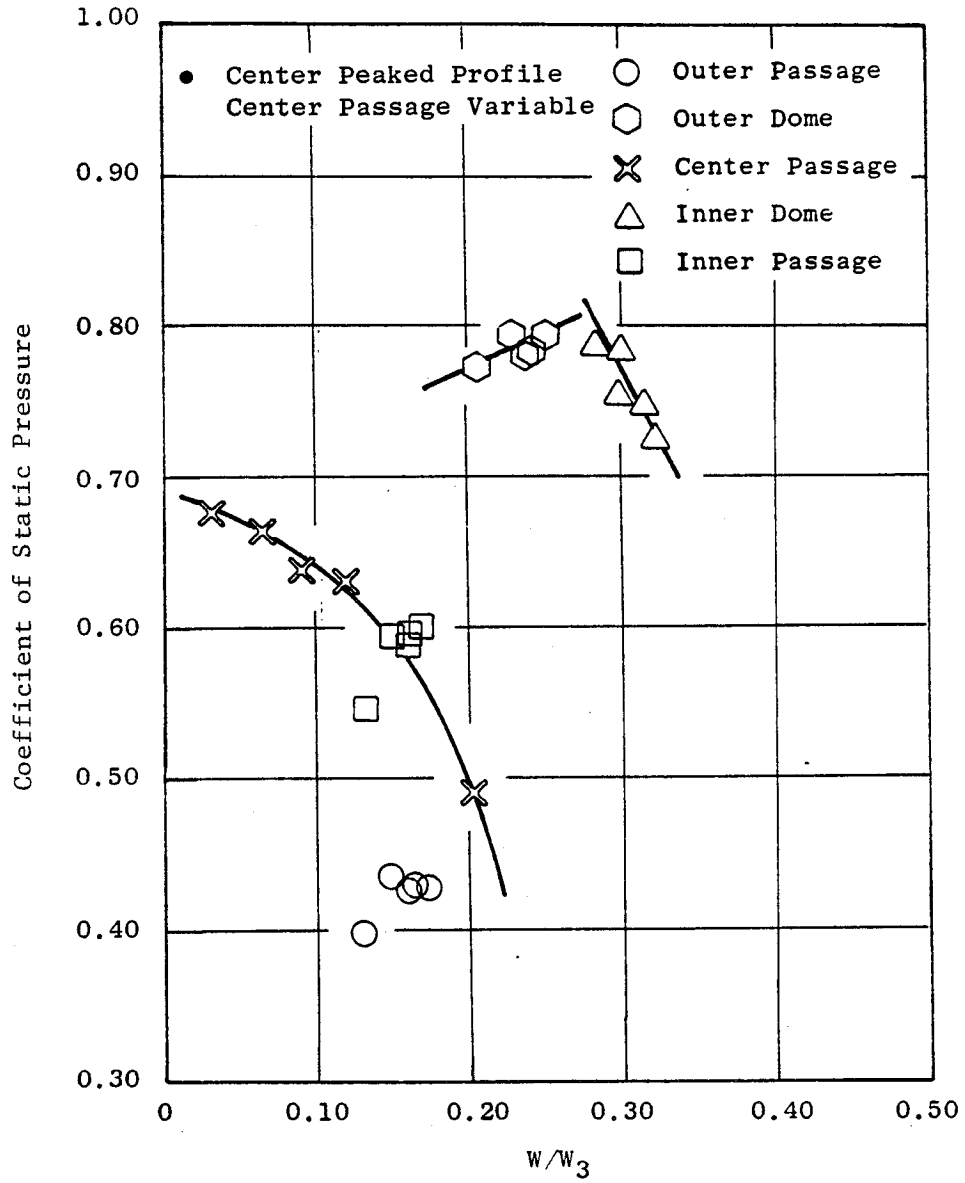


Figure 3B. E³ Combustor Inlet Diffuser CR&D Model Test Data.

ORIGINAL PAGE IS
OF POOR QUALITY

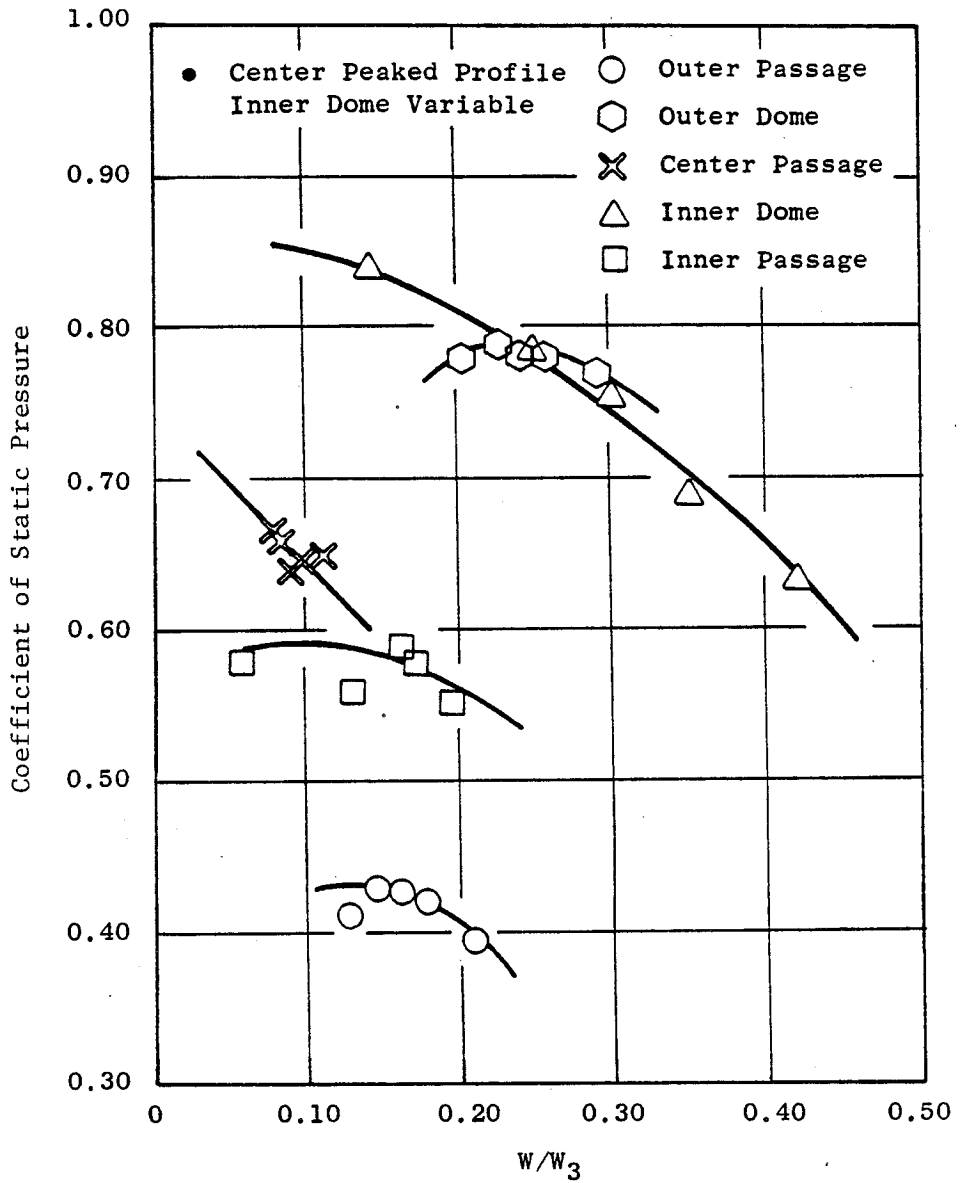


Figure 4B. E^3 Combustor Inlet Diffuser CR&D Model Test Data.

ORIGINAL PAGE IS
OF POOR QUALITY

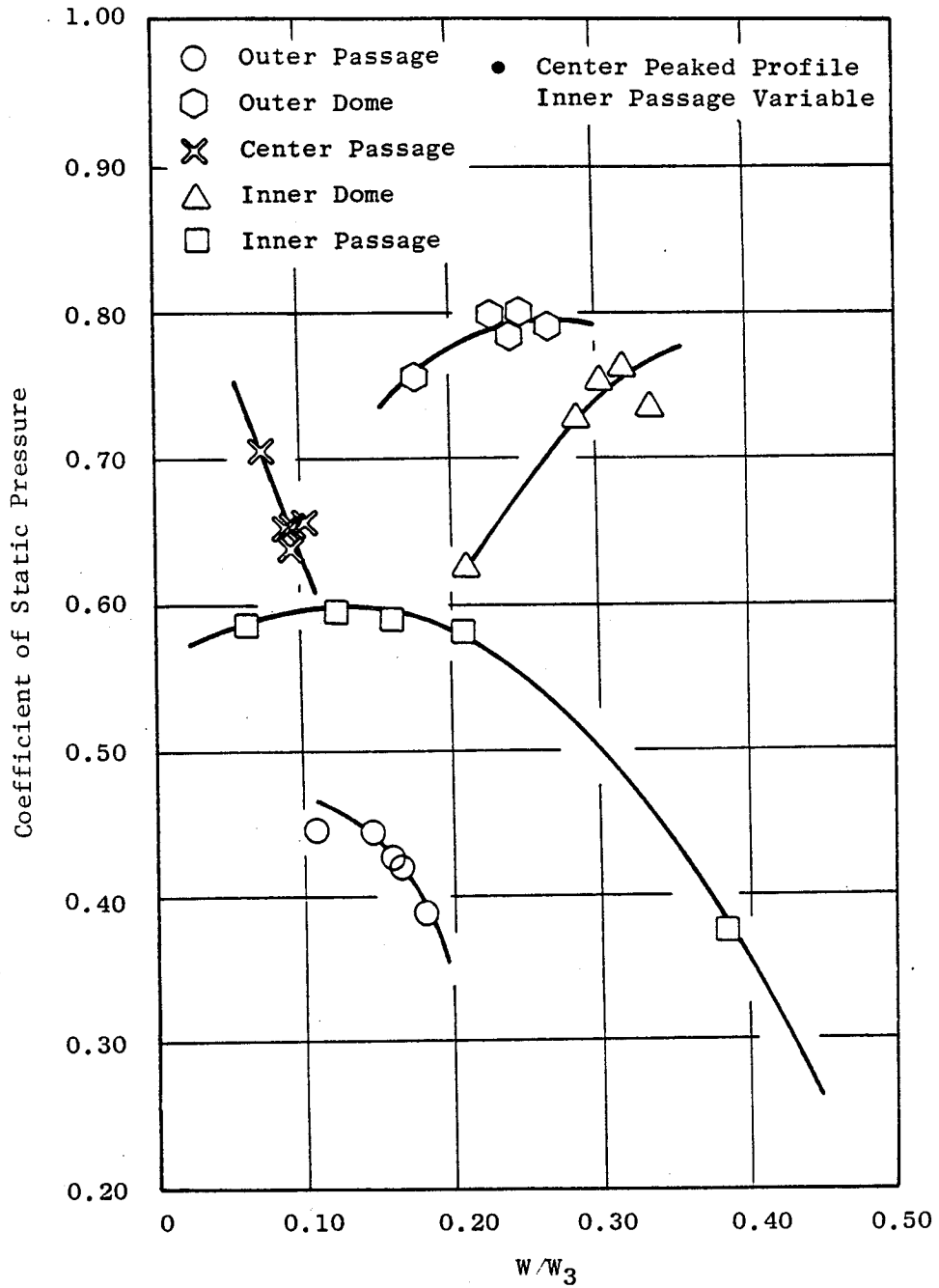


Figure 5B. E³ Combustor Inlet Diffuser CR&D Model Test Data.

ORIGINAL PAGE IS
OF POOR QUALITY

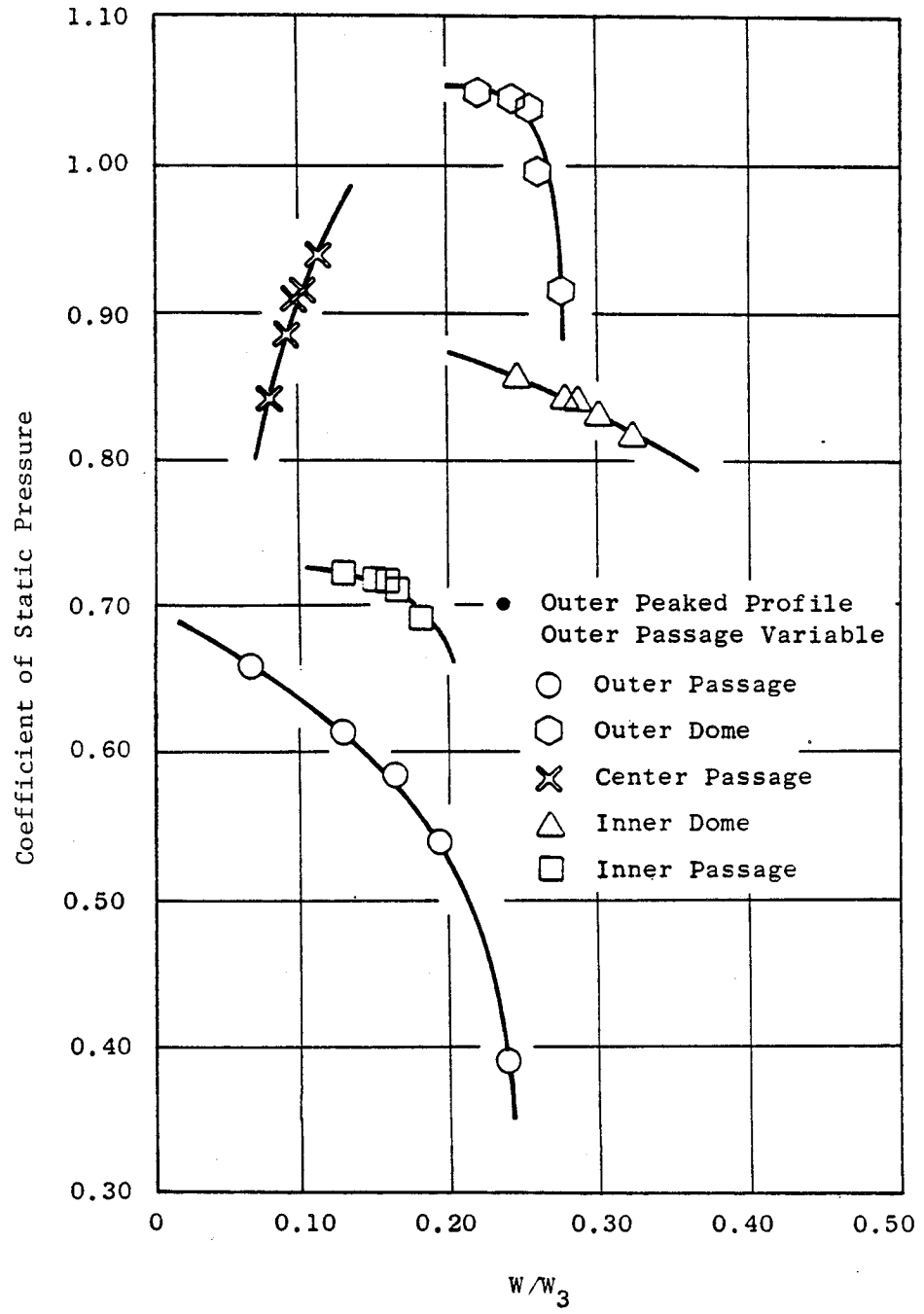


Figure 6B. E³ Combustor Inlet Diffuser CR&D Model Test Data.

EXPERIMENTAL DATA
 CONFIDENTIAL

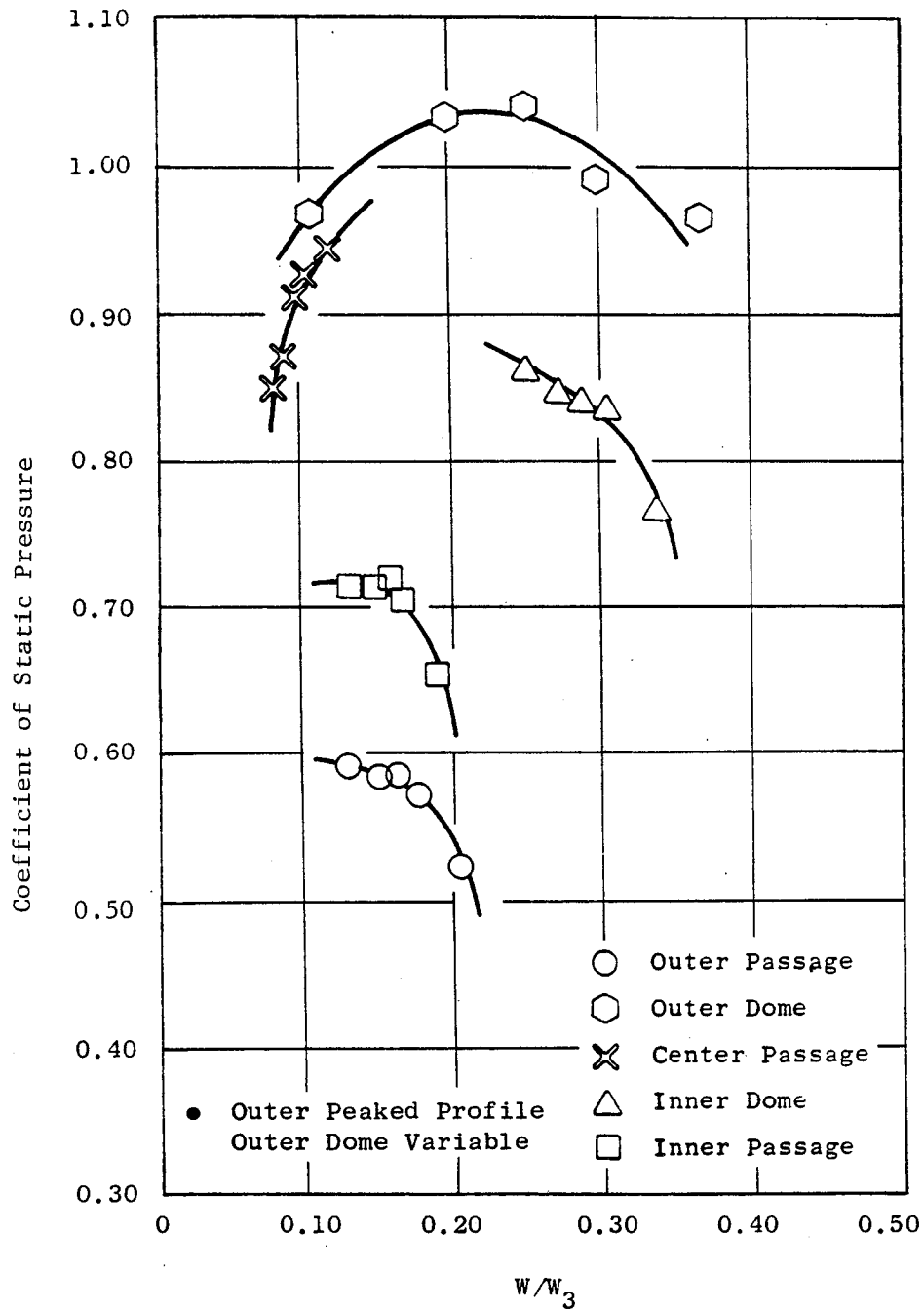


Figure 7B. E³ Combustor Inlet Diffuser CR&D Model Test Data.

ORIGINAL PAGE IS
OF POOR QUALITY

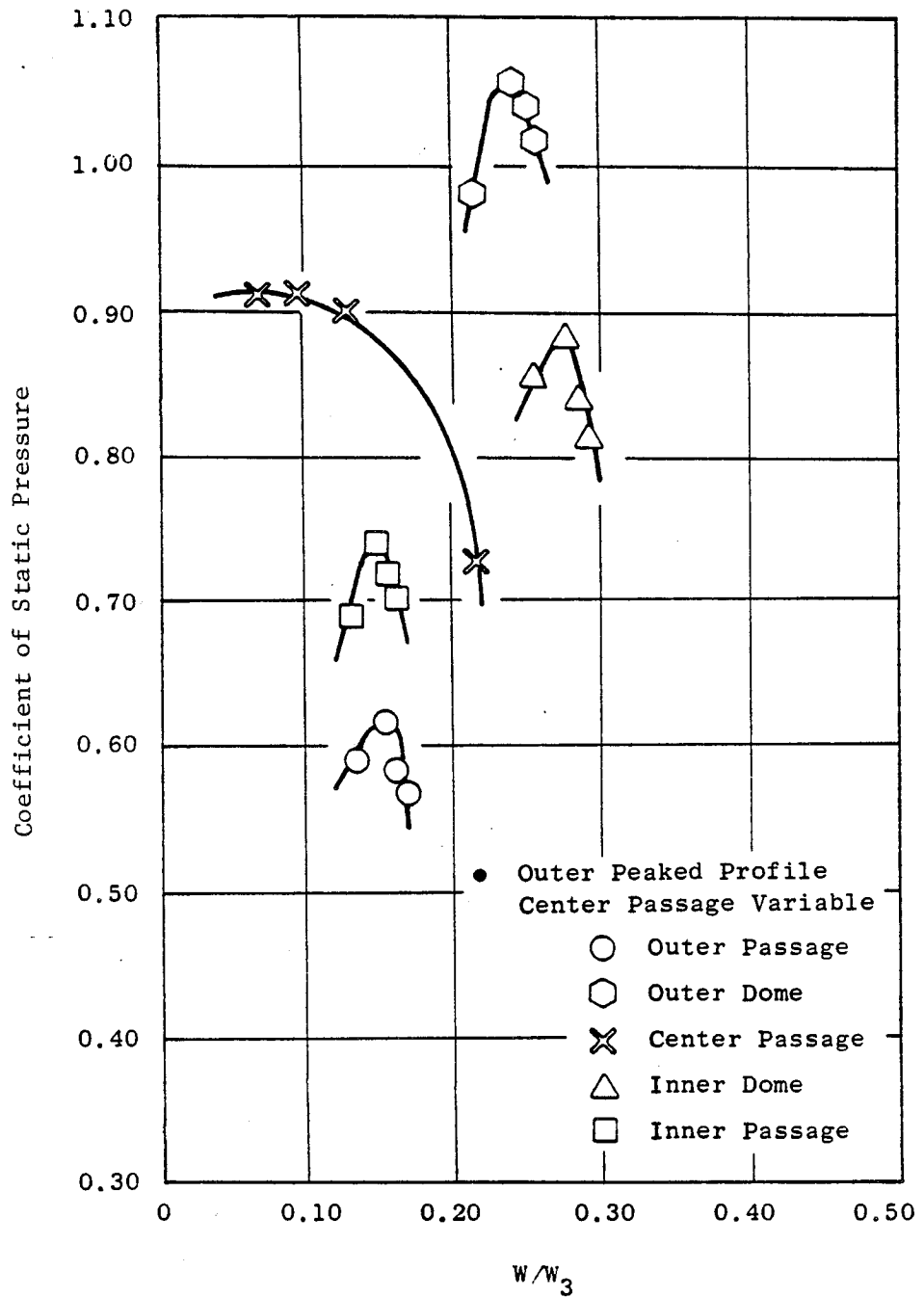


Figure 8B. E³ Combustor Inlet Diffuser CR&D Model Test Data.

ORIGINAL PAGE
OF POOR QUALITY

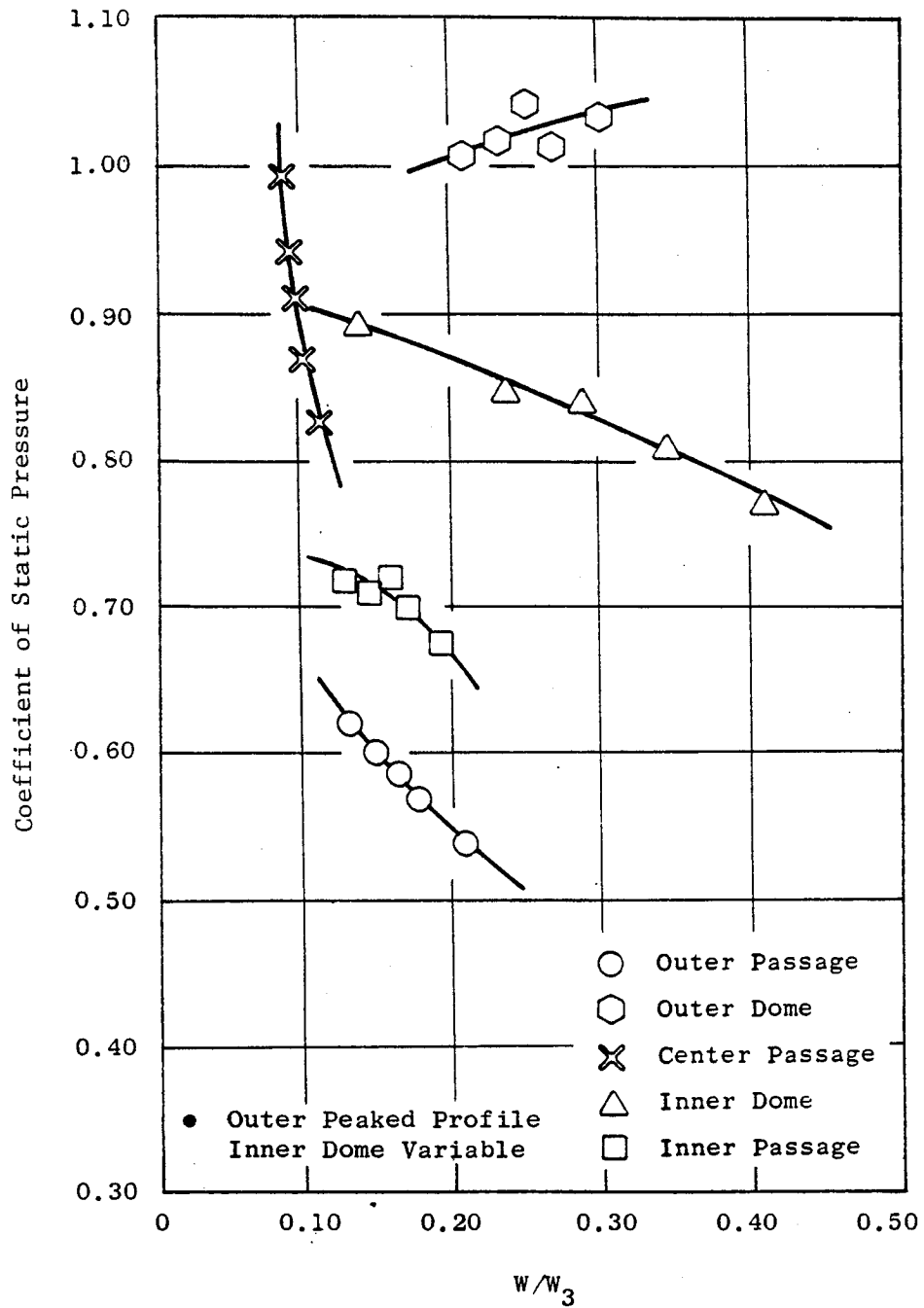


Figure 9B. E³ Combustor Inlet Diffuser CR&D Model Test Data.

ORIGINAL SOURCE OF POCN 0100000

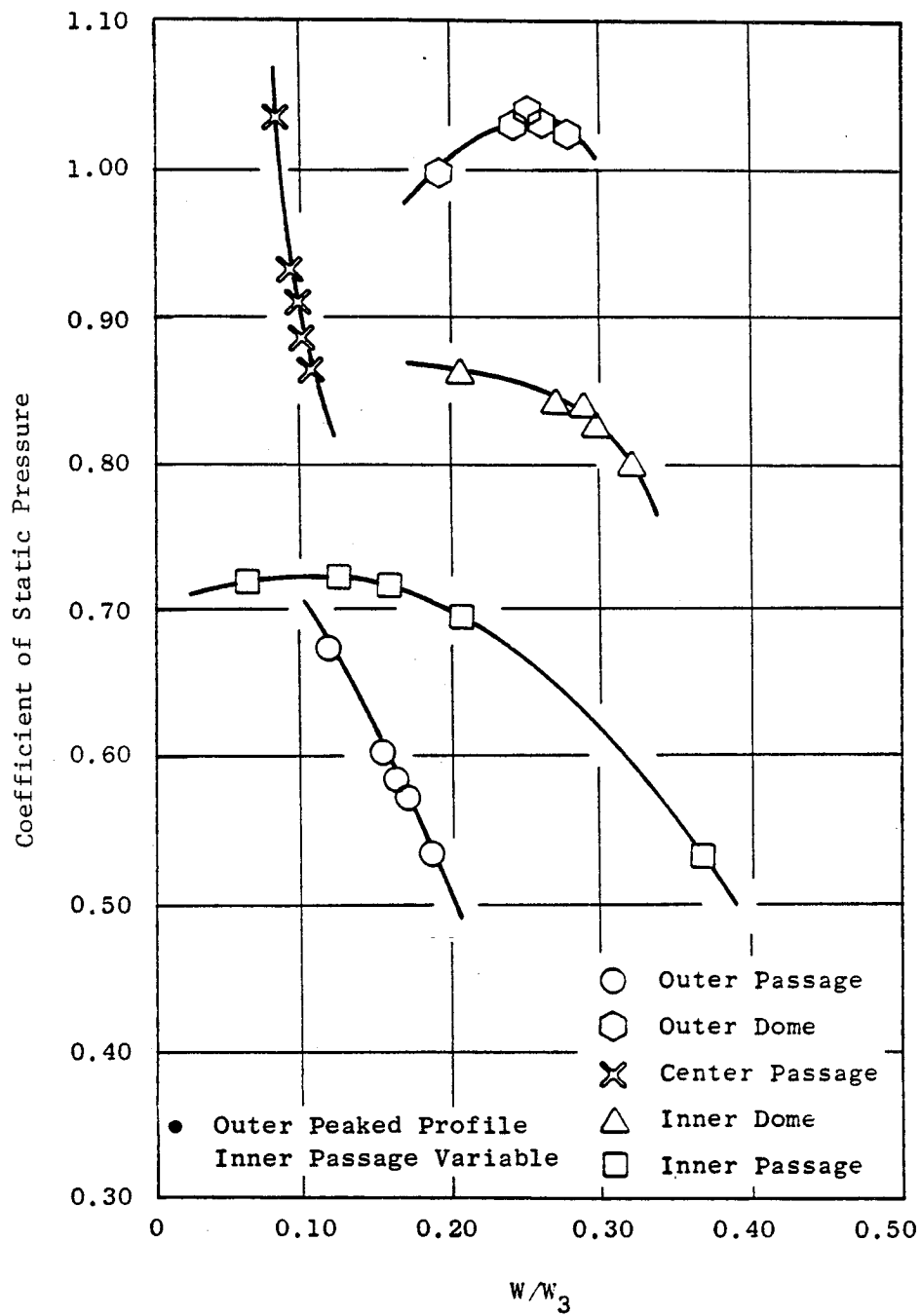


Figure 10B. E³ Combustor Inlet Diffuser CR&D Model Test Data.

ORIGINAL PAGE IS
OF POOR QUALITY

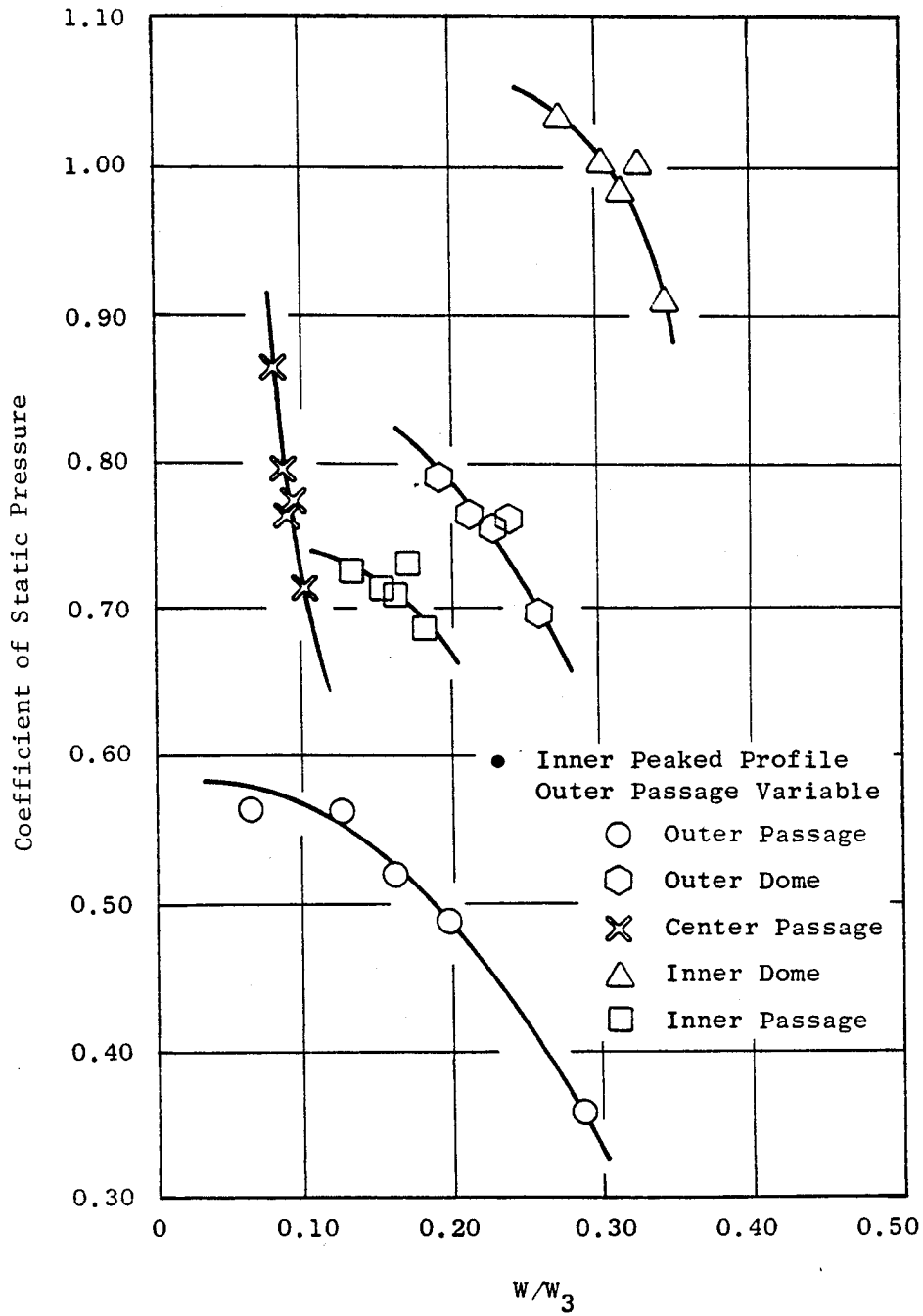


Figure 11B. E³ Combustor Inlet Diffuser CR&D Model Test Data.

ORIGINAL PAGE IS
OF POOR QUALITY

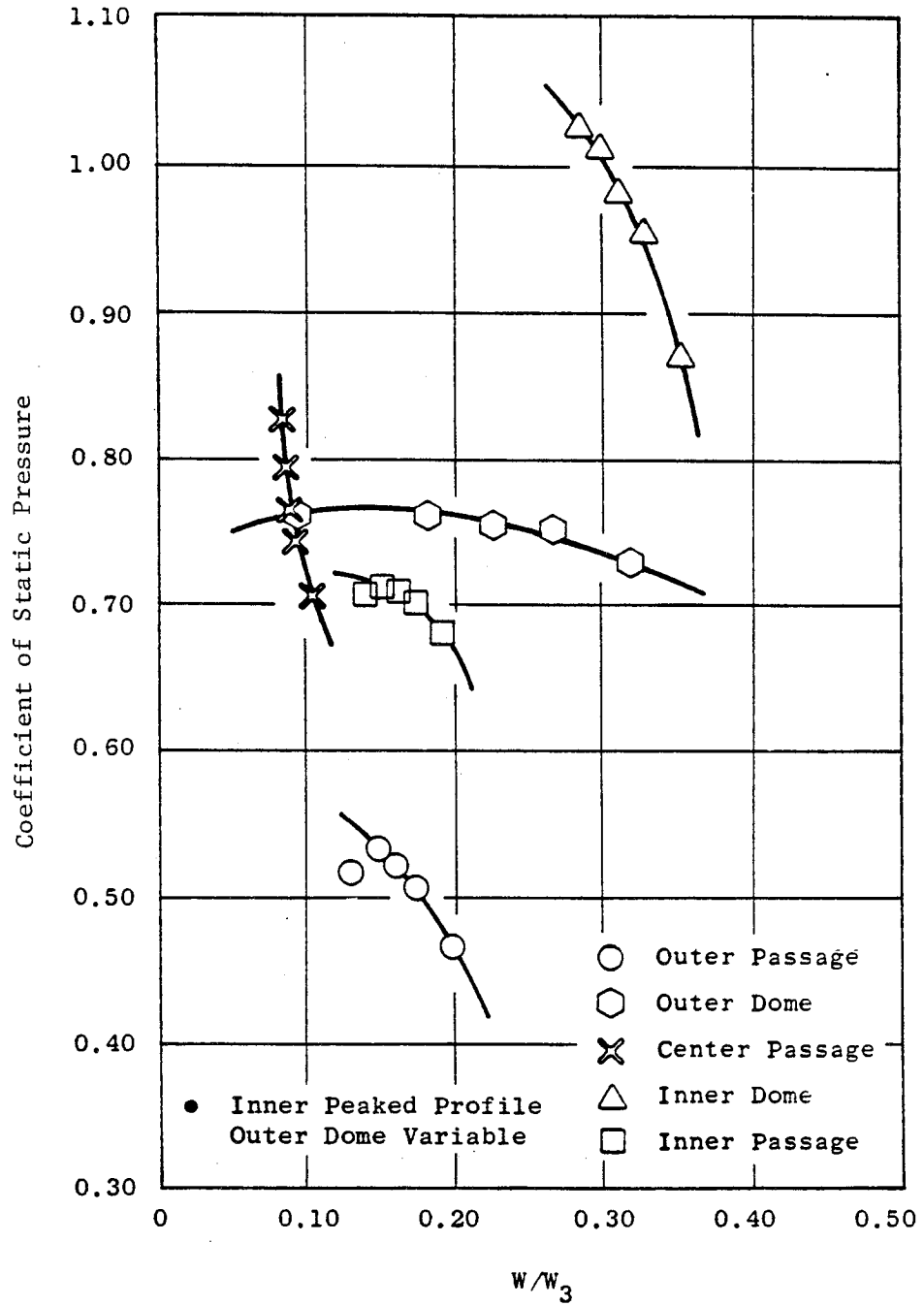


Figure 12B. E^3 Combustor Inlet Diffuser CR&D Model Test Data.

ORIGINAL PAGE IS
OF POOR QUALITY

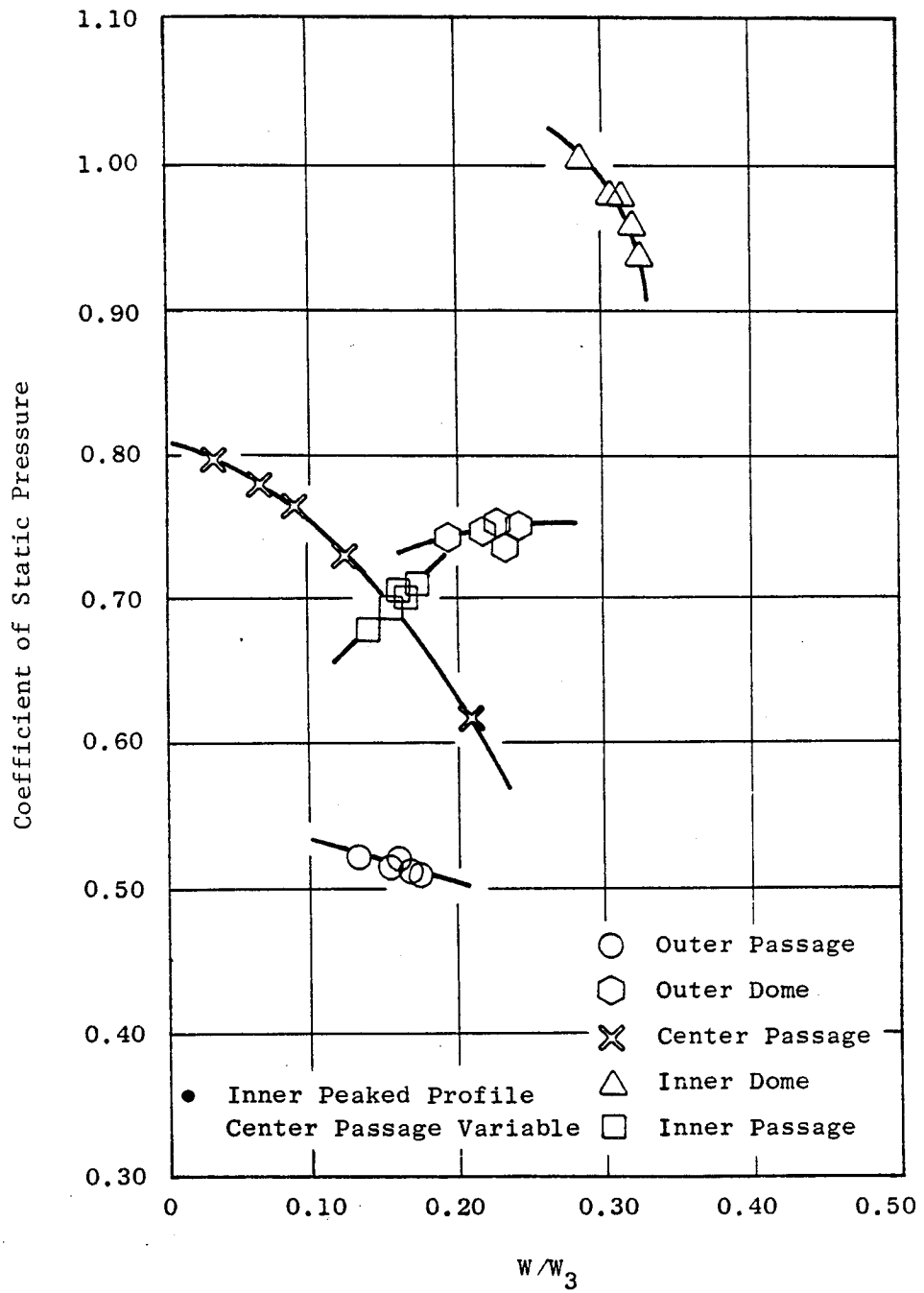


Figure 13B. E³ Combustor Inlet Diffuser CR&D Model Test Data.

ORIGINAL PAGE IS
OF POOR QUALITY

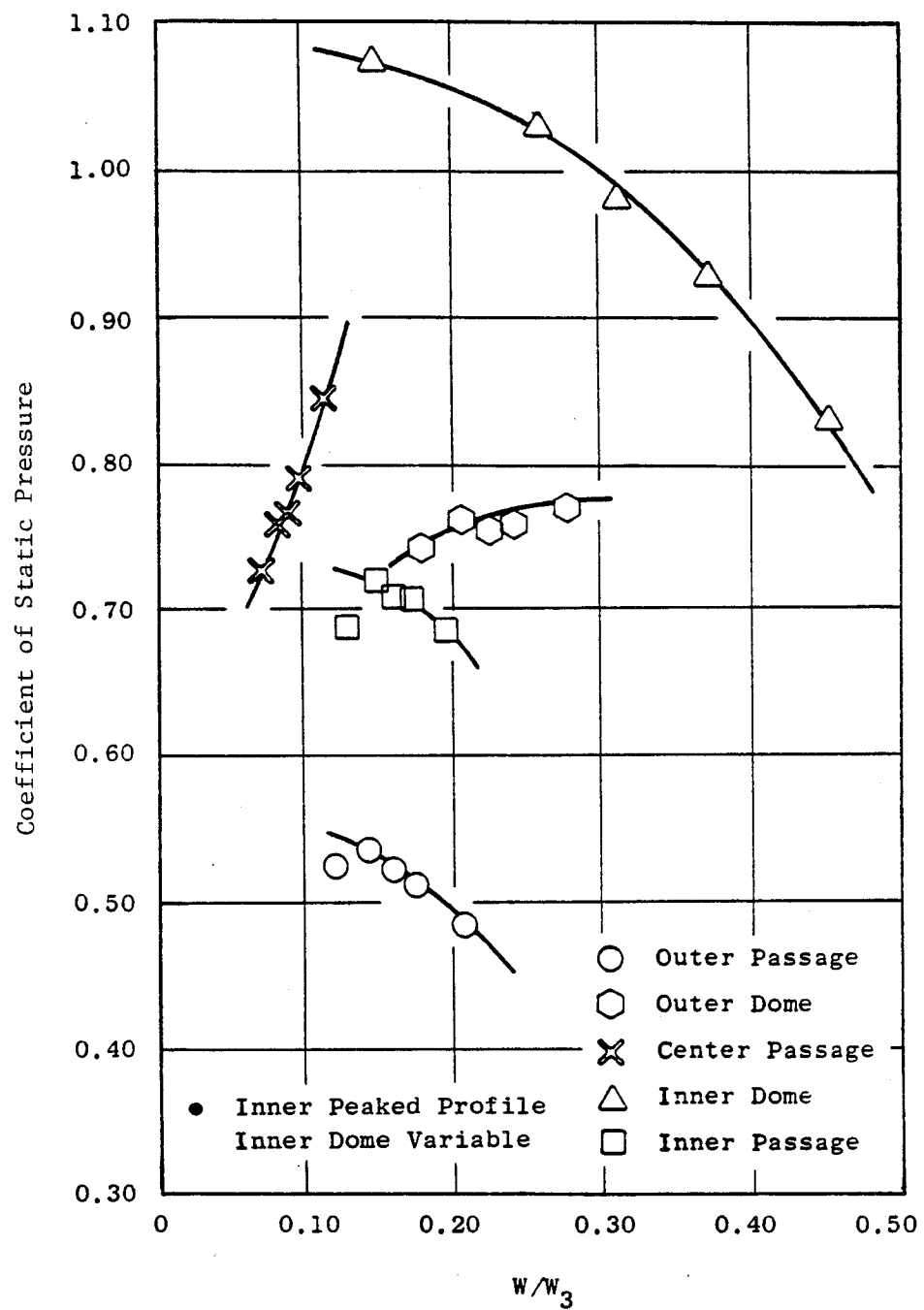


Figure 14B. E³ Combustor Inlet Diffuser CR&D Model Test Data.

ORIGINAL PAGE IS
OF POOR QUALITY

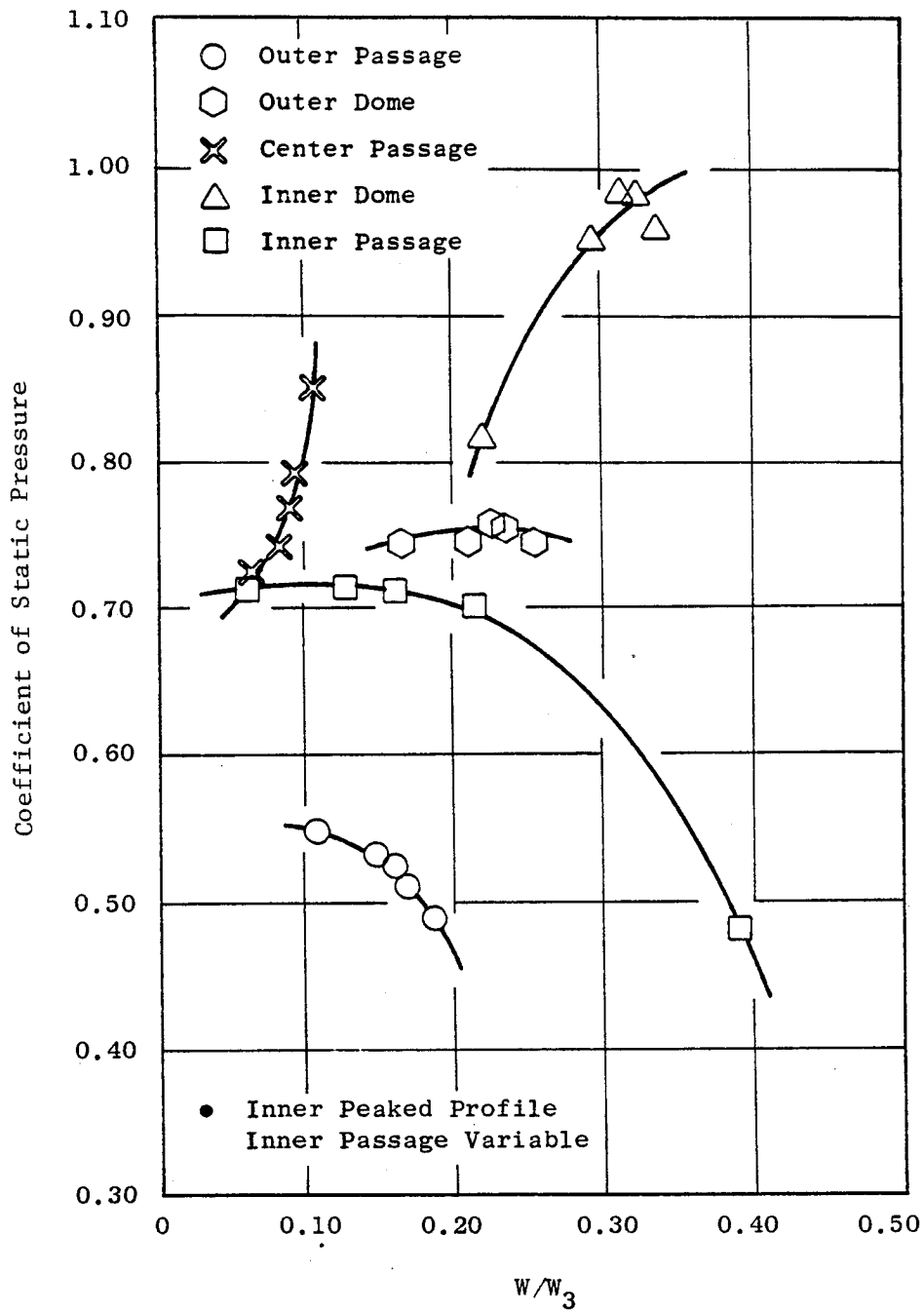


Figure 15B. E³ Combustor Inlet Diffuser CR&D Model Test Data.

APPENDIX C

SUMMARY OF DESCRIPTION OF COMPONENT SECTOR RIG TEST CONFIGURATIONS
AND RESULTS

PRECEDING PAGE BLANK NOT FILMED

439

PAGE 438 INTENTIONALLY BLANK

Table IC. Summary of the E³ Sector Combustor Test Configurations, Features, and Effectiveness.

Configuration	Features	Modification Intended for:	Results
Baseline	<ul style="list-style-type: none"> The primary dilution holes in the outer and inner liners were relocated to between swirl cups from in line with cups. 45° sleeves replaced the 90° sleeves Pilot dome splash plate cooling reduced by 40%. 	<ul style="list-style-type: none"> A more uniform fuel/air distribution. A more dispersed fuel flow. Lower idle emissions. 	<ul style="list-style-type: none"> Poor ignition and emissions performance. Idle emissions reduced. Ignition slightly improved.
Mod II	<ul style="list-style-type: none"> Development type swirl cups replaced the prototype cups. Reduced pilot stage swirl cup airflow. Increased main stage aft dilution airflow. 	<ul style="list-style-type: none"> More closely duplicate the full annular combustor design. Reduced idle emissions. Reduce NO_x emissions at high power. 	<ul style="list-style-type: none"> Idle emissions reduced to meet target levels. NO_x emissions increased. Ignition deteriorated.
Mod III	<ul style="list-style-type: none"> Reduced main stage swirl cup airflow. Development type fuel nozzles replaced the prototype nozzles. Crossfire tube incorporated in the centerbody design. 	<ul style="list-style-type: none"> Improve main stage crossfire performance. Duplicate the full-annular combustor fuel system. 	<ul style="list-style-type: none"> Ignition performance improved significantly. Idle emissions increased.
Mod III-A	<ul style="list-style-type: none"> Blocked the fuel nozzle shroud air. 	<ul style="list-style-type: none"> Reduced idle emissions. 	
Mod III-B	<ul style="list-style-type: none"> Reverted back to prototype fuel nozzles. 	<ul style="list-style-type: none"> Determine effects of fuel nozzle type on idle emissions. 	
Mod III-C	<ul style="list-style-type: none"> Installed larger flow number development type fuel nozzles 		
Mod IV	<ul style="list-style-type: none"> Increased pilot stage primary dilution airflow. Shortened centerbody multijet length. 	<ul style="list-style-type: none"> Reduced idle emissions. Mechanical considerations. 	<ul style="list-style-type: none"> Idle emissions same as Mod III.
Mod V	<ul style="list-style-type: none"> Increased main stage primary dilution airflow. 	<ul style="list-style-type: none"> Reduce NO_x emissions at high power. 	<ul style="list-style-type: none"> NO_x emissions increased.
Mod VI	<ul style="list-style-type: none"> Reduced pilot stage swirl cup airflow. Increased pilot stage primary dilution airflow. Reduced outer liner Row 1 cooling airflow. 	<ul style="list-style-type: none"> Reduce idle emissions. 	<ul style="list-style-type: none"> No improvement on idle emissions.
Mod VI-A	<ul style="list-style-type: none"> Reduced main stage swirl cup and splashplate cooling airflows. 	<ul style="list-style-type: none"> Improve crossfire performance 	<ul style="list-style-type: none"> No improvement in crossfire performance
Mod VI-B	<ul style="list-style-type: none"> Increased pilot stage swirl cup airflow. 	<ul style="list-style-type: none"> Improve crossfire performance. 	<ul style="list-style-type: none"> No improvement in crossfire performance.
Mod VI-C	<ul style="list-style-type: none"> Added an extension to the main stage side of crossfire tube. 	<ul style="list-style-type: none"> Improve crossfire performance 	<ul style="list-style-type: none"> No improvement in crossfire performance
Mod VI-D	<ul style="list-style-type: none"> Added an extension to the pilot stage side of crossfire tube. 	<ul style="list-style-type: none"> Improve crossfire performance 	<ul style="list-style-type: none"> No improvement in crossfire performance
			<ul style="list-style-type: none"> No improvement in crossfire

ORIGINAL COPY IN
OF FOUR COPIES

ORIGINAL PART IN
OF POOR QUALITY

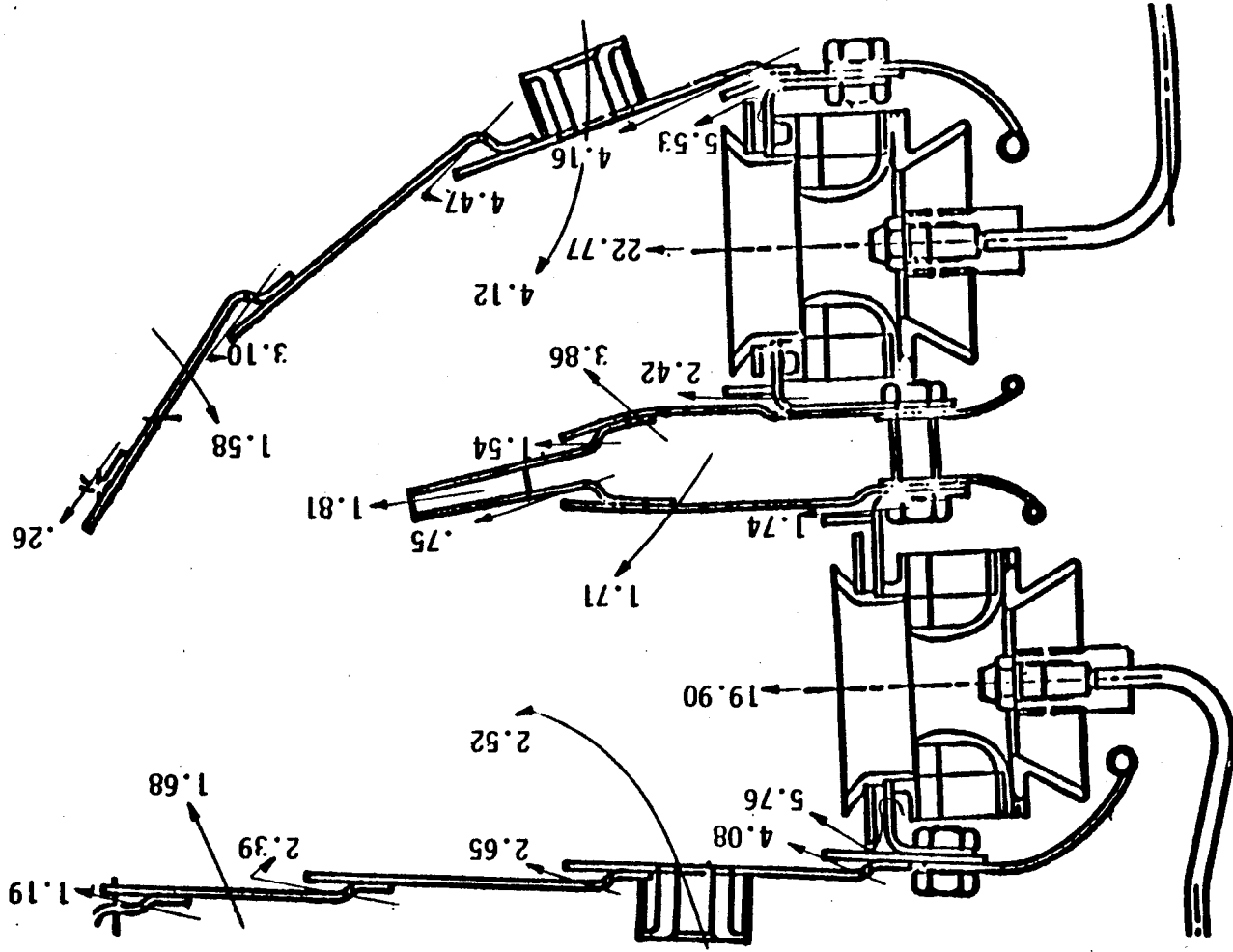
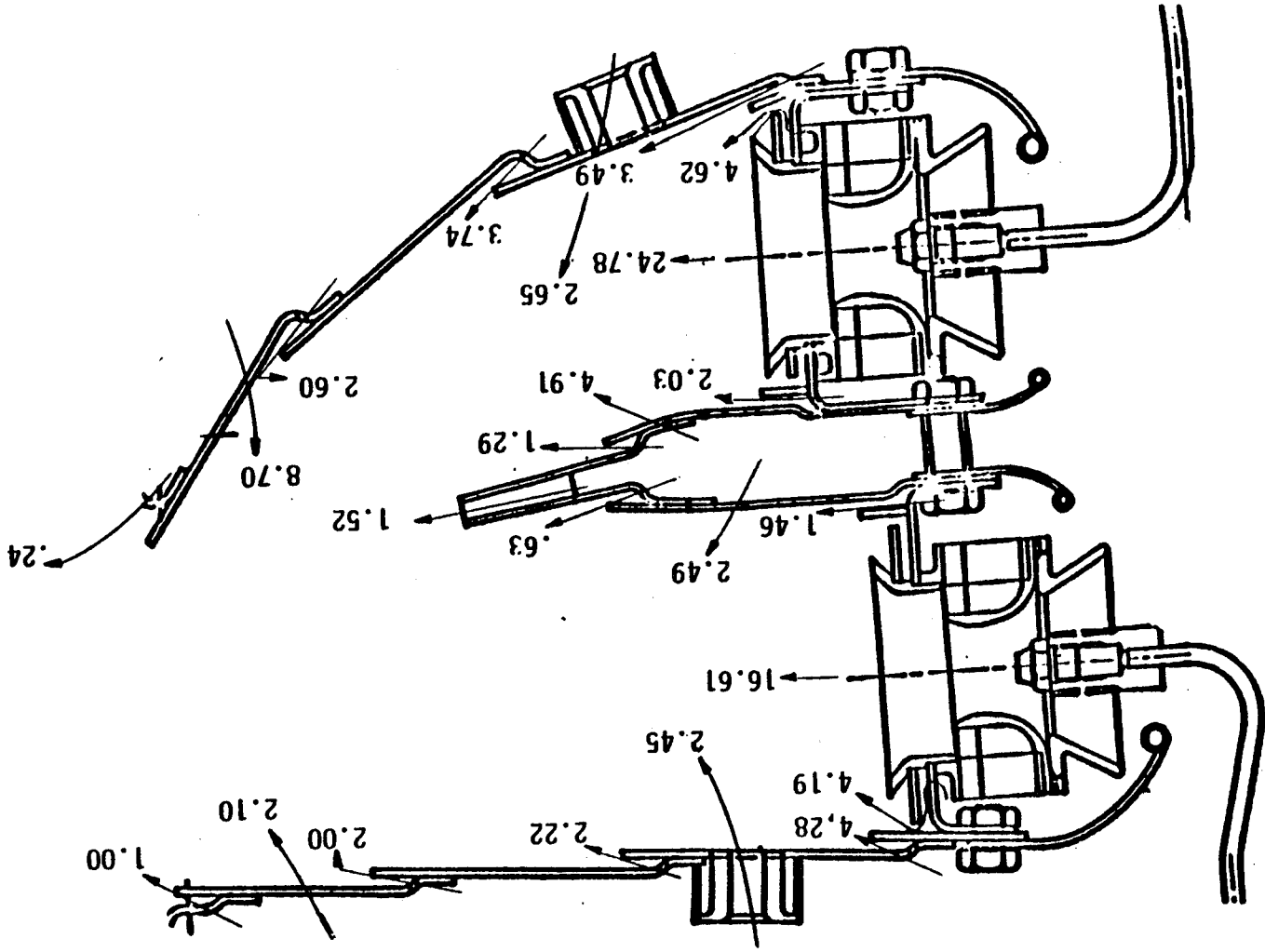


Figure 1C. E³ Sector Combustor Airflow Distribution Mod I Configuration.

Figure 2C. E³ Combustor Airflow Distribution Mod II Configuration.



ORIGINAL DRAWING IS
OF POOR QUALITY

ORIGINAL PAGE IS
OF POOR QUALITY

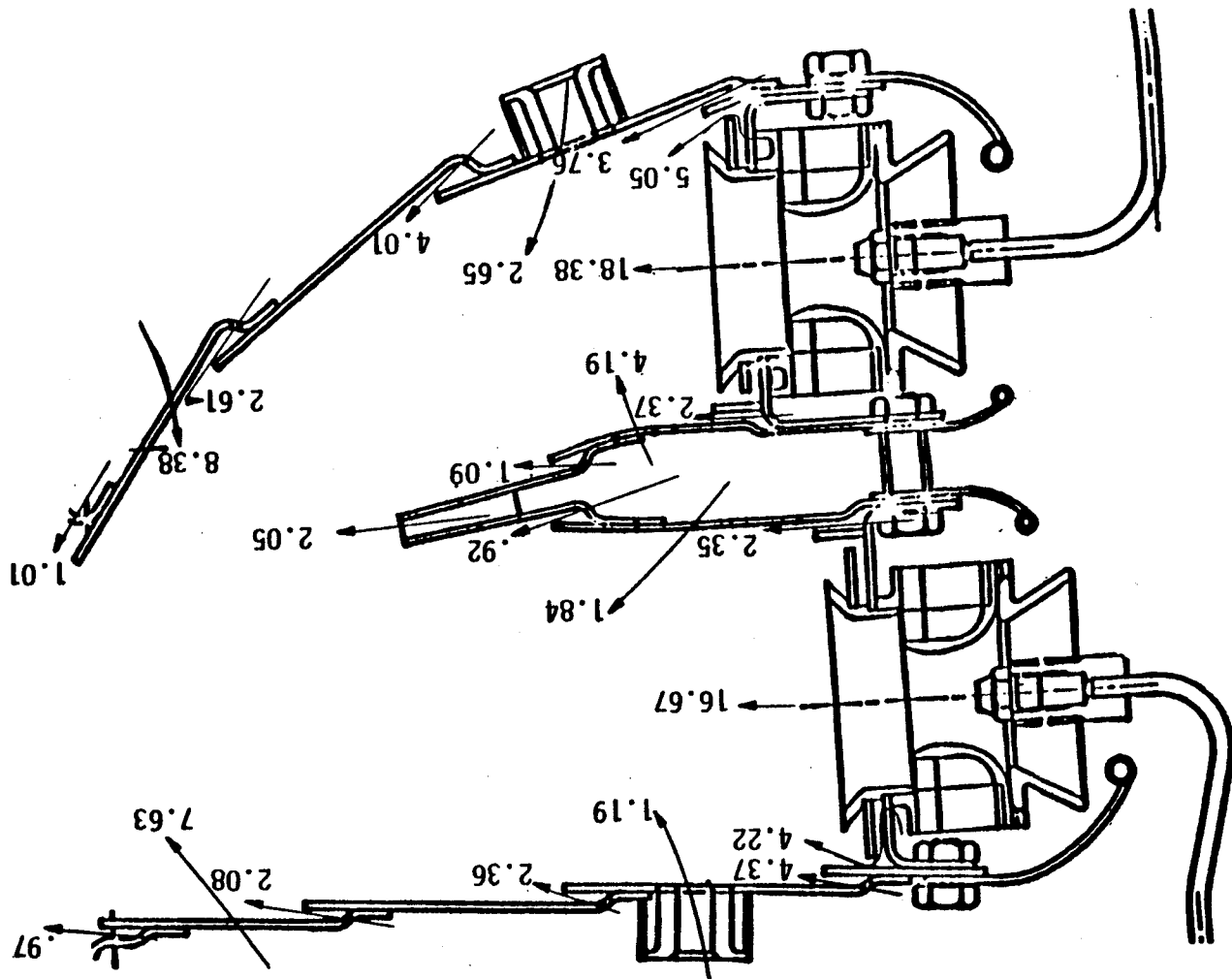


Figure 3C. E3 Sector Combustor Airflow Distribution Mod III Configuration.

ORIGINAL PAGE IS
OF POOR QUALITY

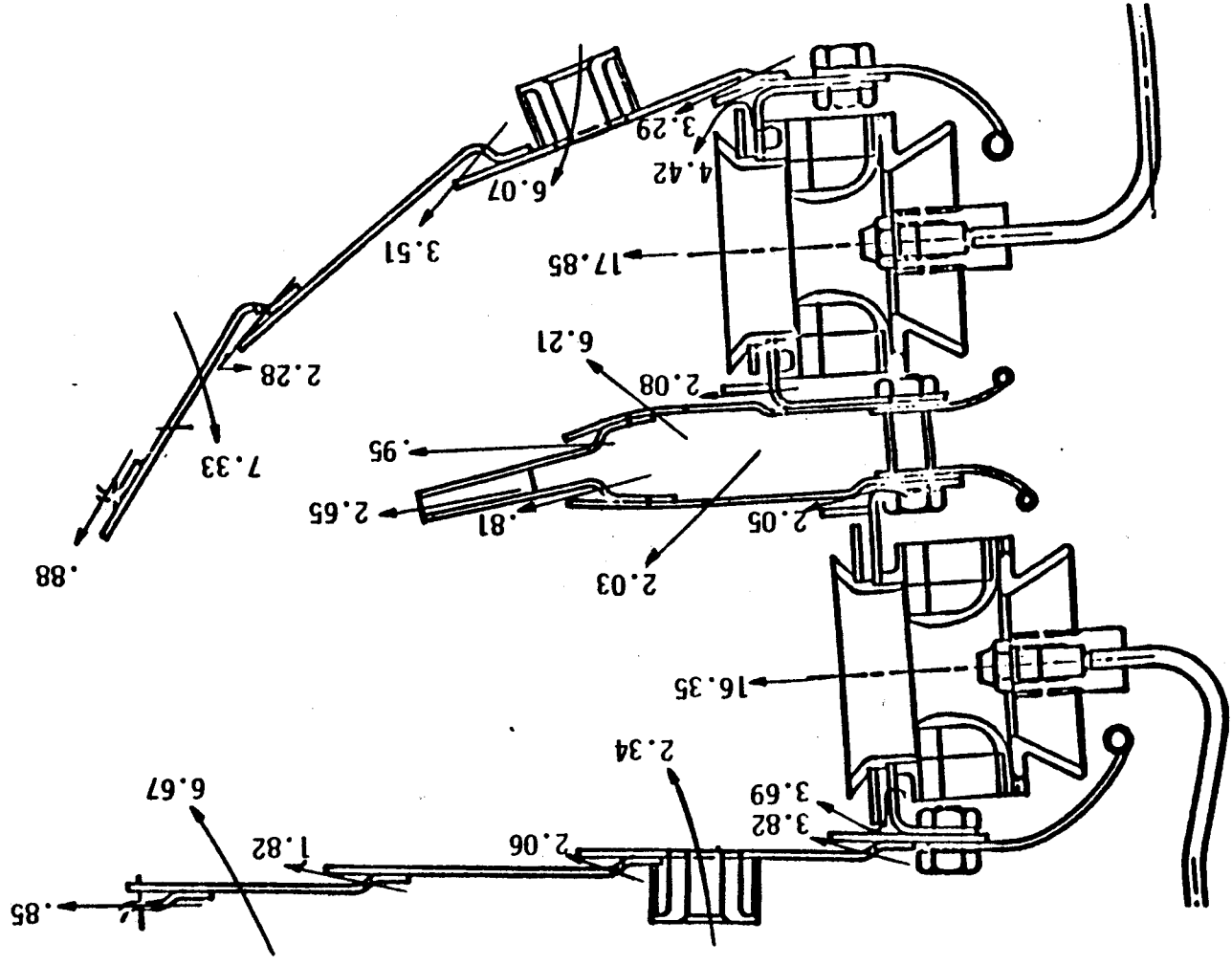
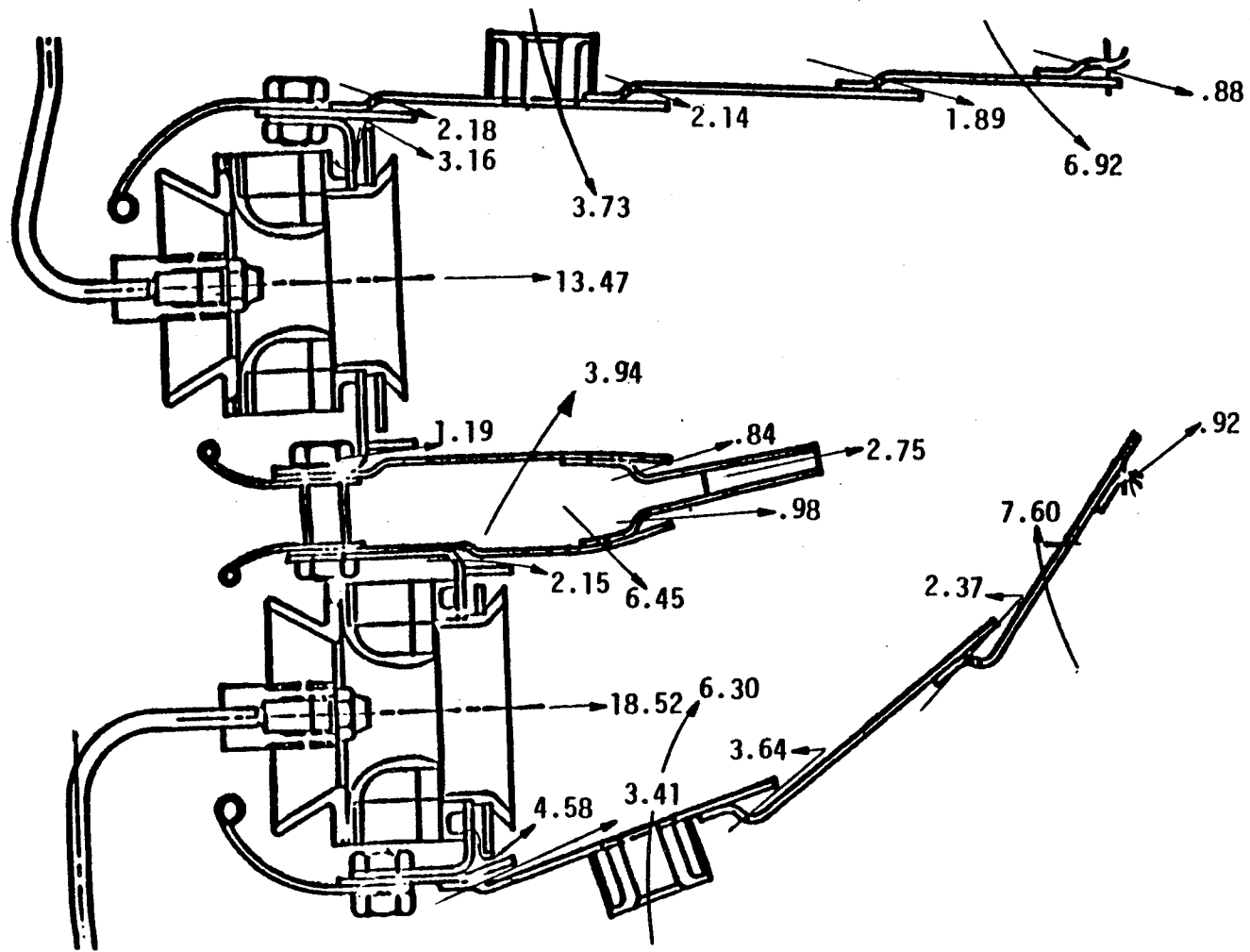


Figure 5C. E³ Sector Combustor Airflow Distribution Mod V Configuration.



ORIGINAL PAGE IS
OF POOR QUALITY

Figure 6C. E³ Sector Combustor Airflow Distribution Mod VI Configuration.

APPENDIX D

EMISSIONS CORRECTION AND CORRELATION EQUATION

This appendix contains adjustment relationships which were used to correct the measured emissions data obtained at derated high-power operating conditions to the actual QCSEE double-annular engine design cycle conditions. These relations were developed as part of the EPA/CFM-56 and NASA/GE ECCP and have generally provided a satisfactory method for adjusting the emissions levels to the correct combustor inlet conditions as specified in an engine cycle.

These relations are defined as follows:

(1) $EI_{CO}(ADJ) = EI_{CO}(MEA) (P_3/P_3 \text{ Cycle})^{1.5} \sim g/kg \text{ fuel}$

(2) $EI_{HC}(ADJ) = EI_{HC}(MEA) (P_3/P_3 \text{ Cycle})^{2.5} \sim g/kg \text{ fuel}$

(3) $EI_{NO_x}(ADJ) = EI_{NO_x}(MEA) (P_3 \text{ Cycle}/P_3)^{0.37} \text{ Exp } \frac{T_3 \text{ Cycle} - T_3}{345} \sim g/kg \text{ fuel}$

(4) NO_x Severity Parameter -

Correlating measured NO_x emissions data with this parameter yields a linear characteristic that allows easy extrapolation of the NO_x levels to high-power operating conditions.

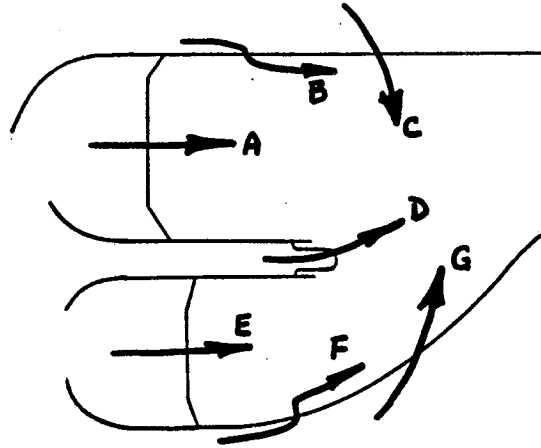
$$\left(\frac{P_3}{P_3^*} \right)^{0.37} \left(\frac{V_{Ref}^*}{V_{Ref}} \right) \left(\frac{f/a \text{ Pilot}}{0.00854} \right)^{0.65} \left(\frac{f/a \text{ Main}}{0.01586} \right)^{0.65} \text{ Exp } \left(\frac{T_3 - T_3^*}{345} \right) + \frac{6.29 - \text{Humidity}}{53.19}$$

Note: The starred values refer to levels at sea level takeoff operating conditions

ORIGINAL PAGE IS
OF POOR QUALITY

APPENDIX E

Estimated Airflow Distribution for Full-Annular
Development Combustor Configurations - % $W_{\text{Combustor}}$



Configu- ration	A	B	C	D	E	F	G
Baseline	33.61	6.23	4.13	11.55	33.09	6.62	4.77
Mod I	25.44	6.43	3.38	11.58	38.28	6.94	7.95
Mod II	25.80	5.75	4.30	12.98	28.78	7.60	14.79
Mod III	23.78	5.39	9.72	12.79	23.37	9.46	15.59
Mod IV	23.26	6.13	11.92	12.43	22.53	8.40	15.33
Mod V	23.00	6.18	14.69	11.11	22.65	8.47	13.90
Mod VI	23.19	6.13	4.50	11.36	32.42	9.23	13.17
Mod VII	23.20	6.12	4.51	11.41	32.30	9.23	13.23

APPENDIX F

DATA SUMMARY TABLES FOR E³ DEVELOPMENT ANNULAR COMBUSTOR TESTS

This Appendix contains test data summaries for all development combustor configurations and the engine combustor tested for component evaluation.

ORIGINAL PAGE IS
OF POOR QUALITY

Table 1F. Development Combustor Baseline Test Data.

ORIGINAL PAGE IS
OF POOR QUALITY

Reading	Test Point	Inlet Total Pressure		Inlet Temperature		Combustor Inlet Airflow		Combustor Exit Airflow		Combustor Total Fuel Flow		Pilot To Total Fuel Split	Combustor Overall Fuel/Air Ratio	Pilot Stage Ignition (f/a)					Main Stage Ignition (f/a)				Emissions Data				Combustor Total Pressure Loss %	Comments	
		psia	MPa	F	K	pps	kg/s	pps	kg/s	pph	kg/h			L/O 1-Cup	L/O 3-Cup	LBO 1-Cup	LBO Total	Steady State and Cross Fire	L/O 1-Cup	L/O 30-Cups	LBO 1-Cup	LBO Total	Co	HC g/Kg	Nox	HC %			
1	1	14.75	0.102	68	293	2.77	1.26	2.77	1.26	---	---	---	---	0.0282	0.0370	---	0.0209	---	---	---	---	N/A	N/A	N/A	N/A	N/A	N/A	Ignition (H2 Torch)	
2	2	14.83	0.102	75	297	3.72	1.69	3.72	1.69	---	---	---	---	0.0218	0.0306	---	0.0172	0.0505	---	---	0.0439	---	---	---	---	---	---	---	
3	3	14.81	0.102	99	310	3.60	1.64	3.60	1.64	---	---	---	---	0.0211	0.0311	---	0.0168	0.0474	---	---	0.0426	---	---	---	---	---	---	---	
4	4	14.86	0.102	164	346	3.71	1.69	3.71	1.69	---	---	---	---	0.0166	0.0294	---	0.0106	0.0467	---	---	---	---	---	---	---	---	---	---	
5	5	14.93	0.103	232	384	4.16	1.89	4.16	1.89	---	---	---	---	0.0124	0.0234	---	0.0077	0.0353	---	---	0.0350	---	---	---	---	---	---	---	
6	6	14.98	0.103	305	425	4.28	1.95	4.28	1.95	---	---	---	---	0.0103	0.0194	---	0.0048	0.0311	*0.0423	---	---	---	---	---	---	---	---	*Partial Propagation	
7	7	15.18	0.105	435	497	5.11	2.32	5.11	2.32	---	---	---	---	0.0079	0.0137	---	0.0037	0.0254	0.0309	---	0.0226	---	---	---	---	---	---	Ignition (electrical ignitor)	
8	8	15.24	0.105	655	508	5.13	2.33	5.13	2.33	---	---	---	---	0.0089	---	---	0.0041	---	---	---	---	---	---	---	---	---	---	---	
9	9	14.99	0.103	310	427	4.17	1.90	4.17	1.90	---	---	---	---	0.0119	---	---	0.0079	---	---	---	---	---	---	---	---	---	---	---	---
10	5	14.93	0.103	228	382	4.04	1.84	4.04	1.84	---	---	---	---	0.0109	---	---	0.0101	---	---	---	---	---	---	---	---	---	---	---	---
1	1	49.6	0.342	375	464	21.53	9.79	17.53	7.97	566	257	1.0	0.0089	---	---	---	---	---	---	---	146.3	117.2	0.8	86.40	5.54	---	---	Emissions	
2	2	49.2	0.339	374	463	20.96	9.53	16.96	7.71	745	339	1.0	0.0122	---	---	---	---	---	---	---	80.5	53.2	1.4	93.49	5.38	---	---	---	
3	3	49.7	0.342	379	466	21.46	9.75	17.33	7.88	845	384	1.0	0.0136	---	---	---	---	---	---	---	61.4	37.9	1.8	95.28	5.23	---	---	4Z G-Idle	
4	4	49.6	0.342	375	464	21.56	9.80	17.55	7.98	1235	561	1.0	0.0196	---	---	---	---	---	---	---	77.7	7.5	3.1	97.53	5.26	---	---	---	
5	5	49.9	0.344	378	465	21.10	9.59	16.99	7.72	1350	614	1.0	0.0221	---	---	---	---	---	---	---	105.8	4.5	3.3	97.14	5.41	---	---	---	
6	6	63.2	0.436	423	490	28.16	12.77	22.93	10.42	716	325	1.0	0.0087	---	---	---	---	---	---	---	139.6	72.9	1.7	90.40	5.96	---	---	---	
7	7	62.8	0.433	427	493	27.89	12.68	22.93	10.42	886	403	1.0	0.0107	---	---	---	---	---	---	---	85.1	37.1	2.1	94.79	5.82	---	---	---	
8	8	62.8	0.433	427	493	28.47	12.94	23.74	10.79	990	450	1.0	0.0115	---	---	---	---	---	---	---	65.4	28.4	2.5	96.00	5.84	---	---	5Z G-Idle	
9	9	62.8	0.433	427	493	28.47	12.94	23.74	10.79	990	450	1.0	0.0115	---	---	---	---	---	---	---	80.9	40.1	2.5	94.63	5.84	---	---	A-Rake U* - 66*	
10	10	62.8	0.433	427	493	28.47	12.94	23.74	10.79	990	450	1.0	0.0115	---	---	---	---	---	---	---	68.6	28.5	2.5	95.92	5.84	---	---	B-Rake 72* - 136*	
11	11	62.8	0.433	427	493	28.50	12.95	23.77	10.80	990	450	1.0	0.0115	---	---	---	---	---	---	---	62.3	29.0	2.6	96.02	5.85	---	---	C-Rake 144* - 210*	
12	12	62.8	0.433	425	491	28.53	12.97	23.80	10.82	991	450	1.0	0.0115	---	---	---	---	---	---	---	65.1	26.0	2.8	96.22	5.85	---	---	D-Rake 216* - 282*	
13	13	62.8	0.433	426	492	28.53	12.97	23.80	10.82	991	450	1.0	0.0115	---	---	---	---	---	---	---	68.1	29.7	2.8	95.83	5.84	---	---	E-Rake 288* - 354*	
14	14	63.1	0.435	427	493	28.55	12.98	23.64	10.75	1202	546	1.0	0.0141	---	---	---	---	---	---	---	39.8	12.1	3.4	98.02	6.19	---	---	---	
15	15	63.1	0.435	429	494	27.04	12.29	21.94	9.97	1611	732	1.0	0.0203	---	---	---	---	---	---	---	68.8	2.3	4.6	98.20	6.0	---	---	---	
16	16	175.3	1.209	689	638	70.74	32.15	57.67	26.21	2934	1334	0.5	0.0141	---	---	---	---	---	---	---	183.8	57.5	3.4	90.71	6.2	---	---	30Z Approach	
17	17	175.1	1.207	686	636	71.00	32.27	58.63	26.65	2936	1335	0.4	0.0139	---	---	---	---	---	---	---	171.0	37.4	3.3	92.76	6.0	---	---	---	
18	18	174.4	1.202	686	636	71.14	32.34	58.83	26.74	2946	1339	0.3	0.0139	---	---	---	---	---	---	---	112.4	89.9	3.4	91.30	6.1	---	---	---	
1	11	175.0	1.207	681	634	69.82	31.74	57.94	26.34	2916	1325	1.0	0.0140	---	---	---	---	---	---	---	5.7	0.7	8.7	99.81	6.5	---	---	---	
2	11	175.4	1.209	683	635	69.88	31.76	58.01	26.37	2908	1322	1.0	0.0139	---	---	---	---	---	---	---	9.3	1.4	6.9	99.66	6.1	---	---	A-Rake U* - 66*	
3	11	176.0	1.213	686	636	70.51	32.05	58.68	26.67	2930	1332	1.0	0.0139	---	---	---	---	---	---	---	7.4	0.7	7.9	99.77	6.20	---	---	B-Rake 72* - 136*	
4	11	175.2	1.208	682	634	69.90	31.77	58.14	26.43	2930	1332	1.0	0.0140	---	---	---	---	---	---	---	4.7	0.5	8.5	99.85	6.10	---	---	C-Rake 144* - 210*	
5	11	175.6	1.211	685	636	69.94	31.79	57.81	26.28	2934	1334	1.0	0.0141	---	---	---	---	---	---	---	7.9	0.8	7.8	99.75	6.02	---	---	D-Rake 216* - 282*	
6	11	175.3	1.209	681	634	69.98	31.81	58.03	26.38	2935	1334	1.0	0.0140	---	---	---	---	---	---	---	6.0	0.3	10.6	99.83	5.98	---	---	E-Rake 288* - 304*	
7	15	222.1	1.531	798	699	81.57	37.08	67.62	30.74	4159	1890	0.4	0.0171	---	---	---	---	---	---	---	34.5	1.8	6.8	99.04	5.22	---	---	50Z Fn Unadjusted	
8	16	240.6	1.659	882	745	82.23	37.38	67.75	30.80	5097	2317	0.4	0.0209	---	---	---	---	---	---	---	6.9	0.2	10.2	99.82	4.92	---	---	70Z Fn Unadjusted	
9	17	241.7	1.666	941	778	82.17	37.35	67.79	30.77	5566	2530	0.5	0.0228	---	---	---	---	---	---	---	4.3	0.1	12.9	99.89	5.05	---	---	85Z Fn Unadjusted	
10	18	240.7	1.660	947	781	82.19	37.36	68.33	31.06	5590	2541	0.35	0.0228	---	---	---	---	---	---	---	3.5	0.1	13.3	99.91	5.55	---	---	Unadjusted	
11	20	241.3	1.664	959	788	82.10	37.32	67.78	30.81	5683	2583	0.35	0.0233	---	---	---	---	---	---	---	3.4	0.1	14.1	99.92	5.12	---	---	93Z Fn Unadjusted	
12	21	241.9	1.668	1002	812	79.96	36.35	66.34	30.15	5939	2700	0.45	0.0249	---	---	---	---	---	---	---	1.9	0.1	15.6	99.95	5.09	---	---	100Z Fn Unadjusted	
13	22	241.5	1.665	1005	814	81.30	36.95	67.48	30.67	5961	2710	0.40	0.0246	---	---	---	---	---	---	---	2.4	0.1	16.4	99.94	5.17	---	---	Unadjusted	
14	23	241.4	1.664	1008	815	80.27	36.49	65.92	29.96	4789	2181	0.50	0.0203	---	---	---	---	---	---	---	6.3	0.1	13.8	99.84	5.10	---	---	Unadjusted	

PRECEDING PAGE BLANK NOT FILMED

FOLDOUT FRAME

FOLDOUT FRAME

Table 2F. Development Combustor Mod I Test Data.

Reading	Test Point	Inlet Total Pressure		Inlet Temperature		Combustor Inlet Airflow		Combustor Exit Airflow		Combustor Total Fuel Flow		Pilot To Total Fuel Split	Combustor Overall Fuel/Air Ratio	Pilot Stage Ignition (f/a)					Main Stage Ignition (f/a)				Emissions Data				Combustor Total Pressure Loss %	Comments
		psia	MPa	F	K	pps	kg/s	pps	kg/s	pph	kg/h			L/O 1-Cup	L/O 3-Cup	LBO 1-Cup	LBO Total	Steady State and Cross Fire	L/O 1-Cup	L/O 30-Cups	LBO 1-Cup	LBO Total	Co	HC g/Kg	No _x	nc %		
1	1	14.66	0.101	80	300	2.75	1.25	2.75	1.25	---	---			0.0262	0.0307	---	---	---	---	---	---	N/A	N/A	N/A	N/A	N/A	Ignition	
2	1	14.68	0.101	80	300	2.75	1.25	2.75	1.25	---	---			0.0263	0.0311	---	0.0205	0.0303	0.0390	---	---	---	---	---	---	Main 15 Un/15 Off		
3	2	14.77	0.102	78	299	3.79	1.72	3.79	1.72	---	---			0.0187	0.0237	---	0.0137	0.0237	0.0395	---	---	---	---	---	---	Main 30 On/0 Off		
4	2	14.79	0.102	79	299	3.77	1.71	3.77	1.71	---	---			0.0189	0.0271	---	0.0130	0.0256	0.0483	---	---	---	---	---	---	Main 15 Un/15 Off		
5	3	14.74	0.102	109	316	3.43	1.56	3.43	1.56	---	---			0.0204	0.0248	---	0.0129	0.0238	0.0507	---	---	---	---	---	---	Main 30 On/0 Off		
6	3	14.77	0.102	119	321	3.41	1.55	3.41	1.55	---	---			0.0145	0.0220	---	0.0088	0.0176	0.0304	---	---	---	---	---	---	*Partial Propagation		
7	4	14.78	0.102	161	345	3.81	1.73	3.81	1.73	---	---			0.0145	0.0206	---	0.0082	0.0184	0.0441	*0.0646	---	---	---	---	---	Main 30 On/0 Off		
8	4	14.82	0.102	166	348	3.64	1.65	3.64	1.65	---	---			0.0141	0.0158	---	0.0063	0.0163	0.0309	*0.0572	---	---	---	---	---	*Partial Propagation		
9	5	14.92	0.103	231	384	4.11	1.87	4.11	1.87	---	---			0.0138	0.0138	---	0.0046	0.0122	0.0370	*0.0528	---	---	---	---	---			
10	6	14.98	0.103	321	434	4.27	1.94	4.27	1.94	---	---			0.0138	0.0138	---	0.0046	0.0122	0.0370	*0.0528	---	---	---	---	---			
11	7	15.29	0.105	447	504	5.12	2.33	5.12	2.33	---	---			0.0115	0.0115	---	0.0023	0.0101	0.0296	0.0444	---	---	---	---	---	Ignition		
1	1	14.93	0.103	89	305	3.11	1.41	3.11	1.41	---	---			0.0197	0.0263	---	0.0148	---	---	---	---	---	---	---	---	Ignition		
2	2	20.73	0.143	162	345	4.69	2.13	4.69	2.13	---	---			0.0122	0.0160	---	0.0092	0.0160	N/L	---	---	---	---	---	---			
3	3	27.1	0.187	236	386	7.51	3.41	7.51	3.41	---	---			0.0070	0.0100	---	0.0048	0.0100	0.0298	0.0339	---	---	---	---	---			
4	4	49.4	0.341	374	463	21.00	9.55	21.00	9.55	---	---			0.0114	0.0114	---	0.0042	0.0079	0.0207	0.0219	---	---	---	---	---	Emissions		
5	6	49.7	0.343	384	469	20.97	9.53	17.33	7.88	852	387	1.0	0.0136								30.6	8.3	1.8	98.57	N/A	A-Rake 0° - 66°		
6	6	49.7	0.343	388	471	21.09	9.59	17.56	7.98	847	385	1.0	0.0134								39.9	3.9	3.2	98.73	5.30	B-Rake 72° - 138°		
7	6	49.7	0.343	390	472	21.04	9.56	17.51	7.96	853	388	1.0	0.0135								34.2	4.4	3.2	98.82	---	C-Rake 144° - 210°		
8	6	49.7	0.343	379	466	21.11	9.60	17.44	7.93	855	389	1.0	0.0135								51.9	6.0	3.6	98.27	---	E-Rake 288° - 354°		
9	6	49.7	0.343	381	467	21.21	9.64	17.73	8.06	858	390	1.0	0.0134								44.6	5.2	3.9	98.50	4.80	42 G-Idle		
10	5	49.7	0.343	382	468	21.29	9.68	17.65	8.02	860	390	1.0	0.0087								95.8	30.9	2.2	94.38	5.22			
11	5	49.7	0.343	382	468	21.03	9.56	17.39	7.90	1245	566	1.0	0.0197								164.6	4.2	4.0	95.80	5.46			
12	7	49.8	0.343	382	468	21.31	9.69	17.68	8.04	1049	477	1.0	0.0164								88.5	4.9	4.6	97.51	5.63			
13	10	63.3	0.436	431	495	27.26	12.39	22.56	10.25	863	392	1.0	0.0108								31.8	6.0	3.3	98.73	---	62 G-Idle		
14	11	63.3	0.436	430	494	26.72	12.15	22.11	10.05	994	452	1.0	0.0124								31.5	4.0	4.0	98.91	---			
15	12	63.2	0.436	432	495	26.97	12.26	22.35	10.16	1208	549	1.0	0.0149								175.1	1.7	3.5	95.77	6.33			
16	13	63.2	0.436	435	497	26.83	12.20	22.15	10.07	1607	730	1.0	0.0200								51.0	16.2	2.1	97.40	6.00			
17	9	63.4	0.437	434	496	26.88	12.22	22.21	10.10	725	330	1.0	0.0090								23.4	1.1	9.0	99.36	---	Unadjusted		
18	14	241.3	1.664	803	701	76.63	34.83	61.95	28.16	4380	1991	0.4	0.0197								12.7	0.4	9.9	99.67	---	Unadjusted		
19	15	241.7	1.667	797	698	76.54	34.79	62.06	28.21	5033	2288	0.4	0.0226															

Table 3F. Development Combustor Mod II Test Data.

Reading	Test Point	Inlet Total Pressure		Inlet Temperature		Combustor Inlet Airflow		Combustor Exit Airflow		Combustor Total Fuel Flow		Pilot To Total Fuel Split	Combustor Overall Fuel/Air Ratio	Pilot Stage Ignition (f/a)					Main Stage Ignition (f/a)				Emissions Data				Combustor Total Pressure Loss %	Comments		
		psia	MPa	F	K	pps	kg/s	pps	kg/s	pph	kg/h			L/O 1-Cup	L/O 3-Cup	LBO 1-Cup	LBO Total	Steady State and Cross Fire	L/O 1-Cup	L/O 30-Cups	LBO 1-Cup	LBO Total	Co	HC g/Kg	No _x	nc %				
1	1	14.55	0.100	64	291	2.82	1.28	2.82	1.28	---	---			0.0217	0.0381	0.0314	0.0143	0.0370	N/L	---	---	---	---	---	N/A	N/A	N/A	N/A	N/A	Mod II-A Ignition
2	2	14.63	0.101	60	289	3.71	1.69	3.71	1.69	---	---			0.0202	0.0302	0.0260	0.0142	0.0284	N/L	---	---	---	---	---	---	---	---	---	---	
3	3	14.65	0.101	101	311	3.44	1.56	3.44	1.56	---	---			0.0192	0.0306	0.0267	0.0151	0.0287	N/L	---	---	---	---	---	---	---	---	---	---	
4	4	14.71	0.101	160	344	3.72	1.69	3.72	1.69	---	---			0.0149	0.0243	0.0209	0.0123	0.0223	N/L	---	---	---	---	---	---	---	---	---	---	
5	5	14.81	0.102	228	382	4.09	1.86	4.09	1.86	---	---			0.0122	0.0193	0.0154	0.0060	0.0177	0.0344	*0.0587	---	0.0352	---	---	---	---	---	---	*Partial Propagation	
6	6	14.91	0.103	307	426	4.48	2.04	4.48	2.04	---	---			0.0105	0.0149	0.0110	0.0018	0.0123	0.0247	*0.0464	---	0.0223	---	---	---	---	---	---		
7	7	15.20	0.105	439	499	5.16	2.35	5.16	2.35	---	---			0.0083	0.0092	0.0062	0.0010	0.0073	0.0197	0.0263	0.0188	0.0120	---	---	---	---	---	---		
1	1	14.66	0.101	107	315	2.81	1.28	2.81	1.28	---	---			0.0276	0.0323	0.0231	0.0174	0.0276	N/L	---	---	---	---	---	---	---	---	---	---	
2	2	14.76	0.102	96	309	3.82	1.74	3.82	1.74	---	---			0.0156	0.0260	0.0177	0.0134	0.0209	N/L	---	---	---	---	---	---	---	---	---	---	
3	3	14.73	0.102	107	315	3.41	1.55	3.41	1.55	---	---			0.0224	0.0286	0.0189	0.0141	0.0208	N/L	---	---	---	---	---	---	---	---	---	---	
4	4	14.78	0.102	156	342	3.60	1.64	3.60	1.64	---	---			0.0164	0.0259	0.0186	0.0107	0.0194	0.0560	*0.0683	---	0.0366	---	---	---	---	---	---	*Partial Propagation	
5	5	14.86	0.103	228	382	4.07	1.85	4.07	1.85	---	---			0.0131	0.0216	0.0124	0.0033	0.0143	0.0397	*0.0625	---	0.0260	---	---	---	---	---	---		
6	6	14.94	0.103	312	429	4.32	1.96	4.32	1.96	---	---			0.0108	0.0169	0.0075	0	0.0107	0.0256	0.0480	0.0411	0.0202	---	---	---	---	---	---		
7	7	15.23	0.105	442	501	5.20	2.36	5.20	2.36	---	---			0.0070	0.0113	0.0065	0.0024	0.0084	0.0243	0.0251	0.0155	0.0135	---	---	---	---	---	---		

ORIGINAL PAGE 19
OF POOR QUALITY

Table 4F. Development Combustor Mod III Test Data.

ORIGINAL PAGE 19
OF POOR QUALITY

Reading	Test Point	Inlet Total Pressure		Inlet Temperature		Combustor Inlet Airflow		Combustor Exit Airflow		Combustor Total Fuel Flow		Pilot To Total Fuel Split	Combustor Overall Fuel/Air Ratio	Pilot Stage Ignition (f/a)					Main Stage Ignition (f/a)				Emissions Data				Combustor Total Pressure Loss %	Comments
														L/O 1-Cup	L/O 3-Cup	LBO 1-Cup	LBO Total	Steady State and Cross Fire	L/O 1-Cup	L/O 30-Cups	LBO 1-Cup	LBO Total	CO	HC g/Kg	NOx	η _c %		
		psia	MPa	°F	K	pps	kg/s	pps	kg/s	pph	kg/h			---	---	---	---	---	---	---	---	---	---	---	---	---		
1	1	14.62	0.101	79	299	2.77	1.26	2.77	1.26	---	---	---	---	0.0292	0.0383	0.0318	0.0202	0.0350	N/L	---	---	---	N/A	N/A	N/A	N/A	N/A	Mod III-A Ignition
2	2	14.71	0.101	86	303	3.79	1.72	3.79	1.72	---	---	---	---	0.0213	0.0272	0.0258	0.0155	0.0285	N/L	---	---	---	N/A	N/A	N/A	N/A	N/A	Mod III-A Ignition
3	3	14.68	0.101	112	318	3.41	1.55	3.41	1.55	---	---	---	---	0.0206	0.0283	0.0232	0.0135	0.0255	---	0.0179	0.0565	0.0390	N/A	N/A	N/A	N/A	N/A	Mod III-A Ignition
4	4	14.72	0.102	167	354	3.56	1.62	3.56	1.62	---	---	---	---	0.0196	0.0269	0.0172	0.0130	0.0200	---	0.0565	0.0428	0.0261	N/A	N/A	N/A	N/A	N/A	Mod III-A Ignition
5	4	14.73	0.102	162	345	3.63	1.65	3.63	1.65	---	---	---	---	0.0174	0.0264	0.0202	0.0129	0.0225	0.0411	0.0526	0.0390	0.0261	N/A	N/A	N/A	N/A	N/A	Mod III-A Ignition
6	5	14.83	0.102	233	385	4.10	1.86	4.10	1.86	---	---	---	---	0.0135	0.0190	0.0161	0.0068	0.0178	---	0.0437	0.0327	0.0253	N/A	N/A	N/A	N/A	N/A	Mod III-A Ignition
7	6	14.90	0.102	313	429	4.33	1.97	4.33	1.97	---	---	---	---	0.0123	0.0151	0.0140	0.0041	0.0120	0.0244	0.0342	0.0247	0.0178	N/A	N/A	N/A	N/A	N/A	Mod III-A Ignition
8	7	15.13	0.104	444	502	5.08	2.31	5.08	2.31	---	---	---	---	0.0083	0.0094	0.0073	0.0025	0.0083	---	0.0317	0.0110	0.0089	N/A	N/A	N/A	N/A	N/A	Mod III-A Ignition
1	1	14.51	0.100	93	307	2.80	1.27	2.80	1.27	---	---	---	---	0.0202	0.0384	0.0318	0.0196	0.0352	0.0653	*0.0694	---	0.0583	N/A	N/A	N/A	N/A	N/A	Mod III-b Ignition
2	3	14.55	0.100	108	315	3.12	1.42	3.12	1.42	---	---	---	---	0.0191	0.0325	0.0266	0.0175	0.0288	0.0538	0.0749	0.0680	0.0507	N/A	N/A	N/A	N/A	N/A	Mod III-b Ignition
3	4	14.62	0.101	106	314	3.78	1.72	3.78	1.72	---	---	---	---	0.0154	0.0261	0.0227	0.0147	0.0245	0.0453	*0.0655	---	0.0431	N/A	N/A	N/A	N/A	N/A	*Partial Propagation
4	5	14.67	0.101	104	313	4.26	1.94	4.26	1.94	---	---	---	---	0.0144	0.0240	0.0191	0.0129	0.0211	0.0419	*0.0582	---	0.0399	N/A	N/A	N/A	N/A	N/A	*Partial Propagation
5	6	14.60	0.101	156	342	3.40	1.55	3.40	1.55	---	---	---	---	0.0161	0.0295	0.0232	0.0140	0.0256	0.0482	0.0632	0.0607	0.0394	N/A	N/A	N/A	N/A	N/A	*Partial Propagation
6	7	14.66	0.101	153	340	3.86	1.75	3.86	1.75	---	---	---	---	0.0140	0.0254	0.0212	0.0129	0.0233	0.0432	0.0610	0.0568	0.0357	N/A	N/A	N/A	N/A	N/A	*Partial Propagation
8	8	14.76	0.102	151	339	4.60	2.09	4.60	2.09	---	---	---	---	0.0123	0.0216	0.0168	0.0091	0.0186	0.0347	0.0512	0.0487	0.0296	N/A	N/A	N/A	N/A	N/A	*Partial Propagation
8	9	14.73	0.102	226	381	4.16	1.89	4.16	1.89	---	---	---	---	0.0135	0.0214	0.0147	0.0078	0.0162	0.0308	0.0433	0.0338	0.0259	N/A	N/A	N/A	N/A	N/A	*Partial Propagation
9	10	14.78	0.102	307	426	4.33	1.97	4.33	1.97	---	---	---	---	0.0146	0.0169	0.0114	0.0046	0.0125	0.0339	0.0339	0.0252	0.0192	N/A	N/A	N/A	N/A	N/A	*Partial Propagation
10	11	15.06	0.104	441	500	5.16	2.35	5.16	2.35	---	---	---	---	0.0093	0.0098	0.0075	0.0010	0.0082	0.0234	0.0234	0.0151	0.0100	N/A	N/A	N/A	N/A	N/A	*Partial Propagation
11	12	15.20	0.105	440	500	5.61	2.55	5.61	2.55	---	---	---	---	0.0069	0.0090	0.0073	0.0025	0.0081	0.0190	0.0223	0.0175	0.0124	N/A	N/A	N/A	N/A	N/A	*Partial Propagation
12	13	15.40	0.106	440	500	6.36	2.89	6.36	2.89	---	---	---	---	0.0065	0.0089	0.0068	0.0038	0.0074	0.0186	0.0198	0.0155	0.0111	N/A	N/A	N/A	N/A	N/A	*Partial Propagation

Table 5F. Development Combustor Mod IV Test Data.

Reading	Test Point	Inlet Total Pressure		Inlet Temperature		Combustor Inlet Airflow		Combustor Exit Airflow		Combustor Total Fuel Flow		Pilot To Total Fuel Split	Combustor Overall Fuel/Air Ratio	Pilot Stage Ignition (f/a)					Main Stage Ignition (f/a)				Emissions Data				Combustor Total Pressure Loss %	Comments
														L/O 1-Cup	L/O 3-Cup	LBO 1-Cup	LBO Total	Steady State and Cross Fire	L/O 1-Cup	L/O 30-Cups	LBO 1-Cup	LBO Total	CO	HC g/Kg	NOx	η _c %		
		psia	MPa	°F	K	pps	kg/s	pps	kg/s	pph	kg/h			---	---	---	---	---	---	---	---	---	---	---	---	---		
1	1	N/A	N/A	78	299	2.87	1.30	2.87	1.30	---	---	---	---	0.0173	0.0375	0.0276	0.0186	0.0328	0.0784	0.0784	0.0742	0.0521	N/A	N/A	N/A	N/A	N/A	Ignition
2	2	N/A	N/A	74	296	3.71	1.69	3.71	1.69	---	---	---	---	0.0249	0.0298	0.0258	0.0156	0.0278	0.0760	*0.0760	---	0.0409	N/A	N/A	N/A	N/A	N/A	*Partial Propagation
3	3	N/A	N/A	104	313	3.56	1.62	3.56	1.62	---	---	---	---	0.0202	0.0293	0.0254	0.0160	0.0285	0.0755	0.0755	0.0634	0.0448	N/A	N/A	N/A	N/A	N/A	*Partial Propagation
4	4	N/A	N/A	156	342	3.73	1.70	3.73	1.70	---	---	---	---	0.0187	0.0253	0.0224	0.0139	0.0241	0.0648	0.0648	0.0549	0.0354	N/A	N/A	N/A	N/A	N/A	*Partial Propagation
5	5	N/A	N/A	226	381	4.04	1.84	4.04	1.84	---	---	---	---	0.0159	0.0204	0.0149	0.0085	0.0158	0.0453	0.0453	0.0353	0.0240	N/A	N/A	N/A	N/A	N/A	*Partial Propagation
6	6	N/A	N/A	310	428	4.27	1.94	4.27	1.94	---	---	---	---	0.0130	0.0155	0.0109	0.0051	0.0122	0.0388	0.0388	0.0283	0.0214	N/A	N/A	N/A	N/A	N/A	*Partial Propagation
7	7	N/A	N/A	442	501	5.16	2.35	5.16	2.35	---	---	---	---	0.0107	0.0110	0.0071	0	0.0081	0.0265	0.0265	0.0188	0.0138	N/A	N/A	N/A	N/A	N/A	*Partial Propagation
8	4	N/A	N/A	160	344	3.66	1.66	3.66	1.66	---	---	---	---	0.0197	0.0247	0.0218	0.0146	0.0246	0.0591	0.0598	0.0527	0.0364	N/A	N/A	N/A	N/A	N/A	*Partial Propagation

Table 6F. Development Combustor Mod V Test Data.

Reading	Test Point	Inlet Total Pressure		Inlet Temperature		Combustor Inlet Airflow		Combustor Exit Airflow		Combustor Total Fuel Flow		Pilot To Total Fuel Split	Combustor Overall Fuel/Air Ratio	Pilot Stage Ignition (f/a)					Main Stage Ignition (f/a)				Emissions Data				Combustor Total Pressure Loss %	Comments
														L/O 1-Cup	L/O 3-Cup	LBO 1-Cup	LBO Total	Steady State and Cross Fire	L/O 1-Cup	L/O 30-Cups	LBO 1-Cup	LBO Total	CO	HC g/Kg	NOx	η _c %		
		psia	MPa	°F	K	pps	kg/s	pps	kg/s	pph	kg/h			---	---	---	---	---	---	---	---	---	---	---	---	---		
1	1	14.57	0.101	78	299	2.77	1.26	2.77	1.26	---	---	---	---	0.0291	0.0366	0.0323	0.0187	0.0356	N/L	---	---	---	N/A	N/A	N/A	N/A	N/A	Ignition
2	2	14.68	0.101	77	298	3.69	1.68	3.69	1.68	---	---	---	---	0.0204	0.0287	0.0259	0.0167	0.0283	---	0.0231	0.0619	0.0425	N/A	N/A	N/A	N/A	N/A	Ignition
3	3	14.66	0.101	99	310	3.46	1.57	3.46	1.57	---	---	---	---	0.0189	0.0290	0.0271	0.0166	0.0293	---	0.0768	0.0551	0.0461	N/A	N/A	N/A	N/A	N/A	Ignition
4	4	14.70	0.101	157	343	3.62	1.65	3.62	1.65	---	---	---	---	0.0210	0.0265	0.0237	0.0116	0.0265	---	0.0640	0.0513	0.0417	N/A	N/A	N/A	N/A	N/A	Ignition
5	5	14.78	0.102	223	379	4.04	1.84	4.04	1.84	---	---	---	---	0.0184	0.0214	0.0172	0.0078	0.0190	0.0428	0.0673	0.0422	0.0309	N/A	N/A	N/A	N/A	N/A	Ignition
6	6	14.85	0.102	308	426	4.31	1.96	4.31	1.96	---	---	---	---	0.0125	0.0168	0.0117	0.0035	0.0128	0.0280	0.0364	0.0264	0.0223	N/A	N/A	N/A	N/A	N/A	Ignition
7	7	15.10	0.104	434	496	5.10	2.32	5.10	2.32	---	---	---	---	0.0110	0.0134	0.0066	0.0028	0.0091	0.0205	0.0225	0.0200	0.0149	N/A	N/A	N/A	N/A	N/A	Ignition
8	4	14.69	0.101	155	341	3.63	1.65	3.63	1.65	---	---	---	---	0.0208	0.0268	0.0211	0.0109	0.0230	---	0.0606	0.0461	0.0371	N/A	N/A	N/A	N/A	N/A	Ignition

ORIGINAL PAGE IS
OF POOR QUALITY

Table 7F. Development Combustor Mod VI Test Data.

ORIGINAL PAGE IS
OF POOR QUALITY

Reading	Test Point	Inlet Total Pressure		Inlet Temperature		Combustor Inlet Airflow		Combustor Exit Airflow		Combustor Total Fuel Flow		Pilot To Total Fuel Split	Combustor Overall Fuel/Air Ratio	Pilot Stage Ignition (f/a)					Main Stage Ignition (f/a)				Emissions Data				Combustor Total Pressure Loss %	Comments		
		psia	MPa	°F	K	pps	kg/s	pps	kg/s	pph	kg/h			L/O 1-Cup	L/O 3-Cup	LBO 1-Cup	LBO Total	Steady State and Cross Fire	L/O 1-Cup	L/O 30-Cups	LBO 1-Cup	LBO Total	Co	HC g/Kg	Nox	HC %				
1	1	14.79	0.102	87	304	4.77	2.17	4.77	2.17	----	----			0.0153	0.0208	0.0162	0.0102	----	----	----	----	----	----	N/A	N/A	N/A	N/A	N/A		Ignition
2	2	14.78	0.102	87	304	4.65	2.11	4.65	2.11	----	----			0.0142	0.0211	0.0149	0.0108	----	----	----	----	----	----							
3	3	14.92	0.103	95	308	5.50	2.50	5.50	2.50	----	----			0.0115	0.0190	0.0131	0.0091	----	----	----	----	----	----							
4	4	14.89	0.103	96	309	5.32	2.42	5.32	2.42	----	----			0.0122	0.0190	0.0132	0.0094	----	----	----	----	----	----							
5	5	15.09	0.104	130	328	6.28	2.85	6.28	2.85	----	----			0.0104	0.0162	0.0102	0.0064	0.0124	N/L	----	----	----	----							
6	6	15.04	0.104	138	332	5.98	2.72	5.98	2.72	----	----			0.0122	0.0173	0.0096	0.0066	0.0118	N/L	----	----	----	----							
7	7	15.31	0.106	157	343	7.06	3.21	7.06	3.21	----	----			0.0100	0.0147	0.0086	0.0060	----	----	----	----	----	----							
8	8	15.28	0.105	167	348	6.90	3.14	6.90	3.14	----	----			0.0096	0.0144	0.0086	0.0060	----	----	----	----	----	----							
9	9	15.10	0.104	376	464	5.25	2.39	5.25	2.39	----	----			0.0071	0.0113	0.0066	0.0040	0.0080	0.0377	*0.0481	----	0.0325								
10	10	15.06	0.104	402	479	5.10	2.32	5.10	2.32	----	----			0.0092	0.0108	0.0063	0.0032	0.0071	0.0394	0.0465	0.0288	0.0145								
11	11	15.21	0.105	428	493	5.41	2.46	5.41	2.46	----	----			0.0075	0.0108	0.0060	0.0031	0.0072	0.0353	0.0362	0.0195	0.0108								
12	12	15.27	0.105	504	535	5.34	2.43	5.34	2.43	----	----			0.0068	0.0095	0.0058	0.0034	0.0068	0.0318	0.0318	0.0149	0.0106								
13	13	15.27	0.105	678	632	4.95	2.25	4.95	2.25	----	----			0.0062	0.0175	0.0061	0.0017	0.0070	0.0305	0.0322	0.0121	0.0095								

Table 8F. Development Combustor Mod VII Test Data.

Reading	Test Point	Inlet Total Pressure		Inlet Temperature		Combustor Inlet Airflow		Combustor Exit Airflow		Combustor Total Fuel Flow		Pilot To Total Fuel Split	Combustor Overall Fuel/Air Ratio	Pilot Stage Ignition (f/a)					Main Stage Ignition (f/a)				Emissions Data				Combustor Total Pressure Loss %	Comments		
		psia	MPa	°F	K	pps	kg/s	pps	kg/s	pph	kg/h			L/O 1-Cup	L/O 3-Cup	LBO 1-Cup	LBO Total	Steady State and Cross Fire	L/O 1-Cup	L/O 30-Cups	LBO 1-Cup	LBO Total	Co	HC g/Kg	Nox	HC %				
1	1	18.0	0.124	85	303	5.38	2.45	5.38	2.45	----	----			0.0171	0.0202	0.0146	0.0104	----	----	----	----	----	----	N/A	N/A	N/A	N/A	N/A		Ignition
2	2	18.5	0.128	98	310	6.25	2.84	6.25	2.84	----	----			0.0156	0.0172	0.0120	0.0071	----	----	----	----	----	----							
3	3	20.4	0.141	117	320	7.64	3.47	7.64	3.47	----	----			0.0129	0.0143	0.0086	0.0058	0.0095	N/L	----	----	----	----							
4	4	22.5	0.155	171	350	8.86	4.03	8.86	4.03	----	----			0.0105	0.0118	0.0064	0.0058	0.0095	0.0255	0.0396	----	0.0141								
5	5	50.9	0.351	365	458	17.83	8.10	17.83	8.10	----	----			0.0069	0.0073	0.0038	0.0033	0.0047	0.0216	0.0216	0.0147	0.0144								
6	6	62.7	0.432	420	489	23.16	10.53	23.16	10.53	----	----			0.0094	0.0094	0.0038	0.0032	0.0045	0.0184	0.0184	0.0143	0.0137								
7	7	85.8	0.592	500	533	31.03	14.10	31.03	14.10	----	----			0.0084	0.0084	0.0035	0.0031	0.0038	0.0179	0.0179	----	0.0072								
8	8	49.9	0.344	368	460	21.38	9.72	17.42	7.92	594	270	1.0	0.0095	N/A	N/A	N/A	N/A	N/A	N/A	N/A	N/A	N/A	81.6	32.5	1.9	94.85	4.02		Emissions	
9	9	50.2	0.346	368	460	21.62	9.83	17.82	8.10	703	320	1.0	0.0110										41.4	12.7	2.5	97.76	4.55			
10	10	50.1	0.345	369	460	21.43	9.74	17.77	8.08	808	367	1.0	0.0126										29.1	7.2	2.9	98.60	4.29		4% G-Idle	
11	11	50.2	0.346	366	459	21.57	9.80	18.08	8.22	1015	461	1.0	0.0156										33.9	5.8	3.4	98.63	4.30			
12	12	50.1	0.345	369	460	21.45	9.75	17.60	8.00	1138	517	1.0	0.0180										57.6	3.3	3.5	98.33	4.46			
13	13	63.2	0.436	420	489	26.95	12.25	21.23	9.65	821	373	1.0	0.0102										35.7	8.0	3.4	98.37	4.80			
14	14	63.0	0.434	428	493	27.22	12.37	22.79	10.36	943	429	1.0	0.0115										23.3	4.3	3.9	99.03	4.73			
15	15	63.1	0.435	425	491	27.01	12.28	22.64	10.29	981	446	1.0	0.0120										31.4	6.1	2.9	98.06	4.92			
16	16	63.4	0.437	425	491	27.44	12.47	22.94	10.43	1165	530	1.0	0.0141										23.6	2.7	4.3	99.18	4.91			
17	17	63.0	0.434	425	491	27.06	12.30	22.82	10.37	1318	599	1.0	0.0160										35.2	1.6	4.5	99.02	5.74			
18	18	99.7	0.687	692	640	40.68	18.49	32.45	14.75	1624	738	0.3	0.0139										130.3	166.5	1.8	80.31	N/A		Unadjusted	
19	19	98.6	0.680	694	641	40.86	18.57	33.04	15.02	1631	741	0.4	0.0137										127.7	96.0	2.2	87.42	N/A		Unadjusted	
20	20	99.9	0.689	687	637	40.16	18.25	32.39	14.72	1560	709	1.0	0.0134										6.8	1.8	4.2	99.66	N/A		Unadjusted	

FOLDOUT FRAME

FOLDOUT FRAME

REFERENCES

1. Bahr, D.W., Gleason, L.C., and Rogers, D.W., "Experimental Clean Combustor Program."
2. Bahr, D.W., Burrus, D.W., and Sabla, P.E., "QCSEE Double-Annular Clean Combustor Technology Department Report," NASA CR-159483, May 1979.
3. "Control of Air Pollution from Aircraft and Aircraft Engines," U.S. Environmental Protection Agency, Federal Register Vol. 38, No. 136, July 1973.
4. Reneau, L.R., Johnston, J.P., and Kline, S.J., "Diffuser Design Manual," Dept. of Mechanical Engineering, Stanford University, Report PD-8, September 1964.
5. Waitman, B.A., Reneau, L.R., and Kline, S.J. "Effects of Inlet Conditions on Performance of Two-Dimensional Diffusers," Dept. of Mechanical Engineering, Stanford University, Report PD-5, August 1960.
6. Livesey, J.L. and Turner, J.T., "The Dependence on Diffuser Performance Upon Inlet Flow Conditions," Journal of Royal Aeronautical Society, Vol. 69, 1965.

PRECEDING PAGE BLANK NOT FILMED

